

Towards Synthesis of Simplified Analogues of Pateamine A

by

Tao Xu

*A thesis submitted to the Victoria University of Wellington in fulfilment of
the requirements for the degree of Doctor of Philosophy*



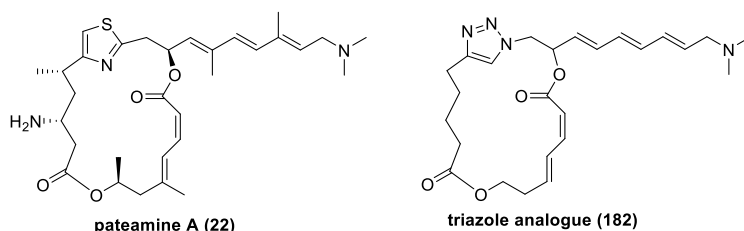
Victoria University of Wellington

2020

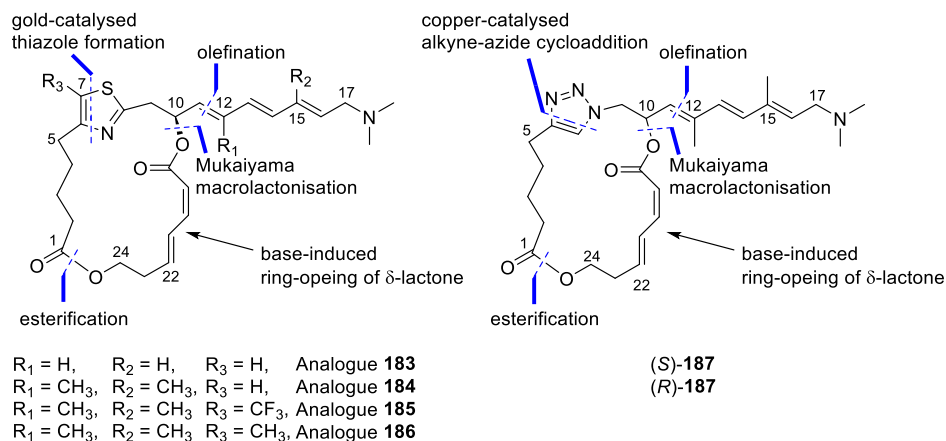
Abstract

Pateamine A (**22**) is a natural product that was isolated from a marine sponge inhabiting the coast of New Zealand. It exhibits potent inhibition of protein synthesis and nonsense-mediated mRNA decay through binding with eIF4A isoforms. Due to the scarcity of pateamine A (**22**) in the natural source and the low yield of total synthesis of pateamine A, it is necessary to prepare structurally simplified analogues which would allow further research on structure-activity relationships (SAR) of pateamine A (**22**).

Based on the structure-activity relationship studies reported by Romo and co-workers, a simplified triazole analogue **182** lacking methyl groups was synthesized by Hemi Cumming, a previous Ph.D. student who studied at Victoria University of Wellington. The antiproliferative activity of this analogue was found to be significantly lower than that of pateamine A, suggesting that the thiazole embedded within the molecule or the excised methyl groups are crucial for its potency.



Therefore, to further explore the necessary features for its selective activity for eIF4A isoforms, new thiazole analogues **183** – **186** and triazole analogues (10*S*)- and (10*R*)-analogue **187** were targeted in this project.



The preparation of the thiazole-containing macrocyclic core of analogues **183** and **184** was achieved. It features: (1) gold-catalysed thiazole formation through coupling between an alkyne fragment and a thioamide fragment; (2) preparation of the *Z,E*-dienoate moiety by base-induced ring-opening of a δ -substituted- α,β -unsaturated lactone; and (3) a modified Mukaiyama macrolactonisation. The synthesis of the triazole-containing macrocyclic core of (10*S*)-analogue **187** was completed. It features: (1) a copper-catalysed triazole formation through 1,3-dipolar cycloaddition between an alkyne fragment and an azide fragment; (2) preparation of the *Z,E*-dienoate moiety by base-induced ring-opening of a δ -substituted- α,β -unsaturated lactone; and (3) a modified Mukaiyama macrolactonisation. Studies on the preparation of a side-chain fragment with suitable functionalities to allow coupling with the various macrocycles through olefination reactions were also conducted.

The attachment of the side-chain fragment onto the macrocyclic cores for the synthesis of the targeted analogues **183** and **184** and (10*S*)-analogue **187** will be investigated in the future work. These experimental results will inform the synthesis of new generation analogues to further study the key structures required for effective binding to the protein target eIF4A and selectivity between isoforms.

Acknowledgements

In my PhD journey, I've encountered many unexpected challenges. Although it was filled with stress and frustration sometimes, it has also been very enjoyable and enriching. It is now very satisfying that I can finally be able to share what I have learnt and achieved in these few years and thank those who have helped me succeed.

First, I would like to thank my supervisors, Joanne Harvey and Paul Teesdale-Spittle. Thank you very much for your guidance, encouragement, patience and immense knowledge throughout these years. Paul, your inspiring ideas; and Joanne, your enthusiasm for chemistry, has helped me tremendously succeeding my goals. Also, I really appreciate your proofreading my thesis and invaluable suggestions.

I was very lucky to get financial support for most of my time of study. Many thanks to Worldwide Cancer Research for offering my scholarship, Faculty Strategic Research Grants from Faculty of Science and New Zealand Institute Travel Grant (allowing me to attend 22nd International Conference on Organic Synthesis at Florence) and Victoria PhD Submission Scholarship (allowing to survive in my last months). Big thanks again to Joanne for offering me a part-time research assistant job to help me get through all those days when my scholarship was running out.

Furthermore, I would like to acknowledge Ian Vorster for his help to keeping the NMR facilities working nicely and running NOE experiments for my samples, and Sophie and Ethan for their time running my samples on the mass spectrometer. I want to thank Sarah Andreassend for running samples on the 600 NMR.

To Chao, I probably wouldn't have been able to finish my Ph.D. project if you weren't by my side. Thank you for accompanying me when I was working in lab on the weekends to make me feel safe, and driving me to university or picking me up after working hours.

I'm really thankful for the members of "ECAT". Claire, Amira, Ethan. Thank you for being very supportive to me, and making the "boring" lab to be such a fun place to work. Also, big thanks to Claire Cuyamendous and Sarah Brown, for helping me out at the early days of my project, and contributing a lot to the pateamine project.

To all the past and present members of our group - Jordan, Ben, Tom, Dan, Hedley, Sophie, Chris, Matt, Olly, thanks for all the great discussions and all the help.

To my mum and dad, thank you so much for encouraging me to pursue my future overseas and supporting me to complete this long and stressful journey. I'm so blessed that I can have you in my life. Everything I have and will achieve is because of you both.

ABSTRACT	II
ACKNOWLEDGEMENTS	IV
ABBREVIATIONS	X
CHAPTER ONE: INTRODUCTION	1
1.1 Natural Products and Analogues as Anticancer Agents	1
1.2 Discovery of Pateamine A	10
1.3 Biological Activity of Pateamine A	11
1.4 Syntheses of Pateamine A and Analogues	15
1.4.1 Total Syntheses of Pateamine A	15
1.4.2 Pateamine A Analogues Synthesis	37
1.5 Structure-Activity Relationship Studies of PatA and Analogues	45
1.5.1 Studies on Immunosuppressive Activity of PatA Analogues	45
1.5.2 Studies on Anti-proliferative Activity of PatA Analogues	47
1.5.2 Summary	51
1.6 Cumming's Synthesis of Triazole Analogue	52
1.7 Research Aim	54
1.7.1 Analogue Design	54
1.7.2 Retrosynthetic Analysis	56
CHAPTER TWO: TOWARDS THE SYNTHESIS OF THIAZOLE ANALOGUE WITH NON-METHYLATED SIDE CHAIN	59
2.1 Retrosynthesis	59
2.2 Synthesis of C8-C11 Thioamide (Fragment IV)	61
2.2.1 Introduction	61
2.2.2 Initial Attempts Towards Synthesis of Nitrile 206	64
2.2.3 Preparation of Thioamide Fragment IV	66

2.3 Synthesis of Thiazole Fragment 232	77
2.3.1 Introduction	77
2.3.2 Synthesis of Thiazole Fragment 232 Using Gold Catalysis	83
2.4 Coupling of Side Chain Fragment	92
2.4.1 Introduction	92
2.4.2 Preparation of Sulfone 277	93
2.4.3 Synthesis of Side Chain Fragment 297	94
2.4.4 Model Julia-Kocienski Olefination	96
2.5 Revised Synthesis of Sulfone 316	101
2.5.1 Attempted Synthesis of Thioamide 317	101
2.5.2 Attempted Preparation of Air-Stable Thioamides	110
2.6 Revised Synthesis of Analogue 183	118
2.7 Conclusion	120
 CHAPTER THREE: TOWARDS SYNTHESIS OF THIAZOLE ANALOGUE WITH METHYLATED SIDE CHAIN	 123
3.1 Retrosynthetic Analysis	123
3.2 Preparation of Air-stable Thioamide 382	124
3.3 Preparation of Alkyne 364	130
3.4 Preparation of Thiazole And C7-Substituted Thiazole	133
3.4.1 Preparation of Thiazoles 392 and 393	133
3.4.2 Preparation of C-7 Substituted Thiazole	135
3.4.3 Summary	138
3.5 Construction of macrocycle	139
3.5.1 Synthesis of <i>E,Z</i> -Dienoic Acid	139
3.5.2 Macrolatonisation	153
3.6 Synthesis of Side Chain Fragment	162
3.6.1 Wittig Olefination and Horner-Wadsworth-Emmons Reaction	162
3.6.2 Preparation of Side Chain Fragments	165

3.7 Conclusion	177
 CHAPTER FOUR: TOWARDS SYNTHESIS OF TRIAZOLE ANALOGUE WITH METHYLATED SIDE CHAIN	 179
4.1 Introduction	179
4.1.1 Synthesis of Triazole Analogue 182	179
4.1.2 Reintroduction of Methyl Groups to Side Chain	182
4.2 Retrosynthetic Analysis	183
4.3 Attempted Preparation of Aldehyde (<i>R</i>)-509	186
4.4 Revised Synthetic Route for Synthesis of Analogue (<i>S</i>)-187	188
4.5 Construction of Macrocyclic Compound 523	189
4.6 Conclusion	195
 CHAPTER FIVE: SUMMARY AND FUTURE WORK	 197
5.1 Summary	197
5.1.1 Attempted Synthesis of Thiazole Analogue 183	197
5.1.2 Towards Synthesis of Thiazole Analogue 184	200
5.1.3 Towards Synthesis of Analogue (<i>S</i>)-187	204
5.1.4 Closing Remarks	205
5.2 Future Work	206
5.2.1 Synthesis of Analogues 184 and 187	206
5.2.2 Role of the Thiazole and Methyl Groups on the Macrocycle	209
5.2.3 Role of Methyl Groups on Side Chain	211
5.2.4 Importance of the C-10 Configuration	212
 CHAPTER SIX: EXPERIMENTAL	 213
6.1 General Experimental Details	213
6.2 Experimental for Chapter Two	215
6.2.1 Preparation of Thioamide 223	215
6.2.2 Gold-catalysed Preparation of Thiazole 276	224

6.2.3 Julia-Kocienski Coupling with Side Chain	232
6.2.3 Towards Synthesis of Thioamide 317	243
6.2.4 Attempted Preparation of Air-stable Thioamides	248
6.3 Experimental for Chapter Three	257
6.3.1 Synthesis of Thioamide 382	257
6.3.2 Synthesis of Alkyne 364	261
6.3.4 Synthesis of Thiazoles 392, 393 and 394	266
6.3.5 Synthesis of Macrocyclic Alcohol 441	269
6.3.5 Synthesis of the Side Chain Fragments	276
6.4 Experimental for Chapter Four	286
6.4.1 Attempted Synthesis of Aldehyde (<i>R</i>)-509	286
6.4.2 Synthesis of Macrocyclic Alcohol 523	290
NMR Spectra of Novel Compounds	296
Spectra of Chapter Two	296
Spectra of Chapter Three	331
Spectra of Chapter Four	355
BIBLIOGRAPHY	361

Abbreviations

18-crown-6	1,4,7,10,13,16-Hexaoxacyclooctadecane
2D	Two-dimensional
4Å	4 Angstrom
<i>aq.</i>	Aqueous
Ac	Acetyl
BAIB	(Diacetoxyiodo)benzene
Boc	<i>tert</i> -Butyloxycarbonyl
BRSM	Based on recovered starting material
<i>c.f.</i>	<i>confer</i> (“compare to”)
<i>ca.</i>	<i>circa</i> (“approximately”)
CAN	Ceric ammonium nitrate
cat.	Catalytic
Cbz	Carboxybenzyl
DBU	1,8-Diazabicyclo[5.4.0]undec-7-ene
DCC	<i>N,N'</i> -Dicyclohexylcarbodiimide
DCE	1,2-Dichloroethane
DCM	Dichloromethane
DDQ	2,3-Dichloro-5,6-dicyano-1,4-benzoquinone
DIAD	Diisopropyl azodicarboxylate

DIBAL-H	Diisobutylaluminium hydride
DIPEA	<i>N,N</i> -Diisopropylethylamine
DMAP	4-Dimethylaminopyridine
DME	1,2-Dimethoxyethane
DMF	<i>N,N</i> -Dimethylformamide
DMP	Dess–Martin periodinane
DMSO	Dimethyl sulfoxide
<i>e.e.</i>	Enantiomeric excess
<i>e.g.</i>	<i>exempli gratia</i> (“for example”)
EDCI	<i>N</i> -(3-Dimethylaminopropyl)- <i>N'</i> -ethylcarbodiimide hydrochloride
EJC	Exon junction complex
equiv.	Equivalent
Et	Ethyl
Et ₂ O	Diethyl ether
EtOAc	Ethyl acetate
gCOSY	Gradient correlation spectroscopy
<i>gem</i> -	Geminal
h	Hour(s)
HMBC	Heteronuclear multiple bond correlation
HSQC	Heteronuclear single quantum correlation
HMPA	Hexamethylphosphoramide

HRMS	High resolution mass spectrometry
HWE	Horner–Wadsworth–Emmons
IC ₅₀	Inhibitory concentration for 50% effect
IR	Infrared
KHMDS	Potassium bis(trimethylsilyl)amide
LiHMDS	Lithium bis(trimethylsilyl)amide
M	Molar
<i>m</i> -CPBA	3-Chloroperoxybenzoic acid
Me	Methyl
MOM	Methoxymethyl
MS	Molecular sieves
Ms	Mesylate
MsOH	Methanesulfonic acid
MTPA	α -Methoxy- α -trifluoromethylphenylacetic acid
MTT assay	((3-(4,5-Dimethylthiazol-2-yl)-2,5-diphenyltetrazolium bromide) tetrazolium reduction assay
NBS	<i>N</i> -Bromosuccinimide
NMD	Nonsense-mediated decay
NMR	Nuclear magnetic resonance
NOE	Nuclear overhauser effect
-OTf	Trifluoromethanesulfonate (triflate)

pet. ether	Petroleum ether
PG	Unspecified protecting group
Ph	Phenyl
PKC	Protein kinase C
PMB	<i>para</i> -Methoxybenzyl
PPTS	Pyridinium <i>para</i> -toluenesulfonate
Pr	Propyl
PT	Phenyl tetrazole
<i>p</i> -TSA	<i>para</i> -Toluenesulfonic acid
quant.	Quantitative
R	Unspecified Substituent
R _f	Retardation factor
rt	Room temperature
TBAF	Tetra- <i>n</i> -butylammonium fluoride
TBAI	Tetra- <i>n</i> -butylammonium iodide
TBDPS	<i>tert</i> -butyldiphenyl silyl
TBS	<i>tert</i> -butyldimethyl silyl
TcBoc	Trichloro- <i>tert</i> -butoxy carbamate
TEA	Triethylamine
TEMPO	2,2,6,6-Tetramethylpiperidine 1-oxyl
TES	Triethyl silyl

Tf ₂ O	Trifluoromethanesulfonic anhydride
TFA	Trifluoroacetic acid
TFAA	Trifluoroacetic anhydride
THF	Tetrahydrofuran
TIPS	Triisopropyl silyl
TLC	Thin-layer chromatography
Tr	Trityl
Ts	<i>para</i> -Toluenesulfonate (Tosyl)
UV	Ultraviolet
<i>viz.</i>	<i>videlicet</i> (“namely”)

Chapter One: Introduction

This thesis presents efforts directed towards the synthesis of simplified analogues of the marine natural product, pateamine A. This chapter will begin by introducing the importance of marine-sourced natural products in the discovery of anticancer agents. The precedent for design and synthesis of structurally simplified analogues of marine natural products in drug development will be discussed. The discovery of pateamine A and its biological activity will be described. This is followed by a review of previous total syntheses of pateamine A, syntheses of its analogues, and the analysis of its structure-activity relationship. Finally, the research aim of this thesis and the retrosynthetic analysis of target analogues will be presented.

1.1 Natural Products and Analogues as Anticancer Agents

Natural products, by definition, are secondary metabolites naturally produced by plants, animals, and microbes. Historically, they have provided numerous agents of great value for medicines, such as aspirin (**1**), penicillin G (**2**), and paclitaxel (**3**) (Figure 1.1).¹ Natural products are very important for drug discovery because they possess enormous structural and chemical diversity, and can exhibit diverse bioactivities. In addition, they are evolutionarily optimised to have drug-like properties with regard to absorption, distribution, metabolism, excretion, and toxicity (ADMET) characteristics,² which influence the performance and pharmacological activity of a drug compound.

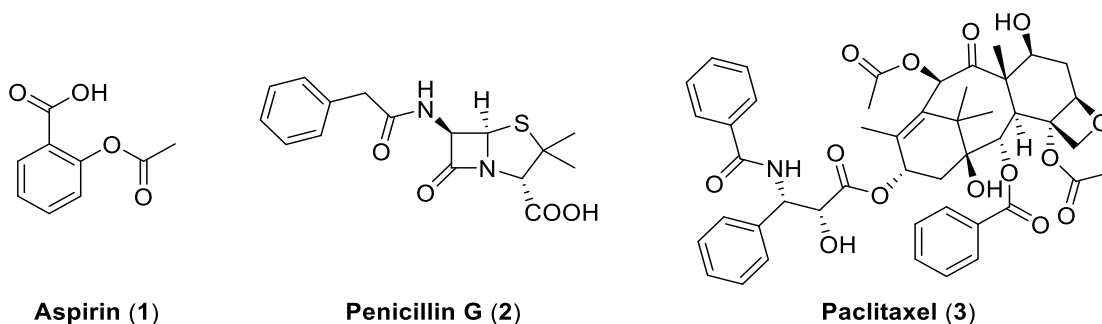


Figure 1.1 Chemical structures of aspirin (**1**), penicillin G (**2**) and paclitaxel (**3**).¹

Despite these advantages, it is undeniable that screening natural products for drug discovery is associated with some disadvantages. First, the process of isolation and characterisation of active compounds from a crude extract is time-consuming and

sometimes lacking in efficiency for finding novel chemical entities due to the high rediscovery rate. Second, identifying a pharmacophore of a structurally complex natural product through structure-activity studies is very challenging. Last but most importantly, scale-up for process chemistry to deliver sufficient quantities of structurally complex natural products is a significant obstacle for medicinal chemists.³ Consequently, the major pharmaceutical companies have been less enthusiastic about participation in natural product research since the 1990s after the advent of high-throughput screening (HTS) and combinatorial chemistry, which can rapidly generate large libraries of novel compounds for various bioactivity screening through diversity-oriented syntheses. Disappointingly, high-throughput screening of large numbers of purposely synthesised compounds imbued with high randomness has failed to deliver new lead compounds in significant numbers.⁴ A scan of drugs approved by the U.S. FDA (and similar organisations) from 1981–2014 shows that only 3 approved drugs, sorafenib (**4**), ataluren (**5**), and vemurafenib (**6**) (Figure 1.2), could be ascribed to combinatorial chemistry.⁴ In contrast, about 50% of drugs in the scan are naturally derived or naturally inspired. In the case of cancer, 77% of the anticancer drugs from the late 1930s to 2014 are related to natural products.⁴ This comprehensive analysis has demonstrated that natural products and structures related to natural products have played and will continue to play a very important role in the development of novel therapeutic treatments, which explains the recent trend of revisiting natural products for the discovery of new drug candidates in pharmaceutical companies and institutions.⁵

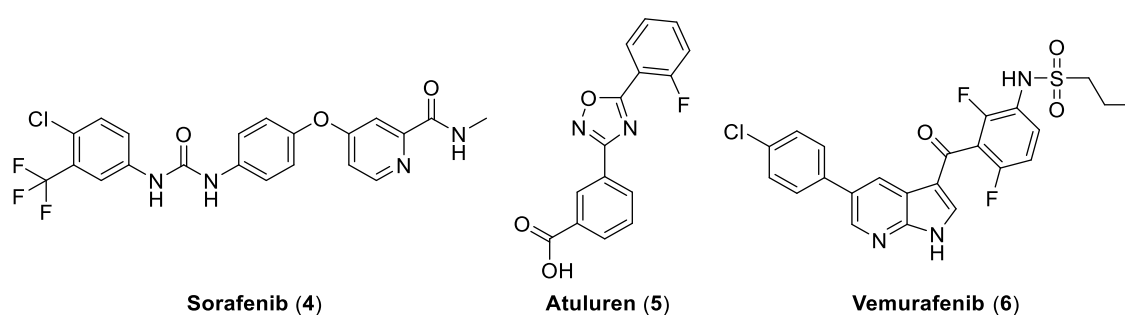


Figure 1.2 Chemical structures of sorafenib (**4**), ataluren (**5**), and vemurafenib (**6**).

In this area of research, the exploration of new anticancer agents from organisms living in the sea, such as sponges, alga, ascidians, coral, etc., has attracted increasing interests. The oceans are vast and cover more than 70% of the surface of the earth, and marine species are estimated to approach one to two million species. However, the majority

cohabit in the ocean fringe. Competition from such a high concentration of species in a narrow range of habitats makes them promotes greater evolutionary variation. Therefore, many species have evolved to be capable of producing chemicals to defend against predators, to suppress competing species, or to prey on other species for survival.⁶ These chemical adaptations involve a wide variety of primary and secondary metabolites, including nucleosides, sugars, steroids, terpenoids, alkaloids, polyketides and compounds of mixed structural origins, some of which exhibit potent anticancer effects. For example, didemnin B (**7**) (Figure 1.3), a cyclic depsipeptide isolated from the tunicate *Trididemnum solidum* living in the Caribbean area, showed *in vivo* cytotoxicity and could effectively increase the life-span of P388 leukemia-bearing mice.^{7, 8} It was the first marine natural product that successfully entered clinical trials as an anticarcinoma agent, although clinical trials against breast cancer, small-cell lung cancer, central nervous system tumors, and several other cancers were suspended due to significant neuromuscular toxicity and no positive responses.⁹⁻¹⁹

Another good example of the development of marine-derived antitumor agents is ecteinascidin-743 (ET-743) (**8**) (Figure 1.3), the structure of which was published by Rinehart²⁰ and Wright²¹ in 1990, 20 years after the first report about the antitumor activity of the extracts of the Caribbean tunicate *Ecteinascidia turbinata*. Its distinguishing structural characteristic is a 10-membered lactone containing a thioether bridge connecting the tetrahydroisoquinoline ring and the base scaffold. Ecteinascidins were found to display cytotoxicity against L1210 leukemia cells (IC₅₀ value of 0.5 ng/mL) and to possess significant *in vivo* antitumor activity in several mice models bearing P388 leukemia, B16 melanoma and colon carcinoma 26.²⁰ The mechanism of action of ET-743 is accredited to its covalent modification of DNA by acting as an alkylating agent, a property similar to another natural-product-based successful anticancer drug, anthramycin (**9**) (Figure 1.3).²² In 2007, ET-743, under the trade name Yondelis, was approved by the European Union for the treatment of patients with refractory soft tissue sarcoma, meaning that it became the first marine-derived marketable anticancer drug.

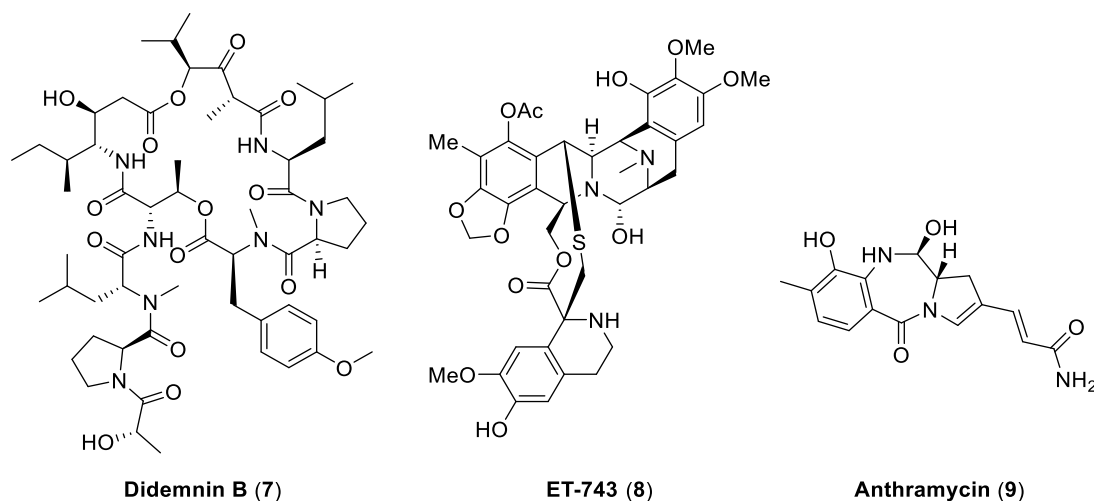


Figure 1.3 Chemical structures of didemnin B (7), ET-743 (8) and

anthramycin (9).^{8, 20, 21, 23}

Recently, marine bacteria have been considered as new potential sources for the discovery of drug leads.²⁴ Actually, many compounds isolated from marine invertebrates are considered to be produced by as-yet-uncultured symbiotic marine bacteria in larger host organisms, such as marine sponges, marine hares, and tunicates.²⁵ Metagenomics, or “genome mining”, has provided a promising method to search for novel natural product skeletons from free-living marine bacteria or endosymbiotic marine bacteria. The exploration of metagenomics has shown that the genetic information related to the biosynthesis of bioactive metabolites could be “abstracted” from uncultured microbes and in some cases successfully heterologously expressed in cultivable host microorganisms to achieve the desired secondary metabolites.²⁴

Nevertheless, it is obvious that a major difficulty for developing anticancer drugs from marine sources is to ensure a sustainable supply of adequate quantities of these rare compounds. Indeed, many marine natural products with interesting pharmacological properties can only be obtained in minute amounts. The extremely low yields of isolation and purification are already a forbidding challenge for preclinical and clinical trials with patients, not to mention the immense supply problem faced by the pharmaceutical industry once a bioactive compound successfully enters the market as a drug. To solve this pressing problem, several strategies appear to be feasible: 1. aquaculture of marine invertebrates;²⁶ 2. cloning and heterologous expression of key biosynthetic gene clusters of marine microbes to facilitate large-scale fermentation for production;^{24, 26} 3. semi-

synthesis; 4. total synthesis. For example, the breakthrough in the supply of ET-743 (**8**) was achieved by PharmaMar through large-scale semi-synthesis starting from cyanosafracin B (**10**) (Figure 1.4), an antibiotic that can be obtained in bulk by fermentation of *Pseudomonas fluorescens*.²⁷ Recently, Ma and co-workers reported the scalable 26-step total synthesis of ET-743 (**8**) starting from commercially available carbamate benzyloxy (Cbz) protected (*S*)-tyrosine, which could also potentially solve the supply issue of this potent antitumor drug.²⁸

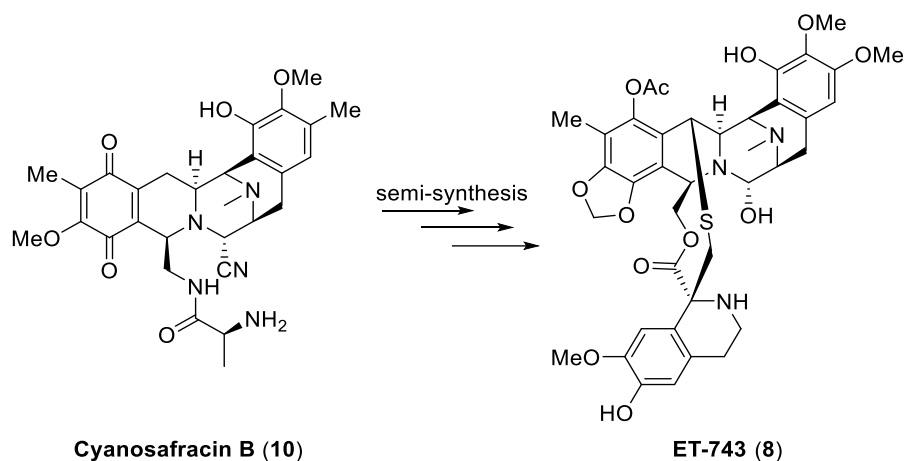


Figure 1.4 Scalable semi-synthesis of ET-743 (**8**) from cyanosafracin B (**10**).^{27, 29}

Although the total synthesis of many marine natural products has been achieved, in many cases, it is not economically pragmatic for large-scale production because of the intrinsic structural complexity and low yields. Design and synthesis of analogues with simplified structures but retaining the crucial pharmacophores for target binding, can reduce the number of synthetic steps and improve the yield.

Halichondrin B (**11**) is a classic example of a complex marine natural product that was converted into a significantly simplified analogue eribulin mesylate (**12**) to produce a drug candidate (Figure 1.5). Halichondrin B is a polyether macrolide originally isolated from the marine sponge *Halichondria okadai*,^{30, 31} which binds to tubulin and inhibits tubulin assembly, thereby, preventing cell division, and thus, tumor growth.^{32, 33} However, the scarcity of this natural product hampered its sustainable supply for drug development. Its total synthesis required about 90 steps starting from commercially available starting materials,³⁴ which is obviously unfeasible for scale-up production. Mass culture of source sponges was also carried out and indeed provided halichondrin B, but it could only address partially the problem because the growth of sponges is highly dependent on

environmental conditions.³⁵ A significant breakthrough was the discovery and scale-up production of structurally simplified analogues, especially eribulin mesylate,³⁶⁻³⁸ which displays antiproliferative activity against a diverse variety of human tumor cells,³⁹ and has undergone phase II and phase III clinical trials,⁴⁰ and is approved for clinical use in treatment of metastatic breast cancer and liposarcoma.

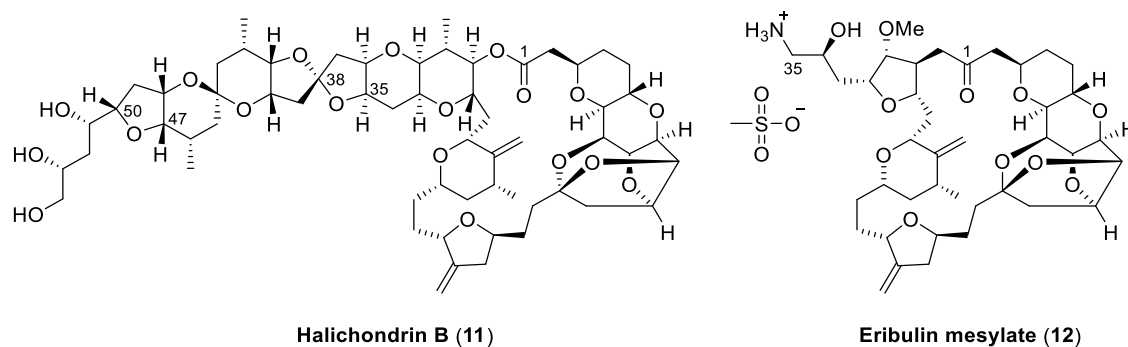


Figure 1.5 Chemical structures of halichondrin B (**11**) and its analogue eribulin mesylate (**12**).^{31, 37}

Another example of preparing analogues for clinical development is provided by bryostatin 1 and its synthetic analogue. Bryostatin 1 (**13**) (Figure 1.6), a 26-membered macrocyclic lactone, was produced by a symbiotic bacteria in marine bryozoan *Bugula neritina*.^{41, 42} Early studies have shown that bryostatin 1 exhibited remarkable anticancer activity,⁴¹ and it was identified as a modulator of protein kinase C (PKC).⁴³ In addition, bryostatin 1 has shown promising activity related to other diseases, including stroke,⁴⁴ diabetes,⁴⁵ and Alzheimer's disease.⁴⁶ This wide range of potentials in medicinal applications makes it an intriguing drug candidate. Unfortunately, the extremely low abundance of this compound in the source organism (18 g isolated from about 10,000 gallons of *Bugula neritina* L)⁴⁷ restricted its supply for preclinical and clinical studies. The reported total synthesis (52 total steps)⁴⁸ is not economically practical for scalable production, either. Hence, a simplified analogue was sought to resolve the supply problem. Based on computational modelling studies, C1, C19, and C26 oxygen atoms are suggested to be critical elements for the binding of bryostatin to PKC.⁴⁹ Following this hypothesis, a bryostatin analogue (**14**) (Figure 1.6) was prepared in 27 steps for the longest linear sequence starting from (*R*)-(+)-methyl lactate.⁵⁰ It can be seen that the important features have been maintained while the complexity of the skeleton has been reduced. As expected, this analogue has a similar affinity for PKC and shows significant

levels of *in vitro* antiproliferative activity against several human tumour cell lines.⁵¹

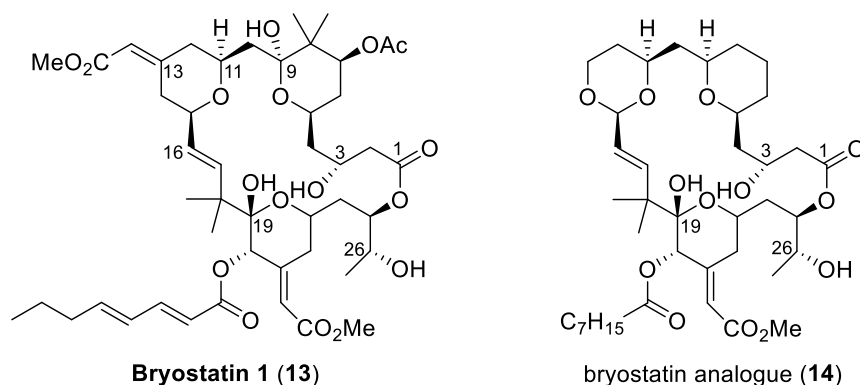


Figure 1.6 Chemical structures of bryostatin 1 (**13**) and its analogue (**14**).^{41, 52}

The value of analogue preparation for drug development of marine natural products is not only to facilitate economical chemical synthesis for large-scale manufacture but also to provide solutions for another major question in developing anticancer drugs based on marine natural products, which is how to optimise structures to access new chemical entities with enhanced desirable biological and/or pharmacokinetic properties for human therapies.

Dolastatin 10 (**15**) and its analogue TZT-1027 (**16**) (Figure 1.7) provide a good example in this case. Dolastatin 10, isolated from the sea hare *Dolabella auricularia*,⁵³ is a very potent antimitotic pentapeptide originally produced by the marine cyanobacteria *Symploca*, which is the main diet of a sea hare species.^{54, 55} Its absolute configuration was determined unequivocally through total synthesis.⁵⁶ Further studies showed that dolastatin 10 inhibits microtubule assembly and tubulin polymerisation through binding to tubulin near the vinca binding site, resulting in cell cycle arrest and apoptosis.⁵⁷⁻⁵⁹ However, phase I and phase II clinical trials revealed that dolastatin could induce peripheral neuropathy and exhibit no clinically significant activity.⁶⁰⁻⁶² Therefore, in efforts to reduce the clinical toxicity while maintaining the antitumor activity, a series of analogues were synthesised, of which TZT-1027 was the most promising molecule.⁶³ The structural modification of TZT-1027 is the omission of the thiazole ring from the parent compound. Intermittent injections of TZT-1027 in mice showed it has equivalent or greater potency than dolastatin 10 against several cancer models.⁶⁴ TZT-1027 shares its same mechanism of action with dolastatin 10 and it has been evaluated in phase I and phase II clinical trials in Japan,^{65, 66} USA,⁶⁷ and Europe.⁶⁸

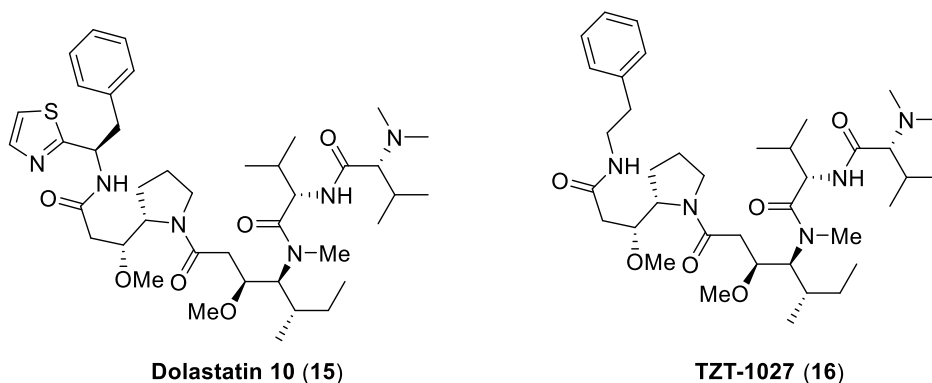


Figure 1.7 Chemical structures of dolastatin 10 (**15**) and TZZ-1027 (**16**).^{53, 69}

Another example of an analogue that provided improved biological activity is hemiasterlin (**17**) and its analogue HTI-286 (**18**) (Figure 1.8). Hemiasterlin was a tripeptide molecule isolated from marine sponge *Hemiusrerellu minor*, and it shows high cytotoxicity and antimitotic activity with an IC_{50} value of *ca.* 0.01 $\mu\text{g/ml}$ against P388 leukaemia cells.⁷⁰ Similar to dolastatin 10, hemiasterlin binds to the vinca binding site on tubulin.^{70, 71} To further explore the important portions of the molecule that are indispensable for the bioactivity, the *N*-methylindole was replaced by a phenyl group to afford a structurally simplified analogue HTI-286 (Figure 1.8), which displays greater *in vitro* potency than hemiasterlin against human mammary carcinoma MCF-7 cells.⁷² Furthermore, it has substantially less interaction with P-glycoproteins than other anticancer drugs, like paclitaxel and vinblastine. In this way, HTI-286 maintains high efficacy at inhibiting growth even in P-glycoprotein-mediated multi-drug resistant tumor cells.⁷³

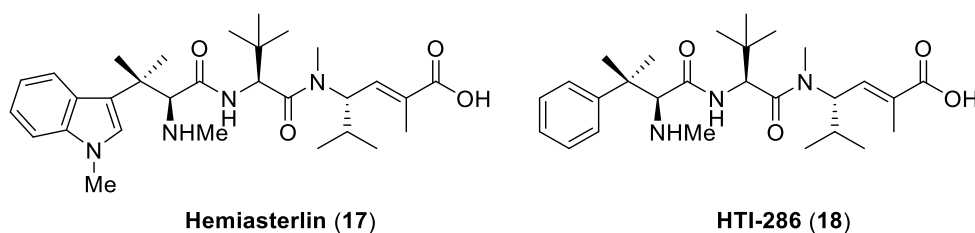


Figure 1.8 Chemical structures of hemiasterlin (**17**) and HIT-286 (**18**).^{70, 73}

Cryptophycin-52 (**19**) (Figure 1.9), an analogue of cryptophycin 1 (**20**) (Figure 1.9), gives an example of an analogue with improved pharmacological properties. Cryptophycin 1 was first isolated from cultured cyanobacteria *Nostoc sp.* strain ATCC 53789⁷⁴ and then re-isolated from cyanobacteria *Nostoc sp.* strain GSV 224 by Moore *et al.*⁷⁵ It was found

to be extremely potent against KB carcinoma and LoVo adenocarcinoma tumor cells.⁷⁵ However, the ester functionalities of cryptophycin 1 are very susceptible to basic conditions, especially the ester bond shown in the box in Figure 1.9, which is readily hydrolysed at pH = 11 to afford cryptophycin-13 (**21**) (Figure 1.9) within one hour, suggesting that this ester bond may be susceptible to esterases.⁷⁶ To reduce this susceptibility, a dimethyl substituted analogue, cryptophycin-52 (**19**), was developed by Eli Lilly. As expected, this modification improves its chemical stability. Interestingly, this modification also enhances its efficacy. Cryptophycin 52 displays exceptionally potent cytotoxicity against several human tumour cell lines, including leukaemia HL-60, mammary carcinoma MCF-7, and colon carcinoma HT-29 cells.⁷⁷

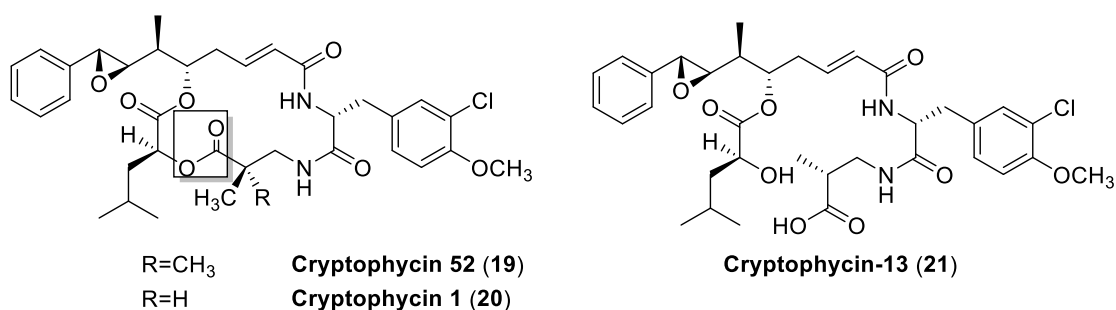


Figure 1.9 Chemical structures of hemiasterlin cryptophycin-52 (**19**), cryptophycin-1 (**20**) and cryptophycin-13 (**21**).⁷⁶

In summary, marine organisms have provided many promising antitumor agents with potential therapeutic applications. The continued exploration of marine natural products will continue to provide exciting drug leads due to advances in analytical spectroscopy and developments in metagenomics, which now allows researchers to probe bacteria with broad diversity from seawater, benthic sediment or in the marine invertebrate host. Simplification of complex marine natural products makes it possible to prepare analogues with limited loss of anticancer activity for pharmaceutical industry manufacture in a practical and economical way. Synthetic analogues also provide efficient methods to regulate the bioactivity of parent marine natural products to improve potency or pharmacology.

1.2 Discovery of Pateamine A

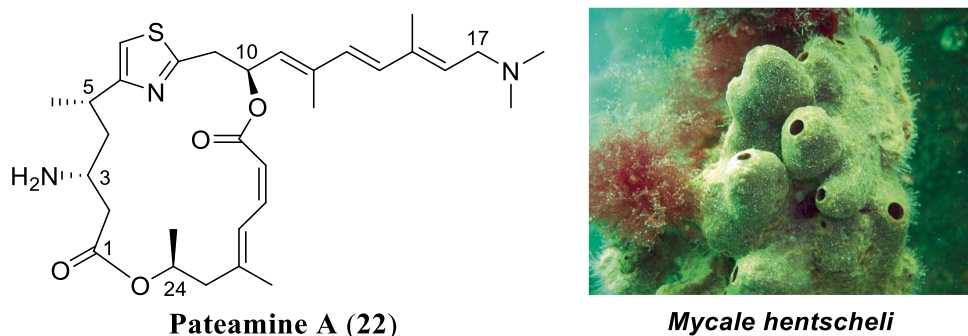


Figure 1.10 Structure of pateamine A (22) and a photo of the marine sponge *Mycale hentscheli*.*

The isolation of pateamine A (22) (Figure 1.10), a macrodiolide, was first reported in 1991 from specimens of the marine sponge *Mycale hentscheli*, which were collected in Thompson Sound on the southwest coast of the South Island of New Zealand.⁷⁸ Its unique structural features include a 2,4-disubstituted thiazole ring, and an isomerisation-prone *Z,E*-dienoate within a 19-membered *bis*-lactone macrocycle attached to an all-*E* trienylamine side chain.

The stereochemical assignment of C24 was then determined as *S* by Romo's synthetic studies on the C18-C24 fragment.⁷⁹ This assignment combined with modelling studies, extensive 2D-NMR experiments, and further chemical derivatisation provided the tentative stereochemical assignment as 3*R*, 5*S*, 10*S*, 24*S*.^{80, 81} In 1998, the first total synthesis by Romo's group finally unequivocally confirmed the absolute stereochemistry of pateamine A as 3*R*, 5*S*, 10*S*, 24*S*.⁸²

The original isolation by Northcote *et al.* was directed by cytotoxic activity of extracts from the marine sponge, resulting in the finding that pateamine A was a potent cytotoxin against fast-growing P388 leukemia murine cells with an IC₅₀ value of 0.15 ng / mL based on an MTT assay. Interestingly, pateamine A was shown to be largely inactive against BSC-1 cells under static growth with an IC₅₀ value of 300 ng / mL.⁷⁸ This selectivity between proliferating cells and quiescent cells has suggested that pateamine A could act as a selective antitumor agent against different tumor cells. Pateamine A was also reported

* Photo taken from <https://www.niwa.co.nz/sites/niwa.co.nz/files/w-a14-3handley.pdf>

to have *in vitro* antifungal activity in a preliminary screening assay.⁷⁸ The abbreviated name ‘PatA’ will be used for the remainder of this thesis to represent pateamine A.

1.3 Biological Activity of Pateamine A

Early studies suggested PatA exerted its dose-dependent cytotoxic effects by an apoptotic mechanism.⁸³ PatA was also found to display immunosuppressive activity through a signaling pathway involved in T-cell receptor-mediated IL-2 production.^{82, 84} It is now established that PatA blocks protein synthesis through inhibition of translation initiation, thereby inducing programmed cell death. The primary binding target for PatA was identified as the eukaryotic initiation factor 4A (eIF4A) family by two independent research groups, Bordeleau *et al.* and Liu *et al.* in 2005.^{85, 86}

The eIF4A family is a member of the DEAD-box protein family of RNA helicases, whose members are defined by the presence of nine highly conserved amino acid motifs.⁸⁷ It plays a critical role in the translation initiation process, which is the rate-determining step for protein synthesis. In humans, the eIF4A family consists of three isoforms: eIF4AI, eIF4AII, and eIF4AIII. EIF4AI and eIF4AII are 90-95% identical at the amino acid level and largely functionally equivalent in translation initiation.⁸⁸⁻⁹¹ EIF4AIII shows 65% similarity to the other isoforms and exhibits a function distinct from eIF4I/II.^{92, 93}

The pivotal process at the initiation stage of cap-dependent eukaryotic translation is the recruitment of the 43S ribosome subunit to the mRNA template. This process is accomplished through the concerted and systematic action of a number of proteins, including the eIF4F complex.⁹⁴ This eIF4F complex is comprised of three subunits (as shown in the box in Figure 1.11): eIF4E, which binds with 5' cap structure on the mRNA (m^7GpppN , where N is any nucleotide); eIF4AI/II, a protein that possesses RNA-dependent ATPase activity and ATP-dependent RNA helicase activity;⁹⁵ and eIF4G, an important scaffolding protein that mediates the interaction between eIF4AI/II and eIF4E.⁹⁶ The eIF4AI/II is the most abundant initiation factor and it exists in two different forms: a free form (eIF4A_f) and a complexed form (eIF4A_c) as a subunit of eIF4F complex; and it is thought that there is a dynamic exchange between the two forms through the eIF4F complex during the initiation process (Figure 1.11).⁹⁰ The complexed form eIF4_c is responsible for unwinding the local secondary structure of mRNA to facilitate the binding of the ribosome preinitiation complex (Figure 1.11).⁹⁷ It was

observed that eIF4A_c has a 20-fold more efficient helicase activity than the free form of eIF4A, which suggested that the “active” conformation of eIF4A may be stabilised when bound with eIF4G.⁹⁸

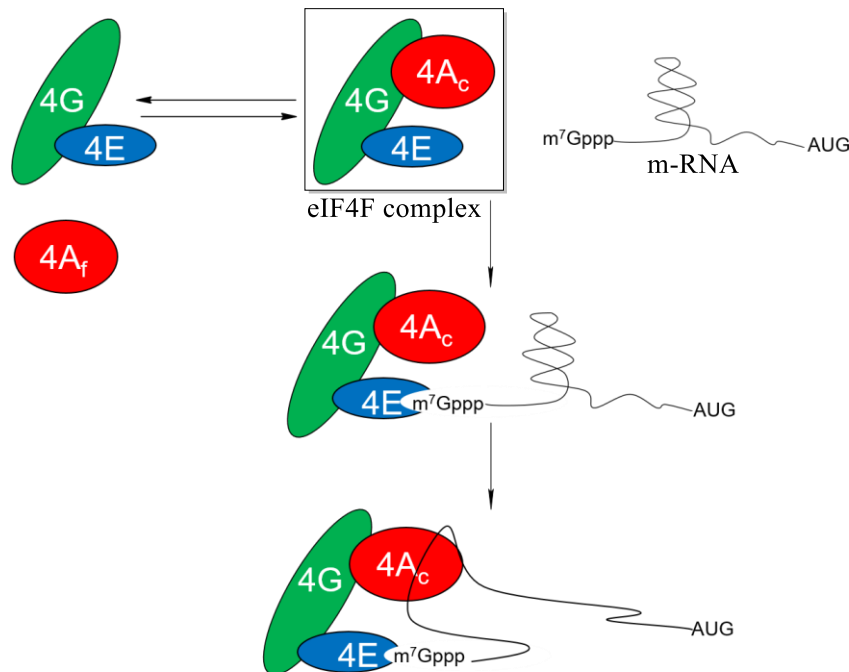


Figure 1.11 Reversible association of subunits of eIF4F complex and its function in the initiation process .⁹⁹

Key: 4A, 4G and 4E represent eIF4A, eIF4G and eIF4E, respectively. 4A_f and 4A_c represent the free and complexed forms of eIF4A. m⁷GpppN represents the cap structure of mRNA. AUG represents the start codon of mRNA.

The mode of action of PatA is that it specifically binds to the free form eIF4A_f (Figure 1.12). Interestingly, PatA also increases the ATPase and helicase activity of eIF4A_f, which means that its ATP-stimulated RNA-binding activity is activated.^{85, 86} Consequently, eIF4A_f bound with PatA is sequestered by RNA and kept away from the interaction with eIF4G (Figure 1.12), which is necessary for the formation of the pivotal apparatus for cap-dependent translation initiation – the eIF4F complex.⁹⁹ This would decrease the levels of eIF4_f available for recycling into the complexed form eIF4A_c. At high intracellular levels of PatA, this leads to an absence of eIF4A_c and the consequent loss of eIF4F complex for cap-dependent translation initiation, causing the stalling of protein synthesis.⁹⁹

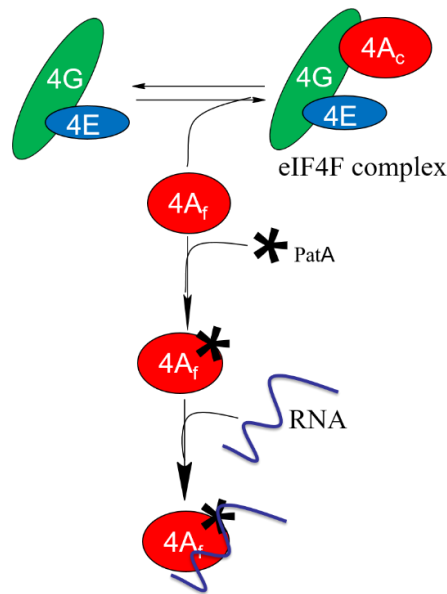


Figure 1.12 Proposed mode of action of PatA for inhibition of translation initiation.⁹⁹

Key: See Figure 1.11.

EIF4AIII is a key component of the exon junction complex (EJC) core, which also includes Y14-MAGOH heterodimer and MLN51 (Figure 1.13).¹⁰⁰ Within the EJC core, ATP-bound eIF4AIII and MLN51 directly bind with RNA while Y14-MAGOH heterodimer inhibits eIF4AIII ATPase activity and locks it into a conformation that can tightly clamp RNA (Figure 1.13).^{100, 101} These four proteins are assembled onto mRNAs to form the EJC core in the nucleus during splicing and the EJC complex is deposited by spliceosomes at a fixed position located 20 – 24 nucleotides upstream of exon-exon junctions.¹⁰² Afterwards, the EJC complex remains on spliced mRNAs and accompanies mRNAs as it is transported to the cytoplasm until it is eventually dissociated from mRNAs and disassembled during the first round of translation.^{103, 104} During this period, the composition of the EJC is highly dynamic as the EJC core constitutes a binding platform for the recruitment of numerous EJC peripheral factors, most of which interact with the EJC core only transiently.¹⁰⁵ This capacity grants the EJC a variety of functions in several post-transcriptional processes, including mRNA transport, translation and nonsense-mediated decay (NMD).¹⁰⁶

This image is unavailable. Please consult the reference list for further details.

Figure 1.13 A mode of four proteins (eIF4AIII, Y14, MAGOH, and MLN51) forming the RNA-binding EJC core.¹⁰⁷

NMD is a translation-dependent mRNA surveillance mechanism to maintain a high level of fidelity in gene expression, which is crucial for cellular homeostasis and survival.¹⁰⁶ NMD specifically promotes the degradation of aberrant mRNAs containing premature termination codons (PTCs) to minimise the synthesis of dysfunctional or even harmful truncated proteins.¹⁰⁸ In mammalian cells, NMD is mainly EJC-dependent.¹⁰⁹

In addition to its aforementioned inhibitory activity in protein synthesis, PatA displays an inhibitory effect on NMD through its direct binding to eIF4AIII, which is independent of its inhibition of translation initiation. It was proposed that PatA may initiate the conformational change of eIF4AIII, causing the perturbation of the dynamic EJC-UPF1 interaction and the eventual inhibition of NMD.¹¹⁰ Although the important role of the EJC in NMD is unveiled, a thorough understanding of the details of the mechanism are still lacking.¹⁰⁶ In this circumstance, PatA may serve as a molecular probe to explore the mechanism of the EJC-dependent NMD.¹¹⁰

More recently, eIF4I/II and eIF4AIII were reported to be important for efficient replication of human cytomegalovirus (HCMV), suggesting that eIF4A family helicases may be a potential class of targets for the development of new therapeutics for viral diseases.¹¹¹ As an inhibitor of both eIF4I/II and eIF4AIII, PatA displayed potent antiviral activity against different RNA and DNA viruses, raising the possibility that PatA may be used as a broad-spectrum antiviral drug.¹¹¹

1.4 Syntheses of Pateamine A and Analogues

The high potency of PatA as a cytotoxin and its selective activity against cancer cell lines has garnered much attention from both chemists and biologists.¹¹² A major concern in the development of PatA-based anticancer drugs is the difficulty in obtaining adequate amounts for preclinical and clinical trials due to its scarcity in the natural source *Mycale* sponges. Therefore, chemical synthesis is required to resolve the supply problem for further research.

1.4.1 Total Syntheses of Pateamine A

1.4.1.1 Romo's Total Synthesis

Romo and co-workers reported the first total synthesis of PatA in 1998.⁸² As shown in Figure 1.14, their synthetic strategy involved the initial construction of the macrocycle, followed by the attachment of the side chain fragment by Stille coupling reaction. The macrocycle was constructed by a combination of a Mitsunobu esterification and a β -lactam-based macrolactonisation. To minimise the risk of isomerisation, the *Z, E*-dienoate was delivered by a Lindlar reduction of the corresponding enyne. The 2,4-disubstituted thiazole ring was furnished by the Hantzsch thiazole synthesis between an α -bromoketone and a thioamide fragment.

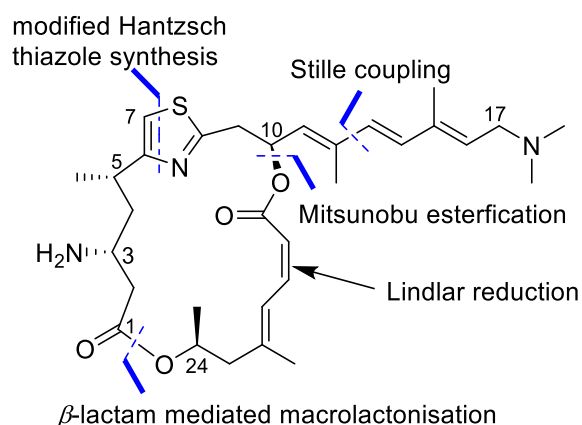


Figure 1.14 Key connections and features in Romo's synthetic strategy.^{82, 84}

Romo's total synthesis started with the preparation of three major fragments – the β -lactam fragment **23**, the dienyl stannane fragment **24** and the enynoic acid fragment **25** (Figure 1.15).

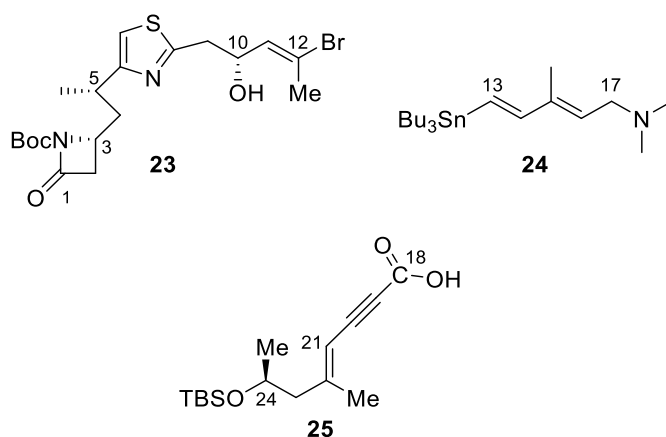
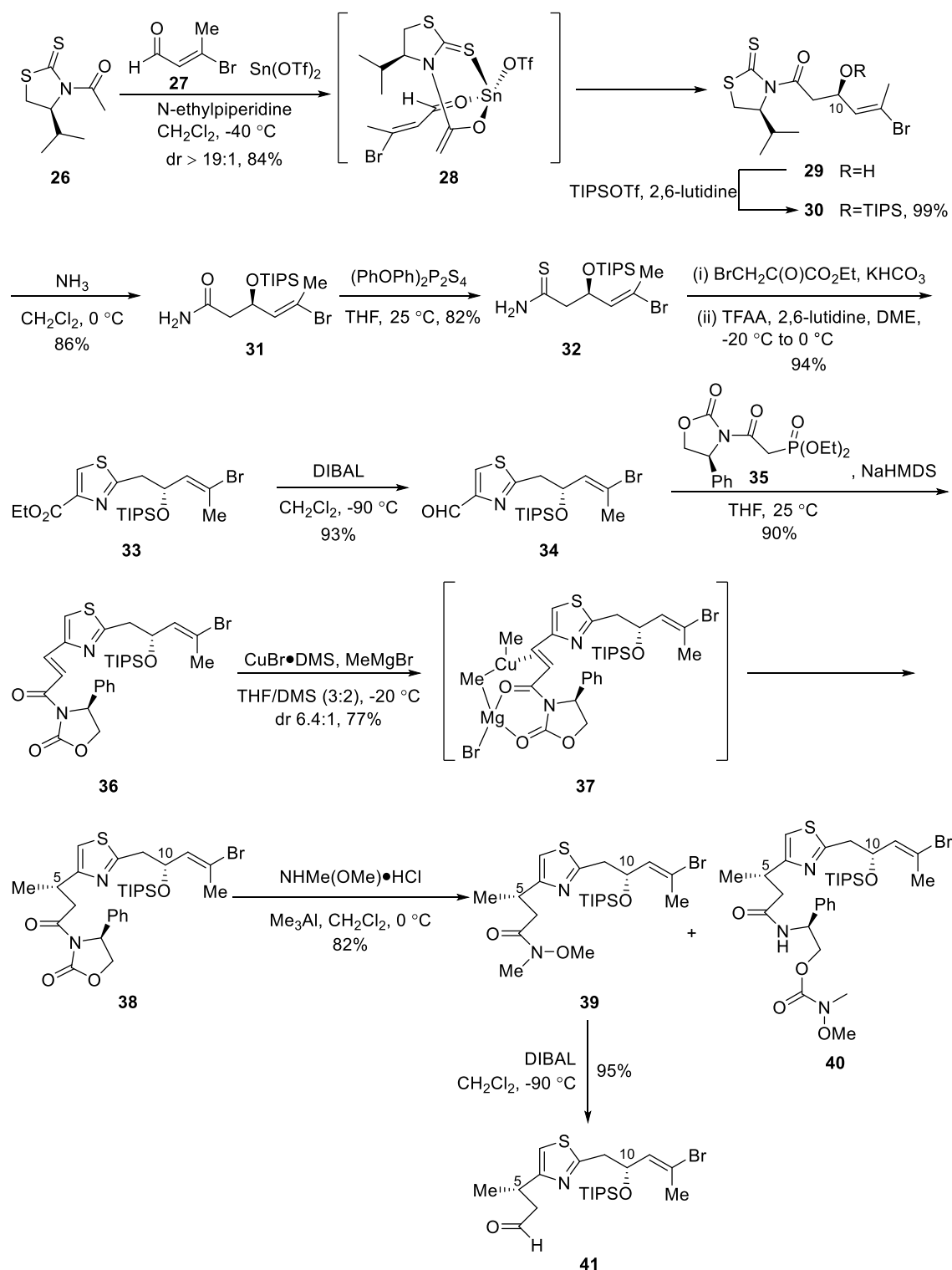


Figure 1.15 Major fragments in Romo's total synthesis of PatA.

Preparation of β -Lactam Fragment 23

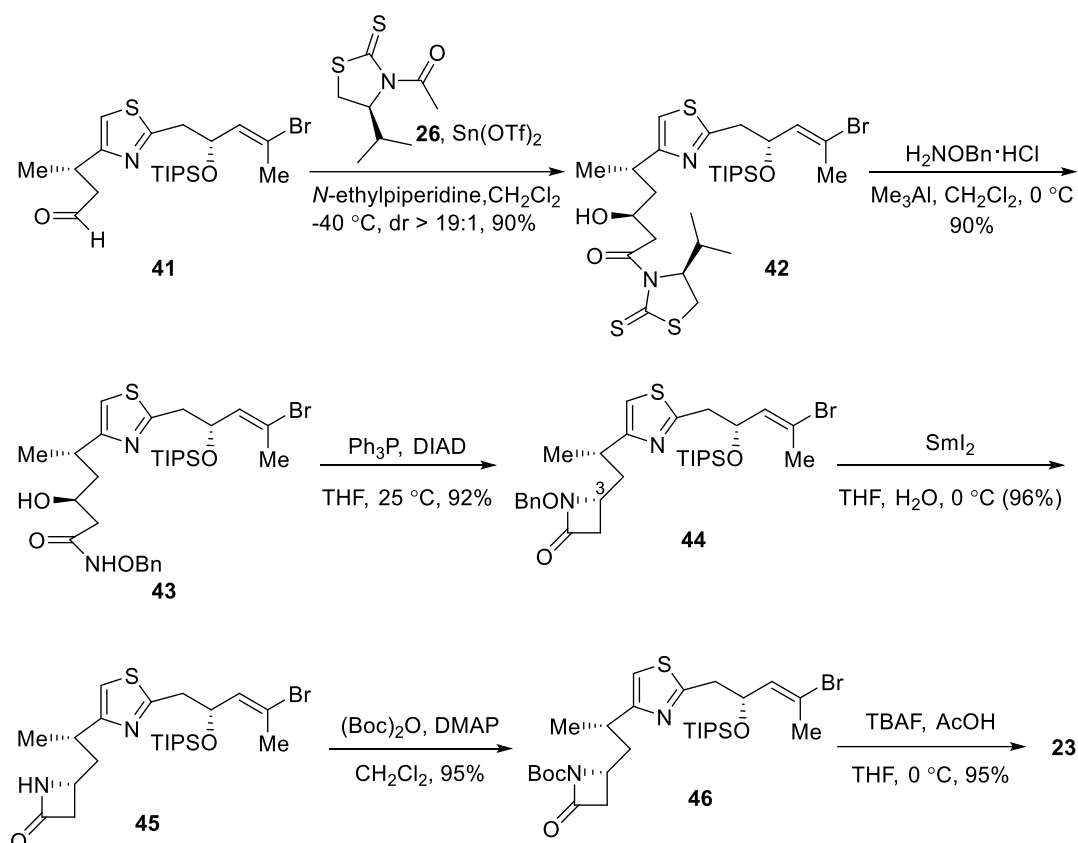
As shown in Scheme 1.1, the preparation of fragment **23** started from a Nagao aldol reaction between thiazolidinone **26** and aldehyde **27** to afford alcohol **29** with good diastereoselectivity ($dr > 9:1$), *via* the presumed tin complex **28**. The stereochemistry at C10 position (PatA numbering) was inverted when compared to PatA. Silyl protection and aminolysis with gaseous ammonia cleaved the auxiliary to afford the amide **31**, which was converted to thioamide **32** with Belleau's reagent. Thiazole **33** was formed in an excellent yield following Meyers' modified Hantzsch conditions.¹¹³ Partial reduction of ester **33** to aldehyde **34** followed by a Horner-Wadsworth-Emmons reaction with an oxazolidinone-containing phosphonate **35** provided the homologated product **36**. Compound **36** was treated with an excess of methyl magnesium bromide and an equivalent amount of copper(I) bromide dimethyl sulfide complex according to the method developed by Hruby¹¹⁴ to deliver the desired methyl adduct **38** in good diastereoselectivity ($dr = 6.4:1$). The selectivity was proposed to be induced by the formation of a Cu(I) π -olefin Mg(II) complex **37**. The methyl group added from the less hindered side – the opposite side to the phenyl group of the auxiliary. The auxiliary was transamidated with *N*, *O*-dimethylhydroxylamine hydrochloride and trimethyl aluminum to provide Weinreb amide **39**. During the process of transamidation, a crystalline by-product, amide **40**, was obtained as a result of the Weinreb amine attacking at the oxazolidinone carbonyl, which fortuitously allowed the verification of the stereochemistry at C5 and C10 position (PatA numbering) by X-ray crystallography.⁸⁴ Weinreb amide **39** was partially reduced by diisobutylaluminum hydride (DIBAL-H) to deliver aldehyde **41**.



Scheme 1.1 Introduction of stereochemistry at C5 and C10 in the preparation of **41**.

A second Nagao acetate aldol reaction between **41** and the *N*-acetylthiazolidinethione **26** afforded the alcohol **42** with high stereoselectivity (dr > 19:1) (Scheme 1.2). Transamidation with *O*-benzylhydroxylamine hydrochloride cleaved the auxiliary to afford the *N*-benzyloxy amide **43**. The following intramolecular Mitsunobu reaction

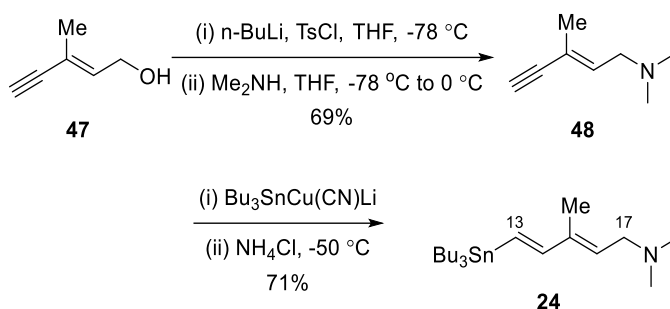
inverted the configuration of C3 (PatA numbering) and gave the β -lactam **44** with the correct stereochemistry. In order to utilise a more compatible deprotection condition with later intermediates, the *N*-*O* bond of the benzoyl-protected β -lactam was reductively cleaved by samarium(II) iodide (SmI_2) in the presence of water to afford the unprotected β -lactam **45**, which was subsequently reprotected as the *tert*-butyl carbamate **46**. Compound **46** was desilylated to give the desired β -lactam fragment **23**.



Scheme 1.2 Preparation of β -lactam fragment **23**.

Preparation of Dienyl Stannane Fragment **24**

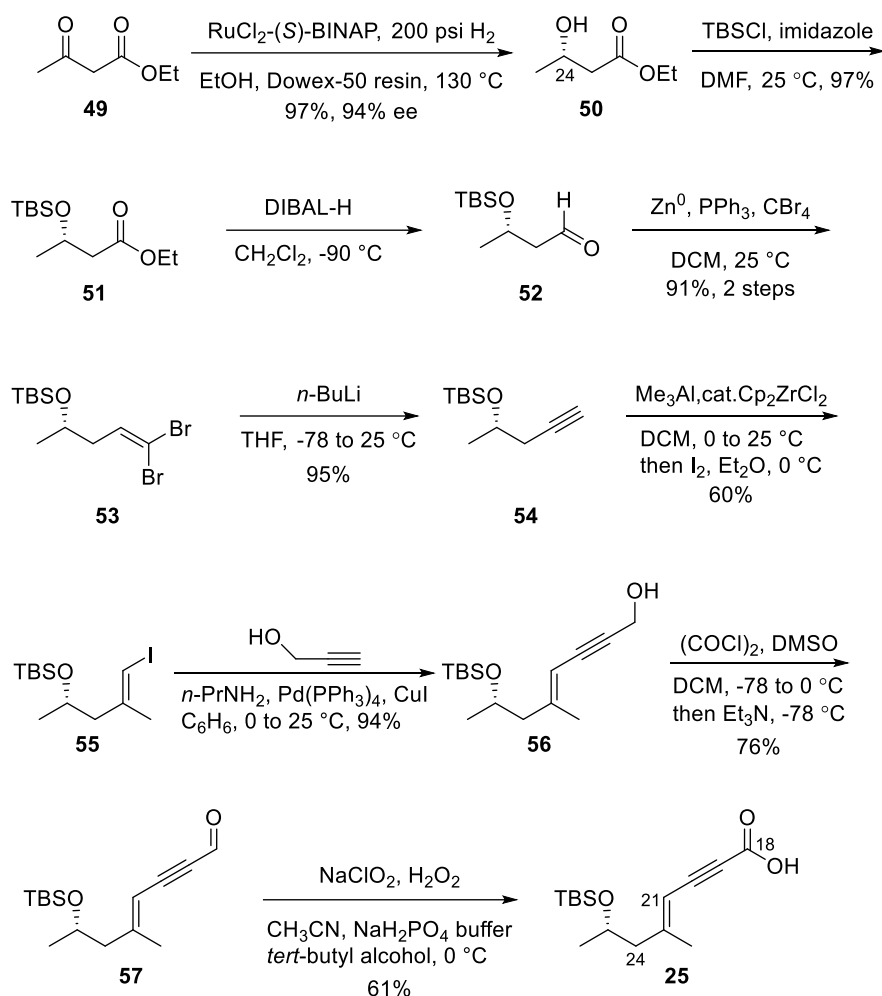
The preparation of the dienyl stannane fragment **24** started with one-pot tosylation of the enyne alcohol **47** and substitution with dimethylamine (Scheme 1.3). The resulting alkyne **48** was stannylated, according to Aksela and Oehlschlager's method,¹¹⁵ to afford the desired stannane **24** for the intermolecular Stille coupling reaction.



Scheme 1.3 Preparation of the stannane fragment **24**.

Preparation of Enynioic Acid Fragment 25

The preparation of the precursor for the *E,Z*-dienoate motif, the enynioic acid **25**, is shown in Scheme 1.4. Ethyl acetoacetate **49** was asymmetrically hydrogenated by the modified Noyori method to set the desired stereochemical configuration at C24 (PatA numbering) with excellent enantioselectivity (94% ee). Silyl protection and partial reduction afforded the aldehyde **52**, which was subjected to the Corey-Fuchs procedure to provide the alkyne **54** via a dibromoalkene intermediate **53**.¹¹⁶ Alkyne **54** was converted to the vinyl iodide **55** by a zirconium catalysed carboalumination/iodination sequence. Sonogashira coupling with propargyl alcohol delivered the enyne alcohol **56**, which was subjected to sequential Swern and Pinnick oxidations to provide the pivotal enynioic acid **25**.

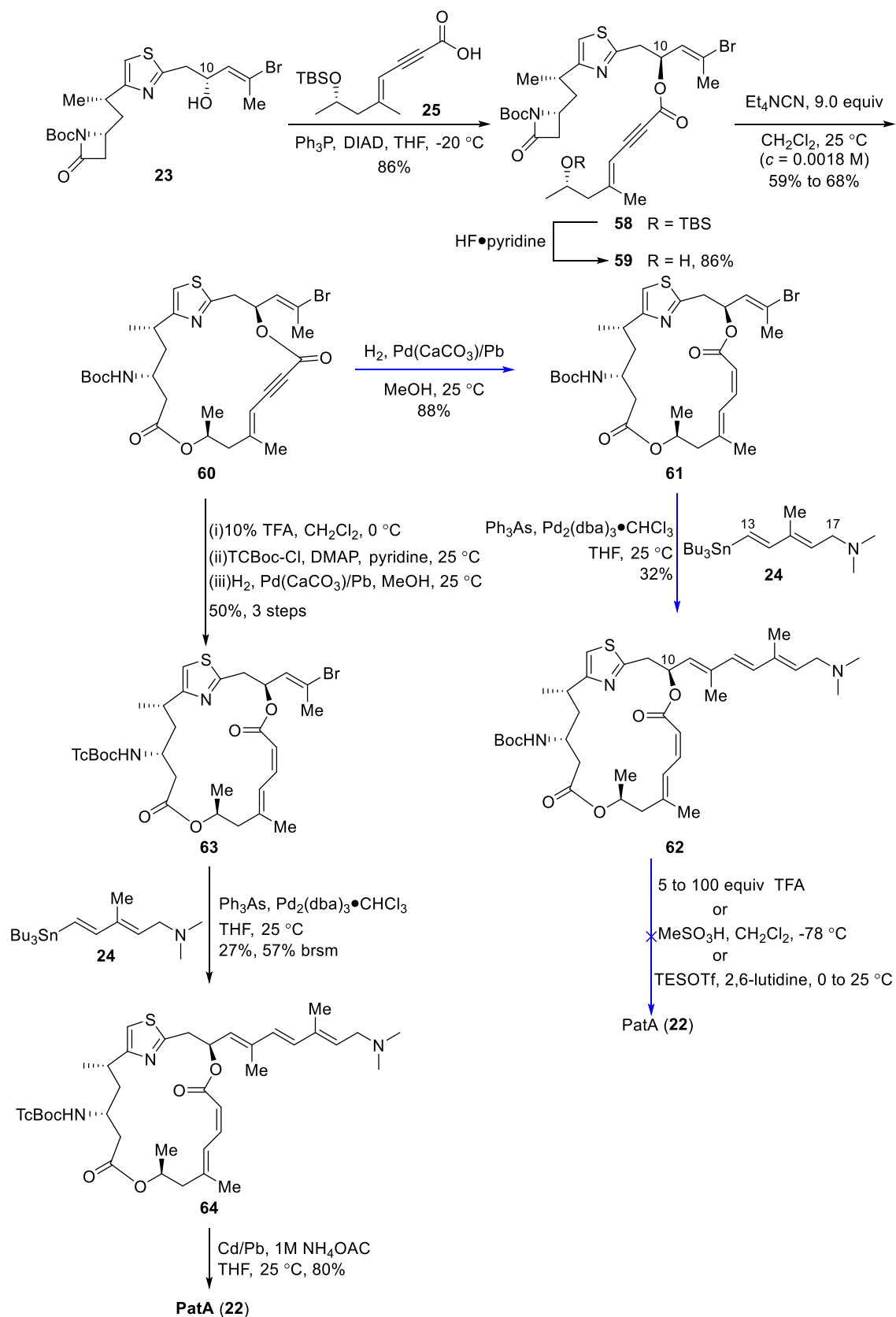


Scheme 1.4 Preparation of enynoic acid **25** as the precursor of *Z,E*-dienoate.

Coupling of Fragments

As shown in Scheme 1.5, β -lactam fragment **23** was coupled with enynoic acid **25** under Mitsunobu conditions to invert the configuration of C10 to afford the required (*S*) configuration in PatA (Scheme 1.5). Desilylation of compound **58** with hydrogen fluoride-pyridine complex was followed by the intramolecular alcoholysis of the β -lactam using modified Palomo conditions to provide the macrocycle core **60**.¹¹⁷ The initial attempt, as outlined with blue arrows, utilised Lindlar's catalyst to reduce the alkyne and the resulting *Z,E*-diene **61** was coupled with the dienyl stannane fragment **24** to provide the Boc-protected PatA **62** in 32% yield. Unfortunately, deprotection of the Boc group under acidic conditions (*e.g.*, 5 to 100 equiv of trifluoroacetic acid (TFA); MeSO_3H , CH_2Cl_2 , $-78\text{ } ^\circ\text{C}$; TESOTf , 2,6-lutidine, $0 \text{ to } 25\text{ } ^\circ\text{C}$) led to decomposition of PatA, which was plausibly caused by the elimination of the ester group at C10.⁸⁴ To avoid using acidic conditions for the deprotection reaction, the trichloro-*tert*-butoxycarbamate (TcBoc)

group, which could be removed under neutral conditions, was chosen as an alternative amine protecting group. Therefore, the *tert*-butyl carbamate group was removed and the free amine group was re-protected as a trichloro-*tert*-butoxycarbamate (TcBoc) protecting group. The resulting TcBoc-protected product underwent Lindlar reduction to provide the *Z,E*-diene **63**. Stille coupling with **24** and treatment with a cadmium-lead couple to remove the TcBoc group from **64** eventually gave the PatA (**22**) in 24 steps (based on the longest linear sequence starting from aldehyde **27**) with a 2.5 % overall yield.



Scheme 1.5 Coupling of fragments **23**, **24**, and **25** to complete the synthesis of PatA.

1.4.1.2 Pattenden's Total Synthesis

In 2000, Pattenden and co-workers disclosed their total synthesis of PatA based on a chiral pool approach.¹¹⁸ As shown in Figure 1.16, their synthetic strategy involved the initial formation of the macrocycle core *via* a combination of a sulfinimine directed aldol reaction, a Yamaguchi esterification, and an intramolecular Stille coupling. Similarly to Romo's approach, the construction of the thiazole fragment was accomplished by the modified Hantzsch thiazole synthesis. The side chain was elongated with a combination of Wittig homologation and intermolecular Stille coupling.

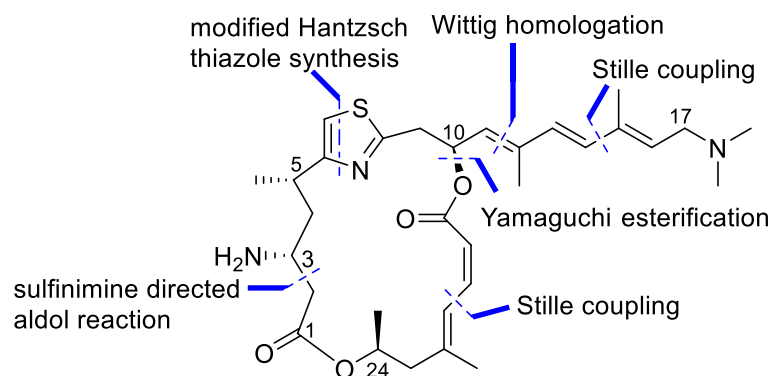


Figure 1.16 Key connections and features in Pattenden's synthetic strategy.¹¹⁸

Therefore, Pattenden's total synthesis utilised five smaller fragments **65**, **66**, **67**, **68** and **69**, and started from the preparation of sulfinimine fragment **65** and ester fragment **68** (Figure 1.17).

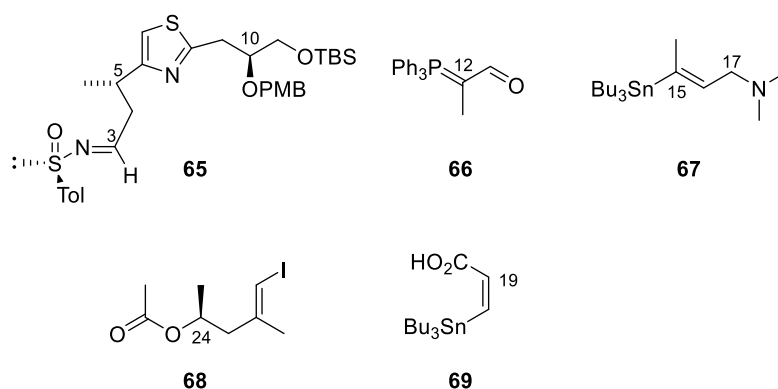
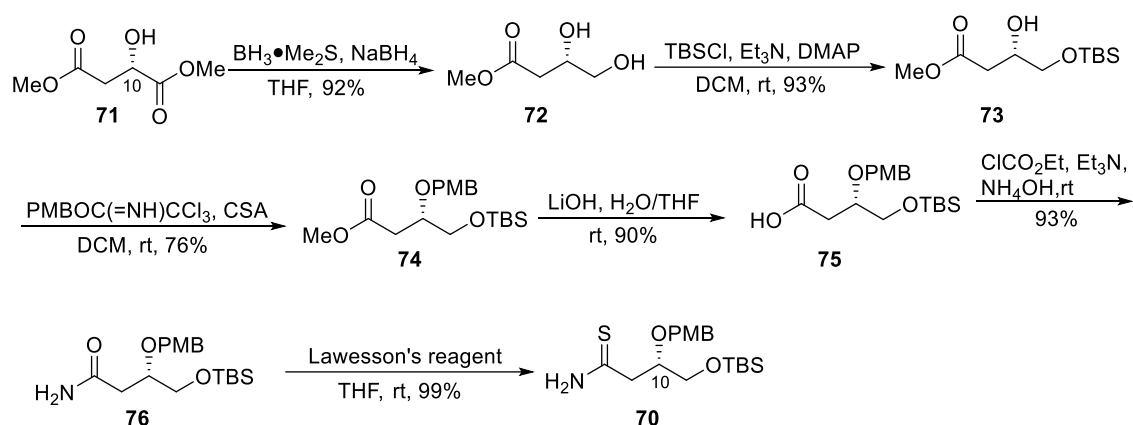


Figure 1.17 Major fragments in Pattenden's total synthesis.¹¹⁸

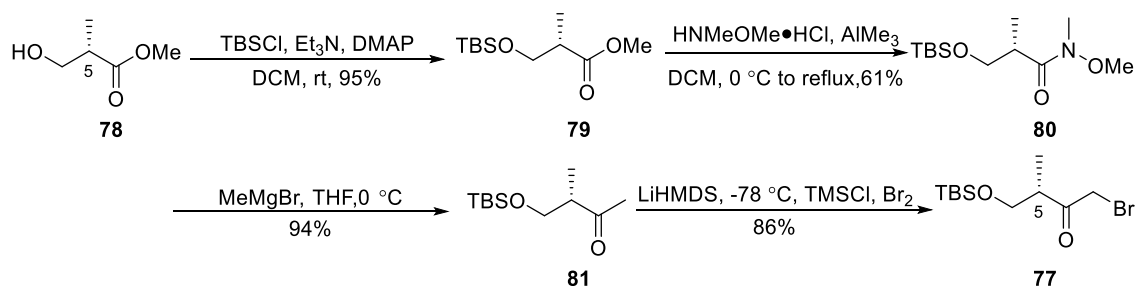
Preparation of Sulfinimine Fragment 65

The preparation of sulfinimine fragment **65** started with the construction of the thiazole ring. The preparation of thioamide **70** (Scheme 1.6) required for the Hantzsch thiazole synthesis began from commercially available L-malate **71**, which sets the required (*S*) configuration at the C10 position in PatA. Selective reduction of compound **71** by treatment with a combination of borane dimethyl sulfide and sodium borohydride provided diol **72**, which was then subjected to a sequential mono-silyl protection and *para*-methoxybenzyl (PMB) protection procedure to afford the ester **74**. Saponification of **74** and subsequent amidation *via* a mixed anhydride intermediate provided amide **76**, and this underwent thionation with Lawesson's reagent to deliver thioamide **70**.

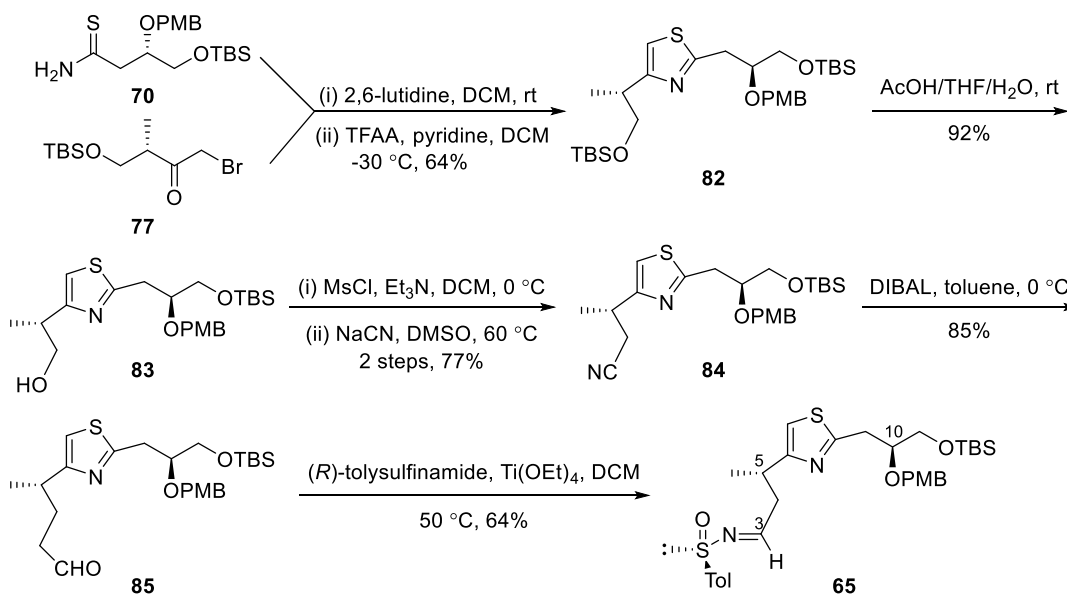


Scheme 1.6 Preparation of thioamide **70**.

The synthesis of the α -bromoketone partner **77** (Scheme 1.7) started with commercially available (*S*)-methyl 3-hydroxy-2-methylpropanoate **78**, which provided the stereochemistry at C5 in PatA. Silylation of the alcohol group and treatment with *N,O*-dimethylhydroxylamine hydrochloride and trimethyl aluminum gave Weinreb amide **80**. Conversion to methyl ketone **81** with a Grignard reagent followed by regioselective bromination mediated by the bulky base LiHMDS gave the α -bromoketone **77**.

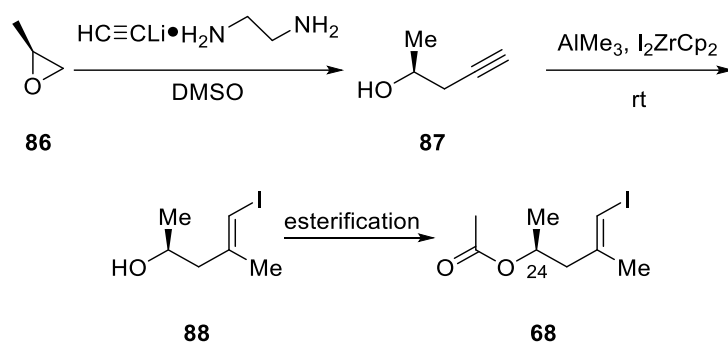
**Scheme 1.7** Preparation of α -bromoketone **77**.

As outlined in Scheme 1.8, the modified Hantzsch reaction following Meyers' conditions¹¹³ between **70** and **77** gave thiazole **82** in high optical purity. Regioselective desilylation of **82** followed by mesylation and cyanation with sodium cyanide afforded nitrile **84**, which was reduced by DIBAL-H to provide aldehyde **85**. Treatment of **85** with (*R*)-*p*-toluenesulfinamide and titanium tetraethoxide led to the formation of the enantiopure sulfinimine **65**.

**Scheme 1.8** Preparation of sulfinimine **65**.

Preparation of Chiral Ester Fragment 68

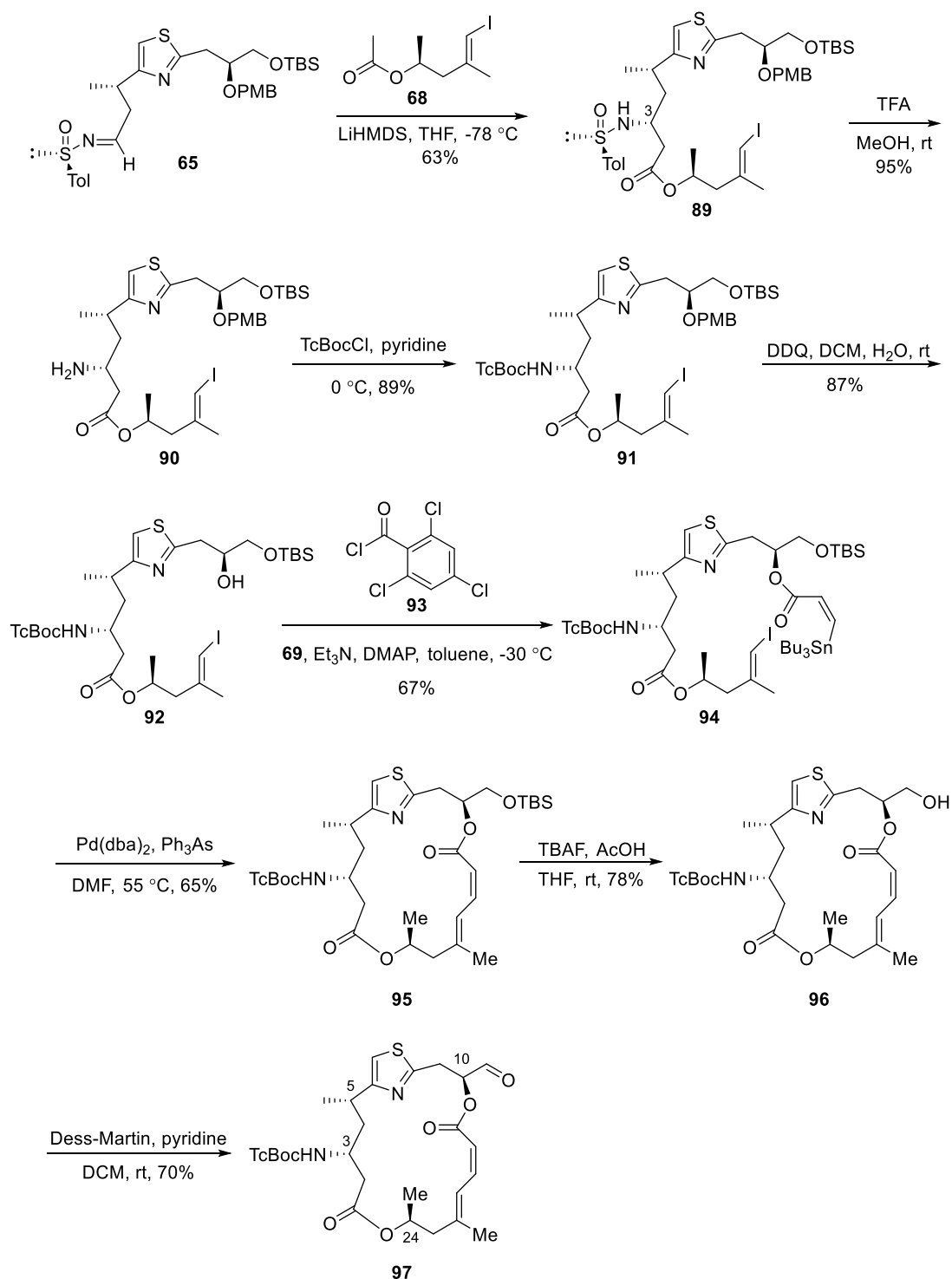
As shown in Scheme 1.9, epoxide ring-opening of the commercially available (*S*)-(-)-propylene oxide **86** by the ethylenediamine complex of lithium acetylide provided the chiral alkyne **87** in high enantiopurity, which sets the stereochemistry at C24 position (PatA numbering). Alkyne **87** then underwent a zirconium-catalysed carboalumination and iodination reaction to afford the iodide **88**, which was then esterified to deliver the desired ester fragment **68**.¹¹⁹ The yields for these three steps were not provided in the publication and the reagents for the esterification step were not specified either.¹¹⁹



Scheme 1.9 Preparation of chiral alcohol fragment **68**.

Preparation of Macrocyclic Aldehyde 97

As shown in Scheme 1.10, sulfinimine **65** was coupled with chiral ester **68** upon treatment with LiHMDS, *via* its derived enolate, to give substituted β -amino ester **89** in about 90% diastereoselectivity for the (*R*)-configuration at the C3 position (PatA numbering). Treatment with TFA-methanol cleaved the *p*-toluenesulfinyl group to give amine **90**, which was protected with 2,2,2-trichloro-1,1-dimethylethyl chloroformate to provide the corresponding TcBoc carbamate **91**. Removal of the *p*-methoxybenzyl (PMB) protecting group with 2,3-dichloro-5,6-dicyano-1,4-benzoquinone (DDQ), followed by esterification with *Z*-3-tri-*n*-butylstannylpropenoic acid **69** using the Yamaguchi activating reagent **93**, provided the key stannane-iodide **94**. Intramolecular Stille coupling furnished the 19-membered *bis*-lactone macrocycle **95** with the complete preservation of the desired *E/Z* stereochemistry. Deprotection with tetra-*n*-butylammonium fluoride (TBAF) and acetic acid followed by oxidation with pyridine-buffered Dess–Martin periodinane afforded aldehyde **97**.

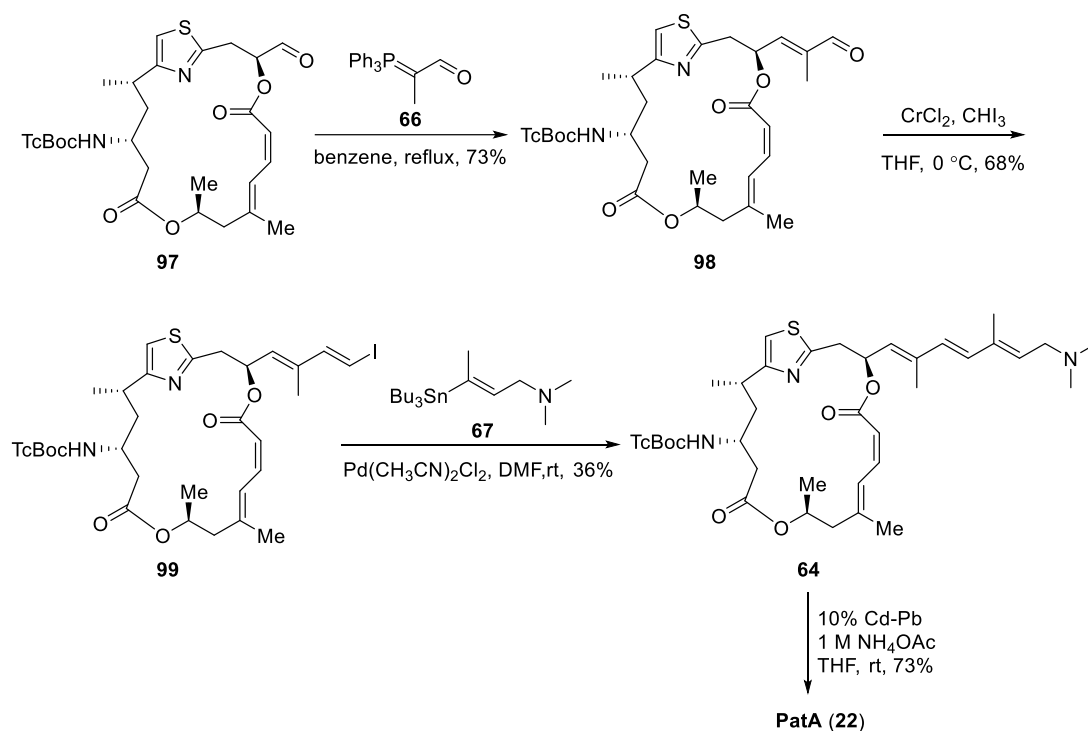


Scheme 1.10 Coupling of fragment **65**, **68** and **69** to furnish the macrocycle core.

Attachment of the Side Chain Fragments 66 and 67

Aldehyde **97** was homologated with 2-(triphenylphosphoranylidene)propionaldehyde **66** to exclusively provide *E*-unsaturated enal **98** (Scheme 1.11). Treatment of aldehyde **98** under Takai conditions, followed by Stille coupling with vinyl stannane **67**, resulted in

the formation of TcBoc-protected PatA **64**. Finally, removal of the TcBoc protecting group using a Cd/Pb couple with ammonium acetate afforded PatA (**22**). This synthetic route provided PatA over 25 steps (the longest linear sequence from starting material **70**) with an overall yield of 0.19%.



Scheme 1.11 Coupling of side chain fragments **66** and **67** to complete synthesis of PatA (**22**).

1.4.1.3 Fürstner and Zhuo's Total Synthesis

Recently, Fürstner and Zhuo reported their robust and efficient total synthesis of PatA, which centres on utilising iron-catalysed ring-opening of a 2-pyrone for the formation of the highly isomerisation-prone *Z,E*-dienoate motif (Figure 1.18).¹²⁰ The macrocycle core was formed *via* a combination of Steglich esterification and modified Mukaiyama macrolactonisation. The attachment of the side chain followed the previous synthetic strategy reported by Pattenden and co-workers.¹¹⁸

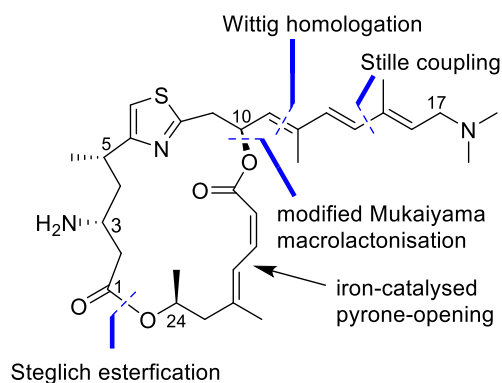


Figure 1.18 Key connections and features in Fürstner and Zhuo's synthetic strategy.¹²⁰

Fürstner's synthetic work started with the preparation of the two major fragments – thiazole-containing fragment **100** and 2-pyrone fragment **101** (Figure 1.19).

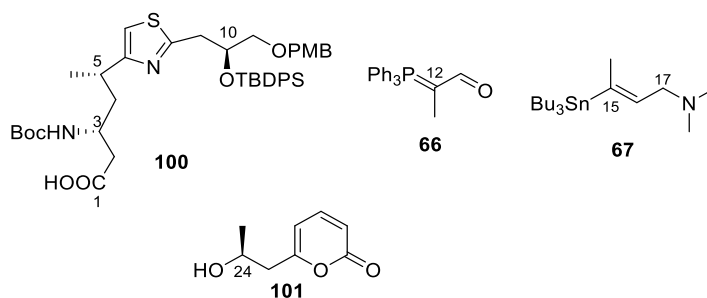
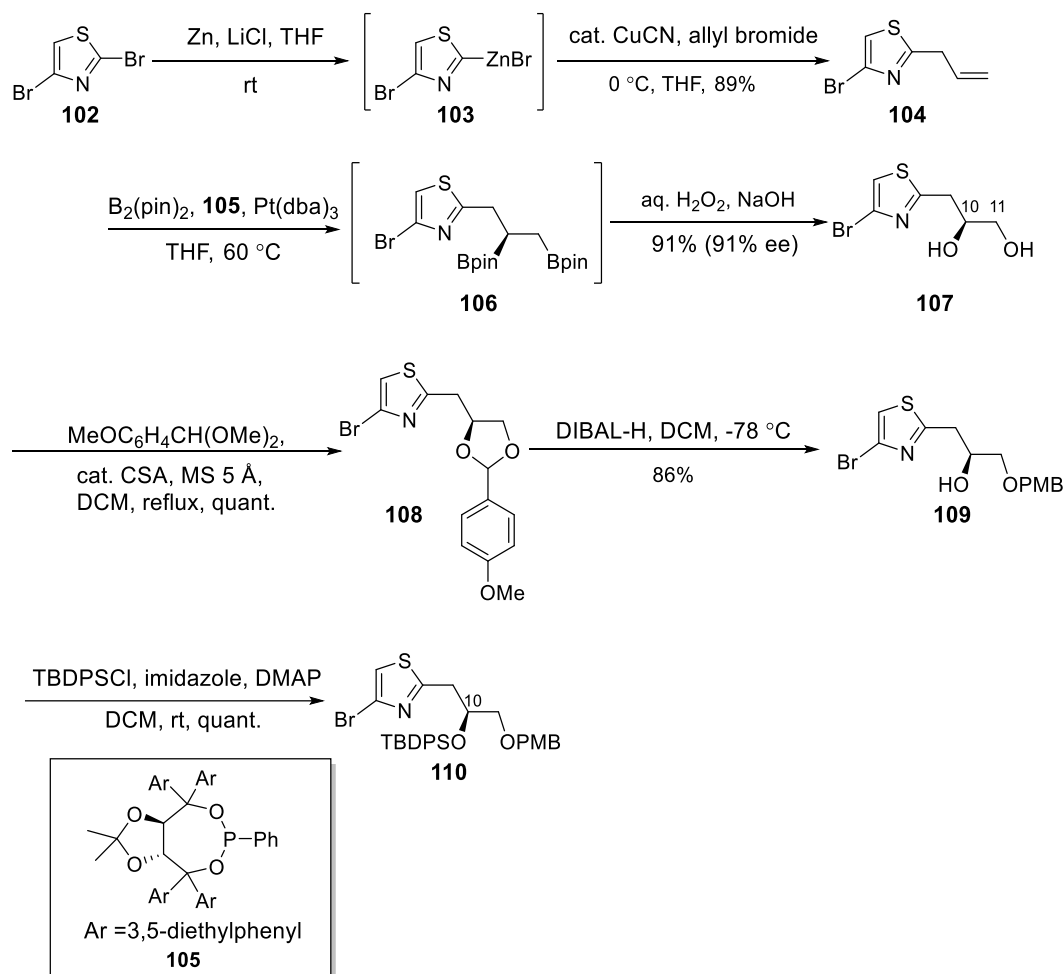


Figure 1.19 Major fragments in Fürstner and Zhuo's total synthesis.

Synthesis of Thiazole-containing Fragment 100

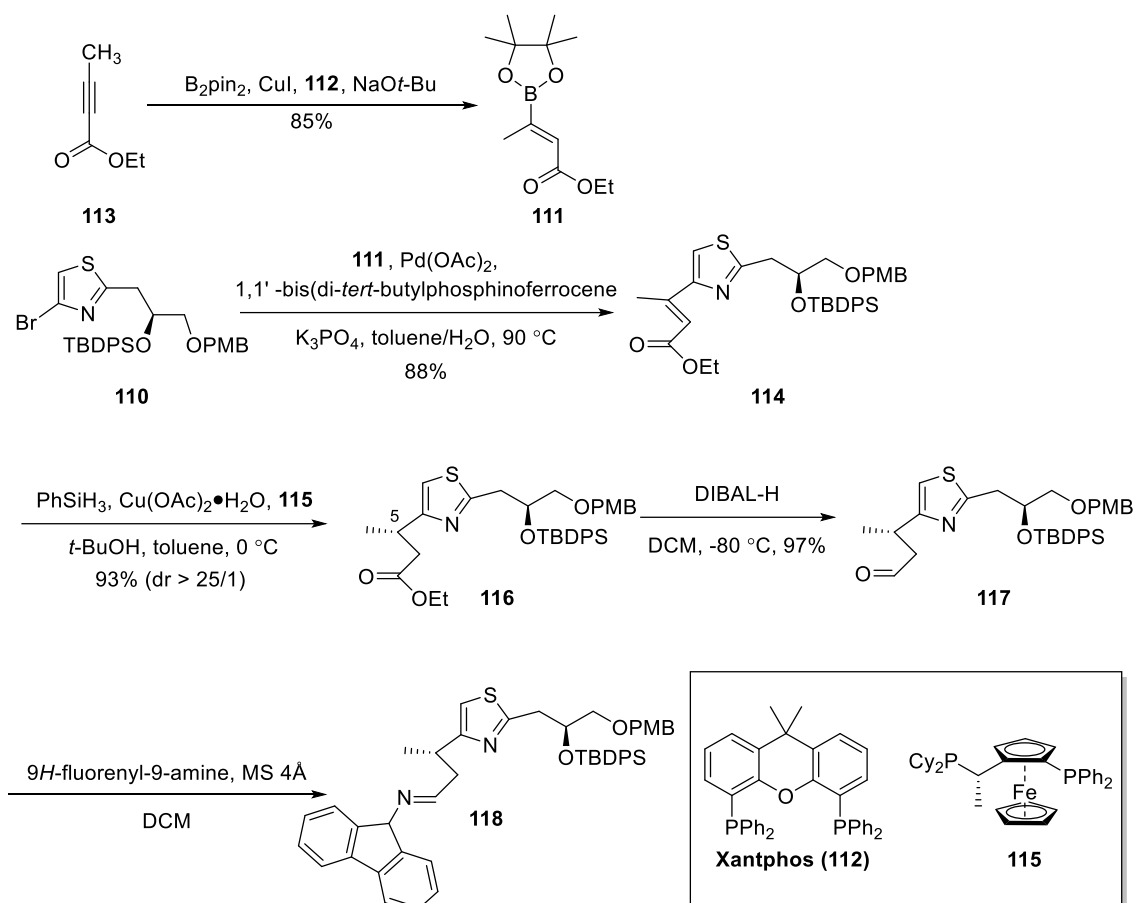
In contrast to Romo and Pattenden's previous synthetic work, in which the 2,4-disubstituted thiazole ring was formed using modified Hantzsch conditions, dibromothiazole **102** was chosen as the starting material in Fürstner and Zhuo's total synthesis (Scheme 1.12). Dibromothiazole **102** was first treated with lithium chloride and activated zinc to form the organozinc species **103**, which was quenched with allyl bromide in the presence of catalytic copper(I) cyanide to give the mono-allylated product **104**. Vicinal boronate species **106** was then formed upon exposure to bis(pinacolato)diboron (B_2pin_2) and a catalyst complex generated *in situ* from tris(dibenzylideneacetone)platinum(0) ($Pt(dba)_3$) and a chiral phosphonite ligand **105**. The primary product **106** was then oxidised to deliver diol **107**. This two-step/one-pot procedure introduced the correct stereochemical configuration at C10 (PatA numbering) with high enantioselectivity (91% *e.e.*). The diol **107** was then transformed into *p*-methoxybenzylidene acetal **108**. Regioselective opening of the acetal **108** and subsequent

silylation furnished thiazole **110**.

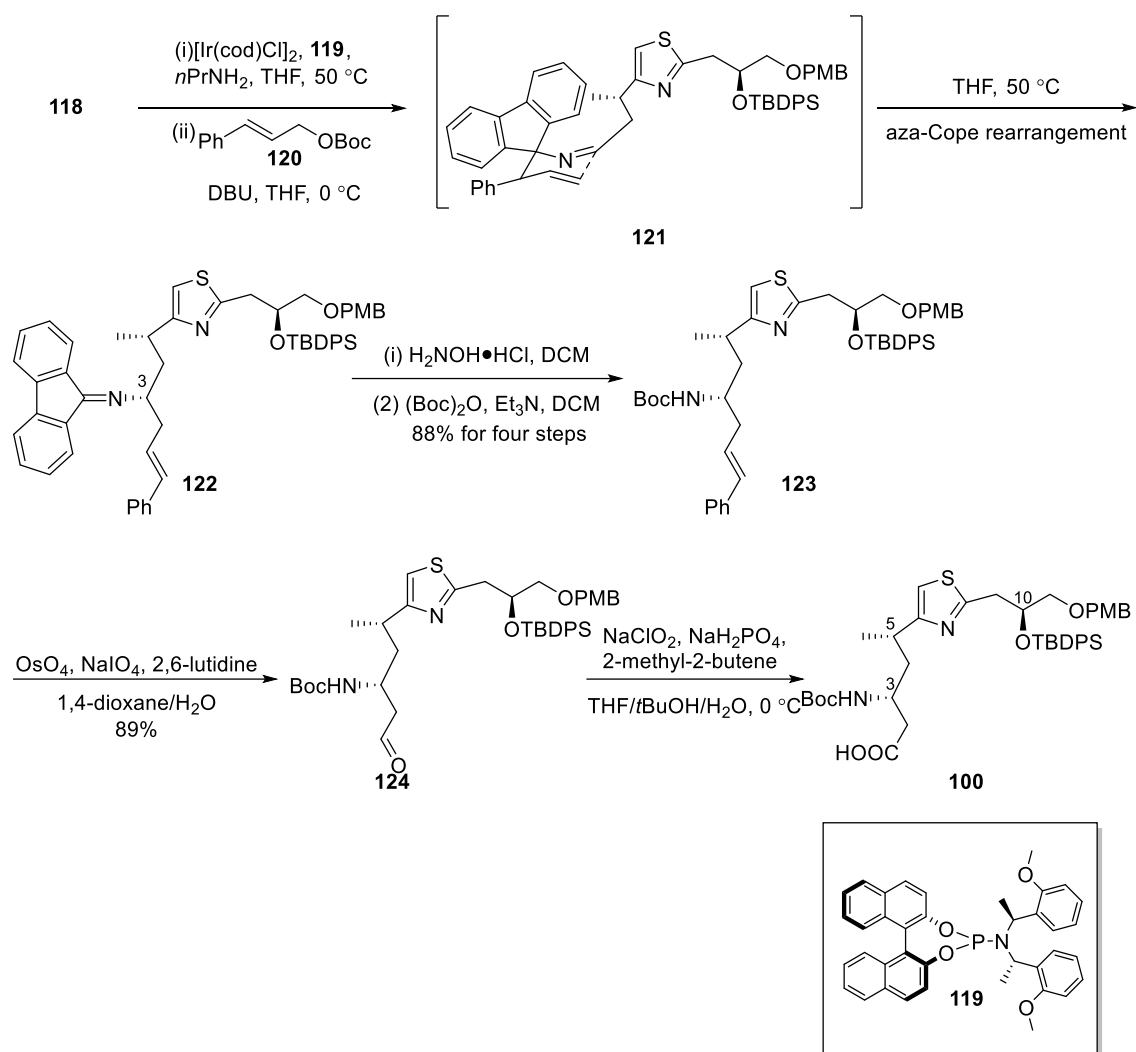


Scheme 1.12 Introduction of stereochemistry at C10 in preparation of thiazole **110**.

As shown in Scheme 1.13, the Suzuki coupling reaction between brominated thiazole **110** and the nucleophilic boronate partner **111**, which was derived from alkynoate **113** via a stereoselective borylation reaction catalysed by the copper catalyst generated *in situ* from copper(I) iodide and xantphos **112**,¹²¹ afforded enoate **114**. Following the conditions of Lam and co-workers,¹²² the C=C bond of compound **114** was asymmetrically reduced with phenylsilane in the presence of copper(II) acetate monohydrate and (*S,R*)-Josiphos **115** as the catalyst to set the stereochemical configuration at C5 (PatA numbering) with excellent diastereoselectivity (*dr* > 25/1). Ester **116** was then reduced to form aldehyde **117**, which reacted with 9*H*-fluorenyl-9-amine to give the imine intermediate **118**.

Scheme 1.13 Preparation of imine **118**.

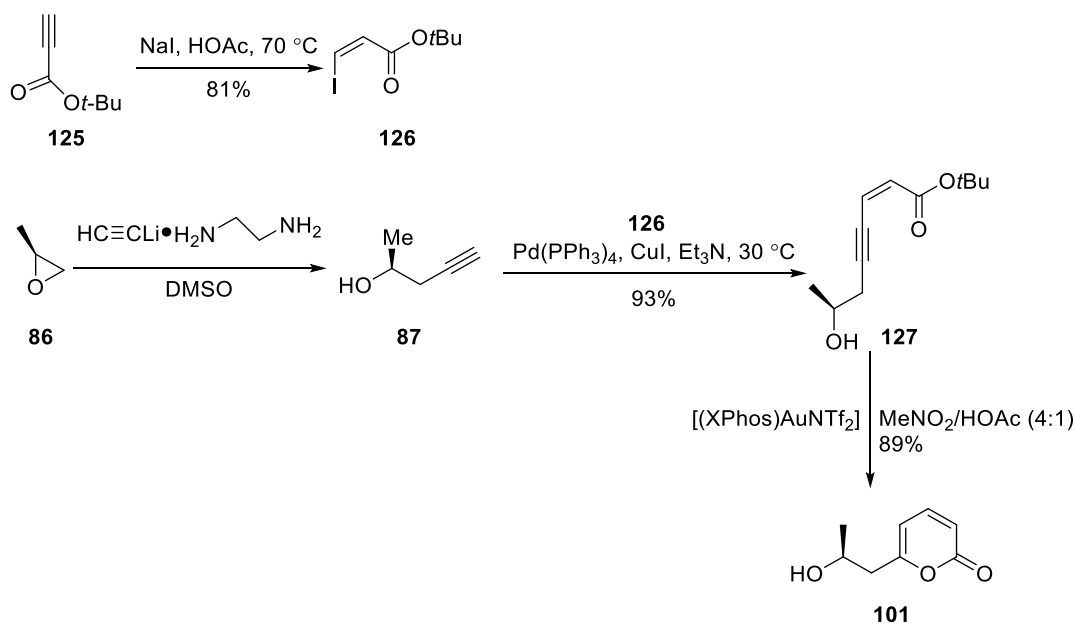
The fluorenyl imine **118** was then deprotonated to give a nucleophilic partner, which engaged in an iridium-catalysed asymmetric allylation reaction with compound **120** (Scheme 1.14). The resulting intermediate **121** underwent an aza-Cope rearrangement in THF at 50 °C to deliver imine **122**. The imine **122** was hydrolysed by treatment with hydroxylamine hydrochloride to provide the resulting amine. This three-step sequence successfully afforded the desired (*R*)-configuration at the C3 position (PatA numbering) in excellent diastereoselectivity (dr > 25:1). The primary amino group was protected by using di-*tert*-butyl dicarbonate ((*Boc*)₂O) and triethylamine. The C=C bond of the Boc-protected product **123** was then cleaved under modified Lemieux-Johnson conditions to afford aldehyde **124**, which underwent Pinnick oxidation to provide the desired thiazole fragment **100**.



Scheme 1.14 Synthesis of thiazole fragment **100**.

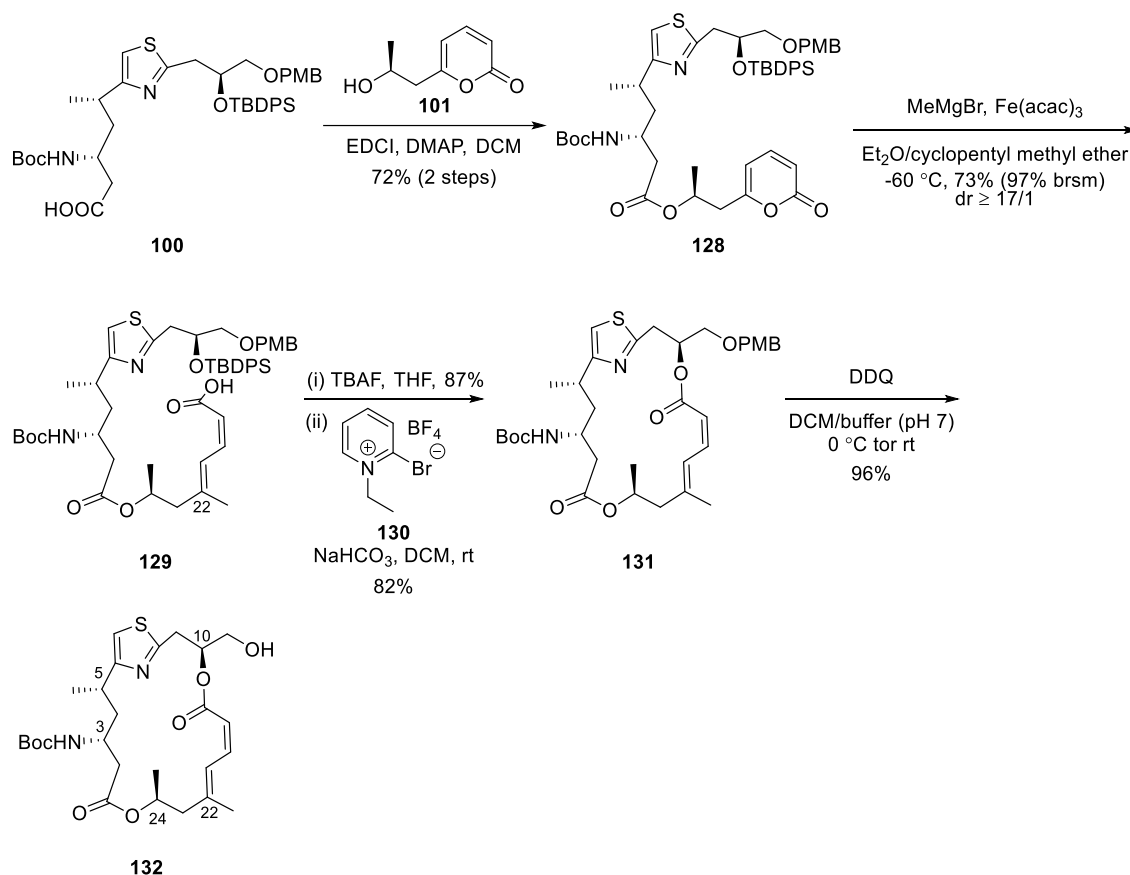
Preparation of 2-Pyrone Fragment **101**

To introduce the desired stereochemistry at C24 position (PatA numbering), the preparation of the 2-pyrone fragment **101** started from (*S*)-(-)-propylene oxide **86** (Scheme 1.15), the same chiral starting material used in Pattenden's total synthesis.¹¹⁸ Similarly, epoxide **86** was first opened by the ethylenediamine complex of lithium acetylide to provide alkyne **87**. Sonogashira coupling between the chiral alkyne **87** and the iodide **126**, which was prepared from propiolate **125**, delivered alcohol **127** in 93% yield. Gold-catalysed 6-*endo*-dig cyclisation of compound **127** provided the desired 2-pyrone fragment **101**. Fürstner and Zhuo mentioned that using the *tert*-butyl ester was very important to ensure the exclusive formation of a 2-pyrone rather than a 4-pyrone.

Scheme 1.15 Preparation of 2-pyrone fragment **101**.

Synthesis of the Macrocyclic Core

Modified Steglich esterification of the acid fragment **100** with the 2-pyrone fragment **101** provided compound **128** (Scheme 1.16). Methyl magnesium bromide opened the pyrone ring to give the isomerisation-prone *Z,E*-dienoic acid motif and install the methyl group at C22 position simultaneously in the presence of iron(III) acetylacetonate as the catalyst. Fürstner and co-workers reported that it was necessary to perform this reaction at $-60\text{ }^\circ\text{C}$ to minimise the undesired attack of the Grignard reagent onto the -NHBoc group. The resulting *Z,E*-configured diennoic acid **129** was desilylated and the macrolactonisation of the resulting seco-acid under modified Mukaiyama conditions¹²³ provided the macrocyclic compound **131** in good yield. Use of a Mukaiyama reagent **130**, which was accompanied by a non-nucleophilic counterion, was critical to avoid massive isomerisation of the *Z*-double bond. Subsequent cleavage of the PMB-ether under treatment with DDQ provided alcohol **132**.



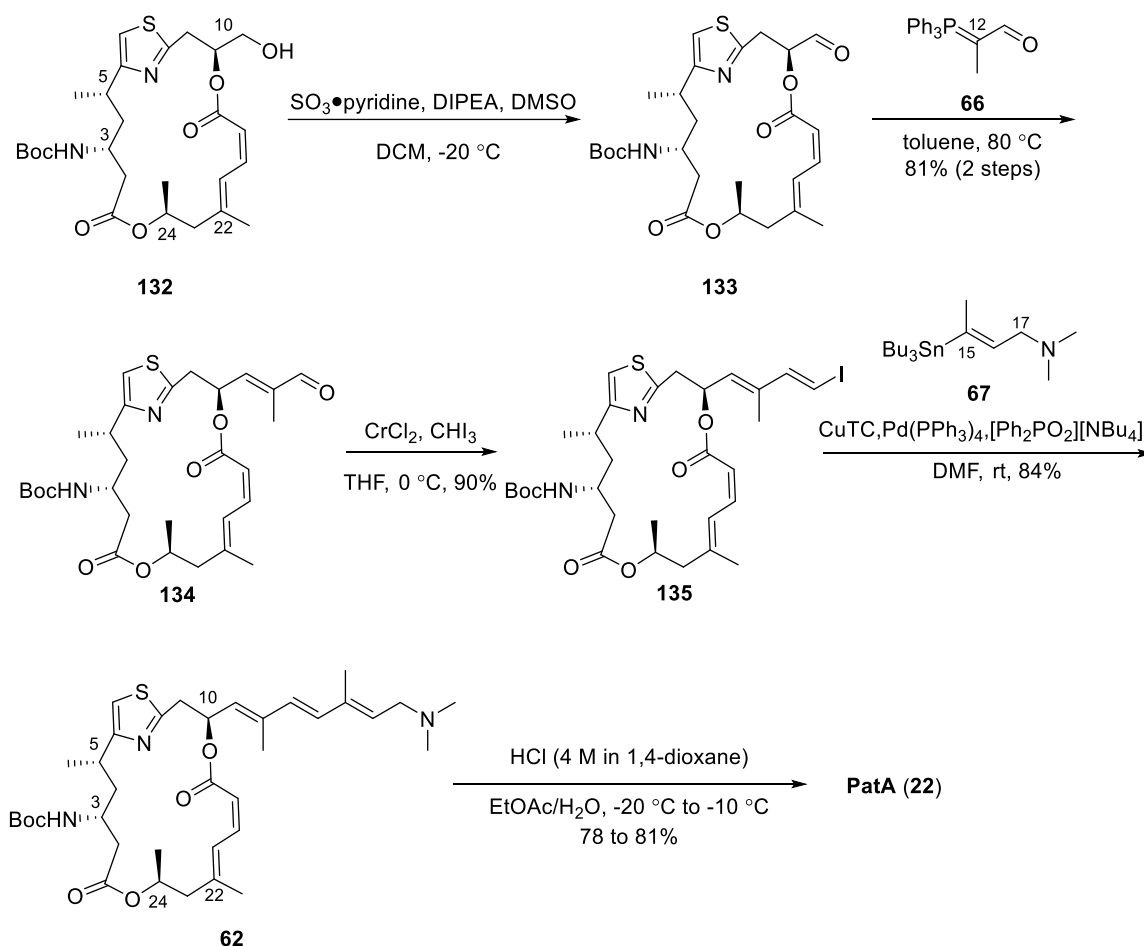
Scheme 1.16 Coupling of major fragments **100** and **101** to form macrocycle core.

Attachment of Side Chain Fragments

Oxidation of alcohol **132** under Parikh-Doering conditions provided aldehyde **133** (Scheme 1.17). Following Pattenden's previous synthetic work,¹¹⁸ Wittig reaction with stabilised ylide **66** provided homologated aldehyde **134**, which was subjected to Takai conditions to afford iodide **135**. According to the modified Stille-Migita protocol developed by Fürstner's research group,¹²⁴ the coupling reaction with vinyl stannane **67**, in the presence of copper thiophene carboxylate (CuTC) and tetrakis(triphenylphosphine)palladium(0) as catalysts and tetra-*n*-butylammonium diphenylphosphinate ([Ph₂PO₂][NBu₄]) as the neutral tin species scavenger,¹²⁵ provided Boc-protected PatA **62** in 84% yield. Compared to the analogous Stille reactions performed in previous Romo's and Pattenden's total synthesis,^{82, 118} the yield was improved considerably. Although Romo reported that attempts to cleave the -NHBoc group under acidic conditions resulted in decomposition,⁸⁴ Fürstner and Zhuo reinvestigated this attractive possibility. Interestingly, they found the use of HCl in dioxane and ethyl acetate could cleave the Boc-protecting group cleanly without

destroying this sensitive material and PatA (**22**) was obtained in reproducibly good yields.

This synthetic route provided PatA with 24 steps in the longest linear sequence from starting material dibromothiazole **102** and an overall yield of 5.3%, which is much higher than the yields reported by Romo (2.5%) and Pattenden (0.19%).



Scheme 1.17 Attachment of side chain fragments and deprotection of -NHBoc group in Fürstner and Zhuo's total synthesis.

1.4.1.4 Comparison of Syntheses

The common feature in Romo's, Pattenden's and Fürstner's strategies is that the *bis*-lactone macrocycle core is constructed prior to the attachment of the conjugated side chain. To form the macrocycle core, Romo used an intramolecular alcoholysis of the β -lactam intermediate with a 59 – 68% yield (*vide supra*, Scheme 1.5), Pattenden employed a Stille coupling with a similar yield (65%) (*vide supra*, Scheme 1.10), and Fürstner obtained a better yield (82%) using modified Mukaiyama macrolactonisation conditions

(*vide supra*, Scheme 1.16). In terms of the addition of the conjugated side chain, Pattenden and Fürstner both adopted a more linear reaction sequence, which involves the connection of smaller fragments through a combination of Wittig olefination, Takai reaction and Stille coupling (*vide supra*, Scheme 1.11 and Scheme 1.17). However, Fürstner obtained an improved yield due to the use of advanced Stille coupling conditions. To prepare the isomerisation-prone *Z,E*-dienoate motif, Romo utilised Sonogashira conditions to couple an *E*-vinyl iodide and an alkyne to form an enyne, the triple carbon-carbon bond of which was reduced by Lindlar catalyst after the formation of the macrocycle to afford the *Z,E*-dienoate (*vide supra*, Scheme 1.11 and Scheme 1.17); Pattenden employed a Stille coupling between a *Z*-configured vinyl stannane and an *E*-configured vinyl iodide (*vide supra*, Scheme 1.10); and Fürstner used a 2-pyrone as the surrogate, which was unfolded under iron-catalysed ring-opening/cross-coupling conditions to provide the desired *Z,E*-dienoate (*vide supra*, Scheme 1.16).

PatA contains four chiral centres at C3, C5, C10 and C24, for which Romo and co-workers used auxiliary-based asymmetric aldol reactions to obtain chiral centres at C3 and C10, an asymmetric hydrogenation in the presence of a chiral ligand to obtain the chiral centre at C24 and an auxiliary-based asymmetric methylation to introduce the desired stereochemistry at C5 (Figure 1.20). Fürstner and Zhuo utilised metal-catalysed asymmetric reactions with the involvement of chiral ligands to obtain three of these chiral centres (at C3, C5, and C10) and incorporated a commercially available chiral starting material to obtain the chiral centre at C24 (Figure 1.20). In contrast, Pattenden's group used the chiral pool strategy to introduce the stereochemistries at C5, C10, and C24, and an auxiliary-based aldol-like asymmetric reaction to obtain the desired stereocentre at C3 (Figure 1.20).

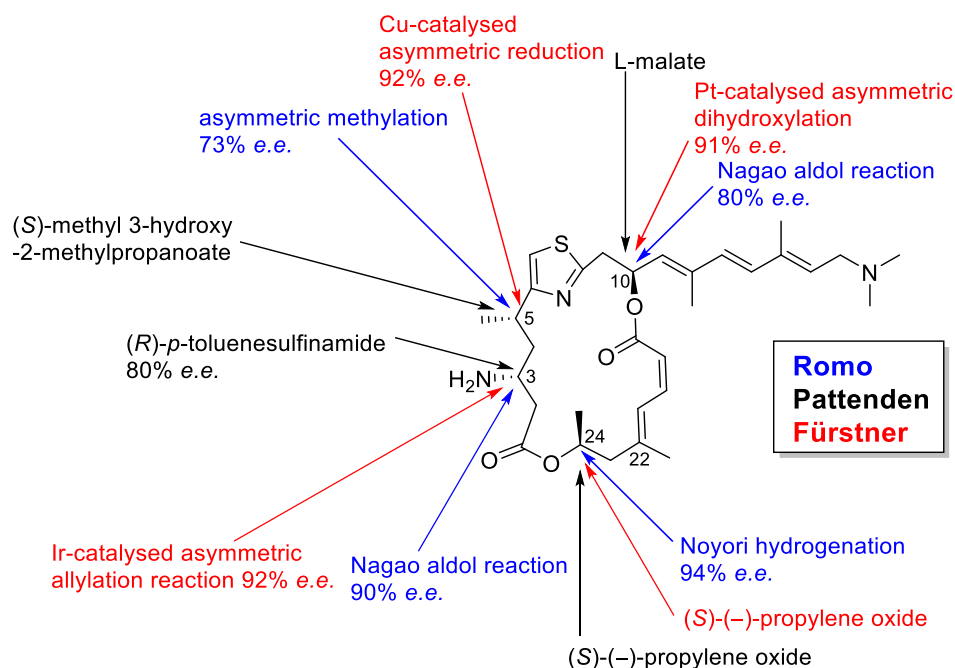


Figure 1.20 Comparison of the introduction of stereochemistries in Romo's, Pattenden and Fürstner's total synthesis of PatA, showing obtained enantiomeric excess (*e.e.*).

1.4.2 Pateamine A Analogues Synthesis

1.4.2.1 Romo's Synthesis of DMDA PatA Analogue

Based on the structural analysis and preliminary molecular modelling studies of PatA, Romo hypothesised that PatA is comprised of two structural domains, a more flexible 'scaffolding domain' (C1 – C5) responsible for defining the conformation of the macrocycle, and the rigid highly unsaturated 'binding domain' (C6 – C24) crucial for protein binding (Figure 1.21).¹²⁶ This hypothesis was also bolstered by Liu and co-workers' findings that the activity of Boc-protected PatA was only 5 – 10 times lower than that of PatA in human mixed lymphocyte reaction.⁸² Accordingly, it was supposed that the C3-amino group, as well as the C5-methyl group, might be omitted without significant loss of activity. To provide more evidence for this hypothesis, Romo's laboratory used a similar strategy to that used in their first total synthesis of PatA and synthesised the simplified derivative des-methyl, des-amino PatA (DMDA PatA) **136** (Figure 1.21), which is devoid of the C3-amino group and C5-methyl group.

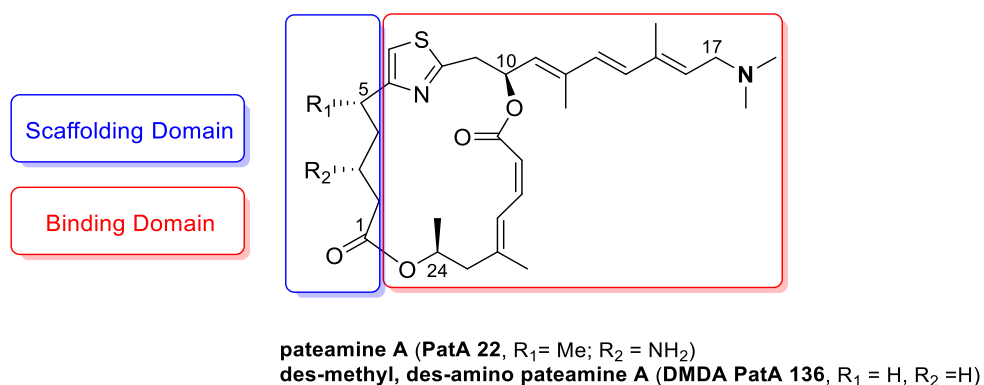


Figure 1.21 Structures of PatA (**22**) and DMDA PatA (**42**) showing hypothesised ‘scaffolding domain’ (blue box) and ‘binding domain’ (red box).¹²⁷

Comparing to Romo and co-workers’ synthetic strategy for PatA (Figure 1.14), the major two modifications in their strategy for DMDA PatA are firstly in the preparation of C1 – C7 fragment and secondly in the macrolactonisation step, where a Yamaguchi esterification was applied instead of the β -lactam mediated macrolactonisation (Figure 1.22).¹²⁶

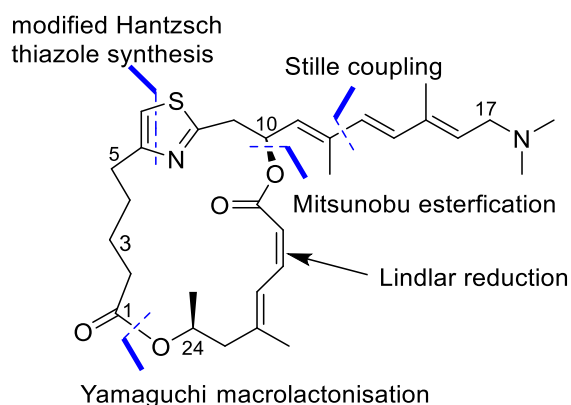
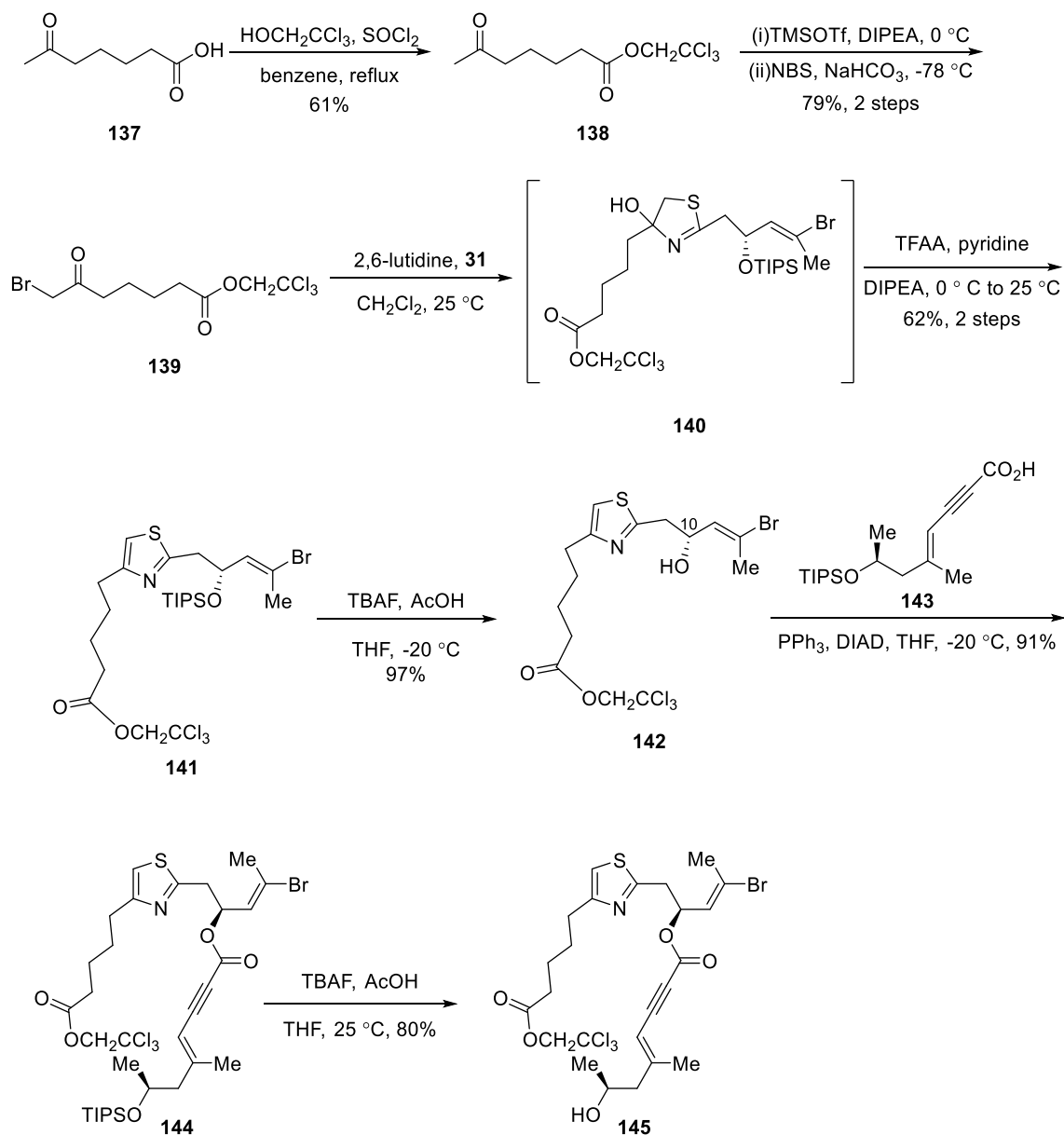


Figure 1.22 Key connections and features in Romo’s synthetic strategy for DMDA PatA.¹²⁶

As shown in Scheme 1.18, the synthesis of DMDA PatA (**136**) started from esterification of commercially available 6-oxoheptanoic acid **137** with commercially available 2,2,2-trichloroethanol, which served as the C1 – C7 fragment. The resulting trichloroethyl ester **138** was regioselectively brominated to give α -bromoketone **139**. Modified Hantzsch thiazole coupling between **139** and thioamide **31**, the same building block used in Romo’s synthesis of PatA (Scheme 1.1), provided thiazole **141** via the formation of thiazoline intermediate **140**. Subsequent desilylation gave secondary alcohol **142** with *R*

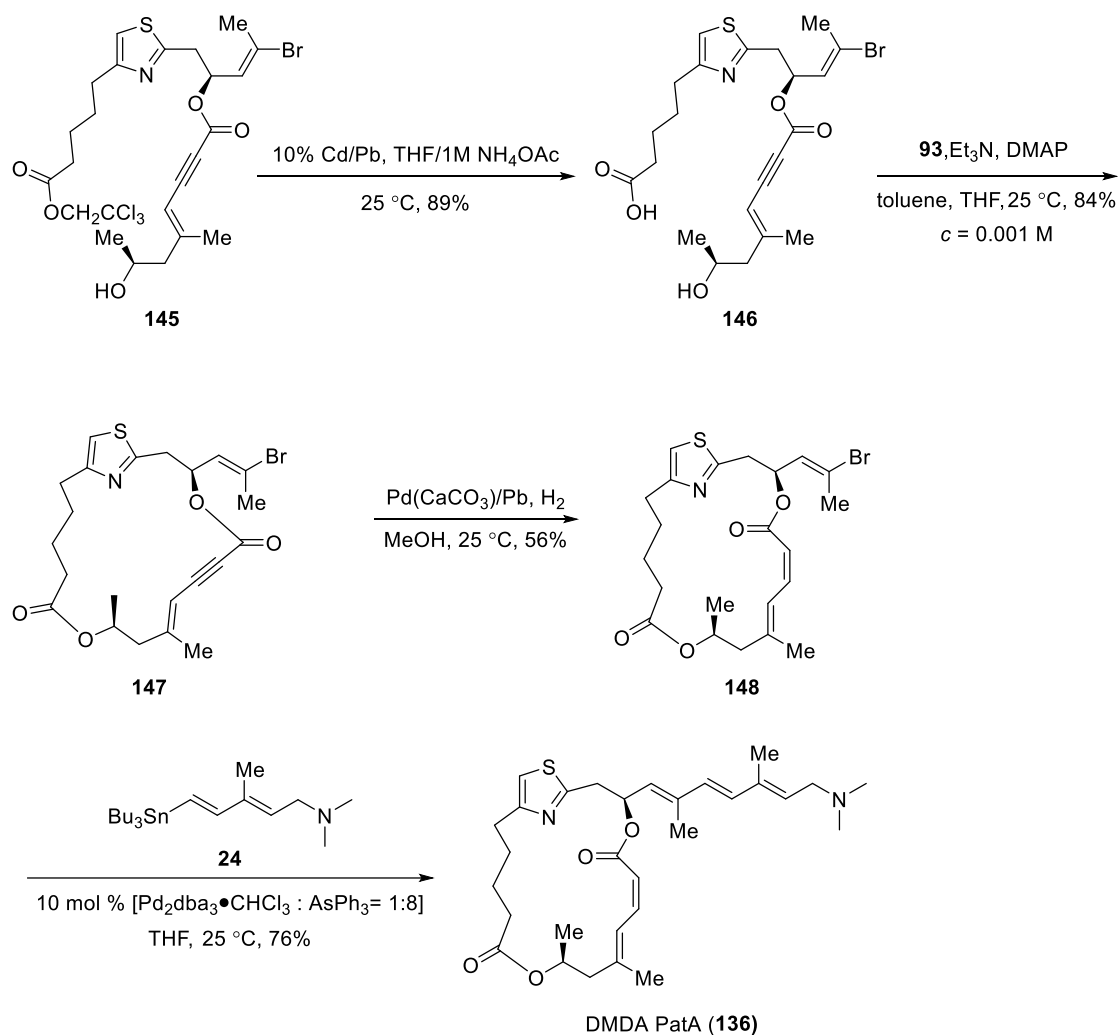
configuration at the C10 position (PatA numbering). Mitsunobu coupling with triisopropylsilyl (TIPS)-protected enynoic acid **143**, which could be prepared using a similar sequence to that for acid **25** (Scheme 1.4), inverted the undesired *R* configuration to the desired *S* configuration and gave compound **144**. Subsequent desilylation provided alcohol **145**.



Scheme 1.18 Preparation of alcohol **145** in the synthesis of DMDA PatA.

Deprotection of the trichloroethyl ester provided compound **146**, which set the stage for the lactonisation step (Scheme 1.19). Yamaguchi macrolactonisation followed by treatment with Lindlar's catalyst afforded the *Z*, *E*-dienoate **148**. Stille coupling with

dienyl stannane **24** delivered DMDA PatA (**136**).



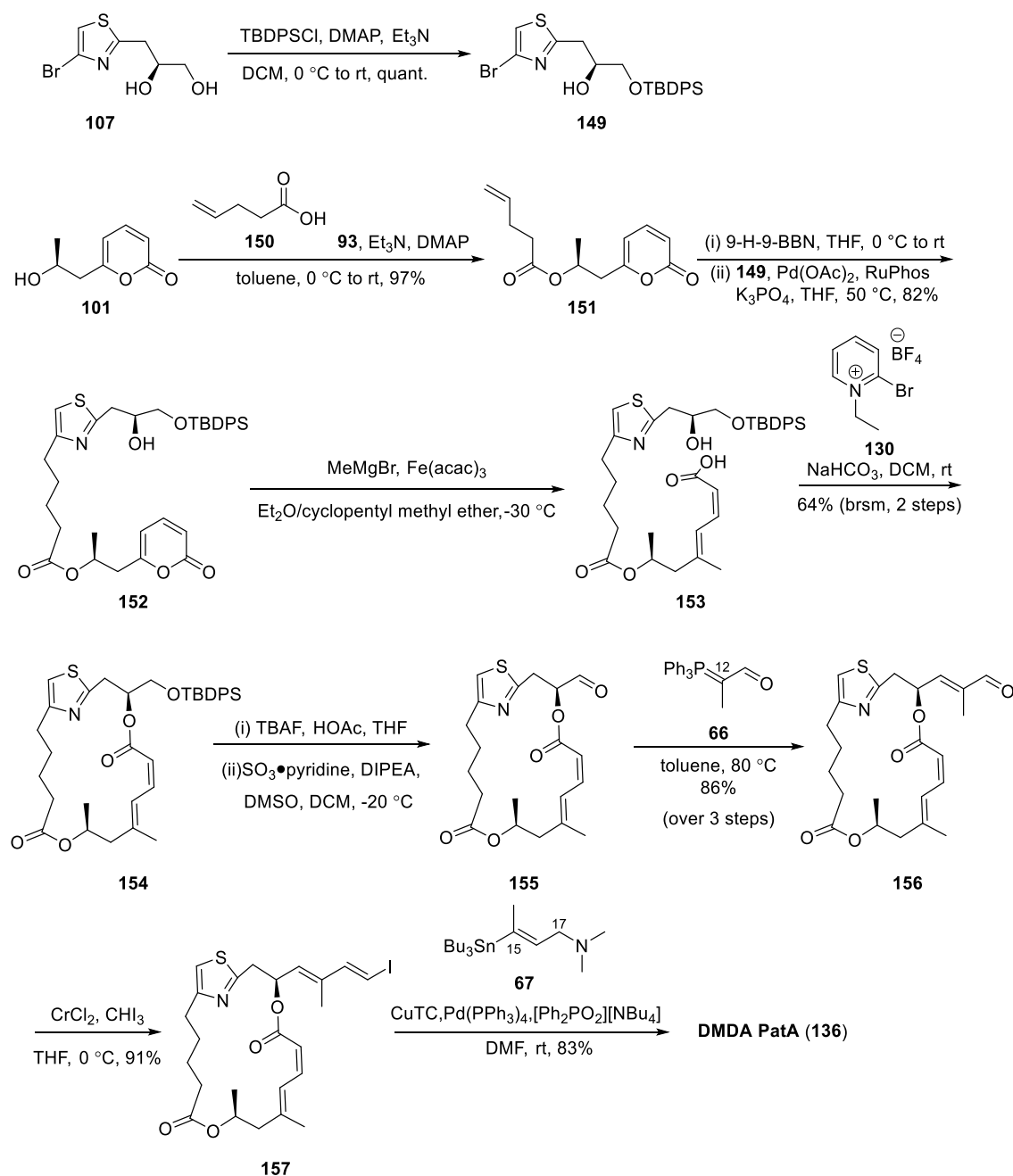
Scheme 1.19 Preparation of DMDA PatA.

This synthetic route for DMDA PatA is only 14 steps starting from aldehyde **25** (*cf.* 24 steps for Romo's synthesis of PatA) and the overall yield is 13% (*cf.* 2.5% for Romo's synthesis of PatA).

Apart from being chemically more accessible, DMDA PatA was also found to display similar potency relative to PatA in its ability to inhibit cell proliferation across a number of cancer lines,¹²⁷ which provides direct evidence supporting the proposed scaffolding domain and binding domain hypothesis (Figure 1.21). In addition, it displays better chemical stability than PatA.¹²⁶ Therefore, it is necessary to develop more efficient synthesis for this promising anticancer agent.

1.4.2.2 Fürstner and Zhuo's Synthesis of DMDA PatA

In similar fashion to Fürstner and Zhuo's total synthesis of PatA, their synthesis of DMDA PatA utilised the diol fragment **107** and 2-pyrone fragment **101** (Scheme 1.20), the same building blocks derived from dibromothiazole **102** and (*S*)-(-)-propylene oxide **86**, respectively (*vide supra*, Schemes 1.12 and 1.15).¹²⁸ As the amino group at C3 and the methyl group at C5 are excised in DMDA PatA, the commercially available 4-pentenoic acid **150** was chosen to serve as the C1 – C5 fragment. Yamaguchi esterification of 2-pyrone **101** with acid **150** provided ester **151**. Hydroboration of the terminal double bond of ester **151** gave the trialkylborane intermediate, which was coupled with mono-silylated thiazole **149** to afford compound **152**. Interestingly, although a free hydroxyl group is present in compound **152**, iron-catalysed ring-opening/cross-coupling reaction with excess methyl Grignard reagent proceeded well. The 2-pyrone ring was unfolded cleanly and the desired methylated *Z,E*-dienoic acid **153** was obtained in high isomeric purity. Modified Mukaiyama macrolactonisation, desilylation, and subsequent Parikh-Doering oxidation gave aldehyde **155**, which was found to be rather sensitive and prone to epimerisation. Therefore, aldehyde **155** production was telescoped with Wittig olefination to provide homologated aldehyde **156**. Treatment with Takai conditions and subsequent modified Stille-Migita coupling¹²⁴ with fragment **67** afforded the complete DMDA PatA. Overall, this synthetic route for DMDA PatA is only 12 steps in the longest sequence (*cf.* 24 steps for Fürstner's synthesis of PatA) and the overall yield is 18% (*cf.* 5.3% for Fürstner's synthesis of PatA).



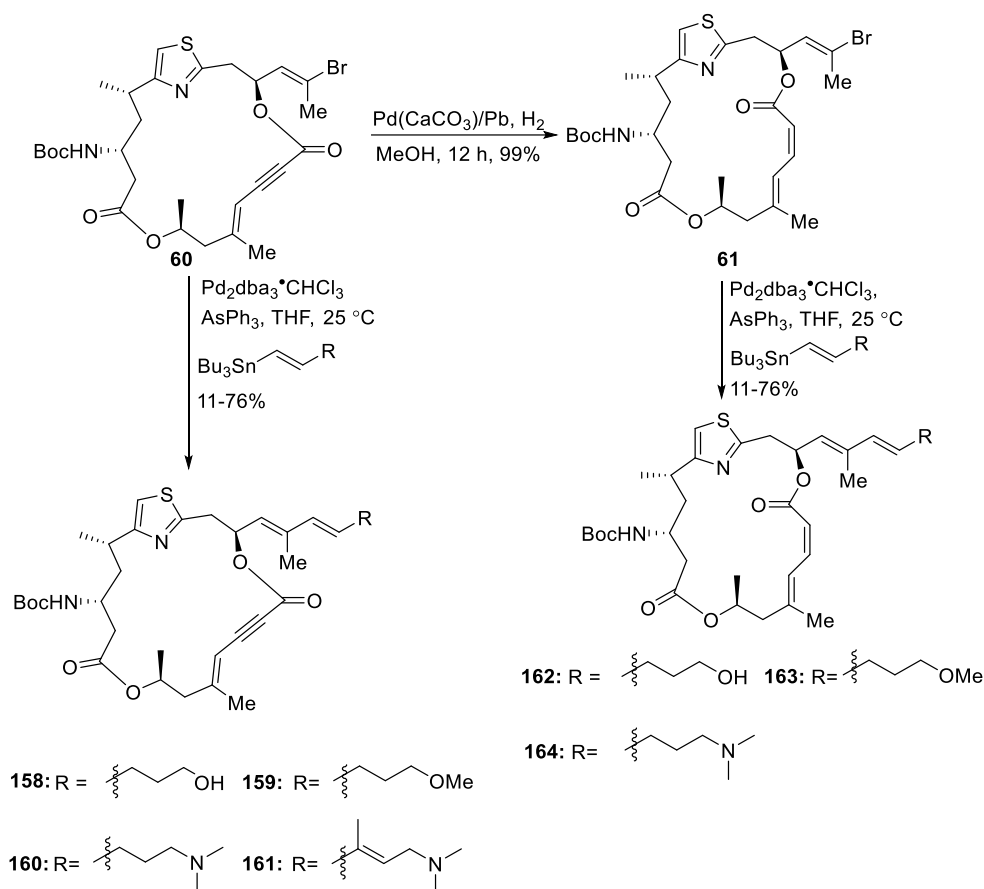
Scheme 1.20 Fürstner and Zhuo's synthesis of DMDA PatA.¹²⁸

1.4.2.3 Romo's Analogue Synthesis Based on PatA

To explore the importance of the side chain in the identified 'binding domain' of PatA, Romo and co-workers synthesised analogues with minor structural variations on the side chain. To investigate whether or not the dienoate motif is essential for the bioactivity, they also synthesised enynoate analogues, in which the Z-olefin at C19 – C20 (PatA numbering) was replaced with a carbon-carbon triple bond. As C3-Boc protected PatA **62** was found to only have a 3-4 fold reduction in activity and to be more stable when

compared to the parent natural product,⁸² the Boc-protecting groups were retained in all these derivatives.¹²⁶

As shown in Scheme 1.21, synthesis of enynoate analogues **158** – **161** was completed through Stille coupling between the *bis*-lactone macrocyclic core **60** and a series of vinylstannanes, respectively. Analogues **162** – **164** with variant side chains were synthesised in a two-step sequence comprising Lindlar reduction of macrocycle **60** followed by attachment of a series of vinylstannanes to bromoalkene **61** through Stille coupling.

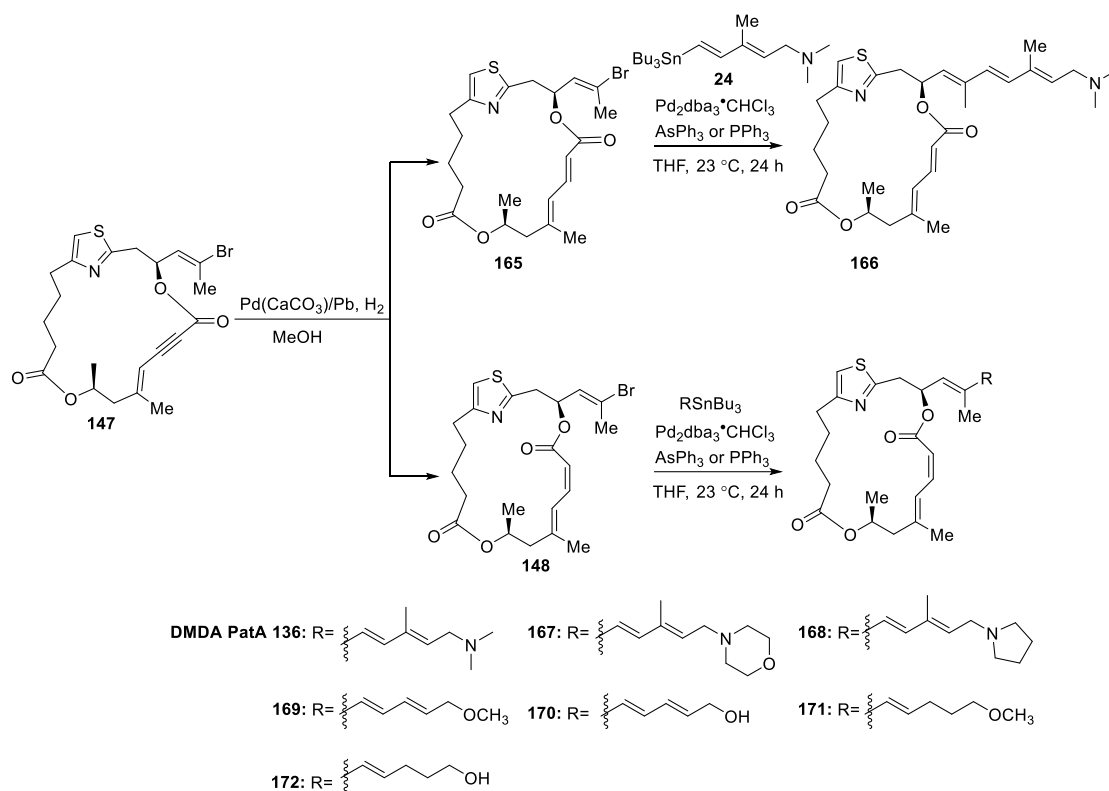


Scheme 1.21 Preparation of analogues **158** – **164** of PatA.

1.4.2.4 Romo's Analogue Synthesis Based on DMDA PatA

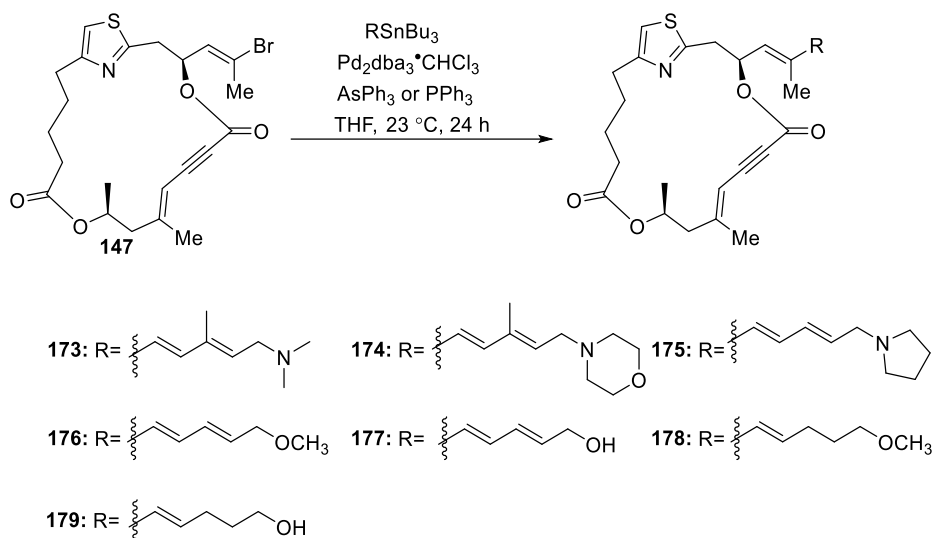
Given that the simplified derivative DMDA PatA is almost equipotent to Pat A and is simpler to synthesise, a series of analogues based on DMDA PatA were designed and synthesised in order to further examine the importance of the side chain and the diene system in the identified 'binding domain' of DMDA PatA.^{126, 127}

As shown in Scheme 1.22, the enyne macrocycle core **147** was reduced by Lindlar's catalyst under particular conditions to provide a mixture of *Z,E*-dienoate **148** and *E,E*-dienoate **165** (*Z,E* : *E,E* = 5:1) that were separable by silica gel chromatography. To synthesise the analogue with an *E, E*-configured dienoate system, bromoalkene **165** was coupled with the vinylstannane **24** to provide analogue **166**. Analogues **167** – **172** with structural variations in the side chain were synthesised through Stille coupling with the *Z, E*-dienoate macrocycle **148** and a series of vinyl stannanes.¹²⁷



Scheme 1.22 Preparation of analogues **166** – **172** based on DMDA PatA.

Enynoate analogues of DMDA PatA **173** – **179** were prepared through the Stille coupling reaction between the enyne macrocycle **147** and a series of vinyl stannanes (Scheme 1.23).



Scheme 1.23 Preparation of enynone analogues **173** – **179** based on DMDA PatA.

1.5 Structure-Activity Relationship Studies of PatA and Analogues

1.5.1 Studies on Immunosuppressive Activity of PatA Analogues

Preliminary studies by Dr. Glynn Faircloth from PharmaMar found that PatA exerted potent inhibitory effects on both murine and human mixed lymphocyte reactions, suggesting it has immunosuppressive activity.⁸² Romo and co-workers found that PatA inhibited T-cell receptor-mediated IL-2 production, which led to inhibition in T cell activation.⁸⁴

In order to examine the effects of structural modifications on the immunosuppressive activity, analogues **158** – **164**, two C3-acylated derivatives **180** and **181**, and DMDA PatA **136** were tested in the same IL-2 gene assay as PatA.¹²⁶ Although analogues listed in Table 1.1 were less active than PatA, DMDA PatA **136** (not listed in Table 1.1) exhibited greater potency (IC_{50} 0.8 ± 0.3 nM) when compared to PatA **22** (IC_{50} 4.0 ± 0.94 nM). Analogue **164** was less active than PatA **22**, indicating the unsaturation or the methyl on the side chain is necessary for the potency. Enyne analogues with the partially saturated side chain **160** or the natural conjugated side chain **161** were not active. Conversely, enyne derivatives (**158** and **159**) with oxygen terminus in the side chain were found to retain a degree of activity in the IL-2 reporter gene assay (340 nM and 55 nM, respectively). This inconsistency may suggest that the oxygenated side chain has compensatory effects for the conformational change of the macrocycle caused by the

introduction of the enyne motif. Another possibility is that **158** and **159** may display immunosuppressive activity through binding to a different protein target.¹²⁶

The immune system is a surveillance mechanism that maintains homeostasis outside cells while NMD is a counterpart mechanism inside the cells. These two mechanisms are closely related. By degrading aberrant immunoglobulin (Ig) and T-cell receptor (TCR) transcripts generated from non-productively rearranged Ig and TCR genes, NMD largely decreases the production of dysfunctional or even deleterious molecules in lymphocytes, which is crucial for the survival of B and T lymphocytes.¹²⁹ Therefore, inhibition of NMD would impact the immune system indirectly. Given that eIF4AIII plays a crucial role in NMD (refer to Section 1.3), the conformational change of eIF4AIII generated from binding with PatA would affect NMD and possibly cause immunosuppression. We proposed that these inhibitory activities in the IL-2 gene assay reported by Romo and co-workers may indirectly reveal the real activities of PatA and its analogues in inhibition of NMD.

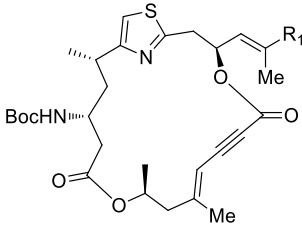
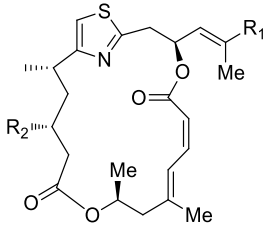
						
Compound	R ₁	IC ₅₀ (nM)	Compound	R ₁	R ₂	IC ₅₀ (nM)
158		340 ± 180	PatA 22		NH ₂	4.0 ± 0.94
159		55 ± 16	162		NHBoc	>1000
160		Not Active	163		NHBoc	>1000
161		Not Active	164		NHBoc	330 ± 120
			180		NHC(O)OPh	15 ± 6.1
			181		NHC(O)CF ₃	300 ± 93

Table 1.1 Comparison of IC₅₀ values for analogues of PatA from IL-2 reporter assay.¹²⁶

1.5.2 Studies on Anti-proliferative Activity of PatA Analogues

Intriguingly, Romo and co-workers found that the structurally simplified analogue DMDA PatA was only slightly less active than PatA in all human cell lines tested for *in vitro* cytotoxicity (Hela (a cervical carcinoma cell line), RKO (a poorly differentiated colon carcinoma cell line), and Jurkat immortalised T cells)(Table 1.2).¹²⁷ DMDA PatA exhibited similar potent anti-proliferative activity in the immortalised human keratinocyte cell line HaCaT and in primary proliferating bovine aortic endothelial (BAEC) cell line (Table 1.2).¹²⁷ DMDA PatA was also found to have the same mechanism of action as the parental PatA.¹²⁷ These results provided convincing evidence for the ‘scaffolding’ and ‘binding’ domain hypothesis (Figure 1.21). DMDA PatA is considered to be a promising natural product-based anticancer agent that requires further research for drug development.

Compound	IC ₅₀ (nM)				
	HeLa	RKO	Jurkat T	HaCaT	BAEC
PatA 22	0.72 ± 0.88	0.38 ± 0.02	0.60 ± 0.02	0.42 ± 0.03	0.5 ± 0.04
DMDA PatA 136	4.5 ± 0.4	1.2 ± 0.05	3.0 ± 0.1	0.9 ± 0.1	1.97 ± 0.1

Table 1.2 IC₅₀ values for PatA 22 and DMDA PatA 42 from cell proliferation assays.¹²⁷

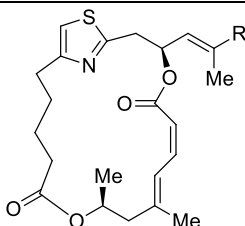
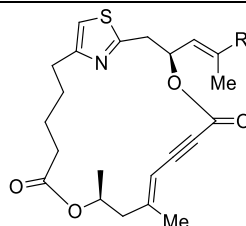
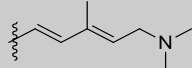
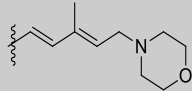
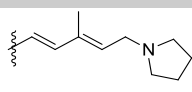
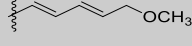
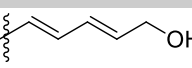
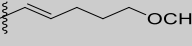
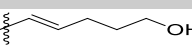
Intensive studies on DMDA PatA showed that it exhibited little differential growth inhibitory activity in a panel of 32 human cancer cell lines including both solid tumours and hematologic malignancies.¹³⁰ Surprisingly, DMDA PatA exerted anticancer effects in two different melanoma xenograft models (MDA-MB-435 and LOX), resulting in significant tumour regression, whereas it did not show a significant effect in either MiaPaca-2 pancreatic cancer or an HT-29 colon cancer xenograft model.¹³⁰ Future studies are required to figure out why this analogue is indiscriminately potent amongst a broad range of human cancer cell lines *in vitro* but is selectively effective *in vivo*. What is also encouraging is that DMDA PatA was found to retain its potency against P-glycoprotein (PgP)-overexpressing human uterine sarcoma cells, suggesting that it is insensitive to PgP-mediated drug efflux.¹³⁰ More intriguingly, DMDA PatA at low nanomolar concentration has no cell-killing ability for quiescent human fibroblasts, indicating that the observed inhibitory activity against human cell growth results from inhibited proliferative processes rather than indiscriminate proliferation-independent cytotoxicity.¹³⁰ Although the mechanism of action of DMDA PatA was considered to be the same as its parental counterpart,¹²⁷ this simplified analogue was found to inhibit S-phase DNA synthesis in some cell lines, although giving no specific cell cycle blockade in others. Where observed, S-phase blockade is proposed to be through direct inhibition of DNA polymerases, which provides an additional impetus for further research on the mechanism of action of DMDA PatA.¹³⁰

On the basis of the established research described above, DMDA PatA is considered to be an intriguing anticancer agent worthy of further structure-activity relationship (SAR) studies.

To find out more information about DMDA PatA's structure-activity relationship, the side chain truncated analogues **147** and **148** and analogues **167** – **179** based on DMDA PatA were tested by Romo's research group for cell proliferation activity in two cell lines (HeLa and Jurkat T).¹²⁷

As shown in Table 1.3, the brominated derivative **148** displays no activity for HeLa cells and Jurkat T cells even at the highest concentration tested, indicating that the trienyl amine side chain plays a crucial role in binding with the protein target.¹²⁷ When the terminal *N,N*-dimethylamine group is replaced with other tertiary amines – a 6-membered morpholine ring (analogue **167**) or a 5-membered pyrrolidine ring (analogue **168**) — it is noteworthy that the morpholine substitution shows a greater loss of activity than the pyrrolidine substitution (400-fold loss for **167** in HeLa cells versus 2-fold loss for **168**). The conjugate acid of pyrrolidine has a similar p*K*_a value of approximately 11 to that of *N,N*-dimethylamine whereas the morpholine ring is significantly less basic, with a p*K*_a value of 8.36 (conjugate acid). In addition, replacement of the *N,N*-dimethyl tertiary amine with ether and alcohol functionalities resulted in significant losses of activity (analogues **169** – **172**). These results suggest that the basic terminal in the side chain is also important for the high potency. It is of interest that analogue **167** displays differential degrees of loss of activity in HeLa cells and Jurkat T cells, suggesting that replacement of the *N,N*-dimethyl tertiary amine with different basic substitutions may increase selectivity between different proliferating cell lines.¹²⁷ Moreover, the different activity of **170** and **172** is due to their only structural difference – the loss of unsaturation at C15 and C16. Therefore, the rigidity generated from double bonds of the side chain may also be crucial for the potency.¹²⁷

Analogues (**173** – **179**) with enyne structures demonstrate a drastic decrease in activity (Table 1.3). The reason for the loss of activity is likely to be that the enyne replacement results in a significant change in the preferred conformations of the macrocycle, which is critical for binding with eIF4A.¹²⁷ Not surprisingly, *E,E*-dienoate analogue **166** (Scheme 1.22) with the alteration at the geometry of the olefin at C19-C20 in the dienolate unit, which was proposed to act as a Michael acceptor for biological nucleophiles,^{86, 110, 131} was found to be inactive in the tested cell lines.¹²⁷

R					
Compound	IC ₅₀ (nM) ^a	Compound	IC ₅₀ (nM) ^a		
	Jurkat T HeLa		Jurkat T HeLa		
	136 11 9.8	173 N.E. (10 ⁴) N.E. (500)			
Br	148 >10 ⁴ N.E. (500)	147 N.E. (10 ⁴) N.E. (500)			
	167 N.E. (10 ⁴) 430	174 N.E. (10 ⁴) N.E. (500)			
	168 25 23	175 N.E. (10 ⁴) N.E. (500)			
	169 N.E. (10 ⁴) N.E. (500)	176 N.E. (10 ⁴) N.E. (500)			
	170 >10 ⁴ >5 × 10 ³	177 N.E. (10 ⁴) N.E. (500)			
	171 N.E. (10 ⁴) N.E. (500)	178 N.E. (10 ⁴) N.E. (500)			
	172 >5 × 10 ³ N.E. (500)	179 N.E. (10 ⁴) N.E. (500)			

^a‘N.E.’ means that no effect was observed up to the concentration tested shown in parentheses.

Table 1.3 Comparison of IC₅₀ values for analogues of DMDA PatA from two different cell proliferation assays.¹²⁷

1.5.2 Summary

In brief, based on the previous structure-activity studies,^{126, 127} the crucial structures residing in the ‘binding domain’ for the potency of PatA (**22**)/DMDA PatA (**136**) include the basic terminus and the unsaturation in the side chain, the conformation of the macrocycle and the *Z,E*-dienoate motif. The roles of the heterocycle, the methyl groups on the side chain, and the methyl groups on the macrocycle core (at C22 and C24 position, PatA numbering) still need to be further examined.

Additionally, considering that DMDA PatA is slightly less potent than PatA in the anti-proliferation assay but more potent than PatA in the IL-2 reporter gene assay,¹²⁷ it is conceivable that the elimination of the C3 methyl and C5 amino may enhance the immunosuppressive activity while slightly weakening the anti-proliferative activity. When comparing the activity data of all analogues synthesised by Romo’s group, an obvious discrepancy was that analogues **158** and **159** still demonstrated some activity in the IL-2 reporter assay (Table 1.1),¹²⁶ but the derivatives **179** and **178** with the same enyne structure and the identical side chains did not display any significant anti-proliferative activity in tested cell lines (Table 1.3).¹²⁷ Romo and co-workers proposed that one possibility is that PatA and its analogues only display cell growth inhibition at low concentrations but possess both IL-2 production inhibition activity and antiproliferative activity at higher concentrations. After eliminating anti-proliferative activity through structural modification, IL-2 transcriptional inhibition activity would become the primary biological activity.¹²⁷ This led to the idea that it is possible to design an analogue of PatA that could regulate the immune system without any significant impact on cell proliferation, and *vice versa*.

In view of the interaction between NMD and the immune system, it is favourable to explore the possibility of synthesising an analogue that selectively binds to eIF4AIII over eIF4AI/II. This analogue would impact NMD directly and may act as a probe to further explore the NMD mechanism based on the EJC model. Furthermore, this may also provide potential regulatory molecules for the immune system and NMD, which may benefit further studies on treatments for autoimmune diseases (*e.g.*, rheumatoid arthritis and lupus)¹³² and inherited genetic diseases related to NMD (*e.g.*, β -thalassemia and Marfan syndrome).¹³³ To achieve this goal, it is necessary to further explore PatA’s mode of binding to different eIF4A isoforms — eIF4AI/II and eIF4AIII.

1.6 Cumming's Synthesis of Triazole Analogue

To examine the role of the heterocycle ring in the binding process of PatA and to probe the possibility of selective binding to either eIF4AI/II or eIF4AIII isoforms, Hemi Cumming, a former Ph.D. student in our research group, designed and synthesised a simplified 1,2,3-triazole-containing analogue **182** (Figure 1.23) based on DMDA PatA.¹³⁴ In this analogue, the thiazole ring embedded within the molecule was replaced with a triazole ring while the key structural features including the size of the macrocycle, the *bis*-lactone functionalities, the *Z,E*-dienoate, the all *E*-configured triene and the tertiary amine terminus were retained. Under the assumption that losses of methyl substituents on the side chain would not significantly impact target protein binding, the methyl groups at C12 and C15 (PatA numbering) were excised. To further reduce the structural complexity, the methyl groups at C22 and C24 (PatA numbering), which were proposed to be not critical for the biological activity, were also omitted. Based on the molecular modelling studies results collected by Cumming, there was no significant change in conformations of DMDA PatA and this simplified triazole analogue **182**.¹³⁵ However, calculation of electrostatic potential surface for DMDA PatA **136** and the triazole analogue **182** showed that the replacement of the thiazole ring with a triazole ring could cause significant differences in charge distribution in the macrocycle.¹³⁵

As summarised in Figure 1.23, Cumming's synthesis of analogue **182** involved a Julia-Kocienski olefination reaction between a sulfone and an aldehyde to connect the side chain fragment, a base-induced ring-opening reaction of a δ -valerolactone to provide the *E,Z*-dienoate motif and a copper-catalysed azide-alkyne cycloaddition reaction to construct the triazole ring. Steglich esterification and Yamaguchi macrolactonisation were utilised to construct the macrocycle. The synthesis of the non-methylated side chain fragment from furan will be covered in Chapter 2 and the preparation of the α,β -unsaturated δ -lactone will be covered in Chapter 3. The remainder of the details of the synthesis will be covered in Chapter 4.

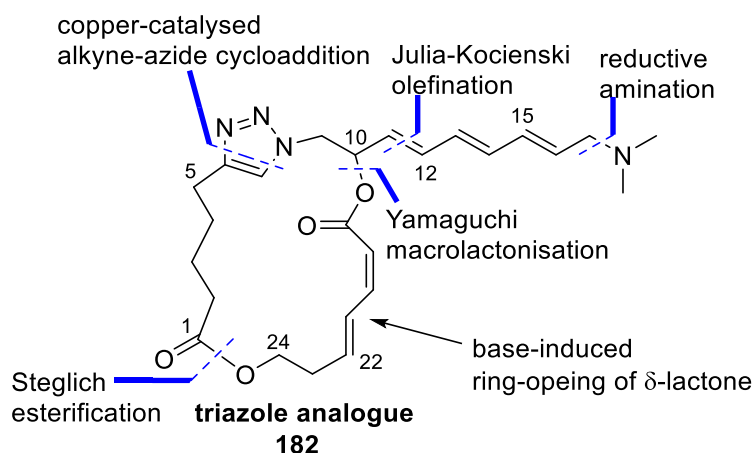


Figure 1.23 Key connections and features in Cumming's synthesis of triazole analogue **182**.¹³⁴

This triazole analogue **182** was tested in two cell lines: HL-60 (human acute myeloid leukaemia cells) and 1A9 (human ovarian carcinoma cells). Compared to DMDA PatA with an IC_{50} value of approximately 1.0 nM in NALM-6 pre-B leukaemia cells,¹³⁰ analogue **182** displayed a drastic reduction in anti-proliferative activity with an IC_{50} value of 34600 nM and 51100 nM in HL-60 and 1A9 cells respectively (Table 1.4).¹³⁵ It is of note that analogue **182** was tested as a mixture of enantiomers, in which the (10*S*)-enantiomer could be completely inactive. However, this still does not rationalise the significant loss in bioactivity relative to PatA/DMDA PatA. Due to the fact that several changes were made simultaneously in this analogue, namely thiazole replacement and removal of four methyl groups, it is difficult to assess the individual contributions to the reduction in the activity for each of the altered structural features.

Compound	IC_{50} (nM)	
	HL-60	1A9
Triazole Analogue (\pm)- 182	34600	51100

Table 1.4 IC_{50} values for analogue **182** based on MTT assay.¹³⁵

1.7 Research Aim

The aim of this project is to design and synthesise new simplified PatA analogues as probes to further explore its mode of binding with eIF4A isoforms. There are two main facets of this research project: firstly, to synthesise new analogues of PatA with fewer structural modifications than Cumming's triazole analogue **182** to explore the structure-activity relationship of simplified PatA analogues and so reveal the individual contributions of the structure modifications to the significant reduction in activity; secondly, to examine the scope and efficiency of the novel synthetic methodology and develop new analogues which can be prepared in a more tractable synthetic route than the natural product.

1.7.1 Analogue Design

As shown in Figure 1.24, the conjugate acid of 2,5-dimethylthiazole has a pK_a value of 3.91¹³⁶ whereas the conjugate acid of 1-methyl-1,2,3-triazole has a significantly lower pK_a value of 1.25.¹³⁷ This means that the basicity of the nitrogen atom in 1,2,3-triazole is lower than the nitrogen atom in thiazole and therefore 1,2,3-triazole is not an easily protonable functional group when compared to thiazole. We considered that the protonation of the nitrogen atom of the thiazole ring residing in PatA is crucial for its efficient binding to eIF4A isoforms. The substitution of the thiazole for the triazole may affect its binding ability to the target protein, and this modification could be the major cause of the significant loss in the activity.

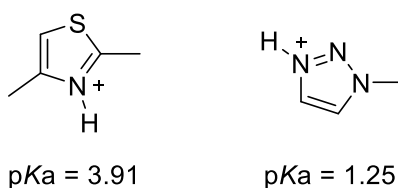


Figure 1.24 Comparison of the pK_a values of the conjugate acids of 2,5-dimethylthiazole¹³⁶ and 1-methyltriazole.¹³⁷

To provide evidence for this hypothesis, it is necessary to reintroduce the thiazole ring into the analogue scaffold, and therefore, thiazole analogue **183** would be the first target (Figure 1.25) in this project. The comparison of activities of 1,2,3-triazole analogue **182** and thiazole analogue **183** would reveal whether the thiazole ring is the key requirement

for binding to eIF4A.

Compared to the potent simplified analogue DMDA PatA (**136**), the other major change in the structure of triazole analogue **182** is the absence of the methyl groups at the C12, C15, C22 and C24 positions (PatA numbering). As the so-called ‘magic’ methyl effects have been proven to be very important in molecular recognition by bioreceptors in medicinal chemistry,^{138, 139} we propose that the absence of methyl groups may also contribute to the reduction in the activity. To examine the importance of the methyl groups at the C12 and C15 positions, the 1,2,3-triazole analogue with the methylated side chain, analogue **187** (Figure 1.25), would also be prepared. Since analogues with the (*R*)-configuration at C10 (PatA numbering) have not yet been synthesised in Romo’s previous structure-activity relationship studies,^{126, 127} preparing a stereoisomeric analogue at C10 would be of interest. As triazoles are synthetically more accessible than thiazoles, we decided to prepare both enantiomers of analogue **187**, namely the (10*R*)-analogue (*R*)-**187** and the (10*S*)-analogue (*S*)-**187**. The comparison of bioactivities of triazole analogues **182**, (*R*)-**187** and (*S*)-**187** would provide information on the importance of the methyl groups on the side chain and the stereochemistry of C10 (PatA numbering).

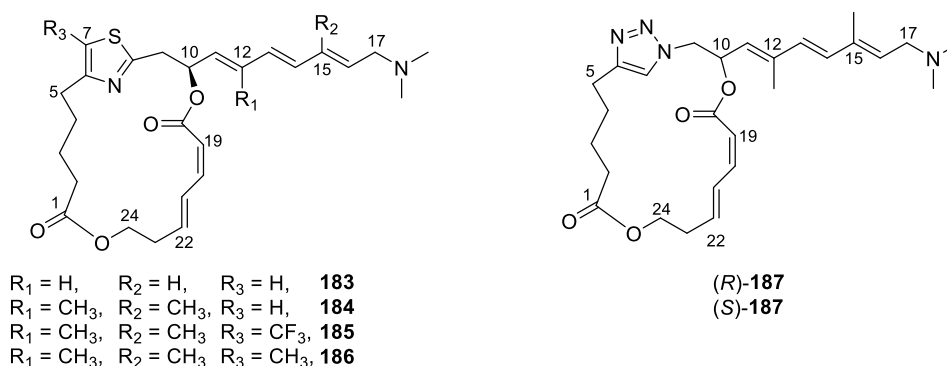


Figure 1.25 Chemical structures of targeted analogues **183** – **187**.

Based on the previous structure-activity studies showing that the modifications of the configuration of the *E,Z*-diene resulted in a drastic decrease in activity,^{126, 127} we propose that the methyl at C22 may have modulatory effects when the diene acts as a Michael acceptor in the binding to the target protein.^{86, 110, 131} In addition, the methyl group at the C24 chiral centre could modify the conformation of the macrocycle to that required for binding to the active site of the protein. To examine the importance of these two methyl groups on the macrocycle, thiazole analogue **184** with the methylated side chain of the

natural product would also be prepared. Comparison of the bioactivities of analogue **184** and DMDA PatA (**136**) would disclose whether or not the removal of these two methyl groups is also responsible for the erosion of activity.

In this project, we would like to further explore the role of the heterocycle in the activity. To examine whether the basicity of the thiazole ring is important for binding to its protein target or not, one viable modification would be to introduce an electron-withdrawing group (*e.g.* a trifluoromethyl group – analogue **185**) or an electron-donating group (*e.g.* a methyl group – analogue **186**) on C7 (PatA numbering) to reduce or increase the basicity of the nitrogen atom of the thiazole ring. The difference in activities of analogues **184**, **185** and **186** would provide more information on the importance of the heterocycle protonation in the activity.

It was hoped that a scaffold that possesses reduced structural complexity while retaining similar bioactivity relative to PatA could be finally determined through all these studies. This would provide a solid foundation for the future design of analogues.

1.7.2 Retrosynthetic Analysis

We envisioned a strategy that could allow the collective synthesis of our designed thiazole analogues **183** – **186** and triazole analogue **187**. In other words, we wanted a synthesis of these analogues that would employ the same building blocks wherever possible.

Figure 1.26 shows our first-generation general retrosynthetic analysis of thiazole analogues **183** – **186** and triazole analogue **187**. In order to converge retrosynthetically with the highly favoured cycloaddition strategy for forming triazoles by coupling an alkyne with an azide,¹⁴⁰ a method that would similarly couple an alkyne with a thioamide in forming a thiazole was sought. We envisioned that the thiazole ring in analogues **183** – **186** could be formed *via* a gold-catalysed coupling reaction between the alkyne fragment (Fragment **I**) and an appropriate thioamide.¹⁴¹ The C7-substituent (PatA numbering) could be introduced onto the thiazole ring after its formation in the synthesis of analogues **185** and **186**. The triazole ring in analogue **187** could be prepared by copper-catalysed cycloaddition between the same alkyne fragment (Fragment **I**) and an appropriate azide fragment (Fragment **V**).^{142, 143} As Julia-Kocienski olefination (an olefination reaction between a phenyl tetrazolyl sulfone and an aldehyde or a ketone) has been utilised successfully to attach the side fragment in the synthesis of the triazole

analogue **182**,¹³⁴ we decided to employ this olefination method to connect the non-methylated side chain fragment (Fragment **II**) or the methylated side chain fragment (Fragment **II'**) to further evaluate their performance. The *E,Z*-dienoate motifs in these analogues would be prepared by the base-induced ring-opening reaction of δ -lactone (Fragment **III**), a methodology already used in the synthesis of the triazole analogue **182**.¹³⁴ The macrocyclic core of these analogues would be constructed by a combination of esterification and macrolactonisation, using appropriate conditions. Therefore, we envisioned the synthesis of thiazole analogues **183** – **186** would require fragment **I**, **II** or **II'**, **III** and the thioamide **IV** (Figure 1.26), while the major fragments for the synthesis of triazole analogue **187** would include fragment **I**, **II'**, **III** and the azide **V** (Figure 1.26). Since there are different orders in which these fragments could be coupled into the desired analogues, the coupling sequence would be investigated individually for different analogues. Our work towards the synthesis of thiazole analogues **183** – **186** will be presented in chapter two and chapter three and the work towards the synthesis of triazole analogue **187** will be presented in chapter four.

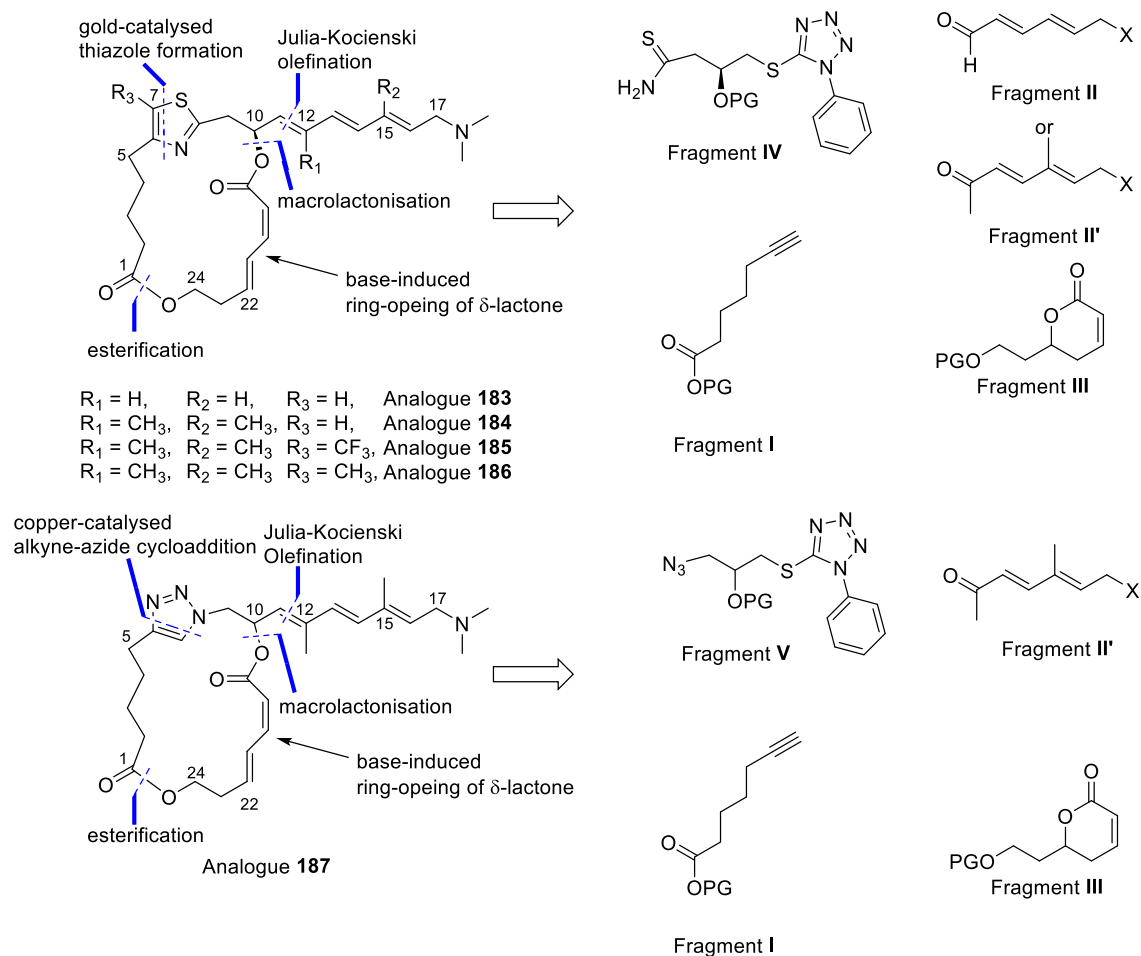


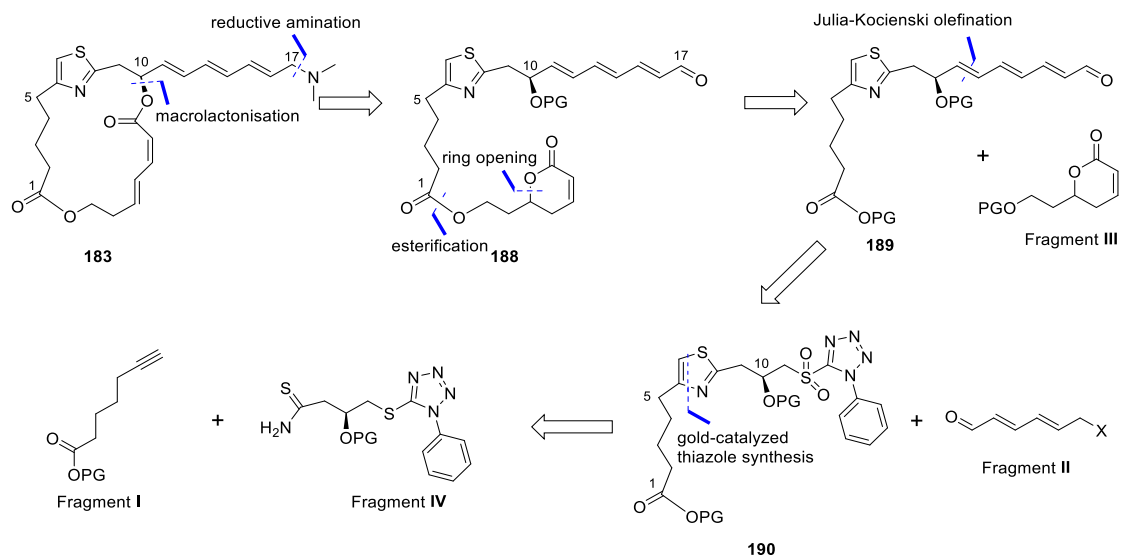
Figure 1.26 First generation retrosynthetic analysis of thiazole analogues **183** – **186** and triazole analogue **187**

Chapter Two: Towards the Synthesis of Thiazole Analogue with Non-Methylated Side Chain

As discussed in Section 1.7.1, the synthesis of thiazole analogue **183** (Figure 1.23) with non-methylated side -chain could help to examine whether or not the absence of a thiazole ring in the triazole analogue **182** (Figure 1.23) is the primary cause of the observed significant loss in cytostatic activity.¹³⁴ This chapter describes the work towards the synthesis of analogue **183**.

2.1 Retrosynthesis

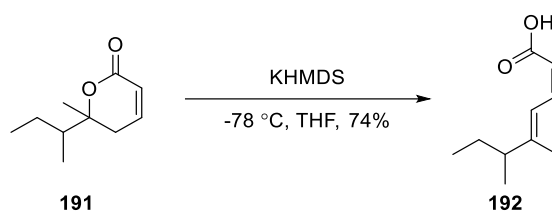
Our proposed synthesis of analogue **183** (Scheme 2.1) was designed to be easily directed towards other five-membered heterocyclic analogues of PatA, such as those containing an oxazole or imidazole ring. Also, we envisioned that our synthesis could evaluate the performance of a new synthetic methodology for thiazole formation¹⁴¹ in a scaffold with structural complexity, which would expand the scope of its applicability.



Scheme 2.1 Retrosynthesis of analogue **183**.

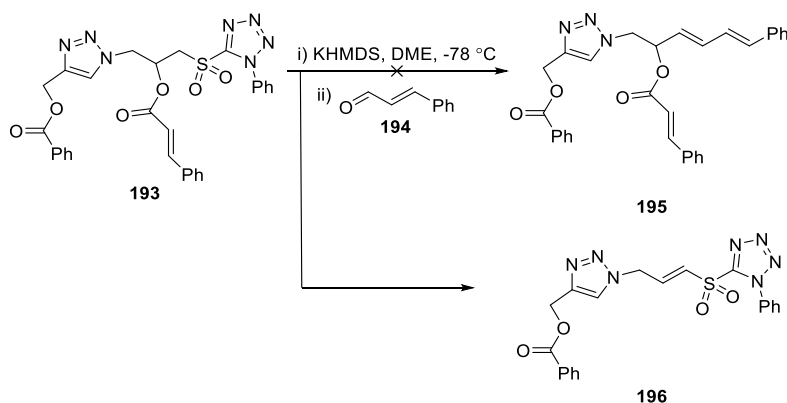
As shown in Scheme 2.1, the *E,Z*-dienoate motif could be formed *via* a base-induced ring opening of δ -valerolactone (Fragment **III**), a methodology well-established in Cumming's synthesis of the triazole analogue **182** (See Scheme 2.2 for a representative example).¹³⁵ The conjugated aldehyde (Fragment **II**) could be attached to the macrocyclic core through a Julia-Kocienski olefination reaction. The thiazole ring could be prepared

by a recently developed gold-catalysed coupling reaction between the terminal alkyne (Fragment **I**) and the primary thioamide (Fragment **IV**).¹⁴¹



Scheme 2.2 Example of preparation of *E,Z*-dienoic acid *via* base-induced ring opening of α,β -unsaturated δ -lactone.¹³⁵

These four fragments (**I**, **II**, **III**, **IV**) may be coupled in different orders to synthesise the thiazole analogue **183**, and a coupling route that could minimise the occurrence of side reactions was sought. Julia-Kocienski reaction requires a strong base (*e.g.*, KHMDS), which means that the esterification step to attach the *E,Z*-dienoate surrogate (Fragment **III**) onto **190** should be performed later than the olefination step. Given that the formation of alkene product **196** was observed by Cumming in the reaction between **193** and cinnamaldehyde **194** (Scheme 2.3),¹³⁵ the macrolactonisation reaction should be performed after side chain attachment to avoid potential degradation resulting from β -elimination of the lactone functional group.

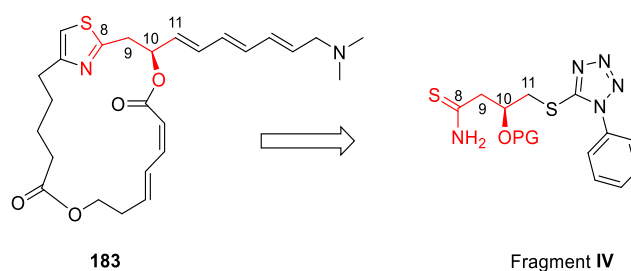


Scheme 2.3 Cumming's attempted Julia-Kocienski reaction with acyclic model substrate **193**.¹³⁵

As gold-alkene complexes have been extensively studied in the area of organometallic chemistry,¹⁴⁴ presuming that the coordination between the gold-centred catalyst required for the thiazole formation and the multiple alkenes in fragment **II** might lead to

undesirable side reactions, the coupling of fragment **I** and fragment **IV** should be carried out before Julia-Kocienski olefination. Finally, we envisioned the terminal tertiary amine group in the side chain could be generated from the reductive amination of an aldehyde intermediate in the final step using a mild boron reductant (*e.g.*, tetramethylammonium triacetoxyborohydride). Hence, we planned to accomplish the construction of the 2,4-disubstituted thiazole **190** in the first place. Preparation of fragments **IV**, **I** and, thiazole **190** will be first discussed in the following sections.

2.2 Synthesis of C8-C11 Thioamide (Fragment IV)



The C8 – C11 fragment **IV** is a central linker involved in three attachment points to the proposed macrocycle analogue **183**: at the thiazole core, the *E*, *Z*-dienoate and the conjugated side chain. Accordingly, it requires three functional groups, a thioamide, an alcohol, and a thioether that is readily oxidised to form a sulfone, on a four-carbon molecule, making it a densely functionalised compound.

2.2.1 Introduction

In general, thioamides are more reactive than their corresponding amides, and the sulfur atom in the C=S group can act as an electrophile and a nucleophile because the sulfur atom and the carbon atom in thioamides have more similar electronegativities.¹⁴⁵ The nitrogen atom in primary and secondary thioamides can also react with electrophiles (*e.g.*, carbonyls).¹⁴⁶ Therefore, thioamides have been increasingly recognised as valuable intermediates in the synthesis of a variety of functional groups¹⁴⁷ and used as organosulfur ligands in transition metal-catalysed functionalisation to perform a range of reactions, including C-H activation,¹⁴⁸ Suzuki-Miyaura coupling,¹⁴⁹ and ruthenium catalysed hydrogenation.¹⁵⁰

A range of different methods has been reported to prepare primary thioamides,¹⁵¹ which can be classified based on substrates. The first method, which has been called the

Willgerodt-Kindler reaction,¹⁵² makes use of the direct incorporation of elemental sulfur to a combination of ketones and amines at high reaction temperatures (Figure 2.1a). Although various methods and variants (*e.g.*, using sulfated polyborate¹⁵³ or ferrous chloride¹⁵⁴ as a catalyst) have been developed to allow for lower reaction temperatures, most of those conditions proceed well for aromatic ketone substrates but are highly problematic for the preparation of aliphatic thioamides. The second strategy employs thiohydrolysis of the corresponding nitriles to give primary thioamides (Figure 2.1b). Compounds bearing P=S bonds, such as Lawesson's reagent **198** in combination with a Lewis acid, diphenylphosphinodithioic acid, ammonium phosphorodithioate, and alkali metal hydrogen sulfides or ammonium sulfide, are widely utilised in this type of reaction instead of elemental sulfur. In most cases, aromatic and aliphatic primary thioamides are obtained in reasonable yields.¹⁵⁵ The third method is the exchange of the oxygen of amides for the sulfur atom of thioamides (Figure 2.1c). It is this third method that has attracted the most attention of the approaches to thioamide formation. A wide range of agents bearing P=S compounds has been developed, such as Berzelius reagent (P₄S₁₀) **197**,¹⁵⁶ Davy's reagent¹⁵⁷ and Lawesson's reagent **198**,¹⁵⁸ and these have been extensively used in this one-step transformation of amides to thioamides.

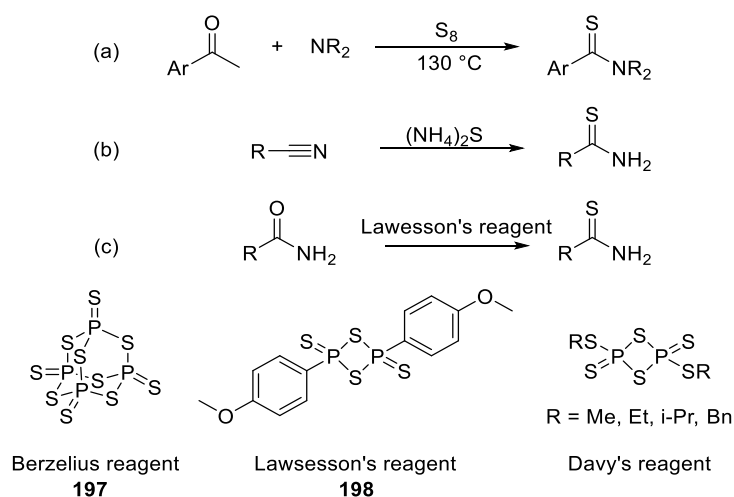
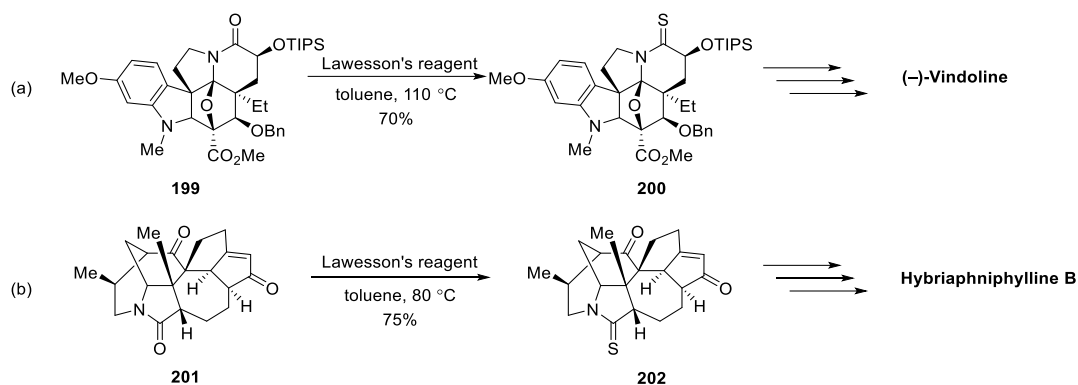


Figure 2.1 Examples of thioamide preparation using (a) ketones, (b) nitriles and (c) amides, and structures of Berzelius reagent **197**, Lawesson's reagent **198** and Davy's reagent.

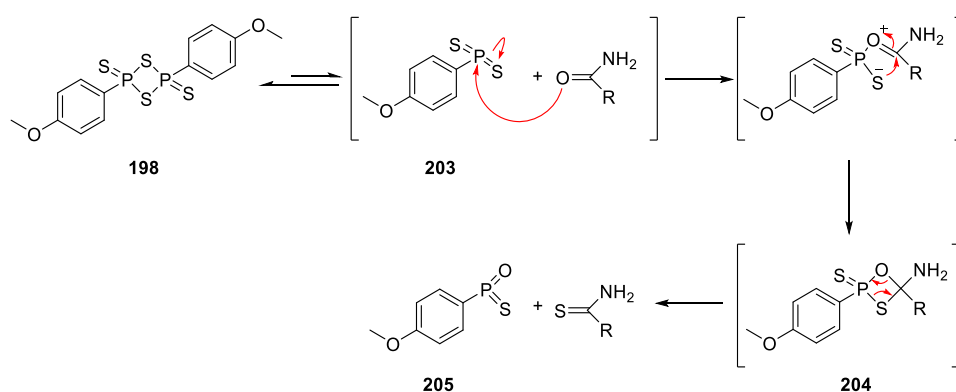
One of the most frequently used agents is Lawesson's reagent **198**. Because of its commercial availability, mild reaction temperature, excellent functional group compatibility, and high efficiency and chemoselectivity, it has been widely applied in

syntheses of complex natural products and biologically active molecules. Two representative examples demonstrating its excellent functional group selectivity and tolerance are shown in Scheme 2.4.^{159, 160}



Scheme 2.4 Thionation using Lawesson's reagent in the total synthesis of (a) (-)-vindoline¹⁵⁹ and (b) hybriaphniphylline B.¹⁶⁰

Lawesson's reagent **198** breaks down in an equilibrium process to the more active dithiophosphine **203**, which reacts with primary amides to form a four-membered cyclic oxathiaphosphetane intermediate **204** (Scheme 2.5). Subsequent retro [2+2] cycloaddition liberates the thioxophosphine oxide **205** to provide the primary thioamide.^{161, 162} Thermodynamically, the P=O bond is more stable than the P=S bond. This could be the most important driving force for the decomposition of the four-membered intermediate **204**.¹⁶³



Scheme 2.5 Proposed reaction mechanism for thioamide formation with Lawesson's reagent.

With regards to the formation of the thioamide fragment **IV**, the second and third methods were chosen for exploration because both of them are appropriate for aliphatic primary

thioamide synthesis. Since nitriles could be easily hydrated to provide amides,¹⁶⁴ nitrile **206** could serve as an intermediate for both strategies (Figure 2.2).

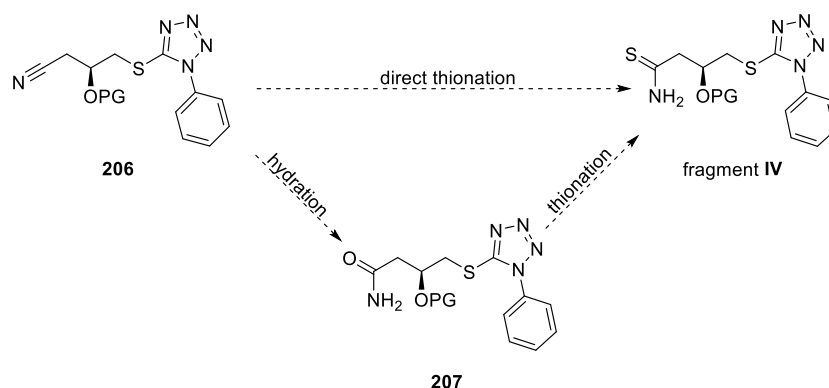


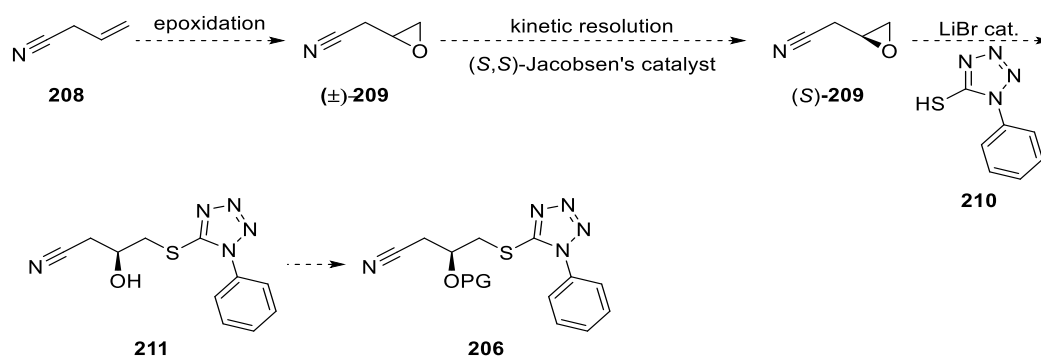
Figure 2.2 Two possible pathways to synthesise thioamide fragment **IV** from nitrile **206**.

The following section describes the synthesis of the thioamide fragment **IV** utilising these two methods.

2.2.2 Initial Attempts Towards Synthesis of Nitrile **206**

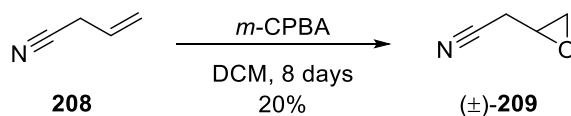
A literature search[†] suggested that the opening of epoxide (*S*)-**209** (Scheme 2.6) with 1-phenyl-1*H*-tetrazole-5-thiol **210** as the nucleophile by using catalytic lithium bromide¹⁶⁵ or Montmorillonite¹⁶⁶ can provide the desired difunctional compound **211**. Hydrolytic kinetic resolution of terminal epoxides using Jacobsen's catalyst has been demonstrated to be an efficient methodology to produce optically pure epoxides with a wide range of functional groups.^{167, 168} Therefore, we envisioned that 3-butenenitrile **208** could serve as an appealing starting material for the desired nitrile intermediate **211** (Scheme 2.6).

[†]Using *SciFinder* database; <https://scifinder.cas.org> (accessed December 2015)



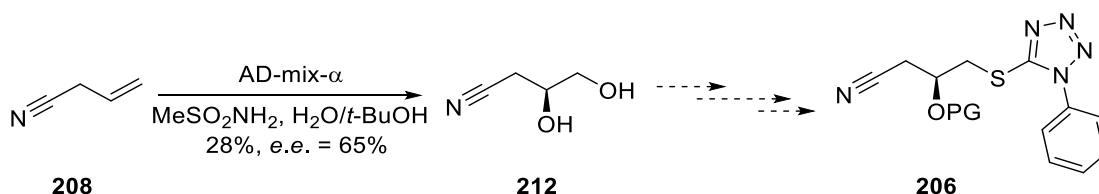
Scheme 2.6 Proposed synthetic route starting from 3-butenitrile **208**.

The synthesis of epoxide **(±)-209** by epoxidation of nitrile **208** had been reported with variable yields from 61% to 77% although the reaction requires a rather long reaction time (variable from two to fourteen days).¹⁶⁹⁻¹⁷¹ Unfortunately, in our hands, the epoxidation was found to be sluggish; and it had not gone to completion with the continuous addition of excess oxidant over eight days (Scheme 2.7). Not surprisingly, the isolated yield after silica gel chromatography purification was only 20%.



Scheme 2.7 Preparation of epoxide **(±)-209**.

Alongside this work, postdoctoral research fellow Claire Cuyamendous in our research group also trialled Sharpless asymmetric dihydroxylation of nitrile **208** to synthesise chiral diol **212**, which could also be an appealing precursor. However, the enantiomeric excess (*e.e.*) of obtained diol **212** was determined to be unsatisfactory by Mosher ester analysis (Scheme 2.8).¹⁷²

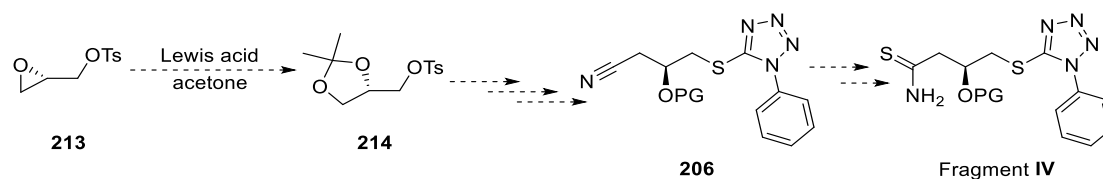


Scheme 2.8 Cuyamendous' preparation of diol **212**.

This inability to effectively synthesise epoxide **(±)-209** and optically pure diol **212** prompted us to adopt a chiral pool strategy, a classic synthetic strategy starting from

readily available enantiopure substances that allows efficient enantioselective synthesis.

The direct transformation of terminal epoxides into 1,3-dioxolanes, which are well-known precursors for 1,2-diols and could be further converted into a wide range of multifunctional molecules, has been demonstrated using a wide range of Lewis acid catalysts. Accordingly, we envisioned (*S*)-epoxide **213**, a readily available enantiopure compound, could be a convenient point of departure (Scheme 2.9).

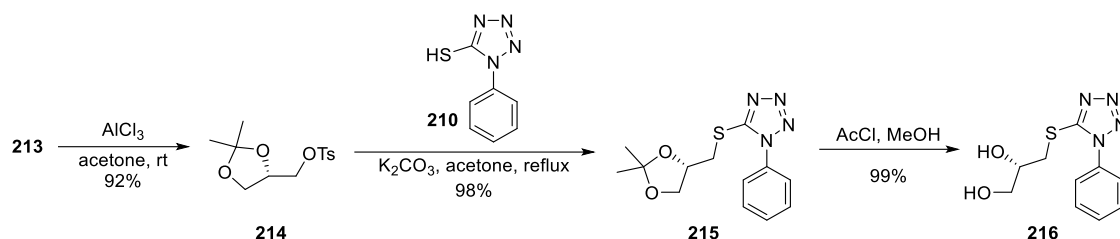


Scheme 2.9 Proposed synthetic route starting from enantiopure epoxide **213**.

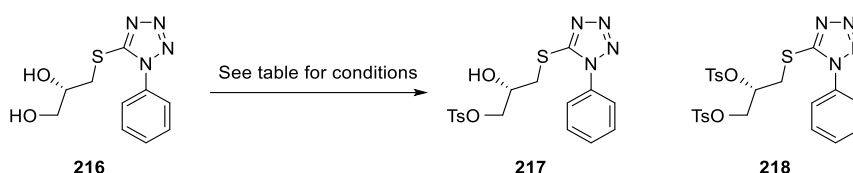
2.2.3 Preparation of Thioamide Fragment IV

2.2.3.1 Preparation of Alcohol **217**

Direct transformation of the enantiopure (*S*)-epoxide **213** into acetonide **214** with acetone as the nucleophile, in the presence of several reported Lewis acid catalyst such as $\text{BF}_3 \cdot \text{Et}_2\text{O}$,¹⁷³ FeCl_3 ,¹⁷⁴ and AlCl_3 ,¹⁷⁵ was explored (Scheme 2.10). In this work, AlCl_3 was found to be the optimal catalyst to provide reproducible excellent yield for both small-scale (*e.g.*, 0.1 gram) and large-scale (*e.g.*, 10 grams) reactions. As acid-catalysed attack on an epoxide by acetone has been reported to result in partial or complete racemisation at the chiral carbon centre, the enantiomeric purity of the acetonide **214** was determined by Mosher ester analysis of compound **217**, the product of a later step in the synthesis,¹⁷⁶ and the stereochemical integrity was mostly preserved relative to the starting material **213**. (see section 2.2.3.2 for details). Substitution of tosylate **214** by 1-phenyl-1*H*-tetrazole-5-thiol **210**, followed by deprotection with acetyl chloride in methanol, provided diol **216** in nearly quantitative yield in three steps.

Scheme 2.10 Synthesis of diol **216**.

Attempted selective tosylation of the primary alcohol in the diol **216** using triethylamine (TEA) and tosyl chloride resulted in a mixture of mono-tosylate **217** and *bis*-tosylate **218**,[‡] as determined by ¹H NMR analysis of isolated products by silica gel chromatoghy (Table 2.1, entry 1). When catalytic dibutyl tin (IV) oxide (Bu₂SnO) was used to promote the selectivity (as reported by Martinelli and co-workers),¹⁷⁷ the mono-tosylate **217** was obtained as the sole product in excellent yield (entry 2).



Entry	Conditions (equiv.) ^a	Ratio ^b 217 : 218	Yield ^c (%)
1	TsCl (1.0), Et ₃ N (1.0), DCM, 0 °C	2:1	31%
2	TsCl (1.0), Et ₃ N (1.0), Bu ₂ SnO (0.2), DCM, rt	1:0	93%

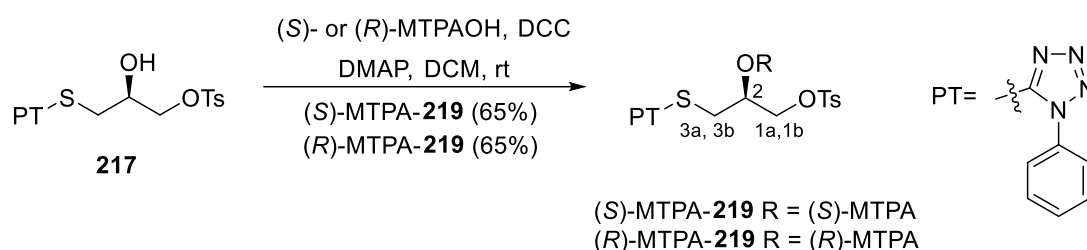
^art = room temperature. ^bDetermined by ¹H NMR spectroscopy on reaction product mixture. ^cIsolated yield of **217** after purification by silica chromatography.

Table 2.1 Reaction screening for selective tosylation of diol **216**.

[‡]Characterised using 1D ¹H NMR spectroscopy, with peaks at (500 MHz, CDCl₃) δ 7.80 – 7.75 (m, 2H), 7.72 – 7.66 (m, 2H), 7.61 – 7.55 (m, 3H), 7.50 – 7.45 (m, 2H), 7.37 (d, *J* = 8.0 Hz, 2H), 7.23 – 7.18 (m, 2H), 5.20 – 5.11 (m, 1H), 4.30 (d, *J* = 3.5 Hz, 2H), 3.62 (dd, *J* = 14.7, 4.5 Hz, 1H), 3.41 (dd, *J* = 14.7, 8.2 Hz, 1H), 2.47 (s, 3H), 2.32 (s, 3H).

2.2.3.2 Mosher Ester Analysis of Alcohol **217**

The enantiomeric purity of the secondary alcohol **217** was assayed by ^1H NMR spectroscopy following the modified Mosher's method.^{172, 178} The alcohol **217** was acylated with (*S*)-(+)- α -methoxy- α -trifluoromethylphenylacetic acid and (*R*)-(+)- α -methoxy- α -trifluoromethylphenylacetic acid to give Mosher ester (*S*)-MTPA-**219** and (*R*)-MTPA-**219**, respectively. As shown in Table 2.2, the stereochemistry of the major enantiomer of the secondary alcohol **217** was confirmed to be *S* configuration.



Proton	δ (<i>S</i>)-MTPA ester (ppm)	δ (<i>R</i>)-MTPA ester (ppm)	$\Delta \delta^{\text{SR}} = \delta_{\text{S}} - \delta_{\text{R}}$ (ppm)
1a	4.29	4.37	-0.08
1b	4.24	4.28	-0.04
2	5.51	5.64	-0.13
3a	3.80	3.72	0.08
3b	3.49	3.39	0.10

Table 2.2 Analysis of $\Delta \delta^{\text{SR}}$ data for diastereomeric MTPA ester derivatives of alcohol **217**.

However, the ^1H NMR spectrum of the (*S*)-MTPA-**219** obtained at 500 MHz showed a doublet of doublets centred at δ 3.80 with an integration of 1.00 and another doublet of doublets centred at δ 3.72 with an integration of 0.04 (see Figure 2.3), indicating that the enantiomeric excess of the alcohol had decreased to about 92%. Therefore, a small degree of racemisation has taken place, most likely in the direct transformation of the epoxide **213** into the acetonide **214**.

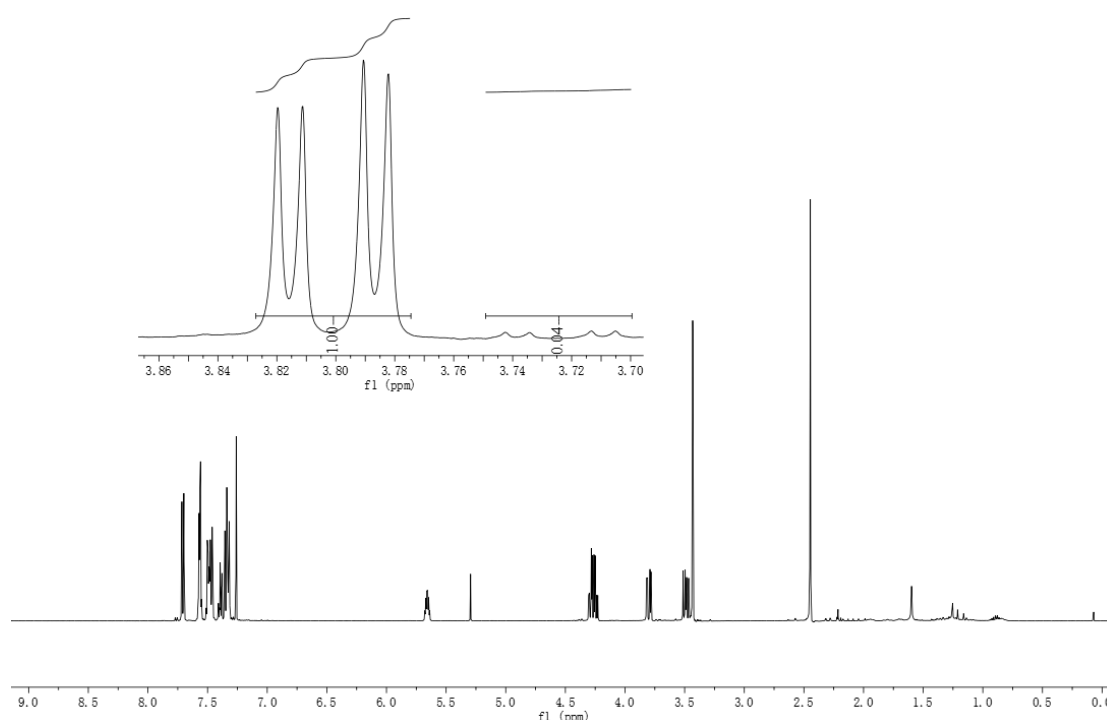
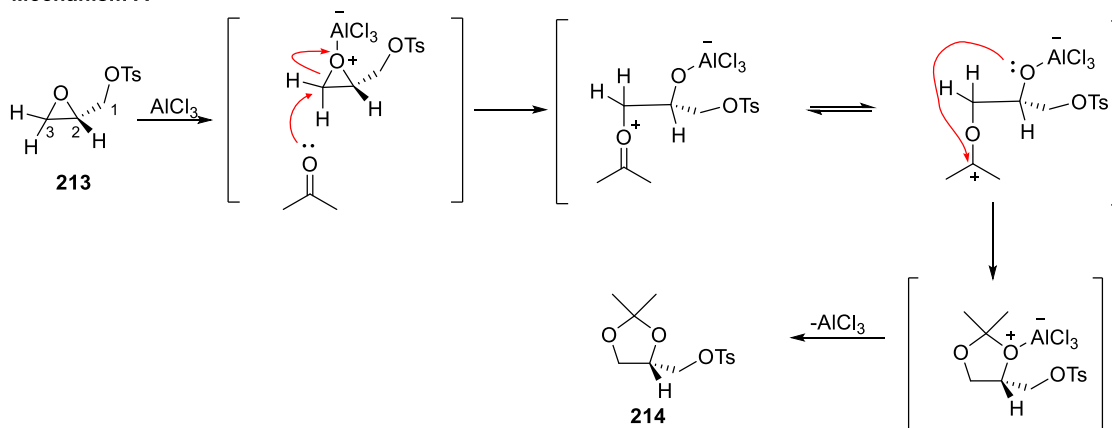
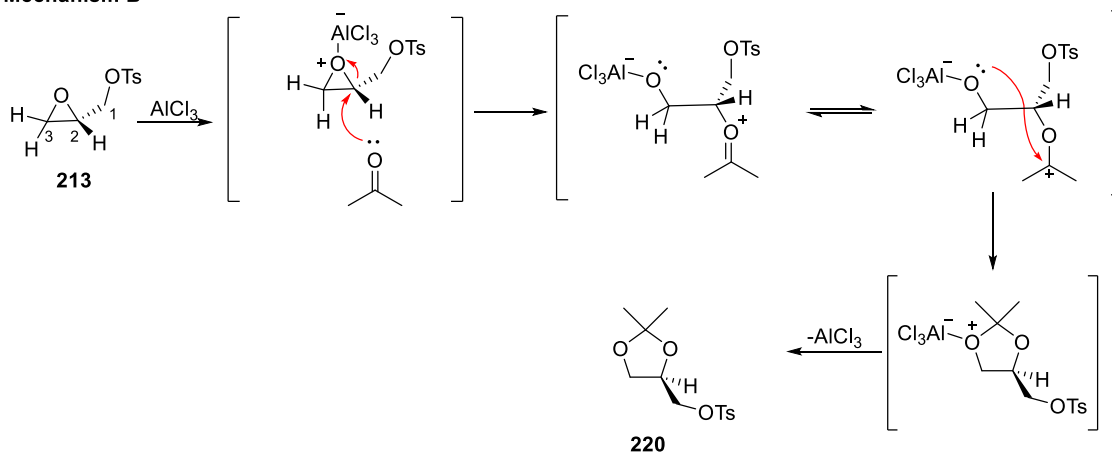


Figure 2.3 500 MHz ^1H NMR spectrum of (S)-MTPA-**219** and expansion of δ 3.70 – 3.86.

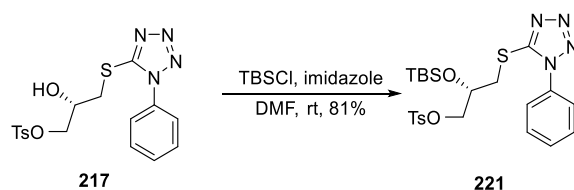
Presuming that opening of an epoxide by the carbonyl oxygen of a ketone goes *via* an $\text{S}_{\text{N}}2$ -like mechanism, a nucleophilic attack at either carbon of the epoxide could result in the different enantiomers. As shown in mechanism A (Scheme 2.11), after coordination of the epoxide oxygen to AlCl_3 , the activated oxirane could be opened by the carbonyl oxygen of acetone at C3, and the dioxolane ring would form in a two-step manner to give the product **214** with enantiomeric integrity relative to the starting material **213**. Alternatively, the selectively complexed epoxide could be attacked at the stereogenic C2 position with inversion of configuration to afford the oxiranium intermediate (mechanism B) and would give the enantiomeric product **220**. As the C3 position is more electron-deficient and less sterically hindered than the C2 position, the nucleophilic C3 opening should be mostly preferential to the other, which matches experimental observation.

Mechanism A**Mechanism B**

Scheme 2.11 Proposed mechanism for the observed partial racemisation in acetonide formation.

2.2.3.3 Preparation of Nitrile **222**

Although the enantiomeric fidelity of epoxide **213** was not completely preserved, *e.e.* of alcohol **217** (92%) was still acceptable. Thus, alcohol **217** was silylated using *tert*-butyldimethylsilyl chloride (TBSCl) to give compound **221** (Scheme 2.12).



Scheme 2.12 Preparation of silyl ether **221**.

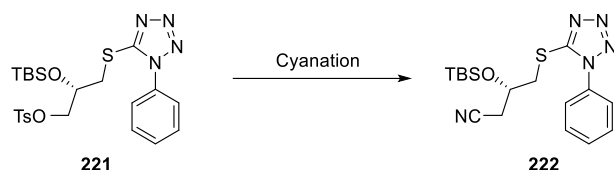
The subsequent substitution to form nitrile **222** was initially attempted by treatment with potassium cyanide at 90 °C (Table 2.3, entry 1). Although tosylate **221** was consumed

completely, nitrile **222** was obtained in poor yield, and a mixture of by-products was observed, one of which was revealed to be structurally related to phenyl tetrazole,[§] suggesting that phenyl tetrazole could possibly be cleaved by cyanide at high temperature. Lowering the reaction temperature to 60 °C did not reduce the formation of side products significantly, and it resulted in a mixture of nitrile **222** and tosylate **221** (entry 2), which was inseparable by silica gel chromatography, prompting the need to optimise reaction conditions to increase the conversion rate whilst minimising the side reactions. Assuming that the poor yield could be a result of potassium cyanide not being sufficiently homogeneous in the DMF solvent, we then trialled using phase transfer catalysts at different reaction temperatures (entries 3 – 7). Increasing the equivalents of 18-crown-6 catalyst (0.3 to 3 equiv., entries 3 – 5) and lowering temperature (60 °C to 40 °C, compare entries 3 & 4, and also entries 6 & 7) did improve the conversion rate, however, it did not suppress the side reactions significantly and the yield of nitrile **222** remained unsatisfying.

Given that the accessible cyanide sources were old legacy chemicals, it was plausible that the KOH impurity resulting from slow hydrolysis of KCN over long-term storage might be the cause of side reactions. Attention was then directed towards using LiCN prepared *in situ* by mixing acetone cyanohydrin and lithium hydride,¹⁷⁹ which could also help to reduce the risk of direct cyanide exposure. This protocol did reduce the formation of the side product to some extent; however, it also resulted in a lower conversion rate even after prolonged reaction time (entries 8, 9 and 10). Since hexamethylphosphoramide (HMPA) was reported to be able to increase the reactivity of different organolithium reagents through the coordination between its three nitrogen atoms and lithium cation,¹⁸⁰ we supposed that using HMPA as the co-solvent could increase the reactivity of LiCN. The conversion rate of compound **221** was indeed increased as expected (compare entries 8 and 11). Nonetheless, the attempt to enhance the conversion rate by raising reaction temperature resulted in poor yield (entry 12), which might be a consequence of increased cleaving of the phenyl tetrazole at the higher temperature. Presuming that the small amount of impurity (*e.g.*, LiOH) in the commercially available LiH from Sigma-Aldrich (purity 95%) could potentially play an important role in the side reaction, using a mixture of LiHMDS and acetone cyanohydrin as a surrogate of high quality of LiCN was trialled

[§]Characterised using 1D ¹H NMR with peaks at (500 MHz, CDCl₃) δ 8.99 (s, 1H), 7.75 – 7.69 (m, 2H), 7.63 – 7.57 (m, 2H), 7.57 – 7.52 (m, 1H).

at 70 °C. Gratifyingly, the yield was increased from 24% to 76% accompanied by the complete conversion of tosylate **221** (entry 13).



Entry	Cyanide (equiv.)	Catalyst (equiv.)	Solvent	T (°C)	Time ^c (hrs)	Ratio 222:221	Yield (%)
1	KCN (1.5)	-	DMF	90	o/n	1:0	7.0 ^d
2	KCN (1.5)	-	DMF	60	o/n	6:1	31 ^e
3	KCN (1.5)	18-crown-6 (0.3)	DMF	60	o/n	4:1	-
4	KCN (1.5)	18-crown-6 (0.3)	DMF	40	o/n	5:1	-
5	KCN (1.5)	18-crown-6 (3)	DMF	40	o/n	30:1	46 ^e
6	KCN (1.5)	TBAI (0.3)	DMF	60	o/n	7:1	45 ^e
7	KCN (1.5)	TBAI (0.3)	DMF	40	o/n	20:1	48 ^e
8^a	LiCN (4.4)	-	THF	70	o/n	1,1:1	-
9^a	LiCN (4.4)	-	THF	70	34	2.5:1	-
10^a	LiCN (4.4)	-	THF	70	72	3:1	-
11^a	LiCN (2.0)		HMPA/THF	rt	o/n	2:1	-
12^a	LiCN (2.0)	-	HMPA/THF	50	o/n	1:0	24 ^d
13^b	LiCN (2.0)		THF	70	o/n	1:0	76^d

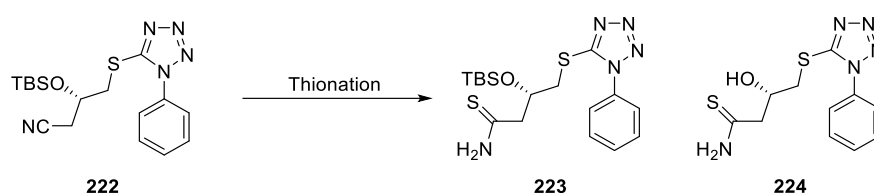
^aPrepared *in situ* by pre-mixed acetone cyanohydrin and LiH. ^bPrepared *in situ* by pre-mixed acetone cyanohydrin and LiHMDS. This result was obtained by research assistant Sarah Andreassend. ^crt = room temperature, o/n = overnight (i.e. 16 – 20 hours). ^dDetermined after purification by silica gel chromatography. ^eDetermined by ¹H NMR of an isolated mixture of **222** and **223** obtained by silica gel chromatography.

Table 2.3 Trialled conditions for the formation of nitrile **222**.

2.2.3.4 Preparation of Thioamide 223

With nitrile **222** in hand, in order to make our synthetic sequence more atom-efficient, we first attempted thiohydrolysis of nitrile **222** using ammonium sulfide and pyridine, conditions reported by Spsychala.¹⁸¹ A literature search suggested that chemical shifts of α -protons of thioamides are normally downfield relative to those of nitriles. As chemical shifts of α -protons of nitrile **222** are at 2.71 ppm, the α -proton signals of desired thioamide **223** should move downfield. Unfortunately, no desired thionation product **223** was observed by ¹H NMR analysis of the crude material after work-up, and instead, a mixture of unidentified products was obtained (Table 2.4, entry 1). Following the conditions

optimised by Schmid and co-workers,¹⁸² thiohydrolysis of nitrile **222** was then attempted with a combination of Lawesson's reagent and $\text{BF}_3 \cdot \text{Et}_2\text{O}$. ^1H NMR analysis of the crude material after work-up showed that the proton signals at 2.71 ppm disappeared completely while two new doublet of doublets peaks appeared at 3.09 and 2.98 ppm, respectively, suggesting that the conversion might be successful. However, the isolated product was proved to be unexpected desilylated thioamide **224**.** (Table 2.4, entry 2). In the absence of success in the one-step preparation of the thioamide **223** from nitrile **222**, we decided to move onto the alternative method comprising thionation of amides to prepare the desired thioamide.



Entry	Conditions (equiv.) ^a	Result ^b
1	$(\text{NH}_4)_2\text{S}$ (5.0), pyridine, H_2O , rt	A mixture of unidentified products
2	Lawesson's reagent (1.5), $\text{BF}_3 \cdot \text{Et}_2\text{O}$ (2.4), toluene-diethyl ether, 50 °C	224 57% yield

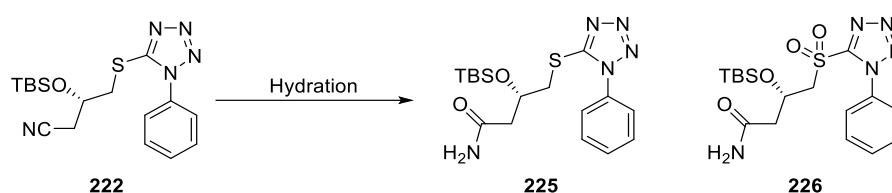
^art = room temperature. ^bIsolated yield after purification by silica chromatography.

Table 2.4 Trialled conditions for one-step conversion of nitrile **222** to thiamide **223**.

A well-known procedure for amide preparation involves treating nitriles with alkaline solutions of hydrogen peroxide.¹⁸³ Thus, nitrile **222** was treated with a solution of hydrogen peroxide and potassium carbonate in ethanol (Table 2.5, entry 1), with the hope that excess hydrogen peroxide would oxidise the sulfur atom to afford sulfone **226** simultaneously. This would be expedient, given the requirements of the intended Julia-Kocienski reaction later in the sequence. Interestingly, only amide **225** accompanied by a tiny amount of inseparable sulfone **226** was obtained. Considering that amide **225** was

**This was characterised by 1D ^1H NMR through observing the disappearance of peaks corresponding to the TBS group: at (500 MHz, CDCl_3) δ 8.12 (br. s, 1H), 7.72 (br. s, 1H), 7.61 – 7.54 (m, 5H), 4.52 (ddt, J = 8.0, 6.9, 3.5 Hz, 1H), 3.63 (dd, J = 14.3, 3.9 Hz, 1H), 3.51 (dd, J = 14.2, 6.8 Hz, 1H), 3.09 (dd, J = 15.0, 3.1 Hz, 1H), 2.98 (dd, J = 15.0, 8.3 Hz, 1H).

very polar based on observation by TLC analysis, it was plausible that the low yield was a consequence of significant material loss in the aqueous work-up procedure. Therefore, to circumvent this material recovery problem, the hydration of nitrile **222** using acetaldoxime (freshly prepared from hydroxylamine hydrochloride and sodium hydroxide, see Section 6.2.1 for experimental details) as the source of water was performed following mild conditions reported by Lee and co-workers.¹⁸⁴ Upon completion, the solvent toluene was evaporated and the resulting crude product was directly purified by silica gel chromatography to provide amide **225** in good yield (entry 2).



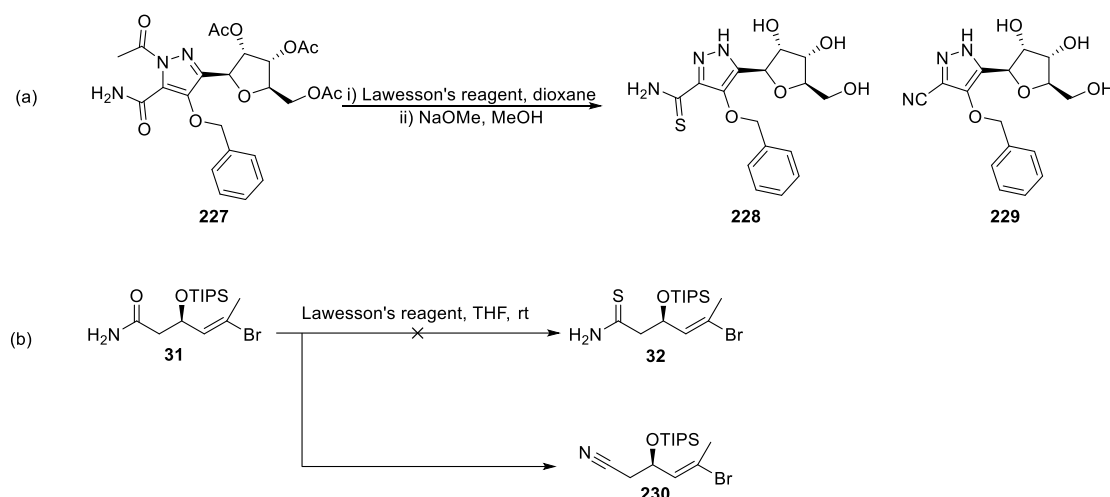
Entry	Conditions (equiv.) ^a	Result
1^b	H ₂ O ₂ (15), K ₂ CO ₃ (5.0), ethanol, 0 °C to rt	225 26% yield
2^c	Acetaldoxime (15), RhCl(PPh ₃) ₃ , toluene, 110 °C	225 88% yield

^art = room temperature. ^bYield based on the calculation of an inseparable mixture of **225** and **226** after purification by silica chromatography. The ratio of **225** and **226** in the isolated mixture was determined to be 1:0.03 based on the ¹H NMR spectrum. ^cIsolated yield after silica gel chromatography purification.

Table 2.5 Trialled conditions for hydration of nitrile **222**.

The thionation of amide **225** was first trialled with Lawesson's reagent under heating (Table 2.6, entry 1). ¹H NMR analysis of the crude material after work-up showed that the α-proton signals of amide **225** at 2.63 and 2.54 ppm disappeared completely while two new strongly downfield doublet of doublets peaks appeared at 3.67 and 3.49 ppm, indicating that the conversion of amide to thioamide should proceed well. However, thioamide **223** was obtained in only modest yield (23%). In addition to it, the by-product nitrile **222** resulting from dehydration of amide **225** was also observed. A similar dehydration process has been reported by Robins and co-workers in their synthesis of nucleoside derivatives,¹⁸⁵ where a mixture of thioamide **228** and nitrile **229** was obtained from the thionation reaction of amide **227** (Scheme 2.13a). Romo's research group also experienced the exclusive formation of nitrile product **230** resulting from dehydration in

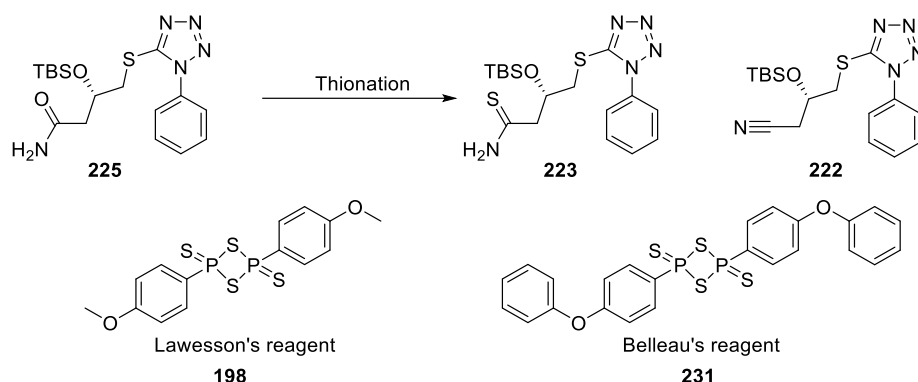
their attempt to synthesise thioamide intermediate **32** for Hantzsch thiazole formation in their PatA synthesis (Scheme 2.13b).⁸⁴ It was then later discovered that using Belleau's reagent **231** instead of Lawesson's reagent **198** could significantly reduce the formation of nitrile **230** and the desired thioamide **32** was obtained in high yield (*vide supra*, Scheme 1.1 in Section 1.4.1.1).^{82, 84}



Scheme 2.13 Dehydration caused by the use of Lawesson's reagent reported by (a) Robins¹⁸⁵ and (b) Romo.⁸⁴

Therefore, Belleau's reagent **231** was prepared from diphenyl ether following Belleau and co-workers' original procedure¹⁸⁶ and then tested. Although using Belleau's reagent **231** provided thioamide **223** as the sole product, the rate of the reaction decreased drastically (entry 2). Following Charette and Grenon's mild thionating conditions,¹⁸⁷ a combination of ammonium sulfide, Tf₂O, and pyridine was also trialled, which gave no desired product but instead a mixture of unidentified products (entry 3). A comprehensive investigation revealed that Lawesson's reagent could decompose under heating due to polymerisation,¹⁸⁸ which might be the cause of the low yield in entry 1, therefore, we then decided to go back to test Lawesson's reagent at a lower reaction temperature. It is also worth noting that the typical impurity in the commercial Lawesson's reagent is P₄S₁₀ (**197**), which has been utilised as a dehydrating reagent.¹⁸⁹ Assuming that the P₄S₁₀ impurity in the excess Lawesson's reagent could be the stimulus for the side reaction, we decided to reduce the equivalents of Lawesson's reagent to 0.54 equivalent and lower the reaction temperature to room temperature to suppress the dehydration (entry 4). This practice did reduce the formation of nitrile **222** and the yield was improved as well, prompting us to move forward to purify the reagent. Following the purification procedure

in the original preparation reported by Lawesson and co-workers,¹⁹⁰ the Lawesson's reagent purchased from suppliers was washed with anhydrous Et₂O and anhydrous DCM, and then recrystallised from boiling anhydrous toluene. Gratifyingly, when purified Lawesson's reagent was used, full conversion of amide **225** was observed within 30 minutes, and thioamide **223** was obtained in 62% with a small amount of nitrile product **222** on both small-scale (entry 5) and gram-scale (entry 6) reactions, which were judged to be the optimal results.

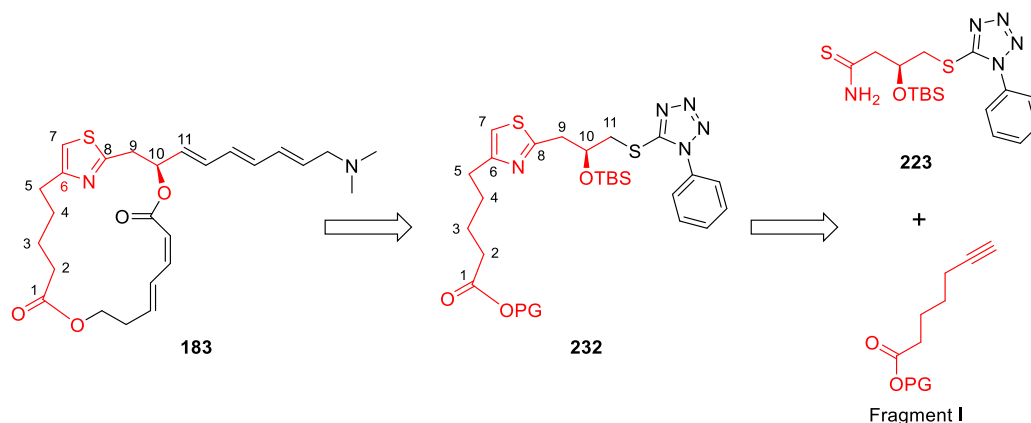


Entry	Reagent (equiv.)	Solvent	T (°C) ^a	Time (h)	Conversion (%)	Ratio ^b 223:222	Yield ^c (%)
1	198 (3.0)	THF	60	0.5	100	1.8:1	23
2	231 (0.7)	THF	rt	48	69	1:0	21
3	(NH ₄) ₂ S (1.5), Tf ₂ O (1.2), pyridine (3.0)	DCM	-40 to rt	2	100	-	0
4	198 (0.54)	THF	rt	48	66	5.6:1	39
5^d	198^f (0.7)	THF	rt	0.5	100	3.8:1	62
6^e	198^f (0.7)	THF	rt	0.5	100	4.4:1	62

^art = room temperature. ^bRatio based on the calculation of isolated thioamide **223** and nitrile **222** after purification by silica chromatography. ^cIsolated yield of **223**. ^dReaction carried out on 50 milligrams. ^eReaction carried out on 3 grams. ^fReaction carried out using purified Lawesson's reagent.

Table 2.6 Reaction screening for thionation of amide **225**.

2.3 Synthesis of Thiazole Fragment 232



2.3.1 Introduction

Thiazoles are heterocyclic compounds possessing sites for both electrophilic substitution and nucleophilic substitution, meaning that they are able to provide ligand points for multiple types of bioreceptors.¹⁹¹ Hence, thiazoles are considered to be privileged scaffolds in drug discovery and a significant amount of drugs containing thiazole subunits are currently on the market or in clinical trials.¹⁹² Recent studies have revealed that substituents at position-2 and position-4 of a thiazole ring could significantly affect its molecular electrostatic potential surface, which plays a critical role in interactions between drugs and protein targets.¹⁹³ Therefore, the 2,4-disubstituted thiazole motif has been considered to be an important pharmacophore in various active synthetic and natural products.¹⁹⁴ Natural products containing 2,4-disubstituted thiazole subunits (see Figure 2.4 for some examples) have been reported to exhibit remarkably diverse biological activities, such as anticancer, antibacterial, antifungal, anti-inflammatory, anthelmintic and antihypertensive activities.¹⁹⁵

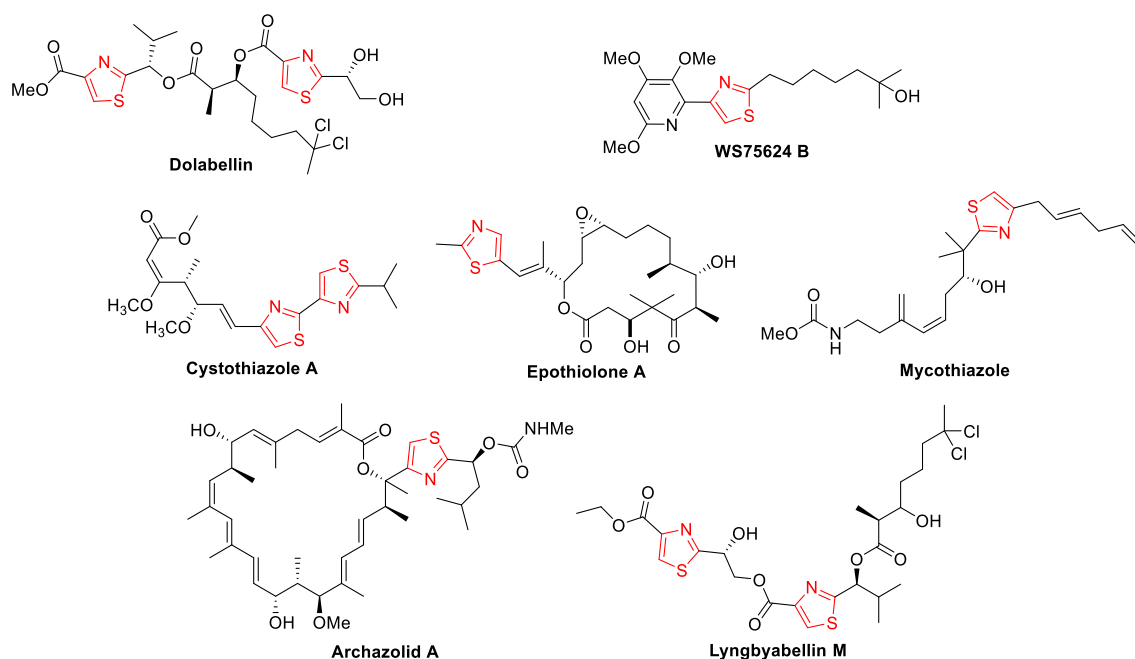
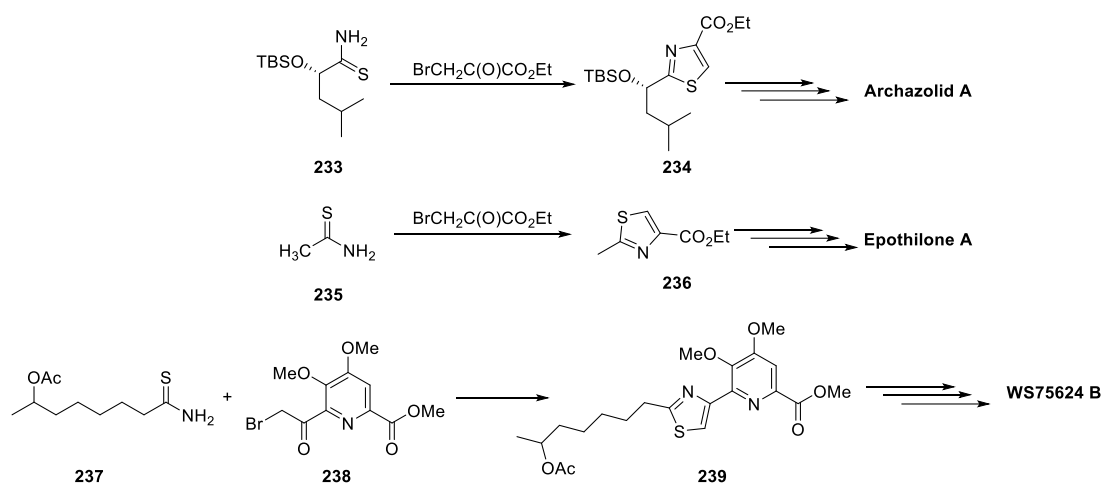


Figure 2.4 Examples of natural products containing 2,4-disubstituted thiazoles.

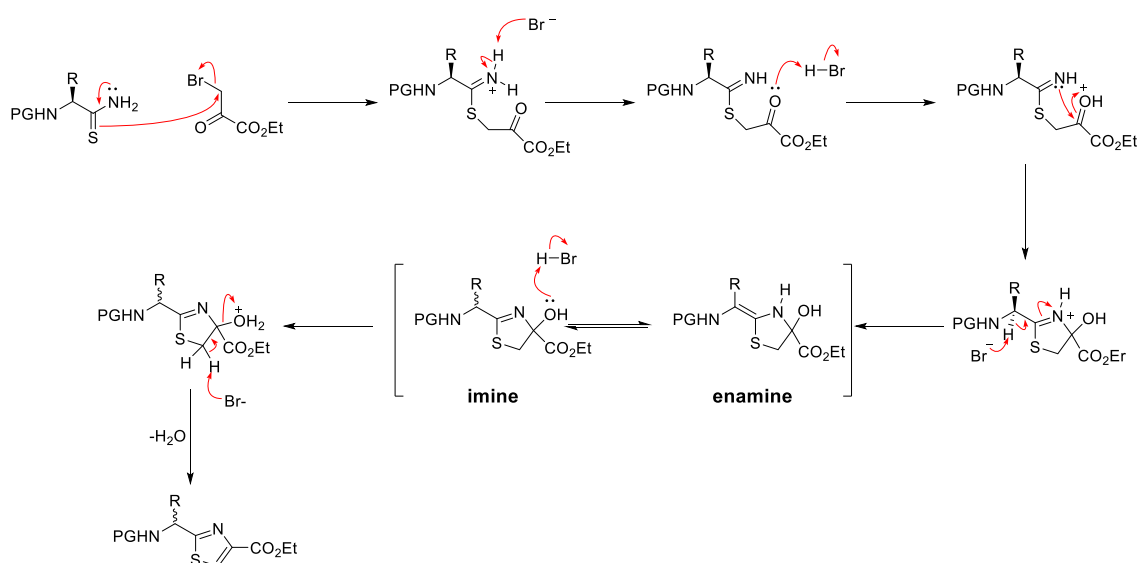
Given that compounds containing 2,4-disubstituted thiazoles display a wide range of pharmacological activities, this motif has attracted many synthetic endeavours. A range of synthetic methodologies has been developed and they can be roughly classed as follows: (a) Hantzsch method and modifications involving condensation between primary thioamides and α -bromoketo esters; and (b) oxidation of thiazoline intermediates generated from condensation of vicinal amino thiols with various partners (*e.g.*, aldehydes, cyanides, carboxylic acids or esters); and (c) transition-metal-catalysed cross-coupling reactions between halo-substituted thiazoles and appropriate partners (*e.g.*, organoboron or organotin species).

The Hantzsch method has been used widely in the synthesis of organic molecules containing a 2,4-disubstituted thiazole,¹⁹⁶ such as archazolid A,¹⁹⁷ epothilone A¹⁹⁸ and WS75624B¹⁹⁹ (Scheme 2.14).



Scheme 2.14 Examples of application of the Hantzsch method in the total synthesis of natural products.

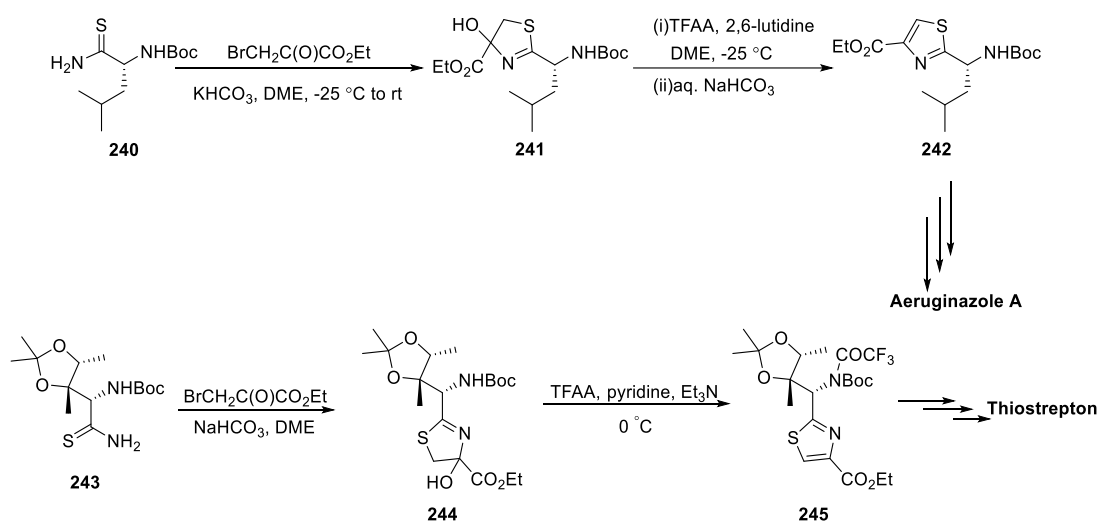
However, as shown in Scheme 2.15, the typical Hantzsch reaction concomitantly forms one equivalent of hydrogen bromide, which can cause significant loss of optical purity in substrates prone to racemisation *via* the formation of enamine intermediates.²⁰⁰



Scheme 2.15 Proposed mechanism of racemisation occurring in Hantzsch thiazole formation.

To overcome this racemisation problem and improve the suitability for chiral thiazole synthesis, a modified protocol using a two-step procedure, called the Holzapfel-Meyers-Nicolaou modification,^{113, 201, 202} has been developed. The first step of this modified method is the reaction between a thioamide and an α -bromoketo ester in the presence of

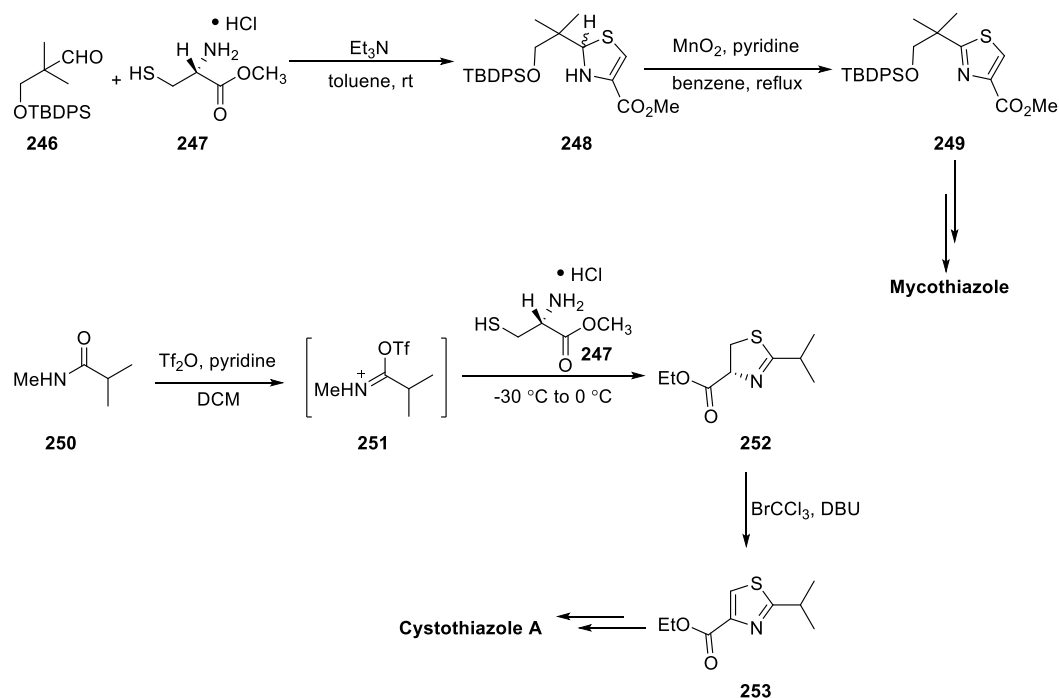
a mild base (*e.g.*, KHCO_3 or NaHCO_3) as the acid scavenger to form a hydroxythiazoline intermediate. The second step is the activation of this intermediate by the addition of reagents (*e.g.*, TFAA) to facilitate the necessary elimination. This method has been applied in the preparation of chiral thiazole building blocks with complete stereocontrol in the synthesis of natural products and their analogues (see Scheme 2.16 for examples). In the total synthesis of aeruginazole A, the cyclocondensation of thioamide **240** and ethyl bromopyruvate provided hydroxythiazoline intermediate **241**, which was then treated by TFAA and 2,6-lutidine, following Meyers' conditions, to furnish thiazole building block **242**.²⁰³ Under similar conditions, in the synthesis of thiostrepton, a combination of TFAA, pyridine, and triethylamine, instead of 2,6-lutidine, was used to promote the elimination step of hydroxythioazoline **244** and thiazole **245** was obtained in optically pure form.²⁰⁴



Scheme 2.16 Examples of application of Holzapfel-Meyers-Nicolaou modified method in the total synthesis of natural products.

Another method for the preparation of 2,4-disubstituted thiazoles is oxidation of the corresponding thiazoline precursors. From the biosynthetic point of view, thiazole moieties in natural products are derived from cysteine-containing peptides.²⁰⁵ Therefore, cysteine and its derivatives are often used as vicinal amino thiol agents to provide 2,4-disubstituted thiazoline intermediates *via* condensation with suitable partners. Since the sulfur atoms of thiazolines are prone to oxidation by strong oxidants to afford undesired products, *e.g.*, sulfones, sulfinic acids or sulfonic acids, only a few mild oxidation conditions, such as manganese dioxide and a combination of bromotrichloromethane and DBU, have been proven to be useful in this transformation of thiazolines into thiazoles.²⁰⁶

Similarly, racemisation could also occur in the formation of thiazolines when substrates prone to epimerisation are exposed to strong basic or acidic conditions,^{207, 208} which remains a major challenge for the stereocontrolled synthesis of 2,4-disubstituted thiazoles through this method. As shown in Scheme 2.17, this approach was utilised effectively in the synthesis of mycothiazole²⁰⁹ and cystothiazole A (Scheme 2.17).²¹⁰



Scheme 2.17 Examples of thiazole formation *via* oxidation of thiazoline.

These two methods mentioned above have several disadvantages: (1) limited substrate scope; for example, Hantzsch and its modified methods require using α -bromoketo esters as starting materials and they are normally prepared by bromination, which can cause serious environmental pollution; (2) time-loss and yield-loss associated with the isolation and purification of thiazoline intermediates in two-step sequences; and (3) potential risk of racemisation when chiral substrates are used. In order to overcome these disadvantages, a range of metal-catalysed methodologies to form 2,4-disubstituted thiazoles has been reported, such as copper-catalysed condensation from oximes, anhydrides and potassium thiocyanate,²¹¹ and iron-catalysed condensation from azides and potassium thiocyanate.²¹² Among all these studies, a novel gold-catalysed methodology for 2,4-disubstituted thiazole formation *via* coupling between terminal alkynes and primary thioamides appeared attractive because of its versatility and good tolerance of a range of functional groups, such as chloroalkyl, silyl ether, alkene and cyclopropane.¹⁴¹

1,2,3-triazoles can be prepared from the well-known copper-catalysed 1,3-dipolar cycloaddition reactions between terminal alkynes and azides (Figure 2.5).^{142, 143} Oxazoles can be formed through gold-catalysed coupling reactions between terminal alkynes and amides.²¹³ Imidazoles can be constructed through rhodium-catalysed transannulation reactions between nitriles and *N*-sulfonyl 1,2,3-triazoles, which can be prepared from reactions between terminal alkynes and sulfonyl azides.²¹⁴ Therefore, a synthetic strategy for thiazole formation that relies on using terminal alkynes as building blocks enables the versatile generation of PatA heterocycle variants, such as oxazole and imidazole-containing analogues. Also, to the best of our knowledge, this methodology has not been utilised yet in the total synthesis of natural products or analogues related to natural products. Thus, our synthetic work assesses the feasibility of this approach to thiazoles from terminal alkynes with multiple functionalities, expands the reaction scope further with chiral substrates, and enhances the use of the gold catalyst in the total synthesis of structurally complex natural products.

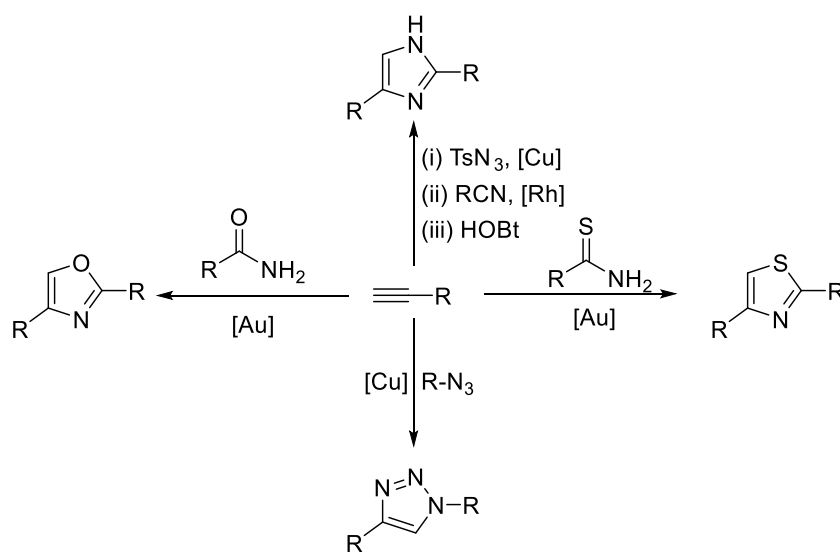


Figure 2.5 Representative of metal-catalysed preparations of thiazoles, oxazoles, imidazoles, and triazoles starting from terminal alkynes.

2.3.2 Synthesis of Thiazole Fragment 232 Using Gold Catalysis

2.3.2.1 Proposed Mechanism of Gold-catalysed Thiazole Formation

In 2012, Zhang and co-workers reported that α -oxo gold carbenes generated by oxidation of terminal alkynes were highly electrophilic and could even abstract halogen atoms from 1,2-dichloroethane or 1,2-dibromoethane to give α -chloro/bromo ketones.²¹⁵ As shown in Figure 2.6, it was later discovered that the electrophilicity of α -oxo gold carbenes (A) could be tempered through the formation of a tricoordinated gold intermediate (B/B'), achieved with an electron-rich *P,N*-bidentate ligand such as di(1-adamantyl)-2-morpholinophenylphosphine (Mol-DalPhos). This modulation of the electrophilicity allows chemoselective intermolecular trapping of gold carbenes by amides²¹³ or carboxylic acids²¹⁶ to form oxazoles or esters.

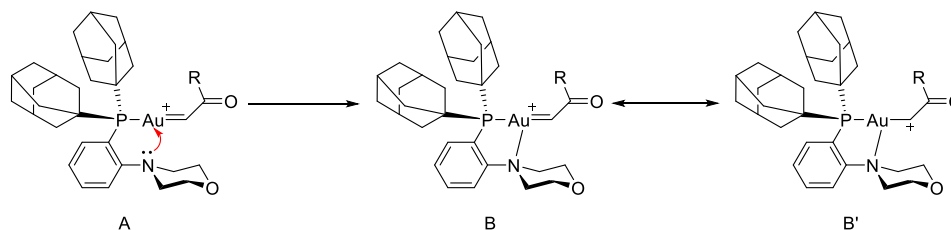
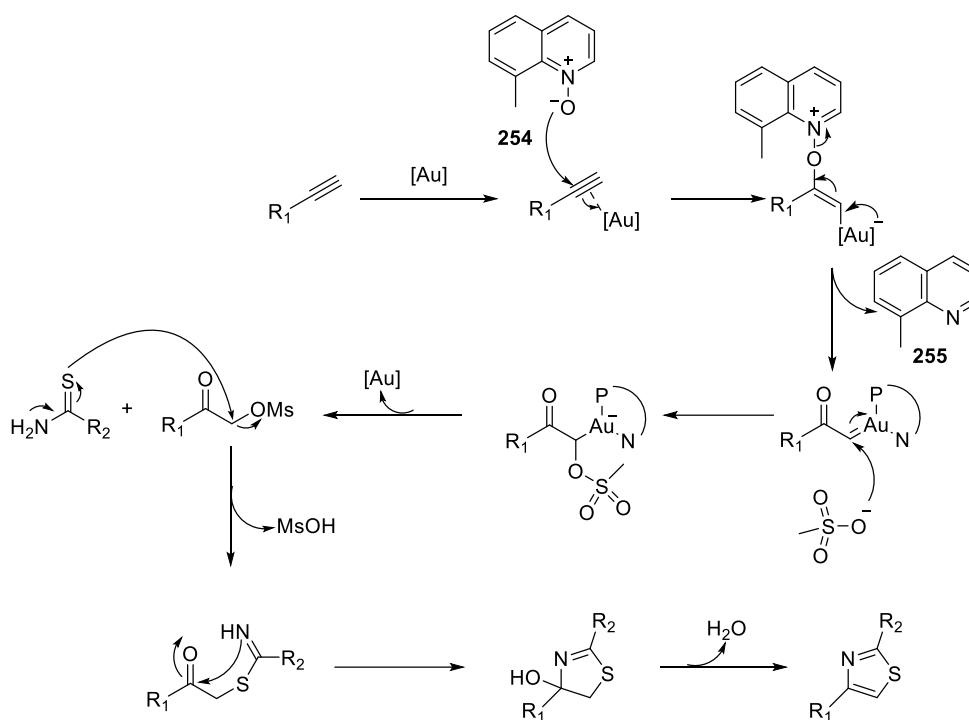


Figure 2.6 Proposed role of Mol-DalPhos in the stabilisation of the α -oxo gold carbene, as presented by Zhang.²¹³

Similarly, in the presence of Mol-DalPhosAuOMs, the tricoordinated gold carbene generated *via* intermolecular oxidation of terminal alkynes by 8-methylquinoline *N*-oxide **254** could be trapped by methanesulfonic acid (MsOH) to provide the methanesulfonyloxymethyl ketone intermediate, which could be reacted *in situ* with primary thioamide to give the 2,4-disubstituted thiazole by cyclocondensation (Scheme 2.18).

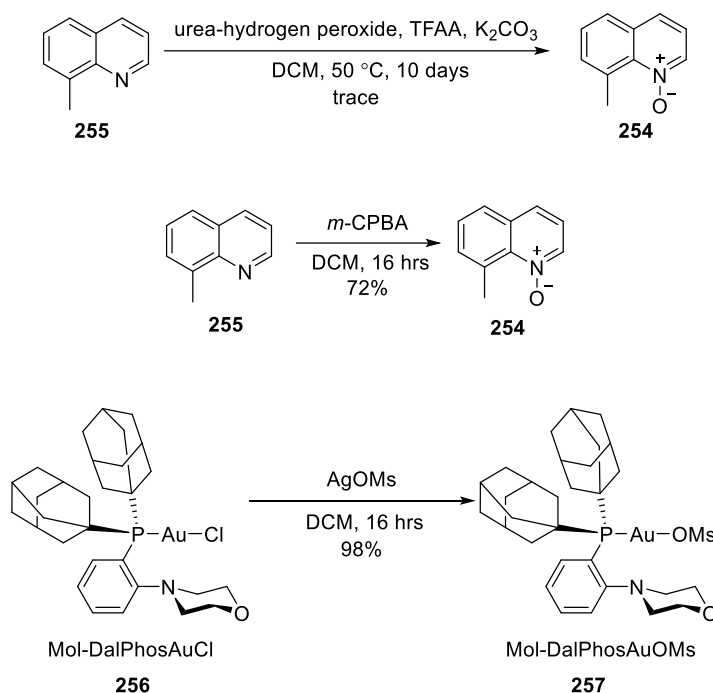


Scheme 2.18 Proposed mechanism of formation of 2,4-disubstituted thiazoles through trapping of an *in-situ* generated gold carbene by MsO^- (modified from Zhang).¹⁴¹

2.3.2.2 Synthesis of *N*-Oxide **254** and Mol-DalPhosAuOMs **257**

From a practical point of view, it is more cost-effective to prepare 8-methylquinoline *N*-oxide **254** by oxidation of 8-methyl quinoline **255** than purchasing it from suppliers.^{††} We first attempted using trifluoroperacetic acid, which was generated *in situ* from the reaction between urea hydrogen peroxide and trifluoroacetic anhydride in the presence of K_2CO_3 ,²¹⁷ to avoid the awkward purification associated with the use of *m*-CPBA.²¹⁸ Unfortunately, these conditions were found to result in a sluggish reaction with little conversion, prompting us to go back to using the conventional oxidant *m*-CPBA to prepare *N*-oxide **254** for thiazole synthesis (Scheme 2.19). Following the procedure reported by Zhang and co-workers,¹⁴¹ Mol-DalPhosAuOMs **257** was prepared from commercially available Mol-DalPhosAuCl **256** in excellent yield (Scheme 2.19).

^{††}\$ (NZ)389 for 5 grams of 8-methylquinoline *N*-Oxide **254**, \$ (NZ)67.50 for 5 grams of 8-methylquinoline. Prices taken from Sigma-Aldrich catalogue (February 2016). <https://www.sigmaaldrich.com/new-zealand.html>

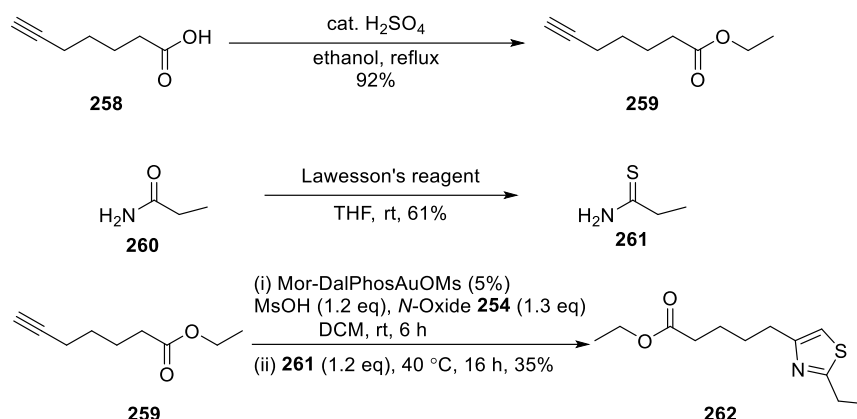


Scheme 2.19 Preparation of 8-methyl quinoline *N*-oxide **254** and Mol-DalPhosAuOMs **257**.

2.3.2.3 Gold-catalysed Preparation of Thiazole 276

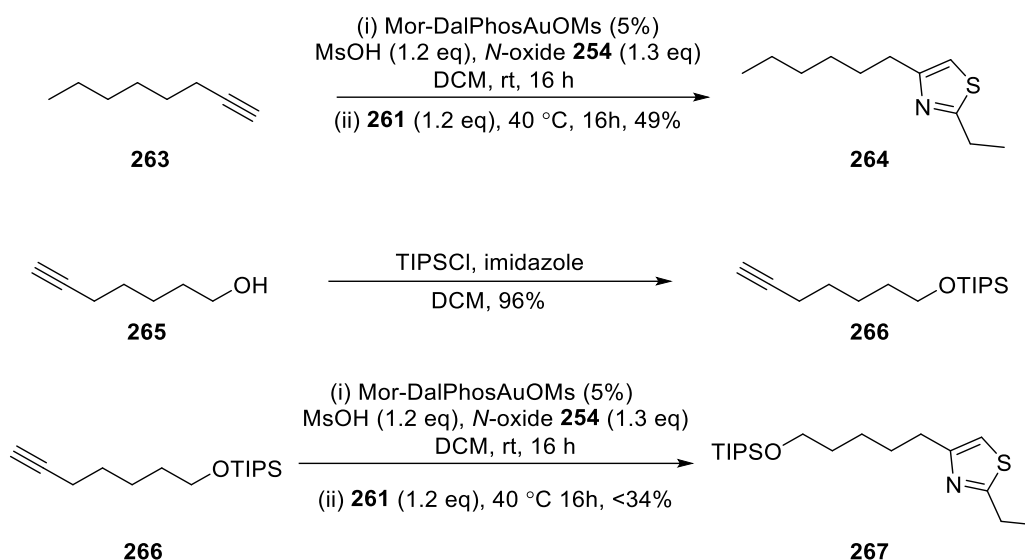
As the α -oxo gold carbene can be trapped with carboxylic acids,²¹⁶ commercially available 6-heptynoic acid **258** was protected by esterification to afford the ethyl ester **259** (Scheme 2.19) which could serve as the C1 – C7 fragment (Fragment **I**, see Scheme 2.1) in the PatA analogue **183**. In order to assess the compatibility of the ester alkyne substrate **259** with the gold-catalysed method, propanethioamide **261** was synthesised (Scheme 2.20) and used as the thioamide partner for model reactions. The one-pot thiazole formation reaction was performed following the conditions optimised by Zhang and co-workers. After the addition of the mixture of MsOH and *N*-oxide **254** to the solution of alkyne **259** and Mol-DalPhosAuOMs by a syringe pump, the proton signals of the terminal alkyne at 1.95 ppm disappeared, as determined by ¹H NMR analysis of the aliquot sample of the reaction mixture. This indicated that the alkyne substrate was consumed completely. Then propanethioamide **261** was added and the resulting mixture was heated at 40 °C for sixteen hours. To our delight, ¹H NMR analysis of the crude material showed an indicative singlet peak at 6.79 ppm, which was consistent with the reported proton signals of the 2,4-thiazoles prepared by Zhang and co-workers.¹⁴¹ This suggested that the formation of the desired thiazole should be successful. However,

thiazole **262** was obtained in only 35% yield after purification by silica gel chromatography (Scheme 2.20).

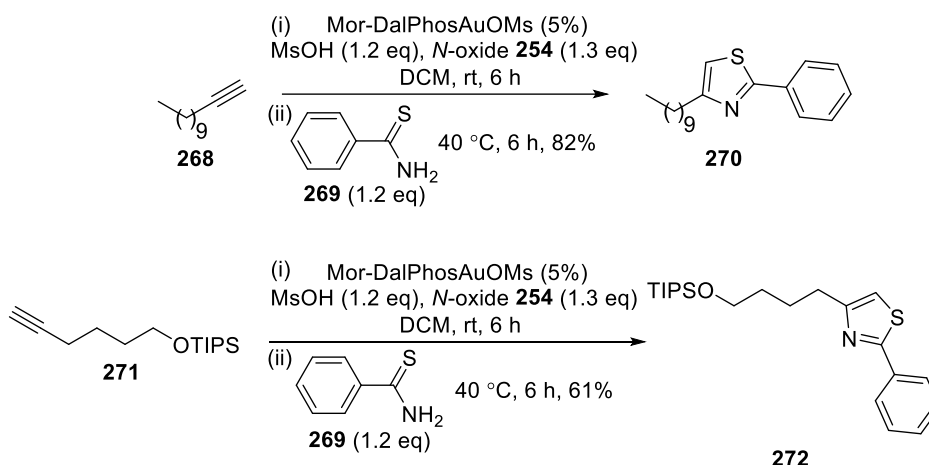


Scheme 2.20 Preparation of ester **259**, propanethioamide **261** and thiazole **262**.

Given that the oxygen atom of homopropargylic ether has been reported to be capable of trapping a gold carbene center,²¹⁹ it was surmised that the nucleophilic oxygens in the ester functional group of alkyne **259** might also participate in intramolecular trapping of the gold carbene. To determine whether the low yield of thiazole **262** was attributed to the presence of the ester group in the alkyne substrate, 1-octyne **263** and alkyne **266**, which was synthesised from 6-heptyn-1-ol **265** (Scheme 2.21), were chosen as substrates for comparative experiments. The gold-catalysed coupling reactions were carried out by postdoctoral fellow Claire Cuyamendous following the same conditions, and thiazole **264** and thiazole **267** accompanied with a small amount of inseparable unidentified by-products were obtained in 49% and 34% yield, respectively (Scheme 2.21).

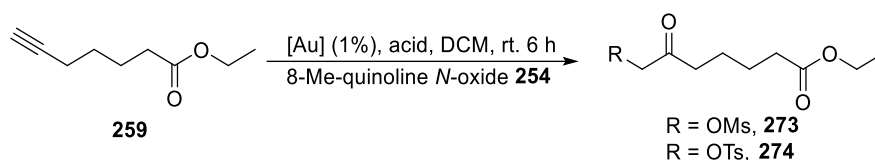
Scheme 2.21 Preparation of thiazoles **266** and **267**.

Our yields for these reactions were lower than the reported yields of thiazoles prepared from alkynes with similar structural features (*viz.* thiazole **264** versus **270**, thiazole **267** versus **272**) (see Scheme 2.22). Therefore, we assumed that the introduction of a small amount of water from methanesulfonic acid, a notoriously hygroscopic chemical, could disrupt the generation of gold carbene, resulting in the low yields of thiazole formation.

Scheme 2.22 Preparation of thiazole **270** and **272** reported by Zhang.¹⁴¹

Given that methanesulfonic acid is difficult to handle for small-scale reactions and is hard to purify, *para*-toluenesulfonic acid (*p*-TSA) was considered to be a potential replacement, which was supported by the precedent literature about the formation of thiazoles *via* condensation reactions between α -tosyloxy ketones and thioamides.²²⁰ *p*-TSA was

recrystallised from ethanol and water, and azeotropically dried with toluene to ensure that anhydrous *p*-TSA was used for the thiazole synthesis. Simultaneously, a new bottle of extra pure MsOH was purchased from Acros Organics, which was the exactly same supplier of MsOH for Zhang's work. As, in theory, α -oxo gold carbenes only participate in the first stage – the formation of α -mesyloxy ketones – experiments were stopped at the first stage to exclude the influence of thioamides. As shown in Table 2.7, using purified *p*-TSA did not give a better yield (entry 2). As expected, using a new bottle of MsOH provided a slight increase in the yield from 45% to 58% (compare entries 1 and 3), indicating that the water content level of MsOH was an influencing factor of the reaction yield.



Entry	[Au]	254 (equiv.)	Acid (equiv.)	Yield ^a (%)
1	Mor-DalPhosAuOMs	1.3	MsOH ^b (1.2)	273 45
2	Mor-DalPhosAuOMs	1.3	<i>p</i> -TSA ^c (1.2)	274 29
3	Mol-DalPhosAuOMs	1.3	MsOH ^d (1.2)	273 58

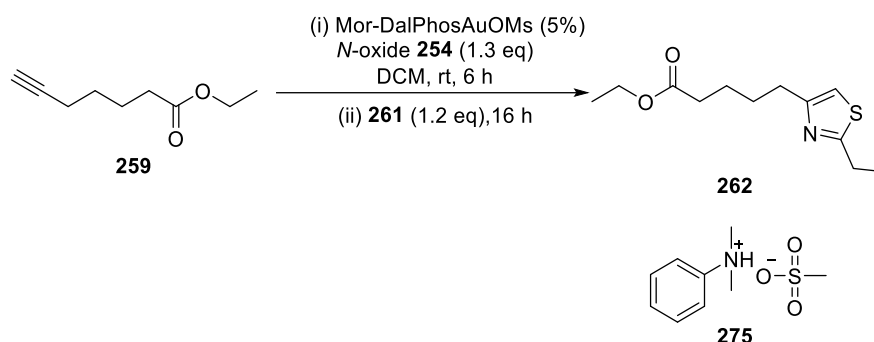
^aIsolated yield after silica gel chromatography. ^bOld bottle of MsOH was used. ^cRecrystallised *p*-TSA was used. ^dNew bottle of MsOH from Acros Organics was used.

Table 2.7 Investigation of gold-catalysed oxidation of alkyne **259** for using different acids.

As discussed by Zhang and co-workers, the gold carbene intermediate could be further oxidised to form an α -ketoaldehyde by the remaining 8-methylquinoline *N*-oxide.¹⁴¹ In order to avoid over-oxidation, it is necessary to add the mixture of oxidant and MsOH to the reaction vessel by a syringe pump to maintain a low concentration of the oxidant during the reaction, which could be a time-consuming process for a large-scale reaction. To overcome this deficiency, a modified one-pot methodology was developed by Wu and co-workers, in which ammonium sulfonate salt **275** was used as the trapping reagent for

the gold carbene.²²¹ The benefit of this methodology was that, except for the thioamides, other reaction components – alkyne, gold catalyst, oxidant, and ammonium sulfonate – could be added into the reaction vessel at the same time. In addition, the low-acidity of the ammonium sulfonate makes this reaction more suitable for acid-sensitive substrates. Last, but not least, the yield was reported to be slightly improved over Zhang's results when using substrates **268** and **269** on a larger scale (86% versus 82%, see Scheme 2.22). Therefore, this new reaction system was tested with alkyne ester **259** and simple thioamide **261** in the hope that this could improve the yield of the thiazole formation.

To our dismay, using the modified methodology provided thiazole **262** in only 27% yield (Table 2.8, entry 1). Adding the solution of salt **275** and the oxidant **254** slowly by a syringe pump and raising the reaction temperature to 40 °C resulted in a drastic decrease in the yield (compare entries 1 and 2). It was not clear whether these uninspiring yields were due to changes in reaction temperature, addition rate or mesylate source. Therefore, previously optimised conditions using MsOH were replicated in the reaction between alkyne **259** and thioamide **261**, and thiazole **262** was obtained in an improved yield (entry 3), albeit similar to those encountered by us earlier.

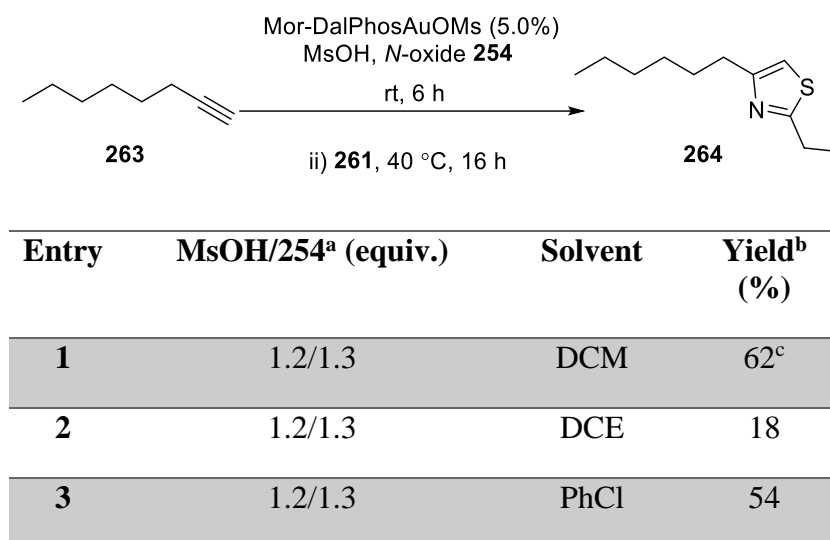


Entry	Reagent (equiv.)	Addition <i>via</i> Syringe Pump	T ^a (°C)	Yield ^b (%)
1^c	275 (1.2)	No	rt	27
2^c	275 (1.2)	Yes	40	3
3^d	MsOH (1.2)	Yes	40	53

^art = room temperature. ^bIsolated yield of thiazole **262** after silica gel chromatography. ^cSalt **275** was prepared from *N,N*-dimethylaniline and methanesulfonic acid. ^dNew bottle of MsOH from Acros Organics was used.

Table 2.8 Reaction screening with different sources of MsO⁻.

Since the effect of different solvents, which could play an important role in the performance of the gold catalyst,²²² was not reported in Zhang's work,¹⁴¹ halogenated solvents—dichloromethane (DCM), dichloroethane (DCE), and chlorobenzene, which are widely used for gold catalysed oxidation of alkynes, were chosen for screening of conditions in the formation of thiazole **264** (Table 2.9).



^aNew bottle of MsOH from Acros Organics was used. ^bIsolated yield after silica gel chromatography. ^cYield was obtained by postdoctoral fellow Claire Cuyamendous.

Table 2.9 Reaction screening with different solvents.

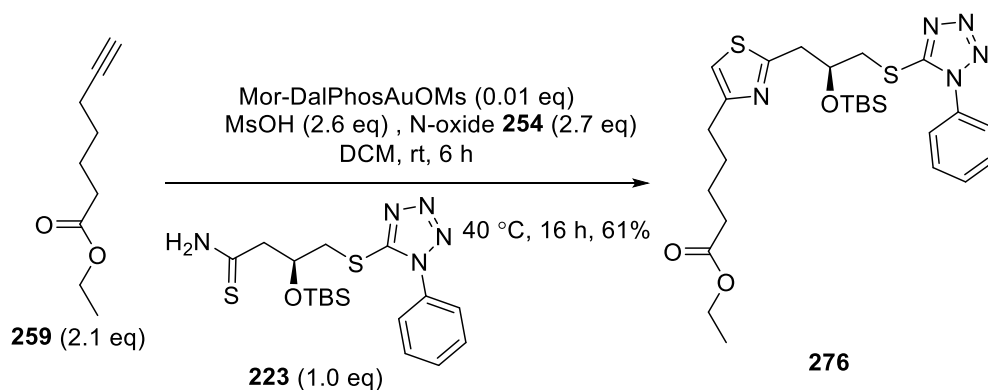
From the results listed above, it was clear that DCM was the optimal solvent for this transformation, which was in agreement with Wu's reported experimental observations in 2016.²²¹

Despite the lack of major improvements in yield, we could still draw some useful information from all these optimisation attempts. It is worth noting that the yields of thiazole **262** (Table 2.8, entry 3) and mesylate **273** (Table 2.7, entry 3) are close to each other (53% versus 58%); and the yield of thiazole **264** (Table 2.9, entry 1) was significantly lower than the reported yield of thiazole **270** by Zhang (62% versus 82%). Therefore, we assumed that the possible cause of the inefficient catalytic results was that there are problems with the methodology when using aliphatic thioamides because the thioamide substrates used in Zhang and co-worker's reaction scope studies, apart from ethanethioamide and cyclohexanecarbothioamides, are all aromatic thioamides. Additionally, the interference of the two oxygen atoms of the ester functional group in alkyne **259** with the intermolecular trapping of α -oxo gold carbene by MsO^- could not be

ruled out by our experimental results.

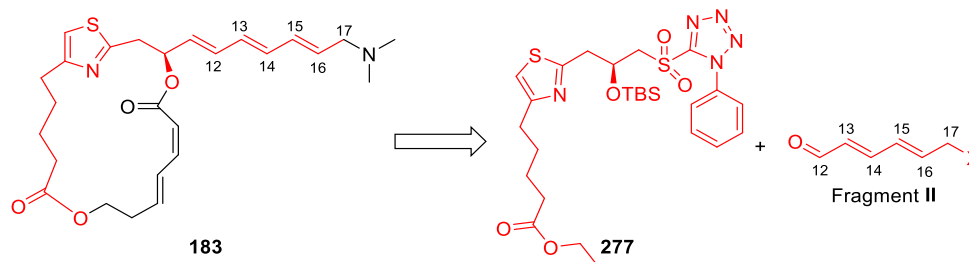
Nonetheless, our optimised conditions gave yields of up to 62% in the model reaction between alkyne **263** and thioamide **261**, which was sufficient to continue with their application to the preparation of desired thiazole **276**.

The preparation of thiazole **276** was performed with modifications of Zhang's optimised conditions using functionalised thioamide **223** (Scheme 2.23, the loading of the gold catalyst was lowered to be 1 mol% instead of 5 mol%). ¹H NMR investigation of the aliquot sample of the reaction mixture after 16-hours heating showed a sharp singlet peak at 6.25 ppm, which was considered to be an obvious sign of the formation of desired thiazole **276**. To our delight, thiazole **276** was obtained with a 61% yield, which was higher than the 30% yield of five steps required for the preparation of the α -bromoketone **139** and thiazole **141** in Romo's synthesis of DMDA PatA (*vide supra*, Scheme 1.18 in Section 1.4.2.1).¹²⁶



Scheme 2.23 Synthesis of thiazole **276**.

2.4 Coupling of Side Chain Fragment



As discussed earlier in our retrosynthetic analysis in Section 2.1, Julia-Kocienski reaction between the thiazole-containing sulfone **277** and the fragment **II** was chosen for the attachment of the side chain fragment.

2.4.1 Introduction

The modified Julia-Kocienski reaction has emerged as one of the premiere alkene forming reactions in organic synthesis because of its tolerance of base-sensitive aldehyde substrates.²²³ As shown in Figure 2.7, the reaction mechanism begins with the metalation of phenyl tetrazolyl sulfone **278** with an appropriate metal base to give the nucleophilic sulfone anion **279**, which couples with an aldehyde to form the β -alkoxysulfone (*syn*-**280** or *anti*-**280**). This unstable intermediate then rearranges *via* a facile Smiles rearrangement to give sulfinic acid salt (**281** or **282**), which spontaneously eliminates sulfur dioxide and metallated phenyltetrazole to provide the alkene product. The *Z/E*-selectivity of the alkene product is highly dependent on the substrates, the base used to form the sulfone anion, the metal cation, and solvents in most cases.²²⁴ When larger metal cation (K^+) and polar solvents are involved, the non-chelated open transition state becomes predominant and the transition state **II** is of lower energy because it lacks the unfavourable interaction between R and R' which is present in the alternative transition state **I**.²²⁵ Progression of the olefination process *via* the favoured transition state leads to the formation of *anti*-intermediate alkoxide **280** and thence to the *E*-alkene product. In addition, the selectivity can also be influenced to some extent by the steric hindrance imparted by the phenyltetrazole in Smiles rearrangement (Figure 2.7).²²⁶

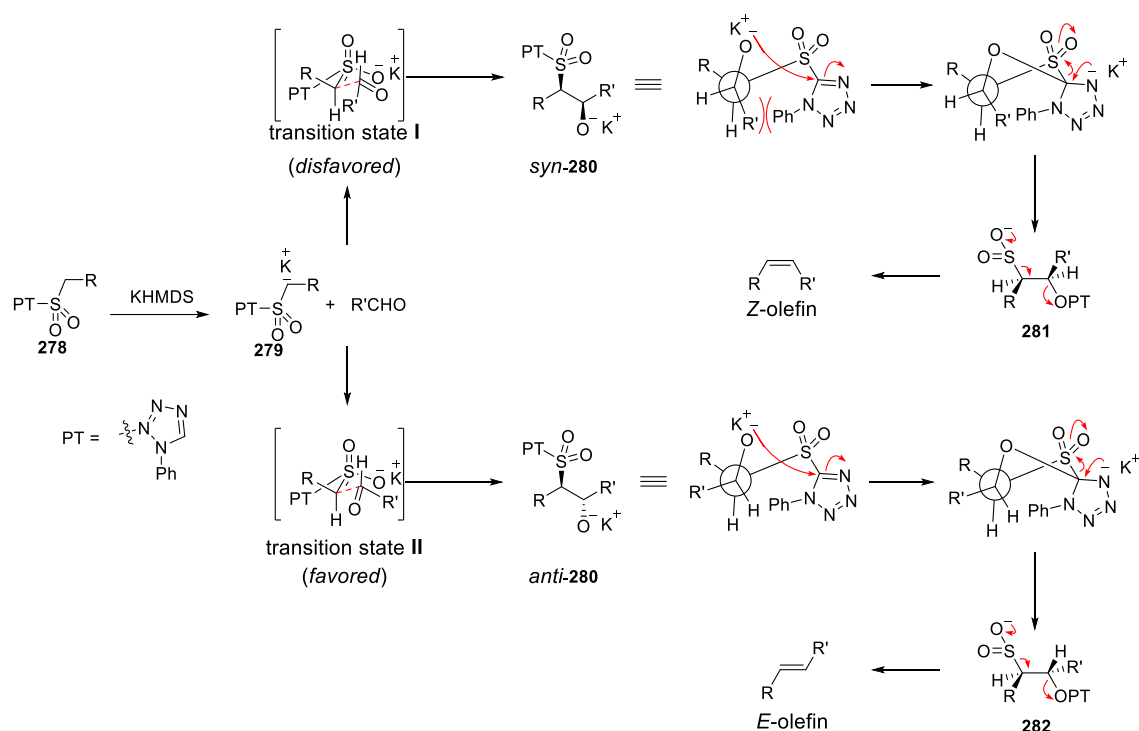


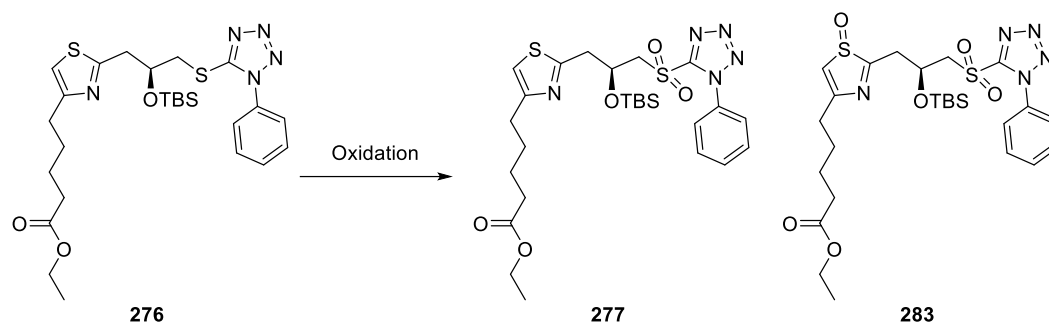
Figure 2.7 Proposed mechanism of Julia-Kocienski olefination and rationale for stereocontrol of olefins.

2.4.2 Preparation of Sulfone 277

With thiazole **276** in hand, we then set out to prepare sulfone **277** required for Julia-Kocienski reaction. Thiazole **276** has two oxidisable sulfur atoms. We anticipated that the thioether sulfur atom would be the most prone to oxidation. In the preparation of sulfones from thioethers, up to 3 equivalents of *m*-CPBA are commonly used in the literature. However, to minimise unwanted oxidation at the sulfur atom of the thiazole ring, the oxidation of thioether **276** was first attempted with 2.0 equivalents of *m*-CPBA (Table 2.10, entry 1). Interestingly, only the over-oxidised product **283** was isolated,^{‡‡} along with the recovery of unreacted starting material. The oxidation reaction was then tested in treatment with catalytic ammonium heptamolybdate and aqueous hydrogen peroxide as the terminal oxidant, a chemoselective oxidation method which has enjoyed widespread use for the synthesis of sulfones.²²⁷ Thankfully, the desired sulfone **277** was

^{‡‡} Characterised by HR-MS investigation. The base peak in the HR-MS spectrum of the isolated product was at $m/z = 610.2181$, which matches with the calculated mass for compound **283** plus one hydrogen ion ($C_{26}H_{40}N_5O_6S_2Si^+ [M+H]^+ 610.2189$).

obtained as the sole product in 71% yield, albeit in a slower reaction rate (entry 2).



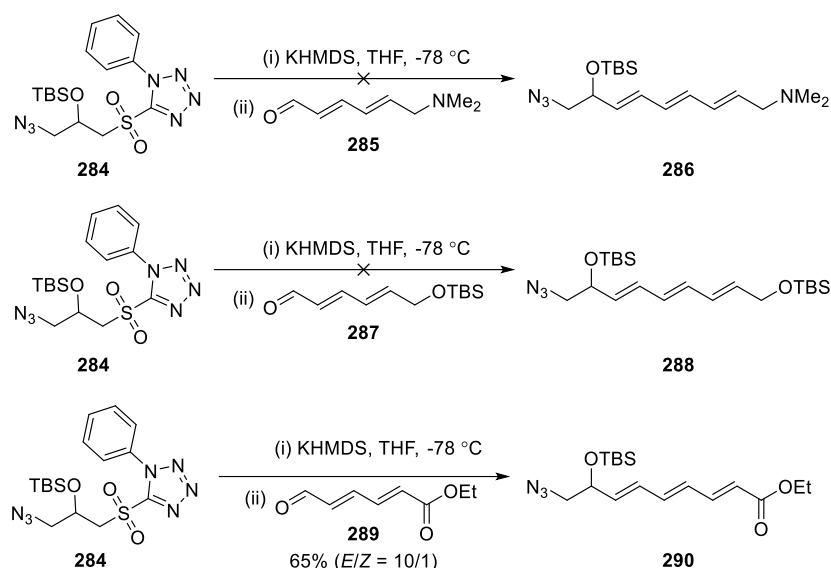
Entry	Conditions (equiv.) ^a	Time (hrs)	Yield ^b
1	<i>m</i> -CPBA (2.0), NaHCO ₃ (5.2), DCM, 0 °C to rt	18	283 36%
2	H ₂ O ₂ (30), (NH ₄) ₆ Mo ₇ O ₂₄ (0.5), ethanol, 0 °C to rt	38	277 71%

^art = room temperature. ^bIsolated yield after silica gel chromatography.

Table 2.10 Trialled conditions for the formation of sulfone **277**.

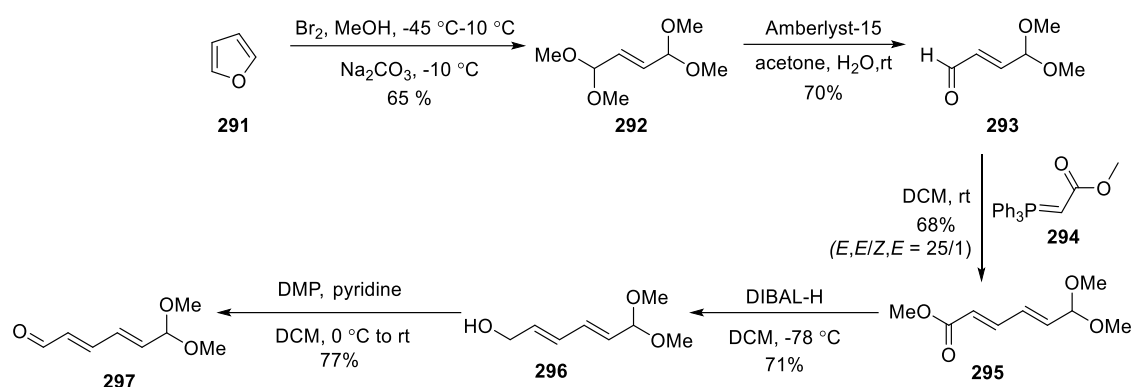
2.4.3 Synthesis of Side Chain Fragment 297

In Cumming's endeavours to synthesise thtriazole analogue **182** (see Figure 1.23 in Section 1.6), he found that reactions between sulfone **284** and aldehydes **285** or **287** under Julia-Kocienski olefination conditions did not provide desired triene products, but resulted in mixtures of degradation products (Scheme 2.24). He proposed that these failures were possibly due to the presence of an enolisable centre in these aldehyde substrates. Therefore, conjugated ester **289** was then trialled in his project under the same conditions and triene **290** was obtained with good *E*-selectivity.¹³⁵ Informed by Cumming's work, we proposed that a non-enolisable conjugated fragment could serve as an appropriate substrate for Julia-Kocienski reaction in the synthesis of PatA analogue **183**.



Scheme 2.24 Julia-Kocienski olefination with sulfone **284** and aldehydes in Cumming's previous work.¹³⁵

The synthetic strategy of the side chain fragment in Cumming's synthesis of the triazole analogue **182**¹³⁴ was incorporated with modifications in the preparation of the desired fragment for coupling with sulfone **277**. Cheap commercial available starting material furan **291** was treated with bromine and methanol to provide *bis*-dimethyl acetal **292** via oxidative ring-opening (Scheme 2.25),²²⁸ subsequent mono-deprotection catalysed by Amberlyst-15, a resin with strongly acidic sulfonic acid groups, in acetone and water gave aldehyde **293**, and Wittig reaction with stabilised triphenylphosphoryl ylide **294** (prepared from 2-bromoacetate and triphenylphosphine, see Section 6.2.3 for experimental details) provided *E,E*-dienoate **295** as the major product in good yield. The attempted partial reduction of methyl ester **295** to aldehyde **297** using one equivalent of DIBAL-H resulted in a mixture of alcohol **296** and aldehyde **297**. The methyl ester **295** was instead subjected to a two-step protocol. Reduction to the corresponding primary alcohol **296** occurred in 71% yield. Considering that the acetal was sensitive to the acidic environment, pyridine was used as an acid scavenger in the following Dess-Martin oxidation, and the aldehyde **297** was obtained in 17% yield over 5 steps. It was proposed that enal **297** was unlikely to be able to enolise under Julia-Kocienski olefination conditions. Therefore, enal **297** was targeted as a potential candidate for the side chain fragment, which would also allow progress to the terminal dimethyl amine for PatA analogue synthesis.

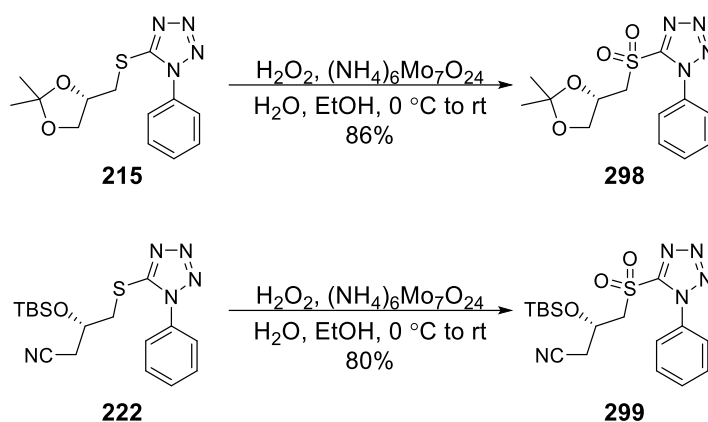


Scheme 2.25 Synthesis of enal **297**.

It is worth mentioning that the acetal functional group of enal **297** rapidly deprotected in deuterated chloroform used for NMR analysis. This unexpected deprotection process was prompted by the tiny amount of HCl impurity generated by chloroform degradation in air, indicating that the terminal acetal could be converted into the terminal aldehyde when required by very mild acidic conditions. The acid-lability of the acetal would be beneficial for the late-stage progression of PatA analogues.

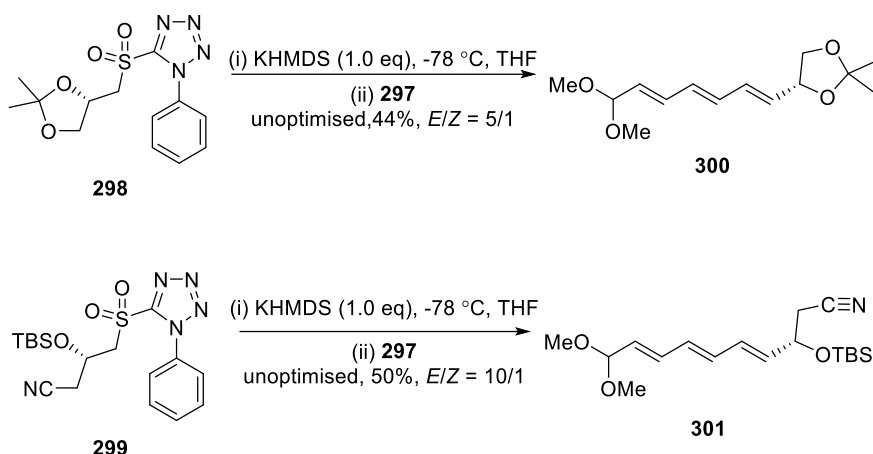
2.4.4 Model Julia-Kocienski Olefination

Given that there are few published examples of enals containing acetal functional groups that successfully couple in Julia-Kocienski reactions, sulfones **298** and **299** were prepared by oxidation of corresponding thioethers **215** and **222** with hydrogen peroxide and catalytic ammonium heptamolybdate (Scheme 2.26), which would allow assessment of the performance of enal **297** in model versions of this olefination method.



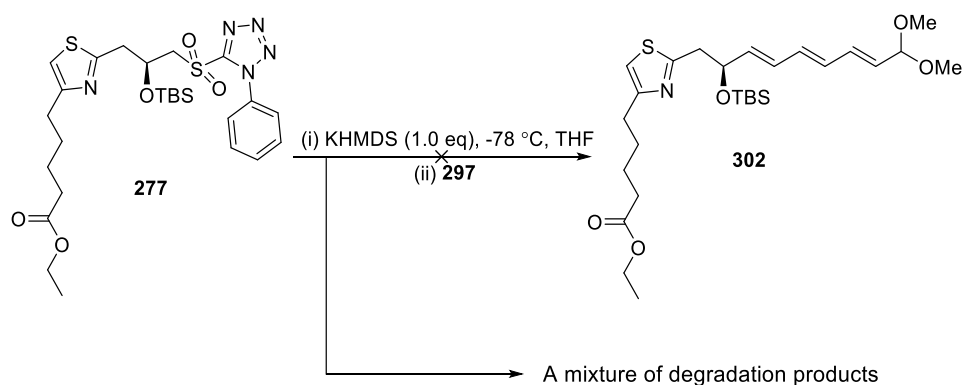
Scheme 2.26 Preparation of sulfone **298** and **299**.

Presuming that enal **297** could be unstable in a strongly basic environment, KHMDS used in pre-treating the sulfones was strictly limited to one equivalent to ensure that no excess KHMDS would be present in the reaction vessels when the enal **297** was added to couple with the deprotonated sulfone partners. Gratifyingly, the Julia-Kocienski reactions with sulfones **298** and **299** afforded triene products **300** and **301** in inseparable (*E,Z*) mixtures with good *E*-selectivity, respectively (Scheme 2.27).



Scheme 2.27 Model Julia-Kocienski reactions with sulfones **298** and **299**.

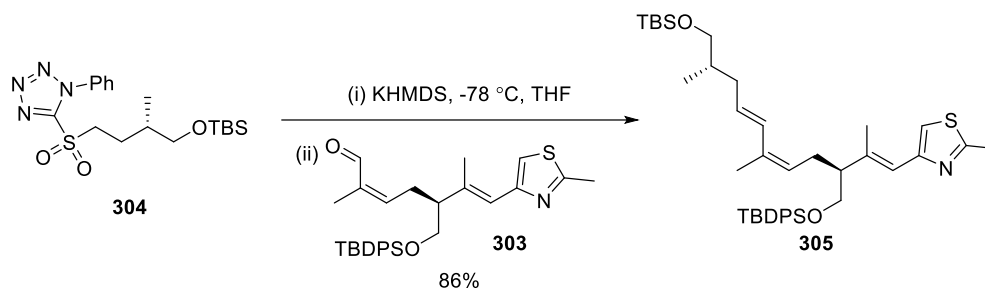
Encouraged by these successful results, we then attempted coupling sulfone **277** with enal **297** using the same conditions (Scheme 2.28). Disappointingly, instead of desired triene product **302**, a mixture of unidentified products was obtained, which were possibly derived from degradation of enal **297**.



Scheme 2.28 Attempted Julia-Kocienski reaction with sulfone **277** and enal **297**.

There are some reported examples of aldehydes containing 2,4-disubstituted thiazole moieties that were efficiently reacted with sulfone partners under Julia-Kocienski's

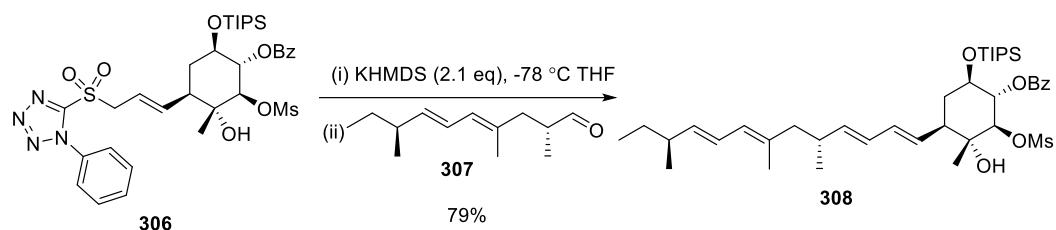
optimised conditions, for example, the coupling of aldehyde **303** with sulfone **304** to provide diene **305** in the synthesis of epothilone (Scheme 2.29).²²⁹ Therefore, the interference of thiazole with the reaction between enal **297** and the sulfone anion derived from **277** was presumed not to be the major cause of the failure.



Scheme 2.29 Julia-Kocienski reaction of thiazole-containing aldehyde **303** in the synthesis of epothilone.²²⁹

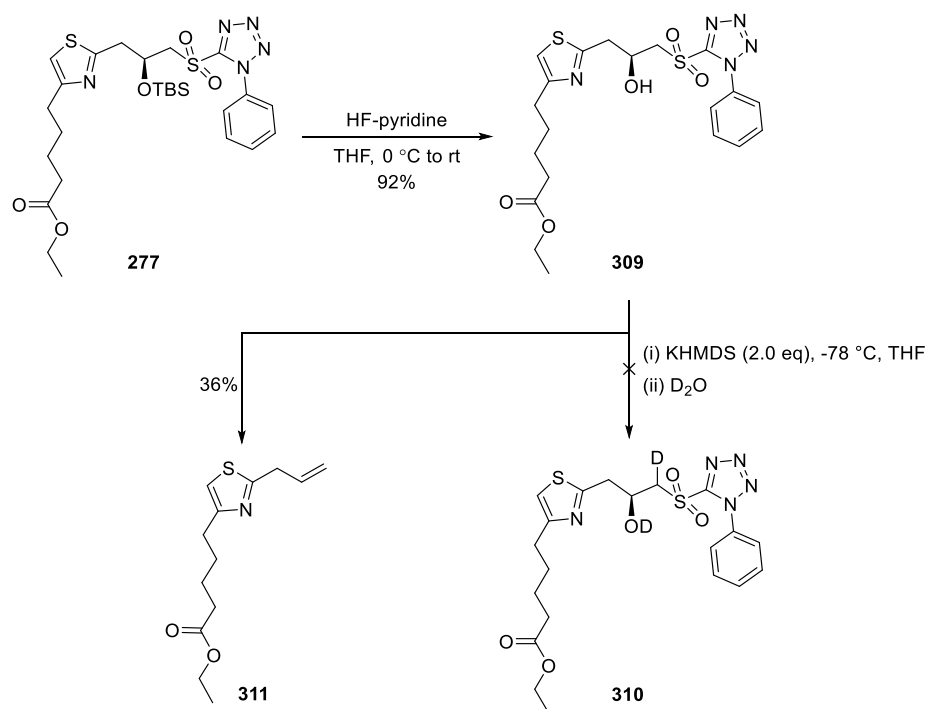
It was of note that sulfone starting material **277** could be partially recovered and the Julia-Kocienski reaction of TBS-protected sulfone **299** had provided the olefination product **301** with enal **297** in moderate yield (Scheme 2.27). It was then proposed that the steric effect of the protecting group in sulfone **277** could be enhanced dramatically by the presence of a relatively rigidified thiazole ring, which would make access of the bulky base KHMDS to the proton at the α -position of the sulfone slow. Consequently, the nucleophilic sulfone anion was probably not produced in the first phase, and then the treatment of enal **297** with unreacted KHMDS could have led to significant degradation. Hence, we assumed that using a free hydroxy group or replacing the TBS group with a less bulky protecting group could benefit the deprotonation process. In view of the step economy, it would be ideal that the Julia-Kocienski reaction could work with an unprotected hydroxyl group.

To our delight, a scan through the literature disclosed that Omura and co-workers, en route to the synthesis of nafuredin, utilised sulfone **306** with a free hydroxyl group in their pivotal Julia-Kocienski reaction (Scheme 2.30).



Scheme 2.30 Julia-Kocienski reaction with sulfone **306** containing free -OH group.²³⁰

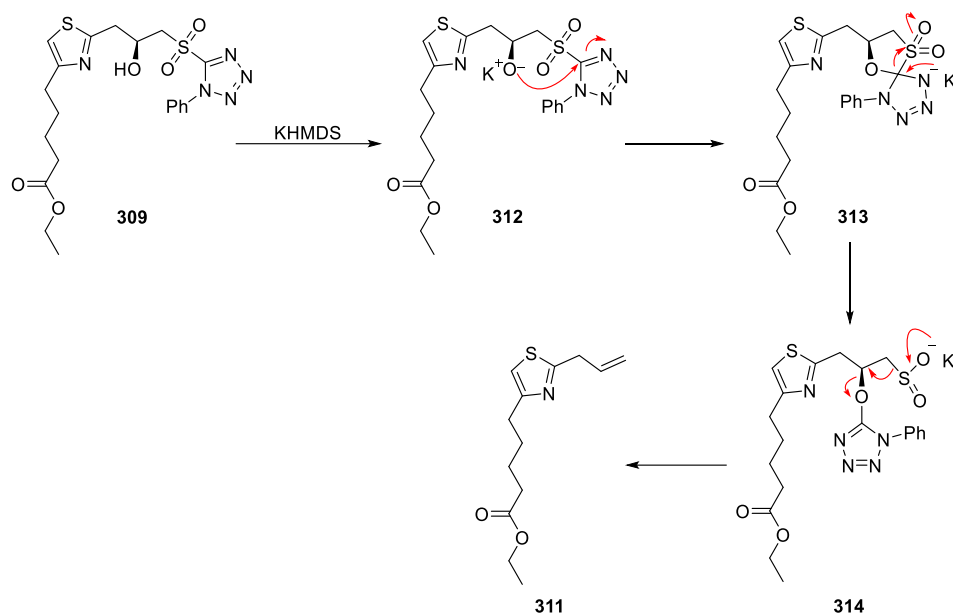
Therefore, sulfone **277** was desilylated by HF-pyridine to provide sulfone **309** (Scheme 2.31). To test whether the removal of the TBS group was beneficial for the Julia-Kocienski reaction, we attempted to prepare the deuterated sulfone **310** first, which would be unequivocal evidence that the efficiency of the deprotonation process had been improved. Interestingly, no desired deuterated product **310** was observed, and instead, allylic thiazole **311**, the structure of which was determined by 2D NMR and HR-MS investigation, was obtained in moderate yield, (Scheme 2.31). This experimental result suggested that compound **309** containing a free -OH group was not an appropriate sulfone partner for coupling with enal fragment **297** under Julia-Kocienski conditions.



Scheme 2.31 Attempted preparation of deuterated sulfone **310**.

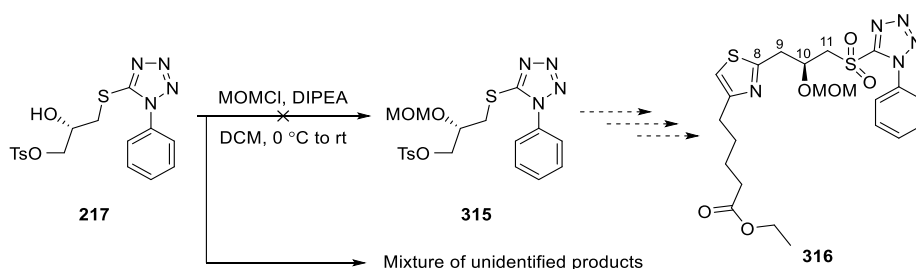
On the basis of the proposed mechanism of Julia-Kocienski olefination, as shown in Scheme 2.32, we conceived that unstable β -alkoxide **312** derived from sulfone **309** may

have experienced similar Smiles rearrangement *via* the formation of a spirocyclic intermediate **313** to give the unexpected eliminated thiazole **311**.



Scheme 2.32 Proposed mechanism for the formation of thiazole **311**.

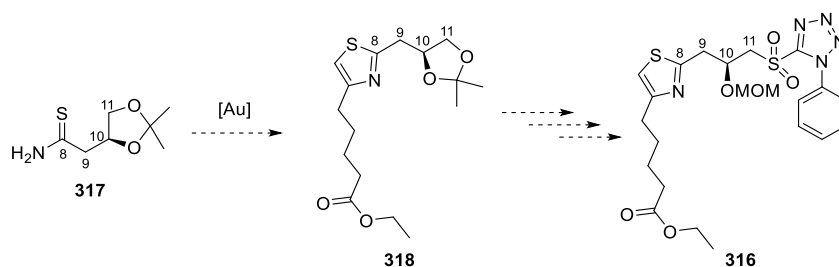
To avoid the tedious deprotection-protection at this stage, we then opted to go back to replace the protecting group at an early stage (Scheme 2.33). Given that the methoxymethyl (MOM) group is considered to be less bulky than the TBS group, we attempted to prepare the methoxymethyl ether **315** following classic conditions²³¹ for the preparation of methoxymethyl (MOM)-protected sulfone **316**. However, this resulted in a mixture of unidentified products, with no sign of the desired compound **315** observed by ¹H NMR and HRMS analysis.



Scheme 2.33 Attempted preparation of methoxymethyl protected alcohol **315** for the synthesis of sulfone **316**.

2.5 Revised Synthesis of Sulfone 316

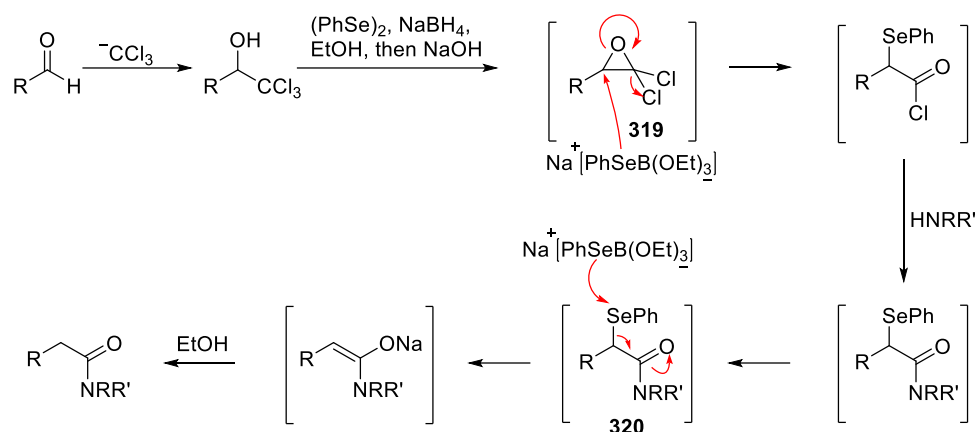
Given that the formation of methoxymethyl ether **315** in the early stage was unsuccessful, it was necessary to develop a new synthetic route for sulfone **316** which could be a suitable substrate for the Julia-Kocienski olefination. The present synthetic route utilised a chemist-unfriendly cyanation step for one-carbon homologation, which required an awkward procedure for quenching cyanide residue. Besides, the one-step conversion of epoxide **213** to acetone **214** resulted in a degree of racemisation at the stereocentre based on Mosher analysis (*vide supra*, Section 2.2.3.2). To overcome these disadvantages, a chiral thioamide **317** that possesses sites for the connection with both alkyne fragment **259** and enal fragment **297** was targeted as a potential building block for the alternative route (Scheme 2.34).



Scheme 2.34 Proposed synthetic route for sulfone **316** starting from thioamide **317**.

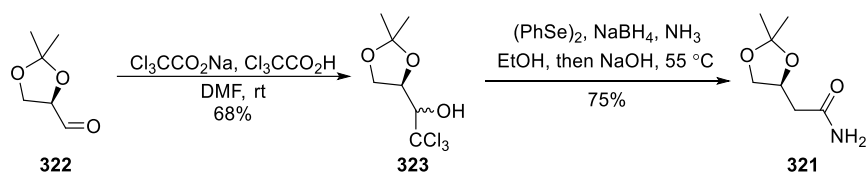
2.5.1 Attempted Synthesis of Thioamide 317

In 2014, Snowden and co-workers reported that the transformation of aldehydes into one-carbon homologated amides could be achieved in two steps *via* a Jovic-Reeve type reaction.^{232, 233} As shown in Scheme 2.35, the plausible reaction mechanism starts with the trichloromethylation of an aldehyde. The trichloromethyl carbinol intermediate is then slowly deprotonated by NaOH in a protic solvent to form a highly electrophilic *gem*-dichloroepoxide **319**, which is then quickly regioselectively substituted by the phenylseleno(triethyl)borate complex, a nucleophile prepared *in situ* by mixing diphenyl diselenide and NaBH₄ in argon-purged ethanol. The opening of epoxide gives a reactive acid chloride intermediate, which allows for rapid acyl substitution by the available amine in the reaction system. The resultant α -phenylselenoamide **320** slowly undergoes *in situ* deselenylation to afford the enolate intermediate, which is immediately protonated by the protic solvent to provide a one-carbon homologated amide product.



Scheme 2.35 Proposed mechanism of homologated amide formation *via gem*-dichloroepoxide by Snowden and co-workers.²³²

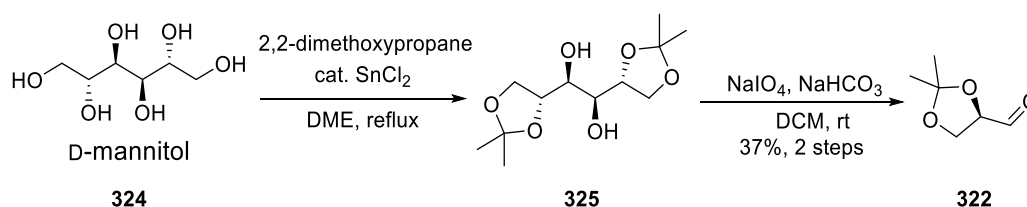
The typical transformation of aldehydes to one-carbon homologated amides involves reduction to primary alcohols, conversion to leaving groups, substitution by cyanides and nitrile hydration to amides. In comparison, the benefit of this novel method is that it can avoid the use of hazardous cyanide and furnish the transformation in two steps. In addition, based on Snowden and co-worker's experimental observations, diphenyl diselenide used in the reaction could be completely recovered after work-up procedures and the recycled diphenyl diselenide could be reused in the subsequent homologations without decrease in reaction efficiency, making this two-step reaction sequence to be an environmental benign methodology. Furthermore, this approach was found to have broad substrate scope and be capable of converting enolisable aldehydes into the corresponding one-carbon homologated amides without racemisation. For example, butanamide **321**, a potential precursor for thioamide **317**, was reported to be conveniently obtained in 51% yield with high optical purity (Scheme 2.36). Therefore, we opted to utilise this novel synthetic method, which would enable a more step-economic synthesis for thioamide **317**.



Scheme 2.36 Preparation of chiral amide **321** from aldehyde **322** reported by Snowden.²³²

2.5.1.1 Preparation of Trichloromethyl Carbinol **323**

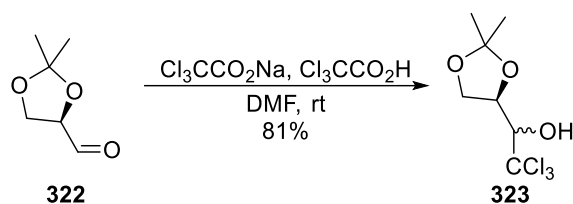
It was reported that the monomeric stability of chiral aldehyde **322** is highly dependent on storage conditions and its polymerisation process can cause a slight deviation in its optical purity.²³⁴ Also, from a practical point of view, it is more sustainable to prepare chiral aldehyde **322** from cheap starting material D-mannitol **324**^{§§} following the highly reliable two-step protocol reported by Schmid and co-workers.²³⁴ Thus, we decided to use freshly prepared aldehyde **322** rather than purchasing it from suppliers. As shown in Scheme 2.37, D-mannitol **324** was first ketalised with catalytic stannous chloride and 2,2-dimethoxypropane to provide diacetonide **325**, followed by oxidative cleavage, providing aldehyde **322**. The high optical purity of aldehyde **322** was determined by the comparison between the observed specific rotation and reported specific rotation in previous literature (See section 6.2.3 for details).



Scheme 2.37 Preparation of chiral aldehyde **322** from D-mannitol **324**.

Based on the proposed mechanism by Snowden and co-workers (Scheme 2.35), neither the trichloromethyl carbinol nor the homologated amide should be enolisable in the basic reaction conditions as the stereogenic hydrogen in either compound lacks activation by an adjacent electron-attracting functional group (*e.g.*, the carbonyl group in the aldehyde). Thus, in terms of stereochemical fidelity, the only step of concern was the trichloromethylation of aldehyde **322**. As reported by Snowden, the mild buffered Corey-Link trichloromethylation protocol²³⁵ was utilised to retain the enantiomeric purity, giving a mixture of diastereomers **323** in 81% yield (Scheme 2.38).

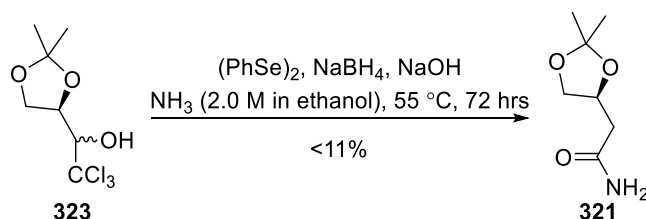
^{§§}Chiral aldehyde **322**, \$(NZ)134\$ for 0.5 gram, compared to D-mannitol, \$(NZ)64\$ for 500 grams. Prices taken from Sigma-Aldrich catalogue (July 2017). <https://www.sigmaaldrich.com/new-zealand.html>



Scheme 2.38 Preparation of trichloromethyl carbinol **323**.

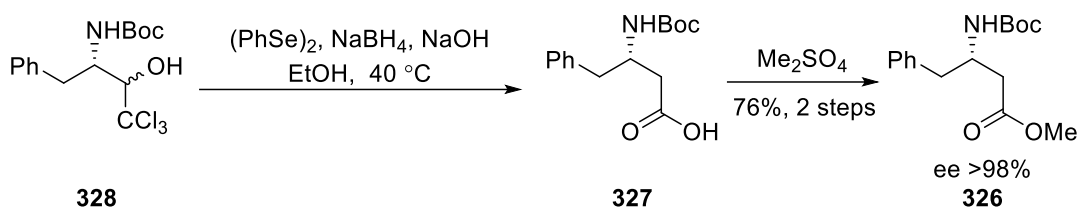
2.5.1.2 Preparation of Butanamide **321**

As reported in Snowden and co-workers' experimental procedures, ethanol saturated by gaseous ammonia was used as the reaction media in their synthesis of butanamide **321**. Given that an ammonia cylinder was unavailable in our laboratory and the reaction was performed in a sealed pressure tube, we initially reckoned that commercially available ammonia solution in ethanol could be a feasible substitute. Disappointingly, after three days, the reaction had not gone to completion even when excess ammonia solution (2.0 M in ethanol) was used, and the butanamide **321** was obtained in poor yield (Scheme 2.39), suggesting that the high concentration of ammonia could be essential to help out-compete other nucleophiles in the reaction system ($\text{PhSeB}(\text{OEt})_3^-$, HO^- , EtO^- , Cl^-). Therefore, exploring an alternative synthetic method for the amide **321** was deemed necessary.



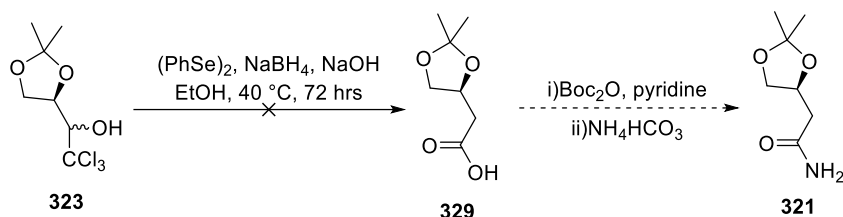
Scheme 2.39 One-step synthesis of amide **321**.

A scan through Snowden and co-workers' research related to transformations of trichloromethyl carbinols revealed that they could be also converted to one-carbon homologated carboxylic acid in one-step *via* the similar Jovic-Reeve type mechanism.²³⁶ Motivated by the fact that methyl ester **326** was synthesised *via* carboxylic acid intermediate **327** with no detectable decrease in *e.e.* (Scheme 2.40), our attention was focused on a potential alternative approach to amide **321**, which involved aminolysis of an anhydride intermediate.



Scheme 2.40 Preparation of chiral methyl ester **326** reported by Snowden and co-workers.²³⁶

Following Snowden and co-workers' optimised conditions,²³⁶ trichloromethyl carbinol **323** was treated with a mixture of diphenyl diselenide, NaBH₄ and NaOH in argon-purged ethanol at 40 °C. The reported chemical shifts of α -protons of carboxylic acid **329** ((300 MHz, CDCl₃) δ 2.71 (dd, J = 16.2, 6.7 Hz), 2.53 (dd, J = 16.2, 6.8 Hz))²³⁷ were used as the reference in monitoring the formation of the acid by ¹H NMR analysis of reaction aliquots. After three-day heating, although the starting material was consumed completely based on observation by TLC plates, there was no evidence of the formation of the desired acid **329** over the reaction period (Scheme 2.41).

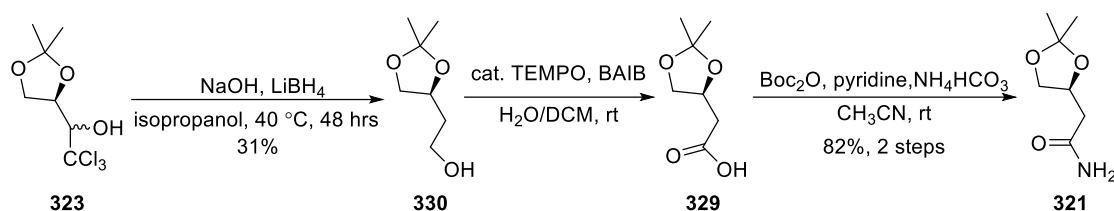


Scheme 2.41 Attempted synthesis of amide **321** *via* carboxylic acid intermediate **329**.

With the failed preparation of the carboxylic acid **329** after multiple attempts, primary alcohol **330**, which could be prepared *via* reductive homologation of the trichloromethyl carbinol **323**,²³⁸ was targeted as the appropriate precursor for acid **329**.

Gratifyingly, treatment with a mixture of LiBH₄ and NaOH in isopropanol provided the alcohol **330** in 31% yield (Scheme 2.42). Although the yield obtained in our hands was significantly lower than the reported yield in the literature (31% versus 75%),²³⁸ it was proven to be reliable and reproducible on both small-scale (*e.g.*, 0.1 gram) and large-scale (*e.g.*, 1.4 gram) reactions. Subsequent mild oxidation reaction, in which a catalytic amount of TEMPO worked as the oxidant and a stoichiometric amount of BAIB was used to regenerate TEMPO, afforded carboxylic acid **329**.²³⁹ The resultant carboxylic acid was then treated with Boc₂O and pyridine to give an anhydride intermediate, which was

inherently unstable and underwent aminolysis to provide desired amide **321**.



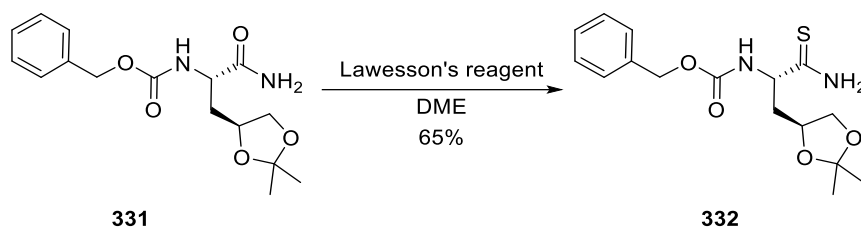
Scheme 2.42 Preparation of amide **321** via primary alcohol intermediate **330**.

2.5.1.3 Attempted Preparation of Thioamide **317**

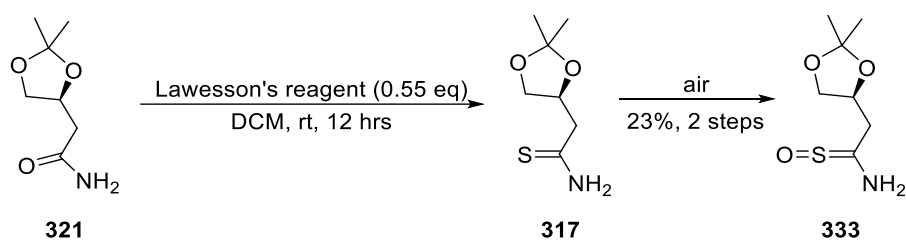
As there were only a handful of reported examples in which amides containing an acetonide functional group were transformed into thioamides successfully (see Scheme 2.43 for one example),^{***} we were concerned about the compatibility of the acetonide functionality in amide **321** with Lawesson's reagent. To avoid possible side-reactions caused by unreacted Lawesson's reagent, we decided to minimise the equivalents of Lawesson's reagent. Therefore, the thionation of amide **321** was first attempted by treating with 0.55 equivalent of Lawesson's reagent. As the amide starting material and the by-product generated from Lawesson's reagent were indistinguishable on TLC plates, the reaction was monitored by intensive ¹H NMR analysis of the aliquot samples of the reaction mixture. After 12-hour stirring at room temperature, the α-proton signals of amide **321** at 2.55 and 2.47 ppm disappeared, indicating the conversion was completed. The reaction was then quenched with saturated NaHCO₃ solution and a thionation product was isolated in a moderate yield (Scheme 2.44). Whilst this product was initially believed to be the desired thioamide **317** based on ¹H NMR analysis, HR-MS investigation revealed that the major line with peak height of about 92% was at *m/z* = 192.0685, which matches with the mass of the desired thioamide product plus the mass of one oxygen atom (Figure 2.8). This result suggested that the major component of the obtained product was, in fact, thioamide *S*-oxide **333**, which is most likely the result of oxidation *via* the addition of atmospheric oxygen. Interestingly, Pattenden and co-workers reported that they successfully prepared thioamide **317** in their initial synthetic studies towards PatA, but they did not report any characterisation data.¹¹⁹ Therefore, we assumed that they also encountered this instability problem caused by aerobic oxidation. Given that the thionation reaction was performed under argon atmosphere in our hands, it was proposed

^{***} Using *SciFinder* database; <https://scifinder.cas.org> (accessed November 2017)

that the aerobic oxidation occurred in the work-up procedure.



Scheme 2.43 Example of thionation of amide with acetonide functionality.²⁴⁰



Scheme 2.44 Attempted preparation of thioamide **317**.

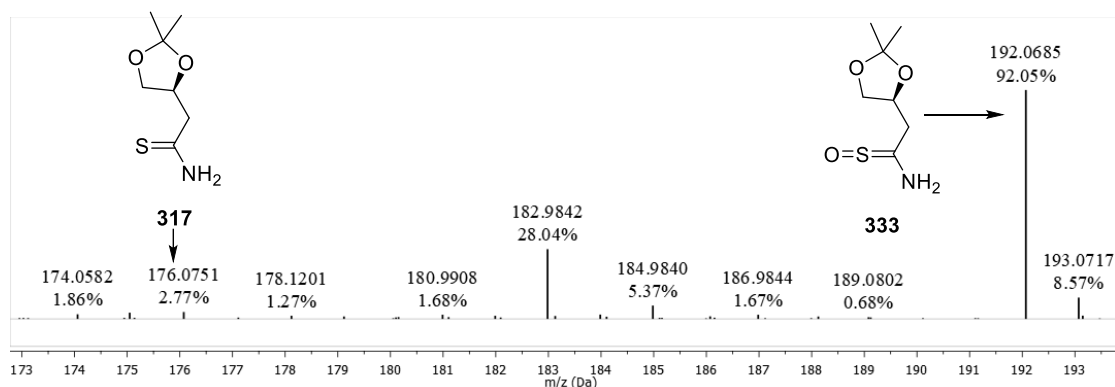
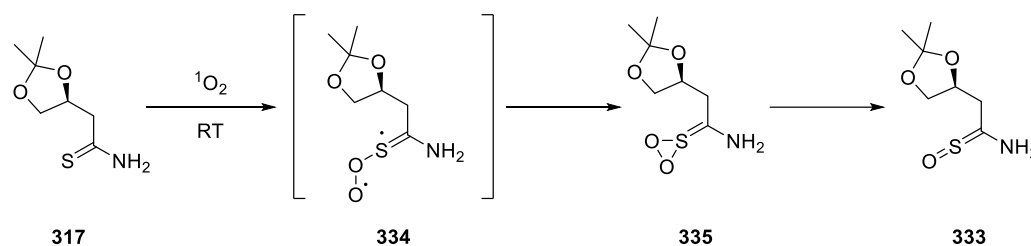


Figure 2.8 HR-MS of thioamide *S*-oxide **333**.

Mass of protonated thioamide **317** at $m/z = 176.0751$, calculated for $C_7H_{14}NO_2S^+$, 176.0740 and protonated thioamide *S*-oxide **333** at $m/z = 192.0685$, calculated for $C_7H_{14}NO_3S^+$, 192.0689.

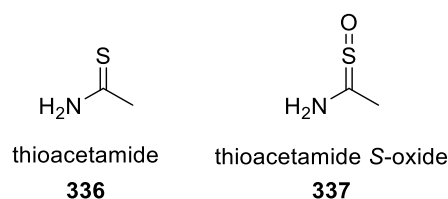
As the photochemical *S*-oxidation of thiobenzamides by singlet oxygen is well established,^{241, 242} it was conceived that the existence of singlet oxygen in air may be the cause of the oxidative degradation of thioamide **317**. A mechanism for reactions between sulfides and singlet oxygen was proposed by Jensen and co-workers based on calculations,²⁴³ and the aerobic oxidation of thioamide **317** may undergo a similar process. Thus, as described in Scheme 2.45, thioamide **317** reacts readily with single oxygen to

form a highly reactive thiadioxirane **335** via a diradical peroxy sulfoxide intermediate **334**, which then rapidly breaks down to provide thioamide S-oxide.



Scheme 2.45 Proposed mechanism of oxidation of thioamide **317** by singlet oxygen.

As shown in Table 2.11, the proton signal of thioacetamide **336** appears at 2.40 ppm in deuterated DMSO^{†††} while the proton signal of thioacetamide S-oxide **337**, reported by Sarma and Hanzlik,²⁴⁴ appears at 1.94 ppm in the same deuterated solvent. Therefore, the chemical shifts of protons at the α -position of thioamide S-oxide **333** were supposed to also be shifted upfield comparing to those of desired thioamide **317**.



Compound	Thioacetamide 336	S-oxide 337
¹ H NMR δ (ppm)	2.40, s	1.94, s

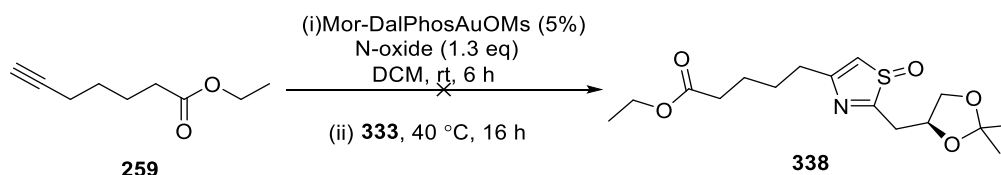
Table 2.11 Comparison of ¹H NMR of thioacetamide **336** and thioacetamide S-oxide **337** in DMSO-d₆.

In the literature, the chemical shifts of protons at the α -position of thioamides appear at 2.7 – 3.7 ppm in deuterated chloroform. The obtained proton shifts of the α -position of thioamide S-oxide **333** in deuterated chloroform appears at 3.04 and 2.91 ppm. Therefore, we reviewed the 2.9 – 4.0 ppm region in the ¹H NMR spectra of reaction aliquots at various time points of the reaction. Surprisingly, we could not find any evidence of the existence of thioamide **317**. This suggested that the oxidation process occurred so rapidly that the sulfur atom of thioamide **317** was fully oxidised in the preparation of aliquot

^{†††}¹H NMR data obtained in our laboratory using thioacetamide purchased from suppliers.

samples for NMR analysis. Such a rate of oxidation was unexpected because the photochemical oxidation of thioamide normally requires use of photosensitiser to speed up the reaction rate.²⁴¹

However, in the interest of examining whether the oxidised thioamide **333** could be transformed into the thiazole *S*-oxide product **338**, which could potentially allow access to a novel oxidised analogue of PatA, we then attempted to couple *S*-oxide **333** and the alkyne **259** following the gold-catalysed conditions reported by Zhang.¹⁴¹ Unfortunately, no sign of formation of the desired product was observed and only the mesylate intermediate **273** (*vide supra*, Table 2.7) was recovered (Scheme 2.46). Consequently, it would be reasonable to propose that the decreased nucleophilicity of the sulfur atom resulting from the electron-withdrawing S=O bond renders it incapable of reacting in the cyclocondensation step of the thiazole formation.



Scheme 2.46 Attempted synthesis of thiazole *S*-oxide **338**.

2.5.2 Attempted Preparation of Air-Stable Thioamides

In light of the finding that the thioamide **317** was oxidised rapidly when exposed to air, attention was then focused on structural modifications of the thioamide which could potentially improve its stability. After reviewing structures of thioamides reported in Romo's⁸² and Pattenden's²⁴⁵ studies on the total synthesis of PatA, and **223** in our work (Figure 2.9), we hypothesised that the presence of bulky protecting groups, like TIPS and TBS, could be a stabilising factor against oxidation.

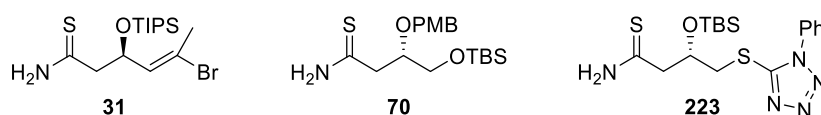
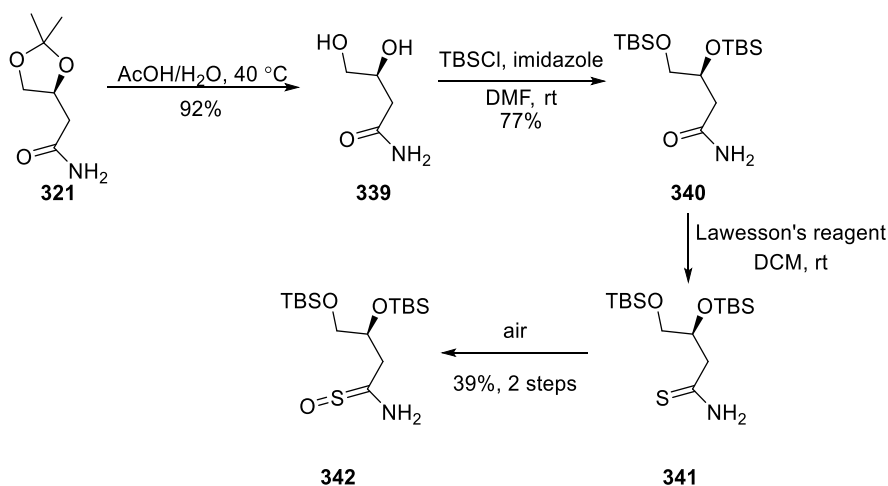


Figure 2.9 Structures of air-stable thioamides in Romo's,⁸² Pattenden's²⁴⁵ and this work.

To test whether the introduction of two TBS groups could protect the sulfur atom from the undesired oxidation, we set out to prepare thioamide **341**. Amide **321** was reacted with acetic acid and water, followed by double-silylation to provide amide **340**. Bis-silylated amide **340** was then treated with Lawesson's reagent. (Scheme 2.47).



Scheme 2.47 Attempted preparation of thioamide **341**.

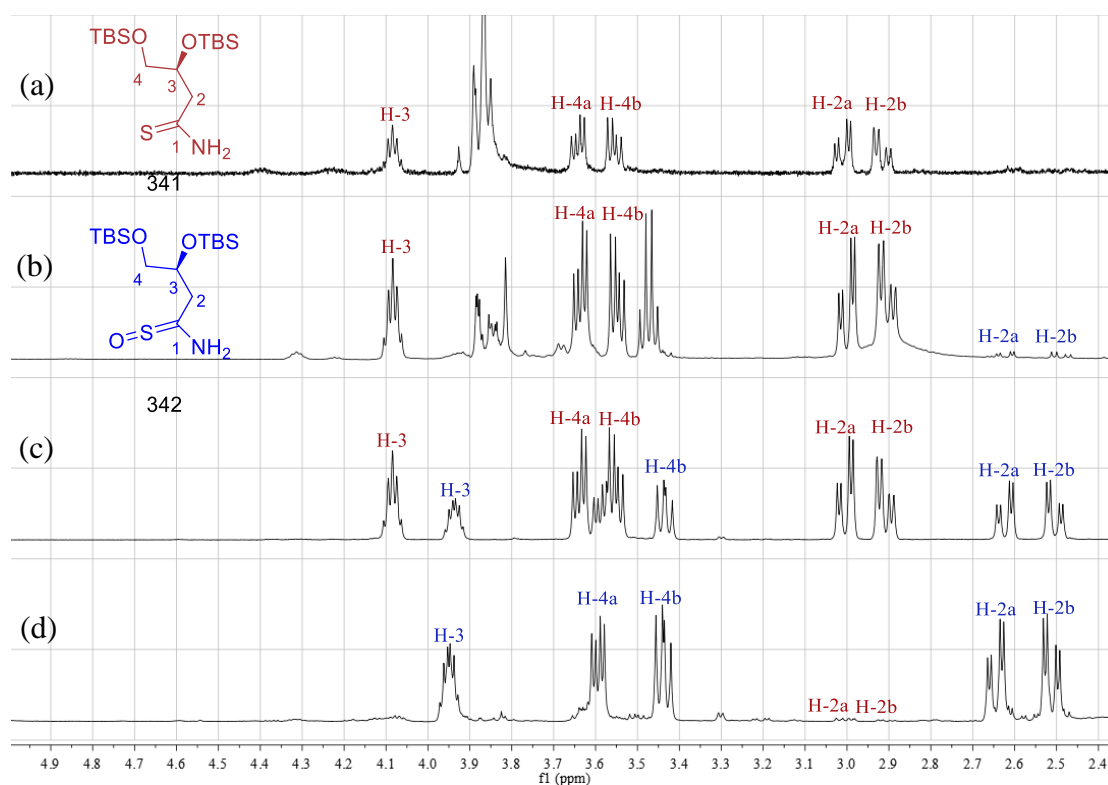
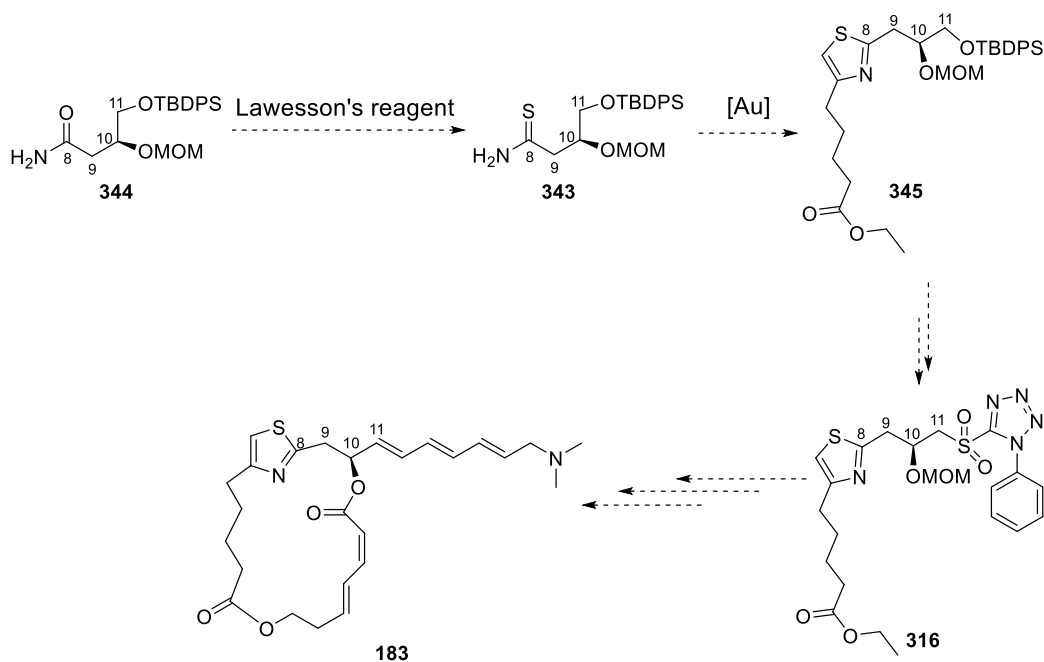


Figure 2.10 Observed oxidation of thioamide **341** based on analysis of ^1H NMR spectra of mixtures at different time points: (a) before quenching by aqueous NaHCO_3 solution; (b) after extraction by ethyl acetate; (c) during purification by silica gel chromatography; and (d) post-column concentration under vacuum at room temperature.^{†††}

Gratifyingly, as shown in Figure 2.10, aerobic oxidation of the thioamide **341** was clearly slowed down to some extent based on intensive ^1H NMR investigation throughout the work-up and purification process. Consequently, it was reasonable to propose that replacing the TBS group with bulkier *tert*-butyldiphenylsilyl (TBDPS) protecting group would further retard the oxidation. The synthetic route for sulfone **316** was then modified to use a potential air-stable thioamide **343** as the major fragment, which could be prepared from amide **344** (Scheme 2.48).

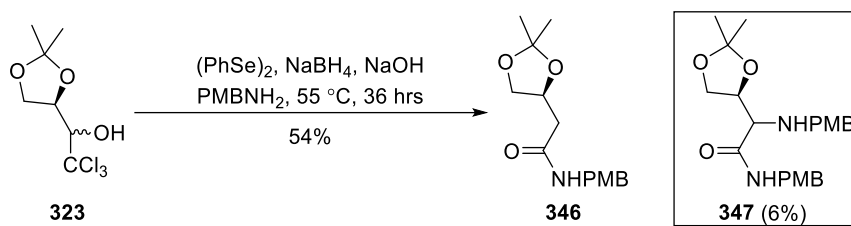
^{†††}Thioamide **341** with peaks at (500 MHz, CDCl_3) δ 4.12 – 4.04 (m), 3.64 (dd, J = 10.3, 5.1 Hz), 3.55 (dd, J = 10.3, 5.9 Hz), 3.00 (dd, J = 14.4, 4.5 Hz) and 2.91 (dd, J = 14.4, 5.6 Hz), compared to thioamide S-oxide **342** with peaks at (500 MHz, CDCl_3) δ 3.97 – 3.90 (m), 3.59 (dd, J = 10.2, 4.9 Hz), 3.43 (dd, J = 10.1, 7.8 Hz), 2.62 (dd, J = 15.0, 4.5 Hz), and 2.50 (dd, J = 15.0, 4.4 Hz).



Scheme 2.48 Proposed synthetic route for PatA analogue **183** using thioamide **343**.

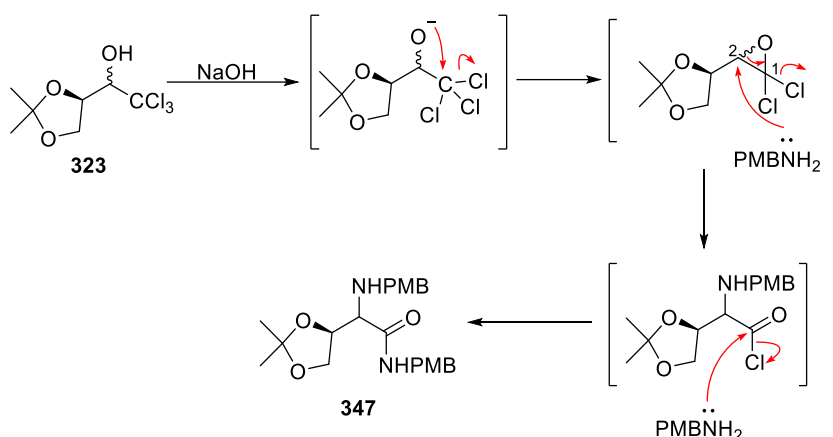
It has been reported that the *para*-methoxybenzyl (PMB) protecting groups of amides could be cleaved by treatment with one-electron oxidising agent ceric ammonium nitrate,²⁴⁶ which could be compatible with the MOM protecting group. Therefore, to avoid the likely chemoselectivity issues with MOM protection between a primary amide and a secondary alcohol, we decided to use *para*-methoxybenzylamine (PMBNH₂) as opposed to ammonia in ethanol to prepare secondary amide **346** (Scheme 2.49). Another benefit is that the PMB-protecting group could also facilitate the reaction monitoring and purification process because of it being a chromophore easily visualised by UV on TLC plates.

To our delight, following Snowden and co-workers' optimised condition,²³² the one-pot reaction provided amide **346** in reasonable yield. In addition, a minor product was isolated in isomerically pure form, and 2D NMR and HRMS investigations revealed it to be α -substituted amide **347** (Scheme 2.49).



Scheme 2.49 Preparation of PMB-protected amide **346**.

The formation of the side product **347** could be attributed to the nucleophilicity of the nitrogen atom resulting from the strong electron-donating effect of the PMB group. As shown in Scheme 2.50, PMBNH_2 acts as a nucleophile to attack the highly electrophilic *gem*-dichloroepoxide intermediate at C2 to give the acid chloride intermediate, which rapidly reacted again with PMBNH_2 to provide the substituted amide **347**.

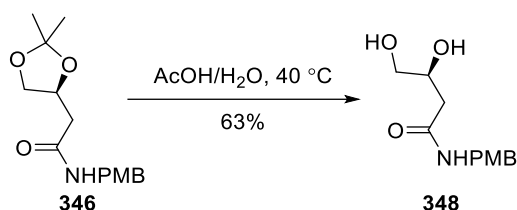


Scheme 2.50 Proposed mechanism for formation of α -substituted amide **347**.

Since a mixture of diastereomers **323** was used in the reaction, it was conceived that a mixture of diastereomers of **347** would be generated through the proposed mechanism but only one stereoisomer was obtained. Considering that the other isomer of amide **347** might be lost in the purification process, the reaction was then repeated on a larger scale and intensive ^1H NMR experiments of aliquot samples were conducted. However, no evidence of formation of the other diastereomer of **347** was observed. This indicates stereospecificity in the by-product formation, which is possibly due to different reaction rates of epoxide formation from **323**. To unambiguously determine the stereoselectivity of this concomitant side reaction, it would be necessary to assign the configuration of the new-forming chiral centre of the isolated by-product through chiral derivatisation of the primary amine,²⁴⁷ which could be readily prepared by selective removal of the PMB

protecting group. However, due to time constraints, this was not further explored during the course of this Ph.D. project.

With the PMB-protected amide in hand, we then attempted to prepare amide **342**, the precursor of thioamide **343**. Amide **346** was first treated with acetic acid in water to give diol product **348** (Scheme 2.51).



Scheme 2.51 Preparation of diol **348**.

¹H NMR spectrum of the diol product **348** obtained in deuterated chloroform showed a broadened singlet centred at δ 2.19 with an integration of 1.00 and another broadened singlet centred at δ 4.00 with an integration of 1.00 (see Figure 2.11), and the large downfield chemical shift was possibly due to the internal hydrogen bonding interaction between the secondary alcohol and the carbonyl group. It is well known that hydrogen bonding interactions can reduce the acidity of alcohols and inhibit their reactions with bases.²⁴⁸ Hence, this internal hydrogen bonding could be beneficial for the subsequent selective silylation of the primary OH.

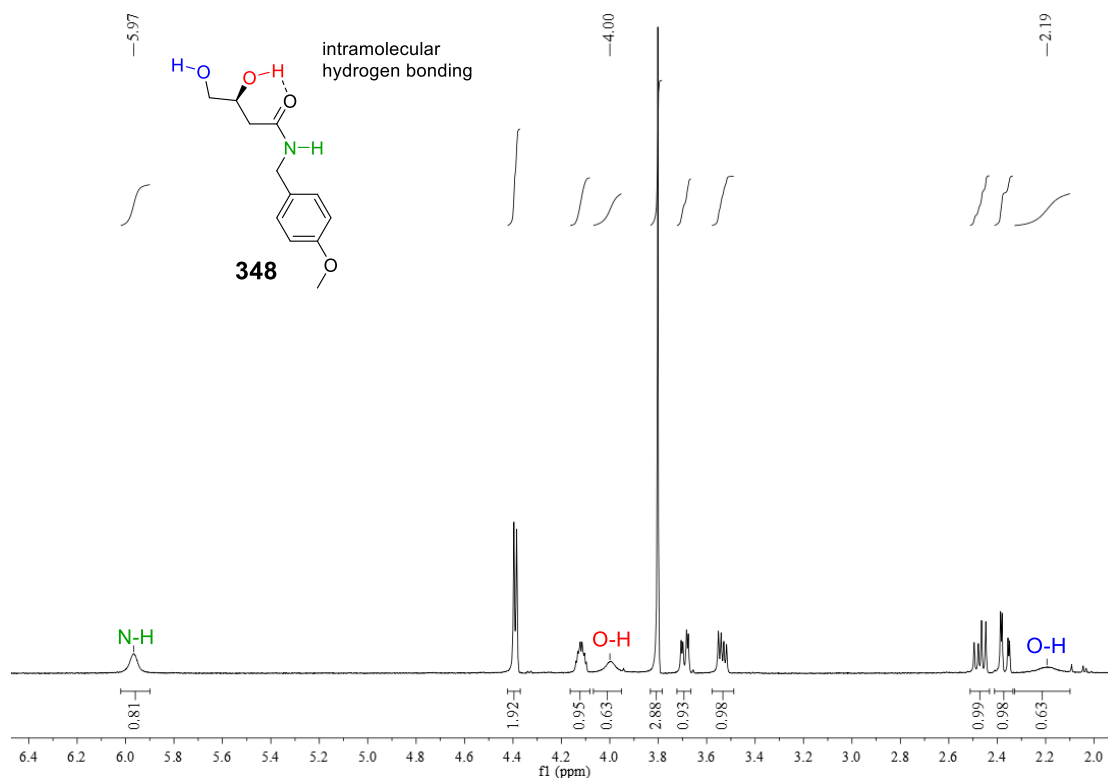
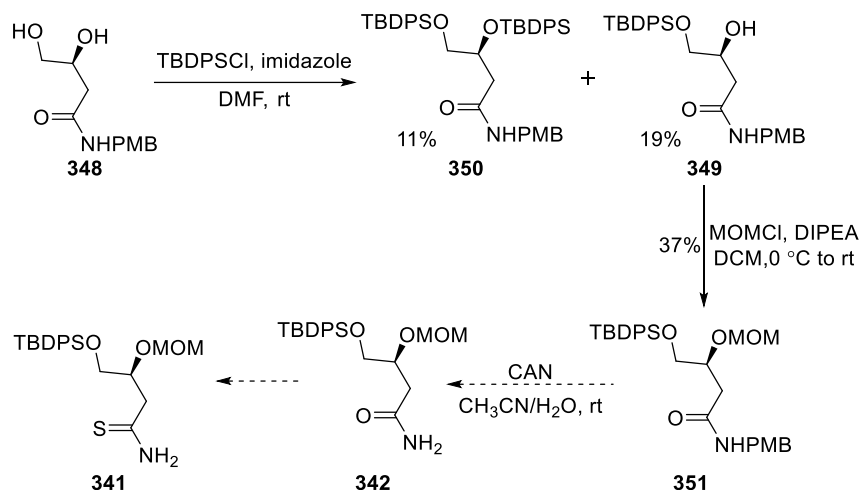


Figure 2.11 ^1H NMR evidence of possible internal hydrogen bonding interaction between secondary OH and carbonyl group in diol **348** (^1H NMR run in CDCl_3). (Assigned using gCOSY NMR)

As the use of a nonpolar solvent would promote such intramolecular hydrogen bonding interaction and facilitate the selectivity, the diol **348** was initially treated with 1 equivalent of TBDPSCl and imidazole in DCM, a relatively nonpolar solvent. Unexpectedly, the desired mono-silylated product **349** was obtained in less than 3% yield with 70% recovery of the diol starting material. The poor yield was possibly because the polar diol was poorly solubilised in DCM. Given that selective TBDPS silylation of 1,2-diols has been used with great regularity in organic synthesis, we then changed to use a polar aprotic solvent DMF, which should sufficiently solubilise diol **348** *via* intermolecular hydrogen bonding, with the thought that the bulkiness of TBDPS could counteract the disrupted intramolecular hydrogen bonding. To our dismay, the reaction in DMF provided both mono-silylated product **349** and *bis*-silylated product **350** in poor yields (Scheme 2.52). However, no further optimisation was performed for this step at this stage, and we moved onto the next step to test the feasibility of this route. Protection of the secondary OH with MOMCl and DIPEA provided the product **351** in an uninspiring yield, which was attributed to the potential internal hydrogen bonding similar to that seen in diol **348**.

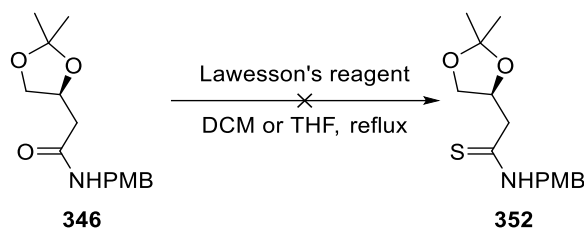
Repeating the reaction with more active methoxymethyl iodide, which was prepared *in situ* by mixing MOMCl and sodium iodide, at higher temperatures resulted in significant degradation of the substrate, with possible cleavage of the PMB protecting group observed and no evidence of forming any desired MOM ether. In light of the lack of high-yielding steps, this route was not pursued.



Scheme 2.52 Attempted preparation of thioamide **343** starting from diol **348**.

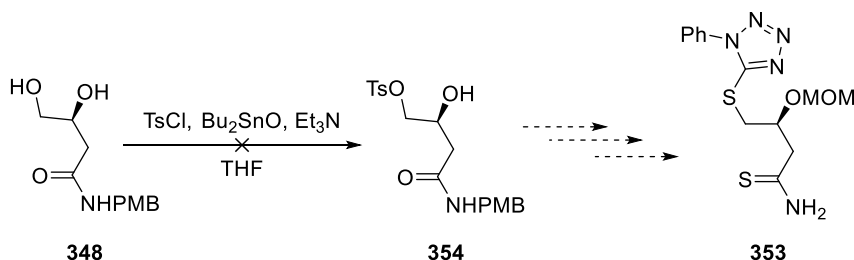
The low yields of these two protection steps were possibly consequences of interference by the intramolecular hydrogen bonding between the secondary OH and the carbonyl group. As sulfur atoms are known to be poor hydrogen bond acceptors,²⁴⁶ we then attempted to transform the amide **346** into thioamide **352** with the hope that the absence of internal hydrogen bonding could improve the yields of the following protection steps. A literature search suggested that thionation reactions of protected amides normally require higher reaction temperatures (*e.g.*, reflux in 1,2-dimethoxyethane or toluene).^{§§§} To avoid the risk of degradation of the acetonide functional group, we first performed the reaction in refluxing DCM. But no significant reaction was observed. When the reaction was repeated in refluxing THF, a mixture of unreacted amide **346**, and unidentified degradation products were obtained, with no sign of thioamide **352** or the *S*-oxide of thioamide **352** observed by HR-MS investigation (Scheme 2.53). This suggested that a further increase in the reaction temperature would possibly lead to significant degradation of the substrate instead of the formation of the desired thioamide.

^{§§§}Using *SciFinder* database; <https://scifinder.cas.org> (accessed April 2018).



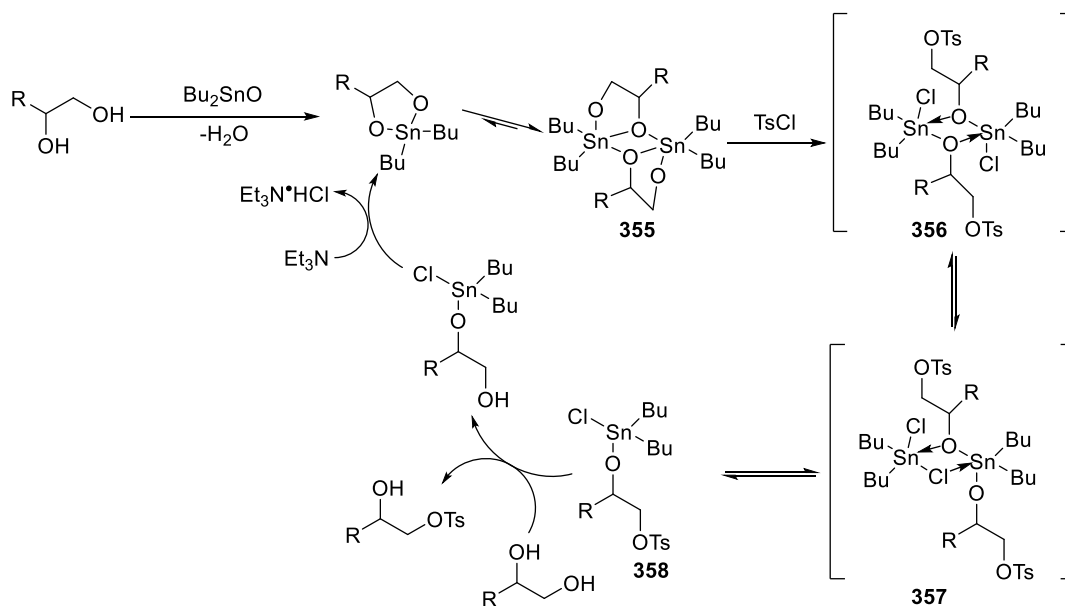
Scheme 2.53 Attempted preparation of thioamide **352**.

With the absence of success in the preparation of the TBDPS-protected thioamide **352**, we decided to move on to the phenyltetrazole functional group as a potential stabiliser for the sulfur atom, even though it is considered to be less bulky than TBDPS protective group. Thus, attempts were made to prepare thioamide **353** starting from mono-tosylation of diol **348**. Surprisingly, when the diol was treated with catalytic Bu_2SnO , TsCl and 1 equivalent of Et_3N , only the starting material **348** was recovered and no evidence of formation of mono-tosylate **354** was observed (Scheme 2.54) by HRMS investigation.



Scheme 2.54 Attempted preparation of mono-tosylated amide **354**.

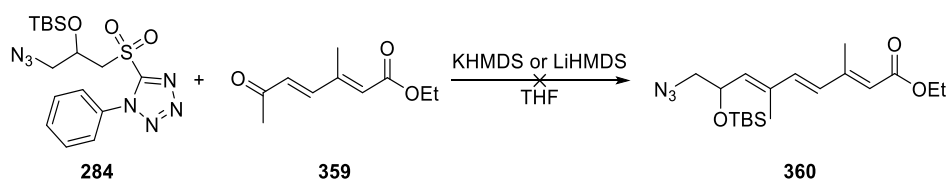
Based on the proposed mechanism of Bu_2SnO catalysed selective tosylation of diol (Scheme 2.55),²⁴⁹ the reaction proceeds *via* a dimeric species **355**, which can be sulfonylated by *p*- TsCl to produce intermediates **356** and **357**. Et_3N acts as a nucleophile and helps to break up dimer intermediates **356** and **357** to furnish intermediate **358**. Thus, it was proposed that the sluggishness of the tosylation reaction of diol **348** was a consequence of the existence of the secondary amide functional group. Normally, the nitrogen atom on an amide is less nucleophilic than the nitrogen of an amine because the amide carbonyl group can provide the resonance stabilisation of the nitrogen lone pair electrons. However, the electron-donating effect of the PMB protective group could possibly make the nitrogen atom on the amide **348** more nucleophilic and to be able to interfere with the break-up process of dimeric intermediates, resulting in the incomplete catalytic cycle.



Scheme 2.55 Proposed mechanism of Bu_2SnO catalysed tosylation by Martinelli and co-workers.²⁴⁹

2.6 Revised Synthesis of Analogue 183

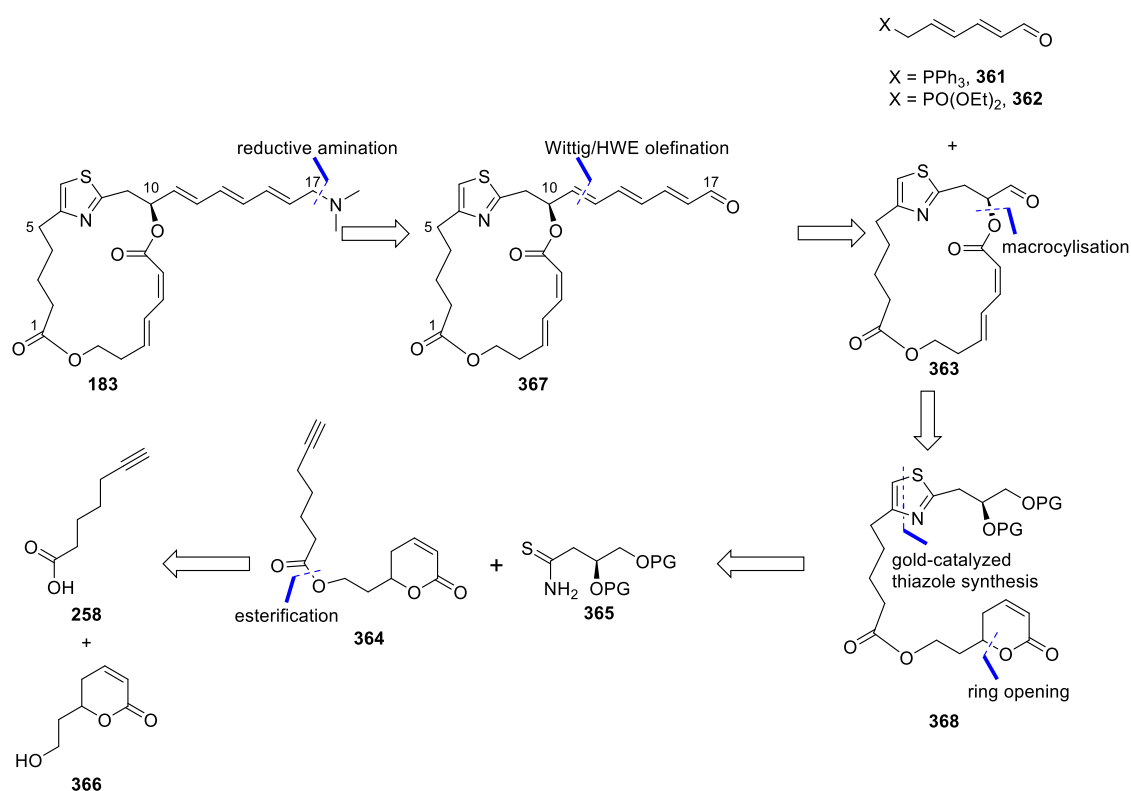
Alongside our efforts to prepare mono-tosylated amide **354** and MOM-protected sulfone fragment **316**, postdoctoral fellow Claire Cuyamendous in our group conducted extensive studies on model reactions between sulfone **284** and ketone **359** to test the feasibility of attaching the methylated side chain fragment (Fragment **II'**, *vide supra*, Section 1.7.2) by Julia-Kocienski olefination, and found that the reaction was sluggish with no conversion (Scheme 2.56).



Scheme 2.56 Cuyamendous' attempted Julia-Kocienski reaction between sulfone **284** and ketone **359**.

Based on this unsuccessful result, it was clear that an alternative strategy for attachment of the side chain fragments was necessary to facilitate the collective syntheses of PaA analogues **183** and **184**.

As shown in Scheme 2.57, to make the most of the existing results from our work, the revised route would involve performing a Wittig/Horner-Wadsworth-Emmons (HWE) olefination with the side chain fragment **361** or **362** and macrocyclic aldehyde **363**. The thiazole core could be constructed *via* the gold-catalysed coupling between alkyne **364** and thioamide **365**. Alkyne **364** could be prepared *via* esterification between 6-heptynoic acid **258** and δ -valerolactone **366**. Owing to the fact that it is no longer necessary to introduce ester protecting groups to avoid inadvertent trapping of the reactive gold carbene with the acid functionality, this route can enable a degree of step economy.²⁵⁰



Scheme 2.57 Revised retrosynthetic analysis of PatA analogue **183**.

As the PatA analogue **184** (see Figure 1.25 in Section 1.7.1) with methylated side chain could provide more information about whether the two methyl groups at C22 and C24 (PatA numbering) on the macrocyclic core are critical for activity, we decided to prioritise the synthesis of analogue **184** rather than the fully non-methylated analogue **183**.

2.7 Conclusion

In conclusion, the key four-carbon fragment, namely thioamide **223**, for the synthesis of thiazole analogue **183** was prepared from an enantiopure epoxide with a 28% yield over 8 steps. However, a degree of racemisation occurred in this reaction sequence, which was determined by Mosher analysis of alcohol intermediate **217**. In the synthesis of nitrile intermediate **222**, a range of reported conditions was screened for the substitution of tosylate **221** with a cyanide source. LiCN generated *in situ* from LiHMDS and acetone cyanohydrin was found to be effective in facilitating this transformation. In the thionation step, it was found the impurities of the purchased Lawesson's reagent could possibly be the cause of the dehydration side reaction and the yield was significantly improved by using further purified Lawesson's reagent.

After optimisation efforts to improve the yield of gold-catalysed thiazole formation, thiazole **276** was obtained in 61% yield. Thiazole-containing sulfone partner **277** required for Julia-Kocienski olefination was prepared successfully using catalytic ammonium heptamolybdate and aqueous hydrogen peroxide.

The side chain fragment **297** was prepared from furan with a 17% yield over 5 steps. However, the reaction of sulfone **277** and aldehyde **297** under Julia-Kocienski reaction conditions resulted in a mixture of degradation products, which was possibly due to the steric hindrance of the TBS group. Attention was then focused on the preparation of an alternative four-carbon fragment, namely, acetonide-protected thioamide **317**. Scalable preparation of amide **321**, the precursor of thioamide **317**, was achieved by employing a 6-step reaction sequence starting from D-mannitol **324**. Thionation of amide **321** was then performed. Unfortunately, thioamide **317** was found to be very unstable and prone to oxidation by air.

It was hypothesised that introducing bulky protecting groups could potentially improve the stability of thioamides. Therefore, attempts to prepare thioamides **341** and **343** were carried out and were found to be unsuccessful. However, the results of these efforts revealed that the presence of bulky protecting groups in thioamides could slow down the aerobic oxidation.

As the Julia-Kocienski olefination was found to be unable to couple the methylated side chain fragment to the sulfone partner in model reactions, the synthetic route was revised

in order to ensure the collective synthesis of targeted analogues. Wittig/HWE reaction would be utilised as opposed to Julia-Kocienski olefination in the new reaction sequence.

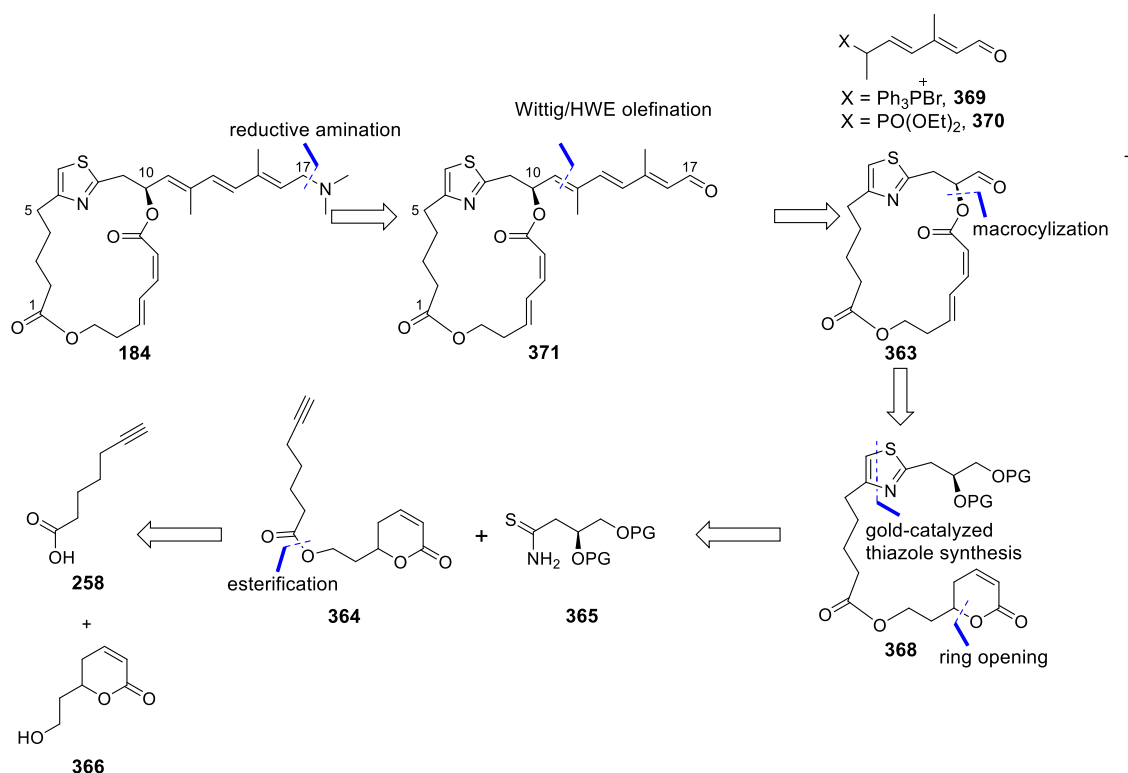
Since analogue **184** could give direct evidence of the importance of the methyl groups on the macrocycle, the synthesis of analogue **184** was prioritised.

Chapter Three: Towards Synthesis of Thiazole Analogue with Methylated Side Chain

As outlined in Section 1.7.1, the synthesis of thiazole analogue **184** with the methylated side chain could help to test whether the two methyl groups at C22 and C24 methyl groups (PatA numbering) are critical for the binding process of PatA to its protein target. This chapter describes the work towards the synthesis of this analogue.

3.1 Retrosynthetic Analysis

As the structural difference between analogue **184** and analogue **183** is the side chain fragment, the synthetic route for analogue **184** could incorporate the same macrocyclic aldehyde intermediate **363**, which was proposed in the retrosynthetic analysis in Section 2.6. As shown in Scheme 3.1, to make the most of our existing synthetic strategy, the thiazole core would be constructed through gold-catalysed thiazole formation using thioamide **365** and alkyne **364** as substrates. The *E*, *Z*-dienoic acid would be produced by base-induced ring opening of δ -valerolactone **368**. The macrocycle would be furnished by using an appropriate macrolactonisation, and the methylated side chain fragment, which could be derived from **369** or **370**, would be coupled with the macrocyclic aldehyde **363** *via* Wittig/HWE olefination. The terminal tertiary amine group in the side chain would be introduced in the final step by reductive amination.



Scheme 3.1 Revised retrosynthetic analysis of PatA analogue **184**.

Preparation of thioamide **365** and alkyne **364**, construction of the macrocycle and synthesis of the side chain fragments will be discussed in the following sections.

3.2 Preparation of Air-stable Thioamide 382

Based on our observations that the aerobic oxidation of sulfur atoms in thioamides could be slowed by introducing bulky protective groups (*vide supra*, Section 2.5.2), compounds **372** and **373** were targeted as potential candidates for air-stable thioamides.

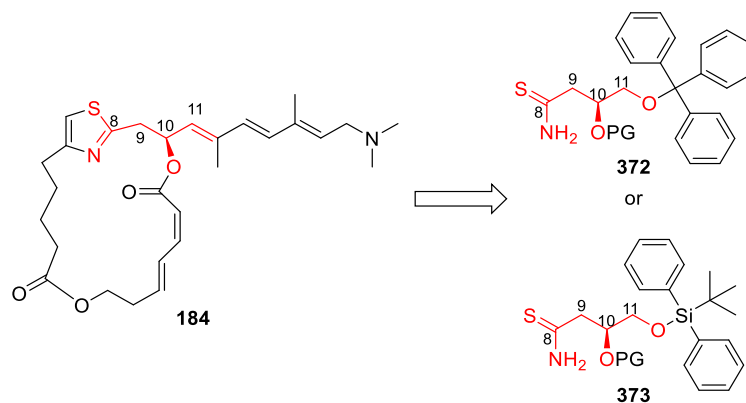
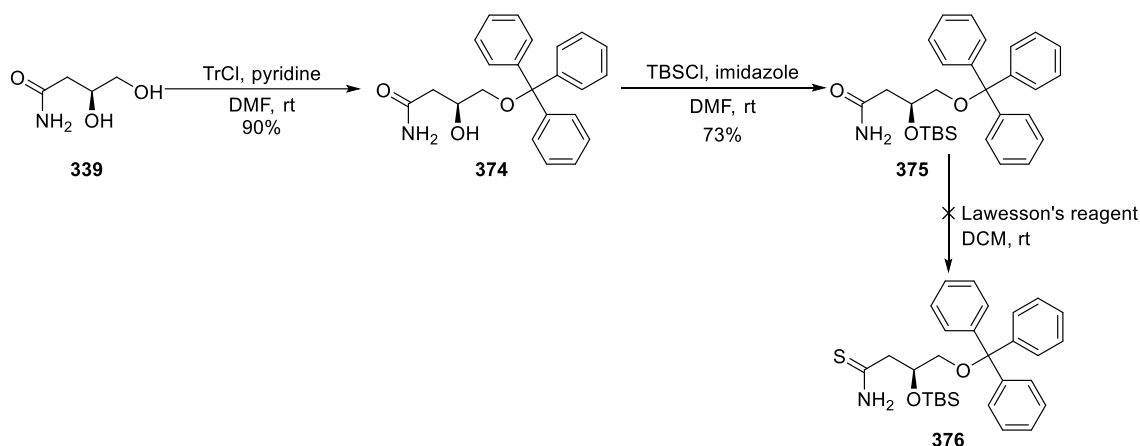


Figure 3.1 Proposed appropriate thioamides **372** and **373** for synthesis of analogue **184**.

As the trityl protecting group is considered to be bulkier than the TBDPS protecting group, we first attempted to prepare tritylated thioamide **372** starting from commercially available amide **339**, which could be also prepared from D-mannitol **324** (*vide supra*, Section 2.5.1).

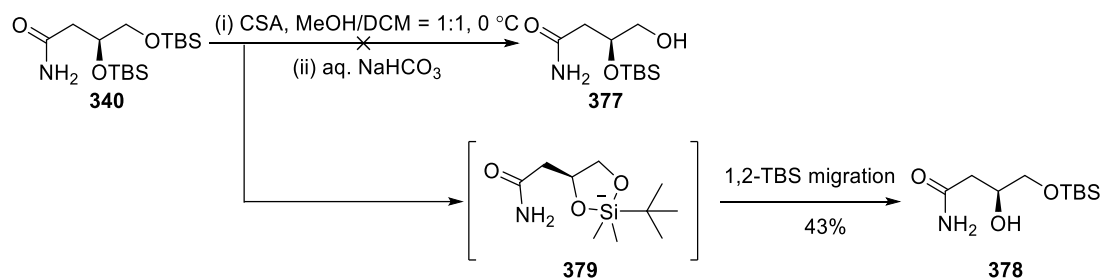
To ensure that the polar amide **339** was fully solubilised to accelerate the tritylation reaction, polar DMF was chosen as the solvent and mono-tritylation of amide **374** was achieved in excellent yield (Scheme 3.2). Considering that the potential hydrogen bonding interaction between the secondary OH and the carbonyl group could interfere with the subsequent silylation reaction, DMF was used again to disrupt the internal hydrogen-bonding and the desired product **375** was obtained in 73% yield. Thionation of amide **375** by treatment with Lawesson's reagent afforded a mixture of degradation products, one of which was identified to be predominately triphenylmethanol by comparison with literature NMR values.²⁵¹ This suggested that the degradation was possibly caused by the incompatibility of the trityl ether with Lawesson's reagent.



Scheme 3.2 Attempted preparation of thioamide **376**.

This unexpected failure prompted us to turn our attention to the synthesis of the TBDPS-protected thioamide **373**. As discussed in Section 2.5.2, we encountered difficulties in mono-silylation of amide **348**, which was possibly due to the intramolecular hydrogen bonding. Assuming that mono-silylation of amide **339** would not provide good regioselectivity between primary OH and secondary OH, we opted to start from selective desilylation of amide **340** for preparation of thioamide **373** because a substantial amount of amide **340** was available from previous work (see Section 2.5.2 for the details for the preparation of amide **340**)

The *bis*-TBS protected amide **340** was treated with (\pm)-10-camphorsulfonic acid (CSA) and the formation of desired amide **377** was observed by ^1H NMR analysis of reaction aliquots. However, it rapidly isomerised to amide **378** when saturated NaHCO_3 aqueous solution was used to quench the reaction (See Figure 3.2 for comparison of ^1H NMR of amide **377** and **378**). This isomerisation presumably occurred *via* a pentacoordinate silicon intermediate **379**²⁵² and could be explained by less molecular crowding and the formation of the internal hydrogen bonding between the $-\text{NH}_2$ and the secondary OH or between the carbonyl group and the secondary OH. Given that the presence of a base is requisite for silylation reactions, this undesired 1,2-silyl migration prompted by basic conditions would possibly also occur in TBDPS protection of TBS-protected amide **377**. Thus, we abandoned this approach and decided to move on to preparing thioamide **373** from unprotected amide **339**.



Scheme 3.3 Attempted selective desilylation of amide **340**.

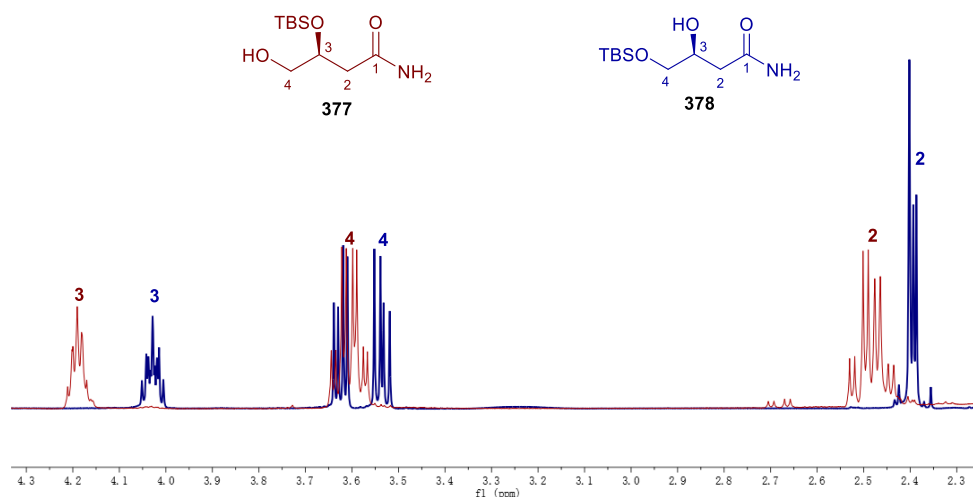
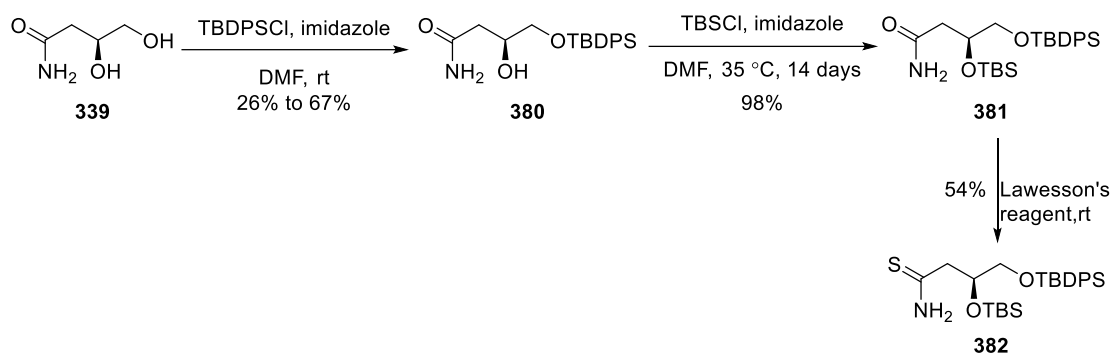


Figure 3.2 Comparison of δ 4.3 – 2.3 ppm region in ^1H NMR of amide **377** (in maroon) and **378** (in blue).****

Gratifyingly, initial treatment of amide **339** with one equivalent of TBDPSCl in DMF provided the desired mono-silylated amide **380** as the sole product, albeit in 26% yield (Scheme 3.4). It was proposed that the uninspiring yield was a consequence of substantial material loss in the aqueous work-up procedure to remove DMF. For this reason, in subsequent attempts, DMF was removed by distillation under reduced pressure and the yield was improved to 67%. Subsequent silylation by treatment with TBSCl produced the desired amide **381** in excellent yield. However, the reaction was sluggish, prompting us to seek an alternative less bulky silyl protecting group for the secondary OH. Given that the trityl protecting group could be cleaved under treatment with Lawesson's reagent, it was reasonable to propose that the trimethylsilyl (TMS) group was not compatible with the following thionation step. Because the triethylsilyl (TES) group was more susceptible to acid hydrolysis when compared to TBS, which could potentially facilitate desilylation

**** Based on analysis of the ^1H NMR and gCofsy spectra. Amide **377** (500 MHz, CDCl_3) δ 4.19 (tt, J = 5.8, 4.6 Hz, 1H, H-3), 3.63 (dd, J = 11.4, 4.8 Hz, 1H, H-4), 3.58 (dd, J = 11.4, 4.3 Hz, 1H, H-4), 2.51 (dd, J = 14.5, 5.6 Hz, 1H, H-2), 2.46 (dd, J = 14.5, 5.9 Hz, 1H, H-2), compared to amide **378** (500 MHz, CDCl_3) δ 4.03 (tt, J = 6.9, 4.7 Hz, 1H, H-3), 3.62 (dd, J = 10.0, 4.6 Hz, 1H, H-4), 3.54 (dd, J = 10.0, 6.6 Hz, 1H, H-4), 2.41 – 2.38 (m, 2H, H-2).

under milder conditions before the macrolactonisation step, the seemingly less bulky TES group was chosen to substitute TBS. Unfortunately, treatment of amide **380** with TESCl and imidazole for 7 days at 35 °C resulted in no significant reaction, suggesting that the TES group was possibly effectively bulkier than the TBS group in this circumstance.



Scheme 3.4 Preparation of thioamide **382**.

Thionation of amide **381** by Lawesson's reagent was performed at room temperature under argon atmosphere. As the amide starting material **381** and the by-product generated from Lawesson's reagent were indistinguishable on TLC plates, the reaction was monitored by ^1H NMR analysis of the reaction aliquots. After 30-minute stirring at room temperature, the α -proton signals of amide **381** at 2.66 and 2.42 ppm disappeared, indicating the conversion was completed. The reaction was then quenched and the desired thioamide **382** was isolated by silica gel chromatography. However, as shown in Figure 3.3a, partial oxidation by air was still observed by ^1H NMR analysis after product fractions from column chromatography being concentrated under reduced pressure at room temperature (18 to 20 °C). Despite that, it was clear that oxidation rate of thioamide **382** was slower than that of the *bis*-TBS protected thioamide **341** (see Section 2.5.2 for observed oxidation of thioamide **341**). Assuming that the concentrated product was more susceptible to oxidation by air than when dissolved (*e.g.*, in column fractions), we then performed solvent evaporation of column fractions at 10 °C under vacuum, and used nitrogen to backfill the rotary evaporator when opening the stopcock on the rotary evaporator after column fractions had completed evaporating to reduce exposure of the concentrated sample to air. Gratifying, after taking these protective measures, we obtained thioamide **382** in high purity (Figure 3.3b), albeit in moderate yield (54%).

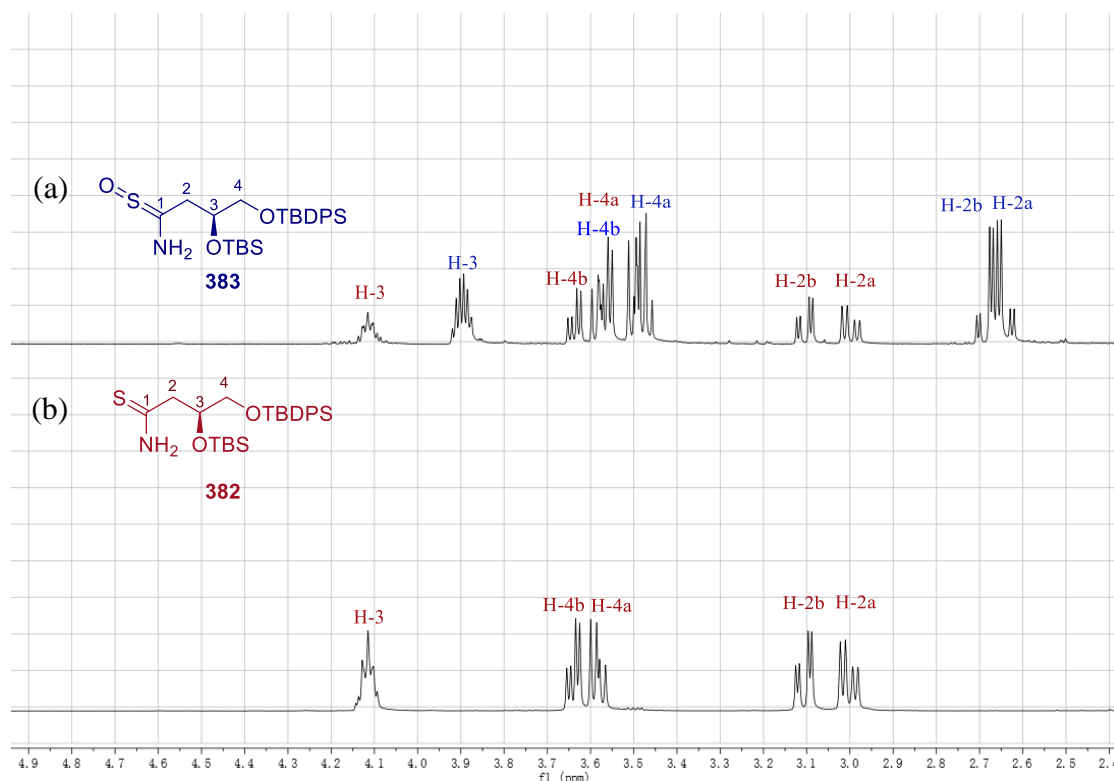


Figure 3.3 Comparison of ^1H NMR spectra of obtained thioamide **382** samples: (a) without exclusion of air in the concentration of column fractions after chromatography; and (b) under an inert atmosphere in the concentration of column fractions after chromatography.^{††††}

In summary, trityl-protected thioamide **376** and TBDPS-protected thioamide **382** were chosen as potential candidates for air-stable thioamides. Efforts to prepare thioamide **376** by thionation of trityl-protected amide **375** were unsuccessful due to the incompatibility of the trityl ether with Lawesson's reagent. In order to prepare thioamide **382**, selective desilylation of *bis*-TBS protected amide **340** was performed and it was found that the desired amide **377** rapidly isomerised to amide **378** under mild basic conditions. Thioamide **382** was then prepared from amide **339** in three steps. However, it was necessary to take extra measures to exclude exposure to air in the concentration of product

^{††††} Based on analysis of the ^1H NMR and gCoty spectra. Thioamide *S*-oxide **383** (500 MHz, CDCl_3) δ 3.93 – 3.86 (m, H-3), 3.57 (dd, $J = 10.3, 4.8$ Hz, H-4b), 3.49 (dd, $J = 12.3, 7.9$ Hz, H-4a), 2.69 (dd, $J = 14.9, 4.0$ Hz, H-2b), 2.64 (dd, $J = 14.9, 4.6$ Hz, H-2a), compared to thioamide **382** (500 MHz, CDCl_3) δ 4.14 – 4.08 (m, H-3), 3.64 (dd, $J = 10.3, 4.6$ Hz, H-4b), 3.58 (dd, $J = 10.4, 6.8$ Hz, H-4a), 3.10 (dd, $J = 14.4, 4.1$ Hz, H-2b) and 3.00 (dd, $J = 14.4, 6.0$ Hz, H-2a).

fractions after chromatography to ensure that thioamide **382** was obtained in high purity.

3.3 Preparation of Alkyne **364**

As mentioned in Section 3.1, alkyne **364** could react with thioamide **382** to furnish the thiazole ring through a gold-catalysed coupling reaction. The δ -lactone motif of the alkyne could be unfolded to provide the *E,Z*-dienoic acid under basic conditions. This fragment could provide most of the skeleton of the macrocycle core for the synthesis of PatA analogue **184** (Figure 3.4) and it has been previously utilised in Cumming's synthesis of triazole analogue **182** (see Figure 1.23 in Section 1.6).¹³⁴ Thus, we largely followed the reported procedures for its synthesis.

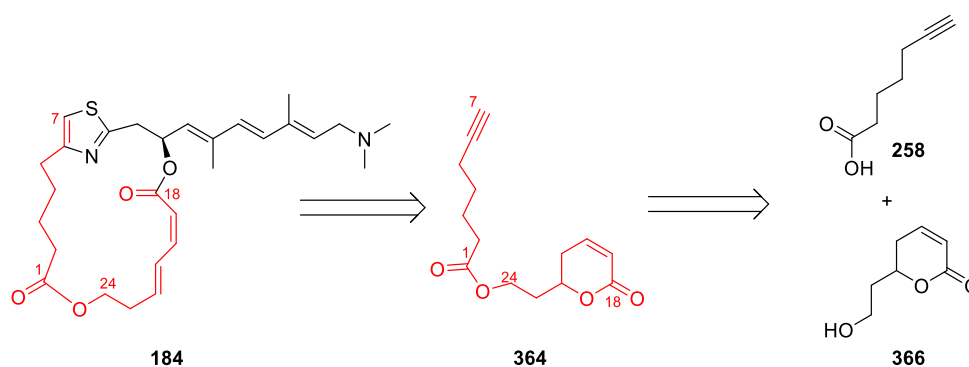
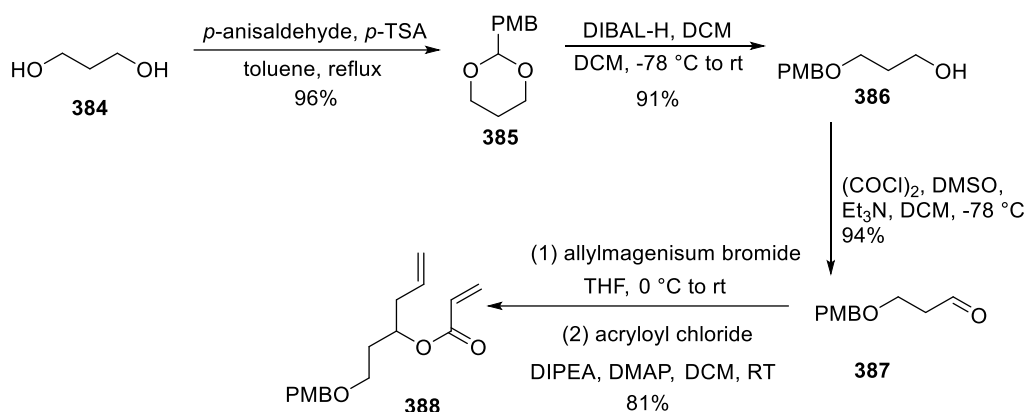


Figure 3.4 Proposed alkyne fragment **364** for the synthesis of PatA analogue **184**.

As shown in Scheme 3.5, in the presence of catalytic *p*-TSA, commercially available 1,3-propanediol **384** was reacted with *para*-anisaldehyde in a Dean-Stark apparatus to provide acetal **385**. Subsequent reductive cleavage of acetal by DIBAL-H at -78 °C afforded mono-alcohol **386**, which was then subjected to typical Swern conditions to provide aldehyde **387**. The one-pot reaction of aldehyde **387** with allylmagnesium bromide and acryloyl chloride gave diene **388** in 81% yield on a modest scale (e.g., 0.59 gram). However, when the reaction was repeated on a larger scale (e.g., 5 gram), it was noticed that the purified diene **388** polymerised when the product fractions after chromatography purification were heated at 40 to 50 °C on a rotary evaporator to remove solvent for a prolonged period of time. In addition, the purified diene **388** from the small-scale reaction was found to polymerise slowly even on storage in the freezer at -20 °C. The polymer was largely insoluble in deuterated solvents, and therefore, the nature of the polymerised products could not be determined by NMR techniques.



Scheme 3.5 Preparation of diene **388** starting from 1,3-propanediol **384**

Since various options for the formation of acrylate polymers, including anionic, cationic and radical polymerisation, have been widely reported and they have been utilised in numerous applications, like plastics and adhesives industry,²⁵³ we initially proposed that self-initiated spontaneous thermal polymerisation without the addition of radical initiators was possibly the cause of the observed polymerisation process.^{254, 255} However, this type of radical polymerisation of acrylates normally requires employing high temperature (>100 °C).²⁵⁵ It seems unlikely that diene **388** could polymerise rapidly at moderate temperatures (*e.g.* 40 to 50 °C) without the involvement of radical initiators.

Instead, we proposed that an alternative potential cause for the degradation of the diene **388** was the acid lability of PMB protective group. A catalytic amount of HCl might be introduced to column fractions by sand used in preparing columns, which was washed by acid in production and could contain up to 0.2% HCl according to its recorded manufacturing parameter. This could cause small amounts of deprotection of product **388**, which could lead to polymerisation by oxa-Michael addition of the unprotected alcohol **389** to the acrylate of the lactone (Figure 3.5).

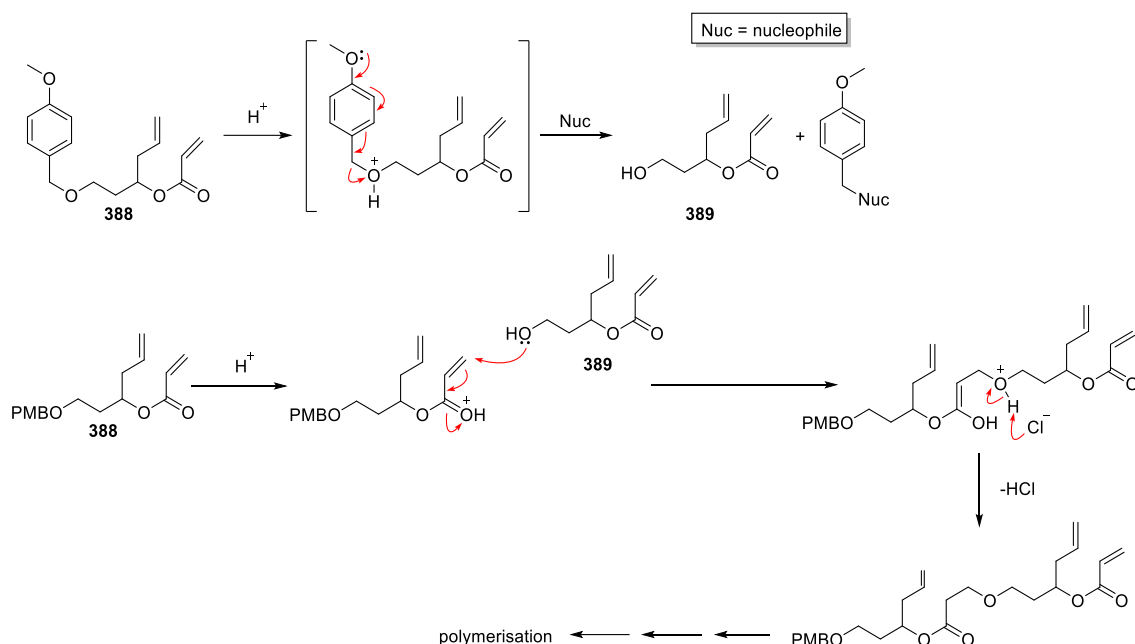
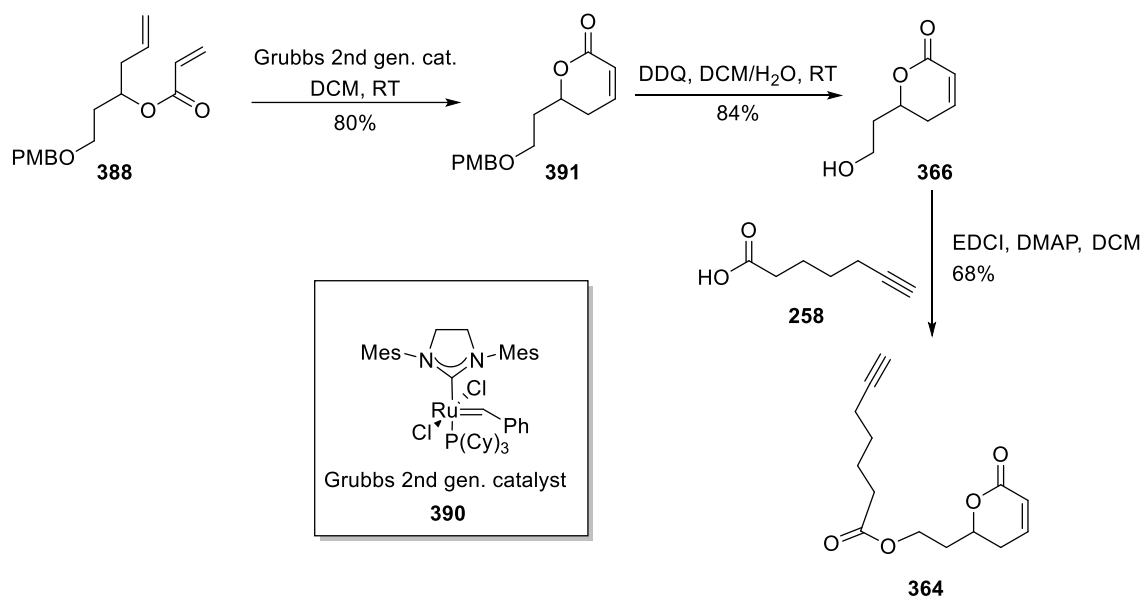


Figure 3.5 Proposed polymerisation of diene **388** caused by cleavage of the PMB group.

In view of the above discussion, acid-washed sand was replaced with neutral sodium sulfate in the following preparation of columns for purification of diene **388**. To our delight, it seemed that this practice did prevent the occurrence of polymerisation, because the pure monomeric diene **388** was obtained on a 5-gram scale with 80% yield even after the concentrated diene was heated at 40 to 50 °C on the rotary evaporator for a relatively prolonged period of time.

Diene **388** then underwent ring-closing metathesis in the catalysis of Grubbs' 2nd generation catalyst **390** to afford δ -lactone **391** (Scheme 3.6). Cleavage of the PMB ether of lactone using DDQ provided alcohol **366**, which was then coupled with hept-6-ynoic acid **258** under modified Steglich esterification conditions to afford the desired alkyne **364**. The yield of alkyne over 7 steps was 30%, which was lower than the 43% global yield reported by Cumming.¹³⁴ It is worth mentioning that alkyne **364** was obtained in racemic form and both isomers were used for the following reaction sequence because the chiral centre will be removed by elimination in the base-induced ring-opening reaction of the δ -lactone.

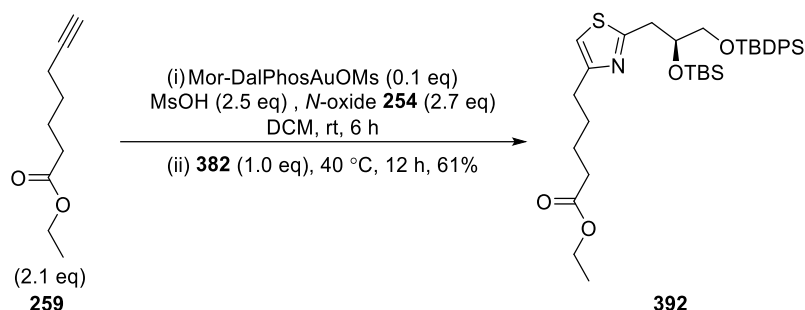
Scheme 3.6 Preparation of alkyne **364**.

3.4 Preparation of Thiazole And C7-Substituted Thiazole

3.4.1 Preparation of Thiazoles **392** and **393**

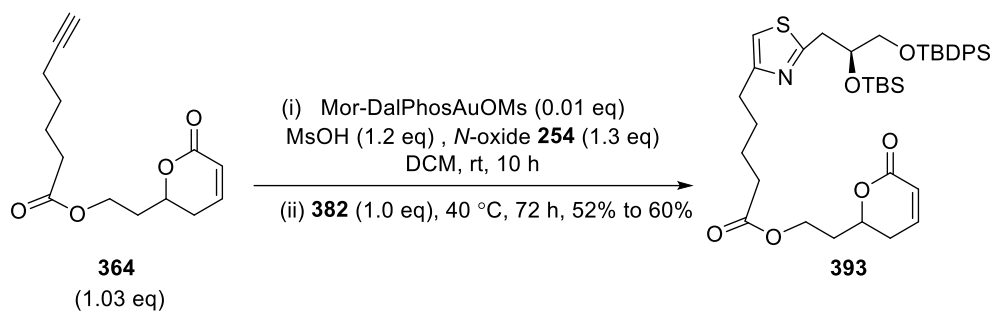
The use of a gold-catalysed formation of the thiazole was discussed in Section 2.3.2. As gold alkene complexes have attracted considerable attention in the area of organometallic chemistry,¹⁴⁴ we were concerned whether the conjugated C=C double bond or the two oxygen atoms in the δ -lactone motif of alkyne **364** could interfere with the function of the gold catalyst. In light of the fact that the *bis*-silylated thioamide **382** could be partially oxidised to form the corresponding thioamide *S*-oxide **383** after a short exposure to air at room temperature (18 to 20 °C), we were also concerned about its stability when heated at 40 °C with a mesylate intermediate in the cyclocondensation stage of the gold-catalysed thiazole formation. Thus, a model reaction using alkyne **259** was first performed to test the compatibility of the thioamide **382** under gold-catalysed conditions. This model reaction was conducted under the optimised conditions (see Section 2.3.2.3). As excess oxidant *N*-oxide **254** was present in the reaction vessel, we were concerned that this could lead to the formation of the undesired thioamide *S*-oxide **383**, which could significantly reduce the efficiency of this transformation. Therefore, intensive ¹H NMR analysis of the reaction aliquots was performed to detect the oxidised by-product after thioamide **3** was added to the reaction mixture. To our delight, the α -proton signals of thioamide *S*-oxide **383** at 2.69 ppm and 2.64 ppm were not observed throughout the heating period,

indicating that the oxidative degradation of thioamide **382** did not occur. Thiazole **392** was obtained in 61% yield and no degradation products of thioamide **382** were observed in this model reaction (Scheme 3.7). This satisfying result suggested that thioamide **382** could serve as a good substrate in this transformation.



Scheme 3.7 Preparation of thiazole **392**.

The gold-catalysed coupling between alkyne **364** and thioamide **382** was first performed on 0.1-gram scale and thiazole **393** was obtained in 60% yield, suggesting that the presence of the lactone motif might have little effect on the performance of the gold carbene. Thus, to test the applicability of this transformation for alkyne **364** on a larger scale, we subjected 0.86-gram of alkyne **364** to the one-pot protocol over 10 hours, following previously optimised conditions used for the preparation of thiazole **276** (see Section 2.3.2.3). As the catalyst loading was lowered to be 1% in this reaction, the consumption rate of thioamide **382** was expectedly slower. ¹H NMR analysis of the reaction aliquots at intervals indicated that the integration of the α-proton signals of thioamide **382** at 3.64 and 3.58 ppm was decreasing while the integration of the proton signal of the thiazole ring at 6.80 ppm was increasing, suggesting that the reaction proceeded smoothly under argon atmosphere. Pleasingly, thiazole **392** was obtained in 52% yield (BRSM yield 57%), with the recovery of a small amount of unreacted thioamide **382** (Scheme 3.8). It is worth mentioning that the diastereomers of thiazole **392** are inseparable by flash chromatography and the isolated product was a mixture of diastereomers.

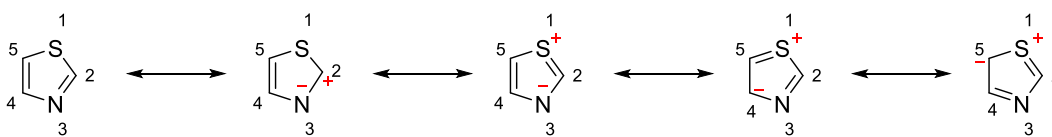
Scheme 3.8 Preparation of thiazole **393**.

3.4.2 Preparation of C-7 Substituted Thiazole

As discussed in Section 1.7.1, we are interested in examining the effects of different substituents of the thiazole ring in PatA on its binding to the protein target. With the thiazole **392** in hand, we were able to explore the feasibility of modifications on the thiazole ring.

3.4.2.1 Preparation of Brominated Thiazole **394**

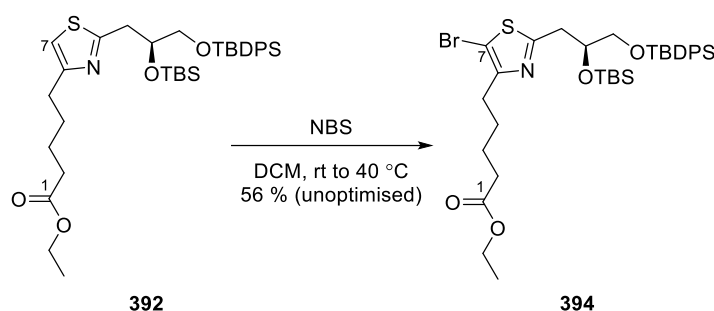
We conceived that a bromo group at the C-5 position (equivalent to the C-7 position of PatA) could be a useful handle to allow the further introduction of an electron-withdrawing or electron-donating group to the thiazole ring for the preparation of PatA analogue **185** or **186** (see Section 1.7.1 for structures). As reflected by the resonance structures of thiazole (Figure 3.6), the C-5 position in the present system of thiazole **392** is the most reactive site for electrophilic substitution.²⁵⁷

Figure 3.6 Resonance structures of thiazole. (Modified from Pola, 2016)²⁵⁸

A literature search^{††††} suggested that the electrophilic phenyl bromination by *N*-bromosuccinimide (NBS) normally requires the addition of activation reagents (*e.g.*, Lewis acid). Thus, we had little concern about the interference of the phenyl groups of the TBDPS protective group in the regioselective bromination of thiazole **392** by solely using NBS. However, the reaction with one equivalent of NBS provided brominated

†††† Using *SciFinder* database; <https://scifinder.cas.org> (accessed July 2018).

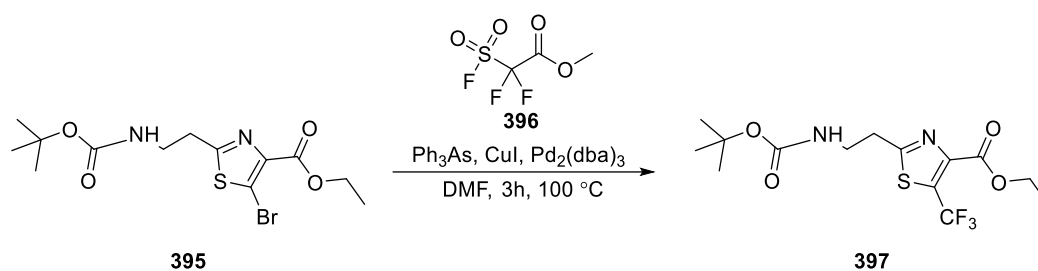
thiazole **394** in only moderate yield (54%) (Scheme 3.9) with an unidentified by-product.



Scheme 3.9 Preparation of brominated thiazole **394**.

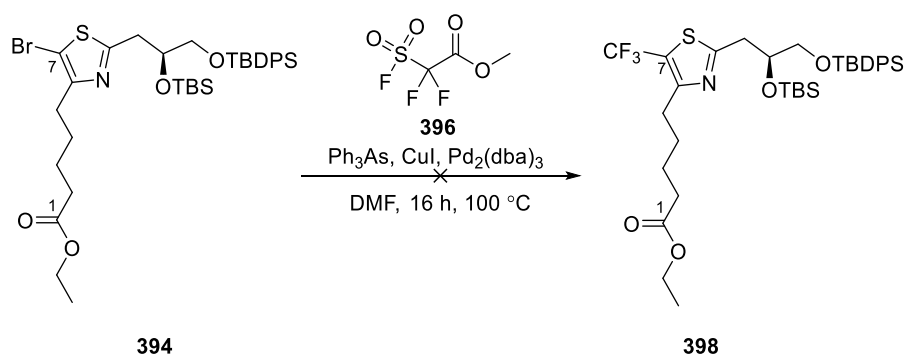
3.4.2.2 Attempted Preparation of Trifluoromethylated Thiazole **398**

As aromatic compounds bearing trifluoromethyl (CF_3) groups have been considered to be privileged motifs in drug discovery because of their unique properties arising from the electron-withdrawing nature, lipophilicity and metabolic stability of CF_3 group,²⁵⁹ a significant number of copper-catalysed methodologies have been developed to achieve formation of aryl- CF_3 bonds, most of which involve formation of reactive $[\text{CuCF}_3]$ species in trifluoromethylation processes and are mainly limited to aryl iodide substrates.^{260, 261} A scan of the literature (see Scheme 3.10 for a selected example) showed that palladium-based methodologies for trifluoromethylation could be appropriate for the preparation of CF_3 -substituted thiazole **395** from brominated thiazole **394**.



Scheme 3.10 Selected example of trifluoromethylation of brominated thiazole.²⁶²

Following the condition used in the synthesis of compound **397**, methyl fluorosulfonyldifluoroacetate **396** was chosen as the CF_3 source, which decarboxylates in the presence of Cu(I) iodide and releases difluorocarbene and fluoride ion to form CF_3^- *in situ*. As shown in Scheme 3.11, trifluoromethylation of thiazole **394** with $\text{Pd}_2(\text{dba})_3$ catalysis in DMF resulted in no significant reaction, with the recovery of bromothiazole **394**.



Scheme 3.11 Attempted preparation of trifluoromethylated thiazole **398**.

The Pd-CF₃ bond in the [Pd(II)(Aryl)(CF₃)] complex has been reported to be relatively inert in the reductive elimination step of the catalytic cycle (Figure 3.7).²⁶¹ For example, Marshall and Grushin discovered that the reductive elimination step required heating in xylene at 145 °C to produce PhCF₃ slowly in their studies on the reactivity of several diphosphine-stabilised trifluoromethyl palladium phenyl complexes.²⁶³ To overcome this limitation, one major strategy is to use sterically and electronically modified phosphine ligands, such as Brettphos (compound **399**),²⁶⁰ and Xantphos (compound **115**, Figure 3.7)²⁶⁴

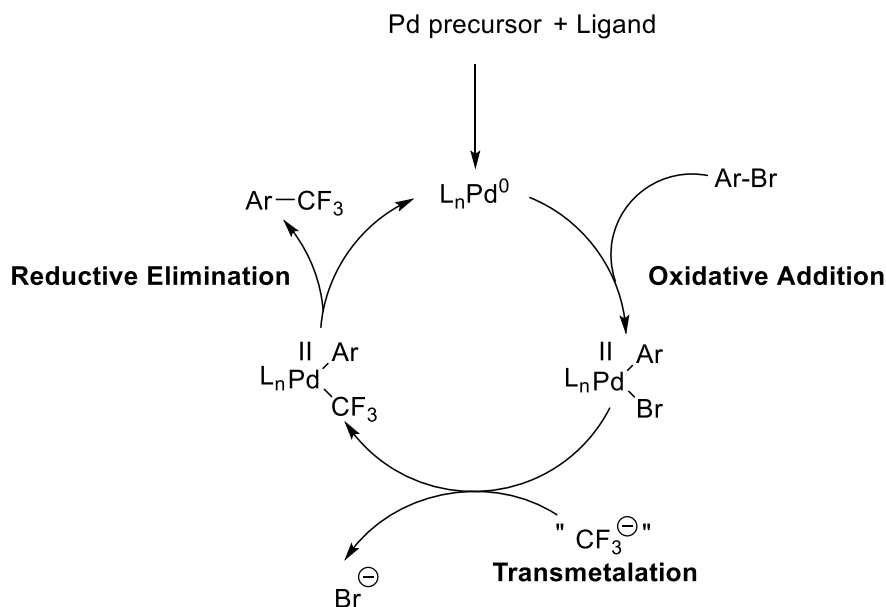


Figure 3.7 Generalised catalytic cycle for trifluoromethylation of aryl bromide (L = ligand; Ar = aryl) (modified from Buchwald *et al.*).²⁶⁰

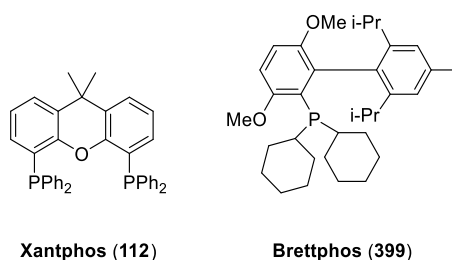


Figure 3.8 Structures of Xantphos (**112**) and Brettphos (**399**).

It has been reported that a possible side reaction associated with the inertness of the reductive elimination step is the dehalogenation of the halide substrate.²⁶⁵ ^1H NMR and HR-MS analysis of the reaction aliquots was performed again to detect the formation of the hydrodebrominated product-thiazole **392**, which would potentially provide further insights into the cause of the sluggishness of the trifluoromethylation reaction. However, no evidence of the formation of thiazole **392** was observed. This raised that the possibility that the failure of the reaction might not be merely due to the activation barrier in the reductive elimination step. The problem with the oxidative addition of the brominated thiazole to the palladium(0) species might also play a role. Therefore, an obvious step forward is to assess the effectiveness of the conditions used in the trifluoromethylation of thiazole **394** by performing model reactions with simple brominated aromatic substrates (*e.g.*, bromobenzene). If these model reactions did provide good results, the next step would be screening for reported combinations of ligand, palladium catalyst and CF_3 source to facilitate reductive elimination of the Pd-CF_3 bond. However, due to time constraints, this was not further explored during the course of this Ph.D. project.

3.4.3 Summary

The gold-catalysed coupling between alkyne **259** and thioamide **382** was performed as the model reaction and thiazole **392** was obtained in 61% yield, suggesting thioamide **382** was compatible with the optimised conditions for the thiazole formation. The coupling reaction between alkyne **364** and thioamide **382** was then carried out and thiazole **393** was obtained in 52% – 60% yield. C7-brominated thiazole **394** was prepared in moderate yield in order to access C7-substituted PatA analogues. The preparation of CF_3 -substituted thiazole **395** by trifluoromethylation of thiazole **394** was unsuccessful, necessitating the need for optimising reaction conditions in the future work.

3.5 Construction of macrocycle

3.5.1 Synthesis of *E,Z*-Dienoic Acid

3.5.1.1 Introduction

Although structures containing a carbonyl group conjugated to one or more alkenes frequently occur in macrocyclic lactone nature products,²⁶⁶ the presence of the *Z,E*-dienoate moiety is relatively rare compared to its counterpart *E,E*-dienoate. Usually, “isolated” *Z,E*-isomers require more energy to form than “isolated” *E,E*-isomers for steric reasons. However, in a complicated chemical environment, the situation may be different. For example, in a macrolide where the constraints of the macrocycle may favour one of the alkenes being *Z*-configuration, so the energy of the entire molecule with the *Z,E*-diene may be lower than that with the *E,E*-diene. The selected examples of natural products possessing *Z,E*-dienoate motif are presented in Figure 3.9, which include roridin E, dictyostatin, macrolactin A, zampanolide and salarin C. All of these compounds except roridin E (an extract from the black mold-*Stachybotrys chartarum*)²⁶⁷ are isolated from marine microorganisms.

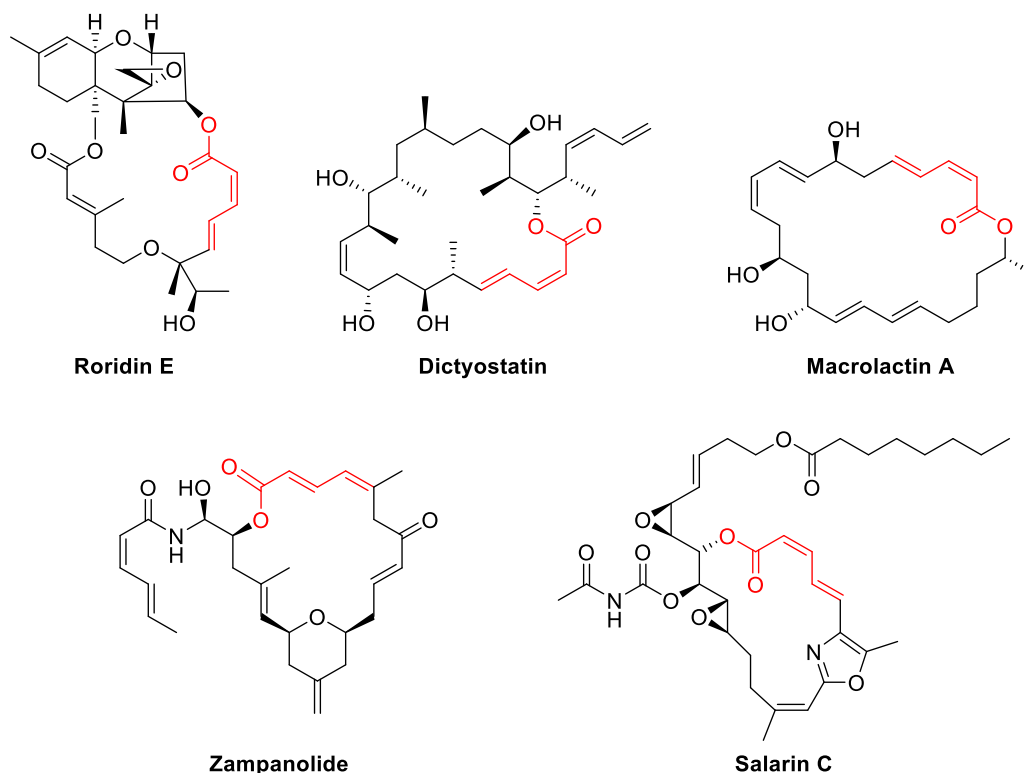
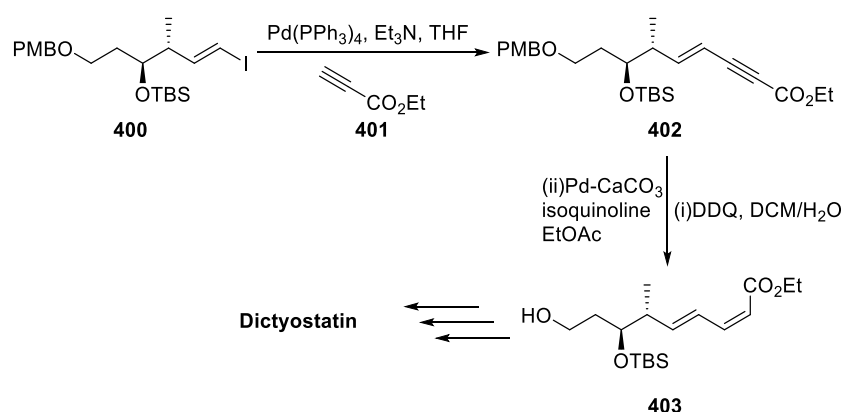


Figure 3.9 Examples of natural products possessing *Z,E*-dienoate motif.

The major challenge in the synthesis of *Z,E*-dienoates is their tendency to isomerise to energetically more favoured *E,E*-dienoates. The most reliable methodologies for the stereoselective preparation of *Z,E*-dienoates can be roughly classified as follows: (a) cross-coupling reactions between an *E*- or *Z*-vinyl stannane and a *Z*- or *E*-vinyl halide, which has been utilised in Pattenden's total synthesis of PatA (*vide supra*, Section 1.4.1.2); (b) *Z*-selective olefination reactions, like Still-Gennari olefination and its modifications; (c) Sonogashira coupling reaction between an *E*-vinyl iodide and an alkyne, followed by subsequent selective hydrogenation of the alkyne by Lindlar catalyst, which has been applied in Romo's synthesis of PatA and its analogue DMDA PatA (*vide supra*, Section 1.4.1.1 and Section 1.4.2.1); and (d) the base-induced ring opening of α,β -unsaturated lactone.

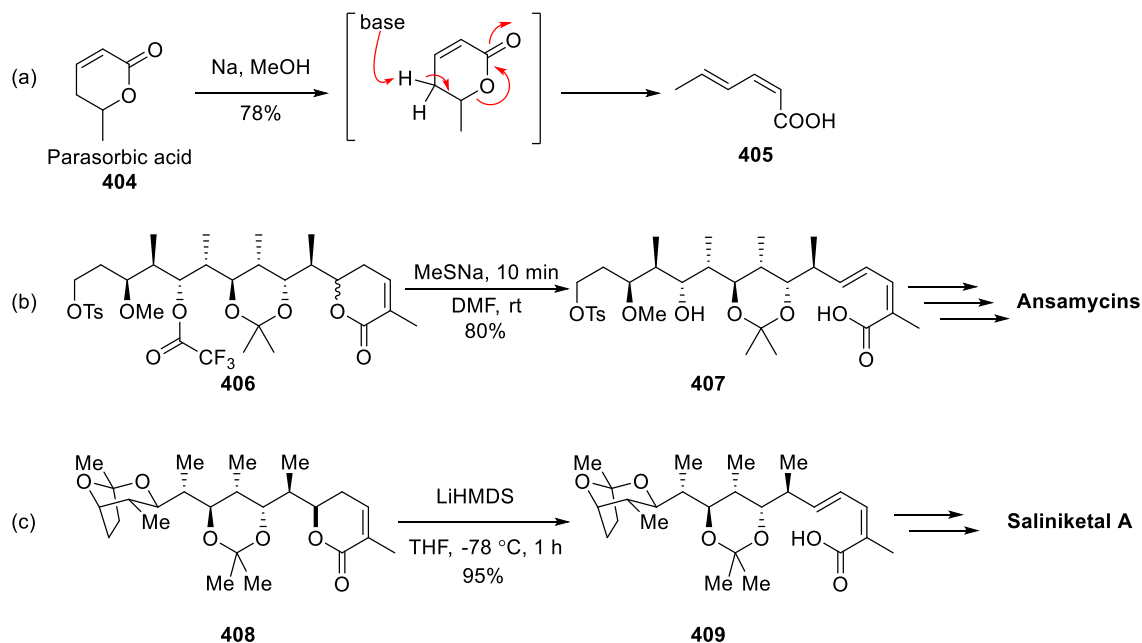
For example, in the synthesis of dictyostatin, to prevent the risk of isomerisation, *E*-vinyl iodide **400** was coupled with terminal alkyne **401** under Sonogashira conditions, whereby the resultant alkyne **402** could be reduced to the *Z*-alkene by Lindlar catalyst to give *Z,E*-dienoate **403**.²⁶⁸



Scheme 3.12 Preparation of *Z,E*-dienoate **403** through a combination of Sonogashira coupling and Lindlar reduction in synthesis of dictyostatin.²⁶⁸

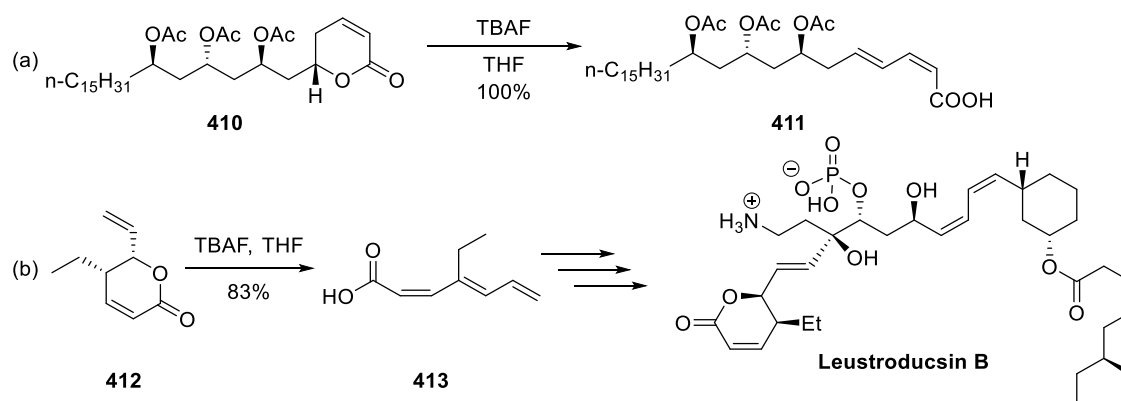
An alternative method to prepare *Z,E*-dienoic acid moieties is base-induced ring opening of α,β -unsaturated δ -lactones. This was first reported by Eisner and co-workers when they discovered that treatment of racemic parasorbic acid **404** with methanolic sodium methoxide yielded (2*Z*,4*E*)-hexadienoic acid **405** (Scheme 3.13a).²⁶⁹ Following their discovery, it has been reported that other bases, such as *t*-BuOK,²⁷⁰ MeSNa,²⁷¹ NaOH,²⁷² and LiHMDS,²⁷³ can also induce this transformation. This method has been used in the

synthesis of the ansamycins (Scheme 3.13b)²⁷¹ and saliniketal A (Scheme 3.13c).²⁷³ As shown in Scheme 3.13, the most intriguing features of this reaction are its complete stereospecificity in these examples.



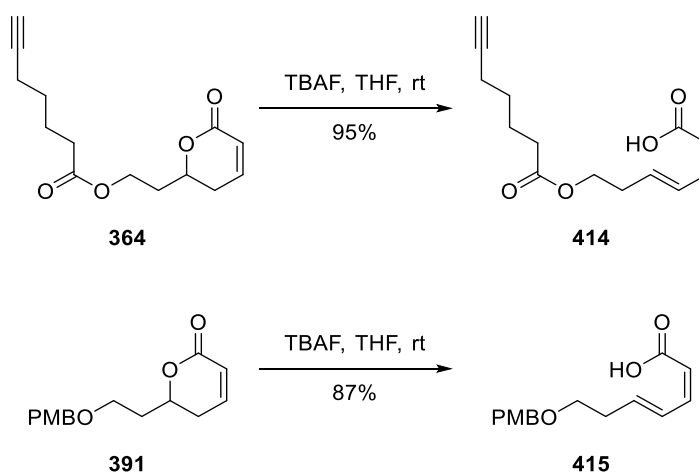
Scheme 3.13 Ring-opening reactions of α,β -unsaturated lactones induced by strong base: (a) of parasorbic acid;²⁶⁹ (b) in the synthesis of ansamycins;²⁷¹ and (c) in the synthesis of saliniketal.²⁷³

However, functional groups susceptible to strong basic conditions are not compatible with the conditions mentioned above. In an effort to search much milder conditions, Oishi and co-workers found that the mild base TBAF could act effectively in this transformation.²⁷⁴ For example, the acetoxyl groups in compound **410** remained completely intact in the ring-opening reaction induced by TBAF (Scheme 3.14a). This method was also used effectively towards the synthesis of leustroducsin B (Scheme 3.14b).²⁷⁵ As TBAF has enjoyed widespread use for desilylation,²⁷⁶ silyl protecting groups are not compatible with this method.



Scheme 3.14 TBAF induced ring-opening reactions of lactones: (a) in preparation of triacylated compound **411**,²⁷⁴ and (b) towards the synthesis of leustroducsin B.²⁷⁵

Despite these reported excellent stereoselectivities and good yields for *Z,E*-dienoic acids, this method has not attracted lots of attention from the synthetic community. Therefore, to explore the practicality of this method in the synthesis of PatA triazole analogue **182** (*vide supra*, Section 1.6) lacking a methyl group at the C22 position, previous Ph.D. student Hemmi Cumming in our research group conducted extensive studies on ring-opening reactions of α,β -unsaturated lactones, and found that the treatment of lactones **364** and **391** with TBAF provided the desired *E,Z*-dienoic acids **414** and **415** as single isomers, respectively.



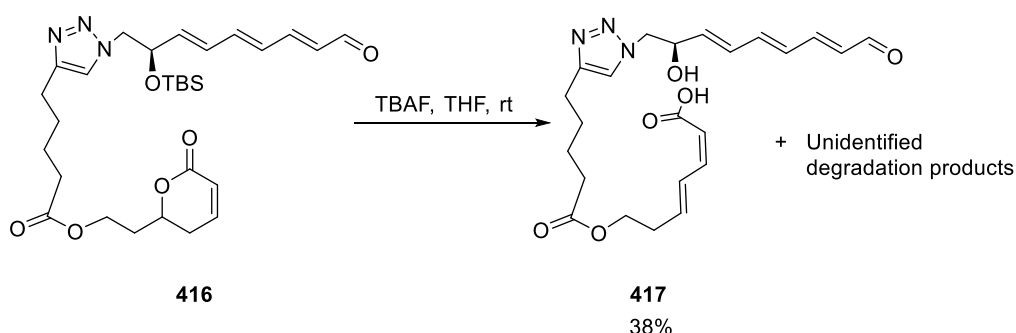
Scheme 3.15 TBAF induced ring-opening reactions of lactone **364** and **391** conducted by Cumming.¹³⁵

3.5.1.2 Initial Synthesis of *E,Z*-Dienoic Acid 419

In light of the excellent stereoselectivities and yields obtained in the preparation of *E,Z*-

dienoic acids **414** and **415** through ring opening of lactones **364** and **391** (Scheme 3.15), we decided to adopt this base-induced ring-opening strategy in the preparation of *E,Z*-dienoic acid **419** required for the macrolactonisation step.

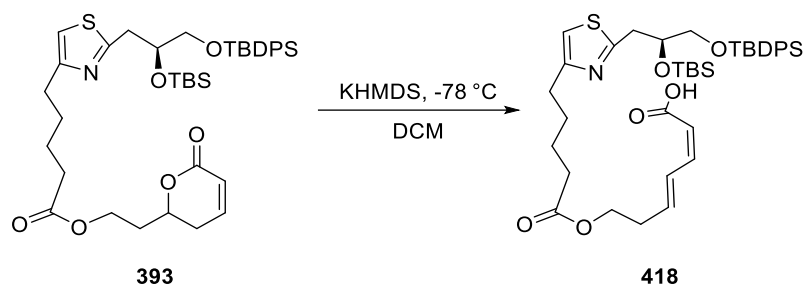
Although treatment with TBAF could theoretically cleave the silyl protecting groups simultaneously with the lactone ring-opening reaction, we were concerned that this one-pot protocol could cause significant side-reactions on the basis of Cumming's discovery that the treatment of lactone **416** with TBAF led to the formation of a considerable amount of degradation products (Scheme 3.16). Thus, we decided to first test the validity of using KHMDS for the lactone ring-opening transformation.



Scheme 3.16 Simultaneous silyl ether deprotection and lactone opening of **416** by treatment with TBAF reported by Cumming.¹³⁵

In 1966, Landesberg and Olofson conducted extensive studies to assess the electron distribution in thiazoles as depicted by the resonance structures in Figure 3.6 by deuteration experiments and discovered that the proton at C-2 position and C-5 position (thiazole numbering) of the unsubstituted thiazole were deprotonated at the same rate under treatment with sodium methoxide in deuterated methanol.²⁷⁷ This means that the acidity of the proton of the thiazole in compound **393** needs to be taken into account when performing the base-induced ring-opening reaction. Nonetheless, the δ -position of the lactone was likely to be more acidic than the proton on the thiazole, and therefore reactions occurring on the thiazole ring might be minimised by limiting the equivalents of KHMDS used in the ring-opening reaction. This should avoid potential side-reactions caused by the nucleophilic attack of the deprotonated thiazole. Initial treatment with 1.1 equivalent of KHMDS (Table 3.1, entry 1) at -78 °C led to incomplete conversion of the lactone **393**. However, the coupling constants of the alkenes of the isolated dienolic acid product were consistent with the reported characterisation data of intermediate **153** in

Fürstner's synthesis of DMDA PatA (*vide supra*, Section 1.4.2.2),¹²⁸ indicating the product was the desired Z, E-dienoic acid **418**. The isolated yield was 43%, and no other geometrical isomer was observed by ¹H NMR analysis. Pleasingly, increasing the usage of KHMDS to 1.3 equivalent successfully drove the reaction to completion and improved the yield to 60% (Table 3.1, entry 2).



Entry	KHMDS (equiv.)	Conversion Rate (%)	Isolated Yield (%)
1	1.1	77	43
2	1.3	100	60

Table 3.1 Optimisation of the base-induced ring opening of lactone **393**.

With *Z,E*-dienoic acid **418** in hand, we were then able to test conditions for chemoselective cleavage of the secondary TBS silyl group. As indicated by Table 3.2, the difference between the lability of primary TBS and TBDPS silyl ethers in acid is greater than that between their fluoride reactivity.^{278, 279} Although these results were obtained with primary silyl ethers, in contrast to the secondary TBS group in the present system, it was reasonable to assume that acid-mediated desilylation could differentiate more effectively between the secondary TBS silyl ether and the primary TBDPS silyl ether than fluoride-induced desilylation. Thus, we then set out to screen for acid methods that allow removal of a secondary TBS ether in the presence of a primary TBDPS ether.

Table 3.2 Comparison of acidic hydrolytic lability and fluoride reactivity of primary TBS and TBDPS silyl ethers.^{278, 279}

Silyl Ether	Half-Lives with 1% HCl-MeOH, 25 °C	Half-Lives with TBAF, 25 °C ^a
<i>n</i> -C ₆ H ₁₃ OTBS	≤1 min	-
<i>n</i> -C ₆ H ₁₃ OTBDPS	225 min	-
<i>n</i> -C ₁₂ H ₂₅ OTBS	-	140 h
<i>n</i> -C ₁₂ H ₂₅ OTBDPS	-	375 h

^a0.01 M in substrate containing TBAF (6 equiv.), DCM/THF (9:1). Half-Lives were determined by ¹H NMR monitoring quenched reaction aliquots.

A range of acidic conditions that may be suitable for the desired chemoselectivity has been reported. These included the use of *p*-TSA,²⁸⁰ camphorsulfonic acid,²⁸¹ a mixture of AcOH-H₂O-THF (3:1:1),²⁸² HCl in MeOH,²⁸³ and pyridinium *p*-toluenesulfonate (PPTS) (rt or heat).²⁸⁴ As we were concerned that the treatment of compound **418** with more strongly acidic conditions could lead to degradation of *Z,E*-dienoic acid, we decided to first test the weakly acidic salt PPTS in the selective desilylation reaction.

Following the original conditions of Blair and co-workers,²⁸⁴ the removal of the TBS group was first attempted with 2 equivalents of PPTS in MeOH at room temperature, but after 1 day, only little consumption of the starting material was observed (Table 3.3, entry 1). This suggested that we needed to seriously consider the impacts of the basicity of the thiazole ring in the following experiments.²⁸⁵ We then proposed that increasing the equivalents of PPTS could drive the reaction to completion. However, using 4 equivalents of PPTS at room temperature resulted in no significant reaction neither (entry 2). Raising the reaction temperature to 55 °C did provide desired product **419**, but after 1 day the reaction had not gone to completion (entry 3). Increasing PPTS equivalents at 55 °C did not drive the reaction to completion, nor did it appreciably improve the yield (entry 4).



Entry ^a	Reagent (equiv.)	Solvent	T (°C) ^b	Time (h)	Consumption Rate of SM ^c (%)	Yield ^d (%)
1	PPTS (2.0)	MeOH	rt	27	little	-
2	PPTS (4.0)	MeOH	rt	27	little	-
3	PPTS (4.0)	MeOH	55	27	68	27 (BRSM 40)
4	PPTS (10.0)	MeOH	55	27	71	30 (BRSM 43)

^aAll reactions were carried out at concentrations of 0.014 M. ^brt = room temperature. ^cSM = starting material. Consumption rate was calculated based on the amount of recovered *bis*-silylated starting material after purification by silica gel chromatography. ^dIsolated yields of **419** purified by silica gel chromatography. (BRSM yields are in parentheses).

Table 3.3 Trialled conditions for selective desilylation of compound **418**.

HR-MS investigation of the aliquot samples from the reaction mixture after 27 hours heating at 55 °C revealed that it contained a mixture of the *bis*-silylated starting material **418** ([M-H]⁻ ion at m/z = 734.3372), desired TBS-deprotected product **419** ([M-H]⁻ ion at m/z = 620.2525), undesired TBDPS-deprotected product **420** ([M-H]⁻ ion at m/z = 496.2168) and *bis*-desilylated product **421** ([M-H]⁻ ion at m/z = 382.1339) (see Figure 3.10 for HR-MS spectrum).

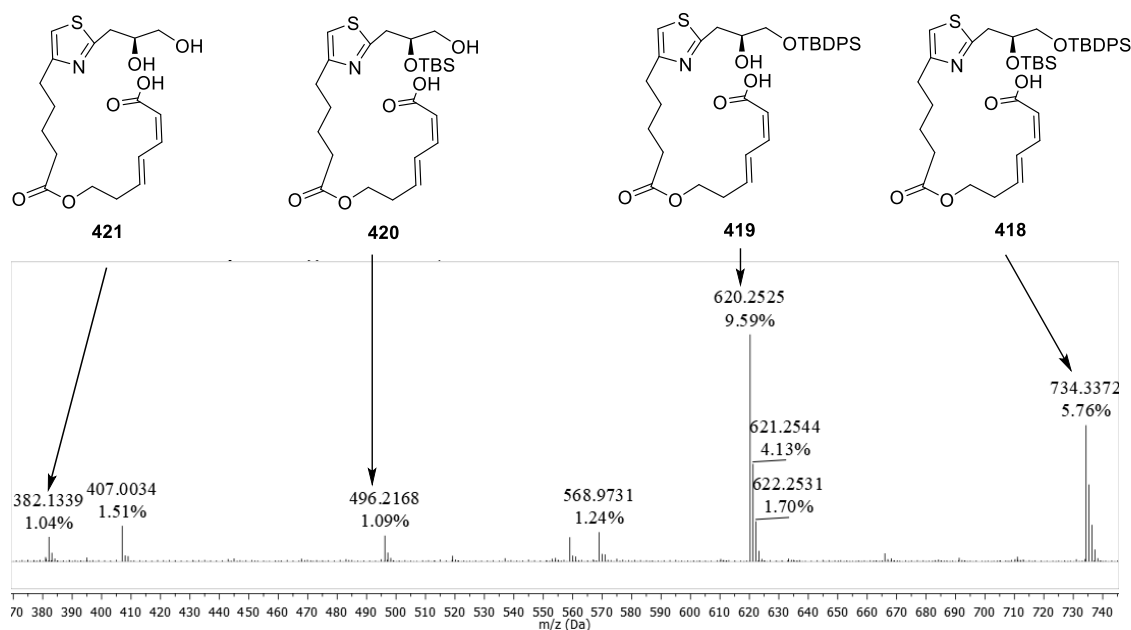


Figure 3.10 HR-MS for the reaction mixture of mono-desilylation of **418** using 10 equivalents of PPTS.^{§§§§}

Given that the formation of doubly desilylated product **421** was detected by HR-MS, attention then turned to the possibility of recovery of compound **421** and reprotection of the primary hydroxyl. This would potentially provide more desired product **419**. However, there was a risk that the use of base (*e.g.*, imidazole or pyridine) in selective re-silylation of the primary OH of product **421** could cause isomerisation of the *Z,E*-dienoic acid. We attempted to recover product **421** from the PPTS reaction described above. Unfortunately, *bis*-desilylated product **421** was lost while being purified by flash silica gel chromatography due to its high polarity.

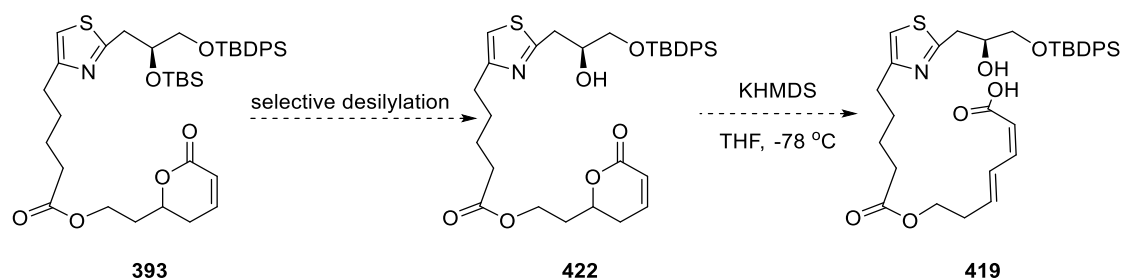
The overall yield of these two steps for the preparation of *Z,E*-dienoic acid **419** was only 18%, which prompted us to explore a more efficient synthetic route.

3.5.1.3 Alternative Routes for Synthesis of *E,Z*-dienoic Acid **419**

As shown in Scheme 3.17, an alternative two-step approach was then considered, in which the TBS removal would be performed ahead of the lactone opening. This would

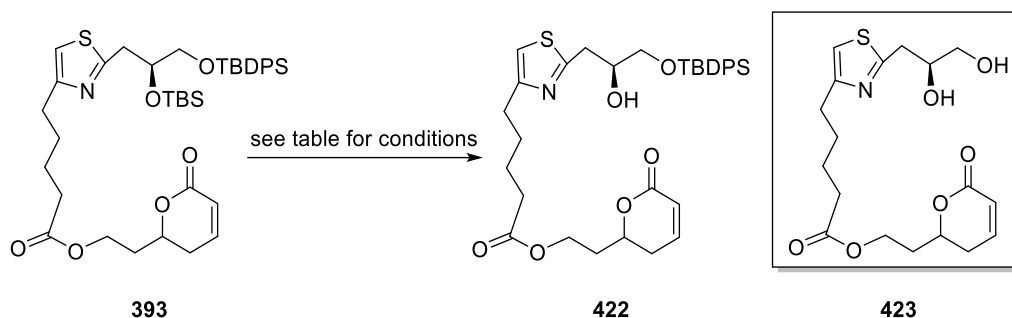
^{§§§§} [M-H]⁻ peak of compound **418** (at 734.3372, calculated for C₄₀H₅₆NO₆SSi₂⁻, 734.3372), compound **419** (at 620.2525, calculated for C₃₄H₄₂NO₆SSi⁻, 620.2508), compound **420** (at 496.2168, calculated for C₂₄H₃₈NO₆SSi⁻, 496.2195) and compound **421** (at 382.1339, calculated for C₁₈H₂₄NO₆S⁻, 382.1330).

allow more options for the acid-mediated selective removal of the secondary TBS silyl ether.



Scheme 3.17 Proposed alternative two-step approach to the synthesis of seco-acid **419**.

The desilylation of compound **393** was first trialled with a catalytic amount of strong acid *p*-TSA in MeOH and DCM at room temperature (Table 3.4, entry 1).²⁸⁶ Surprisingly, little consumption of the starting material was observed after over-night stirring. Increasing *p*-TSA equivalents provided only a trace amount of desired product **422** (entry 2). Instead, a diol product **423** resulting from the removal of both silyl ethers was obtained as the major product. Attention was then directed towards use of milder acidic conditions. Treatment with a mixture of AcOH, H₂O, and THF at room temperature resulted in no significant reaction (entry 3). Performing the reaction at 50 °C cleanly provided the desired product **422** as the sole product, albeit with the recovery of substantial amounts of the starting material (entry 4). Efforts to drive the reaction to completion by extending the reaction time did prompt the consumption of the starting material (entries 5 and 6) but also resulted in substantial formation of diol product **423**. Not surprisingly, the isolated yields of compound **422** were not improved significantly. Two unconventional conditions for selective removal of secondary TBS silyl ether were then explored: one used the oxidising reagent NaIO₄ in THF,²⁸⁷ the second used a 1:1 mixture of TBAF and BF₃·Et₂O in anhydrous acetonitrile.²⁸⁸ Unfortunately, these two conditions were found to be sluggish with little consumption of starting material (entries 7 and 8). Given that reactions with mixtures of AcOH, H₂O and THF under prolonged heating in fact provided mixtures of mono-silylated product **422** and the diol **423**, along with unreacted starting material, we then opted to prepare compound **422** by full deprotection, followed by mono-protection of the primary position, with the hope that this could provide a better overall yield (albeit with more steps).



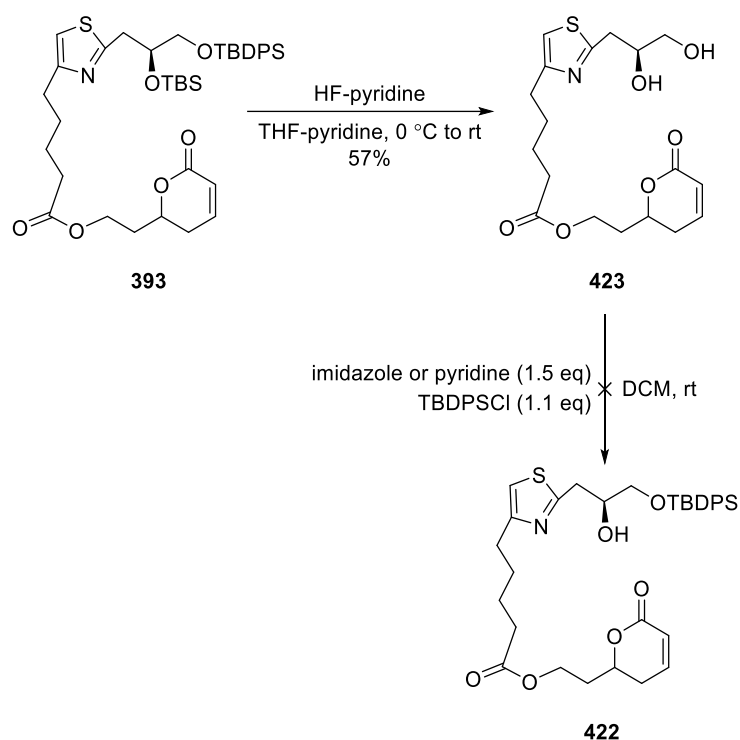
Entry	Reagent (equiv.)	Solvent	T (°C) ^a	Time (h)	Consumption Rate ^b (%)	Yield ^c (%)
1	<i>p</i> -TSA (0.3)	MeOH-DCM	rt	18	little	-
2	<i>p</i> -TSA (2.0)	MeOH-DCM	rt	18	44	422 , trace
3	AcOH	THF-H ₂ O	rt	18	little	-
4	AcOH	THF-H ₂ O	50	3	33	422 , 30 (BRSM 100)
5	AcOH	THF-H ₂ O	50	9	76	422 , 26 (BRSM 35)
6	AcOH	THF-H ₂ O	50	23	88	422 , 34 (BRSM 39)
7	NaIO ₄	EtOH	rt	18	-	-
8	BF ₃ -TBAF	MeCN	rt	18	-	-

^art = room temperature. ^bCalculation based on the amount of recovered *bis*-silylated starting material **393** after purification by silica gel chromatography. ^cYields of purified products by silica gel chromatography. (BRSM yields are in parentheses).

Table 3.4 Trialled conditions for selective desilylation of compound **393**.

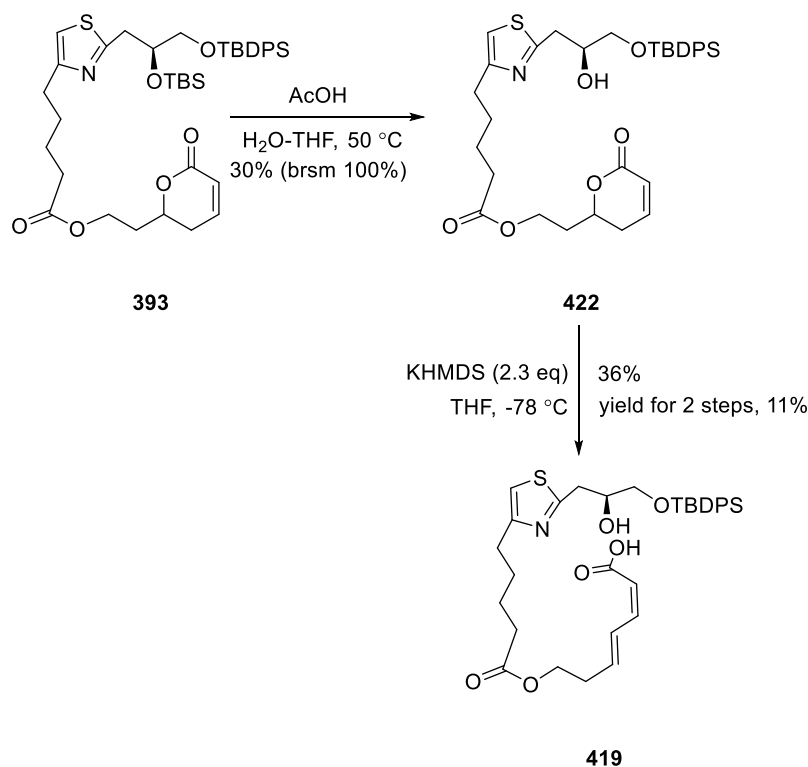
As shown in Scheme 3.18, desilylation of compound **393** by treatment with HF-pyridine provided diol **423** in uninspiring 57% yield. Assuming that this moderate yield was a result of material loss in the aqueous quench with aqueous saturated NaHCO₃ solution, given that the polarity (and likely hydrophilicity) of the diol, we then used trimethylsilanol to quench excess HF instead. But this modification did not give a better yield. Since sufficient diol was obtained for the next step, no further optimisation was performed. We then moved on to perform selective silyl protection of the primary hydroxyl group. The classic conditions using TBDPSCl and imidazole were first trialled.²⁸⁹ Surprisingly, a mixture of unidentified degradation products was obtained, with no sign of the desired product observed by ¹H NMR analysis. Assuming that the unexpected degradation was induced by deprotonation of the highly acidic δ-proton of the lactone by imidazole, we repeated the reaction with TBDPSCl and pyridine, a base considered to be about 100 times less basic than imidazole.²⁹⁰ To our dismay, this reaction

again provided a mixture of degradation products.



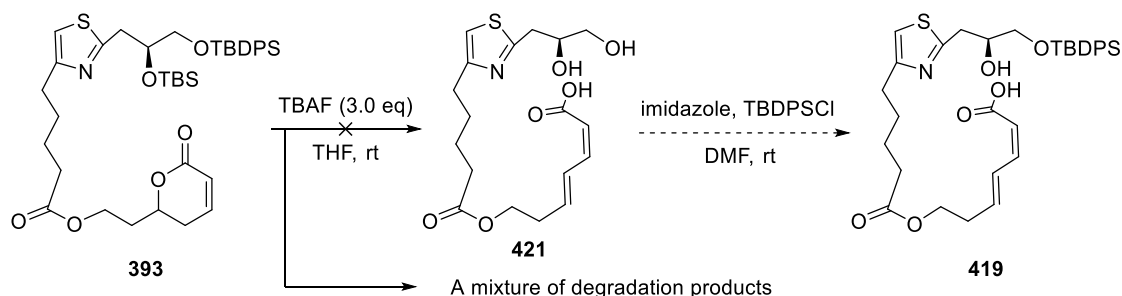
Scheme 3.18 Attempted preparation of compound **422** *via* diol intermediate **423**.

This inability to prepare compound **422** by selective protection of diol **423** prompted us to return to selective desilylation of **393** (Table 3.4, Entry 3) in order to access compound **419**. After obtaining sufficient material by using this method, we then performed the lactone opening reaction using 2.3 equivalents of KHMDS at -78 °C (Scheme 3.19). Unexpectedly, this reaction provided seco-acid **419** in only 36% yield, accompanied by a mixture of unidentified by-products. The obtained overall yield for these two steps was 11%, which was lower than the yield obtained in the initial synthetic route described in Section 3.5.1.2.



Scheme 3.19 Preparation of seco-acid **419** *via* mono-silylated intermediate **422**.

The poor yield then led us to re-consider the feasibility of a one-pot protocol for the preparation of seco-acid **421**. The problem associated with the purification of polar compound **421** would likely be resolved by using reversed-phase chromatography. Thus, we then carried out the double desilylation reaction using 3 equivalents of TBAF in THF with the hope that it would allow the base-induced lactone opening and the silyl cleavage to occur simultaneously (Scheme 3.20). Unfortunately, a mixture of degradation products was obtained, with no sign of compound **421** observed by ¹H NMR investigation.



Scheme 3.20 Attempted preparation of seco-acid **419** *via* intermediate **421**.

Based on experimental results obtained in our endeavours described above, the preparation of seco-acid **419** will require further optimisation. As TBAF has been used to

3.5.2 Macrolatonisation

3.5.2.1 Introduction

Macrocyclic lactones are common and broadly found in natural products from terrestrial and marine sources²⁹² and present a remarkably diverse range of medicinal properties, such as antibiotic, anticancer or antitumoral, antifungal, and immunosuppressive.²⁹³ Thus, it is not surprising that macrocyclic lactone natural products have served as intriguing targets to drive organic chemists to develop new macrocyclisation methodologies for their synthesis. Even though a significant number of diverse macrocyclisation approaches have been reported over the years, such as HWE olefination,²⁹⁴ intramolecular ring-closing metathesis,²⁹⁵ palladium-catalysed carbon-carbon cross-coupling (*e.g.*, Stille coupling),²⁹⁶ and chromium-induced Nozaki-Hiyama-Takai-Kishi reaction,²⁹⁷ the macrolactonisation of seco-acids still remains one of the most often used protocols.

According to Illuminati and Mandolini's comprehensive kinetic investigations of lactonisation with different ring sizes,²⁹⁸ there are three factors directing the $\kappa_{\text{intra}}/\kappa_{\text{inter}}$ ratio in the macrolactonisation: the activation energy (enthalpy), decreased degree of freedom (entropy) and the possibility of end-end encounters. The activation energy is the energy that needs to be provided to overcome the strain energy, which arises from geometric deviations of bond angles (Baeyer strain), steric hindrance due to imperfect staggered conformation (Pitzer strain) and transannular strains due to repulsive interactions between atoms, when a bifunctional open chain precursor is converted to the transition state for the ring to be formed. The internal rotation of single bonds is constrained as the lactone is being formed, meaning that the level of disorder in the system is reduced, and this is entropically disfavoured. As the ring size gets larger, the proportion of conformers that include end-to-end encounters typically decreases

As shown in Figure 3.11, for medium-sized rings ($n = 8\sim 12$), enthalpic factors from the increased strain energy, which decreases the ability to adopt an ideal bond angle and form the reactive conformation, in combination with the entropic factors, make the formation of medium-sized rings the most difficult to achieve. For macrocyclic lactone rings ($n > 13$), although the ring strain is low (enthalpic factor), the entropic factors increases and the probability of the chain terminals encountering each other also decreases. However, the intermolecular reaction may also suffer a similar entropy penalty. Therefore, the

$\kappa_{\text{intra}}/\kappa_{\text{inter}}$ ratio remains relatively constant.

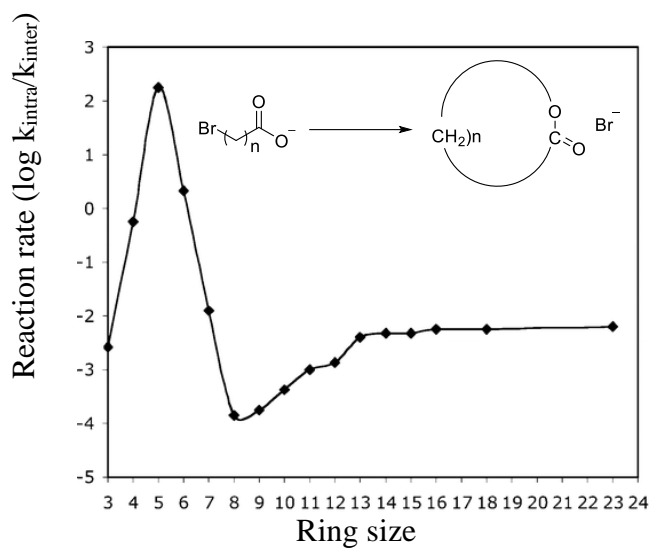


Figure 3.11 Reactivity profile for lactone formation.²⁹⁸

Therefore, to favour intramolecular reactions in the competition between intra- and intermolecular reactions, high-dilution conditions were first introduced by Ruggli and Ziegler,²⁹⁹ which requires adding the substrate at a slow rate, for example by a syringe pump, to a large volume of solvent.

Many reagents and conditions have been developed for the purpose of accelerating the macrolactonisations, most of which work by means of either “acid activation” (path a in Figure 3.12) or “carboxylate attack” on a leaving group (path b in Figure 3.12).

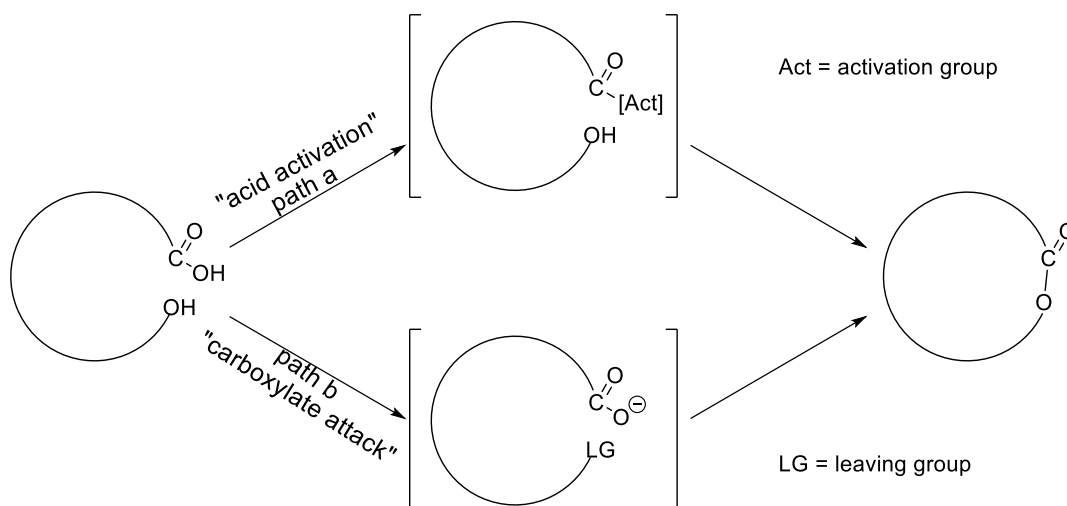


Figure 3.12 Representative scheme of macrolactonisation by “acid activation” or “carboxylate attack” (Modified from Campagne *et al.*)³⁰⁰

Some general macrolactonisation reactions/reagents and their mechanistic intermediates are summarised in Figure 3.13. Each of the reactions exemplifies their respective category of macrolactonisation reactions/reagents, of which a number of variations and modifications have been developed and applied successfully in the synthesis of macrocyclic natural products and their analogues.³⁰⁰

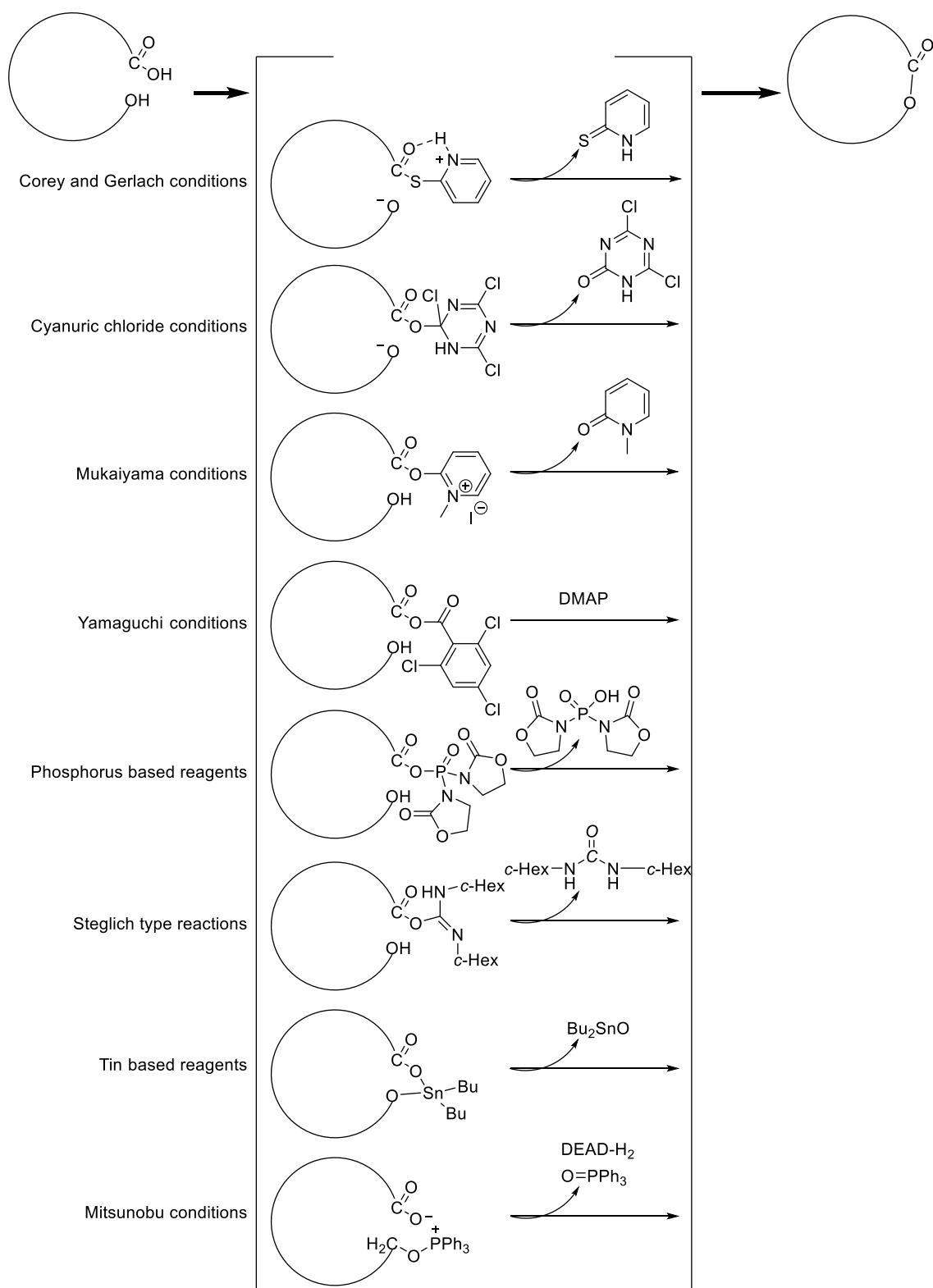
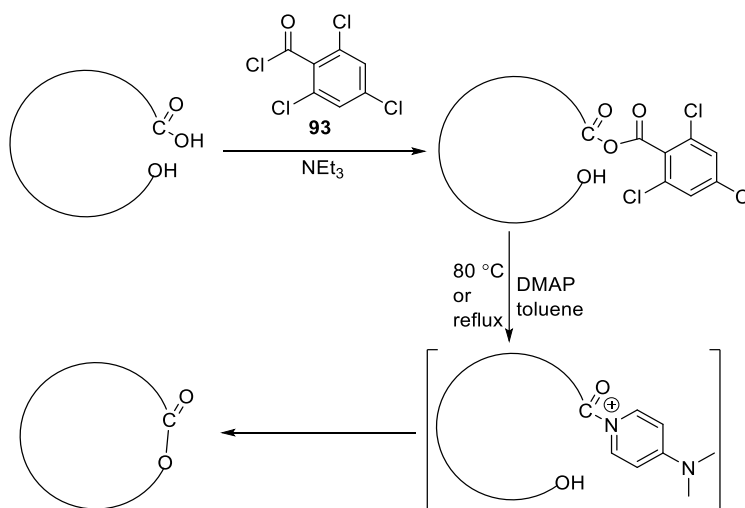


Figure 3.13 Summary of selected macrolactonisation methods.

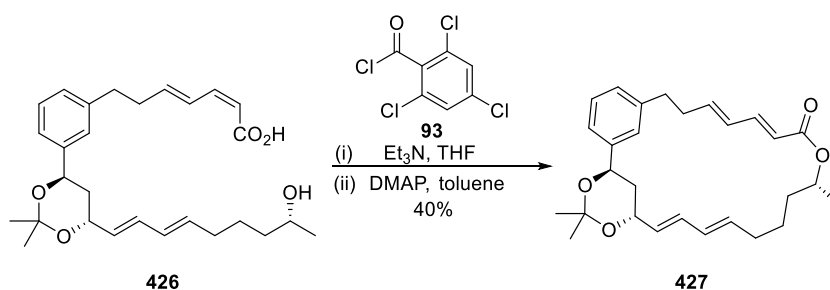
Among all these methods, the original Yamaguchi reaction, which uses 2,4,6-trichlorobenzoyl chloride **93** as “acid activator”,³⁰¹ remains the most popular method for construction of macrocyclic lactones and has been utilised with success in many synthetic

approaches.³⁰⁰ As shown in Scheme 3.22, the carboxylic acid first reacts with Yamaguchi reagent **93** in the presence of triethylamine to provide the mixed anhydride. The anhydride is then added slowly by a syringe pump to a highly diluted solution of DMAP at high temperatures. DMAP acts as a stronger nucleophile than the alcohol and attacks the anhydride to afford the reactive amide intermediate, which reacts rapidly with the alcohol to form the macrocyclic lactone.



Scheme 3.22 Proposed mechanism of Yamaguchi macrolactonisation.³⁰¹

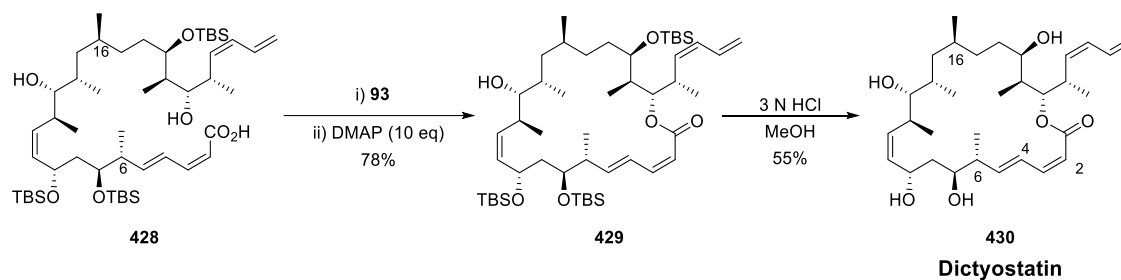
When Yamaguchi procedure is used for lactonisation of an *E,Z*-dienoic acid and an alcohol, significant isomerisation can sometimes occur. For example, in the synthesis of macrolactin A analogue reported by Takemoto *et al.* (Scheme 3.23), the Yamaguchi lactonisation step afforded the undesired (*2E*, *4E*)-lactone **427** as the sole product, instead of the desired (*2Z*, *4E*)-lactone.³⁰²



Scheme 3.23 Isomerisation in lactonisation in synthesis of macrolactin A analogue.³⁰²

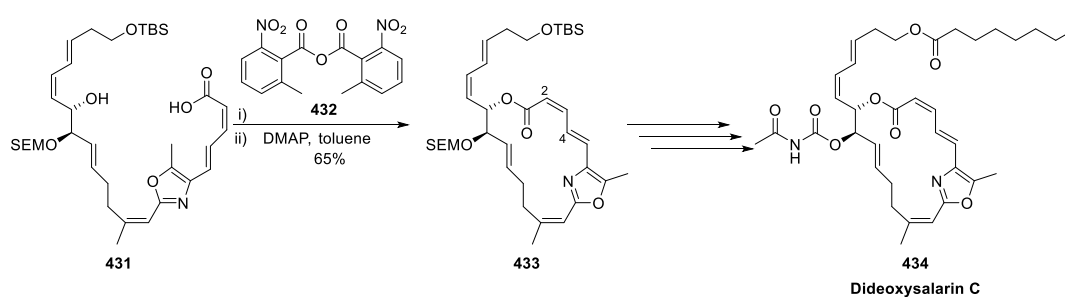
Considering that the isomerisation could be partially attributed to the high reaction temperature required in the second step, Yonemitsu further developed a modification of

Yamaguchi conditions where an excess amount of DMAP (*e.g.*, 10 equivalents) is directly added to the solution of preformed anhydride intermediates at room temperature.³⁰³ In the synthesis of dictyostatin, the macrolactonisation of seco-acid was conducted under these modified conditions and the (2*Z*,4*E*)-lactone **429** was obtained in 78% yield, accompanied by 5 – 10% of the (2*E*, 4*E*)-lactone isomer (Scheme 3.24).³⁰⁴



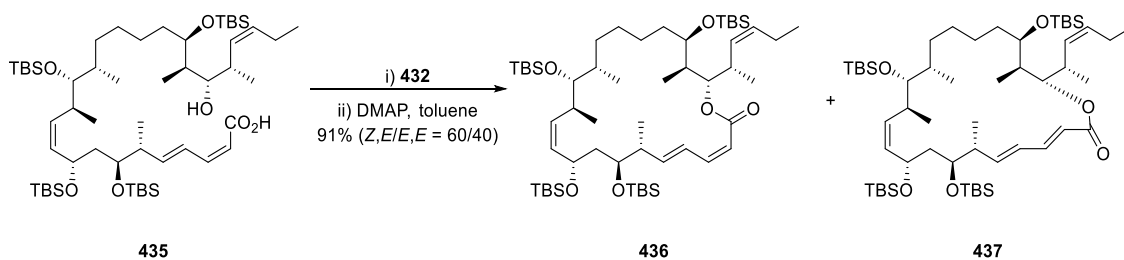
Scheme 3.24 Use of Yonemitsu's modified conditions in synthesis of dictyostatin.³⁰⁴

Similarly, the Shiina reaction, a variation of the Yamaguchi reaction, can be also performed with an excess of DMAP at room temperature. In the synthesis of dideoxysalarin C recently reported by Altmann and Schrof, the desired macrocycle **433** was constructed under Shiina conditions with only about 7% of isomerised (2*E*, 4*E*)-dienoate byproduct observed based on ¹H NMR analysis.³⁰⁵



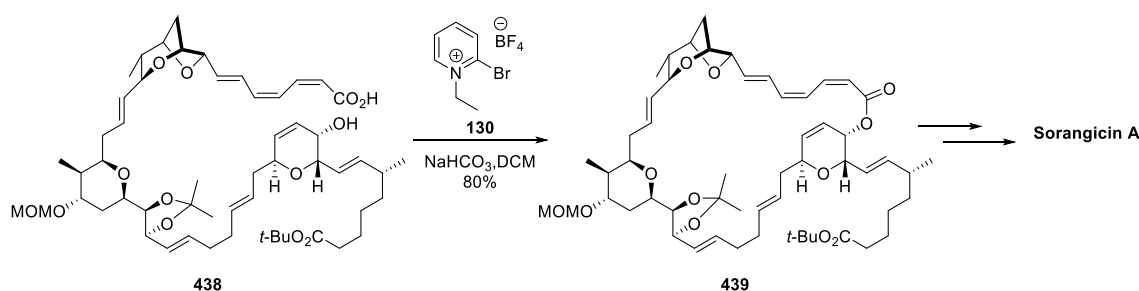
Scheme 3.25 Shiina reaction towards the synthesis of dideoxysalarin C.³⁰⁵

Interestingly, in the synthesis of an analogue of dictyostatin, the Shiina reaction on seco-acid **435** provided a 60/40 ratio of *Z,E*-product **436** and *E,E*-product **437** (Scheme 3.26).³⁰⁶



Scheme 3.26 Isomerisation in Shiina reaction in the synthesis of dictyostatin analogue.³⁰⁶

The isomerisation observed in the classic Yamaguchi reaction and its modifications (*e.g.*, Yonemitsu's and Shiina's conditions) was proposed to be a consequence of a reversible nucleophilic aza-Michael-type addition of DMAP onto the activated acid intermediate.³⁰⁷ Therefore, in the synthesis of sorangicin A, the modified Mukaiyama reagent 2-bromo-1-ethyl-pyridinium tetrafluoroborate **130**,³⁰⁸ which possesses a non-nucleophilic counterion, was tested for the lactonisation step (Scheme 3.27). It was anticipated that this could minimise the isomerisation of the trienoic acid **438**. The desired product **439** was obtained in 80% yield without significant isomerisation.¹²³ This suggests that this coupling reagent could be useful for the synthesis of other macrocyclic lactones containing isomerisation-prone *E,Z*-dienoate motif.

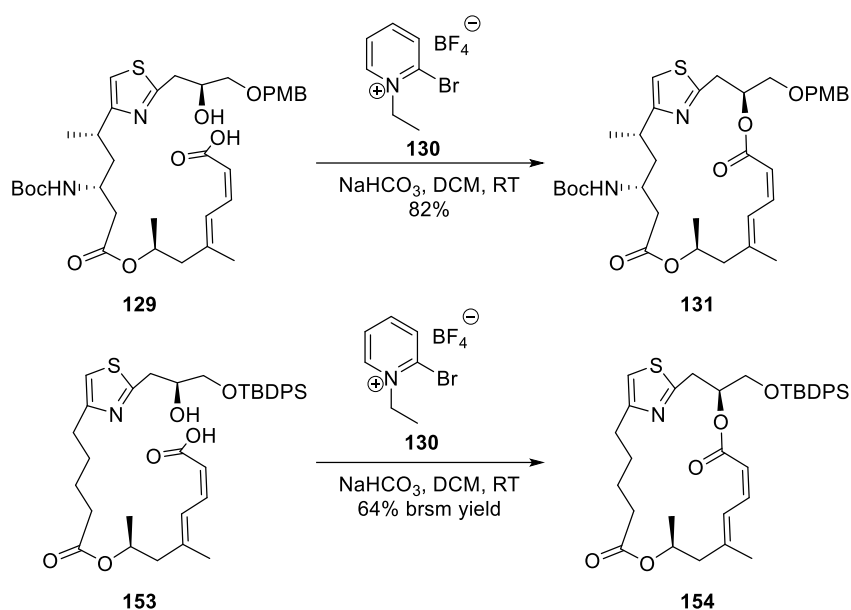


Scheme 3.27 Macrolactonisation in the total synthesis of sorangicin A under modified Mukaiyama conditions.¹²³

3.5.2.2 Preparation of Macrocyclic Alcohol 441

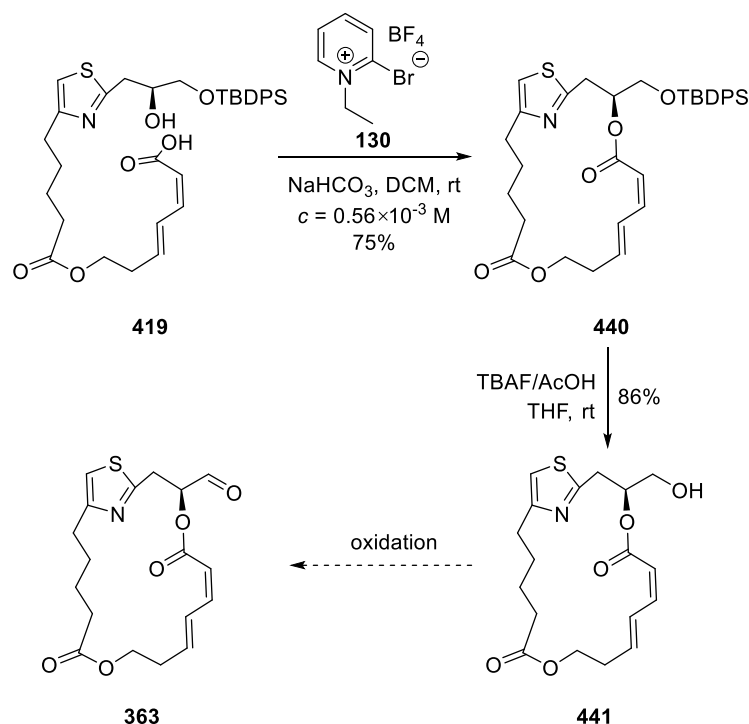
As mentioned in Section 1.4.1.3 and 1.4.2.2, in Fürstner's synthetic work towards PatA and DMDA-PatA, only the modified Mukaiyama protocol proved to give reproducibly good yields for the lactonisation step, whereas other conventional reagents/conditions provided substantial amounts of undesired isomerised products.¹²⁰ Based on their experimental results, the modified Mukaiyama reagent **130** was chosen for the

macrolactonisation step in our synthesis.



Scheme 3.28 Macrolactonisation under modified Mukaiyama conditions in synthesis of PatA and DMDA PatA.¹²⁰

Following the conditions reported by Fürstner and co-workers, highly diluted seco-acid **419** in DCM ($c = 0.56 \times 10^{-3}$ M) was treated with excess NaHCO_3 and reagent **130** in a dark environment, and gratifyingly, the desired *Z,E*-configured macrocycle **440** was obtained as the sole product in 75% yield, with no geometric isomer observed by ^1H NMR analysis (Scheme 3.29). The coupling constants of the alkenes of compound **440** were consistent with the reported characterisation data of the macrocyclic compound **154** in Fürstner's synthesis of DMDA PatA (*vide supra*, Section 1.4.2.2).¹²⁸ Subsequent desilylation of compound **440** with buffered TBAF provided primary alcohol **441** in good yield.



Scheme 3.29 Preparation of macrocyclic alcohol **441**.

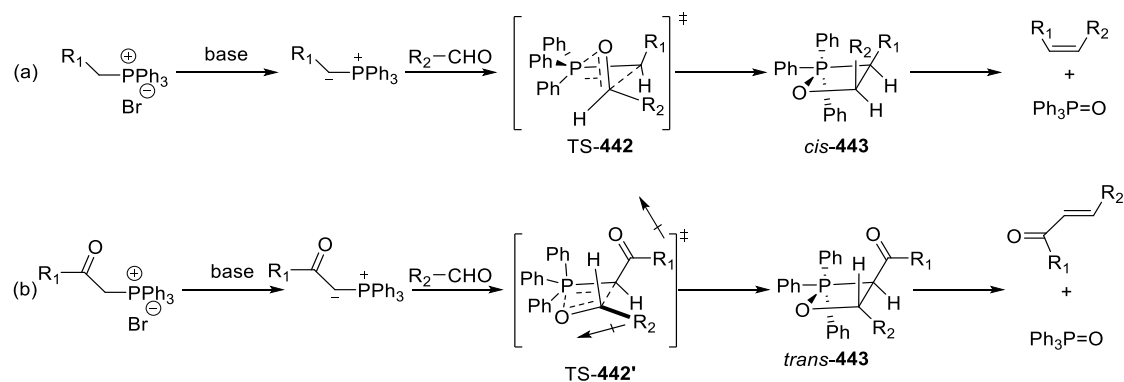
Macrocyclic alcohol **441** was prepared in 12 steps as the longest linear sequence (15 steps total), starting from commercially available chemicals, with an overall yield of 3%. The selective deprotection for compound **418** is the major hurdle to overcome. Aside from this step, the overall yield would be 10%.

As aldehyde **363** prepared from the alcohol **441** is structurally similar to aldehyde **155**, an intermediate in Fürstner's synthesis of DMDA PatA (refer to Section 1.4.2.2),¹²⁸ it is presumed to be rather sensitive and prone to epimerisation on storage. We then decided to stockpile the alcohol **441** and not to perform the oxidation reaction until the side chain fragment was ready for coupling with it. Therefore, at this stage, we moved on to preparing the methylated side chain fragment.

3.6 Synthesis of Side Chain Fragment

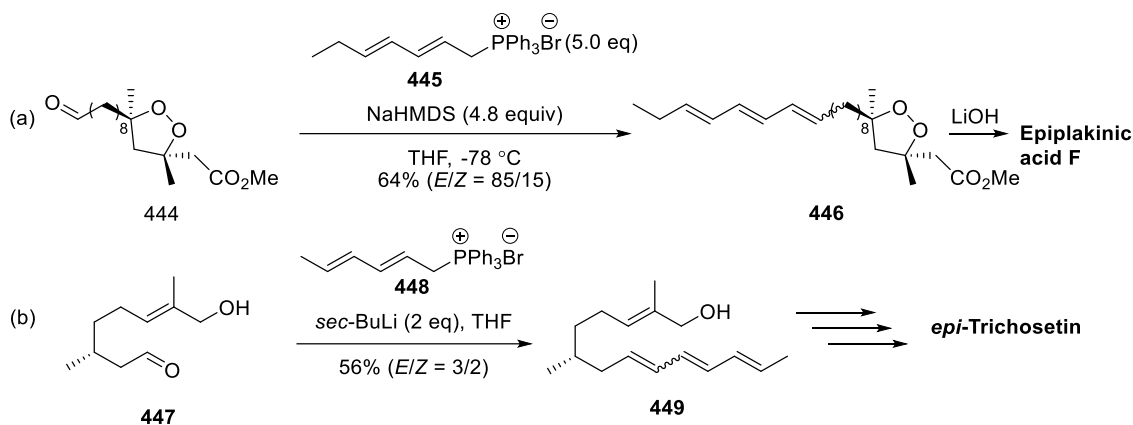
3.6.1 Wittig Olefination and Horner-Wadsworth-Emmons Reaction

Wittig olefination employs the reaction between a phosphonium ylide and an aldehyde or a ketone for alkene synthesis. Triphenylphosphonium ylides are the most often used reagents because of their good air-stability and easy preparation.³⁰⁹ As shown in Scheme 3.30, the stereochemical outcome of Wittig reactions using triphenylphosphonium ylides is highly dependent on whether or not they are stabilised. In the case of unstabilised ylides, the reaction proceeds under kinetic control. The puckered transition state **TS-442** forms at an early stage to minimise steric interactions between R_1 and R_2 (1,2-interaction) and between R_2 and Ph (1,3-interaction). The resulting oxaphosphetane intermediate *cis*-**443** eliminates triphenylphosphine oxide to give the *Z*-olefin.³¹⁰ By contrast, the addition of ylides stabilised by electron-withdrawing functional groups (*e.g.*, alkoxycarbonyl or cyano group) to aldehydes or ketones preferentially proceeds through a late planar transition state **TS-442'** to relieve the steric interaction between R_2 and Ph and the dipole-dipole interaction. The resulting oxaphosphetane *trans*-**443** provides an *E*-olefin.^{310, 311}



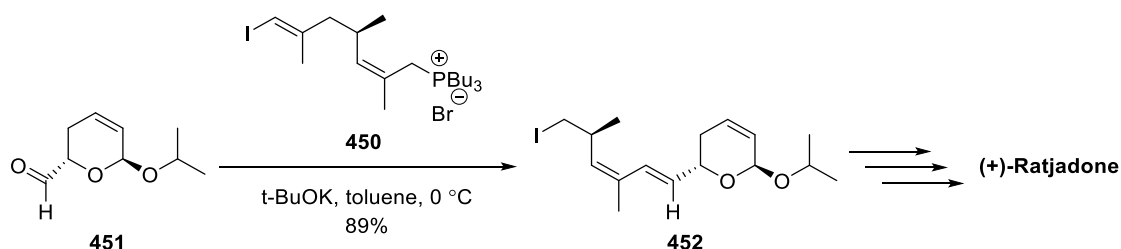
Scheme 3.30 Preferred transition state based on Vedejs model for: (a) non-stabilised triphenylphosphonium ylides; and (b) stabilised triphenylphosphonium ylides.^{310, 311}

Generally speaking, Wittig reactions using ylides semi-stabilised by functional groups (*e.g.*, vinyl or aryl group) provides mixtures of *Z*- and *E*-olefins, and the ratio of *Z*- and *E*-olefins varies on individual cases. The stereochemical outcomes of representative Wittig reactions using vinyl triphenylphosphonium ylides are shown in Scheme 3.31.



Scheme 3.31 Use of vinyl triphenylphosphonium ylide in the synthesis of (a) epiplakinic acid F,³¹² and (b) *epi*-trichosetin.³¹³

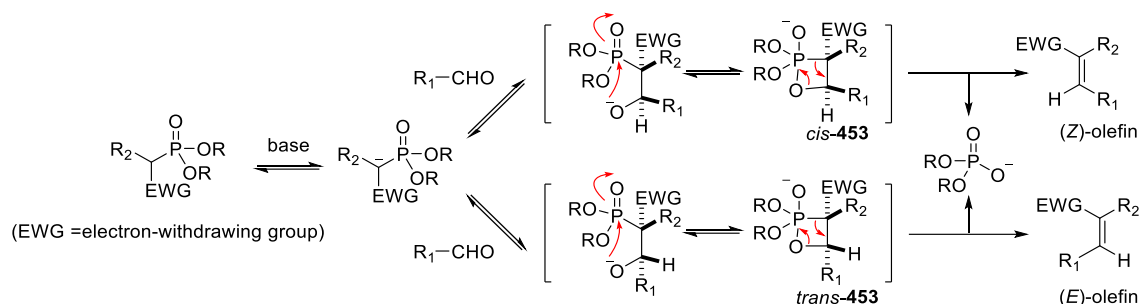
It was found that the *E*-selectivity of Wittig reactions with unstabilised ylides could be dramatically boosted by using trialkylphosphines in place of triphenylphosphines.³¹⁴ For example, in the synthesis of (+)-ratjadone, tributylphosphonium salt **450**, after deprotonation, underwent Wittig reaction between the resulting unstabilised ylide and aldehyde **451** afforded *E*-isomer **452** as the sole product (Scheme 3.32).³¹⁵



Scheme 3.32 Use of tributylphosphonium salt for Wittig olefination.³¹⁵

One of the most important modifications of Wittig reaction is the Horner-Wadsworth-Emmons (HWE) reaction, and its mechanism is closely related to that of Wittig reaction of stabilised ylides.³¹⁶ In the proposed mechanism (Scheme 3.33), the addition of the stabilised phosphonate anion to the carbonyl group provides a mixture of isomeric β -oxido phosphonates, which close to form *cis*- and *trans*-oxaphosphetanes **453**. Both *cis*- and *trans*-oxaphosphetane intermediates then rapidly eliminate dialkylphosphate to afford *Z*- and *E*-olefins. It should be pointed out that the presence of electron-withdrawing groups (*e.g.*, ester, cyano, sulfonyl, vinyl, or aryl) on the phosphonate α -centre is essential for the deprotonation process and the decomposition of the β -oxido phosphonate intermediate.³¹⁷ As the initial addition and the formation of the four-membered cyclic

intermediates are under equilibrium conditions, the ratio of *Z*- and *E*-olefins is controlled by both kinetic and thermodynamic factors. Generally speaking, the conditions that favour the *E*-selectivity include increased bulkiness of phosphonates and α -substitution of aldehydes, higher reaction temperature, and use of lithium or sodium as the counterion.³¹⁷



Scheme 3.33 Proposed mechanism of HWE reaction.

The HWE reaction has a number of advantages over Wittig olefination, one of which is that phosphonate ylides are more nucleophilic but less basic than comparable phosphorus ylides derived from phosphonium salts. Therefore, they have less difficulty in reacting with sterically hindered carbonyl groups and broader substrate range.³¹⁸ However, aldehyde substrates with stereocentres adjacent to carbonyl groups may be prone to epimerisation under treatment of strong anionic bases in the HWE reaction. To obviate the use of any kind of ionic bases, modified protocols have been reported, which employ non-ionic weaker bases such as bicyclic guanidine base **454**³¹⁹ and bicyclic triaminophosphine compound $P(i\text{-BuNCH}_2\text{CH}_2)_3\text{N}$ (**455**) (Figure 3.14).³²⁰

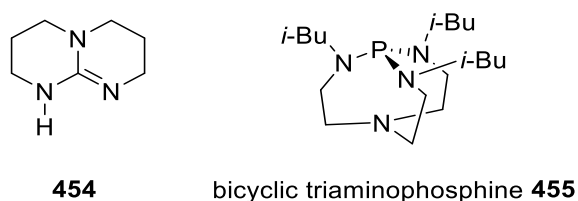
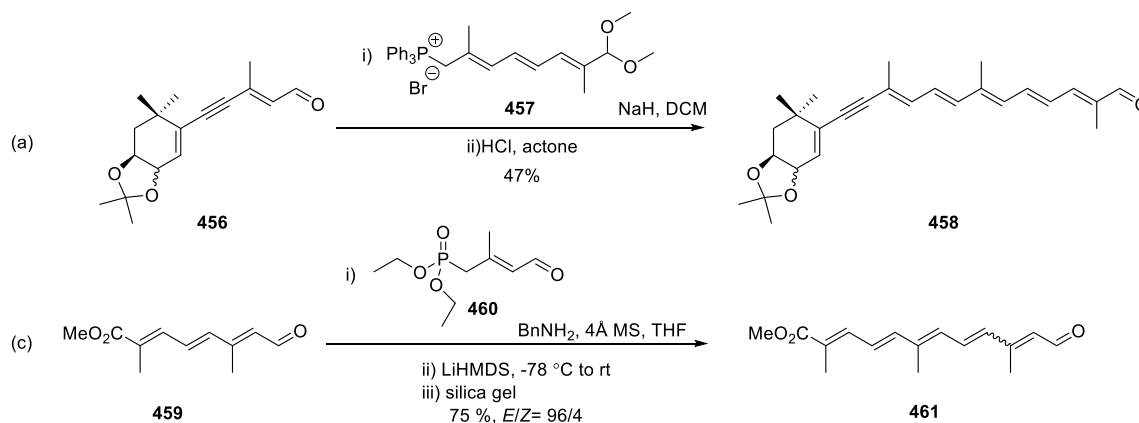


Figure 3.14 Structures of **454** and bicyclic triaminophosphine **455**.

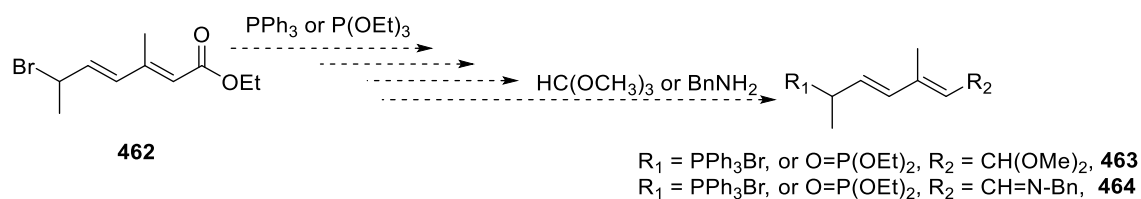
3.6.2 Preparation of Side Chain Fragments

As described in Section 3.1, the terminal tertiary amine functional group would be introduced by reductive amination of the terminal aldehyde and the methylated side chain would be attached to the macrocyclic core with a Wittig/HWE reaction. Since intramolecular Wittig reactions of phosphoryl ylides and carbonyl groups and intramolecular HWE reactions of phosphorylated aldehydes have been used widely for the construction of various five-, six-, seven-membered rings and macrocycles,³²¹ it is necessary to protect the terminal aldehyde to avoid self-condensation. The frequently used protective method is to transform the terminal aldehyde to an acetal,³²² and the other reported method is to temporarily mask the aldehyde as a relatively unstable imine,³²³ which could be easily converted back to the aldehyde in the purification process by silica gel chromatography (see Scheme 3.34 for examples).



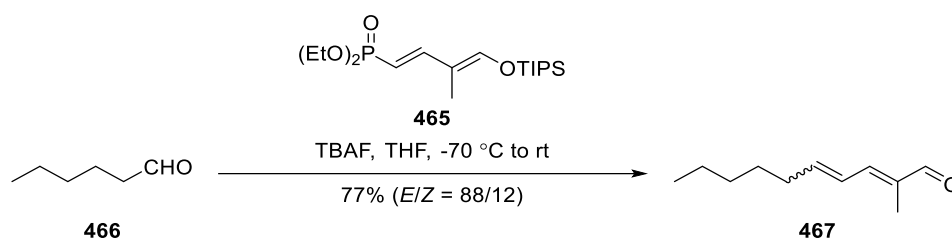
Scheme 3.34 Examples of protection of aldehydes in Wittig/HWE reactions using acetals³²² or imines.³²³

Therefore, as shown in Scheme 3.35, we proposed that compound **463** and **464** with an acetal and an imine functional groups, respectively, could be prepared from the brominated unsaturated ester **462** and could serve as a Wittig/HWE reagent for appending the side chain onto the macrocycle.



Scheme 3.35 Proposed preparation of methylated side chain fragments for Wittig/HWE olefination.

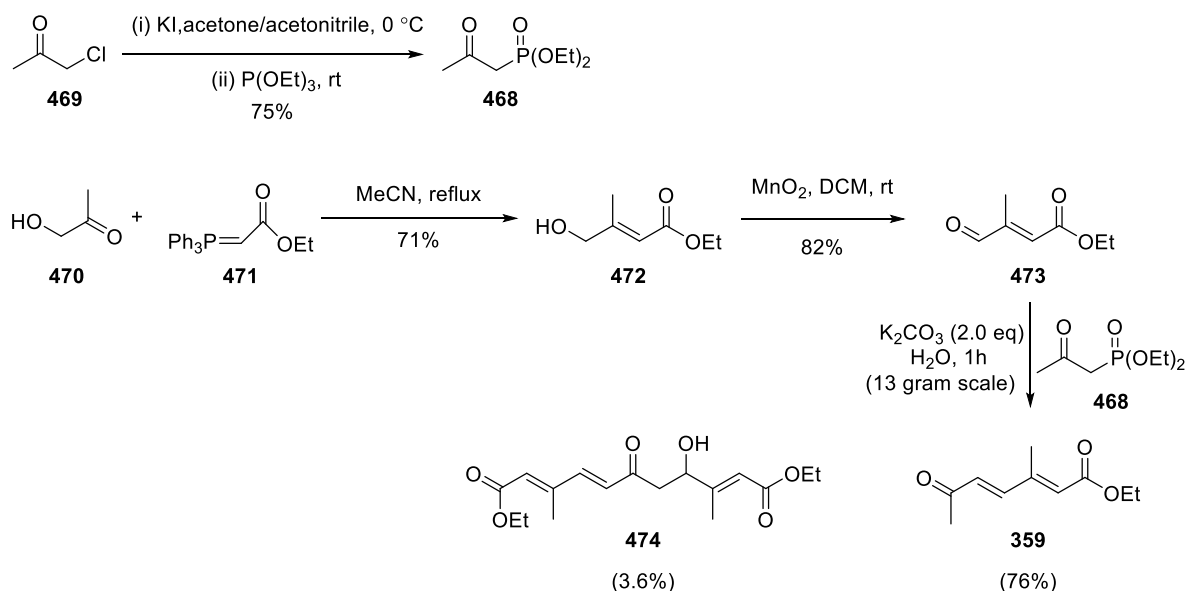
In 1999, Collignon and co-workers reported a methodology for the preparation of dienal compounds.³²⁴ It involves the reaction between an aldehyde and a tetrabutylammonium dienolate, which is generated *in situ* from *O*-triisopropylsilylated (*E, E*)-enol ether under treatment with TBAF (see Scheme 3.36 for a representative example). Based on their experimental results, this reaction showed high *E*-selectivity within non-conjugated aliphatic aldehydes. To the best of our knowledge, this methodology has not yet been utilised in synthetic work since its publication. Therefore, we were interested in testing the feasibility of using this method to attach the methylated side chain onto the macrocycle core.



Scheme 3.36 Use of enol silyl ether **465** in preparation of dienal **467**.³²⁴

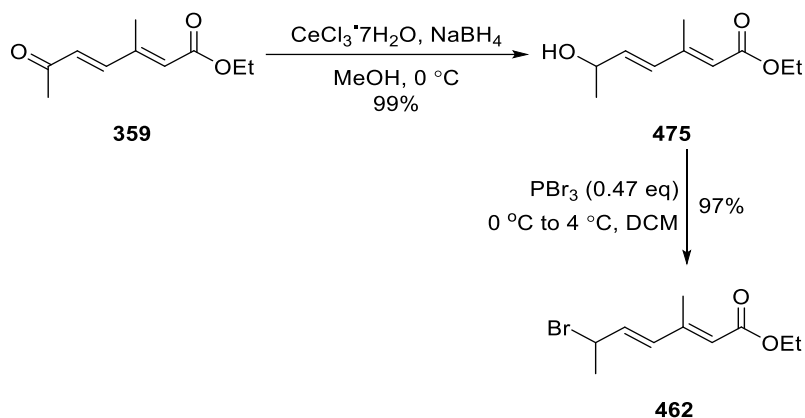
The preparation of brominated ester **462** largely followed a synthetic route designed by postdoctoral fellow Claire Cuyamendous in our research group. As shown in Scheme 3.37, the HWE reagent **468** required for this route was first prepared. This was achieved by Michaelis-Arbuzov reaction of triethylphosphite (P(OEt)_3) and iodoacetone, which was generated *in situ* by iodide substitution of chloroacetone **469**.³²⁵ Wittig reaction of hydroxyacetone **470** with stabilised triphenyl phosphorane **471** provided *E*- α,β -unsaturated ester **472**. Subsequent allylic oxidation by active manganese dioxide, which was freshly prepared from activated carbon and potassium permanganate (see Section 6.3.5 for experimental details), afforded aldehyde **473**. Initial small-scale HWE reaction of aldehyde **473** with the phosphonate **468** in an aqueous potassium carbonate solution

gave desired methyl ketone **359** in almost quantitative yield. However, when the reaction was scaled up, the yield of the ketone decreased and a minor product was observed. 2D NMR investigation revealed it to be compound **474**, which is generated from the aldol reaction between ketone **359** and the aldehyde starting material. The formation of this undesired product was probably prompted by excess K_2CO_3 and the higher concentration of the product ketone **359** in the reaction vessel. Therefore, lowering the equivalents of K_2CO_3 and performing the reaction in a more diluted manner should reduce the formation of the aldol product and improve the yield for large-scale reactions. Nonetheless, a reasonable yield of ketone **359** was obtained, and the optimisation was therefore not attempted.



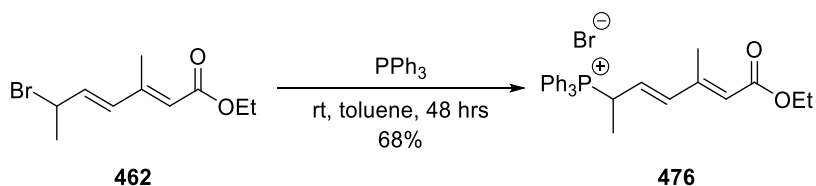
Scheme 3.37 Preparation of methyl ketone **359**.

Selective 1,2-reduction of methyl ketone **359** under Luche conditions provided allylic alcohol **475** in almost quantitative yield (Scheme 3.38).³²⁶ The conversion of allylic alcohol **475** into allylic bromide **462** was achieved by using phosphorus(III) bromide (PBr_3) as the brominating reagent. It is worth mentioning that the slow addition of PBr_3 by a syringe pump at a lower temperature was essential for the excellent yield. Not surprisingly, it was found that the allylic bromide was quite unstable and it could degrade significantly even on storage at $-18\text{ }^\circ\text{C}$. Hence, the bromide needs to be used for the next step immediately.



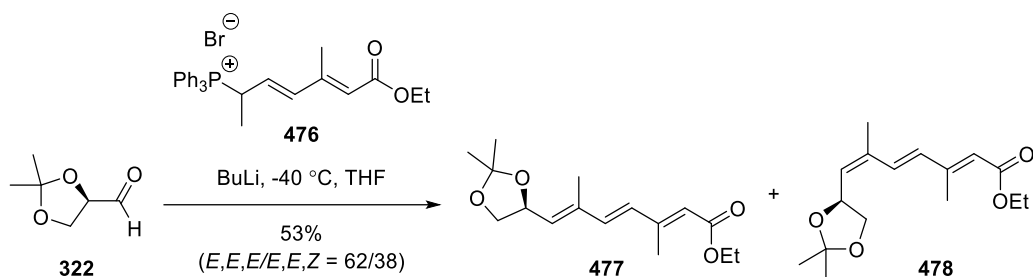
Scheme 3.38 Preparation of bromide **462**.

The bromide **462** was then reacted with triphenylphosphine (PPh_3) at room temperature in toluene to provide the triphenylphosphonium salt **476** in 68% yield (Scheme 3.39).



Scheme 3.39 Synthesis of triphenylphosphonium salt **476**.

Because the phosphorus ylide generated by deprotonation of phosphonium salt **476** could be stabilised by the terminal ester group through the conjugated system, we assumed that the Wittig reaction should have good *E*-selectivity based on Vedejs' model (refer to Section 3.6.1). To investigate its stereochemical outcome, we chose the chiral aldehyde **322** as the substrate for the model reaction. The reaction was carried out by pre-treating phosphonium salt **476** with BuLi at $-40\text{ }^{\circ}\text{C}$ followed by the addition of aldehyde **322**, resulting in an inseparable 62/38 ratio of the desired *E,E,E*-trienoate **477** and the undesired *E,E,Z*-trienoate **478** (Scheme 3.40).



Scheme 3.40 Preparation of trienoate **477** and **478**.

Assignments of proton peaks of the mixture of stereoisomers (Figure 3.15) were made on the basis of COSY, HSQC and HMBC correlations. The COSY spectrum enabled connectivity within the protonated fragments of each isomer to be determined (Figure 3.16). A structural subunit of C7/C8/C9 could be established as an isolated spin-system according to the ¹H-¹H COSY correlations of H7/H8/H9. The HMBC correlations from H2 to C1, C3 and C13, from H4 to C2, C3 and C13, and from H5 to C3 and C6, in combination with the HMBC correlations from H7 to C6, C9 and C14, successfully established the connectivity throughout the full carbon chain for each compound (Figure 3.17).

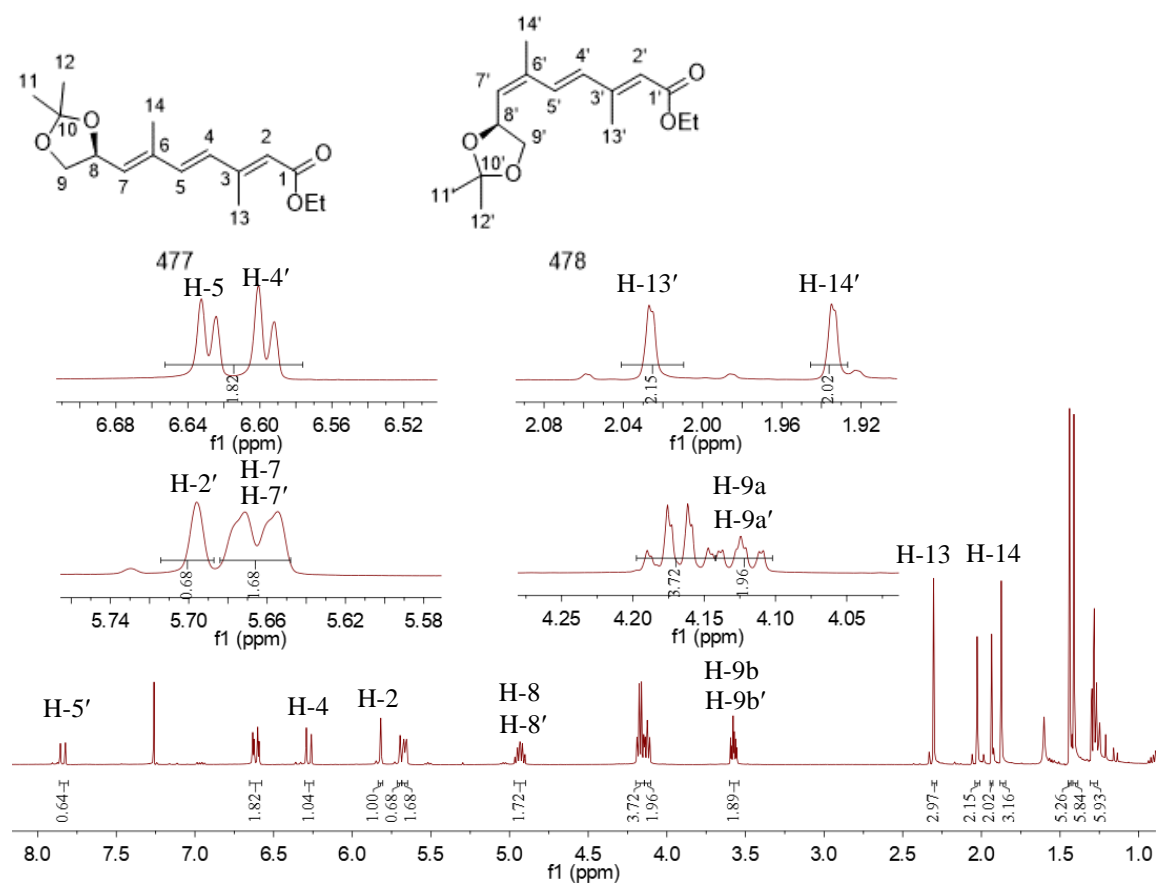


Figure 3.15 Assignment of ^1H NMR of the mixture of trienoate **477** and **478** in CDCl_3

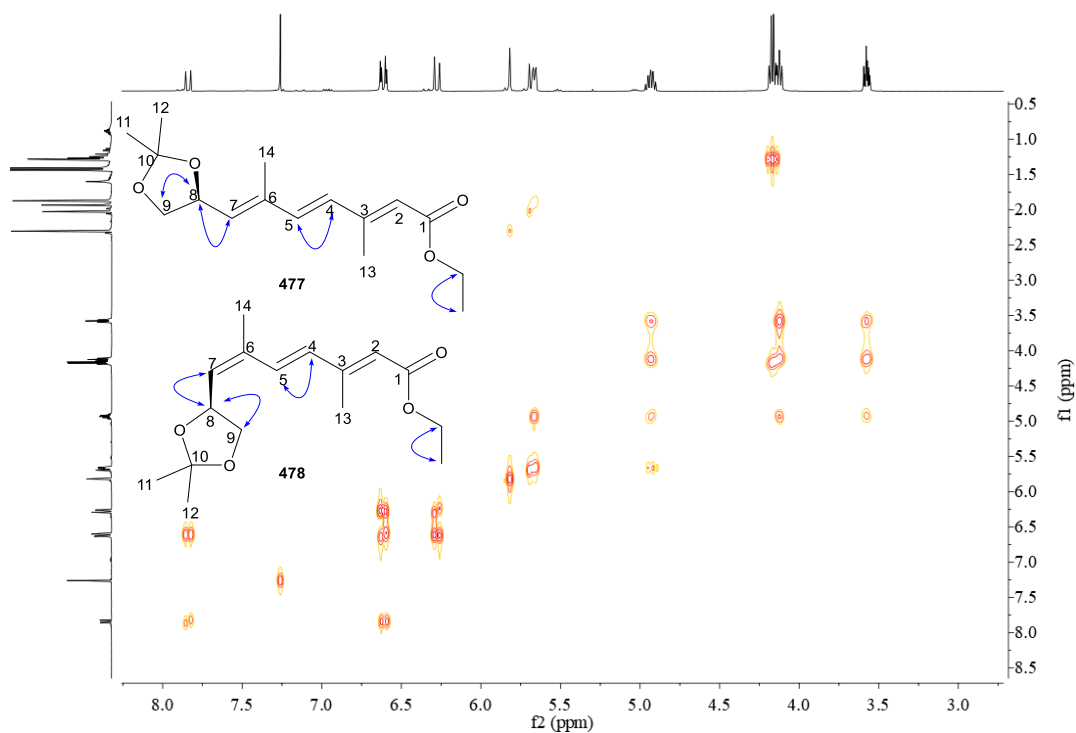


Figure 3.16 COSY correlations in structural elucidation of compounds **477** and **478**

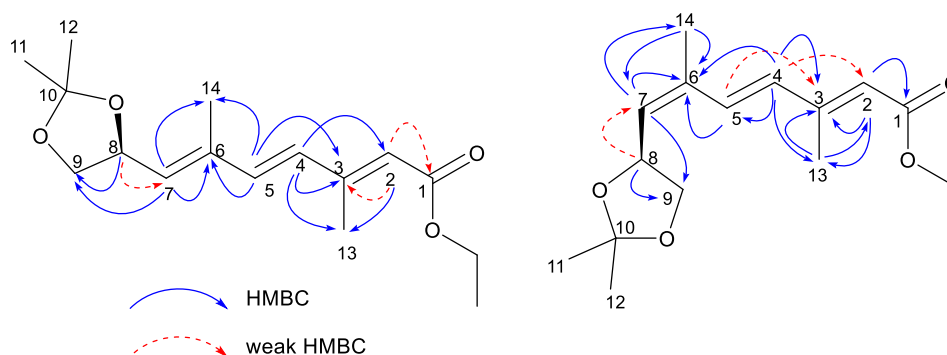
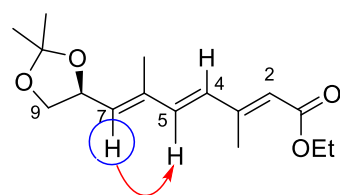


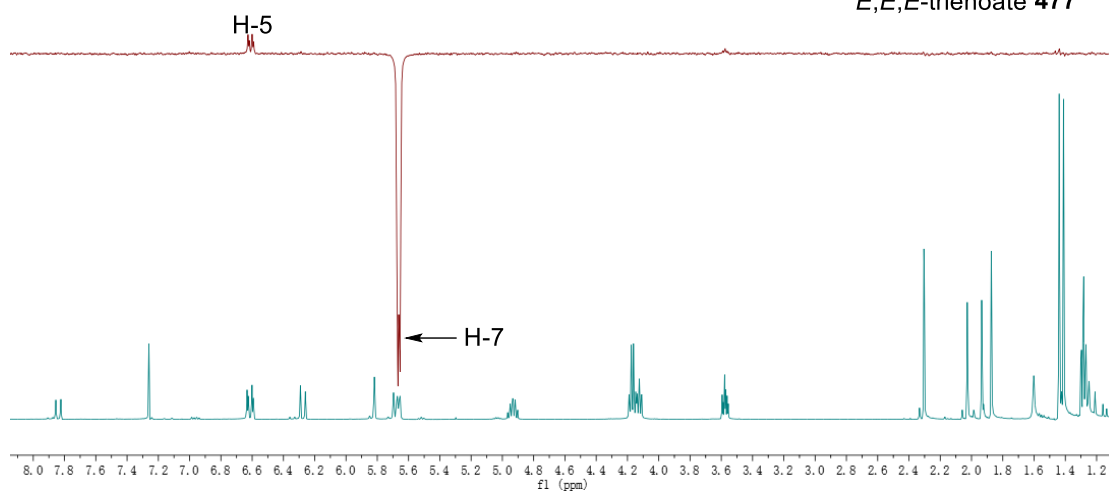
Figure 3.17 Key HMBC correlations in structural elucidation of compounds **477** and **478**

To distinguish the two stereoisomers of the trienoate, it was necessary to perform NOE experiments because the newly-formed double bond was trisubstituted. Unfortunately, the chemical shifts of the protons (between 5.68 and 5.64 ppm) at C7 for the two stereoisomers completely overlap in the ^1H NMR spectrum (Figure 3.15). Nevertheless, attempts were made to distinguish and assign the two stereoisomers by NOE correlations.

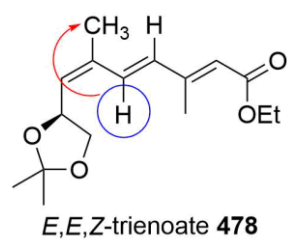
(a)



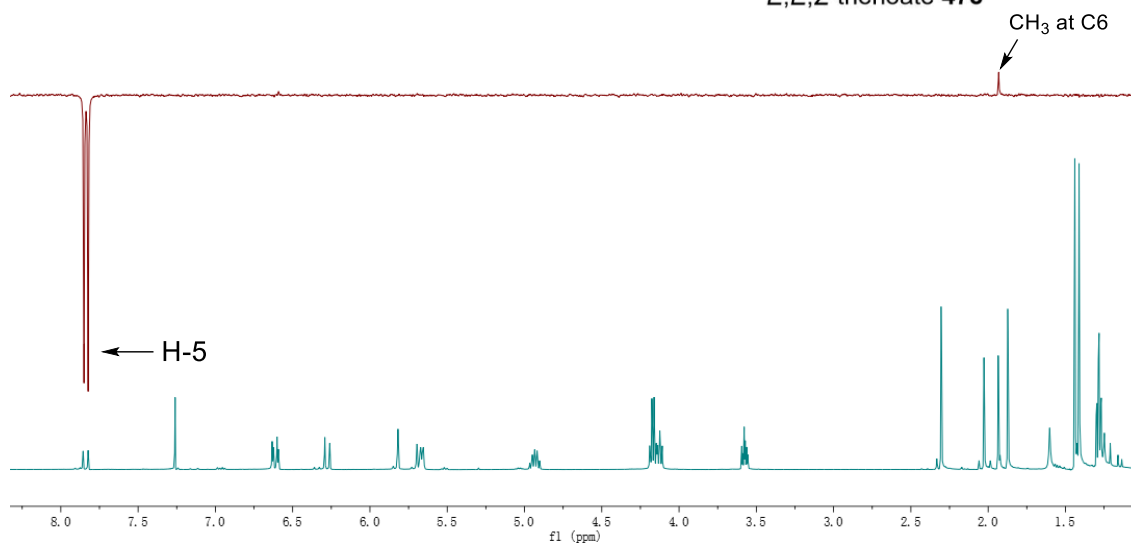
E,E,E-trienoate **477**



(b)



E,E,Z-trienoate **478**



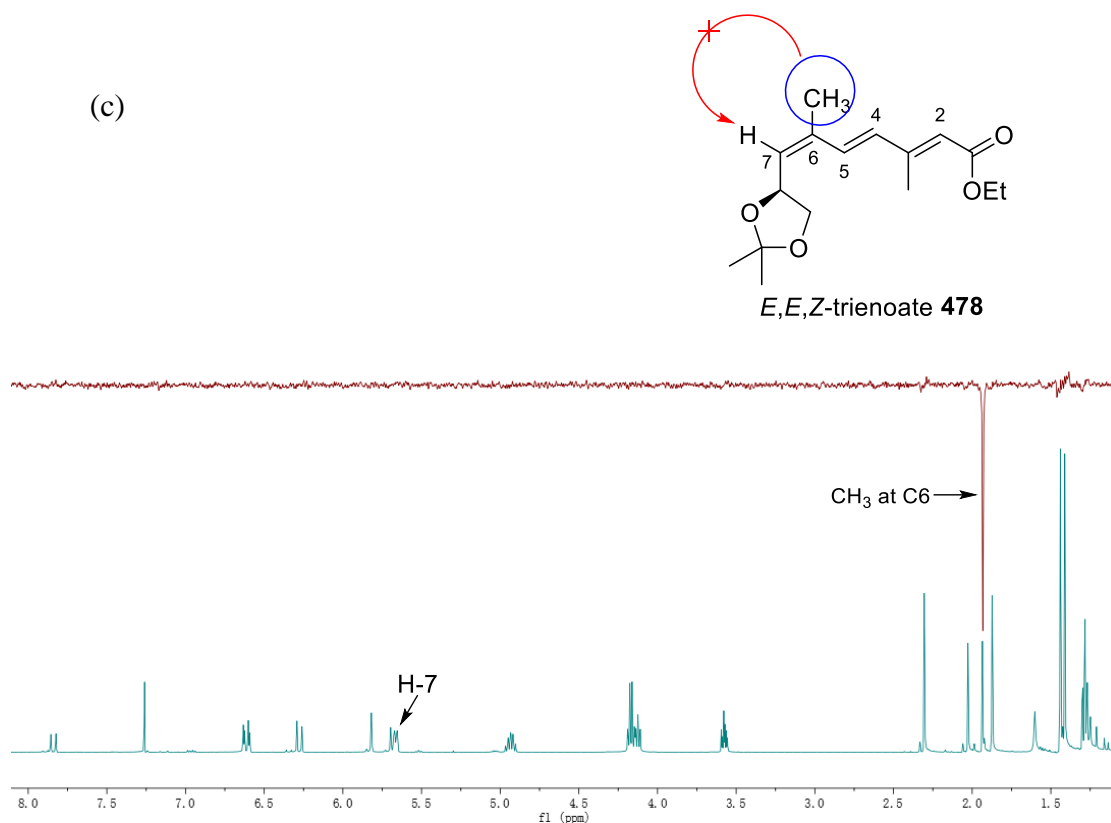


Figure 3.18 NOE correlations (in maroon) and ^1H NMR spectrum (in blue) of the mixture of trienoate **477** and **478** in CDCl_3 . The irradiated proton is shown in the blue circle and any NOE correlation observed is shown with a red arrow.

As shown in Figure 3.18a, irradiation at δ 5.68 ppm (H7) caused enhancement of the signal of the C5 proton (at δ 6.61 ppm) of the major isomer, identifying that the isomer as *E,E,E*-trienoate **477**. An irradiation of the C5 proton of the minor isomer at δ 7.84 ppm caused enhancement of the signal of the C6-methyl group (at δ 1.93 ppm), which is not helpful in identification of the configuration of the C-C double bond (Figure 3.18b). An irradiation of the C6-methyl group of the minor isomer at δ 1.93 ppm did not provide the expected correlation to the C7 proton (Figure 3.18c). However, we were confident that the minor isomer is *E,E,Z*-trienoate **478** based on 2D NMR analysis. It is also worth mentioning that the chemical shifts of the C5 proton allowed some additional confidence in these assignments. The signal of H5 in the major isomer is at δ 6.63 ppm whereas for the minor isomer is at δ 7.84 ppm (Figure 3.15). The significant downfield shift in the minor isomer is consistent with the assignment as *E,E,Z*-trienoate **478** as a result of the through-space deshielding effect due to the electronegative oxygen atom in the acetonide (Figure 3.19).

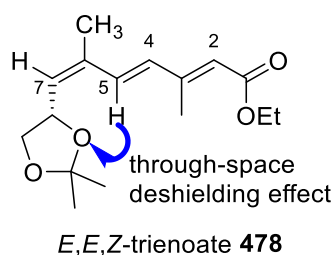


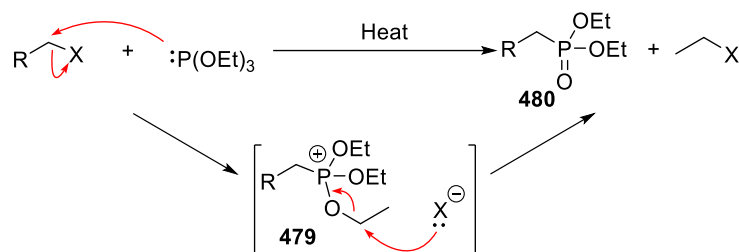
Figure 3.19 Proposed deshielding effect due to the oxygen atom of the acetonide in *E,E,Z*-trienoate **478**.

In view of the moderate *E*-selectivity (*E/Z* = 62/38) of the Wittig reaction with triphenylphosphonium salt **476**, we assumed that the triphenylphosphoryl ylide with a terminal acetal or imine group would afford a similar stereochemical outcome. Whether the use of a trialkylphosphonium salt would improve the *E*-selectivity would need to be further examined. However, an HWE strategy was first pursued.

As a phosphoryl aldehyde can serve as the common intermediate in the synthesis of the phosphoryl acetal or phosphoryl imine for HWE reaction and a phosphoryl silyl ether substrate for the TBAF-mediated aldol condensation, we decided to prioritise preparing phosphonate **481** at this stage. This would be synthesised by an Arbuzov reaction between bromide **462** and triethylphosphite.

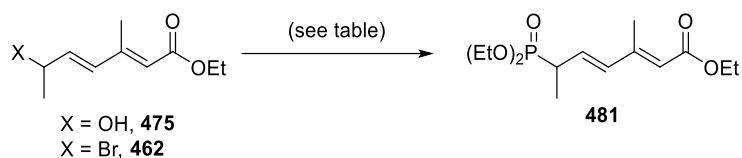
The Arbuzov reaction is a traditional method to prepare organophosphonates from the corresponding halides.³²⁷ In the proposed mechanism (Scheme 3.41), the reaction begins with the S_N2 nucleophilic attack on the alkyl group of the alkyl halide by the triethylphosphite to provide a phosphonium intermediate **479**. A second S_N2 reaction of the displaced halide anion with the phosphonium intermediate **479** resulted in the formation of a phosphonate product **480** accompanied by an alkyl halide.³²⁸ Despite its prevalence, it requires high reaction temperatures (*e.g.*, 140 – 180 °C) for an extended period of time for the activation of the reaction.^{328, 329} Therefore, we were concerned that the degradation of the unstable allylic bromide **462** would likely occur under heating at such high temperature, leading to the formation of unexpected by-products. In addition, traditional Arbuzov reactions with alkyl bromides and triethylphosphite concomitantly generate one equivalent of volatile and toxic ethyl bromide, which is not chemist-friendly. The resulting ethyl bromide could also react with the phosphite at such high temperatures to reduce the reaction efficiency. Therefore, direct conversion of alcohol **475** into

corresponding phosphonate **481** under mild conditions would be attractive as this could limit the risk of degradation and potentially give a higher yield.



Scheme 3.41 Proposed mechanism of the Arbuzov reaction between alkyl halide and triethylphosphite.^{327, 328}

Following the conditions of Iranpoor and co-workers,³³⁰ the direct conversion of allylic alcohol **475** to phosphonate **481** was attempted with a combination of PPh_3 , DDQ and P(OEt)_3 (Table 3.5, entry 1). However, no obvious evidence of formation of the desired phosphonate product **481** was obtained by ^1H NMR and HR-MS investigation. As TBAI has been efficiently used as a catalyst in this type of direct transformation,³³¹ the reaction was repeated with the presence of TBAI at 125 °C (entry 2) but a mixture of unidentified by-products was obtained. The inability to prepare phosphonate **481** by alcohol-based Michaelis-Arbuzov reaction prompted us to go back to attempt the traditional Arbuzov reaction. In order to reduce the risk of degradation of bromide **462**, the reaction was first carried out with P(OEt)_3 at reflux in toluene (at 110 °C) as opposed to 140 – 180 °C (entry 3). However, only a trace amount of the desired phosphonate was obtained after two-days heating. Repeating the reaction in refluxing *m*-xylene resulted in the degradation of the substrate, with the elimination of the allylic bromide observed (Entry 4). However, the desired product was obtained in 26% yield. We assumed that performing the reaction neat could potentially accelerate the desired transformation and therefore limit the degradation or elimination of the bromide substrate. Satisfyingly, when excess triethylphosphite was used as the solvent, the yield of phosphonate **481** improved to 50% (entry 5).

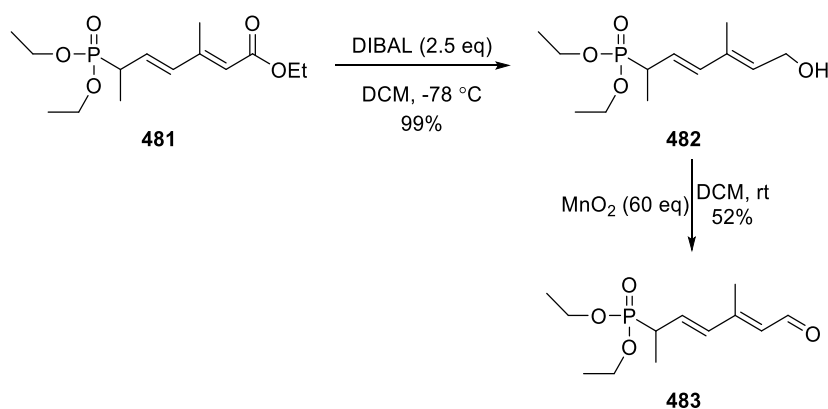


Entry	X	Conditions ^a (equiv.)	Yield ^b (%)
1	OH	P(OEt) ₃ (2.0), PPh ₃ (2.0), DDQ (2.0), MeCN, 80 °C, o/n	No product
2^c	OH	P(OEt) ₃ (1.5), TBAI (0.02), neat, 125 °C, o/n	No product
3	Br	P(OEt) ₃ (1.0), toluene, reflux, 2 d	trace
4	Br	P(OEt) ₃ (1.0), <i>m</i> -xylene, 140 °C, o/n	26
5^c	Br	P(OEt) ₃ (3.0), neat, 140 °C, o/n	50

^ao/n = overnight (i.e. 16 – 20 hours). ^bIsolated yields following silica gel chromatography. ^cP(OEt)₃ was used as solvent.

Table 3.5 Reaction screening for preparation of phosphonate **481**.

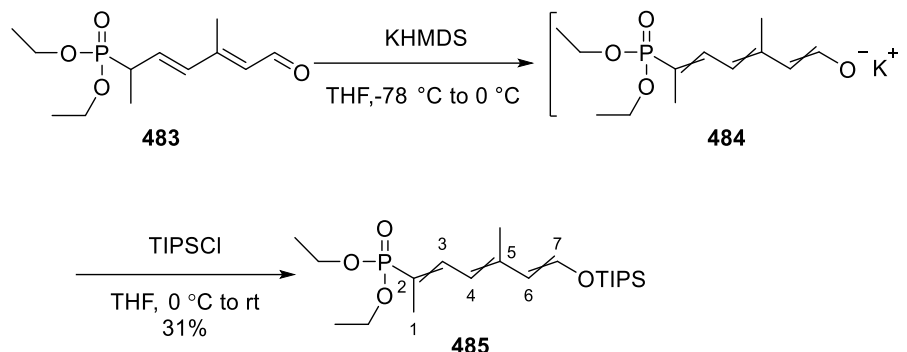
As shown in Scheme 3.42, the phosphoryl ester **481** was then reduced by DIBAL-H to provide alcohol **482** in almost quantitative yield. Subsequent allylic oxidation by active manganese dioxide afforded phosphoryl aldehyde **483** smoothly.



Scheme 3.42 Preparation of phosphoryl aldehyde **483**.

With aldehyde **483** in hand, we then attempted to prepare phosphoryl silyl ether **485**. Following the procedure reported by Collignon and co-workers,³²⁴ aldehyde **483** was deprotonated by KHMDS at -78 °C to 0 °C to form the potassium dienolate **484**. This intermediate displayed low solubility in THF, which matches Collignon's experimental observation.³²⁴ Subsequent reaction between TIPSCl and dienolate intermediate **484** afforded silyl ether **485** (Scheme 3.43). NMR analysis showed that the coupling constant between C6 proton and C7 proton ³J is 11.9 Hz, which is not a solid evidence to support

the desired *E*-configuration. At this point, the time constraints limited further investigation on optimisations to improve the yield and thorough NOE experiments to confirm the configuration of the double bonds of compound **485**.



Scheme 3.43 Preparation of phosphoryl silyl ether **485**.

3.7 Conclusion

In conclusion, the three major fragments, namely thioamide **382**, alkyne **364** and phosphoryl silyl ether **485**, were prepared for the synthesis of thiazole analogue **184**. The C8 – C11 fragment thioamide **382** was prepared from commercially available amide **339** with a 35% yield over 3 steps and the formation of the thioamide (*S*)-oxide impurity by air could be avoided by taking extra measures in the post-purification stage. The alkyne fragment was efficiently accessed from 1,3-propanediol with a 30% yield over 7 steps. In preparation of alkyne **364**, it was found that the observed polymerisation of diene intermediate **388** could be possibly attributed to the inadvertent introduction of acid from sand used for column preparation. The side chain-fragment phosphoryl silyl ether **485** was prepared from hydroxyacetone in an 8% yield over 8 steps and the yield could be potentially further improved after optimising conditions for the formation of the silyl ether.

The one-pot gold-catalysed coupling between alkyne **364** and thioamide **382** provided the desired thiazole **393** in an acceptable yield. KHMDS-induced ring opening of the lactone residing in compound **393** provided the desired *Z,E*-dienoic acid **418** smoothly. However, the subsequent selective desilylation step was found to be low-yielding, there, several alternative routes, including performing the desilylation step prior to the lactone opening, were trialled. Unfortunately, these efforts did not improve the yield significantly. This

means that the preparation of seco-acid **419** will require further investigation. The macrolactonisation of compound **419** under modified Mukaiyama conditions, followed by fluoride-induced desilylation, provided macrocyclic alcohol **441** efficiently. To complete the synthesis of analogue **184**, TBAF-mediated aldol-like condensation between silyl ether **485** and the aldehyde derived from alcohol **441** will be performed.

In order to prepare CF₃-substituted thiazole analogue **185**, attempts to access CF₃-substituted thiazole **395** via brominate thiazole intermediate **394** were made. Unfortunately, the initial palladium-catalysed trimethylation reaction was unsuccessful. Further investigation of appropriate conditions will be conducted.

Chapter Four: Towards Synthesis of Triazole Analogue with Methylated Side Chain

4.1 Introduction

4.1.1 Synthesis of Triazole Analogue 182

As mentioned in Section 1.6, the key features of the synthesis of the racemic analogue **182** included Julia-Kocienski olefination to attach the non-methylated side chain fragment, lactone ring-opening to provide the *Z,E*-dienoate and a copper-catalysed alkyne-azide cycloaddition (CuAAC) to form the triazole ring. Therefore, three major fragments – sulfone fragment **284**, aldehyde fragment **289**, and alkyne fragment **414** were utilised in Cumming's synthesis of analogue **182**.¹³⁴

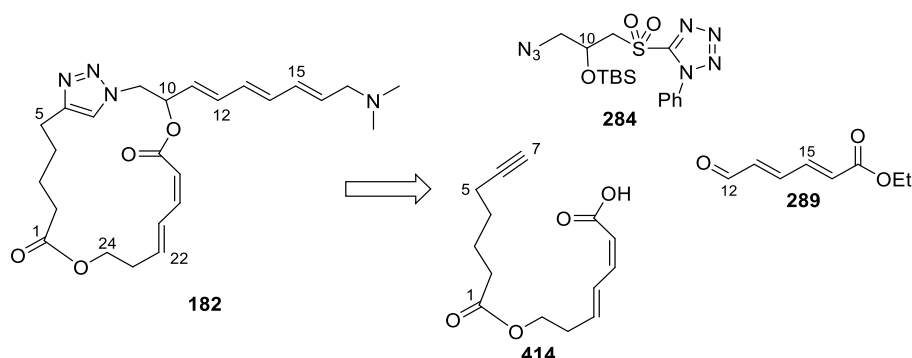
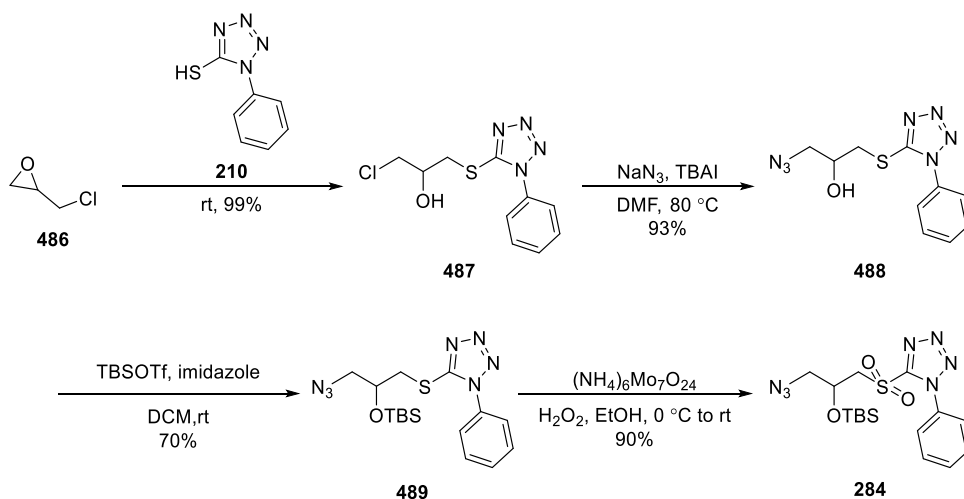


Figure 4.1 Major fragment in Cumming's synthesis of analogue **182**.

Preparation of Sulfone Fragment 284

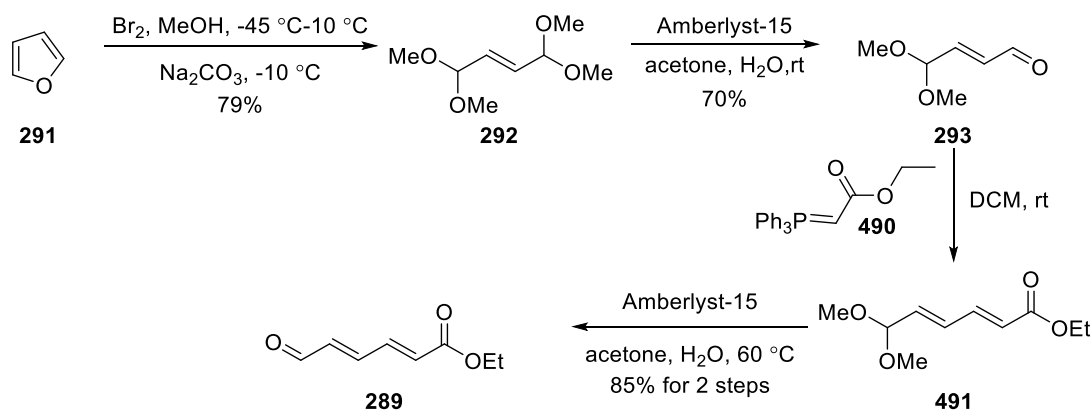
The synthesis of sulfone fragment **284** began with the ring opening of 2-(chloromethyl)oxirane **486** with 1-phenyl-1*H*-tetrazole-5-thiol **210**, giving chloroalkylthioether **487**. The alkyl chloride was then substituted by sodium azide to afford compound **488**. Subsequent silylation, followed by oxidation of the resulting thioether **489**, provided sulfone fragment **284** (Scheme 4.1).



Scheme 4.1 Preparation of sulfone **284** in the synthesis of analogue **182**.

Preparation of Aldehyde Fragment 289

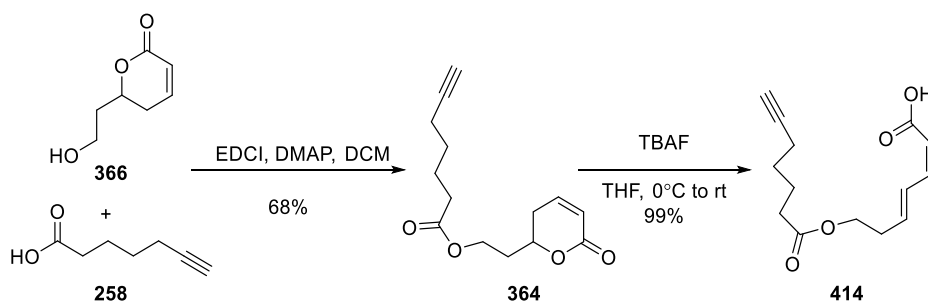
The key acetal intermediate **293** for the synthesis of aldehyde fragment **289** was prepared from furan in 2 steps, which has been described in the synthesis of enal **297** (refer to Section 2.3.3). Wittig reaction with stabilised ylide **490** provided *E,E*-dienoate **491**. Acetal cleavage under treatment with Amberlyst-15, a solid-supported acidic resin, at 60 °C provided the desired dienal **289** (Scheme 4.2).



Scheme 4.2 Synthesis of aldehyde **289** from furan **291**.

Preparation of Alkyne Fragment 414

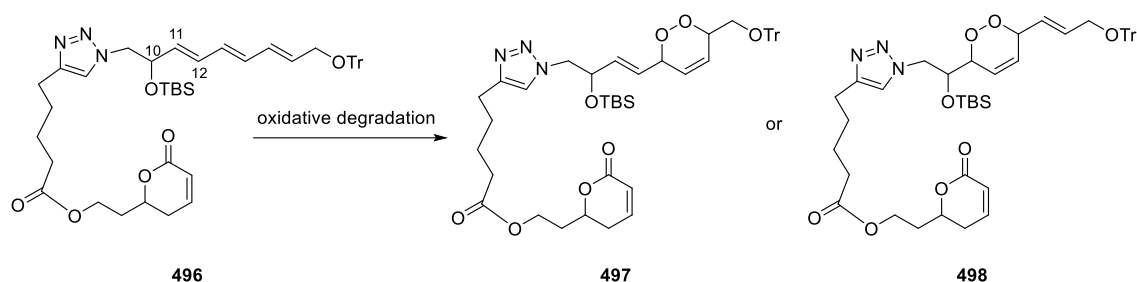
Alkyne fragment **414** was prepared from the TBAF-induced ring opening of alkyne **364** (Scheme 4.3), which was synthesised from the Steglich esterification of 6-heptynoic acid **258** with alcohol **366** (refer to Section 3.3 for the details of the synthesis of **366** from 1,3-propanediol).

Scheme 4.3 Preparation of alkyne fragment **414**.

Coupling of Fragments to Complete Analogue **182**

The side chain fragment enal **289** was coupled with sulfone **284** through Julia-Kocienski olefination to provide trienoate **290** (Scheme 4.4). Ester **290** was reduced by DIBAL-H to give alcohol **492**, which was subjected to Parikh-Doering conditions to afford trienal **493**. As prolonged treatment of trienal **493** under acidic conditions could potentially lead to the formation of a teraene product through the elimination of the hydroxyl group of desilylated product **494**, treatment with HCl in methanol was only conducted for 2 hours and the silyl ether starting material was recovered and recycled in subsequent desilylation reactions. Azid-containing seco-acid **417** was prepared *via* a CuAAC reaction between azide **494** and alkyne fragment **414** (*vide supra*, Scheme 4.3). In the following Yamaguchi macrolactonisation step, to minimise the risk of isomerisation of the *Z,E*-dienoic acid, a catalytic amount of DMAP was added to the highly-diluted anhydride intermediate at -78 °C, which was generated from the reaction with the activating reagent **93**. Although the use of these modified Yamaguchi conditions did prevent the isomerisation, the desired macrocyclic compound **495** was obtained in only 13% yield. Reductive amination of **495** with dimethyl amine and tetramethylammonium triacetoxyborohydride provided racemic triazole analogue **182**.

Cumming's synthetic route provided triazole analogue **182** over 11 steps for the longest linear sequence but the overall yield is only 2.2%. It is worth mentioning that the overall yield before the Yamaguchi macrolactonisation step is 31% and the overall yield after that is only 4%. Therefore, the macrolactonisation step is the major hurdle to improve the yield. Based on the good results obtained in the macrolactonisation step in Fürstner's synthesis of PatA and DMDA PatA (refer to Section 1.4.1.3 and 1.4.2.2), use of the modified Mukaiyama macrolactonisation methodology would potentially enhance the yield for the synthesis of this type of PatA analogues.



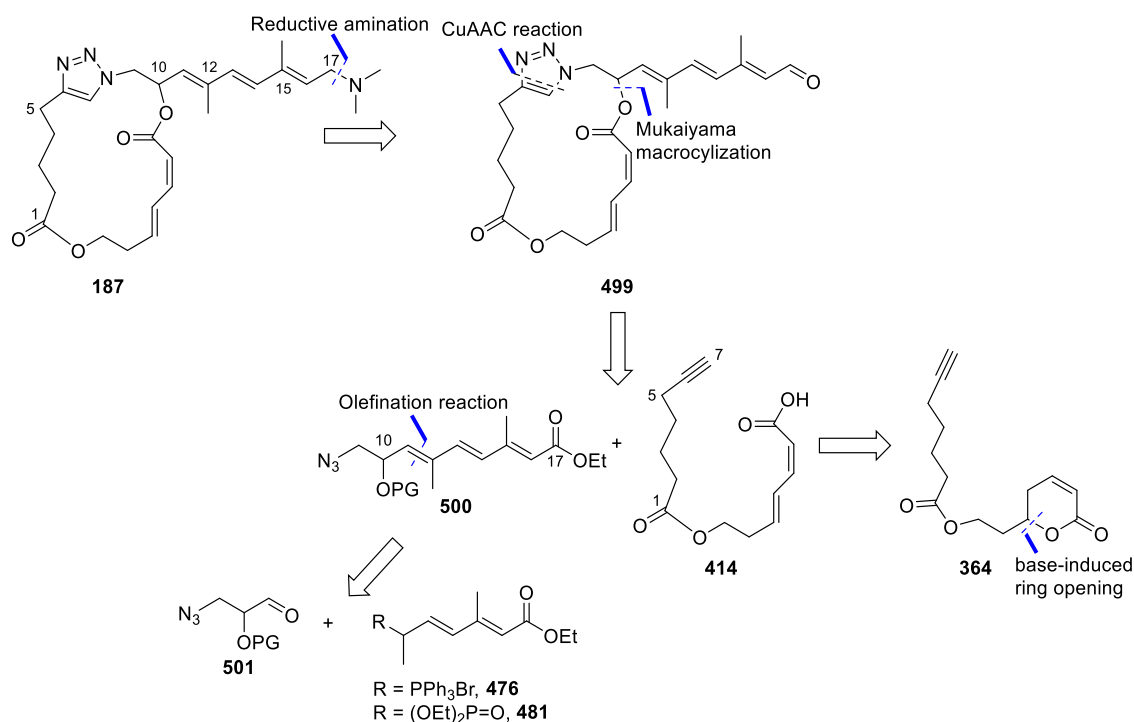
Scheme 4.5 Proposed degradation of compound **496** caused by autoxidation.¹³⁵

As mentioned in Section 1.7.1, investigating the difference between the biological activity of Cumming's triazole analogue **182** and that of a triazole analogue with the methylated side chain would ascertain whether the reintroduction of the methyl groups at C12 and C15 (PatA numbering) could enhance the inhibitory activity. This chapter describes studies towards the synthesis of a novel triazole analogue that we carried out alongside the synthesis of thiazole analogue **184** described in chapter three.

4.2 Retrosynthetic Analysis

In a variation of Cumming's strategy in the synthesis of analogue **182**, the reaction sequence for the synthesis of analogue **187** would use modified Mukaiyama macrolatonisation as opposed to Yamaguchi macrolatonisation to improve the overall yield. Also, the side chain-fragment would be attached through a Wittig/HWE reaction instead of the Julia-Kocienski olefination.

As shown in Scheme 4.6, the terminal tertiary amine group in the side chain would be introduced in the final step by reductive amination of aldehyde **499**. The side chain fragment **476** or **481** would be incorporated into the molecule prior to the construction of the macrocycle. The triazole ring would be synthesised by a CuAAC after the formation of the *E,Z*-dienoic acid. Trienoate fragment **500** could be prepared from a Wittig/HWE reaction between azide **501** and a triphenylphosphonium salt **476** or a phosphoryl ester **481** (see Section 3.6.2 for their synthetic routes). Alkyne fragment **414** could be prepared by a base-induced ring-opening reaction of the lactone **364** (see Section 3.3 for its synthetic route). The macrocycle **499** would be conveniently constructed through a combination of the modified Mukaiyama macrocyclisation and the CuAAC reaction.



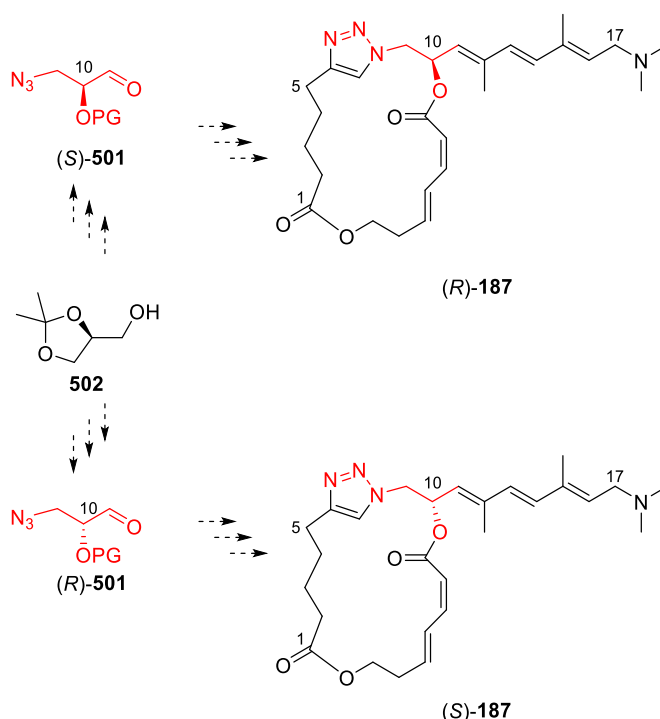
Scheme 4.6 Retrosynthetic analysis of triazole analogue **187**.

The CuAAC reaction is a variant of the Huisgen 1,3-dipolar cycloaddition and was independently discovered by Medal¹⁴³ and Sharpless¹⁴² in 2002. It is a robust reaction that displays extraordinary tolerance towards a wide range of functionalities.¹⁴⁰ Therefore, it has been utilised in various fields such as drug discovery,³³² biochemistry,³³³ and polymer chemistry.³³⁴ It has been identified as one of the reactions that fulfil the prerequisite criteria of “click chemistry”, a terminology introduced by Sharpless and co-workers to describe reactions that are high-yielding, tolerant to a wide range of functionalities, able to generate only by-products which can be removed by non-chromatographic methods, simple to conduct (ideally, the reaction should not be sensitive to water or oxygen) and can be performed without solvents or in benign solvents (such as water).³³⁵

Although Cumming proposed that the stereochemistry of C10 (PatA numbering) is essential for the binding process and that the stereoisomeric analogues of C10 could be completely inactive,¹³⁵ there were no structure-relationship studies on the configuration of C10 reported in the literature. Therefore, in order to compare the bioactivity of stereoisomers at C10, we chose to prepare both enantiomers of the triazole analogue **187**.

Based on Cumming’s unpublished experimental results,¹³⁵ attempts to construct the

macrocycle and simultaneously invert the configuration of C-10 using an intramolecular Mitsunobu reaction would result in significant degradation of substrates. Therefore, it would be attractive to use a switchable starting material for the preparation of (*R*)- and (*S*)-**187**. We envisioned that (*S*)-solketal **502**, a readily available enantiopure building block, could serve the purpose because it could be conveniently transformed to chiral aldehyde (*S*)-**501** or (*R*)-**501** via a few simple steps (Scheme 4.7).

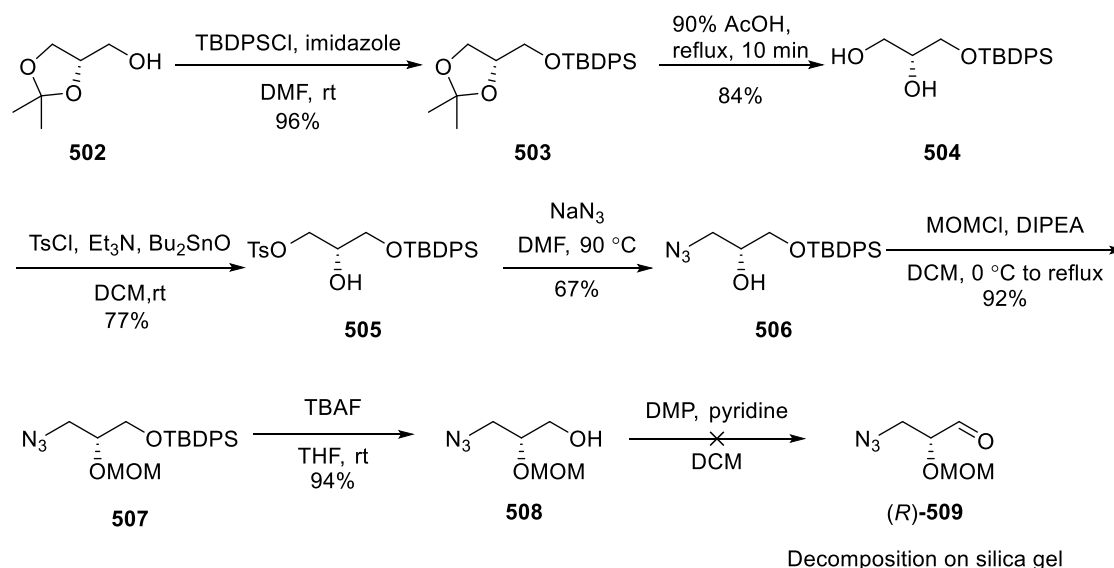


Scheme 4.7 Proposed synthesis of (*R*)-**187** and (*S*)-**187** from the same starting material (*S*)-solketal **502**.

As the preparation of (*R*)-**501** from (*S*)-solketal **502** requires fewer steps than that of (*S*)-**501**, it would be more likely to succeed. In addition, because enantiomers exhibit identical behaviours in achiral chemical reactions, the synthesis of analogue (*S*)-**187** would be informative for the synthesis of (*R*)-**187** analogue. Therefore, attempts to synthesise analogue (*S*)-**187** from aldehyde (*R*)-**501** were first performed.

4.3 Attempted Preparation of Aldehyde (*R*)-509

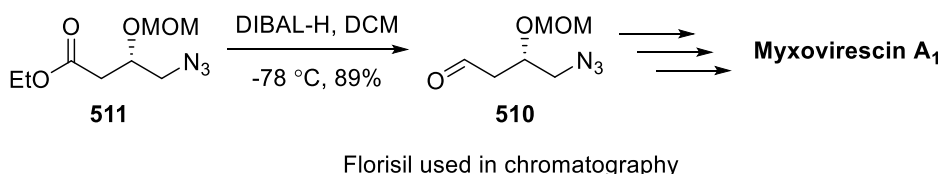
Our attempts to synthesise MOM-protected aldehyde (*R*)-509 began with TBDPS protection of (*S*)-soketal 502 (Scheme 4.8). Subsequent cleavage of the acetonide group in silyl ether 503 was achieved by reflux with 90% acetic acid. Tosylate 505 was formed *via* the Bu₂SnO-catalysed selective tosylation of diol 504. Subsequent substitution of the tosylate by sodium azide was performed in DMF at 90 °C. MOM-protection of the secondary OH of azide 506 using methoxymethyl chloride and DIPEA provided MOM ether 507, which was then treated with TBAF to give primary alcohol 508. Buffered Dess-Martin oxidation was used in our first attempt to prepare chiral aldehyde (*R*)-509. After one-hour stirring at room temperature, ¹H NMR analysis of aliquot samples of the reaction mixture showed that the signals of the α-protons of the -OH group of 508 at 3.68 and 3.63 ppm completely disappeared while a sharp singlet peak at 9.71 ppm appeared, suggesting that the oxidation of the alcohol 508 to the desired aldehyde^{*****} had a good conversion rate. However, purification of the crude product by silica gel flash chromatography to remove impurities generated from Dess-Martin periodinane provided only a mixture of unidentified by-products. 2D TLC analysis of the crude sample was then performed, and it was found that aldehyde (*R*)-509 rapidly decomposed on silica.



Scheme 4.8 Attempted preparation of aldehyde (*R*)-490 from (*S*)-solketal 489.

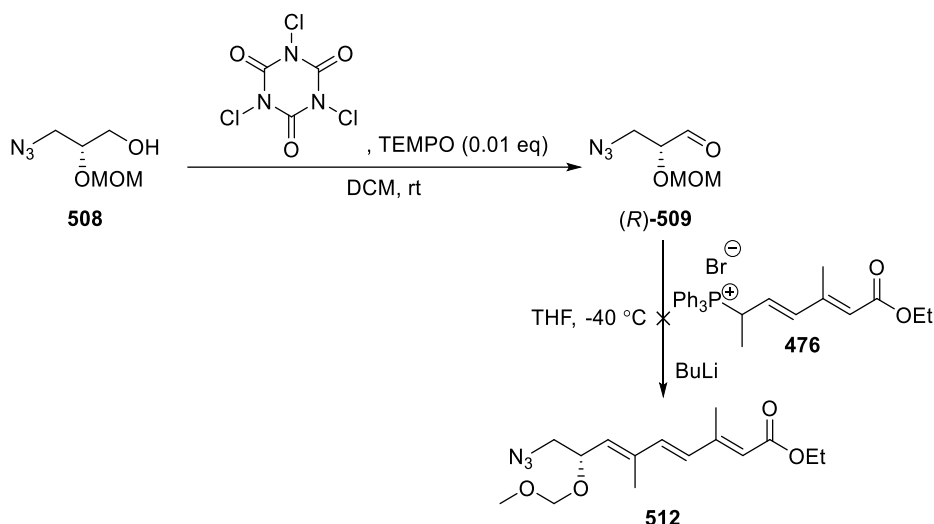
***** This was based on analysis of the ¹H NMR and gCofsy spectra of the crude mixture. With peaks at (500 MHz, CDCl₃) δ 9.71 (s, 1H), 4.83 (s, 2H), 4.13 – 4.09 (m, 1H), 3.59 – 3.55 (m, 2H), 3.48 (s, 3H).

A scan through the literature revealed that aldehyde **510** with a similar structure to (*R*)-**509** was reported by Fürstner and co-workers to be sensitive to silica gel. Instead, activated magnesium silicates for chromatography, like Florisil, were used for its purification (Scheme 4.9).³³⁶ As this type of chromatography material was unavailable in our laboratory, we decided to seek an alternative method to provide the aldehyde in pure form which does not require using chromatographic purification.



Scheme 4.9 Preparation of aldehyde in the total synthesis of myxovirescin A1.³³⁶

In 2001, Giacomelli and co-workers reported that primary alcohols could be efficiently oxidised to the corresponding aldehydes by trichloroisocyanuric acid at room temperature in the presence of catalytic TEMPO.³³⁷ This mild method was very attractive to us because it provided chiral aldehydes with α -stereocenters in high purity after a simple aqueous work-up procedure. Therefore, oxidation of alcohol **508** was performed following their conditions. Unfortunately, in addition to the desired product, a minor unidentified product was observed in the crude sample after work-up. Purification of the aldehyde (*R*)-**509** by distillation was then attempted. Not surprisingly, it was found that aldehyde degraded significantly in the distillation process when it was heated at 40 – 45 °C for a relatively prolonged period of time. As purification of the aldehyde proved to be problematic, the oxidation of alcohol **508** under Giacomelli's conditions was repeated, and the crude aldehyde was used directly after work-up for the Wittig reaction with triphenylphosphonium salt **476** (Scheme 4.10). To our dismay, no sign of the desired product **512** was observed, and instead, a mixture of unidentified products was obtained. This result was possibly due to the instability of the aldehyde in the strongly basic conditions.

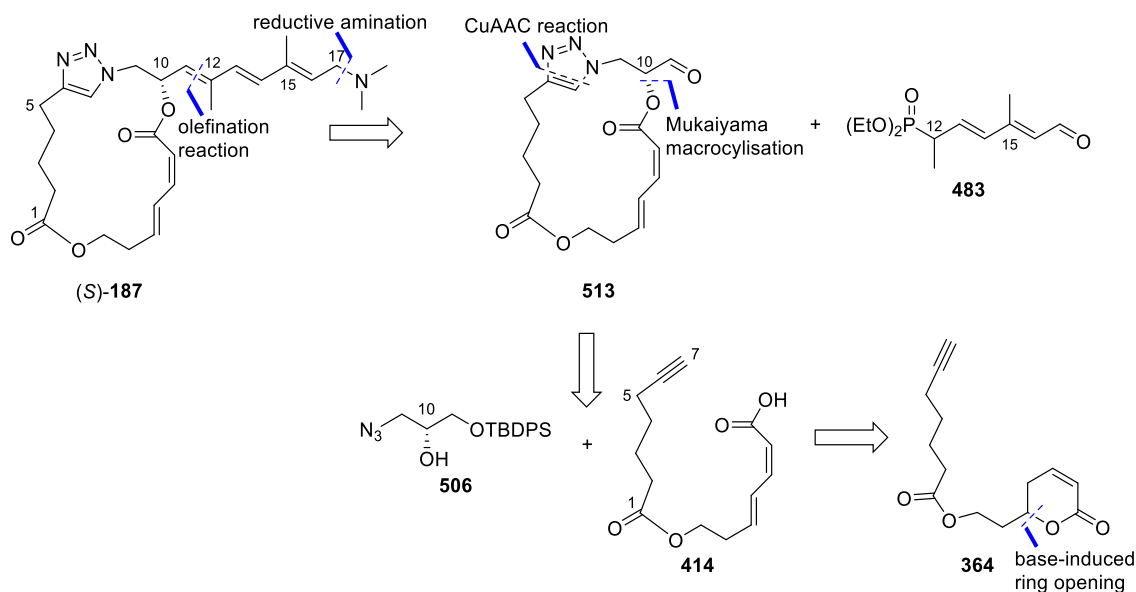


Scheme 4.10 Attempted preparation of trienoate **512** *via* crude aldehyde (*R*)-**509**.

The inability to purify the aldehyde (*R*)-**509**, as well as its potential instability under basic conditions required for Wittig/HWE olefination, led us to abandon this approach. A new synthetic route to triazole analogues (*S*)- and (*R*)-**187** that aligned with the synthesis of the thiazole analogue **184** was designed. In this new design, the macrocyclic core would be constructed prior to the attachment of the side chain fragment.

4.4 Revised Synthetic Route for Synthesis of Analogue (*S*)-**187**

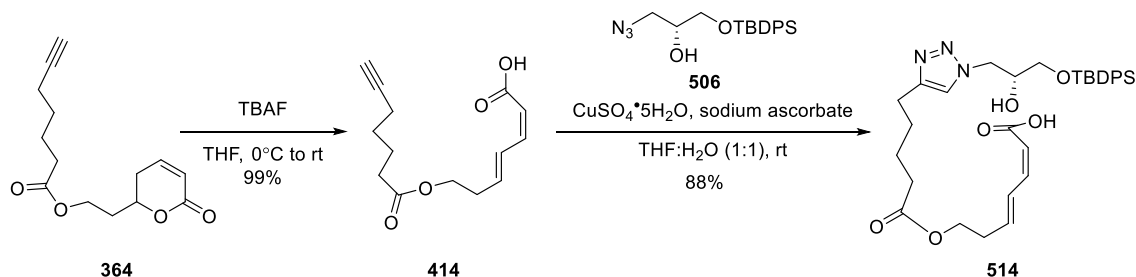
The revised route for the synthesis of (*S*)-**187** would involve a macrocyclic aldehyde partner and a side chain phosphonate (Scheme 4.11). This would mean performing the CuAAC reaction between mono-silylated azide **506** and alkyne **414**. The triazole-containing macrocycle **513** would be constructed at an early stage *via* modified Mukaiyama macrocyclisation. The olefination reaction between triazole-containing macrocyclic aldehyde **513** and an appropriate derivative of phosphoryl aldehyde **483** would be carried out at a late stage to attach the side chain.



Scheme 4.11 Revised retrosynthetic analysis of triazole analogue (*S*)-**187**.

4.5 Construction of Macrocyclic Compound **523**

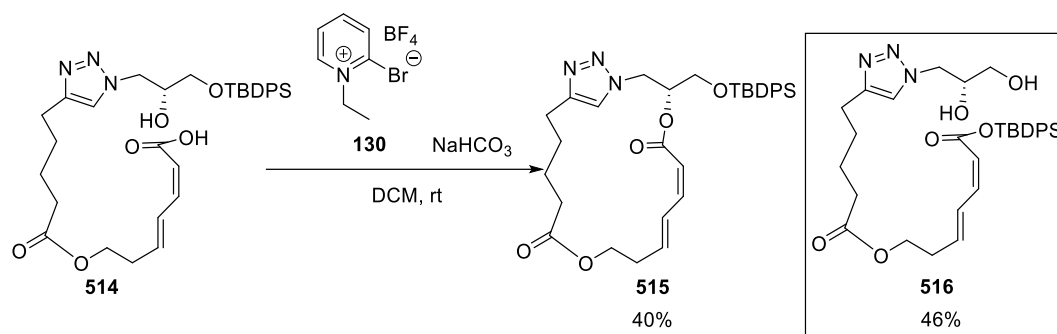
Attention was first turned to the construction of the macrocycle core. The ring opening of lactone **364** facilitated by treatment with TBAF gave *Z,E*-dienoic acid **414** in almost quantitative yield, which was subsequently coupled with azide **506** via a CuAAC process to provide seco-acid **514** (Scheme 4.12).



Scheme 4.12 Preparation of seco-acid **514**.

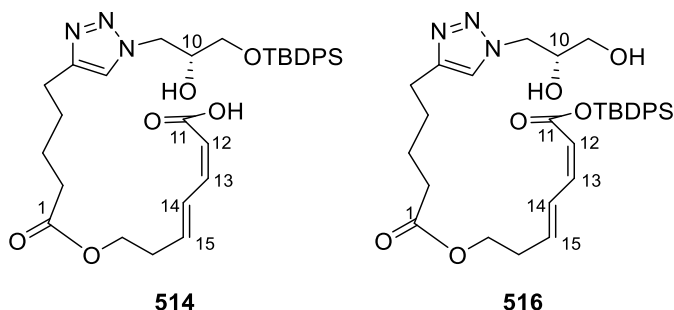
Performing Mukaiyama lactonisation of seco-acid **514** following conditions optimised for the synthesis of thiazole-containing macrocycle **440** (see Scheme 3.29 in Section 3.5.2.2) afforded triazole-containing macrocycle **515** (see entry 1 of Table 4.2 for detailed conditions) in a 40% yield (Scheme 4.13) and no geometric isomer was observed by ¹H NMR analysis. However, in addition to the desired product, an unexpected by-product **516** was observed by ¹H NMR analysis of the aliquot samples and was successfully

isolated by silica gel chromatography.



Scheme 4.13 Preparation of triazole-containing macrocycle **515**.

Careful investigation of the 2D NMR spectra of both seco-acid starting material **514** and the by-product **516** revealed that the changes of proton and carbon chemical shifts, compared to the starting material, mainly appeared in the C11 to C15 region (Table 4.1) and especially, the signal of the carbon at the C11 position was significantly shifted upfield from 169.6 ppm to 161.6 ppm. However, it was of note that there were no significant changes in the coupling constants of the alkenes, suggesting that the *Z,E*-diene motif should be completely retained.



Position	Compound 514 ^1H NMR δ (ppm)/ J (Hz)	Compound 516 ^1H NMR δ (ppm)/ J (Hz)	Compound 514 ^{13}C NMR δ (ppm)	Compound 516 ^{13}C NMR δ (ppm)
11	-	-	169.6	161.6
12	5.63, d, 11.3	5.62, d, 11.1	116.9	115.0
13	6.60, t, 11.3	6.72, t, 11.2	145.5	149.0
14	overlapped	overlapped	129.4	129.2
15	6.04, dt, 14.3, 6.7	6.14, dt, 14.6, 7.1	140.1	143.1

Table 4.1 Comparison of selected ^1H NMR and ^{13}C NMR data of seco-acid **514** with that of silyl ester **516**.

A literature search of TBDPS esters showed that the chemical shifts of carbonyl groups of silyl ester products are normally shifted upfield when compared to those of carbonyl groups of the corresponding carboxylic acids (See Figure 4.2 for selected examples). This was consistent with the observations in the NMR comparison listed in Table 4.1, raising the idea that the silyl migration had led to the formation of product **516**.

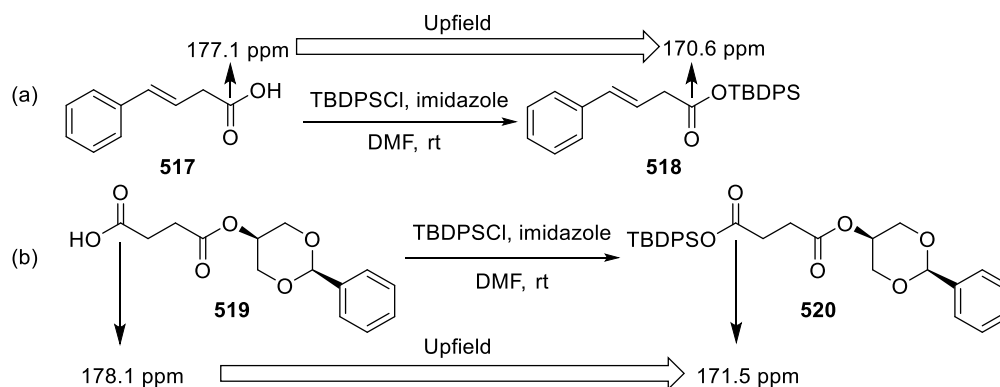


Figure 4.2 Examples of reported upfield chemical shifts of carbonyl groups in preparation of silyl esters.^{338, 339}

HR-MS analysis showed a minor line with peak height of about 20% at $m/z = 606.2974$, which did match with the calculated mass of silyl ester product **516** plus one hydrogen ion (Figure 4.3). However, the obtained base peak at $m/z = 597.2922$ was not explainable in terms of reasonable fragmentation of the molecule of silyl ester **516** or seco-acid starting material **514** (the calculated mass of **514** is 605.2921).

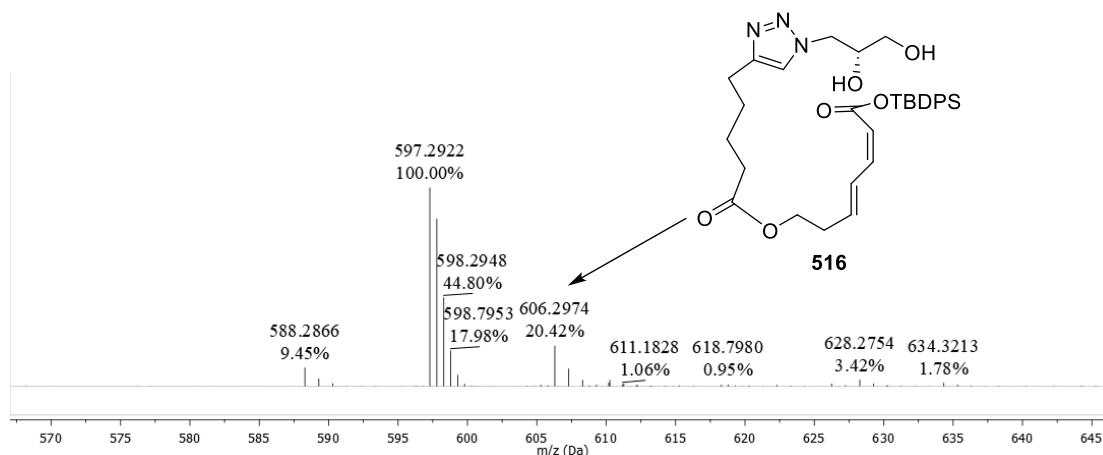
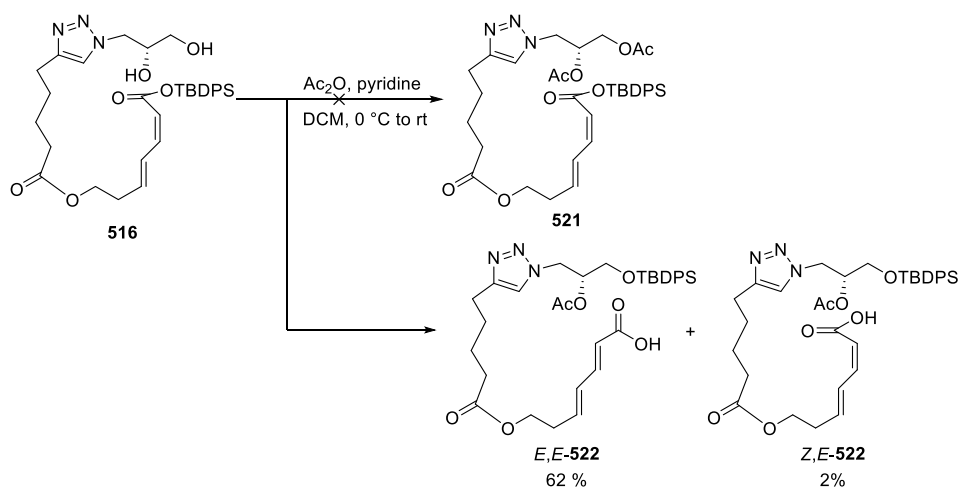


Figure 4.3 HR-MS of by-product **516**.^{†††††}

Acetylation of the isolated by-product was then performed using acetic anhydride and pyridine, with the hope that NMR and HR-MS analysis of the resulting *bis*-acylated product **521** could help to fully confirm that the by-product was the proposed silyl ester **516** (Scheme 4.14).



Scheme 4.14 Attempted preparation of *bis*-acylated product **521**.

Interestingly, based on 2D NMR analysis and HR-MS investigation, mono-acylated products *E,E*-**522** and *Z,E*-**522** were obtained instead. The rational explanation for this experimental result was that the TBDPS group rapidly migrated from the carboxylic acid

^{†††††} Mass of protonated compound **516** is at $m/z = 606.2974$ while the calculated mass for silyl ester product **516** plus one hydrogen ion ($C_{33}H_{44}N_3O_6SSi^+$) is 606.2994.

group back to the primary OH group under treatment with pyridine, meaning that the proposed structure of the by-product **516** was correct. It is also worth mentioning that *E,E*-**522** was obtained as the major product while only a trace amount of *Z,E*-**522** was isolated. As 4-DMAP has been proposed to be a major cause of the observed isomerisation in esterification reactions of *Z,E*-dienoic acids (see Section 3.5.2.1), the significant isomerisation in this acetylation reaction could possibly be triggered by the reversible nucleophilic addition of pyridine onto the mixed anhydride intermediate. These two stereoisomers were clearly distinguished by ^1H NMR spectroscopy in the coupling constant of α -proton of the unsaturated moiety ($J = 15.6$ Hz and 11.4 Hz, respectively) (see Figure 4.4 for the comparison of the proton signals in the alkene region) and their chemical shifts of the alkene protons also matches with the reported characteristic signal shifts of dienoate isomers synthesised by Romo and co-workers in their structural studies of PatA.⁷⁹

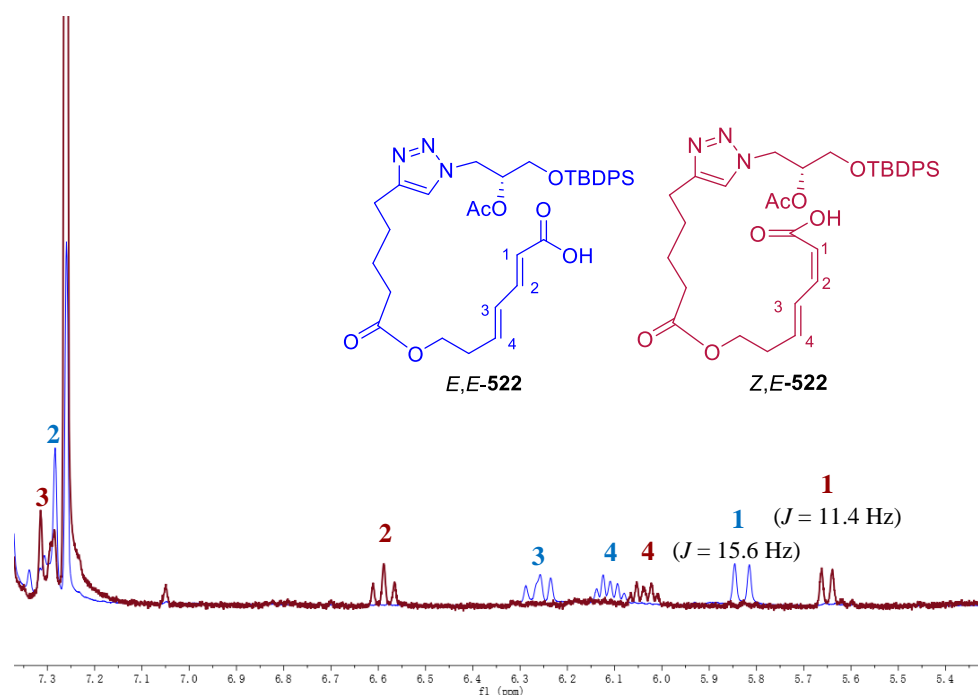
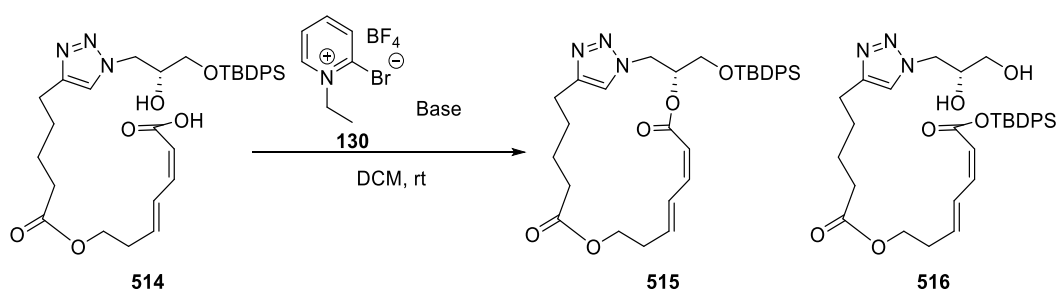


Figure 4.4 Comparison of the alkene region (5.45 ppm – 7.35 ppm) for the ^1H NMR spectra of *Z,E*-**522** (in maroon) and *E,E*-**522** (in blue). (Assigned by gCOSY NMR).^{††††}

^{††††}*Z,E*-**522** with alkene peaks at (500 MHz, CDCl_3) δ 7.32 – 7.27 (m, 1H, H-3), 6.59 (t, $J = 11.4$ Hz, 1H, H-2), 6.04 (dt, $J = 13.9, 6.3$ Hz, 1H, H-4), and 5.65 (d, $J = 11.4$ Hz, 1H, H-1), compared to *E,E*-**522** with alkene peaks at (500 MHz, CDCl_3) δ 7.35 – 7.27 (overlapped, m, 1H, H-2), 6.26 (dd, $J = 15.2, 11.8$ Hz, 1H, H-3), 6.14 – 6.06 (m, 1H, H-4), and 5.83 (d, $J = 15.6$ Hz, 1H, H-1).

In order to improve the synthetic yield of the desired macrocycle **515**, it was necessary to optimise the macrolactonisation conditions to suppress the silyl-migration side reaction. Considering the silyl migration may plausibly have been caused by the presence of excess NaHCO_3 (246 equivalents) in the macrolactonisation, it was proposed that reducing the equivalents of the base used in the reaction could potentially reduce the formation of silyl ester **516**. However, lowering the amount of NaHCO_3 (246 to 17 equiv.) and Mukaiyama reagent (24.6 to 15 equiv.) drastically decreased conversion and provided a 5/1 ratio of seco-acid starting material **514** and the undesired by-product **516** (Table 4.2, entry 2), which could be a consequence of the extremely low solubility of NaHCO_3 in DCM. It was then assumed that maintaining a continuously low concentration of base in the reaction system in a controllable manner should favour the desired lactonisation reaction and limit the side reaction simultaneously because the reaction between the secondary alcohol group and the activated acid intermediate might proceed faster than the base-mediated silyl-migration between the primary alcohol group and the free acid group. Therefore, a soluble base DIPEA was then trialled, and it was added slowly by a syringe pump to the reaction mixture of seco-acid **514** and the activating reagent **130** (Table 4.2, entry 3). Surprisingly, silyl ester **516** was obtained as the sole product. These experimental results suggested that high-yielding macrolactonisation conditions of seco-acid **514** would require further investigation. Nonetheless, a sufficient quantity of macrolactone **515** had been stockpiled for exploring further elaboration.

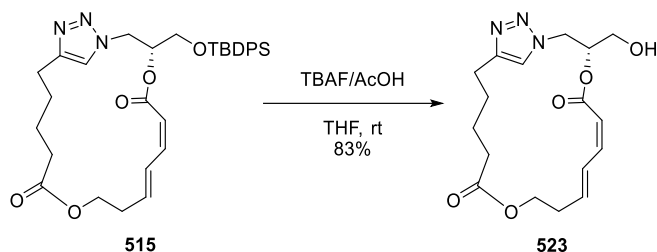


Entry ^a	Compound (equiv.)	Base (equiv.)	Ratio ^b 514 : 515: 516	Time (h)	Yield ^c (%)
1	24.6	NaHCO_3 (246)	0 : 1 : 1.15	16	40
2	15	NaHCO_3 (17)	5 : 0 : 1	16	-
2	15	DIPEA (2)	0 : 0 : 1	16	-

^aAll reactions were carried out at concentrations of 0.56×10^{-3} M. ^bDetermined by ^1H NMR analysis of crude mixture after work-up. ^cIsolated yield of compound **515** by silica gel chromatography.

Table 4.2 Trialled conditions for macrolactonisation of seco-acid **514**.

Desilylation of TBDPS silyl ether **515** using buffered TBAF afforded primary alcohol **51** in good yield (Scheme 4.15). At this point, the time constraints limited further investigations on the oxidation of the alcohol **523** to the aldehyde **513** and the attachment of the side chain fragment on the macrocyclic core.



Scheme 4.15 Preparation of macrocyclic alcohol **523**.

4.6 Conclusion

In conclusion, the initial synthetic route to analogue (*S*)-**187**, which involves using aldehyde (*R*)-**509** as the key fragment, was unsuccessful and a revised synthetic route, in which macrocyclic alcohol **523** acts as the pivotal intermediate, was pursued.

Alcohol **523** was prepared in 11 steps as the longest linear sequence (15 steps total), starting from commercially available chemicals, with an overall yield of 9%. However, in the macrolactonisation step, an unexpected silyl ester by-product **516** was observed. To minimise the formation of this by-product, several reaction conditions were trialled. Unfortunately, these attempts were unsuccessful in reducing the by-product. Therefore, it is necessary to further optimise conditions in order to enhance the yield of the macrocyclic compound **515**.

To complete the synthesis of analogue (*S*)-**187**, coupling of the side chain fragment to the macrocycle core would require further investigation.

Chapter Five: Summary and Future Work

5.1 Summary

Pateamine A has potent antiproliferative activity in cancer cell lines. The mechanism of action of PatA involves binding to the eukaryotic initiation factor 4A (eIF4A) to inhibit the initiation of protein synthesis, thereby inducing programmed cell death.

To further explore the structural features that are most important for its binding to eIF4A protein targets, thiazole analogues **183**, **184**, **185**, **186** and triazole analogue (*S*)-**187** and (*R*)-**187** were designed (Figure 5.1). The work towards the synthesis of analogues **183**, **184** and (*S*)-**187** was first carried out, with the hope that this could be informative for the synthesis of a new generation of analogues.

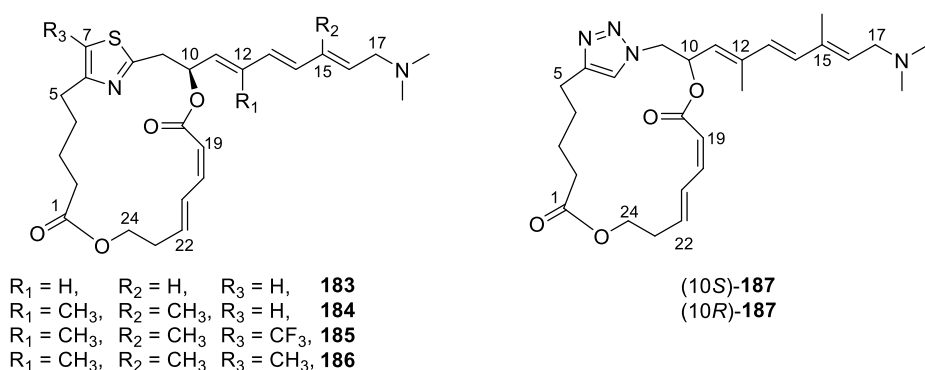


Figure 5.1 Chemical structures of targeted analogues **183** – **187**

5.1.1 Attempted Synthesis of Thiazole Analogue **183**

Our strategy for the synthesis of analogue **183** was to construct the thiazole core by a gold-catalysed coupling reaction between a thioamide and an alkyne. The initial method tested to connect the non-methylated side chain fragment was Julia-Kocienski olefination. Three fragments were successfully prepared for this purpose (Figure 5.2).

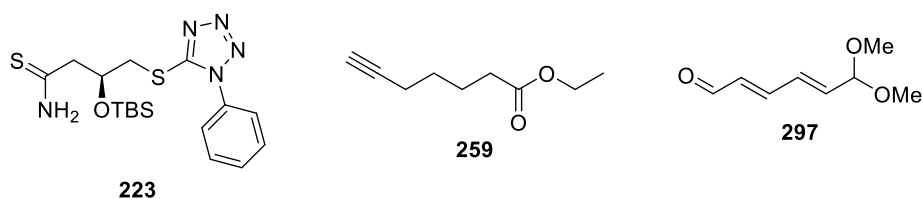
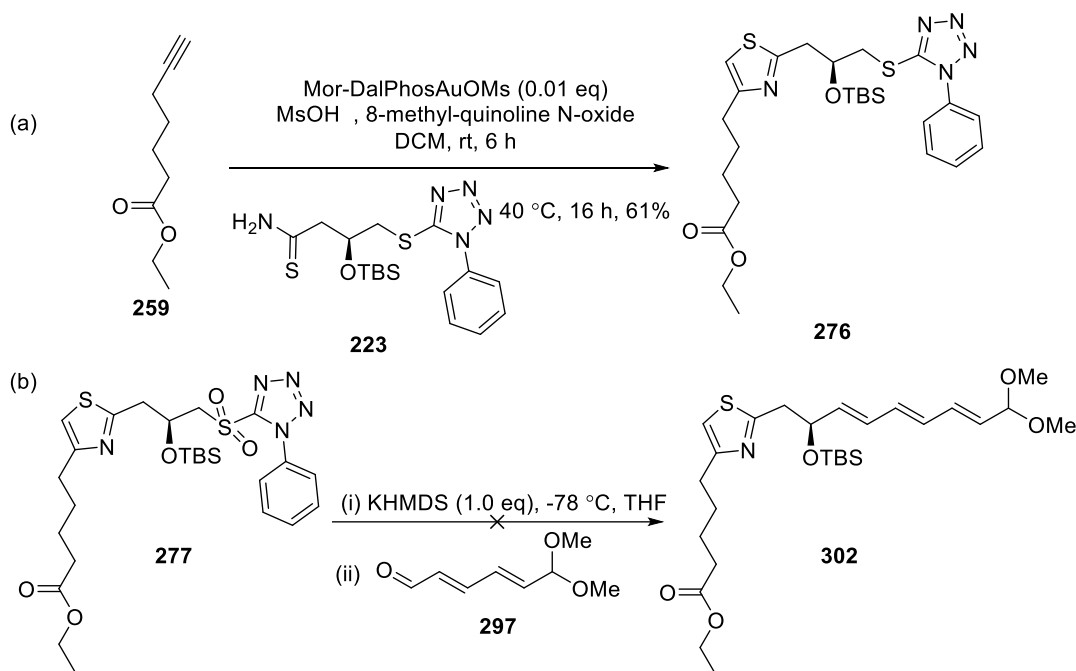


Figure 5.2 Three fragments prepared based on the initial synthetic strategy for analogue **183**.

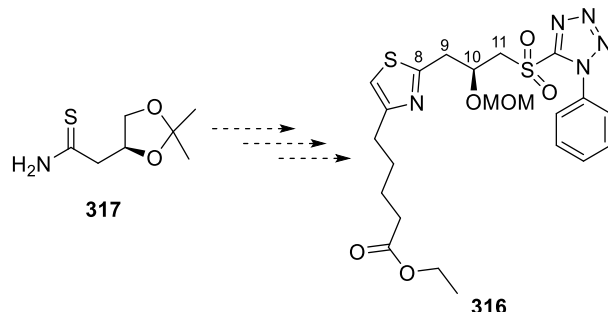
Thioamide fragment **223** was first coupled with the alkyne fragment **259** under optimised gold-catalysed conditions and the desired thiazole **276** was obtained in acceptable yield (Scheme 5.1a). However, the coupling of sulfone **277** with the side chain fragment aldehyde **297** by Julia-Kocienski olefination resulted in a mixture of degradation products with no sign of formation of the desired triene product **302**. This failure was possibly due to the steric effects from the TBS protecting group (Scheme 5.1b).



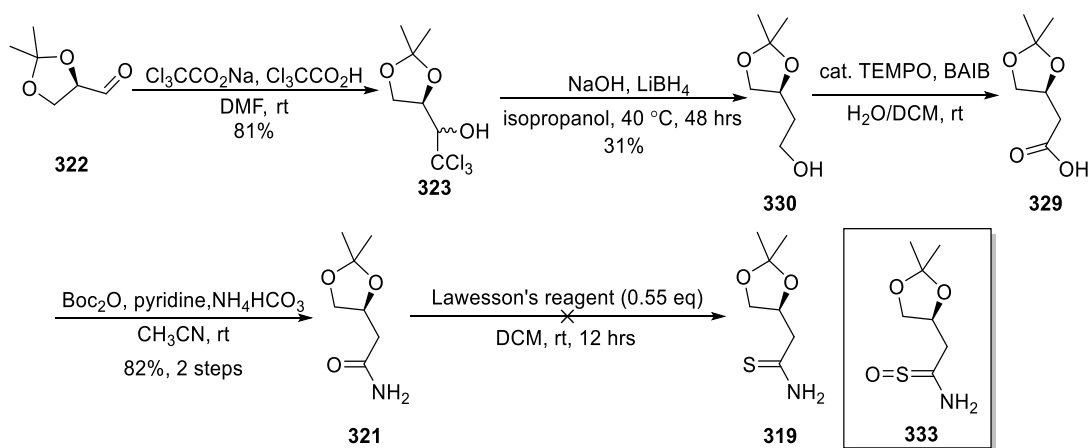
Scheme 5.1 Coupling of fragments for the synthesis of analogue **183**: (a) gold-catalysed thiazole formation; (b) Julia-Kocienski olefination

As the MOM group was considered to be less bulky than the TBS group, MOM-protected sulfone **316** was chosen as the alternative sulfone partner for the Julia-Kocienski reaction with enal **297**. We proposed that sulfone **316** could be prepared from thioamide **317** (Scheme 5.2). The amide precursor **321** was successfully prepared from aldehyde **322** in

four steps (Scheme 5.3). To our dismay, the thionation of **321** only provided the undesired thioamide (*S*)-oxide **333**, as determined by HR-MS investigation. This appeared to be due to the oxidation of the thioamide **319** when exposed to air.



Scheme 5.2 Proposed synthesis of **316** from thioamide **317**.



Scheme 5.3 Attempted synthesis of thioamide **319**.

As introducing bulky protecting groups could potentially retard the undesired oxidation, attempts to prepare *bis*-TBS protected thioamide **341** (Figure 5.3) were carried out first and it was found that the undesired oxidation was indeed slowed down to some extent by the presence of TBS groups. Therefore, TBDPS-protected thioamide **343** (Figure 5.3) was then targeted as a bulkier alternative that might be even more resistant to oxidation. The attempted preparation of thioamide **343** started from PMB-protected amide **346** (Scheme 5.4). However, this synthetic route was eventually abandoned because of the unacceptable yields in the reaction sequence.

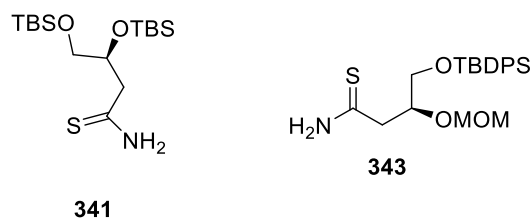
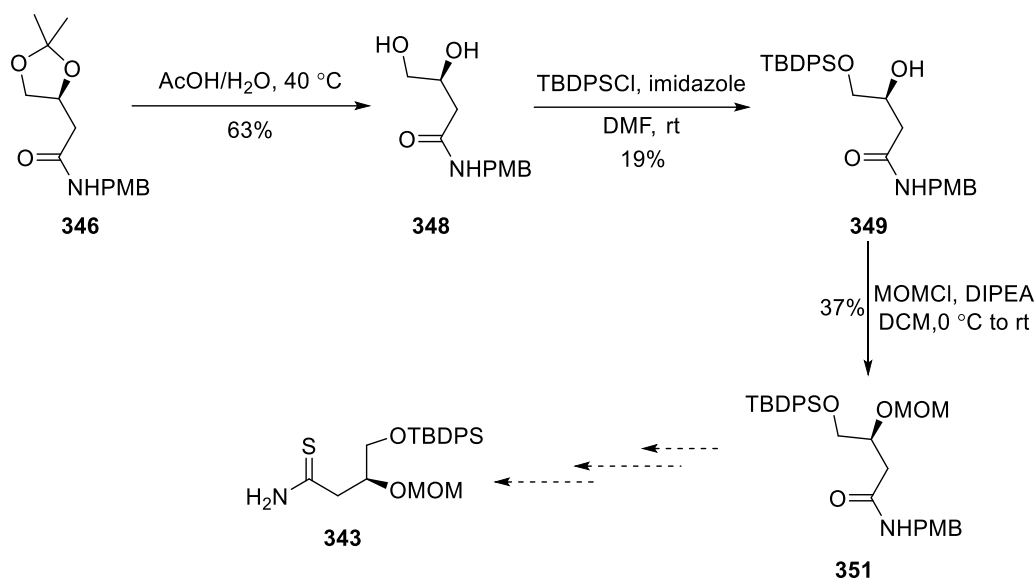


Figure 5.3 Targeted thioamides with bulky protecting groups.



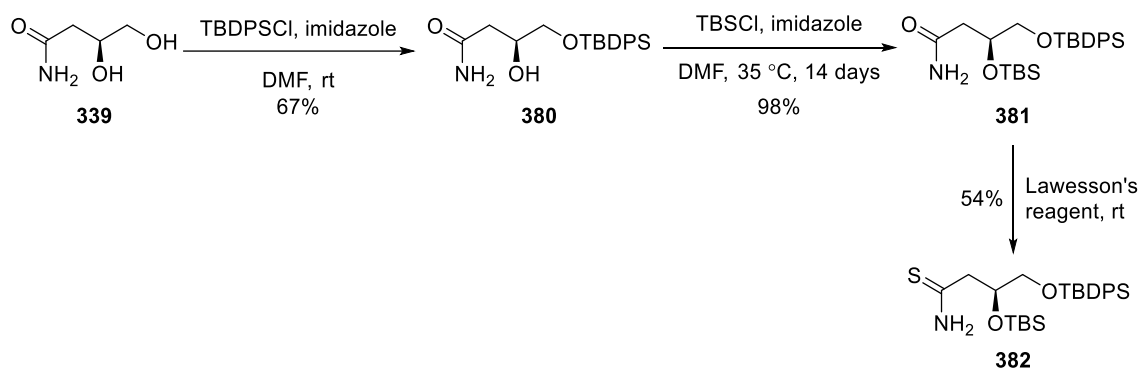
Scheme 5.4 Attempted synthesis of thioamide **343**.

As the Julia-Kocienski olefination was found to be ineffective for coupling the methylated side chain fragment to the sulfone partner in model reactions, we decided to change our initial synthetic strategy and to use Wittig/HWE olefination for the attachment of the side chain in order to ensure the collective synthesis of targeted analogues. As the side chain methylated analogue **184** (Figure 5.1) could provide more specific information about the importance of the methyl groups on the macrocyclic core, the synthesis of analogue **184** was prioritised.

5.1.2 Towards Synthesis of Thiazole Analogue **184**

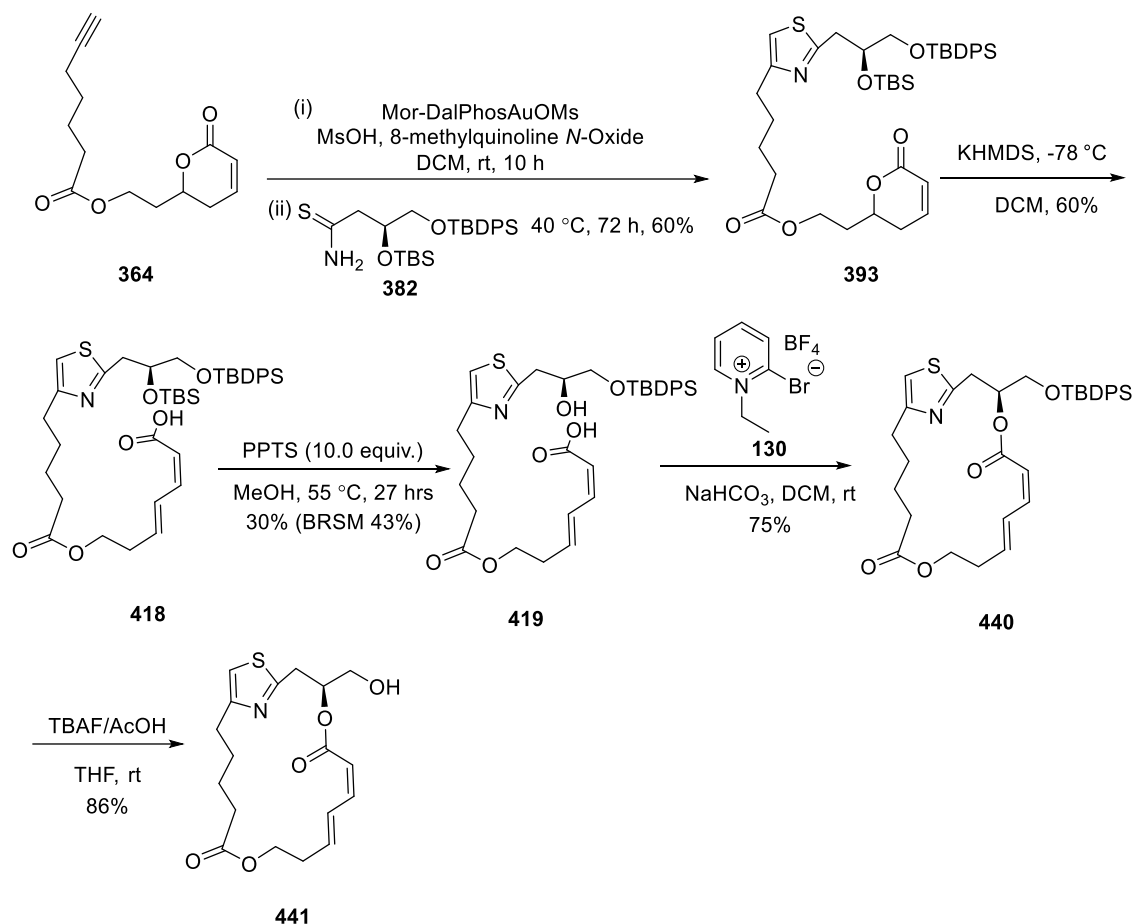
In preparing thiazole analogue **184**, an alternative strategy was employed, whereby the macrocycle would be constructed prior to attachment of the side chain. The macrocyclic core of thiazole analogue **184** was constructed by a combination of gold-catalysed thiazole formation, base-induced ring opening of α,β -unsaturated- δ -lactone, and modified Mukaiyama macrolactonisation. The thioamide fragment **382** required for gold-catalysed

formation was prepared from amide **339** with a 35% yield over 3 steps (Scheme 5.5), and it was found that *bis*-silylated thioamide **382** could be obtained in high purity after taking extra measures at the post-column stage to exclude air exposure. Alkyne fragment **364** was prepared successfully from 1,3-propanediol in 8 steps following Cumming's reported synthetic strategy.¹³⁴



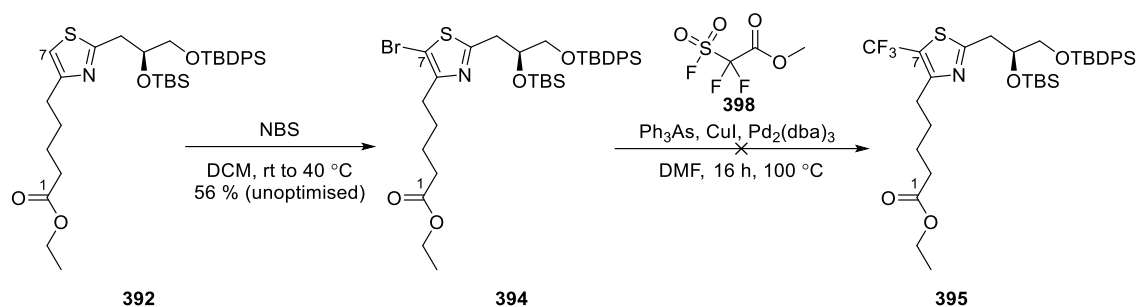
Scheme 5.5 Synthesis of thioamide **382**.

Macrocyclic alcohol **441** was successfully synthesised from the alkyne fragment **364** in 6 steps (Scheme 5.6). However, the overall yield of **441** was only 10%. The low-yielding selective desilylation step to form **419** was the major hurdle to overcome. Therefore, the optimisation for this step will require further investigation. Several alternative synthetic routes were then trialled. However, these efforts did not enhance the yield.



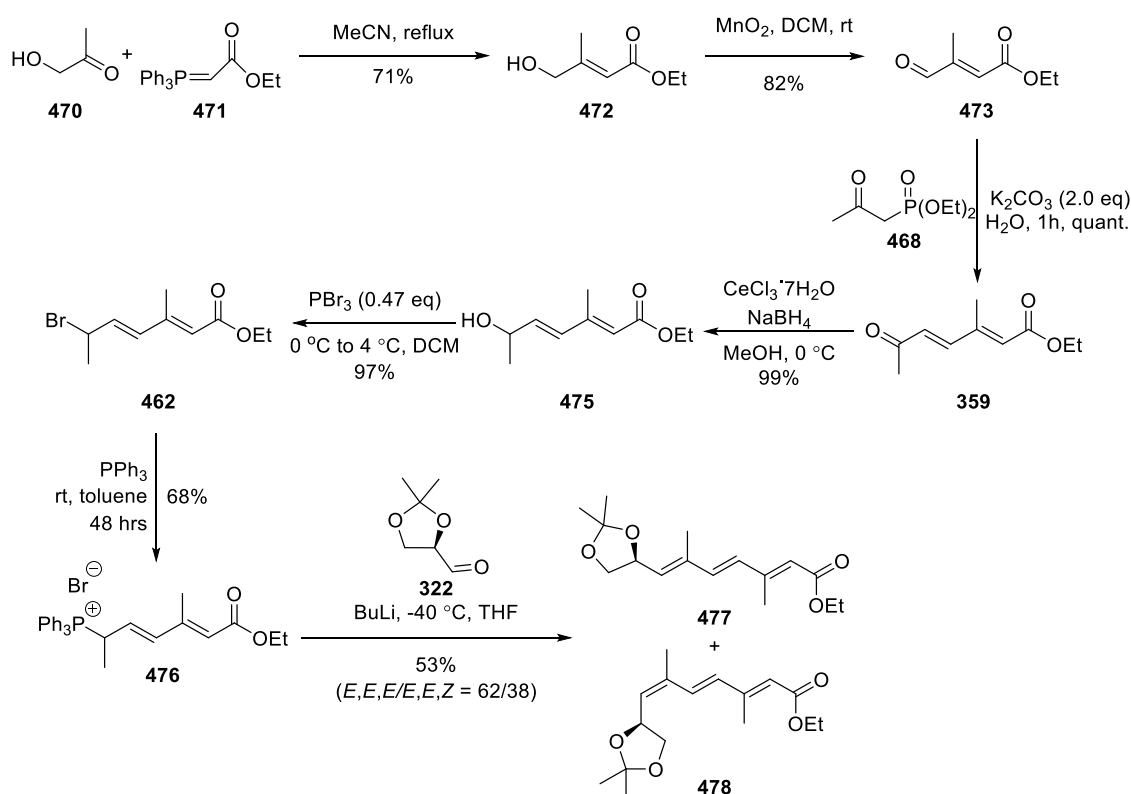
Scheme 5.6 Preparation of the thiazole-containing macrocycle **441** for the synthesis of analogue **184**.

C7-brominated thiazole **394**, a useful intermediate for introducing modifications onto the C7-position, was also prepared successfully (Scheme 5.7). In order to prepare CF₃-substituted analogue **185**, a palladium-catalysed trifluoromethylation of **394** was carried out. However, none of the desired product **395** was obtained. This failure was possibly due to the choice of palladium catalyst or reagents. Therefore, the screening for the appropriate combination of palladium catalyst, ligand, and CF₃ source would also require further investigation.



Scheme 5.7 Attempted preparation of CF_3 -substituted thiazole **395**.

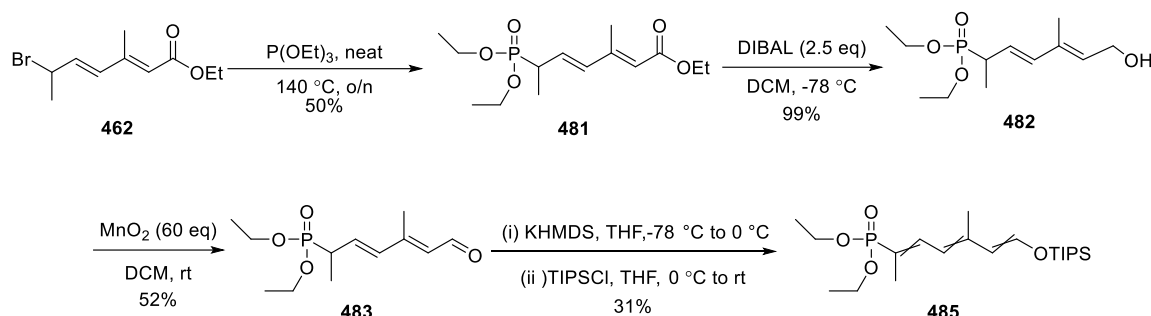
The strategy for the coupling of the side chain fragment through Wittig olefination was first explored. Triphenylphosphonium salt **476** was successfully synthesised from hydroxyacetone **470** with a 56% yield over 6 steps (Scheme 5.8). Aldehyde **322** was used as a model substrate to test the stereochemical outcome of the Wittig reaction with the phosphonium salt **476**. Unfortunately, the model reaction provided a 62/38 ratio of *E,E,E*-trienoate **477** and *E,E,Z*-trienoate **478** products.



Scheme 5.8 Preparation of phosphonium salt **476** and trienoates **477** and **478**.

This moderate *E*-selectivity prompted us to consider using HWE olefination or TBAF-

mediated aldol condensation³²⁴ for the connection with the side chain. Therefore, phosphoryl aldehyde **483**, an intermediate could serve in both strategies, was prepared successfully (Scheme 5.9). Since the TBAF-mediated aldol condensation has not yet been applied in synthetic work towards any natural products or their analogues, the preparation of the requisite enol silyl ether **485** was prioritised in order to test this route. Although NMR analysis suggested that the reaction of aldehyde **483** with KHMDS and TIPSCl did provide silyl ether product **485** in moderate conversion, full confirmation of the double bond configuration would require further NOE experiments on more material. After that, the coupling between the silyl ether **485** and the macrocycle core by the TBAF-mediated aldol condensation could be performed.

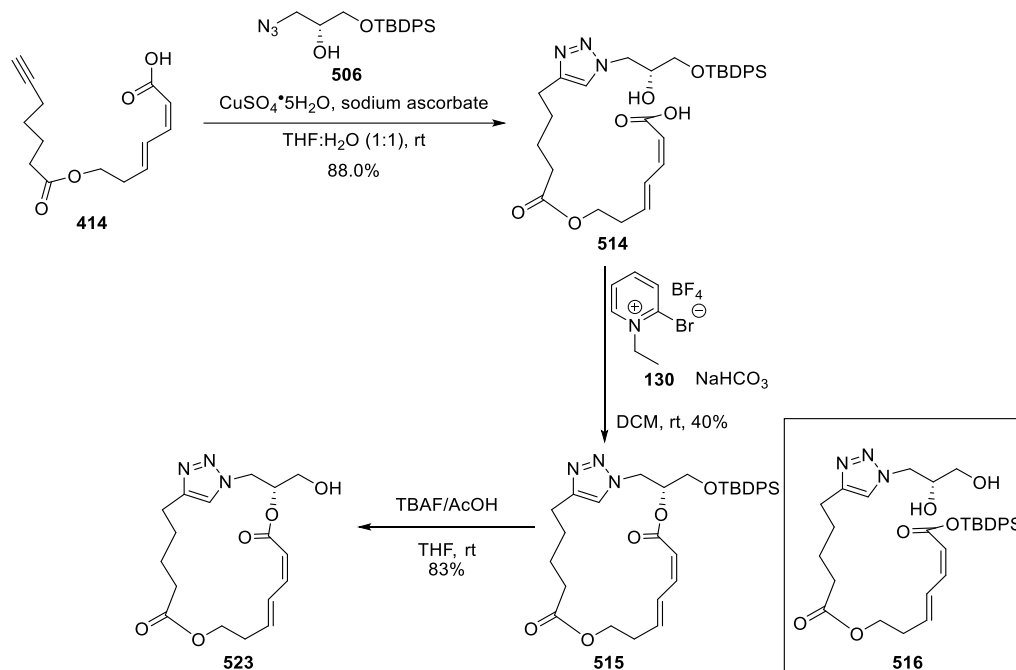


Scheme 5.9 Synthesis of phosphoryl silyl ether **485**.

5.1.3 Towards Synthesis of Analogue (*S*)-**187**

As the synthesis of triazole analogue (*S*)-**187** could employ the same lactone fragment **364** and side chain fragment **485** as with thiazole analogue **184**, attention was focused on the preparation of the azide fragment for the construction of the triazole ring by copper-catalysed azide-alkyne cycloaddition. In our initial synthetic strategy, the coupling between the side chain fragment and the azide fragment was performed prior to the construction of the macrocycle. Therefore, the preparation of azide fragment (*R*)-**509** starting from (*S*)-solketal **502** was first performed (*vide supra*, Section 4.3). However, it was found out that aldehyde (*R*)-**509** degraded significantly when purified by silica gel flash chromatography or by distillation. This inability to purify the aldehyde (*R*)-**509** led us to consider using the crude material for the model Wittig reaction with triphenylphosphonium salt **476**. To our dismay, no desired product was observed, which was possibly due to the instability of the aldehyde in strongly basic conditions. The lack of success in the Wittig reaction, as well as the difficulty in the purification, prompted us

to return to the alternative strategy, in which the macrocycle is prepared before attachment of the side chain, which could allow the collective synthesis of all the desired analogues. Macrocylic alcohol **523** was then prepared from alkyne fragment **414** and azide fragment **506** in three steps (Scheme 5.10).



Scheme 5.10 Preparation of the triazole-containing macrocycle **515** for the synthesis of analogue (*S*)-**187**

An interesting by-product, silyl ester **516**, was observed in the macrolactonisation step and its structure is consistent with the outcomes of NMR analysis and preparation of the acetate derivatives *E,E*-**522** and *E,Z*-**522**. To synthesise triazole analogue (*S*)-**187**, coupling of the aldehyde derived from **523** with the side chain fragment by TBAF-mediated aldol condensation or HWE olefination would require further investigation.

5.1.4 Closing Remarks

The established synthetic route to the thiazole-containing macrocyclic alcohol **440** has 11 steps and the overall yield from the commercially available chemicals was 3.5%. Compared to Fürstner and Zhuo's synthetic route for macrocyclic intermediate **154** with similar structures, although our route has a longer reaction sequence and a lower overall yield, the major strength of this route is the use of an alkyne fragment for the construction of the thiazole ring, which could allow us to conveniently harmonise synthetic routes to

access different heterocyclic rings, like triazoles and oxazoles. This advantage has been demonstrated by the successful preparation of triazole-containing macrocycle **515**.

The synthesis of the methylated side chain fragment, phosphoryl silyl ether **485**, or an alternative derivative from phosphoryl aldehyde **483**, was completed in 6 steps.^{§§§§§} Compared to Pattenden's established step-wise strategy to connect the side chain, our synthetic route employs relatively benign reagents and conditions, and does not involve using chromium-mediated or tin-mediated coupling reactions. This means that it could be more environmentally friendly and be easily scaled up. Also, our strategy could potentially allow us to attach the side chain as a whole fragment, making the synthesis of targeted analogues more convergent.

5.2 Future Work

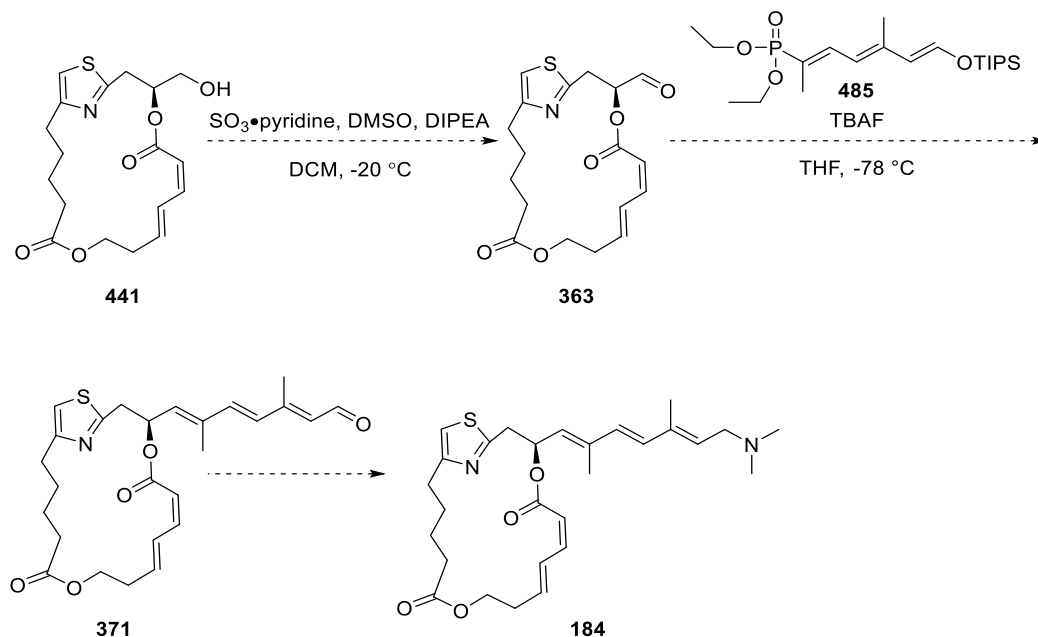
The overall aim of this project was to synthesise thiazole analogues **183**, **184**, **185**, **186** and triazole analogues (*S*)-**187** and (*R*)-**187**, which will help to examine the individual roles of the thiazole ring, the methyl groups on the side chain (at C12 and C15), and the methyl groups on the macrocycle in binding to the protein target of PatA. As the synthesis of thiazole-containing macrocycle **441**, triazole-containing macrocycle **515** and the side chain fragment **485** have been achieved, future work will first focus on the synthesis of analogue **184** and (*S*)-**187** and (*R*)-**187**.

5.2.1 Synthesis of Analogues **184** and **187**

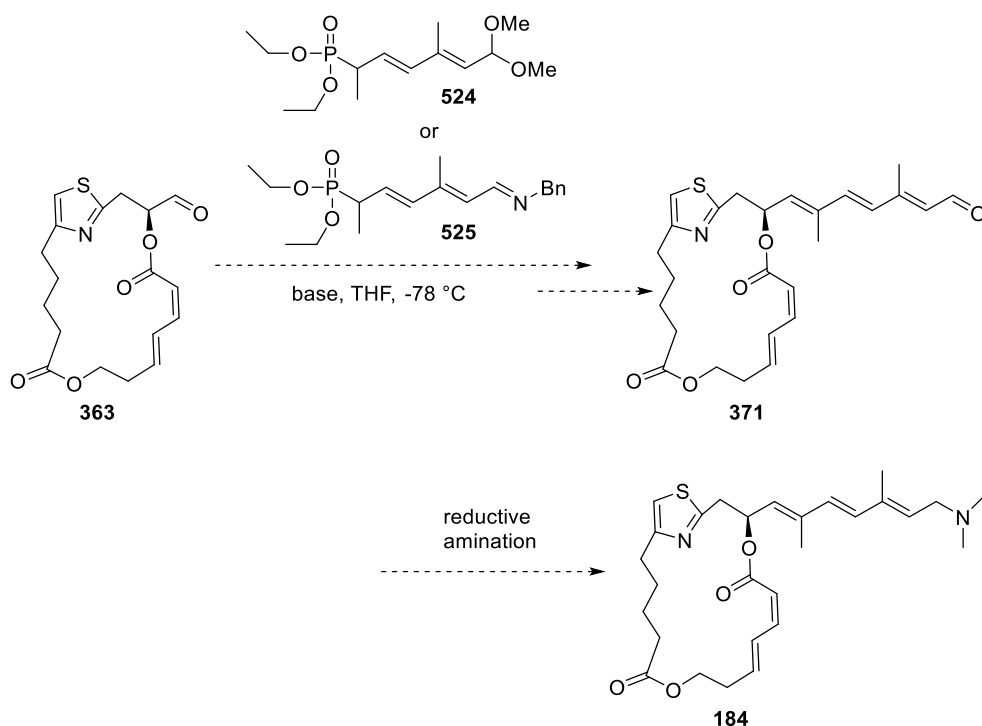
Thorough NOE experiments will be first performed in order to fully confirm that the double bonds of silyl ether **485** are all *E*-configured. If silyl ether **485** is proven to have the desired *E,E,E*-configuration, macrocyclic alcohol **441** will be oxidised to provide the aldehyde **363**. As Fürstner and Zhuo reported that the oxidation under optimised Parikh–Doering conditions provided the macrocyclic aldehyde **155** in reproducibly good yield (*vide supra*, Section 1.4.2.2),¹²⁸ the oxidation step will initially utilise their conditions. The validity of using TBAF-mediated aldol condensation between phosphoryl silyl ether **485** and aldehyde **363** to attach the side chain will then be tested (Scheme 5.11). If the aldol condensation is unsuccessful or the *E*-selectivity of the reaction is not satisfying, phosphoryl aldehyde **483** will be converted into phosphoryl acetal **524** or phosphoryl

^{§§§§§} Taking into account that ethyl (*E*)-3-methyl-4-oxobut-2-enoate **473** is commercially available.

imine **525** and the HWE protocol to couple the side chain would then be tested (Scheme 5.12). Given that the macrocyclic aldehyde **363** is possibly prone to epimerisation (*vide supra*, section 3.5.2.2), the use of relatively weaker non-ionic bases (see Figure 3.14 for examples) will be also investigated to minimise the risk of epimerisation. After suitable conditions for the coupling are found, analogue **184** will be produced by reductive amination of the aldehyde intermediate **371** using a mild boron reductant (*e.g.*, tetramethylammonium triacetoxyborohydride). If neither of these attempts to couple the side chain fragment with the macrocyclic core provides the desired aldehyde **371**, Pattenden's established step-wise strategy to connect the side chain fragment will be incorporated and the efficiency of the optimised conditions for the reaction sequence reported by Fürstner and Zhuo¹²⁸ will also be examined. The synthesis of analogue **184** will be informative for the synthesis of the following other analogues.



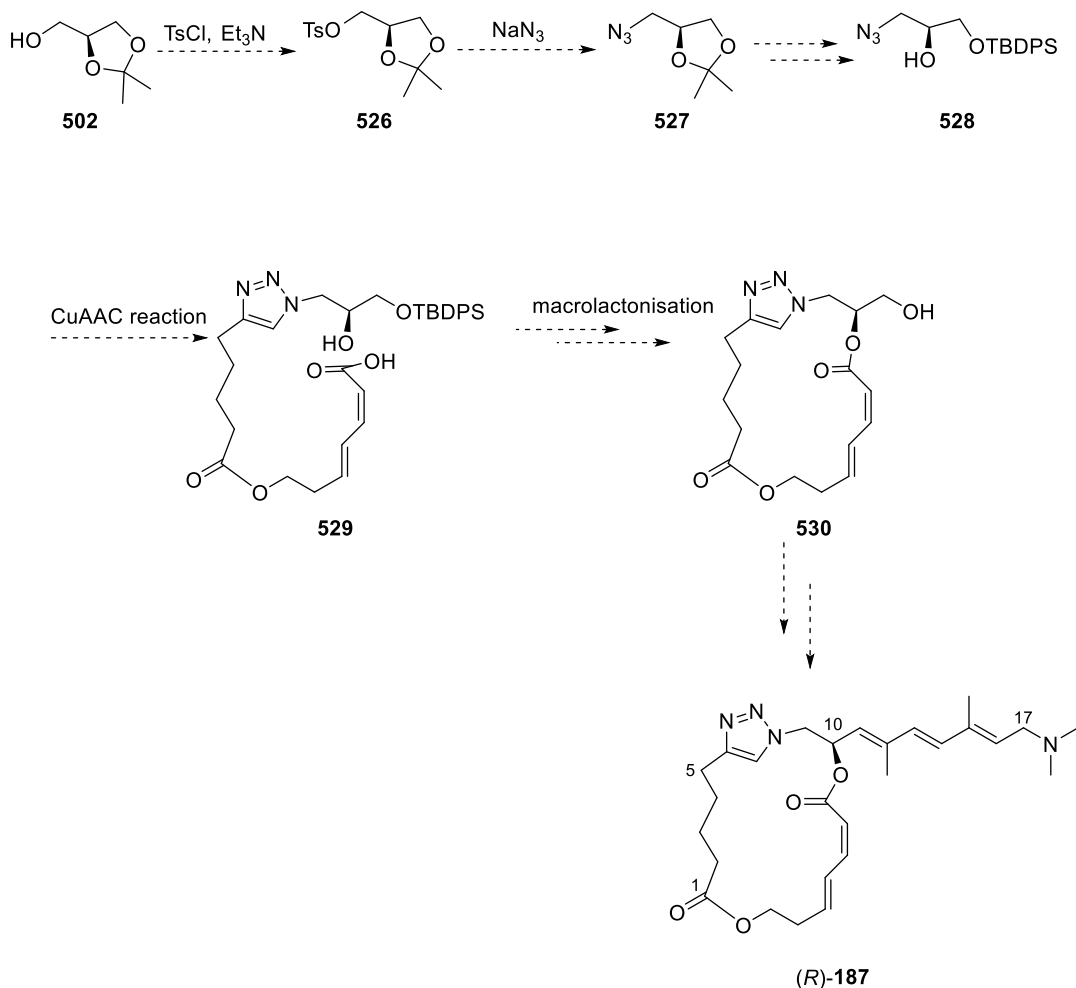
Scheme 5.11 Proposed synthetic route for analogue **184** by TBAF-mediated aldol condensation.



Scheme 5.12 Proposed synthetic route for analogue **184** by HWE olefination.

The synthesis of analogue (*S*)-**187** from macrocyclic alcohol **523** could potentially follow a similar reaction sequence as analogue **184**. However, optimisation for suitable conditions to achieve good results for each step may be required.

In terms of the synthesis of analogue (*R*)-**187**, the key intermediate macrocyclic alcohol **530** could be synthesised from (*S*)-solketal **502** following a similar synthetic route as (*S*)-**187** (Scheme 5.13), which has been discussed in Section 4.5. The attachment of the side chain-fragment could be achieved using exactly the same conditions as for analogue (*S*)-**187**.

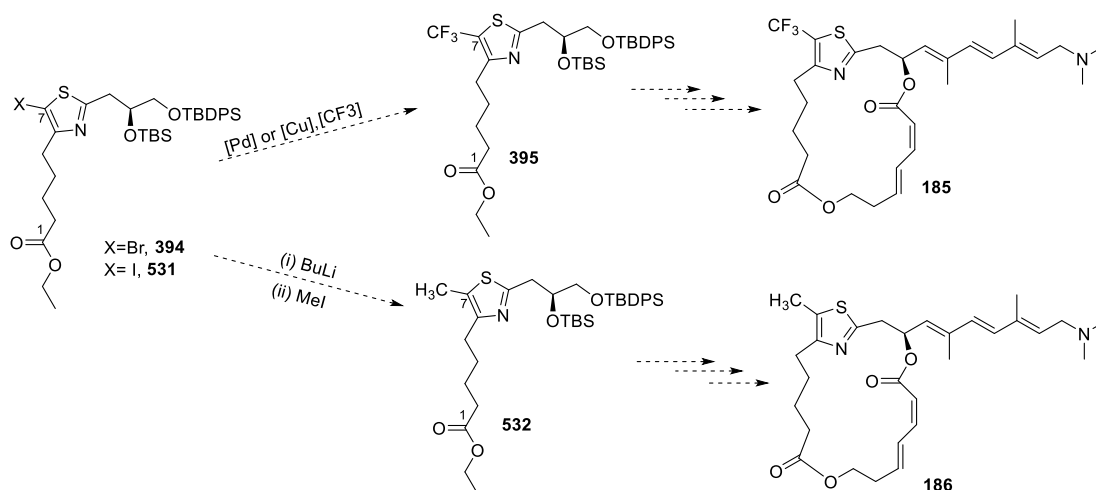


Scheme 5.13 Proposed synthetic route for the synthesis of analogue (R)-**187** via macrocyclic alcohol **530** intermediate.

5.2.2 Role of the Thiazole and Methyl Groups on the Macrocyclic

A comparison of the activities of analogues **184** and (R)-**187** will reveal whether the thiazole ring is critical for binding to the protein target eIF4A. If analogue **184** does indeed exhibit enhanced activity relative to (R)-**187**, this would raise the idea that the protonability or the electron distribution of the heterocycle ring may play an important role in binding to eIF4A. This means modifications on the thiazole ring that could impact its basicity or electron distribution could potentially modulate the activity. Preparation and testing of C7-substituted analogues **185** and **186** will address this issue. To introduce the CF_3 group to the thiazole, the palladium or copper-catalysed conditions for the trifluoromethylation of brominated or iodinated thiazole (**394** or **531**) will be further investigated. A methyl group will be incorporated into the molecule through a two-step protocol. The halogenated thiazole (**394** or **531**) will first undergo a lithium-halide

exchange reaction and the resulting organolithium species can be trapped by methyl iodide. Analogues **185** and **186** will be synthesised from the intermediates **395** and **532**, respectively (Scheme 5.14).



Scheme 5.14 Introduction of trifluoromethyl or methyl group to thiazole ring.

If the activity of analogue **184** is significantly reduced when compared to that of DMDA PatA, this would mean the omitted methyl groups on the macrocycle (at the C22 and C24 position) are required for potent activity. As the *Z,E*-dienoate was proposed to act as a Michael acceptor in binding to eIF4A,^{86, 110, 131} the presence of modifications at the C22 position could modulate its Michael accepting ability. This could be further investigated by the preparation of analogues with a methyl group or a trifluoromethyl group at C22 (Figure 5.4). The influence of the methyl group at the C24 position in favouring an active conformation of the macrocycle required for the binding could be examined by the preparation of stereoisomers of an analogue with a C24 methyl group (Figure 5.5). Synthesis of an analogue with varying C24 substitution, including a *gem*-dimethyl group, could be also of interest. Under these circumstances, the potential to substitute the thiazole for the more synthetically facile triazole will then be reinvestigated.

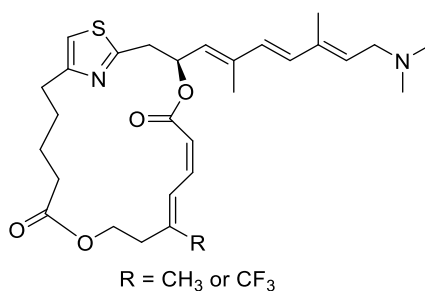


Figure 5.4 Pateamine analogues with modifications at the C22 position.

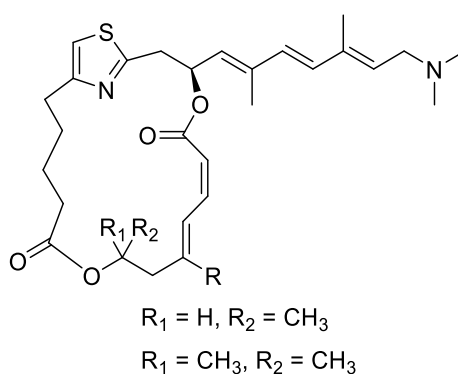
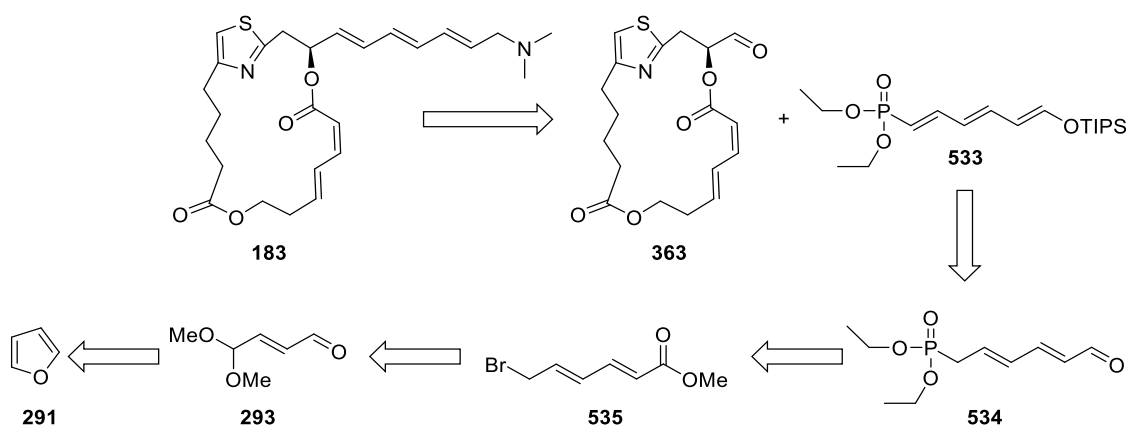


Figure 5.5 Pateamine analogues with modifications at the C24 position.

5.2.3 Role of Methyl Groups on Side Chain

A comparison of the activities of analogues (*R*)-**187** and **182** will potentially provide evidence on whether the reintroduction of the methyl groups on the side chain is advantageous. If analogue (*R*)-**187** does not display significantly improved activity relative to analogue **182**, this would mean that the presence of methyl groups at the C12 and C15 position may play only a minor role in biological activity. The preparation of thiazole-containing analogue **183** will be informative in addressing this problem. As depicted in Scheme 5.15, the existing synthetic route for enal **297** (*vide supra*, Section 2.3.3) could be incorporated in the preparation.



Scheme 5.15 Retrosynthetic analysis for analogue **184**

5.2.4 Importance of the C-10 Configuration

A comparison of the activities of analogues (*R*)-**187** and (*S*)-**187** would give information about the role of the stereochemical configuration at C10 in binding to the protein target. If these two analogues show similar activities in tested cell lines, that would suggest that the configuration of C10 may not be crucial in biological activity. Preparation of a thiazole analogue with an (*R*)-configuration at the C10 position could provide more direct evidence (Figure 5.6). The synthetic route for this analogue will start from the four-carbon amide building block with the (*R*)-configuration, namely (*R*)-amide **339** and utilise the identical reaction sequence that used for the synthesis of analogue **184**.

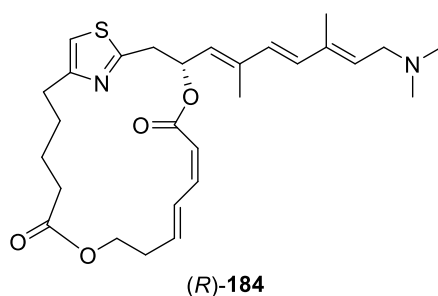


Figure 5.6 Pateamine analogue with (*R*)-configuration at C10 position.

These future works discussed above will provide further insights into the relationship between the structure and the activity of pateamine A, which would provide a solid foundation for the design of a new generation of analogues.

Chapter Six: Experimental

6.1 General Experimental Details

Unless stated otherwise, all reactions were carried out in oven- or heat gun-dried glassware, using anhydrous solvents under argon atmosphere and standard syringe techniques. THF, DCM, Et₂O, and toluene were purified using Innovative Technology's PureSolv system. Other solvents were purified by distillation over the following desiccating reagents and were transferred under argon: acetone (boron trioxide), isopropanol (dried and stored over MS 4 Å); dimethyl sulfoxide (DMSO), dichloroethane (DCE), chlorobenzene, acetonitrile, and 1,2-dimethoxyethane (DME) were distilled over calcium hydride. Anhydrous (99.8%) *N,N*-dimethylformamide (DMF) containing MS 4 Å was purchased from Sigma-Aldrich.

Unless stated otherwise, all commercially available compounds (Alfa Aesar, BDH Chemicals, Sigma-Aldrich, AKSci, Acros Organics) were used as received. Triethylamine (Et₃N) and 2,2-dimethoxypropane were purified by distillation over calcium hydride. Furan was purified by distillation over sodium. Anhydrous *para*-toluenesulfonic acid was obtained by recrystallisation from ethanol and water and azeotropic desiccation with toluene. Lawesson's reagent was purified by washing with anhydrous Et₂O and anhydrous DCM and recrystallisation from anhydrous toluene. Trichloroacetic acid was purified by recrystallisation from hexane. Organic solvents were removed by rotary evaporation with water bath temperature between 40 °C and 50 °C unless otherwise stated.

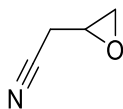
The reaction progress was monitored using TLC plates (Macherey-Nagel pre-coated plates (POLYGRAM®SIL/UV254)) and visualised by UV fluorescence quenching (254 nm), in combination with phosphomolybdic acid (PMA), cerium ammonium molybdate and potassium permanganate (KMNO₄) dip. Purification of products *via* flash chromatography was conducted using a column filled with silica gel 60 (220 – 240 mesh) as the matrix, obtained from Pure Science Ltd, with solvent systems as indicated. Celite used for filtration was obtained from Pure Science Ltd. ¹H and ¹³C NMR spectra were recorded on a Varian Unity Inova 500 spectrometer or a JEOL 500 spectrometer (operating at 500 MHz for ¹H NMR and 125 MHz for ¹³C NMR), or on a Varian Unity

Inova 600 spectrometer or a JEOL 600 spectrometer (operating at 600 MHz for ^1H NMR and 150 MHz for ^{13}C NMR) in the solvents indicated. All chemical shifts (δ) are given in ppm relative to tetramethylsilane (TMS), coupling constants (J) in Hz and multiplicity (s = singlet, d = doublet, t = triplet, q = quartet, quin = quintet, m = multiplet, br = broad). The solvent signals were used as references and the chemical shifts converted to the TMS scale (CDCl_3 : $\delta\text{C} = 77.0$ ppm; residual CHCl_3 in CDCl_3 : $\delta\text{H} = 7.26$ ppm; C_6D_6 : $\delta\text{C} = 128.06$ ppm; residual $\text{C}_6\text{D}_5\text{H}$: $\delta\text{H} = 7.16$ ppm; $(\text{CD}_3)_2\text{CO}$: $\delta\text{C} = 29.84, 206.26$ ppm; residual $(\text{CD}_3)\text{CD}_2\text{HCO}$: $\delta\text{H} = 2.05$ ppm). Melting points were determined using a Gallenkamp or Digimelt SRS melting point apparatus. Optical rotations were measured at the sodium D line on an Autopol II polarimeter from Rudolph Research Analytical and are quoted as specific rotation based on the equation $[\alpha]_D^T = \alpha \times 100 / c \times l$ (where α is rotation in degrees, c is concentration in g/100 mL, $l = 1$ dm). Infrared spectra were obtained on a Bruker Alpha Platinum-ATR. High-resolution mass spectrometry was conducted on a 6530 Accurate Mass Q-TOF LC/MS instrument (Agilent Technologies).

6.2 Experimental for Chapter Two

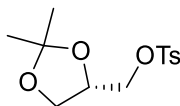
6.2.1 Preparation of Thioamide **223**

Preparation of 2-(oxiran-2-yl)acetonitrile, **209**



To a solution of nitrile **208** (5.0 g, 60.0 mmol, 1.0 equiv) in DCM (50 mL) was added 3-chloroperbenzoic acid (13.4 g, purity 77%, 60.0 mmol, 1.0 equiv.) at room temperature. The reaction mixture was stirred at room temperature while 3-chloroperbenzoic acid (500 mg, 2.2 mmol, 0.037 equiv.) was added to the reaction mixture each day for a total of 8 days. A saturated aqueous solution of NaHSO₃ (30 mL) was added to reduce the unreacted 3-chloroperbenzoic acid and the resulting mixture was stirred vigorously for 20 minutes. Then the organic layers were separated, washed with saturated aqueous NaHCO₃ (10 × 50 mL), dried over anhydrous Na₂SO₄, filtered, and evaporated under reduced pressure. The residue was then purified by silica gel flash chromatography (pet. ether/EtOAc = 2:1) to afford the title compound as a colourless oil (1.0 g, 20%). *R_f*: 0.10 (pet. ether/EtOAc = 10:1). ¹H NMR (500 MHz, CDCl₃), δ: 3.15—3.07 (m, 1 H), 2.77 (t, 1 H, *J* = 4.3 Hz), 2.70—2.56 (m, 3 H). ¹³C NMR (125 MHz, CDCl₃), δ: 115.4, 46.6, 46.1, 21.1. These characterisation data match those reported in the literature.¹⁷⁰

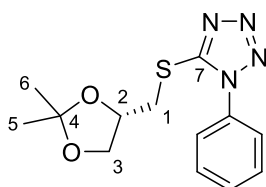
Preparation of (*S*)-(2,2-dimethyl-1,3-dioxolan-4-yl)methyl 4-methylbenzenesulfonate, **214**



To a solution of (*2S*)-(+)-glycidyl tosylate **213** (3.18 g, 13.9 mmol, 1 equiv.) in dry acetone (14 mL) was added aluminium chloride (58.0 mg, 0.435 mmol, 0.03 equiv.), and the solution was stirred at room temperature for 1 hour. The reaction mixture was then cooled to 2 °C and added 30 mL saturated NaHCO₃ aqueous solution slowly. The resulting mixture was then extracted with ethyl acetate (3 × 50 mL). The combined organic fractions were then dried over anhydrous Na₂SO₄, filtered, and then concentrated under reduced pressure. The crude material was purified by silica gel flash

chromatography (pet. ether/EtOAc = 5:1) to provide the title compound (7.00g, 92%) as a colorless oil. **R_f**: 0.50 (pet. ether/EtOAc = 2:1). **Melting point**: 69 – 72 °C. **¹H NMR** (500 MHz, CDCl₃): δ 7.83 – 7.78 (m, 2H), 7.40 – 7.33 (m, 2H), 4.30 – 4.24 (m, 1H), 4.06 – 4.00 (m, 2H), 3.97 (dd, *J* = 10.1, 6.2 Hz, 1H), 3.77 (dd, *J* = 8.8, 5.1 Hz, 1H), 2.45 (s, 3H), 1.34 (s, 3H), 1.31 (s, 3H). **¹³C NMR** (125 MHz, CDCl₃): δ 145.1, 132.6, 129.9, 128.0, 110.1, 72.9, 69.5, 66.2, 26.7, 25.2, 21.7. **FTIR** (thin film) ν 2987, 1598, 1495, 1455, 1359, 1257, 1213, 1189, 1175, 1095, 1054, 974, 788, 664, 554 cm⁻¹. **HRMS** (ESI): Calculated for C₁₃H₁₉O₅S⁺ [M + H]⁺ 287.0948; found 287.0951. [α]_D²⁰ +3.0 (*c* = 1.00, EtOH) (literature [α]_D²⁰ +4.5 (*c* 1.00 EtOH)). These characterisation data match those reported in the literature.³⁴⁰

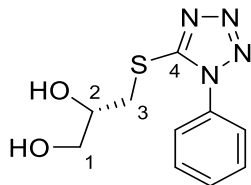
Preparation of (*S*)-5-(((2,2-dimethyl-1,3-dioxolan-4-yl)methyl)thio)-1-phenyl-1*H*-tetrazole, **215**



To a solution of tosylate **214** (8.15 g, 28.5 mmol, 1 equiv.) and 1-phenyl-1*H*-tetrazole-5-thiol **210** (15.66 g, 85.5 mmol, 3.0 equiv.) in acetone (250 mL) was added K₂CO₃ (19.7 g, 0.142 mmol, 5.0 equiv.) at room temperature. The reaction mixture was refluxed for 16 hours and then evaporated to remove solvent under vacuum. The residue was partitioned between ethyl acetate and water. The aqueous phase was extracted with diethyl ether (4 × 100 mL). The combined organic phase was washed with brine, dried over anhydrous Na₂SO₄, filtered and then concentrated under reduced pressure. The crude material was purified by silica gel flash chromatography (pet. ether/EtOAc = 5:1) to provide the title compound (8.14 g, 98%). **R_f**: 0.48 (pet. ether/EtOAc = 2:1). **¹H NMR** (500 MHz, CDCl₃): δ 7.62 – 7.49 (m, 5H), 4.61 – 4.51 (m, 1H, H-2), 4.20 – 4.13 (m, 1H, H-3a), 3.81 (dd, *J* = 8.6, 5.6 Hz, 1H, H-3b), 3.67 (dd, *J* = 13.6, 4.5 Hz, 1H, H-1a), 3.51 (dd, *J* = 13.5, 7.1 Hz, 1H, H-1b), 1.44 (s, 3H, H-5 or H-6), 1.35 (s, 3H, H-6 or H-5). **¹³C NMR** (125 MHz, CDCl₃): δ 153.9 (C-7), 133.5, 130.1, 129.8, 123.7, 110.0 (C-4), 73.7 (C-2), 68.3 (C-3), 36.6 (C-1), 26.8 (C-5 or C-6), 25.2 (C-6 or C-5). **FTIR** (thin film) ν 2981, 2933, 2883, 1596, 1501, 1460, 1389, 1377, 1366, 1280, 1245, 1213, 1190, 1175, 1150, 1090, 1081, 1073, 1051, 1015, 1000, 976, 960, 918, 869, 818, 785, 766, 736, 710,

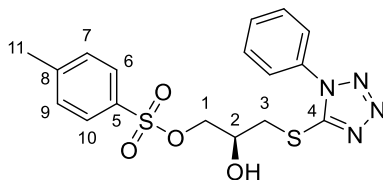
694, 685, 555, 510, 462, 447 cm^{-1} . **HRMS** (ESI): Calculated for $\text{C}_{13}\text{H}_{17}\text{N}_4\text{O}_2\text{S}^+$ $[\text{M}+\text{H}]^+$ 293.1067; found 293.1070. $[\alpha]_D^{25} -360$ ($c = 0.375$, DCM).

Preparation of (*S*)-3-((1-phenyl-1H-tetrazol-5-yl)thio)propane-1,2-diol, **216**



To a solution of acetone **215** (5.12 g, 17.5 mmol, 1.0 equiv.) in methanol (67 mL) was added acetyl chloride (0.37 mL, 5.25 mmol, 0.3 equiv.) at 2 °C. Then the reaction mixture was stirred at room temperature for 24 hours. Then the reaction mixture was evaporated under reduced vacuum and the residue was purified by a short silica plug (pet. ether/EtOAc = 1:2) to provide the title compound (4.4 g, 99.5%) as a colourless oil. **R_f**: 0.13 (pet. ether/EtOAc = 1:2). **¹H NMR** (500 MHz, CDCl_3): δ 7.65 – 7.52 (m, 5H), 4.16 – 4.07 (m, 1H, H-2), 3.81 – 3.68 (m, 2H, H-1), 3.60 (dd, $J = 14.5, 5.6$ Hz, 1H, H-3a), 3.47 (dd, $J = 14.5, 6.1$ Hz, 1H, H-3b), 3.27 (d, $J = 6.1$ Hz, 1H, OH), 3.01 (t, $J = 6.5$ Hz, 1H, OH). **¹³C NMR** (125 MHz, CDCl_3): δ 155.0 (C-4), 130.5, 129.9, 123.9, 71.1 (C-2), 63.9 (C-1), 35.9 (C-3). **FTIR** (thin film) ν 3432, 3396, 3069, 2935, 2882, 1596, 1499, 1461, 1410, 1388, 1318, 1284, 1243, 1176, 1093, 1074, 1038, 1016, 761, 694, 549 cm^{-1} . **HRMS** (ESI): Calculated for $\text{C}_{10}\text{H}_{13}\text{N}_4\text{O}_2\text{S}^+$ $[\text{M}+\text{H}]^+$ 253.0754; found 253.0756. $[\alpha]_D^{23} +3.7$ ($c = 1.16$, CHCl_3).

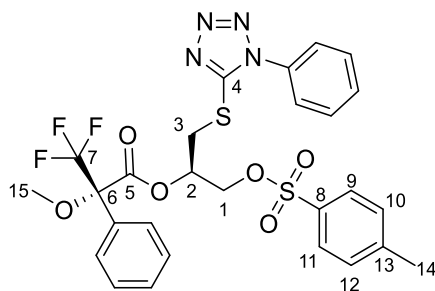
Preparation of (*S*)-2-hydroxy-3-((1-phenyl-1H-tetrazol-5-yl)thio)propyl 4-methylbenzenesulfonate, **217**



To a solution of diol **216** (4.53 g, 17.9 mmol, 1.0 equiv.) in anhydrous DCM (150 mL) were added dibutyltin oxide (0.918 g, 3.59 mmol, 0.2 equiv.) at room temperature. The resulting mixture was stirred at room temperature for 1 hour. Triethylamine (2.50 mL, 17.9 mmol, 1.0 equiv.) was added dropwise to the reaction mixture. Then 4-

toluenesulfonyl chloride (3.5 g, 17.9 mmol, 1.0 equiv.) in anhydrous DCM (50 mL) was added to the reaction mixture by a syringe pump over 1 hr. The reaction mixture was stirred for 8 hours. The reaction was added water (35 mL) and the aqueous phase was extracted with ethyl acetate (3 × 50 mL). The combined organic phase was washed with brine, dried over anhydrous Na₂SO₄, filtered and evaporated under vacuum. The crude material was purified by silica gel flash chromatography (pet. ether/EtOAc = 2:1) to provide the title compound (6.76 g, 93%) as a foamy gel. **R_f**: 0.63 (pet. ether/EtOAc = 1:2). **¹H NMR** (500 MHz, CDCl₃) δ 7.84 – 7.78 (m, 2H, H-6, H-10), 7.62 – 7.53 (m, 5H), 7.36 (d, *J* = 8.0 Hz, 2H, H-7, H-9), 4.36 – 4.29 (m, 1H, H-2), 4.14 (dd, *J* = 5.4, 1.9 Hz, 2H, H-1), 3.59 (dd, *J* = 14.6, 3.6 Hz, 1H, H-3a), 3.44 (dd, *J* = 14.6, 7.0 Hz, 1H, H-3b), 2.45 (s, 3H, H-11). **¹³C NMR** (125 MHz, CDCl₃) δ 154.4 (C-4), 145.3 (C-5), 133.3, 132.3 (C-8), 130.4, 130.0 (C-7, C-9), 129.9, 128.0 (C-6, C-10), 123.8, 71.1 (C-2), 68.6 (C-1), 36.1 (C-3), 21.7 (C-11). **FTIR** (thin film) ν 3255, 3065, 2922, 1595, 1501, 1448, 1418, 1384, 1331, 1289, 1213, 1172, 1121, 1089, 1064, 1033, 1010, 816, 762, 712, 681, 608, 567 cm⁻¹. **HRMS** (ESI): Calculated for C₁₇H₁₉N₄O₄S₂⁺ [M + H]⁺ 407.0842; found 407.0839. [α]_D²³ –46 (*c* = 0.385, DCM).

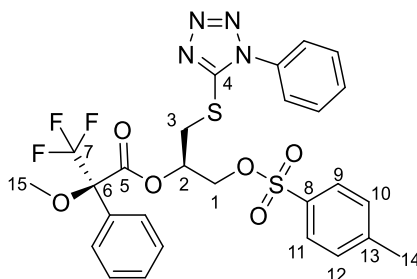
Preparation of (*R*)-1-((1-phenyl-1*H*-tetrazol-5-yl)thio)-3-(tosyloxy)propan-2-yl (*S*)-3,3,3-trifluoro-2-methoxy-2-phenylpropanoate, (*S*)-MTPA-219



To a solution of tosylate **217** (23.2 mg, 0.057 mmol, 1.0 equiv.) in anhydrous DCM (3.0 mL) was added sequentially (*S*)-(+)- α -methoxy- α -trifluoromethylphenylacetic acid (46.0 mg, 0.182 mmol, 3.2 equiv.), *N,N'*-dicyclohexylcarbodiimide (112.3 mg, 0. mmol, 8.8 equiv.) and 4-dimethylaminopyridine (24.2 mg, 0.198 mmol, 3.0 equiv.). The reaction mixture was stirred at room temperature for 5 days. 2 mL waster was added the reaction mixture. Then the aqueous phase was extracted with ethyl acetate (3 × 5 mL). The combined organic phase was washed with brine, dried over anhydrous Na₂SO₄, filtered and evaporated under vacuum. The crude material was purified by silica gel flash

chromatography (pet. ether/EtOAc = 3:1) to provide the title compound (25.7 mg, 65%) as a colourless oil. **R_f**: 0.77 (pet. ether/EtOAc = 1:1). **¹H NMR** (500 MHz, CDCl₃, represents peaks from major diastereomer) δ 7.73 – 7.69 (m, 2H, H-9, H-11), 7.59 – 7.54 (m, 3H), 7.52 – 7.48 (m, 2H), 7.48 – 7.45 (m, 2H), 7.42 – 7.37 (m, 1H), 7.37 – 7.31 (m, 4H, overlapped, H-10, H-12), 5.69 – 5.63 (m, 1H, H-2), 4.29 (dd, *J* = 11.2, 3.2 Hz, 1H, H-1a), 4.24 (dd, *J* = 11.2, 4.7 Hz, 1H, H-1b), 3.80 (dd, *J* = 14.6, 4.2 Hz, 1H, H-3a), 3.43 (s, 3H, H-15), 3.49 (dd, *J* = 14.6, 8.4 Hz, 1H, H-3b), 2.45 (s, 3H, H-14). **¹³C NMR** (125 MHz, CDCl₃, represents peaks from major diastereomer) δ 165.9 (C-5), 152.8 (C-4), 145.4 (C-8), 133.2, 131.9, 131.3 (C-13), 130.4, 130.0 (C-10, C-12), 129.9, 129.8, 128.5, 128.0 (C-9, C-11), 127.4, 122.9 (q, ¹*J*_{C-F} = 287.1 Hz, C-7), 123.8, 84.8 (q, ²*J*_{C-F} = 27.8 Hz, C-6), 71.1 (C-2), 68.0 (C-1), 55.5 (C-15), 32.8 (C-3), 21.7 (C-14). **FTIR** (thin film) ν 2952, 1753, 1597, 1500, 1451, 1366, 1268, 1240, 1189, 1174, 1120, 1107, 1096, 1081, 1052, 1015, 989, 932, 814, 791, 762, 732, 717, 695, 666, 611, 553 cm⁻¹. **HRMS** (ESI): Calculated for C₂₇H₂₆F₃N₄O₆S₂⁺ [M+H]⁺ 623.1246; found 623.1224. [α]_D²⁴ +17.5 (*c* = 1.29, DCM).

Preparation of (*R*)-1-((1-phenyl-1*H*-tetrazol-5-yl)thio)-3-(tosyloxy)propan-2-yl (*R*)-3,3,3-trifluoro-2-methoxy-2-phenylpropanoate, (*R*)-MTPA-219

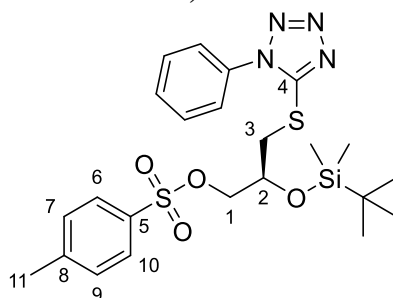


To a solution of tosylate **217** (27.0 mg, 0.066 mmol, 1.0 equiv.) in anhydrous DCM (3.0 mL) was added sequentially (*R*)-(+)-α-methoxy-α-trifluoromethylphenylacetic acid (63.2 mg, 0.25 mmol, 3.79 equiv.), *N,N'*-dicyclohexylcarbodiimide (119.5 mg, 0.579 mmol, 8.8 equiv.) and 4-dimethylaminopyridine (24.2 mg, 0.198 mmol, 3.0 equiv.). The reaction mixture was stirred at room temperature for 5 days. 2 mL waster was added the reaction mixture. Then the aqueous phase was extracted with ethyl acetate (3 × 5 mL). The combined organic phase was washed with brine, dried over anhydrous Na₂SO₄, filtered and evaporated under vacuum. The crude material was purified by silica gel flash chromatography (pet. ether/EtOAc = 3:1) to provide the title compound (26.7 mg,

65%) as a colourless oil.

R_f: 0.77 (pet. ether/EtOAc = 1:1). **¹H NMR** (500 MHz, CDCl₃, represents peaks from major diastereomer) δ 7.79 – 7.74 (m, 2H, H-9, H-11), 7.60 – 7.55 (m, 3H), 7.49 – 7.46 (m, 2H), 7.46 – 7.43 (m, 2H), 7.37 – 7.32 (m, 3H, overlapped, H-10, H-12), 7.31 – 7.26 (m, 2H), 5.67 – 5.61 (m, 1H, H-2), 4.37 (dd, *J* = 11.3, 2.8 Hz, 1H, H-1a), 4.28 (dd, *J* = 11.3, 5.1 Hz, 1H, H-1b), 3.72 (dd, *J* = 14.5, 4.1 Hz, 1H, H-3a), 3.49 (s, 3H, H-15), 3.39 (dd, *J* = 14.5, 8.4 Hz, 1H, H-3b), 2.45 (s, 3H, H-14). **¹³C NMR** (125 MHz, CDCl₃, represents peaks from major diastereomer) δ 165.9 (C-5), 152.9 (C-4), 145.6 (C-8), 133.2, 131.9, 131.6, 130.4, 130.1 (C-10, C-12), 129.9 (C-13), 129.7, 128.4, 128.0 (C-9, C-11), 127.2, 123.8, 123.1 (q, ¹*J*_{C-F} = 287.2 Hz, C-7), 84.6 (q, ²*J*_{C-F} = 27.7 Hz, C-6), 71.0 (C-2), 68.3 (C-1), 55.7 (C-15), 32.8 (C-3), 21.7 (C-14). **FTIR** (thin film) ν 2952, 1753, 1597, 1500, 1451, 1366, 1268, 1238, 1189, 1174, 1120, 1107, 1096, 1081, 1052, 1015, 988, 932, 814, 762, 731, 717, 694, 666, 648, 553 cm⁻¹. **HRMS** (ESI): Calculated for C₂₇H₂₆F₃N₄O₆S₂⁺ [M+H]⁺ 623.1246; found 623.1225. [α]_D²⁴ +63 (*c* = 1.34, DCM).

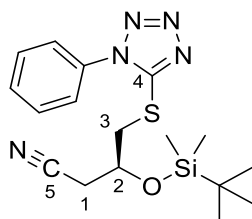
Preparation of (*S*)-2-((*tert*-butyldimethylsilyl)oxy)-3-((1-phenyl-1*H*-tetrazol-5-yl)thio)propyl 4-methylbenzenesulfonate, **221**



To a solution of tosylate **217** (2.86 g, 7.04 mmol, 1.0 equiv.), imidazole (2.88 g, 42.2 mmol, 6.0 equiv.) and 4-dimethylaminopyridine (91.4 mg, 0.704 mmol, 0.1 equiv.) in anhydrous DMF (30 mL) was added *tert*-butyldimethylsilyl chloride (3.18 g, 21.1 mmol, 3.0 equiv.). The reaction mixture was stirred at room temperature for 16 hours. Then the reaction mixture was diluted with ethyl acetate (100 mL), and washed with water (3 × 50 mL). The combined aqueous phase was extracted with ethyl acetate (3 × 50 mL). The combined organic phase was washed with brine, dried over anhydrous Na₂SO₄, filtered and evaporated under vacuum. The crude material was purified by silica gel flash chromatography (pet. ether/EtOAc = 5:1) to provide the title compound (2.96 g, yield 81%) as a white crystal. **R_f**: 0.50 (pet. ether/EtOAc = 2:1). **Melting point**: 122 – 123 °C. **¹H NMR** (500 MHz, CDCl₃): δ 7.81 – 7.75 (m, 2H, H-6, H-10), 7.61 – 7.51 (m, 5H), 7.32

(d, $J = 8.0$ Hz, 2H, H-7, H-9), 4.32 (quin, $J = 5.2$ Hz, 1H, H-2), 4.09 – 4.02 (m, 2H, H-1), 3.53 (dd, $J = 13.7, 5.5$ Hz, 2H, H-3a), 3.45 (dd, $J = 13.7, 6.0$ Hz, 2H, H-3b), 2.43 (s, 3H, H-11), 0.81 (s, 9H), 0.023 (s, 3H), 0.018 (s, 3H). **^{13}C NMR** (125 MHz, CDCl_3): δ 153.8 (C-4), 145.1 (C-5), 133.2, 132.5 (C-8), 130.3, 129.91, 129.86 (C-7, C-9), 128.0 (C-6, C-10), 71.2 (C-2), 68.2 (C-1), 36.6 (C-3), 25.6, 21.7 (C-11), 17.9, -4.77, -4.85. **FTIR** (solid) ν 2951, 2929, 2890, 2855, 1597, 1500, 1473, 1460, 1446, 1423, 1397, 1358, 1307, 1294, 1277, 1255, 1189, 1172, 1110, 1090, 1041, 1017, 997, 976, 929, 865, 841, 824, 809, 778, 764, 738, 692, 666, 609, 573, 553, 489, 469 cm^{-1} . **HRMS** (ESI): Calculated for $\text{C}_{23}\text{H}_{33}\text{N}_4\text{O}_4\text{S}_2\text{Si}^+$ $[\text{M}+\text{H}]^+$ 521.1712; found 521.1735. $[\alpha]_D^{18} +276$ ($c = 0.25$, DCM).

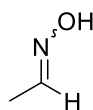
Preparation of (*S*)-3-((*tert*-butyldimethylsilyl)oxy)-4-((1-phenyl-1*H*-tetrazol-5-yl)thio)butanenitrile, **222**



To a solution of silyl ether **221** (104 mg, 0.20 mmol, 1.0 equiv.) and 18-crown-6 (151 mg, 0.57 mmol, 2.85 equiv.) in anhydrous acetonitrile (4 mL) was added potassium cyanide (43.7 mg, 0.67 mmol, 3.35 equiv.) at room temperature. The reaction mixture was heated at 40 °C for 20 hours under argon atmosphere. The reaction mixture was diluted with ethyl acetate (10 mL) and was added saturated aqueous NaHCO_3 solution (5 mL). The aqueous phase was extracted by ethyl acetate (3×10 mL). The combined organic phase was washed with brine, dried over anhydrous Na_2SO_4 , filtered and evaporated under vacuum. The crude material was purified by silica gel flash chromatography (pet. ether/EtOAc = 4:1) to provide the title compound (34.7 mg, yield 46%) as a white solid. **R_f**: 0.45 (pet. ether/EtOAc = 3:1). **Melting point**: 108 – 109 °C **^1H NMR** (500 MHz, CDCl_3): δ 7.62 – 7.53 (m, 5H), 4.51 – 4.45 (m, 1H, H-2), 3.60 (dd, $J = 13.9, 5.7$ Hz, 1H, H-3a), 3.48 (dd, $J = 13.9, 6.0$ Hz, 1H, H-3b), 2.71 (dd, $J = 4.9, 1.3$ Hz, 2H, H-1), 0.90 (s, 9H), 0.15 (s, 3H), 0.12 (s, 3H). **^{13}C NMR** (125 MHz, CDCl_3): δ 153.6 (C-4), 133.4, 130.4, 130.0, 123.8, 116.7 (C-5), 66.5 (C-2), 38.8 (C-3), 25.6, 25.5 (C-1), 17.9, -4.6, -4.8. **FTIR** (thin film) ν 2954, 2929, 2887, 2856, 1597, 1499, 1471, 1463, 1411, 1388, 1363, 1279, 1251, 1099, 1075, 1014, 938, 838, 806, 779, 760, 712, 687, 665, 552 cm^{-1} . **HRMS** (ESI): Calculated for $\text{C}_{17}\text{H}_{26}\text{N}_5\text{OSSi}^+$ $[\text{M}+\text{H}]^+$ 376.1627; found 376.1622. $[\alpha]_D^{18} +93.3$ ($c = 0.15$,

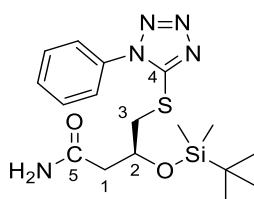
DCM).

Preparation of *cis*- and *trans*-acetaldoxime mixture



A cold solution of sodium hydroxide (21.0 g, 0.53 mol in 60 mL distilled water, 1.5 equiv.) was added slowly to an aqueous solution of hydroxylamine hydrochloride (50 g, 0.7 mol in 100 mL distilled water). Then acetaldehyde (20 mL, 0.35 mol) was added slowly to the reaction mixture. The resulting mixture was stirred at 100 °C for 3 hours and then cooled to room temperature. The reaction mixture was extracted by diethyl ether (4 × 100 mL). The combined organic phase was washed with brine, dried over anhydrous Na₂SO₄, filtered and evaporated under atmospheric pressure. The crude material was purified by distillation to provide the title compound (18.5 g, yield 89%) as a colourless crystal. ¹H NMR (500 MHz, CDCl₃): 8.57 (br. s, 1H), 8.19 (br. s, 1H), 7.46 (q, *J* = 5.8 Hz, 1H), 6.84 (q, *J* = 5.5 Hz, 1H), 1.88 (d, *J* = 5.5 Hz, 3H), 1.86 (d, *J* = 5.8 Hz, 3H). ¹³C NMR (125 MHz, CDCl₃): δ 148.1, 147.8, 15.1, 11.1. These characterisation data match those reported in the literature.³⁴¹

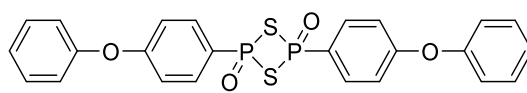
Preparation of (*S*)-3-((*tert*-butyldimethylsilyl)oxy)-4-((1-phenyl-1*H*-tetrazol-5-yl)thio)butanamide, **225**



To an 20 mL vial were added nitrile **222** (0.927 g, 2.47 mmol, 1.0 equiv.), freshly prepared acetaldoxime (0.729 g, 12.4 mmol, 5.0 equiv.), RhCl(PPh₃)₃ (0.026 g, 0.01 equiv.) and anhydrous toluene (8 mL). The reaction mixture was vigorously stirred at 110 °C under argon atmosphere in the sealed vial for 22 hours. Then solvent was removed under vacuum. The crude material was purified by silica gel flash chromatography (pet. ether/EtOAc = 1:1) to provide the title compound (855 mg, yield 88%) as a white solid. **R_f**: 0.11 (pet. ether/EtOAc = 1:1). **Melting point**: 78 – 79 °C. ¹H NMR (500 MHz, CDCl₃): δ 7.62 – 7.51 (m, 5H), 6.26 (br. s, 1H, N-H), 5.48 (br. s, 1H, N-H), 4.54 (quin, *J* = 5.5 Hz,

1H, H-2), , 3.64 (dd, $J = 13.7, 5.5$ Hz, 1H, H-3a), 3.52 (dd, $J = 13.7, 6.2$ Hz, 1H, H-3b), 2.63 (dd, $J = 14.9, 5.2$ Hz, 1H, H-1a), 2.54 (dd, $J = 14.9, 5.4$ Hz, 1H, H-1b), 0.88 (s, 9H), 0.13 (s, 3H), 0.12 (s, 3H). **^{13}C NMR** (125 MHz, CDCl_3): δ 172.1 (C-5), 154.2 (C-4), 133.5, 130.3, 129.9, 123.8, 67.7 (C-2), 42.5 (C-1), 39.1 (C-3), 25.7, 18.0, -4.6, -4.8. **FTIR** (solid) ν 3389, 3339, 3197, 2954, 2929, 2887, 2856, 1673, 1615, 1598, 1499, 1471, 1463, 1407, 1389, 1362, 1335, 1251, 1162, 1090, 1015, 955, 838, 811, 779, 761, 694, 667, 573, 557 cm^{-1} . **HRMS** (ESI): Calculated for $\text{C}_{17}\text{H}_{28}\text{N}_5\text{O}_2\text{SSi}^+$ $[\text{M} + \text{H}]^+$ 394.1728; found 394.1726. $[\alpha]_D^{23} +165$ ($c = 1.65$, DCM).

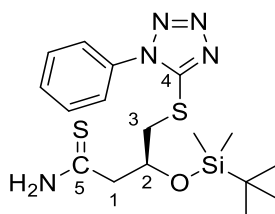
Preparation of Belleau's Reagent (2,4-bis(4-phenoxyphenyl)-1,3,2,4-dithiadiphosphetane 2,4-disulfide),³⁴² 231



231

Phosphorus pentasulfide (6.94 g, 0.016 mmol, 0.1 equiv.) and diphenyl ether (25 mL, 0.16 mmol, 1.0 equiv.) were stirred at 160 °C under argon atmosphere for 9 hours. The reaction mixture was then stirred at room temperature for 15 hours. The yellow precipitate was filtered, washed with anhydrous toluene, and recrystallised from anhydrous toluene (60 mL) to afford the title compound as a yellow powder (3.16 g, yield 37%). **Melting point:** 187-190 °C (sealed tube). This characterisation data match those reported in the literature.^{186, 342}

Preparation of (S)-3-((tert-butyldimethylsilyl)oxy)-4-((1-phenyl-1H-tetrazol-5-yl)thio)butanethioamide, 223

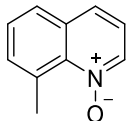


To a solution of amide **225** (1.025 g, 13.7 mmol, 1.0 equiv.) in anhydrous THF (50 mL) was added Lawesson's reagent (3.78 g, 9.5 mmol, 0.7 equiv.). The reaction mixture was stirred at room temperature for 30 minutes. 50 mL saturated aqueous NaHCO_3 solution was added to the reaction mixture and the aqueous phase was extracted with ethyl acetate

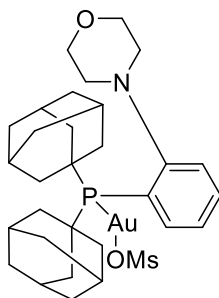
(3 × 100 mL). The combined organic phase was washed with brine, dried over anhydrous Na₂SO₄, filtered and evaporated under vacuum. The crude material was purified by silica gel flash chromatography (pet. ether/EtOAc = 3:1) to provide the title compound (0.661 g, yield 62%) as a yellow oil. **R_f**: 0.4 (pet. ether/EtOAc = 1:1). **¹H NMR** (500 MHz, CDCl₃): δ 8.16 (br.s, 1H, N-H), 7.62 – 7.52 (m, 5H), 7.49 (br.s, 1H, -NH), 4.61 – 4.56 (m, 1H, H-2), 3.67 (dd, *J* = 13.9, 4.8 Hz, 1H, H-1, H-1a), 3.49 (dd, *J* = 13.9, 6.5 Hz, 1H, H-1b), 3.13 (ddd, *J* = 14.4, 4.6, 1.0 Hz, 1H, H-3a), 3.07 (dd, *J* = 14.5, 5.4 Hz, 1H, H-3b), 0.89 (s, 9H), 0.165 (s, 3H), 0.162 (s, 3H). **¹³C NMR** (125 MHz, CDCl₃): δ 205.8, 154.4, 133.4, 130.3, 129.9, 123.8, 69.7, 50.8, 38.5, 25.8, 17.9, -4.6, -4.8. **FTIR** (thin film) ν 3307, 3182, 2953, 2928, 2885, 2855, 1620, 1597, 1499, 1461, 1408, 1388, 1361, 1333, 1316, 1279, 1250, 1209, 1146, 1088, 1014, 939, 917, 836, 809, 778, 730, 692, 663, 552, 465 cm⁻¹. **HRMS** (ESI): Calculated for C₁₇H₂₈N₅OS₂Si⁺ [M + H]⁺ 410.1505; found 410.1479. [α]_D¹⁸ –317 (*c* = 0.23, DCM).

6.2.2 Gold-catalysed Preparation of Thiazole 276

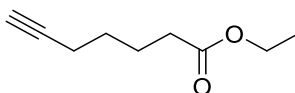
Preparation of 8-methylquinoline *N*-oxide, 254



To a solution of 8-methylquinoline **255** (1.58 g, 11.0 mmol, 1.0 equiv.) in DCM (110 mL) was added 3-chloroperbenzoic acid (3.3 g, 77% purity, 14.3 mmol, 1.3 equiv.). The reaction mixture was stirred at room temperature in dark for 16 hours. Then the reaction mixture was washed with 1M KOH aqueous solution (4 × 50 mL). The combined aqueous phase was extracted with DCM (6 × 100 mL). The combined organic phase was washed with brine, dried over anhydrous Na₂SO₄, filtered and evaporated under vacuum. The crude material was purified by silica gel flash chromatography (DCM/MeOH = 30:1) to provide the title compound (1.268 g, 72%) as a brown oil that solidified upon standing at room temperature. **R_f**: 0.29 (DCM/MeOH = 10:1). **¹H NMR** (500 MHz, CDCl₃): δ 8.40 (dd, *J* = 6.1, 1.1 Hz, 1H), 7.67 – 7.62 (m, 2H), 7.46 – 7.40 (m, 2H), 7.18 (dd, *J* = 8.4, 6.0 Hz, 1H), 3.19 (s, 3H). **¹³C NMR** (125 MHz, CDCl₃): δ 141.5, 137.2, 133.7, 133.3, 132.5, 128.1, 126.8, 126.3, 120.7, 24.9. These characterisation data match those reported in the literature.³⁴³

Preparation of Mor-Dal Phos AuOMs, 257

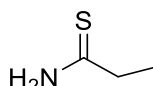
To a suspension of Mor-DalPhos AuCl **256** (50mg, 0.072 mmol, 1.0 equiv.) in 5 mL anhydrous DCM was added silver methanesulfonate (16.5mg mmol, 0.08 mmol, 1.1 equiv.). The mixture was stirred for 1 hour at room temperature under argon atmosphere and the reaction mixture was allowed to settle for 5 min after which silver chloride all precipitated in the bottom. After passing through a Teflon syringe filter (0.2 μm), the solvent was evaporated off under reduced pressure to give the desired gold complex Mor-DalPhos AuOMs in (52.9 mg, 98% yield) as an off-white powder. **^1H NMR** (500 MHz, CDCl_3): δ 7.81 – 7.75 (m, 1H), 7.66 – 7.56 (m, 2H), 7.38 – 7.31 (m, 1H), 4.43 (td, J = 11.5, 2.0 Hz, 2H), 3.86 (dd, J = 11.5, 2.4 Hz, 2H), 3.12 (td, J = 11.5, 3.2 Hz, 2H), 2.98 (s, 3H), 2.66 (d, J = 11.5 Hz, 2H), 2.24 – 2.16 (m, 6H), 2.13 – 2.05 (m, 6H), 2.04 – 1.97 (m, 6H), 1.68 (s, 12H). **^{13}C NMR** (125 MHz, CDCl_3): δ 158.5 (d, $J_{\text{C-P}}$ = 4.6 Hz), 134.5 (d, $J_{\text{C-P}}$ = 2.5 Hz), 132.9 (d, $J_{\text{C-P}}$ = 1.7 Hz), 127.2 (d, $J_{\text{C-P}}$ = 4.9 Hz), 125.1 (d, $J_{\text{C-P}}$ = 6.8 Hz), 121.0 (d, $J_{\text{C-P}}$ = 48.4 Hz), 66.3, 54.5, 42.3 (d, $J_{\text{C-P}}$ = 2.5 Hz), 39.4, 36.2 (d, $J_{\text{C-P}}$ = 1.3 Hz), 28.5 (d, $J_{\text{C-P}}$ = 10.0 Hz). These characterisation data match those reported in the literature.¹⁴¹

Preparation of ethyl hept-6-ynoate, 259

To an oven-dried 20 mL round-bottomed flask outfitted with a stir bar, a condenser, a gas inlet adapter and a rubber septum, absolute ethanol (5.0 mL), hept-6-ynoic acid **258** (99.7 mg, 0.79 mmol) and concentrated H_2SO_4 (1 drop) were added sequentially. The mixture was refluxed for 3 h before cooling to room temperature and the solvent removed under reduced pressure. The crude product was diluted with diethyl ether (50 mL), washed with saturated NaHCO_3 (5 mL) and water (5 mL). The organic layers were dried over

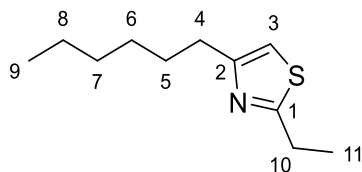
magnesium sulfate, filtered and the solvent removed under reduced pressure. The residue was then purified by flash silica gel chromatography (pet. ether/Et₂O = 10/1) to afford the title compound (112 mg, 92%) as a colourless oil. **R_f**: 0.43 (pet. ether/EtOAc = 5:1). **¹H NMR** (500 MHz, CDCl₃): δ 4.13 (q, *J* = 7.1 Hz, 2H), 2.32 (t, *J* = 7.4 Hz, 2H), 2.21 (td, *J* = 7.0, 2.6 Hz, 2H), 1.95 (t, *J* = 2.7 Hz, 1H), 1.79 – 1.71 (m, 2H), 1.60 – 1.53 (m, 2H), 1.25 (t, *J* = 7.1 Hz, 3H). **¹³C NMR** (125 MHz, CDCl₃): δ 173.4, 84.0, 68.6, 60.3, 33.8, 27.9, 24.0, 18.1, 14.3. These characterisation data match those reported in the literature.³⁴⁴

Preparation of propanethioamide, **261**



To a milky suspension of purified Lawesson's reagent (3.78 g, 9.5 mmol, 0.7 equiv.) in anhydrous THF (50 mL) was added propionamide **260** (1.025 g, 13.5 mmol, 1.0 equiv.). The reaction mixture was stirred at room temperature under argon atmosphere for 30 minutes. Saturated aqueous NaHCO₃ solution (70 mL) was added to the reaction mixture. The combined aqueous phase was extracted with ethyl acetate (3 × 100 mL). The combined organic phase was washed with brine, dried over anhydrous Na₂SO₄, filtered and evaporated under vacuum. The crude material was purified by silica gel flash chromatography (pet. ether/EtOAc = 1:1) to provide the title compound (0.761 g, 61%) as a yellow solid. **Melting point**: 40°C – 41°C **R_f**: 0.4 (pet. ether/EtOAc = 1:1). **¹H NMR** (500 MHz, CDCl₃): δ 7.59 (br. s, 1H), 6.86 (br. s, 1H), 2.69 (q, *J* = 7.5 Hz, 2H), 1.31 (t, *J* = 7.5 Hz, 3H). **¹³C NMR** (125 MHz, CDCl₃): δ 212.2, 38.4, 13.3. These characterisation data match those reported in the literature.³⁴⁵

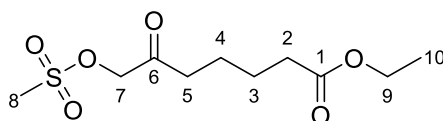
Preparation of 2-ethyl-4-hexylthiazole, **264**



To a solution of Mol-DalPhosAuOMs **257** (17 mg, 0.023 mmol, 0.05 equiv.) in deoxygenated anhydrous DCM (0.9 mL) was added 1-octyne **263** (70 mg, 0.45 mmol, 1.0 equiv.). The resulting mixture was stirred at room temperature under argon atmosphere for 15 minutes. Then a solution of 8-methylquinoline *N*-oxide **254** (94 mg, 0.59 mmol, 1.3 equiv.) and methanesulfonic acid (35 μL, 0.54 mmol, 1.2 equiv.) in deoxygenated

anhydrous DCM (0.9 mL) was added to the reaction mixture via a syringe pump under argon atmosphere in 5 hours. Upon completion, the reaction mixture was further stirred for 1 hour before propanethioamide **261** (48 mg, 0.54 mmol, 1.2 equiv.) in anhydrous DCM (0.5 mL) adding. The resulting mixture was stirred at 40 °C in a sealed vial for 16 hours before concentration under reduced pressure. The crude material was purified by silica gel flash chromatography (pet. ether/EtOAc = 10:1) to provide the title compound (77.6 mg, yield 62 %) as a yellow oil. *R_f*: 0.47 (pet. ether/EtOAc = 5:1). **¹H NMR** (500 MHz, CDCl₃): δ 6.69 (s, 1H, H-3), 3.00 (q, *J* = 7.6 Hz, 2H, H-10), 2.72 (t, *J* = 7.3 Hz, 2H, H-4), 1.72 – 1.65 (m, 2H, H-5), 1.36 (t, *J* = 7.6 Hz, 3H, H-11, overlapped), 1.40 – 1.27 (m, 6H, overlapped, H-6, H-7, H-8), 0.88 (t, *J* = 7.0 Hz, 3H, H-9). **¹³C NMR** (125 MHz, CDCl₃): δ 172.2 (C-1), 157.2 (C-2), 111.3 (C-3), 31.62 (C-7), 31.58 (C-4), 29.2 (C-5), 29.0 (C-6), 26.9 (C-10), 22.6 (C-8), 14.3 (C-11), 14.0 (C-9). **FTIR** (thin film) ν 2956, 2925, 2855, 1522, 1457, 1376, 1320, 1260, 1182, 1131, 1096, 1049, 970, 829, 804, 726. **HRMS** (ESI): Calculated for C₁₁H₂₀NS⁺ [M+H]⁺ 198.1311; found 198.1317.

Preparation of ethyl 7-((methylsulfonyl)oxy)-6-oxoheptanoate, **273**

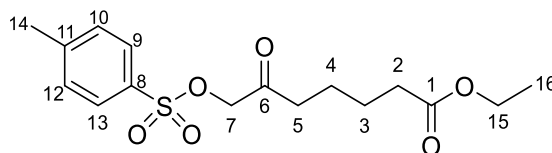


To a solution of alkyne **259** (49.2 mg, 0.324 mmol, 1.0 equiv.) in deoxygenated DCM (0.65 mL) was added Mol-DalPhosAuOMs **257** (2.4 mg, 0.00324, 0.01 equiv.) under argon atmosphere and the resulting mixture was stirred for 15 minutes. The resulting mixture was added a solution of 8-methylquinoline *N*-oxide **254** (67 mg, 0.421 mmol, 1.3 equiv.) and anhydrous methanesulfonic acid (25 μ L, 0.3 mmol, 1.2 equiv.) in deoxygenated DCM (0.65 mL) was added by a syringe pump under argon atmosphere in 5 hours. Upon completion, the reaction mixture was stirred for 1 hour before concentration under reduced pressure. The crude material was purified by silica gel flash chromatography (pet. ether/EtOAc = 2:1) to provide the title compound (38 mg, 45%) as a yellow oil. *R_f*: 0.45 (pet. ether/EtOAc = 1:1). **¹H NMR** (500 MHz, CDCl₃): δ 4.78 (s, 2H, H-7), 4.13 (q, *J* = 7.1 Hz, 2H, H-9), 3.20 (s, 3H, H-8), 2.50 (t, *J* = 6.9 Hz, 2H, H-5), 2.32 (t, *J* = 6.8 Hz, 2H, H-2), 1.71 – 1.60 (m, 4H, H-3, H-4), 1.25 (t, *J* = 7.1 Hz, 3H, H-10). **¹³C NMR** (125 MHz, CDCl₃): δ 202.5 (C-6), 173.2 (C-1), 71.5 (C-7), 60.4 (C-9), 38.9 (C-8), 38.2 (C-5), 33.9 (C-2), 24.2 (C-4), 22.4 (C-3), 14.2 (C-10). **FTIR** (thin film)

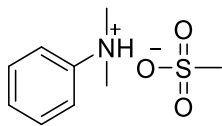
ν 2939, 1723, 1414, 1352, 1253, 1173, 1109, 1060, 1010, 969, 809, 765, 728, 526 cm^{-1} .

HRMS (ESI): Calculated for $\text{C}_{10}\text{H}_{22}\text{NO}_6\text{S}^+$ $[\text{M}+\text{NH}_4]^+$ 284.1168; found 284.1163.

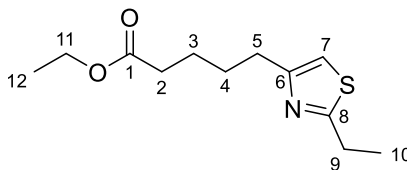
Preparation of ethyl 6-oxo-7-(tosyloxy)heptanoate, **274**



To a solution of ester **259** (49.9 mg, 0.324 mmol, 1.0 equiv.) in deoxygenated DCM (0.65 mL) was added Mol-DalPhosAuOMs **257** (2.4 mg, 0.00324, 0.01 equiv.) under argon atmosphere and the resulting mixture was stirred for 15 minutes. The resulting mixture was added a solution of 8-methylquinoline *N*-oxide **254** (67 mg, 0.421 mmol, 1.3 equiv.) and *p*-toluenesulfonic acid (67 mg, 0.3 mmol, 1.2 equiv.) in deoxygenated DCM (0.65 mL) was added by a syringe pump under argon atmosphere in 5 hours. Upon completion, the reaction mixture was stirred for 1 hour before concentration under reduced pressure. The crude material was purified by silica gel flash chromatography (pet. ether/EtOAc = 4:1) to provide the title compound (32 mg, 29%) as a colourless oil. **R_f**: 0.70 (pet. ether/EtOAc = 1:1). **¹H NMR** (500 MHz, CDCl_3): δ 7.84 – 7.78 (m, 2H, H-9, H-13), 7.40 – 7.35 (m, 2H, H-10, H-12), 4.48 (s, 2H, H-7), 4.11 (q, J = 7.1 Hz, 2H, H-15), 2.53 (t, J = 6.8 Hz, 2H, H-5), 2.46 (s, 3H, H-14), 2.34 (t, J = 6.8 Hz, 2H, H-2), 1.62 – 1.57 (m, 4H, H-3, H-4), 1.25 (t, J = 7.1 Hz, 3H, H-16). **¹³C NMR** (125 MHz, CDCl_3): δ 202.8 (C-6), 173.2 (C-1), 145.5 (C-8), 132.9 (C-11), 130.1 (C-10, C-12), 128.8 (C-9, C-13), 71.8 (C-7), 60.4 (C-15), 38.6 (C-5), 33.9 (C-2), 24.2 (C-4), 22.2 (C-3), 21.7 (C-14), 14.2 (C-16). **FTIR** (thin film) ν 2937, 1729, 1449, 1369, 1292, 1253, 1190, 1177, 1096, 1005, 817, 774, 667, 554 cm^{-1} . **HRMS** (ESI): Calculated for $\text{C}_{16}\text{H}_{22}\text{NaO}_6\text{S}^+$ $[\text{M}+\text{H}]^+$ 365.1035; found 365.1042.

Preparation of *N,N*-dimethylbenzenaminium methanesulfonate, 275

Methanesulfonic acid (1.60 mL, 24.7 mmol, 1.0 equiv.) was dropped to a solution of *N,N*-dimethylaniline (3.20 mL, 25.2 mmol, 1.02 equiv.) in ethanol (50 mL) over 15 minutes. The reaction mixture was then stirred at room temperature for 30 minutes. Ethanol was evaporated under reduced pressure and the crude material was recrystallised in DCM to afford the title compound (1.4 g, yield 26%) as a white solid. $^1\text{H NMR}$ (500 MHz, CDCl_3): 7.64 – 7.59 (m, 2H), 7.58 – 7.46 (m, 3H), 3.26 (s, 6H), 2.90 (s, 3H). $^{13}\text{C NMR}$ (125 MHz, CDCl_3): δ 142.9, 130.7, 130.3, 120.6, 46.9, 39.4. **FTIR** (solid) ν 3036, 2961, 2976, 2519, 2479, 1598, 1515, 1499, 1475, 1429, 1410, 1337, 1222, 1200, 1179, 1164, 1146, 1133, 1076, 1028, 995, 962, 912, 901, 765, 690, 616, 578, 552, 522 cm^{-1} .

Preparation of ethyl 5-(2-ethylthiazol-4-yl)pentanoate, 262

Method A (Use MsOH as MsO^- source and syringe pump for addition)

To a solution of Mol-DalPhosAuOMs **257** (27.5 mg, 0.036 mmol, 0.05 equiv.) in deoxygenated anhydrous DCM (1.4 mL) was added alkyne **259** (111 mg, 0.718 mmol, 1.0 equiv.). The resulting mixture was stirred at room temperature under argon atmosphere for 15 minutes. Then a solution of 8-methylquinoline *N*-oxide **254** (148 mg, 0.93 mmol, 1.30 equiv.) and methanesulfonic acid (56 μL , 0.862 mmol, 1.2 equiv.) in deoxygenated anhydrous DCM (1.4 mL) was added to the reaction mixture via a syringe pump under argon atmosphere in 5 hours. Upon completion, the reaction mixture was further stirred for 1 hour before propanethioamide **261** (74.2 mg, 0.83 mmol, 1.16 equiv.) in anhydrous DCM (0.8 mL) adding. The resulting mixture was stirred at 40 $^\circ\text{C}$ in a sealed vial for 16 hours before concentration under reduced pressure. The crude material was purified by silica gel flash chromatography (pet. ether/EtOAc = 5:1) to provide the title compound (90.8 mg, yield 53%) as a yellow oil. **R_f**: 0.39 (pet. ether/EtOAc = 5:1). $^1\text{H NMR}$ (500 MHz, CDCl_3): δ 6.73 (s, 1H, H-7),

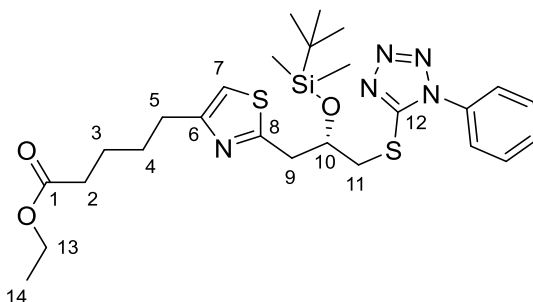
4.12 (q, $J = 7.1$ Hz, 2H, H-11), 3.00 (q, $J = 7.6$ Hz, 2H, H-9), 2.75 (t, $J = 7.0$ Hz, 2H, H-5), 2.33 (t, $J = 7.2$ Hz, 2H, H-2), 1.78 – 1.66 (m, 4H, H-3, H-4), 1.37 (t, $J = 7.6$ Hz, 3H, H-10), 1.25 (t, $J = 7.1$ Hz, 3H, H-12). **^{13}C NMR** (125 MHz, CDCl_3): δ 173.7 (C-1), 172.4 (C-8), 156.5 (C-6), 111.8 (C-7), 60.3 (C-11), 34.2 (C-2), 31.3 (C-5), 28.7 (C-4), 27.0 (C-9), 24.6 (C-3), 14.33 (C-10), 14.27 (C-12). **FTIR** (thin film) ν 2975, 2935, 2870, 1731, 1522, 1458, 1373, 1350, 1313, 1254, 1178, 1140, 1096, 1029, 968, 938, 859, 791, 735. **HRMS** (ESI): Calculated for $\text{C}_{12}\text{H}_{20}\text{NO}_2\text{S}^+$ $[\text{M}+\text{H}]^+$ 242.1209; found 242.1212.

Method B (Use salt **275** as MsO^- source)

To a solution of Mol-DalPhosAuOMs **257** (36.6 mg, 0.048 mmol, 0.05 equiv.) in deoxygenated anhydrous DCM (1.0 mL) was added alkyne **259** (148.3 mg, 0.96 mmol, 1.0 equiv.), 8-methylquinoline *N*-oxide **254** (183 mg, 1.15 mmol, 1.20 equiv.) and *N,N*-dimethylbenzenaminium methanesulfonate **275** (248 mg, 1.14 mmol, 1.18 equiv.) in turn. The resulting reaction mixture was stirred at room temperature under argon atmosphere for 6 hours, then propanethioamide **261** (108 mg, 1.21 mmol, 1.26 equiv.) was added to the reaction mixture. The resulting mixture was stirred at room temperature for 16 hours before concentration under reduced pressure. The crude material was purified by silica gel flash chromatography (pet. ether/EtOAc = 5:1) to provide the title compound (63 mg, yield 27%) as a yellow oil.

Method C (Use **275** as MsO^- source and syringe pump for addition)

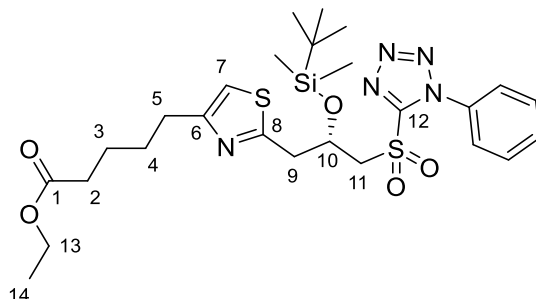
To a solution of Mol-DalPhosAuOMs **257** (13.0 mg, 0.017 mmol, 0.05 equiv.) in deoxygenated anhydrous DCM (0.7 mL) was added alkyne **259** (50 mg, 0.324 mmol, 1.0 equiv.). The resulting mixture was stirred at room temperature for under argon atmosphere 15 minutes. Then a solution of 8-methylquinoline *N*-oxide **254** (61 mg, 0.39 mmol, 1.2 equiv.) and *N,N*-dimethylbenzenaminium methanesulfonate **275** (85 mg, 0.39 mmol, 1.2 equiv.) in deoxygenated anhydrous DCM (4.0 mL) was added to the reaction mixture via a syringe pump under argon atmosphere in 5 hours. Upon completion, the reaction mixture was further stirred for 1 hour before propanethioamide **261** (35 mg, 0.39 mmol, 1.21 equiv.) in anhydrous DCM (0.4 mL) adding. The resulting mixture was stirred at 40 °C in a sealed vial for 16 hours before concentration under reduced pressure. The crude material was purified by silica gel flash chromatography (pet. ether/EtOAc = 5:1) to provide the title compound (2.9 mg, yield 3%) as a yellow oil.

Preparation of ethyl (S)-5-(2-(2-((*tert*-butyldimethylsilyl)oxy)-3-((1-phenyl-1*H*-tetrazol-5-yl)thio)propyl)thiazol-4-yl)pentanoate, **276**

To a solution of Mol-DalPhosAuOMs **257** (35.4 mg, 0.047 mmol, 0.11 equiv.) in deoxygenated anhydrous DCM (2.40 mL) was added alkyne **259** (137 mg, 0.889 mmol, 2.1 equiv.). The resulting mixture was stirred at room temperature for 15 minutes. Then a solution of 8-methylquinoline *N*-oxide **254** (185 mg, 1.16 mmol, 2.73 equiv.) and methanesulfonic acid (74 μ L, 1.14 mmol, 2.68 equiv.) in deoxygenated anhydrous DCM (2.40 mL) was added to the reaction mixture via a syringe pump in 5 hours under argon atmosphere. Upon completion, the reaction mixture was further stirred for 1 hour before propanethioamide **223** (174 mg, 0.425 mmol, 1.0 equiv.) in anhydrous DCM (2.40 mL) adding. The resulting mixture was stirred at 40 °C in a sealed vial for 20 hours under argon atmosphere before concentration under reduced pressure. The crude material was purified by silica gel flash chromatography (pet. ether/EtOAc = 4:1) to provide the title compound (148 mg, yield 61%) as a yellow oil. **R_f**: 0.33 (pet. ether/EtOAc = 3:1). **¹H NMR** (500 MHz, CDCl₃): δ 7.61 – 7.52 (m, 5H), 6.77 (s, 1H, H-7), 4.55 (quin, J = 5.6 Hz, 1H, H-10), 4.11 (q, J = 7.1 Hz, 2H, H-13), 3.59 (dd, J = 13.4, 5.1 Hz, 1H, H-11a), 3.51 (dd, J = 13.4, 6.0 Hz, 1H, H-11b), 3.27 (d, J = 5.3 Hz, 2H, H-9), 2.74 (t, J = 7.1 Hz, 2H, H-5), 2.32 (t, J = 7.0 Hz, 2H, H-2), 1.76 – 1.64 (m, 4H, H-3, H-4), 1.24 (t, J = 7.1 Hz, 3H, H-14), 0.83 (s, 9H), 0.06 (s, 3H), -0.10 (s, 3H). **¹³C NMR** (125 MHz, CDCl₃): δ 173.6 (C-1), 165.1 (C-8), 156.7 (C-6), 154.3 (C-12), 133.6, 130.1, 129.8, 123.8, 113.1 (C-7), 69.8 (C-10), 60.2 (C-13), 39.8 (C-9), 39.3 (C-11), 34.1 (C-2), 31.1 (C-5), 28.7 (C-6), 25.7, 24.6 (C-5), 18.0, 14.2 (C-14), -4.7, -5.0. **FTIR** (thin film) ν 3104, 3068, 3050, 2950, 2918, 1732, 1534, 1462, 1426, 1407, 1275, 1190, 1043, 923, 792, 735. **HRMS** (ESI): Calculated for C₂₆H₄₀N₅OS₂Si⁺ [M+H]⁺ 562.2336; found 562.2344. [α]_D²¹ -4.5 (c = 0.56, CHCl₃).

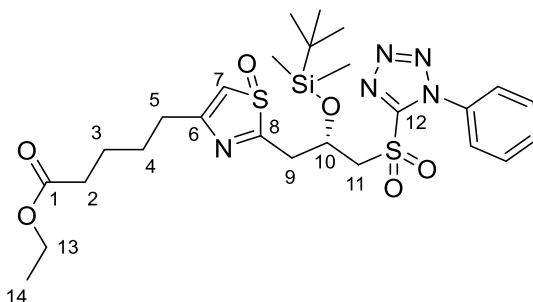
6.2.3 Julia-Kocienski Coupling with Side Chain

Preparation of ethyl (S)-5-(2-(2-((*tert*-butyldimethylsilyl)oxy)-3-((1-phenyl-1*H*-tetrazol-5-yl)sulfonyl)propyl)thiazol-4-yl)pentanoate, **277**



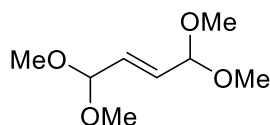
To a solution of thioether **276** (120 mg, 0.21 mmol, 1.0 equiv.) in EtOH (5 mL) was added the prepared oxidant solution of (NH₄)₆Mo₇O₂₄ (135 mg, 0.109 mmol, 0.50 equiv.) in H₂O₂ (0.7 mL, 30% in water, 6.3 mmol, 30 equiv.), and the yellow reaction mixture was stirred for 38 hours at room temperature. Saturated aqueous Na₂S₂O₃ solution (5 mL) was added slowly then ethanol solvent was removed by evaporation under vacuum. The residual aqueous phase was extracted with ethyl acetate (3 × 5 mL). The combined organic phase was washed with brine, dried over anhydrous Na₂SO₄, filtered, concentrated under reduced pressure. The crude material was purified by flash silica gel chromatography (pet. ether/EtOAc = 3/1) to afford the title compound (89.1 mg, 71% yield) as a colourless oil. **R_f**: 0.22 (pet. ether/EtOAc = 3:1). **¹H NMR** (500 MHz, CDCl₃): δ 7.69 – 7.64 (m, 2H), 7.64 – 7.56 (m, 3H), 6.80 (s, 1H, H-7), 4.87 – 4.81 (m, 1H, H-10), 4.14 (dd, *J* = 10.9, 4.1 Hz, 1H, H-11a), 4.11 (q, *J* = 7.1 Hz, 2H, H-13), 4.01 (dd, *J* = 14.9, 6.4 Hz, 1H, H-11b), 3.34 (d, *J* = 5.7 Hz, 2H, H-9), 2.75 (t, *J* = 7.3 Hz, 2H, H-5), 2.33 (t, *J* = 7.1 Hz, 2H, H-2), 1.77 – 1.63 (m, 4H, H-3, H-4), 1.24 (t, *J* = 7.1 Hz, 3H, H-14), 0.82 (s, 9H), 0.04 (s, 3H), 0.01 (s, 3H). **¹³C NMR** (125 MHz, CDCl₃): δ 173.6 (C-1), 163.5 (C-8), 157.1 (C-6), 154.1 (C-12), 133.1, 131.4, 129.7, 125.2, 113.3 (C-7), 66.4 (C-10), 61.4 (C-11), 60.2 (C-13), 40.7 (C-9), 34.1 (C-2), 31.1 (C-5), 28.6 (C-4), 25.7, 24.5 (C-3), 17.8, 14.3 (C-14), -4.8, -4.9. **FTIR** (thin film) ν 3111, 3072, 2930, 2857, 1730, 1595, 1521, 1498, 1463, 1420, 1343, 1299, 1255, 1154, 1122, 1086, 1045, 1015, 937, 918, 839, 827, 810, 779, 762, 688, 662, 621, 569, 523, 484, 451. **HRMS** (ESI): Calculated for C₂₆H₄₀N₅O₅S₂Si⁺ [M+H]⁺ 594.2235; found 594.2242. [α]_D¹⁸ –41.2 (*c* = 0.17, DCM).

Preparation of ethyl 5-(2-((*S*)-2-((*tert*-butyldimethylsilyl)oxy)-3-((1-phenyl-1*H*-tetrazol-5-yl)sulfonyl)propyl)-1-oxidothiazol-4-yl)pentanoate, **283**



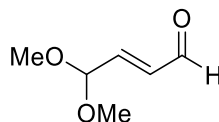
To a stirred solution of thioether **276** (25.3 mg, 0.045 mmol, 1.0 equiv.) in DCM (1.5 mL) were added NaHCO₃ (19.7 mg, 0.234 mmol, 5.2 equiv.) and 3-chloroperbenzoic acid (20.2 mg, 77% purity, 0.09 mmol, 2.0 equiv.) at 0 °C. The suspension was stirred at room temperature for 18 hours. Saturated aqueous Na₂S₂O₃ solution (2 mL) was added slowly then ethanol solvent was removed by evaporation under vacuum. The residual aqueous phase was extracted with ethyl acetate (3 × 5 mL). The combined organic phase was washed with brine, dried over anhydrous Na₂SO₄, filtered, concentrated under reduced pressure. The crude material was purified by flash silica gel chromatography using ethyl acetate to afford the title compound as the major product (10.0 mg, 36% yield) as a colourless oil. *R*_f: 0.40 (ethyl acetate). ¹H NMR (500 MHz, CDCl₃): δ 7.70 – 7.66 (m, 2H, H-16, H-20), 7.64 – 7.56 (m, 3H, H-17, H-18, H-19), 7.01 (s, 1H, H-7), 5.02 – 4.97 (m, 1H, H-10), 4.20 (dd, *J* = 15.1, 4.5 Hz, 1H, H-11a), 4.13 (q, *J* = 7.1 Hz, 2H, H-13), 3.92 (dd, *J* = 15.1, 6.1 Hz, 1H, H-11b), 3.61 (dd, *J* = 15.1, 4.6 Hz, 1H, H-9a), 3.26 (dd, *J* = 15.1, 5.9 Hz, 1H, H-9b), 2.82 – 2.73 (m, 2H, H-5), 2.37 (t, *J* = 6.8 Hz, 2H, H-2), 1.79 – 1.71 (m, 4H, H-3, H-4), 1.25 (t, *J* = 7.1 Hz, 3H, H-14), 0.84 (s, 9H, H-23, H-24, H-25), 0.07 (s, 3H, H-21), 0.04 (s, 3H, H-22). ¹³C NMR (125 MHz, CDCl₃): δ 173.5 (C-1), 154.0 (C-12), 149.0 (C-6), 141.4 (C-8), 133.0, 131.4, 129.6, 125.2, 110.7 (C-7), 64.5 (C-10), 61.3 (C-11), 60.4 (C-13), 35.0 (C-9), 33.8 (C-2), 26.8 (C-5), 25.9 (C-4), 25.7, 24.3 (C-3), 17.8, 14.3 (C-14), -4.9, -5.0. FTIR (thin film) ν 3107, 2930, 2857, 1728, 1595, 1498, 1462, 1423, 1344, 1253, 1180, 1152, 1111, 1077, 939, 902, 838, 826, 809, 779, 763, 735, 689, 662, 622, 567, 522, 478, 462. HRMS (ESI): Calculated for C₂₆H₄₀N₅O₆S₂Si⁺ [M+H]⁺ 610.2189; found 610.2181. [α]_D¹⁶ +60.9 (*c* = 0.45, DCM).

Preparation of (*E*)-1,1,4,4-tetramethoxybut-2-ene, **292**

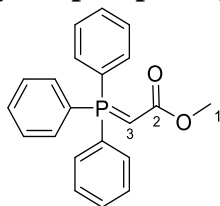


Freshly distilled furan (18.0 mL, 0.233 mol, 1.0 equiv.) and anhydrous MeOH (95 mL) was placed in a 500 mL three-necked flask and cooled to -45 °C under argon atmosphere. A solution of bromine (14.9 mL, 0.289 mol, 1.24 equiv.) in anhydrous MeOH (95 mL) was added dropwise at such a rate that the temperature did not exceed -25 °C. At the end of the addition, the reaction mixture was stirred for 2 h at -10 °C. Powdered anhydrous Na₂CO₃ (76.5 g, 0.722 mol, 3.1 equiv.) was added portion-wise over a period of about 30 min at -10 °C and then the reaction mixture was stirred for 18 h at room temperature. The mixture was then filtered and the solvent was removed under vacuum. The residue was purified by distillation (65-70 °C, 1 mmHg) to afford the title compound (31.8 g, 65%) as a yellow oil. ¹H NMR (500 MHz, CDCl₃): δ 5.78 (br.s, 2H), 4.80 (br.s, 2H), 3.29 (s, 12H). ¹³C NMR (125 MHz, CDCl₃): δ 130.9, 101.8, 52.6. These characterisation data match those reported in the literature.³⁴⁶

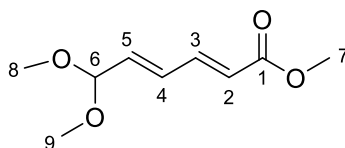
Preparation of (*E*)-4,4-dimethoxybut-2-enal, **293**



To a solution of (*E*)-1,1,4,4-tetramethoxybut-2-ene **292** (8.20 g, 46.5 mmol, 1.0 equiv.) in acetone (150 mL) was added distilled water (2.5 mL), followed by Amberlyst-15 (1.71 g). The reaction mixture was stirred vigorously at room temperature for 10 minutes. Then the acidic resin was removed by filtration and the filtrate was concentrated under reduced pressure. The crude material was purified by flash silica gel chromatography (pet. ether/Et₂O/Et₃N = 5/1/0.05) to afford the title compound (4.23 g, 70%) as a yellow oil. *R*_f: 0.38 (pet. ether/Et₂O = 5:1). ¹H NMR (500 MHz, CDCl₃) δ 9.63 (d, *J* = 7.8 Hz, 1H), 6.63 (dd, *J* = 15.9, 3.9 Hz, 1H), 6.37 (ddd, *J* = 15.9, 7.8, 1.3 Hz, 2H), 5.05 (dd, *J* = 3.9, 1.3 Hz, 1H), 3.36 (s, 6H). ¹³C NMR (125 MHz, CDCl₃): δ 193.2, 150.4, 134.3, 100.5, 53.1. These characterisation data match those reported in the literature.¹³⁴

Preparation of methyl 2-(triphenyl- λ^5 -phosphaneylidene)acetate, 294

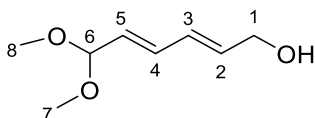
A solution of methyl bromoacetate (5.0 g, 0.0327 mol, 1.0 equiv.) and triphenylphosphine (9.0 g, 0.0340 mol, 1.04 equiv.) was heated at reflux for 4 hours. Then the reaction mixture was cooled to room temperature. The precipitate was separated by filtration and washed with cold Et₂O (3 × 50 mL). The collected phosphonium salt was re-dissolved in DCM (150 mL) and distilled water (100 mL). 2M NaOH aqueous solution was added and the resulting biphasic mixture was stirred at room temperature 12 hours. The organic phase was separated and the aqueous phase was extracted with DCM (3 × 100 mL). The combined organic phase was washed with brine, dried over anhydrous Na₂SO₄, filtered, concentrated under reduced pressure and dried under oil pump vacuum to afford the title compound (10.4 g, 95%) as a white powder. ¹H NMR (500 MHz, CDCl₃) δ 7.70 – 7.60 (m, 6H), 7.57 – 7.50 (m, 3H), 7.46 (m, 6H), 3.52 (br. s, 3H, H-1), 2.90 (br. s, 1H, H-3). ¹³C NMR (125 MHz, CDCl₃): δ 171.7 (C-2), 132.9 (d, *J*_{C-P} = 10.0 Hz), 132.1 (d, *J*_{C-P} = 10.0 Hz), 131.9 (d, *J*_{C-P} = 2.5 Hz), 131.9, 128.7 (d, *J*_{C-P} = 12.5 Hz), 128.5 (d, *J*_{C-P} = 12.5 Hz), 49.8 (C-1), 29.7 (d, *J*_{C-P} = 127.9 Hz, C-3). These characterisation data match those reported in the literature.³⁴⁷

Preparation of methyl (2*E*,4*E*)-6,6-dimethoxyhexa-2,4-dienoate, 295

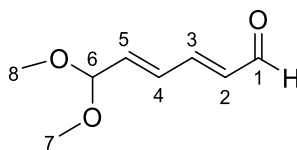
To a solution of aldehyde **293** (3.03 g, 23 mmol, 1.0 equiv.) in anhydrous DCM (20 mL) was added phosphorane (8.0 g, 23.9 mmol, 1.04 equiv.). Then the reaction mixture was stirred at room temperature under argon atmosphere for 16 hours. Solvent was evaporated and the crude material was then purified by flash silica gel chromatography (pet. ether/EtOAc/Et₃N = 10:1:0.1) to afford the title compound (2.95 g, 68%) as a yellow oil. *R*_f: 0.47 (pet. ether/EtOAc = 4:1). ¹H NMR (500 MHz, CDCl₃): δ 7.28 (ddd, *J* = 15.4, 11.2, 0.4 Hz, 1H, H-3), 6.48 (dddd, *J* = 15.5, 11.2, 1.2, 0.7 Hz, 1H, H-4), 6.00 (dd, *J* =

15.5, 4.3 Hz, 1H, H-5), 5.96 (dd, $J = 15.4, 0.4$ Hz, 1H, H-2), 4.91 (dd, $J = 4.3, 1.2$ Hz, 1H, H-6), 3.75 (s, 3H, H-7), 3.33 (s, 6H, H-8, H-9). ^{13}C NMR (125 MHz, CDCl_3): δ 167.1 (C-1), 143.2 (C-3), 137.6 (C-5), 131.0 (C-4), 122.7 (C-2), 101.3 (C-6), 52.7 (C-8, C-9), 51.7 (C-7). **FTIR** (thin film) ν 2951, 2832, 1719, 1651, 1619, 1436, 1359, 1313, 1267, 1234, 1190, 1174, 1126, 1051, 1002, 956, 911, 875, 723 cm^{-1} . **HRMS** (ESI): Calculated for $\text{C}_8\text{H}_{11}\text{O}_3^+$ $[\text{M}-\text{OCH}_3]^+$ 155.0703; found 155.0699.

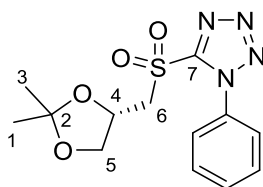
Preparation of (2*E*,4*E*)-6,6-dimethoxyhexa-2,4-dien-1-ol, **296**



To a solution of methyl ester **295** (1.62 g, 8.7 mmol, 1.0 equiv.) in anhydrous DCM (87 mL) was added a solution of diisobutylaluminum hydride (31.0 mL, 1.0 M in cyclohexane, 31.0 mmol, 3.56 equiv.) slowly at -78 °C. The reaction mixture was stirred at -78 °C for 6 hours and then quenched by addition of saturated aqueous potassium sodium tartrate (80 mL). The resulting mixture was stirred at room temperature for 2 hours and the aqueous phase was extracted with ethyl acetate (3×80 mL). The combined organic phase was washed with brine, dried over anhydrous Na_2SO_4 , filtered, concentrated under reduced pressure. The crude material was purified by flash silica gel chromatography (pet. ether/EtOAc/ $\text{Et}_3\text{N} = 2/1/0.02$) to afford the title compound (0.97 g, 71%) as a yellow oil. **R_f**: 0.38 (pet. ether/EtOAc = 2:1). ^1H NMR (500 MHz, CDCl_3): δ 6.37 (dd, $J = 15.2, 10.7$, 1H, H-4), 6.28 (ddt, $J = 15.4, 10.5, 1.6$ Hz, 1H, H-3), 5.92 (dt, $J = 15.1, 5.7$ Hz, 1H, H-2), 5.64 (dd, $J = 15.3, 4.8$ Hz, 1H, H-5), 4.84 (d, $J = 4.8$ Hz, 1H, H-6), 4.21 (t, $J = 5.6$ Hz, 2H, H-1), 3.32 (s, 6H, H-7, H-8). ^{13}C NMR (125 MHz, CDCl_3): δ 134.0 (C-2), 132.9 (C-4), 129.9 (C-3), 129.4 (C-5), 102.4 (C-6), 63.2 (C-1), 52.6 (C-7, C-8). **FTIR** (thin film) ν 3394, 2991, 2936, 1830, 1663, 1629, 1447, 1350, 1298, 1190, 1128, 1072, 1045, 990, 952, 905, 849, 586, 487 cm^{-1} . **HRMS** (ESI): Calculated for $\text{C}_7\text{H}_{11}\text{O}_2^+$ $[\text{M}-\text{OCH}_3]^+$ 127.0754; found 127.0750.

Preparation of (2*E*,4*E*)-6,6-dimethoxyhexa-2,4-dienal, 297

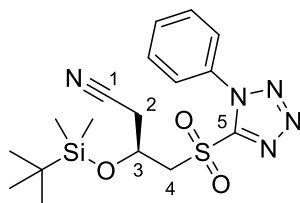
To a solution of alcohol **296** (0.21 g, 1.3 mmol, 1.0 equiv.) in wet DCM (17 mL) was added sequentially pyridine (0.36 mL, 4.55 mmol, 3.5 equiv.) and Dess-Martin periodinane (0.75 g, 1.76 mmol, 1.3 equiv.) at 2 °C. Then the reaction mixture was stirred at 2 – 4 °C for 2 hours. The reaction mixture was diluted with Et₂O (15 mL) and added a mixture of saturated aqueous solution of Na₂S₂O₃ and NaHCO₃ (Na₂S₂O₃/NaHCO₃ = 1/1, 15 mL). The resulting mixture was stirred vigorously for 30 minutes and then the aqueous phase was extracted with Et₂O (3 × 15 mL). The combined organic phase was washed with brine, dried over anhydrous Na₂SO₄, filtered, concentrated under reduced pressure. The crude material was purified by flash silica gel chromatography (pet. ether/Et₂O/Et₃N = 4/1/0.04) to afford the title compound (0.159 g, 76%) as a yellow oil. **R_f**: 0.11 (pet. ether/EtOAc = 9:1). **¹H NMR** (500 MHz, C₆D₆) δ 9.30 (d, *J* = 7.8 Hz, 1H, H-1), 6.34 – 6.25 (m, 1H, H-3), 6.25 – 6.17 (m, 1H, H-4), 5.88 (ddd, *J* = 14.9, 7.8, 2.8 Hz, 1H, H-2), 5.71 (dt, *J* = 15.2, 4.6 Hz, 1H, H-5), 4.64 (d, *J* = 4.3 Hz, 1H, H-6), 3.07 (d, *J* = 1.4 Hz, 6H, H-7, H-8). **¹³C NMR** (125 MHz, C₆D₆) δ 192.5 (C-1), 149.2 (C-3), 139.3 (C-5), 133.3 (C-2), 131.2 (C-4), 101.3 (C-6), 52.2 (C-7, C-8). **FTIR** (thin film) ν 2937, 2830, 1680, 1647, 1602, 1445, 1350, 1188, 1155, 1130, 1103, 1049, 1012, 989, 954, 909, 866, 565, 536 cm⁻¹. **HRMS** (ESI): Calculated for C₇H₈O₂⁺ [M-OCH₃]⁺ 125.0597; found 125.0590.

Preparation of (S)-5-(((2,2-dimethyl-1,3-dioxolan-4-yl)methyl)sulfonyl)-1-phenyl-1*H*-tetrazole, 298

To a solution of thioether **215** (0.35 g, 1.18 mmol, 1.0 equiv.) in EtOH (12 mL) was added the prepared oxidant solution of (NH₄)₆Mo₇O₂₄ (0.34 g, 0.275 mmol, 0.23 equiv.) in H₂O₂ (0.7 mL, 30% in water, 6.18 mmol, 5.2 equiv.), and the yellow reaction mixture was stirred for 20 hours at room temperature. Saturated aqueous Na₂S₂O₃ solution (5 mL) was

added then ethanol solvent was removed by evaporation under vacuum. The residual aqueous phase was extracted with ethyl acetate (3 × 15 mL). The combined organic phase was washed with brine, dried over anhydrous Na₂SO₄, filtered, concentrated under reduced pressure. The crude material was purified by flash silica gel chromatography (pet. ether/EtOAc = 2/1) to afford the title compound (0.33 g, 86%) as a colourless oil that solidified upon standing at room temperature. **R_f**: 0.73 (pet. ether/EtOAc = 1:1). **¹H NMR** (500 MHz, CDCl₃): δ 7.67 – 7.56 (m, 5H), 4.67 (ddt, *J* = 7.6, 6.1, 5.0 Hz 1H, H-4), 4.19 (dd, *J* = 8.9, 6.1 Hz, 1H, H-5a), 4.06 (dd, *J* = 14.7, 7.6 Hz, 1H, H-6a), 3.85 (dd, *J* = 9.0, 5.2 Hz, 1H, H-5b), 3.75 (dd, *J* = 14.7, 4.9 Hz, 1H, H-6b), 1.32 (s, 3H, H-3), 1.30 (s, 3H, H-1). **¹³C NMR** (125 MHz, CDCl₃): δ 153.3 (C-7), 133.0, 131.5, 129.6, 125.5, 110.8 (C-2), 69.6 (C-4), 68.4 (C-5), 59.9 (C-6), 26.6 (C-3), 25.2 (C-1). **FTIR** (thin film) ν 2992, 2914, 1496, 1463, 1379, 1370, 1348, 1338, 1319, 1258, 1229, 1184, 1174, 1146, 1107, 1090, 1081, 1076, 1059, 1021, 1014, 997, 985, 963, 919, 874, 825, 818, 787, 775, 693, 651, 574, 539, 511, 476, 444, 423 cm⁻¹. **HRMS** (ESI): Calculated for C₁₃H₁₆N₄NaO₄S⁺ [M+Na]⁺ 347.0790; found 347.0788. [α]_D²⁴ +21.4 (*c* = 0.37, DCM)

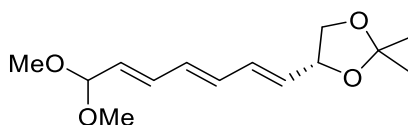
Preparation of (S)-3-((*tert*-butyldimethylsilyl)oxy)-4-((1-phenyl-1*H*-tetrazol-5-yl)sulfonyl)butanenitrile, 299



To a solution of nitrile **222** (102.6 mg, 0.273 mmol, 1.0 equiv.) in EtOH (3 mL) was added a solution of (NH₄)₆Mo₇O₂₄ (31.4 mg, 0.025 mmol, 0.09 equiv.) in H₂O₂ (314 μ L, 30% in water, 2.67 mmol, 9.8 equiv.) at 2 °C, and the yellow reaction mixture was stirred at room temperature for 16 hours. Saturated aqueous Na₂S₂O₃ solution (5 mL) was added then ethanol solvent was removed by evaporation under vacuum. The residual aqueous phase was extracted with ethyl acetate (3 × 5 mL). The combined organic phase was washed with brine, dried over anhydrous Na₂SO₄, filtered, concentrated under reduced pressure. The crude material was purified by flash silica gel chromatography (pet. ether/EtOAc = 4/1) to afford the title compound (88.9 mg, 80%) as a colourless oil that solidified upon standing at room temperature. **R_f**: 0.48 (pet. ether/EtOAc = 2:1). **¹H NMR** (500 MHz, CDCl₃): δ 7.70 – 7.60 (m, 5H), 4.75 – 4.69 (m, 1H, H-3), 4.15 (dd, *J* = 15.0,

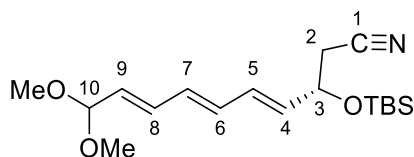
4.8 Hz, 1H, H-4a), 3.98 (dd, $J = 15.0, 6.7$ Hz, 1H, H-4b), 2.89 – 2.78 (m, 2H, H-2), 0.90 (s, 9H), 0.18 (s, 3H), 0.15 (s, 3H). **^{13}C NMR** (125 MHz, CDCl_3): δ 153.6 (C-5), 132.8, 131.7, 129.9, 125.0, 116.0 (C-1), 63.3 (C-3), 61.1 (C-4), 26.7 (C-2), 25.5, 17.8, -4.80, -4.97. **FTIR** (thin film) ν 3402, 2956, 2929, 2858, 1497, 1472, 1463, 1412, 1372, 1344, 1297, 1256, 1220, 1155, 1103, 1068, 1015, 940, 841, 824, 808, 782, 763, 724, 688, 673, 646, 630, 603, 579, 534, 516 cm^{-1} . **HRMS** (ESI): Calculated for $\text{C}_{17}\text{H}_{25}\text{N}_5\text{NaO}_3\text{SSi}^+$ $[\text{M}+\text{Na}]^+$ 430.1340; found 430.1341. $[\alpha]_D^{26} +74.8$ ($c = 0.05$, DCM).

Preparation of (*R*)-4-((2*E*,4*E*,6*E*)-8,8-dimethoxyocta-2,4,6-trien-1-yl)-2,2-dimethyl-1,3-dioxolane, 300



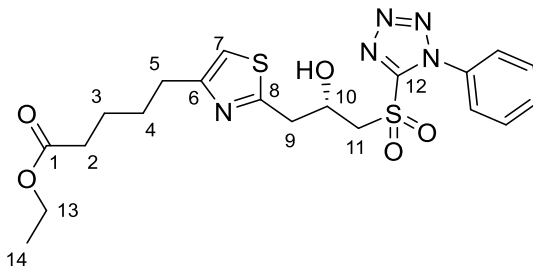
To a solution of sulfone **298** (41.0 mg, 0.126 mmol, 1.0 equiv.) in anhydrous THF (1.2 mL) was added potassium bis(trimethylsilyl)amide (0.28 mL, 0.5 M in toluene, 1.1 equiv.) at $-78\text{ }^{\circ}\text{C}$ under argon atmosphere. The resulting mixture was stirred at $-78\text{ }^{\circ}\text{C}$ for 15 minutes, then a solution of aldehyde (28.0 mg, 0.179 mmol, 1.3 equiv.) in anhydrous THF was added slowly. After that, the resulting mixture was allowed to slowly warm up to $-20\text{ }^{\circ}\text{C}$ over 2 hours. The reaction was then quenched by addition of saturated aqueous NaHCO_3 solution (2 mL). The aqueous layers were separated and extracted with ethyl acetate (3×5 mL). The combined organic phase was washed with brine, dried over anhydrous Na_2SO_4 , filtered, concentrated under reduced pressure. The crude material was purified by flash silica gel chromatography (pet. ether/EtOAc/ $\text{Et}_3\text{N} = 20/1/0.02$) to afford the title compound as a mixture of *E,E,E*- and *E,E,Z*-isomers (18.7 mg, 44%, *E,E,E/E,E,Z* = 5/1). **R_f**: 0.11 (pet. ether/EtOAc = 9:1). **^1H NMR** (500 MHz, CDCl_3 , represents peaks from *E,E,E*-isomer) δ 6.45 – 6.29 (m, 2H), 6.29 – 6.18 (m, 2H), 5.71 – 5.64 (m, overlapped, 1H), 5.66 (overlapped, dd, $J = 15.5, 4.8$ Hz, 1H), 4.85 (dd, $J = 4.9, 1.1$ Hz, 1H), 4.58 – 4.52 (m, 1H), 4.10 (dd, $J = 8.2, 6.2$ Hz, 1H), 3.59 (dd, $J = 15.9, 7.9$ Hz 1H), 3.32 (s, 6H), 1.43 (s, 3H), 1.39 (s, 3H). **^{13}C NMR** (125 MHz, CDCl_3) δ 133.3, 133.1, 131.1, 130.5, 129.9, 129.1, 109.4, 76.8, 69.4, 52.6, 45.7, 26.7, 25.9. **FTIR** (thin film) ν 2955, 2924, 2854, 1460, 1378, 1263, 1123, 1059, 1000, 963 cm^{-1} . **HRMS** (ESI): Calculated for $\text{C}_{13}\text{H}_{19}\text{O}_3^+$ $[\text{M}-\text{OCH}_3]^+$ 223.1329; found 223.1330. $[\alpha]_D^{24} -52.1$ ($c = 0.135$, DCM).

Preparation of (*S*,4*E*,6*E*,8*E*)-3-((*tert*-butyldimethylsilyl)oxy)-10,10-dimethoxydeca-4,6,8-trienenitrile, **301**



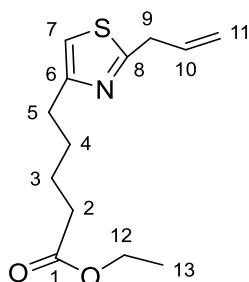
To a solution of sulfone **299** (88.9 mg, 0.218 mmol, 1.0 equiv.) in anhydrous THF (7.3 mL) was added potassium bis(trimethylsilyl)amide (444 μ L, 0.5 M in toluene, 0.222 mmol, 1.02 equiv.) at -78 $^{\circ}$ C under argon atmosphere. The resulting mixture was stirred at -78 $^{\circ}$ C for 15 minutes, then a solution of aldehyde (34.0 mg, 0.262 mmol, 1.2 equiv.) in anhydrous THF was added slowly. After that, the resulting mixture was allowed to slowly warm up to -10 $^{\circ}$ C over 4 hours. The reaction was then quenched by addition of saturated aqueous NaHCO_3 solution (4.5 mL). The aqueous layers were separated and extracted with ethyl acetate (3×5 mL). The combined organic phase was washed with brine, dried over anhydrous Na_2SO_4 , filtered, concentrated under reduced pressure. The crude material was purified by flash silica gel chromatography (pet. ether/EtOAc/ Et_3N = 20/1/0.02) to afford the title compound as a mixture of *E,E,E*- and *E,E,Z*-isomers (36.6 mg, 50%, *E,E,E/E,E,Z* = 10/1). *R_f*: 0.23 (pet. ether/EtOAc = 5:1). **^1H NMR** (500 MHz, C_6D_6 , represents peaks from *E,E,E*-isomer) δ 6.45 (ddd, J = 15.5, 10.6, 1.1 Hz, 1H, H-8), 6.12 – 5.94 (m, 3H, H-5, H-6, H-7), 5.68 (dd, J = 15.5, 4.5 Hz, 1H, H-9), 5.30 (dd, J = 14.8, 6.6 Hz, 1H, H-4), 4.85 (dd, J = 4.4, 1.1 Hz, 1H, H-10), 3.99 – 3.94 (m, 1H, H-3), 3.17 (s, 6H), 1.81 (dd, J = 16.4, 7.0 Hz, 1H, H-2a), 1.72 (dd, J = 16.4, 5.0 Hz, 1H, H-2b), 0.96 (s, 9H), 0.06 (s, 3H), -0.01 (s, 3H). **^{13}C NMR** (125 MHz, C_6D_6) δ 134.0 (C-4), 133.34 (C-7 or C-8), 133.31 (C-8 or C-7), 132.8 (C-5), 131.6 (C-6), 131.4 (C-9), 117.1 (C-1), 102.1 (C-10), 69.5 (C-3), 52.1, 27.0 (C-2), 25.9, 18.3, -4.4, -4.9. **FTIR** (thin film) ν 2954, 2929, 2857, 1463, 1361, 1349, 1255, 1190, 1153, 1122, 1074, 1053, 1001, 940, 908, 880, 837, 809, 779, 687 cm^{-1} . **HRMS** (ESI): Calculated for $\text{C}_{17}\text{H}_{28}\text{NO}_2\text{Si}^+$ [$\text{M}-\text{OCH}_3$] $^+$ 306.1884; found 306.1894. $[\alpha]_D^{22} +57.3$ (c = 0.39, DCM)

Preparation of ethyl (S)-5-(2-(2-hydroxy-3-((1-phenyl-1*H*-tetrazol-5-yl)sulfonyl)propyl)thiazol-4-yl)pentanoate, **309**



To a solution of sulfone **277** (31.7 mg, 0.052 mmol, 1.0 equiv.) in anhydrous THF (0.1 mL) was added a solution of HF-pyridine (135 μ L, 5.15 mmol, 99 equiv.) in anhydrous THF (0.5 mL) dropwise at 0 °C. The reaction mixture was stirred for 2 days at room temperature and 2.0 mL saturated NaHCO₃ aqueous solution was added. Then the aqueous phase was extracted with ethyl acetate (3 \times 5 mL). The combined organic phase was washed with brine, dried over anhydrous Na₂SO₄, filtered, concentrated under reduced pressure. The combined organic phase was washed with brine, dried over anhydrous Na₂SO₄, filtered, concentrated under reduced pressure. The crude material was purified by flash silica gel chromatography (pet. ether/EtOAc = 2/1) to afford the title compound (23.2 mg, 92% yield) as a colourless oil. **R_f**: 0.44 (pet. ether/EtOAc = 1:1). **¹H NMR** (600 MHz, CDCl₃): δ 7.72 – 7.55 (m, 5H, H-16, H-17, H-18, H-19, H-20), 6.81 (s, 1H, H-7), 4.78 – 4.70 (m, 1H, H-10), 4.11 (q, J = 7.1 Hz, 2H, H-13), 3.95 (dd, J = 15.0, 8.7 Hz, 1H, H-11a), 3.78 (dd, J = 15.0, 3.2 Hz, 1H, H-11b), 3.28 (dd, J = 15.7, 3.8 Hz, 1H, H-9a), 3.18 (dd, J = 15.7, 7.3 Hz, 1H, H-9b), 2.74 (t, J = 7.2 Hz, 2H, H-5), 2.34 (t, J = 7.1 Hz, 2H, H-2), 1.76 – 1.62 (m, 4H, H-3, H-4), 1.24 (t, J = 7.1 Hz, 3H, H-14). **¹³C NMR** (150 MHz, CDCl₃): δ 173.6 (C-1), 164.8 (C-8), 156.9 (C-6), 154.0 (C-12), 133.0, 131.5, 129.5, 125.6, 112.9 (C-7), 65.5 (C-10), 61.2 (C-11), 60.3 (C-13), 37.9 (C-9), 34.0 (C-2), 30.9 (C-5), 28.4 (C-4), 24.4 (C-3), 14.2 (C-14). **FTIR** (thin film) ν 3397, 3105, 2937, 2864, 1769, 1728, 1694, 1595, 1523, 1498, 1461, 1434, 1348, 1311, 1280, 1246, 1176, 1152, 1112, 1076, 1032, 1018, 979, 926, 885, 844, 831, 803, 764, 725, 689, 633, 581, 536, 489, 450 cm⁻¹. **HRMS** (ESI): Calculated for C₂₀H₂₆N₅O₅S₂⁺ [M+H]⁺ 480.1370; found 480.1376. [α]_D²⁰ +7.5 (c = 0.99, CHCl₃).

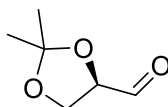
Preparation of ethyl 5-(2-allylthiazol-4-yl)pentanoate, 311



To a solution of alcohol **309** (6.8 mg, 0.014 mmol, 1.0 equiv.) in anhydrous THF (0.5 mL) at -78 °C was added KHMDS (51 μ L, 0.5 M in toluene, 0.026 mmol, 1.8 equiv.) under argon. Then the reaction mixture was stirred at -78 °C for 30 minutes. Deuterium oxide (20 μ L) was added to the reaction mixture at -78 °C and the reaction mixture was stirred at -78 °C for 2 hours. The reaction was quenched with 1 mL saturated aqueous NH_4Cl solution and then extracted with ethyl acetate (3×5 mL). The combined organic phase was washed with brine, dried over anhydrous Na_2SO_4 , filtered, concentrated under reduced pressure. The crude material was purified by flash silica gel chromatography (pet. ether/EtOAc = 3/1) to afford the title compound (1.3 mg, 36% yield) as a colourless oil. **R_f**: 0.50 (pet. ether/EtOAc = 2:1). **¹H NMR** (500 MHz, CDCl_3): δ 6.78 (s, 1H, H-7), 6.04 (ddt, J = 16.9, 10.0, 6.8 Hz, 1H, H-10), 5.30 – 5.17 (m, 2H, H-11), 4.12 (q, J = 7.2 Hz, 2H, H-12), 3.74 (dt, J = 6.9, 1.4 Hz, 1H, H-9), 2.77 (t, J = 7.1 Hz, 2H, H-5), 2.33 (t, J = 7.2 Hz, 2H, H-2), 1.78 – 1.65 (m, 4H, H-3, H-4), 1.25 (t, J = 7.0 Hz, 3H, H-13). **¹³C NMR** (125 MHz, CDCl_3): δ 173.7 (C-1), 168.7 (C-8), 156.9 (C-6), 134.0 (C-10), 118.2 (C-11), 112.6 (C-7), 60.3 (C-12), 37.8 (H-9), 34.1 (C-2), 31.2 (C-5), 29.7 (grease peak), 28.7 (C-4), 24.6 (C-3), 14.3 (C-13). **FTIR** (thin film) ν 2918, 2850, 1731, 1639, 1522, 1461, 1374, 1350, 1299, 1231, 1178, 1136, 1094, 1027, 920, 864, 795, 734, 584, 553 cm^{-1} . **HRMS** (ESI): Calculated for $\text{C}_{13}\text{H}_{20}\text{NO}_2\text{S}^+$ $[\text{M}+\text{H}]^+$ 254.1209; found 254.1212

6.2.3 Towards Synthesis of Thioamide 317

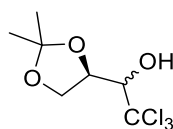
Preparation of (*R*)-2,2-dimethyl-1,3-dioxolane-4-carbaldehyde, 322



To an oven-dried 50 mL two-necked round bottom flask equipped with a stir bar and reflux condenser was added D-mannitol **324** (5.0 g, 27.5 mmol, 1.0 equiv.), anhydrous 1,2-dimethoxyethane (12.0 ml) and anhydrous 2,2-dimethoxypropane (8.0 mL). To this stirred mixture was added SnCl_2 (5 mg, 0.001 equiv.) and the reaction mixture was heated at 75 °C until a clear solution was obtained (ca. 1 hour). The reaction mixture was held at 75 °C for 30 minutes, then cooled to room temperature and was added pyridine (6 μL , 0.075 mmol, 0.002 equiv.). The solvents were removed under reduce pressure (contents heated to 80 – 90 °C). The crude material was slurried in DCM (36 mL) at room temperature for 1 hour and filtered. The filtrate was evaporated under reduced pressure to afford diacetone **325** as a white solid (6.3 g, yield 87%), which was used for the next step without further purification.

To a 100 mL two-necked round bottom flask equipped with a stir bar and thermometer was added diacetone **325** (6.3 g, 24 mmol, 1.0 equiv.) in DCM (57 mL). Saturated aqueous NaHCO_3 (2.27 mL) was then added to the flask, maintaining the temperature at or below 25 °C. NaIO_4 (9.85 g, 46 mmol, 1.9 equiv.) was added over a 10-min period with vigorous stirring. The reaction was stirred for 2 hours while the temperature was maintained below 30 °C. The solids were then removed by filtration and the filtrate was evaporated under atmospheric pressure at a temperature of 55 °C. The residual oil was transferred to a smaller vessel and distilled at 90 mmHg to afford the title compound as a colourless oil (2.83 g, yield 43%). **Boiling point:** 100 – 105 °C (88 – 90 mmHg). **^1H NMR** (500 MHz, CDCl_3): δ 9.72 (dd, J = 1.8 Hz, 0.2 Hz, 2H), 4.39 (ddd, J = 7.5, 4.7, 1.9 Hz, 1H), 4.18 (dd, J = 8.8, 7.5 Hz, 1H), 4.11 (dd, J = 8.8, 4.7 Hz, 1H), 1.49 (s, 3H), 1.42 (s, 3H). **^{13}C NMR** (125 MHz, CDCl_3): 201.9, 111.3, 79.9, 65.6, 26.3, 25.1. $[\alpha]_D^{20} +61$ (c = 1.25, benzene) (literature $[\alpha]_D^{20} +63.3$ (c = 1.25, benzene)). These characterisation data match those reported in the literature.²³⁴

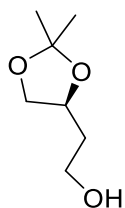
Preparation of 2,2,2-trichloro-1-((*R*)-2,2-dimethyl-1,3-dioxolan-4-yl)ethan-1-ol, **323**



To a 0 °C solution of sodium trichloroacetate (3.89 g, 21 mmol, 1.5 equiv.) and trichloroacetic acid (3.41 g, 21 mmol, 1.5 equiv.) in anhydrous DMF (28 mL) was added aldehyde **322** (1.83 g, 14 mmol, 1.0 equiv.) dissolved in anhydrous DMF (14 mL). After stirring for 15 min, the mixture was warmed to room temperature then stirred rapidly for 17 hours. Upon completion, the mixture was diluted with 80 mL of EtOAc and washed with saturated aqueous NaHCO₃ solution (3 × 40 mL). Precipitated solids were filtered and rinsed three times with EtOAc (3 × 40 mL). The aqueous phase was extracted with EtOAc (3 × 40 mL). The combined organic phase was dried with anhydrous Na₂SO₄, filtered and evaporated under reduced pressure. The crude material was purified by flash chromatography through a plug of silica gel using 9:1 hexanes/EtOAc as eluent. The title compound was obtained as a mixture of (*S,R*)-**323** and (*R,R*)-**323** (2.89 g, yield 81%). A small sample was further purified by silica gel flash chromatography (pet. Ether/EtOAc = 10/1) to characterise (*S,R*)-isomer and (*R,R*)-isomer.

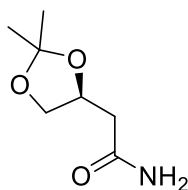
(*S,R*)-**323**: a colourless oil. *R*_f: 0.57 (pet. ether/EtOAc = 5:1). ¹H NMR (500 MHz, CDCl₃): δ 4.58 (td, *J* = 6.8, 2.4 Hz, 1H), 4.25 (dd, *J* = 8.5, 6.6 Hz, 1H), 4.01 – 3.96 (m, 1H), 3.91 (dd, *J* = 8.5, 7.1 Hz, 1H), 3.80 – 3.66 (m, 1H), 1.49 (s, 3H), 1.44 (s, 3H). ¹³C NMR (125 MHz, CDCl₃): 110.9, 101.3, 81.1, 73.2, 68.4, 64.7, 26.0, 25.7. These characterisation data match those reported in the literature.²³²

(*R,R*)-**323**: a white solid. *R*_f: 0.48 (pet. ether/EtOAc = 5:1). ¹H NMR (500 MHz, CDCl₃): δ 4.60 (td, *J* = 6.4, 3.3 Hz, 1H), 4.37 (d, *J* = 3.3 Hz, 1H), 4.27 (dd, *J* = 8.8, 6.3 Hz, 1H), 4.10 (dd, *J* = 8.8, 6.5 Hz, 1H), 3.06 (br.s, 1H), 1.48 (s, 3H), 1.40 (s, 3H). ¹³C NMR (125 MHz, CDCl₃): 109.2, 100.6, 82.3, 75.1, 64.7, 26.3, 25.3. These characterisation data match those reported in the literature.²³²

Preparation of (*S*)-2-(2,2-dimethyl-1,3-dioxolan-4-yl)ethan-1-ol, 330

A mixture of diastereomers (*S,R*)-**323** and (*R,R*)-**323** (1.36 g, 5.48 mmol, 1.0 equiv.) was added to an oven-dried 100 mL two-necked round-bottom flask equipped with a magnetic stir bar and a reflux condenser under argon. Anhydrous deoxygenated isopropanol (20 mL, purged for 30 minutes with argon) was then added, followed by slow addition of LiBH_4 (2.0 M in THF, 12 mL, 24 mmol, 4.4 equiv.) and rapid addition of freshly powdered NaOH (0.66 g, 16.4 mmol, 3.0 equiv.) under a blanket of argon. The reaction mixture was heated in a 40 °C oil bath and allowed to stir at that temperature while being monitored by TLC for the consumption of starting material. It is worth noting that the consumption rate of (*R,R*)-isomer was much faster than (*S,R*)-isomer. The corresponding isopropyl ester intermediate appeared by TLC analysis during the reaction as a spot with a high R_f value ($R_f = 0.9$, pet. ether/EtOAc = 5:1). It was critical for this intermediate to disappear prior to quenching the reaction to ensure the intermediate was converted to the desired product completely. After 48 hours, the reaction mixture was cooled to room temperature and quenched with saturated aqueous NH_4Cl solution (30 mL). The resulting aqueous phase was saturated with solid NaCl and then extracted with ethyl acetate (5×30 mL). The combined organic phase was dried over anhydrous Na_2SO_4 , filtered, and concentrated under reduced pressure. The crude material was purified by flash silica gel chromatography (pet. ether/EtOAc = 1/1) to afford the title compound (244 mg, yield 31%) as a colourless oil. R_f : 0.17 (pet. ether/EtOAc = 2:1). $^1\text{H NMR}$ (500 MHz, CDCl_3): δ 4.32 – 4.24 (m, 1H), 4.10 (dd, $J = 8.1, 6.0$ Hz, 1H), 3.81 (td, $J = 5.9, 2.1$ Hz, 2H), 3.60 (dd, $J = 8.1, 7.3$ Hz, 1H), 1.85 – 1.80 (m, 2H), 1.43 (s, 3H), 1.37 (s, 3H). $^{13}\text{C NMR}$ (125 MHz, CDCl_3): δ 109.2, 75.2, 69.3, 60.5, 35.6, 26.9, 25.6. $[\alpha]_D^{23} +1.08$ ($c = 1.24$, CHCl_3) (literature $[\alpha]_D^{20} +2.45$ ($c = 1.1$, CHCl_3))²³⁸. These characterisation data match those reported in the literature.²³⁸

Preparation of (S)-2-(2,2-dimethyl-1,3-dioxolan-4-yl)acetamide, **321**



Method A (One-step protocol from alcohol **323**)

To a 50 mL dry pressure tube temporarily fit with a rubber septum and equipped with a magnetic stir bar was added diphenyl diselenide (161.4 mg, 0.517 mmol, 1.29 equiv.). Ammonia solution (2.0 M in ethanol, 1.6 mL, 8.0 equiv.) and NaBH₄ (43 mg, 1.12 mmol, 2.8 equiv.) were sequentially rapidly added under argon atmosphere. Shortly after the addition, the initial yellow solution turned to be colourless solution, indicating that diphenyl diselenide was completely reduced. The solution was further stirred at room temperature for 25 minutes, then a mixture of diastereomers (*S,R*)-**323** and (*R,R*)-**323** (99 mg, 0.40 mmol, 1.0 equiv.) was added, followed by the addition of freshly powdered NaOH (43 mg, 1.08 mmol, 2.7 equiv.) under argon. The rubber septum was then quickly replaced with a Teflon screw cap and the solution was heated in a 55 °C oil bath for 36 hours. The ethanolic ammonia was removed by evaporation under vacuum and the amorphous solids were dissolved in 5 mL ethyl acetate and 5 mL saturated aqueous NH₄Cl. The resulting solution was cooled to 0 °C and was carefully adjusted to pH 4 with 1 N HCl and then the resulting solution was saturated by the addition of solid NaCl. The mixture was then extracted with ethyl acetate (6 × 5 mL). The combined organic layers were dried with anhydrous Na₂SO₄ and then concentrated by rotary evaporation. The crude material was purified by flash chromatography through a small plug of triethylamine-saturated silica gel (EtOAc/MeOH = 10/1) to afford the title compound as a white solid (7.1 mg, yield 11%). *R*_f: 0.44 (EtOAc/MeOH = 9:1). ¹H NMR (500 MHz, CDCl₃) δ 6.08 (br. s, 1H), 5.48 (br. s, 1H), 4.47 – 4.39 (m, 1H), 4.15 (dd, *J* = 8.4, 6.0 Hz, 1H), 3.63 (dd, *J* = 8.4, 6.8 Hz, 1H), 2.55 (dd, *J* = 15.4, 7.9 Hz, 1H), 2.47 (dd, *J* = 15.3, 4.5 Hz, 1H), 1.44 (s, 2H), 1.37 (s, 3H). ¹³C NMR (126 MHz, CDCl₃) δ 172.3, 109.5, 72.2, 69.1, 40.1, 26.9, 25.5. These characterisation data match those reported in the literature.²³²

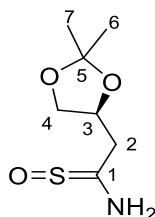
Method B (Two-step protocol from alcohol **330**)

To a solution of alcohol **330** (195.3 mg, 1.34 mmol, 1.0 equiv.) in H₂O-CH₃CN (v:v = 1:1, 10 mL) were added TEMPO (65 mg, 0.4 mmol, 0.3 equiv.) and BAIB (1.30 g, 4.02 mmol, 3.0 equiv.) at 0 °C. Then the reaction mixture was allowed to warm to room

temperature and stirred at room temperature for 24 hours. The reaction was then quenched by addition of saturated aqueous $\text{Na}_2\text{S}_2\text{O}_3$ solution (5 mL) and the resulting mixture was stirred at room temperature for 1 hour. The resulting aqueous phase was saturated with solid NaCl and then extracted with ethyl acetate (7×5 mL). The combined organic phase was dried over anhydrous Na_2SO_4 , filtered, and concentrated under reduced pressure to afford the crude carboxylic acid **329** as a yellow oil, which was used directly for the next step without further purification.

The crude carboxylic acid **329** (1.0 equiv.) was dissolved in acetonitrile (12 mL) and then pyridine (0.43 mL, 5.36 mmol, 4.0 equiv.), di-*tert*-butylbiscarbonate (583 mg, 2.68 mmol, 2.0 equiv.) and NH_4HCO_3 (219 mg, 2.68 mmol, 2.0 equiv.) were added at room temperature. The reaction mixture was stirred for 14 hours. The reaction mixture was concentrated under reduced pressure and the crude material was purified by silica flash chromatography (EtOAc/MeOH = 20/1) to afford the title compound as a white solid (174 mg, two-step yield 82%). **Melting point:** 105 – 106 °C. **R_f:** 0.45 (EtOAc/MeOH = 10/1). **¹H NMR** (500 MHz, CDCl_3): δ 6.10 (br. s, 1H), 5.73 (br. s, 1H), 4.46 – 4.40 (m, 1H), 4.15 (dd, $J = 8.4, 6.0$ Hz, 1H), 3.63 (dd, $J = 8.4, 6.8$ Hz, 1H), 2.55 (dd, $J = 15.4, 7.9$ Hz, 1H), 2.48 (dd, $J = 15.4, 4.6$ Hz, 1H), 1.44 (s, 3H), 1.38 (s, 3H). **¹³C NMR** (125 MHz, CDCl_3): δ 172.5, 109.5, 72.3, 69.1, 40.1, 26.9, 25.5. **FTIR** (solid) ν 3360, 3179, 2991, 2940, 2899, 2858, 1656, 1631, 1431, 1420, 1371, 1328, 1256, 1236, 1213, 1157, 1135, 1097, 1064, 1042, 970, 924, 899, 842, 700, 659, 644, 618, 583, 566, 513, 431 cm^{-1} . **HRMS** (ESI): Calculated for $\text{C}_7\text{H}_{13}\text{NaO}_3\text{N}^+$ $[\text{M}+\text{Na}]^+$ 182.0793; found 182.0785. $[\alpha]_D^{25}$ –17.1 ($c = 1.03$, CHCl_3) (literature $[\alpha]_D^{24}$ –15.4 ($c = 1.0$, CHCl_3)). These characterisation data match those reported in the literature.²³²

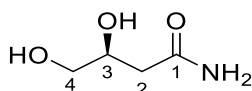
Preparation of (S)-(1-amino-2-(2,2-dimethyl-1,3-dioxolan-4-yl)ethylidene)- λ^4 -sulfanone, 333



Lawesson's reagent (freshly re-purified by washing with DCM and Et₂O, 36.5 mg, 0.09 mmol, 0.55 equiv.) was added to a solution of amide (25.6mg, 0.16 mmol, 1.0 equiv.) in anhydrous DCM. The reaction mixture was stirred vigorously under argon atmosphere at room temperature for 12 hours. Saturated aqueous NaHCO₃ solution (3 mL) was added to the reaction mixture and the aqueous phase was extracted with ethyl acetate (3 × 5 mL). The combined organic phase was dried over anhydrous Na₂SO₄, filtered, and then concentrated under reduced pressure. The crude material was purified by silica flash chromatography (pet. Ether/EtOAc = 2/1) to afford the title compound as a yellow oil (7.2 mg, yield 23%). **R_f**: 0.43 (pet. Ether/EtOAc = 1/1). **¹H NMR** (500 MHz, CDCl₃): δ 7.77 (br. s, 1H, N-H), 7.54 (br. s, 1H, N-H), 4.46 (dtd, *J* = 8.5, 6.5, 3.3 Hz, 1H, H-3), 4.14 (dd, *J* = 8.4, 6.1 Hz, 1H, H-4a), 3.65 (dd, *J* = 8.4, 6.7 Hz, 1H, H-4b), 3.04 (ddd, *J* = 15.3, 3.3, 1.0 Hz, 1H, H-2a), 2.91 (dd, *J* = 15.3, 8.4 Hz, 1H, H-2b), 1.45 (s, 3H, H-6 or H-7), 1.37 (s, 3H, H-7 or H-6). **¹³C NMR** (125 MHz, CDCl₃): δ 206.1 (C-1), 109.9 (C-5), 73.8 (C-3), 68.6 (C-4), 48.8 (C-2), 27.0 (C-6 or C-7), 25.5 (C-7 or C-6). **FTIR** (solid) ν 3312, 3188, 2984, 2933, 1654, 1636, 1629, 1438, 1420, 1381, 1372, 1324, 1249, 1214, 1152, 1106, 1060, 965, 929, 884, 832, 512 cm⁻¹. **HRMS** (ESI): Calculated for C₇H₁₄NO₃S⁺ [M+H]⁺ 192.0689; found 192.0685. [α]_D²² -67.5 (*c* = 0.215, DCM).

6.2.4 Attempted Preparation of Air-stable Thioamides

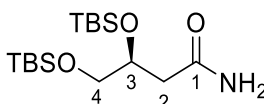
Preparation of (S)-3,4-dihydroxybutanamide, 339



Amide **321** (25.4 mg, 0.091 mmol, 1.0 equiv.) was dissolved in a mixture of acetic acid (0.10 mL) and water (25 μ L). Then the reaction mixture was stirred at 40 °C for 2 hours under argon. The reaction mixture was then cooled to room temperature and saturated NaHCO₃ aqueous solution (1 mL) was slowly added. All solvents were evaporated under reduced pressure at 45 °C and the solids was slurried with acetone and filtered. The filtrate

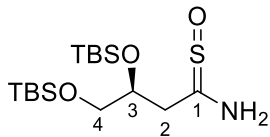
was evaporated to afford the title compound as a white solid (17.5 mg, yield 92%). ^1H NMR ($(\text{CD}_3)_2\text{CO}$, 500 MHz): δ 6.94 (br. s, 1H, -NH), 6.30 (br. s, 1H, -NH), 3.93 – 3.87 (m, 1H, H-3), 3.42 (d, $J = 5.4$ Hz, 2H, H-4), 3.26 (s, 1H, -OH), 2.37 (dd, 1H, $J = 15.1$, 4.0 Hz, H-2a), 2.25 (dd, 1H, $J = 15.0$, 8.3 Hz, H-2b); ^{13}C NMR ($(\text{CD}_3)_2\text{CO}$, 125 MHz): δ 174.8 (C-1), 69.9 (C-3), 66.5 (C-4), 39.4 (C-2). These characterisation data match those reported in the literature.²³²

Preparation of (*S*)-3,4-bis(*tert*-butyldimethylsilyl)oxy)butanamide, **339**

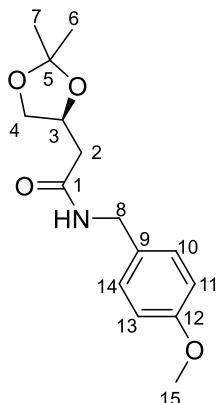


Imidazole (525 mg, 7.71 mmol, 8.0 equiv.) and *tert*-butyldimethylsilyl chloride (859 mg, 5.7 mmol, 6.0 equiv.) were added to a solution of amide **339** (100 mg, 0.95 mmol, 1.0 equiv.) in 5.0 mL anhydrous DMF. The reaction mixture was stirred at room temperature for 16 hours, and the reaction was diluted with 10 mL ethyl acetate, and washed 3 times with 5 mL of water. The combined aqueous phase was then extracted with extracted with ethyl acetate (3×5 mL). The combined organic layers were dried with anhydrous Na_2SO_4 , filtered, and then concentrated by rotary evaporation. The crude material was purified by flash silica chromatography (pet. Ether/EtOAc = 3/1) to afford the title compound as a yellow oil (254 mg, yield 77%). R_f : 0.43 (pet. Ether/EtOAc = 2/1). ^1H NMR (500 MHz, CDCl_3): δ 6.21 (br. s, 1H, N-H), 5.41 (br. s, 1H, N-H), 4.10 – 4.03 (m, 1H, H-3), 3.62 (dd, $J = 10.1$, 5.3 Hz, 1H, H-4a), 3.50 (dd, $J = 10.2$, 6.4 Hz, 1H, H-4b), 2.57 (dd, $J = 14.8$, 4.4 Hz, 1H, H-2a), 2.34 (dd, $J = 14.7$, 6.1 Hz, 1H, H-2b), 0.89 (s, 18H), 0.10 (s, 6H), 0.054 (s, 3H), 0.049 (s, 3H). ^{13}C NMR (125 MHz, CDCl_3): 173.6 (C-1), 70.4 (C-4), 66.5 (C-4), 40.9 (C-2), 25.9, 25.8, 18.3, 18.0, -4.53, -5.01, -5.43, -5.44. **FTIR** (thin film) ν 3324, 3192, 2954, 2929, 2886, 2857, 1668, 1616, 1472, 1463, 1403, 1361, 1253, 1115, 1080, 1005, 982, 939, 830, 811, 775, 728, 667, 573, 452 cm^{-1} . **HRMS** (ESI): Calculated for $\text{C}_{16}\text{H}_{38}\text{NO}_3\text{Si}_2^+$ $[\text{M}+\text{H}]^+$ 348.2385; found 348.2396. $[\alpha]_D^{25}$ -9.5 ($c = 3.81$, EtOAc).

Preparation of (S)-(1-amino-3,4-bis((*tert*-butyldimethylsilyl)oxy)butylidene)- λ^4 -sulfanone, 340



Lawesson's reagent (27.2 mg, 0.067 mmol, 0.7 equiv.) was added to a solution of amide **339** (28.8 mg, 0.083 mmol, 1.0 equiv.) in anhydrous DCM (0.8 mL) under argon. The reaction mixture was stirred vigorously at room temperature for 30 minutes. The reaction was quenched with 2 mL aqueous saturated NaHCO₃ solution and the aqueous solution was extracted with diethyl ether (3 × 5 mL). The combined organic layers were dried with anhydrous Na₂SO₄, filtered and then concentrated by rotary evaporation. The crude material was purified by a short silica plug (pet. Ether/Et₂O = 5/1). The fractions were collected and evaporated at room temperature under vacuum to afford the title compound as a colourless oil (12.3 mg, yield 39%). **¹H NMR** (500 MHz, CDCl₃): δ 7.51 (br. s, 2H, N-H), 4.01 – 3.93 (m, 1H, H-3), 3.61 (dd, *J* = 10.2, 4.9 Hz, 1H, H-4a), 3.46 (dd, *J* = 10.1, 7.7 Hz, 1H, H-4b), 2.67 (dd, *J* = 14.9, 4.4 Hz, 1H, H-2a), 2.53 (dd, *J* = 14.9, 4.6 Hz, 1H, H-2b), 0.92 (s, 9H), 0.91 (s, 9H), 0.13 (s, 3H), 0.11 (s, 3H), 0.09 (s, 3H), 0.08 (s, 3H). **¹³C NMR** (125 MHz, CDCl₃): 191.0 (C-1), 71.53 (C-3), 65.29 (C-4), 32.41 (C-2), 25.84, 25.76, 18.20, 17.95, -4.65, -4.96, -5.41, -5.46. **FTIR** (thin film) ν 2953, 2928, 2856, 1470, 1463, 1361, 1253, 1112, 1078, 1004, 936, 834, 809, 776, 721, 669 cm⁻¹. **HRMS** (ESI): Calculated for C₁₆H₃₈NO₃SSi₂⁺ [M+H]⁺ 380.2105; found 380.2116. [α]_D²² + 19.4 (*c* = 0.57, DCM).

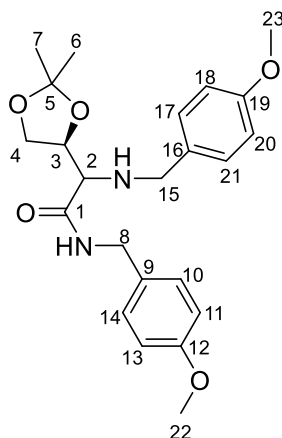
Preparation of (*S*)-2-(2,2-dimethyl-1,3-dioxolan-4-yl)-*N*-(4-methoxybenzyl)acetamide, **346**

Diphenyl diselenide (491 mg, 1.57 mmol, 1.3 equiv.) was added to a dry round-bottom flask equipped with stir bar under a blanket of argon. Deoxygenated absolute ethanol (purged for 30 minutes with argon) was then added, followed by the rapid addition of NaBH₄ (133 mg, 3.5 mmol, 2.87 equiv.). Shortly after the addition, the initial yellow solution turned colourless, indicating that diphenyl diselenide was completely reduced. The solution stirred at room temperature for 30 minutes, then a mixture of diastereomers (304 mg, 1.21 mmol, 1.0 equiv.), freshly powdered NaOH (110 mg, 3.02 mmol, 2.5 equiv.) and 4-methoxybenzylamine (0.19 mL, 1.45 mmol, 1.2 equiv.) were added sequentially under argon. The mixture was heated in a 55 °C oil bath and allowed to react at this temperature for 36 hours while monitoring by TLC for consumption of starting material. Upon completion, ethanol was removed by rotary evaporation under reduced pressure and the amorphous orange solids were dissolved in 5 mL saturated NH₄Cl and extracted with ethyl acetate (5 × 10 mL). The combined organic layers were dried with anhydrous Na₂SO₄, filtered, and then concentrated by rotary evaporation. The crude material was purified by flash silica chromatography (pet. Ether/EtOAc = 1/2) to afford the desired product **346** as a yellow oil (183 mg, yield 54%) and the by-product **347** as a yellow oil (28.3 mg, yield 6%).

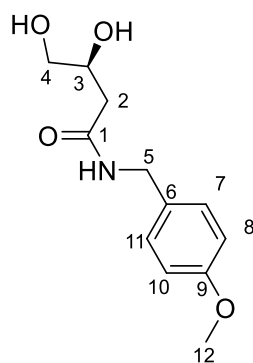
346: *R_f*: 0.6 (pet. Ether/EtOAc = 1/4). ¹H NMR (500 MHz, CDCl₃): δ 7.23 – 7.18 (m, 2H, H-10, H-14), 6.89 – 6.84 (m, 2H, H-11, H-13), 6.25 (br. s, 1H, N-H), 4.47 – 4.41 (m, 1H, H-3), 4.39 (dd, *J* = 5.6, 1.7 Hz, 2H, H-8), 4.14 (dd, *J* = 8.3, 6.0 Hz, 1H, H-4a), 3.80 (s, 3H, H-15), 3.63 (dd, *J* = 8.3, 6.9 Hz, 1H, H-4b), 2.51 (dd, *J* = 6.2, 3.2 Hz, 2H, H-2), 1.38 (s, 3H, H-6 or H-7), 1.35 (s, 3H, H-7 or H-6). ¹³C NMR (125 MHz, CDCl₃): δ 169.7 (C-1), 159.0 (C-12), 130.2 (C-9), 129.0 (C-10, C-14), 114.0 (C-11, C-13), 109.4 (C-5), 72.5 (C-3), 69.1 (C-4), 55.3 (C-15), 43.0 (C-8), 40.5 (C-2), 26.9 (C-6 or C-7), 25.5 (C-7).

or C-6). **FTIR** (thin film) ν 3305, 2985, 2934, 1643, 1613, 1585, 1542, 1511, 1458, 1441, 1370, 1301, 1244, 1176, 1154, 1111, 1062, 1032, 832, 587, 513 cm^{-1} . **HRMS** (ESI): Calculated for $\text{C}_{15}\text{H}_{22}\text{NO}_4^+$ $[\text{M}+\text{H}]^+$ 280.1543; found 280.1541. $[\alpha]_D^{26} -10.3$ ($c = 0.39$, DCM).

2-((S)-2,2-Dimethyl-1,3-dioxolan-4-yl)-N-(4-methoxybenzyl)-2-((4-methoxybenzyl)amino)acetamide, 347

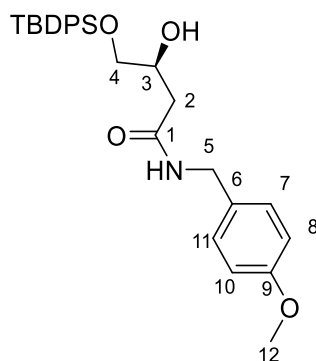


R_f: 0.78 (pet. Ether/EtOAc = 1/4). **¹H NMR** (500 MHz, CDCl_3): δ 7.71 (t, $J = 5.6$ Hz, 1H, N-H), 7.20 – 7.16 (m, 2H, H-10, H-14), 7.14 – 7.10 (m, 2H, H-17, H-21), 6.89 – 6.84 (m, 2H, H-11, H-13), 6.84 – 6.80 (m, 2H, H-18, H-20), 4.40 (dd, $J = 14.6, 6.1$ Hz, 1H, H-8a), 4.33 (dd, $J = 14.6, 5.7$ Hz, 1H, H-8b), 4.20 – 4.15 (m, 1H, H-3), 4.03 (dd, $J = 6.0, 1.3$ Hz, 2H, H-4), 3.80 (s, 3H, H-22 or H-23), 3.79 (s, 3H, H-22 or H-23), 3.70 (d, $J = 13.0$ Hz, 1H, H-15a), 3.61 (d, $J = 13.0$ Hz, 1H, H-15b), 3.19 (d, $J = 7.2$ Hz, 1H, H-2), 1.36 (s, 3H, H-6 or H-7), 1.32 (s, 3H, H-7 or H-6). **¹³C NMR** (125 MHz, CDCl_3): δ 171.2 (C-1), 158.9 (C-12), 158.8 (C-19), 131.3 (C-6), 130.3 (C-9), 129.4 (C-17, C-21), 128.9 (C-10, C-14), 114.1 (C-11, C-13), 113.9 (C-18, C-20), 109.4 (C-5), 76.2 (C-3), 67.1 (C-4), 64.8 (C-2), 55.29 (C-22 or C-23), 55.27 (C-22 or C-23), 52.2 (C-15), 42.5 (C-8), 26.6 (C-6 or C-7), 25.2 (C-7 or C-6). **FTIR** (thin film) ν 3337, 2986, 2932, 2836, 1664, 1612, 1585, 1511, 1461, 1441, 1371, 1301, 1245, 1176, 1154, 1111, 1067, 1034, 820, 755, 572, 514 cm^{-1} . **HRMS** (ESI): Calculated for $\text{C}_{23}\text{H}_{31}\text{N}_2\text{O}_5^+$ $[\text{M}+\text{H}]^+$ 415.2233; found 415.2221. $[\alpha]_D^{26} +19.7$ ($c = 1.42$, DCM).

Preparation of (S)-3,4-dihydroxy-N-(4-methoxybenzyl)butanamide, 348

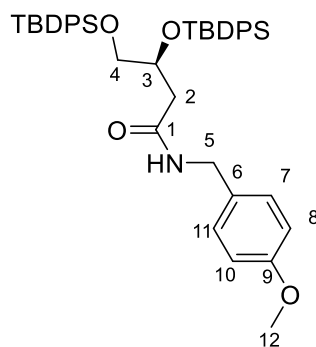
Amide **346** (84.7 mg, 0.3 mmol, 1.0 equiv.) was dissolved in a mixture of acetic acid (0.24 mL) and water (0.06 mL). Then the reaction mixture was stirred at 40 °C for 2 hours. Then acetic acid and water was evaporated under reduced pressure. The crude material was purified by flash silica chromatography (EtOAc/MeOH = 10/1) to afford the title compound as a white solid (45.7 mg, yield 63%). **Melting point:** 117 – 118 °C. **R_f:** 0.25 (EtOAc/MeOH = 10/1). **¹H NMR** (500 MHz, CDCl₃): δ 7.23 – 7.19 (m, 2H, H-7, H-11), 6.90 – 6.85 (m, 2H, H-8, H-10), 5.97 (br. s, 1H, N-H), 4.39 (d, *J* = 5.6 Hz, 2H, H-5), 4.15 – 4.08 (m, 1H, H-3), 4.00 (br. s, 1H, -OH), 3.80 (s, 3H, H-12), 3.69 (dd, *J* = 11.2, 3.7 Hz, 1H, H-4a), 3.53 (dd, *J* = 11.2, 5.6 Hz, 1H, H-4b), 2.47 (dd, *J* = 15.4, 8.7 Hz, 1H, H-2a), 2.37 (dd, *J* = 15.4, 3.3 Hz, 1H, H-2b), 2.19 (br. s, 1H, -OH). **¹³C NMR** (125 MHz, CDCl₃): δ 171.8 (C-1), 159.2 (C-9), 129.8 (C-6), 129.2 (C-7, C-11), 114.2 (C-8, C-10), 68.8 (C-3), 65.9 (C-4), 55.3 (C-12), 43.1 (C-5), 38.6 (C-2). **FTIR** (thin film) ν 3303, 1651, 1631, 1588, 1546, 1515, 1464, 1456, 1441, 1414, 1328, 1305, 1252, 1223, 1181, 1099, 1072, 1034, 820, 809, 745, 585 cm⁻¹. **HRMS** (ESI): Calculated for C₁₂H₁₈NO₄⁺ [M+H]⁺ 240.1230; found 240.1225. [α]_D²² –15.6 (*c* = 0.45, MeOH).

Preparation of (S)-4-((*tert*-butyldiphenylsilyl)oxy)-3-hydroxy-N-(4-methoxybenzyl)butanamide, **349**

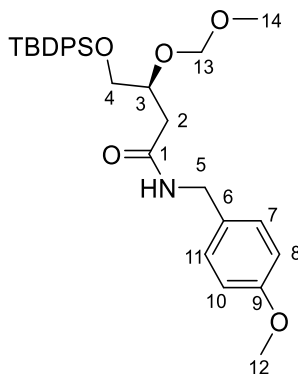


Imidazole (7.9 mg, 0.116 mmol, 1.45 equiv.) and TBDPSCl (23 μ L, 0.088 mmol, 1.05 equiv.) were added to a solution of amide **348** (20 mg, 0.08 mmol, 1.0 equiv.) in 0.8 mL anhydrous DMF. The reaction mixture was stirred at room temperature for 16 hours, and the reaction was diluted with 5 mL ethyl acetate, and washed 3 times with 3 mL of water. The combined aqueous phase was then extracted with extracted with ethyl acetate (3 \times 3 mL). The combined organic layers were dried with anhydrous Na₂SO₄, filtered, and then concentrated by rotary evaporation. The crude material was purified by flash silica chromatography to afford the title compound **349** as a colourless oil (7.6 mg, yield 19%) and bis-TBDPS side-product **350** as a colourless oil (6.5 mg, yield 11%).

349: R_f: 0.34 (pet. Ether/EtOAc = 1/1). **¹H NMR** (500 MHz, CDCl₃): δ 7.65 – 7.61 (m, 4H), 7.46 – 7.34 (m, 6H), 7.23 – 7.18 (m, 2H, H-7, H-11), 6.89 – 6.84 (m, 2H, H-8, H-10), 6.38 (t, J = 5.7 Hz, 1H, -NH), 4.37 (d, J = 5.6 Hz, 2H, H-5), 4.16 – 4.08 (m, 1H, H-3), 3.80 (s, 3H, H-12), 3.64 (dd, J = 10.2, 4.9 Hz, 1H, H-4a), 3.60 (dd, J = 10.2, 6.5 Hz, 1H, H-4b), 2.44 – 2.34 (m, 2H, H-2), 2.08 (s, 1H, -OH), 1.05 (s, 9H). **¹³C NMR** (125 MHz, CDCl₃): 171.3 (C-1), 159.0 (C-9), 135.5, 132.9, 130.1 (C-6), 129.9, 129.1 (C-7, C-11), 127.8, 114.1 (C-8, C-10), 69.1 (C-3), 67.1 (C-4), 55.3 (C-12), 43.0 (C-5), 39.3 (C-2), 26.8, 19.2. **FTIR** (thin film) ν 3309, 2954, 2930, 2857, 1654, 1642, 1613, 1588, 1577, 1560, 1542, 1535, 1513, 1487, 1462, 1438, 1428, 1390, 1362, 1302, 1248, 1175, 1112, 1076, 1035, 998, 823, 741, 702, 692, 614, 504, 489 cm⁻¹. **HRMS** (ESI): Calculated for C₂₈H₃₆NO₄Si⁺ [M+H]⁺ 478.2408; found 478.2359. $[\alpha]_D^{26}$ -11.2 (c = 0.37, DCM).

(S)-3,4-Bis((*tert*-butyldiphenylsilyl)oxy)-N-(4-methoxybenzyl)butanamide, 350

R_f: 0.50 (pet. Ether/EtOAc = 3/1). **¹H NMR** (500 MHz, CDCl₃): δ 7.60 – 7.45 (m, 8H), 7.43 – 7.34 (m, 4H), 7.33 – 7.23 (m, 8H), 7.12 – 7.06 (m, 2H, H-7, H-11), 6.82 – 6.77 (m, 2H, H-8, H-10), 6.23 (t, *J* = 5.4 Hz, 1H, N-H), 4.30 (dd, *J* = 14.3, 5.6 Hz, 1H, H-5a), 4.22 (dd, *J* = 14.7, 5.2 Hz, 1H, H-5b), 4.23 – 4.16 (m, 1H, H-3), 3.79 (s, 3H, H-12), 3.57 – 3.53 (m, 2H, H-4), 2.57 (dd, *J* = 14.8, 5.1 Hz, 1H, H-2a), 2.43 (dd, *J* = 14.8, 5.2 Hz, 1H, H-2b), 0.97 (s, 9H), 0.95 (s, 9H). **¹³C NMR** (125 MHz, CDCl₃): 170.3 (C-1), 159.0 (C-9), 135.8, 135.7, 135.6, 135.5, 133.3, 133.22, 133.21, 133.11, 130.4 (C-6), 129.9, 129.7, 129.60, 129.57, 129.4 (C-7, C-11), 127.7, 127.64, 127.63, 127.59, 114.0 (C-8, C-10), 71.2 (C-3), 66.3 (C-4), 55.3 (C-12), 43.0 (C-5), 40.7 (C-2), 26.9, 26.8, 19.2, 19.1. **FTIR** (thin film) ν 3307, 3070, 3049, 2929, 2856, 1649, 1613, 1588, 1512, 1463, 1427, 1390, 1361, 1302, 1248, 1176, 1111, 1082, 1037, 998, 938, 821, 739, 701, 612, 505, 489, 431 cm⁻¹. **HRMS** (ESI) Calculated for C₄₄H₅₄NO₄Si₂⁺ [M+H]⁺ 716.3586; found 716.3573. [α]_D²⁶ +140.2 (*c* = 0.21, DCM)

Preparation of (S)-4-((*tert*-butyldiphenylsilyl)oxy)-N-(4-methoxybenzyl)-3-(methoxymethoxy)butanamide, 351

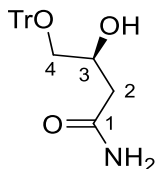
To a solution of amide **349** (6.7 mg, 0.014 mmol, 1.0 equiv.) in anhydrous DCM (0.8 mL) were added sequentially a solution of *N, N*-diisopropylethylamine (185 μ L, 1.06 mmol, 75 equiv.) in anhydrous DCM (1.1 mL) and a solution of methoxymethyl chloride (57 μ L,

technical grade 90% purity, 0.67 mmol, 48 equiv.) in anhydrous DCM (0.75 mL) at 2 °C. Then the reaction mixture was stirred at room temperature for 66 hours. Saturated aqueous NaHCO₃ solution (2 mL) was added slowly and then the resulting mixture was stirred vigorously at room temperature for 15 minutes to destroy residual methoxymethyl chloride. The aqueous phase was extracted with ethyl acetate (3 × 5 mL). The combined organic phase was washed with brine, dried over anhydrous Na₂SO₄, filtered, concentrated under reduced pressure. The crude material was purified by flash silica gel chromatography (pet. ether/EtOAc = 3/1) to afford the title compound (4.8 mg, 37% yield) as a colourless oil. **R_f**: 0.65 (pet. Ether/EtOAc = 1/1). **¹H NMR** (500 MHz, CDCl₃): δ 7.67 – 7.60 (m, 4H), 7.45 – 7.34 (m, 6H), 7.12 – 7.06 (m, 2H, H-7, H-11), 6.88 – 6.80 (m, 2H, H-8, H-10), 6.24 (t, *J* = 5.0 Hz, 1H, N-H), 4.66 – 4.60 (m, 2H, H-13), 4.36 (d, *J* = 5.5 Hz, 2H, H-5), 4.12 – 4.06 (m, 1H, H-3), 3.79 (s, 3H, H-12), 3.71 (dd, *J* = 10.8, 5.1 Hz, 1H, H-4a), 3.66 (dd, *J* = 10.7, 5.0 Hz, 1H, H-4b), 3.22 (s, 3H, H-14), 2.59 (dd, *J* = 14.9, 3.9 Hz, 1H, H-2a), 2.45 (dd, *J* = 15.0, 8.2 Hz, 1H, H-2b), 1.04 (s, 9H). **¹³C NMR** (125 MHz, CDCl₃): 170.4 (C-1), 159.0 (C-9), 135.5, 133.1, 130.3 (C-6), 129.8, 129.2 (C-7, C-11), 127.7, 114.0 (C-8, C-10), 96.4 (C-13), 75.3 (C-3), 65.6 (C-4), 55.6 (C-14), 55.3 (C-12), 43.1 (C-5), 39.5 (C-2), 26.8, 19.2. **FTIR** (thin film) ν 3320, 2927, 2854, 1641, 1559, 1513, 1462, 1451, 1428, 1302, 1248, 1176, 1150, 1112, 1034, 823, 741, 702, 614, 505, 491 cm⁻¹. **HRMS** (ESI): Calculated for C₃₀H₄₀NO₅Si₂⁺ [M + H]⁺ 522.2670; found 522.2688. [α]_D²⁵ – 6.6 (*c* = 0.24, DCM)

6.3 Experimental for Chapter Three

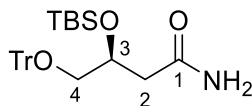
6.3.1 Synthesis of Thioamide **382**

Preparation of (*S*)-3-hydroxy-4-(trityloxy)butanamide, **374**



Amide **339** (64.8 mg, 0.61 mmol, 1.0 equiv.) and trityl chloride (208 mg, 0.74 mmol, 1.2 equiv.) were dissolved in anhydrous DMF (1 mL) under argon atmosphere. Then anhydrous pyridine (0.15 mL) was added to the solution, which was stirred at room temperature for 27 hours. The reaction was quenched by addition of ice water (1.5 mL), and the resulting mixture was diluted with 10 mL ethyl acetate and washed 3 times with 3 mL of water. The combined aqueous phase was then extracted with ethyl acetate (3 × 5 mL). The combined organic layers were dried with anhydrous Na₂SO₄, filtered, and then concentrated by rotary evaporation. The crude material was purified by flash silica chromatography (pet. Ether/EtOAc = 1/4) to afford the desired product as white crystalline solid (201 mg, yield 90%). *R*_f: 0.39 (pet. Ether/EtOAc = 1/4). ¹H NMR (500 MHz, CDCl₃): δ 7.44 – 7.39 (m, 6H), 7.33 – 7.22 (m, 9H), 6.03 (br. s, 1H), 5.39 (br. s, 1H), 4.21 – 4.15 (m, 1H), 3.19 – 3.16 (m, 2H), 2.42 – 2.39 (m, 2H). ¹³C NMR (125 MHz, CDCl₃): 174.1, 143.6, 128.6, 127.7, 127.1, 86.8, 67.7, 66.7, 39.2. These characterisation data match those reported in the literature.³⁴⁸

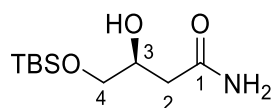
Preparation of (*S*)-3-((*tert*-butyldimethylsilyl)oxy)-4-(trityloxy)butanamide, **375**



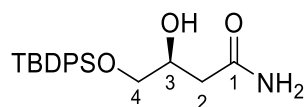
Imidazole (120 mg, 1.77 mmol, 3.18 equiv.) and *tert*-butyldimethylsilyl chloride (119 mg, 0.79 mmol, 1.42 equiv.) were added to a solution of amide **374** (201 mg, 0.556 mmol, 1.0 equiv.) in 1.0 mL anhydrous DMF. The reaction mixture was stirred at room temperature for 16 hours, and the reaction was quenched by addition of 2 mL of distilled water. The resulting mixture was diluted with 10 mL ethyl acetate, and washed 3 times with 3 mL of water. The combined aqueous phase was then extracted with extracted with ethyl acetate (3 × 5 mL). The combined organic layers were dried with anhydrous Na₂SO₄, filtered,

and then concentrated by rotary evaporation. The crude material was purified by flash silica chromatography (pet. Ether/EtOAc = 3/1) to afford the title compound as a colourless oil (193 mg, yield 73%). **R_f**: 0.59 (pet. Ether/EtOAc = 1/1). **¹H NMR** (500 MHz, CDCl₃): δ 7.46 – 7.41 (m, 6H), 7.32 – 7.27 (m, 6H), 7.25 – 7.20 (m, 3H), 6.06 (br.s, 1H, N-H), 5.29 (br. s, 1H, N-H), 4.16 (tt, *J* = 6.4, 4.7 Hz, 1H, H-3), 3.15 (dd, *J* = 9.4, 4.9 Hz, 1H, H-4a), 3.09 (dd, *J* = 9.4, 6.4 Hz, 1H, H-4b), 2.68 (dd, *J* = 14.6, 4.5 Hz, 1H, H-2a), 2.42 (dd, *J* = 14.6, 6.4 Hz, 1H, H-2b), 0.84 (s, 9H), 0.03 (s, 3H), -0.04 (s, 3H). **¹³C NMR** (125 MHz, CDCl₃): 173.6, 143.8, 128.6, 127.8, 127.0, 86.7, 69.0, 66.6, 41.6, 25.7, 17.9, -4.7, -5.1. **FTIR** (thin film) ν 3338, 3187, 3059, 3032, 2953, 2928, 2884, 2856, 1671, 1598, 1490, 1471, 1463, 1448, 1402, 1361, 1253, 1220, 1184, 1154, 1074, 1033, 1000, 954, 899, 832, 812, 776, 746, 704, 646, 632, 574, 532, 501 cm⁻¹. **HRMS** (ESI): Calculated for C₂₉H₃₇NNaO₃Si⁺ [*M*+*H*]⁺ 498.2440; found 498.2433. [α]_D²⁵ -8.1 (*c* = 1.36, DCM).

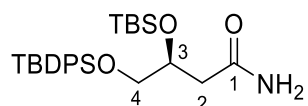
Preparation of (*S*)-4-((*tert*-butyldimethylsilyl)oxy)-3-hydroxybutanamide, **378**



To a solution of amide **339** (75.8 mg, 0.22 mmol, 1.0 equiv.) in MeOH-DCM (v/v = 1/1, 2.4 mL) was added (±)-10-camphorsulfonic acid (51 mg, 0.22 mmol, 1.0 equiv.) over 5 portions over 1 minute at 0 °C. The reaction mixture was stirred at 0 °C for 20 minutes and then added 1 mL saturated aqueous NaHCO₃ solution. All solvents were then evaporated under reduced pressure. The solid residue was slurried with 5 mL ethyl acetate and filtered. The filtrate was evaporated and the crude material was then purified by silica flash chromatography (pet. Ether/EtOAc = 1/4) to afford the title compound as a colourless oil. **R_f**: 0.22 (pet. Ether/EtOAc = 1/2). **¹H NMR** (500 MHz, CDCl₃) δ 6.25 (s, 1H, N-H), 5.51 (s, 1H, N-H), 4.03 (tt, *J* = 6.9, 4.7 Hz, 1H, H-3), 3.62 (dd, *J* = 10.0, 4.6 Hz, 1H, H-4a), 3.54 (dd, *J* = 10.0, 6.6 Hz, 1H, H-4b), 2.41 – 2.38 (m, 2H, H-2), 0.90 (s, 9H), 0.08 (s, 3H). **¹³C NMR** (125 MHz, CDCl₃) δ 173.9 (C-1), 68.7 (C-3), 66.3 (C-4), 38.9 (C-2), 25.8, 18.3, -5.40, -5.43. **FTIR** (solid) ν 3371, 3205, 3125, 2952, 2926, 2877, 2854, 1678, 1656, 1620, 1468, 1435, 1410, 1393, 1362, 1348, 1321, 1279, 1254, 1201, 1120, 1105, 1075, 1047, 1007, 938, 888, 834, 779, 684, 667, 574, 508, 457, 446 cm⁻¹. **HRMS** (ESI): Calculated for C₁₀H₂₄NO₃Si⁺ [*M*+*H*]⁺ 234.1520; found 234.1504. [α]_D²¹ +104(*c* = 0.084, MeOH).

Preparation of (S)-4-((*tert*-butyldiphenylsilyl)oxy)-3-hydroxybutanamide, 380

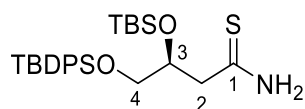
Imidazole (400 mg, 5.87 mmol, 1.55 equiv.) and *tert*-butyldiphenylchlorosilane (1.04 mL, 4.00 mmol, 1.05 equiv.) were added to a solution of amide **339** (400 mg, 3.8 mmol, 1.0 equiv.) in 3.8 mL anhydrous DMF. The reaction mixture was stirred at room temperature for 24 hours, and the reaction was quenched with distilled water (5 mL). Then DMF and water was removed at 60 °C by oil pump. The residue was then purified by flash silica chromatography (pet. ether/EtOAc = 1/2) to afford the title compound as a colourless oil (911 mg, yield 67%). *R_f*: 0.23 (pet. Ether/EtOAc = 1/1). ¹H NMR (500 MHz, CDCl₃): δ 7.67 – 7.60 (m, 4H), 7.47 – 7.36 (m, 6H), 6.21 (br. s, 1H, N-H), 5.72 (br. s, 1H, N-H), 4.16 – 4.05 (m, 1H, H-3), 3.66 (dd, *J* = 10.2, 4.6 Hz, 1H, H-4a), 3.60 (dd, *J* = 10.2, 6.6 Hz, 1H, H-4b), 3.26 (br. s, O-H), 2.42 – 2.37 (m, 2H, H-2), 1.07 (s, 9H). ¹³C NMR (125 MHz, CDCl₃): 174.2 (C-1), 135.4, 132.81, 132.79, 129.946, 129.938, 127.8, 68.8 (C-3), 67.0 (C-4), 38.8 (C-2), 26.8, 19.2. FTIR (thin film) ν 3338, 3202, 2956, 2930, 2857, 1663, 1617, 1589, 1472, 1462, 1427, 1391, 1361, 1111, 1070, 1007, 998, 823, 803, 740, 700, 621, 613, 504, 489 cm⁻¹. HRMS (ESI): Calculated for C₃₀H₄₀NO₅Si₂⁺ [M+H]⁺ 358.1833; found 358.1838. $[\alpha]_D^{25}$ –24.4 (*c* = 0.41, DCM).

Preparation of (S)-3-((*tert*-butyldimethylsilyl)oxy)-4-((*tert*-butyldiphenylsilyl)oxy)butanamide, 381

Imidazole (5.44 g, 79.3 mmol, 6.0 equiv.) and *tert*-butyldimethylsilyl chloride (5.97 g, 39.6 mmol, 3.0 equiv.) were added to a solution of amide **380** (911 mg, 2.55 mmol, 1.0 equiv.) in 50 mL anhydrous DMF. The reaction mixture was stirred at 30 – 35 °C for 14 days under nitrogen atmosphere. Then reaction mixture was quenched by addition of 50 mL ice-water. Then DMF and water was removed at 60 °C by oil pump. The residue was re-dissolved in ethyl acetate (200 mL), and washed with distilled water (3 × 50 mL). The combined aqueous phase was then extracted with ethyl acetate (3 × 50 mL). The combined organic phase was dried with anhydrous Na₂SO₄, filtered, and then concentrated by rotary evaporation. The crude material was purified by flash silica chromatography (pet. ether/EtOAc = 2/1) to afford the title compound as a colorless oil

(6.12 g, yield 98%). **R_f**: 0.30 (pet. Ether/EtOAc = 2/1). **¹H NMR** (500 MHz, CDCl₃): δ 7.68 – 7.62 (m, 4H), 7.46 – 7.34 (m, 6H), 6.11 (br. s, 1H, N-H), 5.29 (br. s, 1H, N-H), 4.15 – 4.05 (m, 1H, H-3), 3.63 (dd, *J* = 10.2, 4.8 Hz, 1H, H-4a), 3.54 (dd, *J* = 10.1, 7.0 Hz, 1H, H-4b), 2.66 (dd, *J* = 14.8, 4.1 Hz, 1H, H-2a), 2.42 (dd, *J* = 14.8, 6.3 Hz, 1H, H-2b), 1.04 (s, 9H), 0.83 (s, 9H), 0.03 (s, 3H), -0.06 (s, 3H). **¹³C NMR** (125 MHz, CDCl₃): 173.4 (C-1), 135.6, 135.5, 133.2, 133.1, 129.8, 129.7, 127.74, 127.73, 70.2 (C-3), 66.9 (C-4), 41.0 (C-2), 26.8, 25.7, 19.2, 17.9, -4.7, -5.1. **FTIR** (thin film) ν 3327, 3190, 3072, 2954, 2929, 2890, 2857, 1670, 1612, 1590, 1472, 1463, 1427, 1390, 1361, 1253, 1189, 1110, 1075, 999, 983, 964, 939, 824, 804, 777, 739, 700, 665, 613, 504, 490 cm⁻¹. **HRMS** (ESI): Calculated for C₂₆H₄₂NO₃Si₂⁺ [M+H]⁺ 472.2698; found 472.2704. [α]_D²⁵ +71.7 (*c* = 0.35, DCM)

Preparation of (*S*)-3-((*tert*-butyldimethylsilyl)oxy)-4-((*tert*-butyldiphenylsilyl)oxy)butanethioamide, **382**



Lawesson's reagent (1.54 g, 3.82 mmol, 0.6 equiv.) was added to a solution of amide **381** (3.06 g, 6.36 mmol, 1.0 equiv.) in anhydrous deoxygenated DCM (63 mL) under argon atmosphere. The reaction mixture was stirred vigorously at room temperature for 20 minutes. Upon completion, the reaction mixture was directly loaded onto a short silica plug and purified using DCM as eluent rapidly. The fractions were immediately collected and evaporated at 10 °C under vacuum to afford the title compound as a yellow oil (1.71 g, yield 54%). **R_f**: 0.37 (DCM).

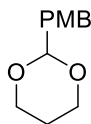
Notes: Tendency towards oxidation by air was observed. Upon purification, the product should be stored in the freezer at -20 °C under argon atmosphere.

¹H NMR (500 MHz, CDCl₃): δ 7.76 (br. s, 1H, N-H), 7.69 – 7.63 (m, 4H), 7.46 – 7.36 (m, 7H), 4.14 – 4.08 (m, 1H, H-3), 3.64 (dd, *J* = 10.3, 4.7 Hz, 1H, H-4a), 3.58 (dd, *J* = 10.4, 6.8 Hz, 1H, H-4b), 3.11 (dd, *J* = 14.4, 4.1 Hz, 1H, H-2a), 3.00 (dd, *J* = 14.4, 6.0 Hz, 1H, H-2b), 1.06 (s, 9H), 0.83 (s, 9H), 0.04 (s, 3H), -0.06 (s, 3H). **¹³C NMR** (125 MHz, CDCl₃): δ 207.7 (C-1), 135.6, 135.5, 133.1, 132.9, 129.81, 129.77, 127.77, 127.74, 72.3 (C-3), 66.4 (C-4), 49.7 (C-2), 26.8, 25.8, 19.2, 17.9, -4.7, -5.0. **FTIR** (thin film) ν 3290, 3169, 3071, 2954, 2929, 2887, 2856, 1618, 1471, 1462, 1427, 1406, 1390, 1361, 1325, 1255, 1188, 1111, 1071, 998, 939, 834, 823, 803, 778, 739, 701, 690, 665, 622, 613, 505,

492 cm⁻¹. **HRMS** (ESI): Calculated for C₂₆H₄₂NO₂SSi₂⁺ [M + H]⁺ 488.2469; found 488.2500. [α]_D²⁵ -97.8 (*c* = 0.92, DCM).

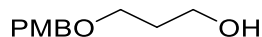
6.3.2 Synthesis of Alkyne 364

Preparation of 2-(4-methoxybenzyl)-1,3-dioxane, 385



To a solution of 1,3-propanediol **384** (6.3 mL, 87.3 mmol, 1.2 equiv.) and *p*-anisaldehyde (8.8 mL, 72.7 mmol, 1.0 equiv.) in toluene (50 mL) was added *p*-toluenesulfonic acid (114 mg, 0.008 equiv.) as a catalyst. The reaction mixture was refluxed at 110 °C in a Dean-Stark apparatus for 17 hours. The reaction mixture was then allowed to cool to room temperature and was quenched by addition of saturated aqueous NaHCO₃ solution (2 mL). The resulting mixture was washed with distilled water (50 mL), and the aqueous fractions were re-extracted with diethyl ether (2 × 50 mL). The combined organic phase was dried with anhydrous Na₂SO₄, filtered, and then concentrated by rotary evaporation. The crude material was purified by flash silica chromatography (pet. ether/EtOAc = 8/1) to afford the title compound as a brown crystal (12.6 g, yield 90%). **R_f**: 0.38 (pet. ether/EtOAc = 5:1). **¹H NMR** (500 MHz, CDCl₃): δ 7.45 – 7.40 (m, 2H), 6.92 – 6.88 (m, 2H), 5.46 (s, 1H), 4.30 – 4.24 (m, 2H), 4.03 – 3.96 (m, 2H), 3.80 (s, 3H), 2.24 (*J* = 13.5, 12.4, 5.0 Hz, 1H), 1.46 (dtt, *J* = 13.5, 2.7, 1.5 Hz, 1H). **¹³C NMR** (125 MHz, CDCl₃): δ 159.9, 131.3, 127.2, 113.4, 101.6, 67.4, 55.3, 25.7. These characterisation data match those reported in the literature.³⁴⁹

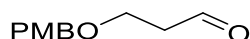
Preparation of 3-((4-methoxybenzyl)oxy)propan-1-ol, 386



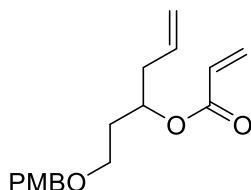
To a solution of acetal **385** (12.6 g, 64.9 mmol, 1.0 equiv.) in anhydrous DCM (400 mL) at -78 °C was a solution of diisobutylaluminium hydride (129.8 mL, 1.0 M in cyclohexane, 129.8 mmol, 2.0 equiv.) slowly at -78 °C. The reaction mixture was allowed to warm to room temperature slowly over 2 hours and stirred at room temperature for 16 hours. The reaction was then quenched by addition of a saturated aqueous solution of potassium sodium tartrate (270 mL) and the resulting mixture was stirred at room temperature for 2 hours until the cloudy suspension turned to be a clear mixture. The aqueous phase was separated and extracted with ethyl acetate (3 × 100 mL). The combined organic phase

was dried with anhydrous Na₂SO₄, filtered, and then concentrated by rotary evaporation to afford the pure title compound as a colourless oil (11.6 g, yield 91%), which was used for the next step without further purification. **R_f**: 0.32 (pet. ether/EtOAc = 1:1). **¹H NMR** (500 MHz, CDCl₃): δ 7.27 (d, *J* = 8.7 Hz, 2H), 6.90 (d, *J* = 8.6 Hz, 2H), 4.47 (s, 2H), 3.82 (s, 3H), 3.79 (t, *J* = 5.6 Hz, 2H), 3.66 (t, *J* = 5.8 Hz, 2H), 1.87 (quin, *J* = 5.7 Hz, 2H). **¹³C NMR** (125 MHz, CDCl₃): δ 159.2, 130.1, 129.3, 113.8, 72.9, 69.2, 62.1, 55.3, 32.0. These characterisation data match those reported in the literature.³⁴⁹

Preparation of 3-((4-methoxybenzyl)oxy)propanal, **387**

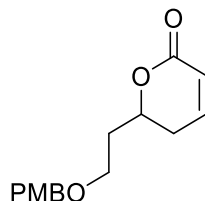


To a solution of anhydrous dimethyl sulfoxide (17.0 mL, 0.234 mol, 4.0 equiv.) in anhydrous DCM (300 mL) at -78 °C was added freshly distilled oxalyl chloride (10.0 mL, 0.118 mol, 2.0 equiv.). The reaction mixture was stirred at that temperature for 30 minutes, then a solution of alcohol **386** (11.6 g, 0.059 mol, 1.0 equiv.) in anhydrous DCM (80 mL) was added at -78 °C. Then anhydrous triethylamine (33 mL, 0.237 mmol, 4.0 equiv.) was added to the reaction mixture in 5 portions over 30 minutes at -78 °C. The reaction mixture was maintained at that temperature for 3 hours, and then was allowed to warm to room temperature slowly over 2 hours. Then the reaction mixture was stirred at room temperature overnight and quenched by addition of 300 mL of saturated aqueous NH₄Cl solution. The aqueous phase was then separated and extracted with DCM (3 × 100 mL). The combined organic phase was dried with anhydrous Na₂SO₄, filtered, and then concentrated by rotary evaporation. The crude material was purified by flash silica chromatography (pet. ether/EtOAc = 5/1) to afford the pure title compound as a yellow oil (10.8 g, yield 94%). **R_f**: 0.25 (pet. ether/EtOAc = 5:1). **¹H NMR** (500 MHz, CDCl₃): δ 9.78 (t, *J* = 1.8 Hz, 1H), 7.26 – 7.24 (m, 2H), 6.90 – 6.84 (m, 2H), 4.46 (s, 2H), 3.80 (s, 3H), 3.78 (t, *J* = 6.1 Hz, 5H), 2.68 (td, *J* = 6.1, 1.8 Hz, 2H). **¹³C NMR** (125 MHz, CDCl₃): δ 201.3, 159.3, 129.9, 129.3, 113.8, 72.9, 63.5, 55.2, 43.8. These characterisation data match those reported in the literature.³⁵⁰

Preparation of 1-((4-methoxybenzyl)oxy)hex-5-en-3-yl acrylate, 388

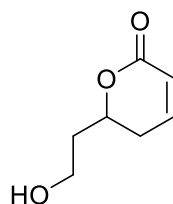
To a solution of aldehyde **387** (0.487g, 2.51 mmol, 1.0 equiv.) in anhydrous THF (25 mL) at 2 °C was added dropwise allylmagnesium bromide solution (3.0 mL, 1.0 M in diethyl ether, 1.2 equiv.). The reaction mixture was allowed to warm up to room temperature and stirred at room temperature overnight. Then anhydrous *N,N*-diisopropylethylamine (1.7 mL, 10.0 mmol, 4.0 equiv.) was added at room temperature and then the reaction mixture was cooled to 2 °C, followed by addition of acryloyl chloride (1.2 mL, 15.1 mmol, 6.0 equiv.) and 4-dimethylaminopyridine (94 mg, 0.75 mmol, 0.3 equiv.). The resulting mixture was stirred at room temperature for 3 hours. The reaction was then quenched by the addition of 15 mL saturated aqueous solution of NH_4Cl and the aqueous phase was then separated and extracted with DCM (3×100 mL). The combined organic phase was dried with anhydrous Na_2SO_4 , filtered, and then concentrated by rotary evaporation. The crude material was purified by flash silica chromatography (pet. ether/diethyl ether = 10/1). (**Note:** Acid-washed sand was replaced with Na_2SO_4 in the preparation of column.) The column fractions were concentrated at room temperature under reduced pressure to afford the provide the title compound as a colourless oil (0.59 g, yield 80%). R_f : 0.43 (pet. ether/EtOAc = 5:1). $^1\text{H NMR}$ (500 MHz, CDCl_3): δ 7.25 – 7.22 (m, 2H), 6.90 – 6.81 (m, 2H), 6.37 (dd, $J = 17.3, 1.4$ Hz, 1H), 6.08 (dd, $J = 17.3, 10.4$ Hz, 1H), 5.82 – 5.70 (m, 2H), 5.21 – 5.13 (m, 1H), 5.10 – 5.02 (m, 2H), 4.40 (s, 2H), 3.80 (s, 3H), 3.52 – 3.42 (m, 2H), 2.45 – 2.32 (m, 2H), 1.94 – 1.84 (m, 2H). $^{13}\text{C NMR}$ (125 MHz, CDCl_3): δ 165.6, 159.1, 133.4, 130.5, 130.4, 129.3, 128.7, 118.0, 113.8, 72.7, 71.0, 66.2, 55.3, 38.8, 33.8. These characterisation data match those reported in the literature.³⁵¹

Preparation of 6-(2-((4-methoxybenzyl)oxy)ethyl)-5,6-dihydro-2H-pyran-2-one, 391



To a solution of diene **388** (1.81 g, 6.2 mmol, 1.0 equiv.) in anhydrous DCM (500 mL) was added Grubbs 2nd generation catalyst **390** (341 mg, 0.4 mmol, 0.065 equiv.). The reaction mixture was stirred at room temperature under argon atmosphere in dark for 21 hours. The solvent was then removed under reduced pressure. The crude material was purified by flash silica chromatography (pet. ether/ethyl acetate = 2/1) to provide the title compound as a colourless oil (1.31 g, yield 80%). *R_f*: 0.37 (pet. ether/EtOAc = 1:1). ¹H NMR (500 MHz, CDCl₃): δ 7.26 – 7.21 (m, 2H), 6.91 – 6.84 (m, 3H), 6.02 (dt, *J* = 9.8, 1.7 Hz, 1H), 4.66 – 4.59 (m, 1H), 4.44 (q, *J* = 11.4 Hz, 2H), 3.80 (s, 3H), 3.70 – 3.64 (m, 1H), 3.63 – 3.58 (m, 1H), 2.38 – 2.33 (m, 2H), 2.10 – 2.02 (m, 1H), 1.98 – 1.90 (m, 1H). ¹³C NMR (125 MHz, CDCl₃): δ 164.4, 159.3, 145.1, 130.2, 129.3, 121.4, 113.8, 75.3, 72.3, 65.3, 55.3, 35.1, 29.6. These characterisation data match those reported in the literature.¹³⁴

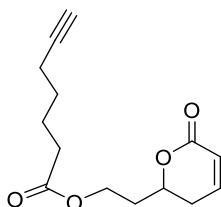
Preparation of 6-(2-hydroxyethyl)-5,6-dihydro-2H-pyran-2-one, 366



DDQ (212 mg, 0.934 mmol, 1.2 equiv.) was added a solution of lactone **391** (204 mg, 0.78 mmol, 1.0 equiv.) in a mixture of DCM (16.2 mL) and distilled water (1.8 mL). The reaction mixture was stirred at room temperature for 1 hour. The reaction mixture was then filtered through filter paper and the filter paper was rinsed with DCM a couple of times. The aqueous phase was separated and extracted with DCM (3 × 5 mL). The combined organic phase was dried with anhydrous Na₂SO₄, filtered, and then concentrated by rotary evaporation. The crude material was purified by flash silica chromatography using ethyl acetate as eluent to afford the title compound as a red oil (89.3 mg, yield 81%). *R_f*: 0.10 (ethyl acetate). ¹H NMR (500 MHz, CDCl₃): δ 6.91 (dt, *J*

= 9.6, 4.3 Hz, 1H), 6.04 (dt, J = 9.8, 1.8 Hz, 1H), 4.71 – 4.65 (m, 1H), 3.94 – 3.88 (m, 1H), 3.87 – 3.81 (m, 1H), 2.42 – 2.38 (m, 2H), 2.09 – 2.00 (m, 1H), 1.96 – 1.88 (m, 1H). ^{13}C NMR (125 MHz, CDCl_3): δ 164.3, 145.2, 121.4, 75.6, 58.6, 37.3, 29.7. These characterisation data match those reported in the literature.³⁵²

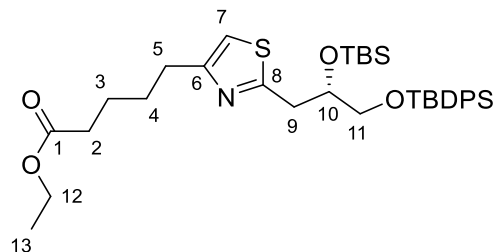
Preparation of (2Z,4E)-7-(hept-6-ynoyloxy)hepta-2,4-dienoic acid, **364**



To a solution of alcohol **366** (1.66 g, 11.7 mmol, 1.0 equiv.) and hept-6-ynoic acid **258** (1.76 g, 14.0 mmol, 1.2 equiv.) in anhydrous DCM (120 mL) was added subsequently EDCI (2.68 g, 14.0 mmol, 1.2 equiv.) and 4-dimethylaminopyridine (0.427 g, 3.5 mmol, 0.3 equiv.) at 1 – 2 °C. Then the reaction mixture was stirred at room temperature overnight. Upon completion, the reaction was quenched by addition of 75 mL of saturated aqueous NH_4Cl solution. The aqueous phase was then separated and extracted with ethyl acetate (3 \times 50 mL). The combined organic phase was dried with anhydrous Na_2SO_4 , filtered, and then concentrated by rotary evaporation. The crude material was purified by flash silica chromatography (pet. ether/ethyl acetate = 3/2) to afford the title compound as a yellow oil (1.98 g, yield 68%). *R_f*: 0.37 (pet. ether/EtOAc = 1:1). ^1H NMR (500 MHz, CDCl_3): δ 6.90 (ddd, J = 9.6, 6.8, 3.7 Hz, 1H), 6.04 (dt, J = 9.8, 1.7 Hz, 1H), 4.60 – 4.53 (m, 1H), 4.34 – 4.28 (m, 1H), 4.27 – 4.21 (m, 1H), 2.41 – 2.36 (m, 2H), 2.34 (t, J = 7.5 Hz, 2H), 2.21 (td, J = 7.0, 2.6 Hz, 2H), 2.16 – 2.08 (m, 1H), 2.06 – 1.96 (m, 1H), 1.95 (t, J = 2.6 Hz, 1H), 1.78 – 1.70 (m, 2H), 1.61 – 1.52 (m, 2H). ^{13}C NMR (125 MHz, CDCl_3): δ 173.2, 163.9, 144.7, 121.5, 83.9, 74.7, 68.6, 59.9, 34.0, 33.6, 29.4, 27.8, 23.9, 18.1. These characterisation data match those reported in the literature.¹³⁴

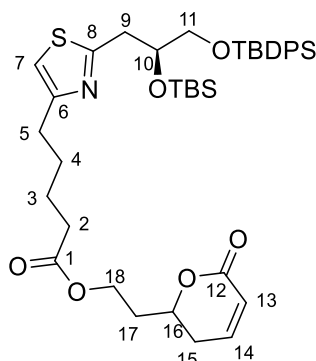
6.3.4 Synthesis of Thiazoles 392, 393 and 394

Preparation of ethyl (S)-5-(2-(2-((*tert*-butyldimethylsilyl)oxy)-3-((*tert*-butyldiphenylsilyl)oxy)propyl)thiazol-4-yl)pentanoate, **392**



To a solution of Mol-DalPhosAuOMs **257** (2.9 mg, 0.00385 mmol, 0.1 equiv.) in anhydrous deoxygenated DCM (0.2 mL) was added alkyne **259** (12 mg, 0.0735 mmol, 2.1 equiv.). The resulting mixture was stirred at room temperature under argon atmosphere for 15 minutes. Then a solution of 8-methylquinoline *N*-oxide **254** (17.0 mg, 0.106 mmol, 2.74 equiv.) and methanesulfonic acid (5.5 μ L, 0.085 mmol, 2.52 equiv.) in degassed anhydrous DCM (0.2 mL) was added to the reaction mixture via a syringe pump under argon atmosphere in 5 hours. Upon completion, the reaction mixture was further stirred for 1 hour before a solution of thioamide **382** (11.9 mg, 0.024 mmol, 1.0 eq) in deoxygenated anhydrous DCM (0.8 mL) adding. The resulting mixture was stirred at 45 °C (oil bath temperature) in a sealed vial under argon atmosphere for 12 hours before concentration under reduced pressure. The crude material was purified by silica gel flash chromatography (pet. ether/EtOAc = 10:1) to provide the title compound (9.5 mg, yield 61 %) as a colourless oil. **R_f**: 0.60 (pet. ether/EtOAc = 5:1). **¹H NMR** (500 MHz, CDCl₃): δ 7.69 – 7.62 (m, 4H), 7.45 – 7.34 (m, 6H), 6.74 (s, 1H, H-7), 4.18 – 4.11 (m, overlapped, 3H, H-10, H-12), 3.63 (dd, *J* = 10.2, 4.7 Hz, 1H, H-11a), 3.54 (dd, *J* = 10.2, 6.7 Hz, 1H, H-11b), 3.39 (dd, *J* = 14.5, 4.0 Hz, 1H, H-9a), 3.11 (dd, *J* = 14.5, 7.8 Hz, 1H, H-9b), 2.75 (t, *J* = 7.2 Hz, 2H, H-5), 2.33 (t, *J* = 7.0 Hz, 2H, H-2), 1.77 – 1.66 (m, 4H, H-3, H-4), 1.25 (t, *J* = 7.1 Hz, 3H, H-13), 1.05 (s, 9H), 0.76 (s, 9H), -0.15 (s, 3H), -0.25 (s, 3H). **¹³C NMR** (125 MHz, CDCl₃): δ 173.7 (C-1), 167.1 (C-8), 156.4 (C-6), 135.62, 135.59, 133.30, 129.67, 129.65, 127.684, 127.678, 112.5 (C-7), 72.8 (C-10), 67.4 (C-11), 60.3 (C-12), 38.6 (C-9), 34.2 (C-2), 31.2 (C-5), 28.8 (C-4), 26.9, 25.8, 24.6 (C-3), 19.2, 18.0, 14.3 (C-13), -4.8, -5.3. **FTIR** (thin film) ν 2954, 2929, 2857, 1735, 1472, 1462, 1428, 1254, 1186, 1112, 1075, 836, 824, 805, 777, 740, 702, 690, 505, 493 cm⁻¹. **HRMS** (ESI): Calculated for C₃₅H₅₄NO₄SSi₂⁺ [M+H]⁺ 640.3307; found 640.3266. [α]_D²⁶ -111.1 (*c* = 0.45, DCM).

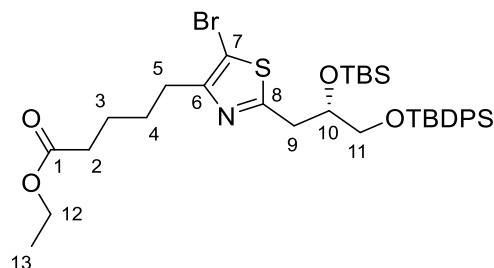
Preparation of 2-(6-oxo-3,6-dihydro-2*H*-pyran-2-yl)ethyl 5-(2-((*S*)-2-((*tert*-butyldimethylsilyl)oxy)-3-((*tert*-butyldiphenylsilyl)oxy)propyl)thiazol-4-yl)pentanoate, **393**



To a solution of Mol-DalPhosAuOMs **257** (26.0 mg, 0.0344 mmol, 0.01 equiv.) in anhydrous deoxygenated DCM (7.0 mL) was added alkyne **364** (862 mg, 3.44 mmol, 1.03 equiv.). The resulting mixture was stirred at room temperature under argon atmosphere for 30 minutes. Then a solution of 8-methylquinoline *N*-oxide **254** (712 mg, 4.47 mmol, 1.34 equiv.) and methanesulfonic acid (268 μ L, 4.13 mmol, 1.24 equiv.) in degassed anhydrous DCM (6.9 mL) was added to the reaction mixture via a syringe pump under argon atmosphere in 9 hours. Upon completion, the reaction mixture was further stirred for 1 hour before a solution of thioamide **382** (1.63 g, 3.34 mmol, 1.0 equiv.) in deoxygenated anhydrous deoxygenated DCM (22 mL) adding. The resulting mixture was stirred at 45 °C in a sealed vial for 72 hours under argon atmosphere before concentration under reduced pressure. The crude material was purified by silica gel flash chromatography (pet. ether/EtOAc = 3:2) to provide the title compound (1.31 g, yield 52%, BRSM yield 57%) as a yellow oil. *R_f*: 0.52 (pet. ether/EtOAc = 1:1). ¹H NMR (500 MHz, CDCl₃): δ 7.69 – 7.62 (m, 4H), 7.46 – 7.33 (m, 6H), 6.94 – 6.82 (m, 1H, H-14), 6.75 (s, 1H, H-7), 6.04 (dt, *J* = 9.9, 1.7 Hz, 1H, H-13), 4.61 – 4.50 (m, 1H, H-16), 4.35 – 4.22 (m, 2H, H-18), 4.17 – 4.09 (m, 1H, H-10), 3.63 (dd, *J* = 10.2, 4.7 Hz, 1H, H-11a), 3.53 (dd, *J* = 10.2, 6.7 Hz, 1H, H-11b), 3.39 (dd, *J* = 14.5, 3.9 Hz, 1H, H-9a), 3.11 (dd, *J* = 14.6, 7.8 Hz, 1H, H-9b), 2.75 (t, *J* = 7.1 Hz, 2H, H-5), 2.43 – 2.31 (m, 2H, H-15), 2.34 (t, *J* = 6.9 Hz, 2H, H-2), 2.16 – 2.09 (m, 1H, H-17a), 2.04 – 1.95 (m, 1H, H-17b), 1.78 – 1.64 (m, 4H, H-3, H-4), 1.05 (s, 9H), 0.76 (s, 9H), -0.15 (s, 3H), -0.25 (s, 3H). ¹³C NMR (125 MHz, CDCl₃): δ 173.4 (C-1), 167.2 (C-8), 163.9 (C-12), 156.3 (C-6), 144.73, 144.72 (C-14), 135.59, 135.56, 133.4, 133.3, 129.65, 129.63, 127.66, 127.65, 121.5 (C-13), 112.6 (C-14), 74.7 (C-16), 72.7 (C-10), 67.3 (C-11), 59.8 (C-18), 38.6 (C-9), 34.02 (C-17), 33.97 (C-2), 31.2 (C-5), 29.4 (C-15), 28.7 (C-4), 26.8, 25.7, 24.5 (C-3), 19.2, 17.9, -4.8, -5.3.

FTIR (thin film) ν 2953, 2929, 2856, 1731, 1472, 1462, 1428, 1389, 1361, 1248, 1155, 1111, 1061, 1006, 998, 938, 835, 822, 776, 739, 701, 690, 662, 622, 614, 505, 489 cm^{-1} . **HRMS** (ESI): Calculated for $\text{C}_{40}\text{H}_{58}\text{NO}_6\text{SSi}_2^+$ $[\text{M}+\text{H}]^+$ 736.3518; found 736.3494. $[\alpha]_D^{25}$ -14.3 ($c = 1.05$, DCM).

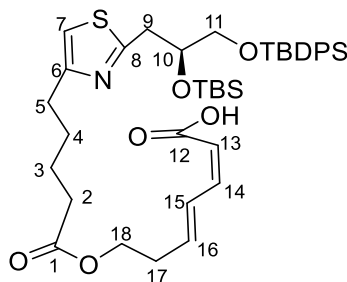
Preparation of ethyl (S)-5-(5-bromo-2-(2-((*tert*-butyldimethylsilyl)oxy)-3-((*tert*-butyldiphenylsilyl)oxy)propyl)thiazol-4-yl)pentanoate, **394**



To a solution of thiazole **392** (7.6 mg, 0.012 mmol, 1.0 equiv.) in anhydrous DCM (0.2 mL) was added *N*-bromosuccinimide (2.1 mg, 0.012 mmol, 1.0 equiv.). The reaction mixture was stirred at room temperature for 20 hours. Solvent was then removed under reduced pressure and at 40 °C, the crude material was purified by flash silica chromatography (pet. ether/EtOAc = 13/1) to afford the title compound as a colourless oil (4.8 mg, yield 56%). **R_f**: 0.57 (pet. ether/EtOAc = 5:1). **¹H NMR** (500 MHz, CDCl_3): δ 7.67 – 7.60 (m, 4H), 7.45 – 7.34 (m, 6H), 4.14 – 4.08 (m, overlapped, 3H, H-10, H-12), 3.60 (dd, $J = 10.2, 4.7$ Hz, 1H, H-11a), 3.51 (dd, $J = 10.2, 7.0$ Hz, 1H, H-11b), 3.30 (dd, $J = 14.7, 4.1$ Hz, 1H, H-9a), 3.11 (dd, $J = 14.7, 7.0$ Hz, 1H, H-9b), 2.74 – 2.67 (m, 2H, H-5), 2.35 – 2.30 (m, 2H, H-2), 1.72 – 1.65 (m, 4H, H-3, H-4), 1.25 (t, $J = 7.1$ Hz, 3H, H-13), 1.04 (s, 9H), 0.79 (s, 9H), -0.13 (s, 3H), -0.18 (s, 3H). **¹³C NMR** (125 MHz, CDCl_3): δ 173.6 (C-1), 166.9 (C-8), 154.4 (C-6), 135.56, 135.53, 133.6, 129.70, 129.68, 127.69, 127.67, 103.0 (C-7), 72.2 (C-10), 66.8 (C-22), 60.2 (C-12), 39.0 (C-9), 34.1 (C-2), 29.1 (C-5), 28.3 (C-4), 26.8, 25.7, 24.6 (C-3), 19.2, 18.0, 14.3 (C-13), -4.8, -5.2. **FTIR** (thin film) ν 2953, 2929, 2857, 1735, 1472, 1462, 1428, 1361, 1256, 1184, 1112, 1080, 1007, 837, 824, 804, 777, 738, 702, 692, 504, 492 cm^{-1} . **HRMS** (ESI): Calculated for $\text{C}_{35}\text{H}_{53}\text{BrNO}_4\text{SSi}_2^+$ $[\text{M}+\text{H}]^+$ 718.2412; found 718.2239. $[\alpha]_D^{24}$ -9.9 ($c = 0.24$, DCM).

6.3.5 Synthesis of Macrocyclic Alcohol **441**

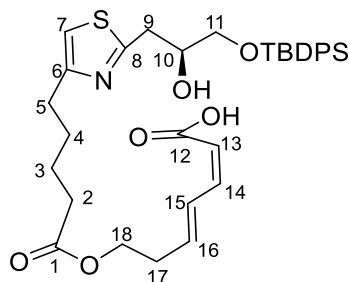
Preparation of (2*Z*,4*E*)-7-((5-(2-((*S*)-2-((*tert*-butyldimethylsilyl)oxy)-3-((*tert*-butyldiphenylsilyl)oxy)propyl)thiazol-4-yl)pentanoyl)oxy)hepta-2,4-dienoic acid, **418**



Potassium bis(trimethylsilyl)amide solution (145 μ L, 1.0 M in THF, 0.145 mmol, 1.3 equiv.) was added dropwise to a solution of thiazole **393** (82.2 mg, 0.112 mmol, 1.0 equiv.) in anhydrous THF (2.0 mL) at $-78\text{ }^{\circ}\text{C}$. The reaction mixture was stirred at that temperature under argon atmosphere for 2 hours. Aqueous sulfuric acid (193 μ L, 2 vol%) was added to the reaction mixture dropwise at $-78\text{ }^{\circ}\text{C}$, and then the resulting mixture was allowed to warm up to room temperature and stir at room temperature for 5 minutes. The mixture was then added ethyl acetate (6 mL) and saturated brine (2 mL). The aqueous phase was extracted by ethyl acetate (3×5 mL). The combined organic phase was dried with anhydrous Na_2SO_4 , filtered, and then concentrated by rotary evaporation. The crude material was purified by flash silica chromatography (pet. ether/EtOAc = 4/1) to afford the title compound as a colourless oil (49.0 mg, yield 60%). **R_f**: 0.27 (pet. ether/EtOAc = 5:1). **¹H NMR** (500 MHz, CDCl_3): δ 7.68 – 7.64 (m, 4H), 7.45 – 7.35 (m, overlapped, 7H), 6.75 (s, 1H, H-7), 6.58 (t, J = 11.3 Hz, 1H, H-14), 6.04 (dt, J = 15.5, 6.4 Hz, 1H, H-16), 5.62 (d, J = 11.4 Hz, 1H, H-13), 4.20 (t, J = 5.7 Hz, 2H, H-18), 4.14 (tt, J = 7.9, 4.2 Hz, 1H, H-10), 3.62 (dd, J = 10.2, 4.5 Hz, 1H, H-11a), 3.53 (dd, J = 10.2, 6.9 Hz, 1H, H-11b), 3.47 (dd, J = 14.5, 3.9 Hz, 1H, H-9a), 3.19 (dd, J = 14.4, 7.9 Hz, 1H, H-9b), 2.77 (t, J = 6.8 Hz, 2H, H-5), 2.54 – 2.48 (m, 2H, H-17), 2.34 (t, J = 6.7 Hz, 2H, H-2), 1.75 – 1.68 (m, 4H, H-3, H-4), 1.05 (s, 9H), 0.75 (s, 9H), -0.17 (s, 3H), -0.25 (s, 3H). **¹³C NMR** (125 MHz, CDCl_3): δ 173.5 (C-1), 169.6 (C-12), 168.1 (C-8), 156.1 (C-6), 144.6 (C-14), 139.3 (C-16), 135.59, 135.58, 133.4, 133.3, 129.65, 129.62, 129.2 (C-15), 127.67, 127.66, 117.3 (C-13), 112.9 (C-7), 72.6 (C-10), 67.2 (C-11), 62.4 (C-18), 38.1 (C-9), 34.2 (C-2), 31.8 (C-17), 30.7 (C-5), 29.2 (C-3), 26.8, 25.8, 24.6 (C-4), 19.2, 17.9, -4.9, -5.4. **FTIR**

(thin film) ν 3070, 3050, 2953, 2929, 2893, 2857, 1736, 1695, 1640, 1602, 1525, 1471, 1463, 1428, 1389, 1361, 1252, 1186, 1112, 1076, 999, 965, 940, 836, 825, 805, 777, 740, 703, 614, 505, 492 cm^{-1} . **HRMS** (ESI): Calculated for $\text{C}_{40}\text{H}_{58}\text{NO}_6\text{SSi}_2^+$ $[\text{M}+\text{H}]^+$ 736.3518; found 735.3446. $[\alpha]_D^{23} -13.7$ ($c = 0.99$, DCM).

Preparation of (2*Z*,4*E*)-7-((5-(2-((*S*)-3-((*tert*-butyldiphenylsilyl)oxy)-2-hydroxypropyl)thiazol-4-yl)pentanoyl)oxy)hepta-2,4-dienoic acid, **419**



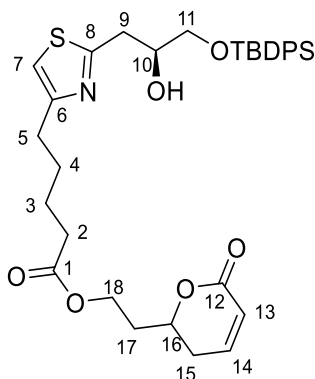
Method A: (Use bis-silylated compound **418** as the starting material)

Pyridinium *p*-toluenesulfonate (156 mg, 0.63 mmol, 10.0 equiv.) was added to a solution of acid **418** (46 mg, 0.063 mmol, 1.0 equiv.) in MeOH (4.5 mL). The reaction mixture was stirred at 45 – 50 °C for 27 hours. Upon completion, the reaction mixture was concentrated under reduced pressure and the residue was directly loaded onto a silica column and purified by flash chromatography using pet. ether/EtOAc = 2/1 as eluent to afford the title compound as a colourless oil (11.9 mg, yield 30%, BRSM 43%). **R_f**: 0.56 (pet. ether/EtOAc = 1/1). **¹H NMR** (500 MHz, CDCl_3): δ 7.68 – 7.62 (m, 4H), 7.45 – 7.32 (m, overlapped, 7H), 6.79 (s, 1H, H-7), 6.59 (t, $J = 11.4$ Hz, 1H, H-14), 6.06 (dt, $J = 15.1$, 6.2 Hz, 1H, H-16), 5.59 (d, $J = 11.4$ Hz, 1H, H-13), 4.22 (t, $J = 5.8$ Hz, 2H, H-18), 4.15 – 4.07 (m, 1H, H-10), 3.72 (dd, $J = 10.3$, 5.5 Hz, 1H, H-11a), 3.67 (dd, $J = 9.7$, 5.3 Hz, 2H, H-11b), 3.31 (dd, $J = 15.6$, 3.1 Hz, 1H, H-9a), 3.20 (dd, $J = 15.1$, 8.7 Hz, 1H, H-9b), 2.74 (t, $J = 7.0$ Hz, 2H, H-5), 2.55 – 2.49 (m, 2H, H-17), 2.35 (t, $J = 6.6$ Hz, 2H, H-2), 1.76 – 1.63 (m, 4H, H-3, H-4), 1.07 (s, 9H). **¹³C NMR** (125 MHz, CDCl_3): δ 173.6 (C-1), 170.1 (C-12), 167.7 (C-8), 156.1 (C-6), 145.4 (C-14), 140.0 (C-16), 135.52, 135.51, 133.10, 133.07, 129.76, 129.75, 129.1 (C-15), 127.74, 127.72, 116.8 (C-13), 112.8 (C-7), 71.3 (C-10), 66.8 (C-11), 62.5 (C-18), 36.3 (C-9), 34.0 (C-2), 31.9 (C-17), 30.6 (C-5), 28.8 (C-4), 26.8, 24.4 (C-3), 19.2. **FTIR** (thin film) ν 3391, 3069, 2929, 2857, 1733, 1640, 1602, 1525, 1461, 1428, 1389, 1361, 1185, 1112, 999, 964, 939, 859, 824, 741, 703, 614, 593, 506, 434, 418 cm^{-1} . **HRMS** (ESI): Calculated for $\text{C}_{40}\text{H}_{58}\text{NO}_6\text{SSi}_2^+$ $[\text{M}+\text{H}]^+$ 622.2659; found 622.2625. $[\alpha]_D^{24} -9.0$ ($c = 0.69$, DCM).

Method B: (Use mono-silylated compound **422** as the starting material)

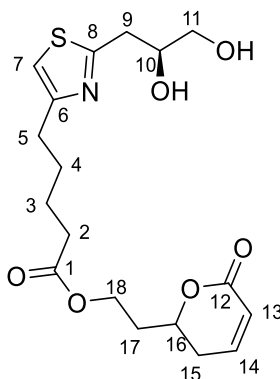
Potassium bis(trimethylsilyl)amide solution (88 μL , 0.5 M in toluene, 0.044 mmol, 2.3 equiv.) was added dropwise to a solution of thiazole **422** (12 mg, 0.019 mmol, 1.0 equiv.) in anhydrous THF (0.8 mL) at $-78\text{ }^{\circ}\text{C}$. The reaction mixture was stirred at that temperature under argon atmosphere for 1 hours. Aqueous sulfuric acid (60 μL , 2 vol%) was added to the reaction mixture dropwise at $-78\text{ }^{\circ}\text{C}$, and then the resulting mixture was allowed to warm up to room temperature and stir at room temperature for 5 minutes. The mixture was then added ethyl acetate (3 mL) and saturated brine (3 mL). The aqueous phase was extracted by ethyl acetate ($3 \times 5\text{ mL}$). The combined organic phase was dried with anhydrous Na_2SO_4 , filtered, and then concentrated by rotary evaporation. The crude material was purified by flash silica chromatography (pet. ether/EtOAc = 4/1) to afford the title compound as a colourless oil (4.3 mg, yield 36%). **R_f**: 0.65 (pet. ether/EtOAc = 2:3). **¹H NMR** (500 MHz, CDCl_3): δ 7.68 – 7.62 (m, 4H), 7.47 – 7.34 (m, overlapped, 7H), 6.80 (s, 1H, H-7), 6.58 (t, $J = 11.4\text{ Hz}$, 1H, H-14), 6.05 (dt, $J = 13.9, 6.2\text{ Hz}$, 1H, H-16), 5.59 (d, $J = 11.4\text{ Hz}$, 1H, H-13), 4.22 (t, $J = 6.0\text{ Hz}$, 2H, H-18), 4.15 – 4.08 (m, 1H, H-10), 3.72 (dd, $J = 10.4, 5.2\text{ Hz}$, 1H, H-11a), 3.67 (dd, $J = 9.7, 5.3\text{ Hz}$, 2H, H-11b), 3.31 (dd, $J = 15.6, 3.1\text{ Hz}$, 1H, H-9a), 3.21 (dd, $J = 15.1, 8.7\text{ Hz}$, 1H, H-9b), 2.74 (t, $J = 7.0\text{ Hz}$, 2H, H-5), 2.55 – 2.49 (m, 2H, H-17), 2.35 (t, $J = 6.8\text{ Hz}$, 2H, H-2), 1.76 – 1.63 (m, 4H, H-3, H-4), 1.07 (s, 9H). **¹³C NMR** (125 MHz, CDCl_3): δ 173.6 (C-1), 170.1 (C-12), 167.7 (C-8), 156.1 (C-6), 145.4 (C-14), 140.0 (C-16), 135.52, 135.51, 133.10, 133.07, 129.76, 129.75, 129.1 (C-15), 127.74, 127.72, 116.8 (C-13), 112.8(C-7), 71.3 (C-10), 66.8 (C-11), 62.5 (C-18), 36.3 (C-9), 34.0 (C-2), 31.9 (C-17), 30.6 (C-5), 28.8 (C-4), 26.8, 24.4 (C-3), 19.2.

Preparation of 2-(6-oxo-3,6-dihydro-2H-pyran-2-yl)ethyl 5-(2-((S)-3-((tert-butyl)diphenylsilyl)oxy)-2-hydroxypropyl)thiazol-4-yl)pentanoate, 422



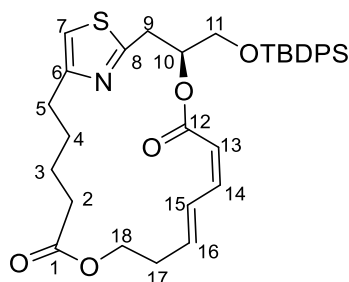
Acetic acid (0.25 mL, 4.43 mmol, 200 equiv.) was added in one portion to a biphasic solution of the thiazole **393** (16.5 mg, 0.022 mmol, 1.0 equiv.) in THF-H₂O (v/v = 1/1, 0.25 mL) and the mixture was stirred at 50 °C for 3 hours. Then the reaction mixture was allowed to cool down to 0 °C and quenched by slow addition of saturated NaHCO₃ solution (10 mL). Then the aqueous phase was separated and extracted by ethyl acetate (3 × 5 mL). The combined organic phase was dried with anhydrous Na₂SO₄, filtered, and then concentrated by rotary evaporation. The crude material was purified by flash silica chromatography (pet. ether/EtOAc = 1/2) to afford the title compound as a colourless oil (4.2 mg, yield 30%, BRSM yield 100%). **R_f**: 0.14 (pet. ether/EtOAc = 1:1). **¹H NMR** (500 MHz, CDCl₃): δ 7.67 – 7.62 (m, 4H), 7.46 – 7.34 (m, 6H), 6.90 – 6.85 (m, 1H, H-14), 6.84 (s, 1H, H-7), 6.03 (d, *J* = 9.7 Hz, 1H, H-13), 4.61 – 4.51 (m, 1H, H-16), 4.33 – 4.20 (m, 2H, H-18), 4.17 – 4.10 (m, 1H, H-10), 3.71 (dd, *J* = 9.9, 5.7 Hz, 1H, H-11a), 3.66 (dd, *J* = 9.9, 5.7 Hz, 1H, H-11b), 3.34 (d, *J* = 14.7 Hz, 1H, H-9a), 3.20 (dd, *J* = 15.1, 8.4 Hz, 1H, H-9b), 2.78 (t, *J* = 7.1 Hz, 2H, H-5), 2.43 – 2.28 (m, overlapped, 4H, H-2, H-15), 2.15 – 2.05 (m, 1H, H-17a), 2.03 – 1.94 (m, 1H, H-17b), 1.77 – 1.61 (m, 4H, H-3, H-4), 1.07 (s, 9H). **¹³C NMR** (125 MHz, CDCl₃): δ 173.3 (C-1), 168.1 (C-8), 163.9 (C-12), 154.9 (C-6), 144.8 (C-14), 135.5, 133.0, 129.8, 127.8, 121.5 (C-13), 113.1 (C-7), 74.7 (C-16), 70.9 (C-10), 66.6 (C-11), 59.9 (C-18), 35.9 (C-9), 34.0 (C-17), 33.8 (C-2), 30.3 (C-5), 29.4 (C-15), 28.3 (C-4), 26.8, 24.3 (C-3), 19.2. **FTIR** (thin film) ν 3353, 3071, 3049, 2930, 2857, 1735, 1731, 1701, 1697, 1654, 1648, 1523, 1472, 1460, 1427, 1389, 1362, 1307, 1245, 1178, 1154, 1112, 1059, 1041, 998, 958, 862, 820, 741, 703, 691, 622, 615, 554, 505, 490, 468, 451, 434 cm⁻¹. **HRMS** (ESI): Calculated for C₃₄H₄₄NO₆SSi₂⁺ [M+H]⁺ 622.2653; found 622.2667. [α]_D²¹ –6.4 (*c* = 0.55, DCM).

Preparation of 2-(6-oxo-3,6-dihydro-2H-pyran-2-yl)ethyl 5-(2-((S)-2,3-dihydroxypropyl)thiazol-4-yl)pentanoate, 423



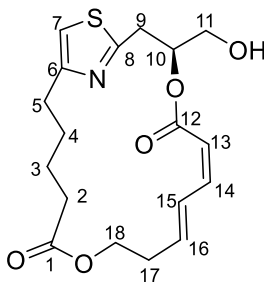
To a solution of **393** (106 mg, 0.144 mmol, 1.0 equiv.) in THF-pyridine (v/v = 4/1, 6.25 mL) was added HF-pyridine (375 μ L) at 0 °C. Then the reaction mixture was stirred for 17 hours at room temperature. Then the reaction was quenched by slow addition of saturated NaHCO₃ aqueous solution (5 mL) at ice-water bath. Then the aqueous layers were separated and extracted by ethyl acetate (3 \times 10 mL). The combined organic phase was dried with anhydrous Na₂SO₄, filtered, and then concentrated by rotary evaporation. The crude material was purified by flash silica chromatography (EtOAc/MeOH = 20/1) to afford the title compound as a colourless oil (31.6 mg, yield 57%). **R_f**: 0.5 (EtOAc/MeOH = 10:1). **¹H NMR** (500 MHz, CDCl₃) δ 6.89 (dt, *J* = 9.2, 3.8 Hz, 1H, H-14), 6.78 (s, 1H, H-7), 6.04 (d, *J* = 10.2 Hz, 1H, H-13), 4.56 (tt, *J* = 9.5, 5.2 Hz, 1H, H-16), 4.33 – 4.19 (m, 2H, H-18), 4.17 – 4.06 (m, 1H, H-10), 3.72 (dd, *J* = 11.5, 3.8 Hz, 1H, H-11a), 3.61 (dd, *J* = 11.4, 5.6 Hz, 1H, H-11b), 3.14 (d, *J* = 6.0 Hz, 2H, H-9), 2.75 (t, *J* = 7.3 Hz, 2H, H-5), 2.40 – 2.36 (m, 2H, H-15), 2.34 (t, *J* = 7.2 Hz, 2H, H-2), 2.16 – 2.06 (m, 1H, H-17a), 2.03 – 1.94 (m, 1H, H-17b), 1.74 – 1.58 (m, 4H, H-3, H-4). **¹³C NMR** (125 MHz, CDCl₃) δ 173.4 (C-1), 167.2 (C-8), 164.0 (C-12), 156.4 (C-6), 144.9 (C-14), 121.5 (C-13), 112.6 (C-7), 74.8 (C-16), 70.8 (C-10), 65.7 (C-11), 59.9 (C-18), 36.0 (C-9), 34.0 (C-17), 33.9 (C-2), 30.8 (C-5), 29.4 (C-15), 28.5 (C-4), 24.3 (C-3). **FTIR** (thin film) ν 3356, 2929, 2867, 1719, 1523, 1459, 1422, 1390, 1362, 1251, 1178, 1125, 1093, 1039, 961, 820 cm⁻¹. **HRMS** (ESI): Calculated for C₁₈H₂₆NO₆S⁺ [M+H]⁺ 384.1475; found 384.1485. [α]_D²² +5.2 (*c* = 0.42, DCM).

Preparation of (*S*,1²*Z*,6*Z*,8*E*)-3-(((*tert*-butyldiphenylsilyl)oxy)methyl)-4,12-dioxal(2,4)-thiazolacycloheptadecaphane-6,8-diene-5,13-dione, 440



To a mixture of acid **419** (12.9 mg, 0.0203 mmol, 1.0 equiv.) and solid NaHCO₃ (419 mg, 4.99 mmol, 246 equiv.) in anhydrous DCM (36 mL) was added 2-bromo-1-ethylpyridinium tetrafluoroborate **130** (141 mg, 0.50 mmol, 24.6 equiv.). The reaction mixture was stirred in dark under argon atmosphere at room temperature for 19 hours. The reaction was quenched by addition of distilled water (3.9 mL). The aqueous phase was separated and extracted by ethyl acetate (4 × 8 mL). The combined organic phase was dried with anhydrous Na₂SO₄, filtered, and then concentrated by rotary evaporation. The crude material was purified by flash silica chromatography (pet. ether/EtOAc = 2/1) to afford the title compound as a colorless oil (9.4 mg, yield 75%). **R_f**: 0.73 (pet. ether/EtOAc = 1:1). **¹H NMR** (600 MHz, CDCl₃): δ 7.70 – 7.64 (m, 4H), 7.45 – 7.36 (m, 6H), 7.19 (dd, *J* = 15.4, 11.3 Hz, 1H, H-15), 6.73 (s, 1H, H-7), 6.46 (t, *J* = 11.4 Hz, 1H, H-14), 5.93 (ddd, *J* = 15.3, 8.9, 5.6 Hz, 1H, H-16), 5.51 – 5.47 (m, overlapped, 2H, H-10, H-13), 4.26 (td, *J* = 10.6, 10.1, 2.8 Hz, 1H, H-18a), 4.22 – 4.18 (m, 1H, H-18b), 3.84 (dd, *J* = 10.8, 5.1 Hz, 1H, H-11a), 3.79 (dd, *J* = 10.8, 4.8 Hz, 1H, H-11b), 3.33 (dd, *J* = 14.6, 2.7 Hz, 1H, H-9a), 3.25 (dd, *J* = 14.7, 11.0 Hz, 1H, H-9b), 2.76 (dt, *J* = 13.7, 6.3 Hz, 1H, H-5a), 2.64 (dt, *J* = 15.0, 7.7 Hz, 1H, H-5b), 2.52 – 2.45 (m, 1H, H-17a), 2.44 – 2.36 (m, 1H, H-17b), 2.29 (t, *J* = 7.6 Hz, 2H, H-2), 1.76 (dt, *J* = 14.5, 7.5 Hz, 1H, H-4a), 1.66 (dt, *J* = 13.9, 6.8 Hz, 1H, H-4b), 1.56 – 1.49 (m, 2H, H-3), 1.07 (s, 9H). **¹³C NMR** (150 MHz, CDCl₃): δ 173.4 (C-1), 165.8 (C-12), 164.7 (C-8), 156.6 (C-6), 144.8 (C-14), 140.1 (C-16), 135.61, 135.56, 133.13, 133.10, 129.8, 129.5 (C-15), 127.8, 127.7, 116.1 (C-13), 113.1 (C-7), 72.7 (C-10), 65.3 (C-11), 61.8 (C-18), 35.2 (C-9), 34.6 (C-2), 32.6 (C-17), 30.8 (C-5), 28.2 (C-4), 26.8, 24.1 (C-3), 19.3. **FTIR** (thin film) ν 2954, 2931, 2858, 1723, 1640, 1602, 1523, 1472, 1461, 1428, 1388, 1361, 1260, 1228, 1173, 1114, 1091, 998, 964, 823, 742, 703, 615, 505 cm⁻¹. **HRMS** (ESI): Calculated for C₃₄H₄₂NO₅SSi₂⁺ [M+H]⁺ 604.2547; found 604.2519. [α]_D²⁵ –32.5 (*c* = 0.07, DCM).

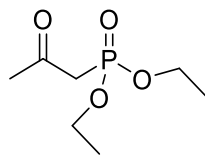
Preparation of (*S*,12*Z*,6*Z*,8*E*)-3-(hydroxymethyl)-4,12-dioxo-1(2,4)-thiazolacycloheptadecaphane-6,8-diene-5,13-dione, **441**



To a solution of macrocyclic compound **440** (35.7 mg, 0.059 mmol, 1.0 equiv.) and acetic acid (16.4 μ L, 0.286 mmol, 4.85 equiv.) in anhydrous THF (3.0 mL) was slowly added tetrabutylammonium fluoride (118 μ L, 1.0 M in THF, 0.118 mmol, 2.0 equiv.) over 20 minutes at 0 °C. Then the reaction mixture was allowed to warm up to room temperature and stirred at room temperature for 17 hours. The reaction mixture was then diluted with ethyl acetate (20 mL) and added saturated aqueous NaHCO₃ solution (2 mL). The aqueous phase was separated and extracted by ethyl acetate (3 \times 5 mL). The combined organic phase was dried with anhydrous Na₂SO₄, filtered, and then concentrated by rotary evaporation. The crude material was purified by flash silica chromatography (pet. ether/EtOAc = 1/2) to afford the title compound (18.5 mg, yield 86%) as a colourless oil. **R_f**: 0.25 (pet. ether/EtOAc = 1/2). **¹H NMR** (500 MHz, CDCl₃) δ 7.17 (dd, *J* = 15.7, 11.7 Hz, 1H, H-15), 6.73 (s, 1H, H-7), 6.48 (t, *J* = 11.3 Hz, 1H, H-14), 5.95 (ddd, *J* = 15.0, 8.7, 5.6 Hz, 1H, H-16), 5.51 (d, *J* = 11.3 Hz, 1H, H-13), 5.49 – 5.44 (m, 1H, H-10), 4.30 – 4.25 (m, 1H, H-18a), 4.20 – 4.15 (m, 1H, H-18b), 3.86 (dd, *J* = 11.9, 4.0 Hz, 1H, H-11a), 3.81 (dd, *J* = 11.9, 5.3 Hz, 1H, H-11b), 3.30 – 3.26 (m, 2H, H-9), 2.78 (dt, *J* = 13.2, 6.3 Hz, 1H, H-5a), 2.64 (dt, *J* = 14.8, 7.6 Hz, 1H, H-5b), 2.53 – 2.37 (m, 2H, H-17), 2.28 (t, *J* = 7.6 Hz, 2H, H-2), 1.81 – 1.60 (m, 2H, H-4), 1.52 – 1.48 (m, 2H, H-3). **¹³C NMR** (125 MHz, CDCl₃) δ 173.4 (C-1), 165.3 (C-12), 164.9 (C-8), 156.7 (C-6), 145.3 (C-14), 140.6 (C-16), 129.2 (C-15), 115.6 (C-13), 113.2 (C-7), 73.1 (C-10), 64.4 (C-11), 61.7 (C-18), 34.7 (C-9), 34.6 (C-2), 32.5 (C-17), 30.8 (C-5), 28.2 (C-4), 24.0 (C-3). **FTIR** (thin film) ν 3355, 2923, 2854, 1719, 1639, 1602, 1524, 1458, 1420, 1380, 1260, 1172, 1131, 1057, 1002, 964, 817, 759 cm⁻¹. **HRMS** (ESI): Calculated for C₁₈H₂₄NO₅S⁺ [M+H]⁺ 366.1370; found 366.1346. [α]_D²⁵ –137 (*c* = 0.125, DCM).

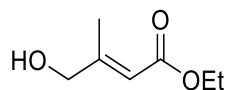
6.3.5 Synthesis of the Side Chain Fragments

Preparation of diethyl (2-oxopropyl)phosphonate, **468**



To a stirred suspension of potassium iodide (22.9 g, 138 mmol, 1.1 equiv.) in acetone/acetonitrile (50 mL/50 mL) was added chloroacetone **469** (10 mL, 125 mmol, 1 equiv.) The mixture was stirred in dark at room temperature for 1 hour, then triethyl phosphite (23.8 mL, 138 mmol, 1 equiv.) was added dropwise over 30 min *via* a dropping funnel. The mixture was stirred at room temperature for 13 hours, then filtered through a plug of Celite and the filtrate was concentrated under reduced pressure. The crude material was then dissolved in 100 mL distilled water and the solution was carefully adjusted to pH 9 to 10 with solid lithium carbonate. Then the aqueous solution was washed with DCM-hexane (v/v= 5/95, 3 × 100 mL) and then extracted with EtOAc (5 × 100 mL). The combined EtOAc extracts were washed with brine, dried over Na₂SO₄, filtered and then concentrated under vacuum to afford the title compound as a yellow oil (18.3 g, yield 75%). **¹H NMR** (500 MHz, CDCl₃) δ 4.19 – 4.10 (m, 4H), 3.09 (d, *J*_{CH-P} = 22.9 Hz, 2H), 2.32 (s, 3H), 1.34 (t, *J* = 7.1 Hz, 6H). **¹³C NMR** (125 MHz, CDCl₃) δ 199.7 (d, *J*_{C-P} = 6.3 Hz), 62.4, 62.3, 43.10 (d, *J*_{C-P} = 127 Hz), 31.1, 16.10, 16.0. **FTIR** (thin film) ν 2984, 1713, 1392, 1361, 1249, 1163, 1098, 1018, 957, 853, 820, 790, 591, 531, 494, 459 cm⁻¹. **HRMS** (ESI): Calculated for C₇H₁₆O₄P⁺ [M+H]⁺ 195.0781; found 195.0776. These characterisation data match those reported in the literature.³⁵³

Preparation of ethyl (*E*)-4-hydroxy-3-methylbut-2-enoate, **472**



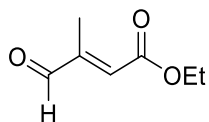
To a solution of alcohol **470** (3.3 mL, purity 90%, 43.6 mmol, 1.0 equiv.) in acetonitrile (100 mL) was added ethyl 2-(triphenyl-λ⁵-phosphaneylidene)acetate **471** (18.3 g, 52.4 mmol, 1.2 equiv.) under nitrogen atmosphere. The reaction was heated at 70 °C for 24 hours and then concentrated under vacuum at room temperature. The residue was slurried with Et₂O for 1 hour and then filtered. The filtrate was then concentrated under vacuum and the crude material was purified by flash silica chromatography (pet. ether/ethyl acetate = 3/1) to afford the title compound as a colourless oil (4.46 g, yield 71%). (**Note:**

The title compound was volatile, therefore the solvents of the product fractions after column chromatography were evaporated at room temperature) **R_f**: 0.60 (pet. ether/EtOAc = 1:1). **¹H NMR** (500 MHz, CDCl₃) δ 6.01 – 5.96 (m, 1H), 4.17 (q, *J* = 7.2 Hz, 2H), 4.16 – 4.12 (m, 2H), 2.09 (s, 3H), 1.28 (t, *J* = 7.1 Hz, 3H). **¹³C NMR** (125 MHz, CDCl₃): δ 166.9, 157.4, 113.5, 66.9, 59.7, 15.5, 14.2. These characterisation data match those reported in the literature.³⁵⁴

Preparation of active manganese dioxide from activated carbon³²⁵

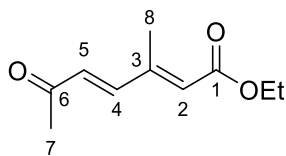
A solution of potassium permanganate (10 g, 0.063 mmol, 1.0 equiv.) in distilled water (250 mL) contained in a one-litre beaker was heated to the boiling point and removed from the source of heat, and then treated with activated carbon (3.13 g, 0.261, 4.1 equiv.) portionwise over 10 minutes. After the complete addition of the activated carbon, the mixture was boiled for another 5 minutes until the purple colour was completely discharged. Then the resulting black suspension was allowed to stand at room temperature for 15 minutes and filtered on a Büchner funnel. The precipitate was washed water (4 × 50 mL) and spread out to dry in the air. The air-dried material was then dried in an oven at 105-110° for 24 hours to afford the oxidant (7.07 g) as a fine powder which could be used directly without grinding.

Preparation of ethyl (*E*)-3-methyl-4-oxobut-2-enoate, **473**



To a solution of alcohol **472** (1.02 g, 7.07 mmol, 1.0 equiv.) in anhydrous DCM (140 mL) was added freshly prepared active manganese dioxide (7.07 g, 71.5 mmol, 10.1 equiv.). Then the reaction mixture was stirred vigorously at room temperature for 1 hour. The reaction mixture was then filtered through a Celite pad and the filtrate was evaporated at room temperature to afford the title product as a yellow oil (0.84 g, yield 82%). **¹H NMR** (500 MHz, CDCl₃) δ 9.54 (s, 1H), 6.49 (q, *J* = 1.8 Hz, 1H), 4.26 (q, *J* = 6.8 Hz, 2H), 2.15 (d, *J* = 1.2 Hz, 3H), 1.33 (t, *J* = 7.2 Hz, 3H). **¹³C NMR** (125 MHz, CDCl₃): δ 194.8, 165.7, 150.6, 135.8, 61.3, 14.4, 11.0. These characterisation data match those reported in the literature.³⁵⁴

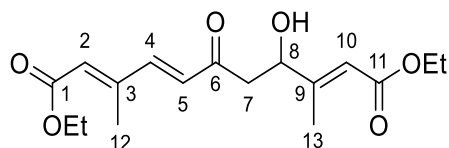
Preparation of ethyl (2*E*,4*E*)-3-methyl-6-oxohepta-2,4-dienoate, **359**



To a solution of aldehyde **473** (13.4 g, 0.094 mol, 1.0 equiv.) in distilled water (187 mL) was added diethyl (2-oxopropyl)phosphonate **468** (18.3 g, 0.094 mol, 1.0 equiv.) and potassium carbonate (26.0 g, 0.188 mol, 2.0 equiv.). The reaction mixture was stirred at room temperature for 18 hours. The reaction mixture was then extracted with Et₂O (3 × 150 mL). The combined organic phase was washed with brine, dried over anhydrous Na₂SO₄, filtered, and then concentrated by rotary evaporation. The crude material was purified by flash silica chromatography (pet. ether/EtOAc = 9/1 to 3/1) to afford the title compound **359** (13.0 g, yield 76%) as a white solid and the by-product **474** (1.10g, yield 3.6%) generated from the undesired aldol reaction as a yellow oil.

359: *R_f*: 0.50 (pet. ether/EtOAc = 1:1). **Melting point**: 48 – 50 °C. **¹H NMR** (500 MHz, CDCl₃) δ 7.10 (d, *J* = 15.0 Hz, 1H, H-4), 6.45 (d, *J* = 15.0 Hz, 1H, H-5), 6.07 (s, 1H, H-2), 4.20 (q, *J* = 7.1 Hz, 2H), 2.33 (s, 3H, H-7), 2.29 (d, *J* = 1.2 Hz, 3H, H-8), 1.30 (t, *J* = 7.1 Hz, 3H). **¹³C NMR** (125 MHz, CDCl₃) δ 198.2 (C-6), 166.1 (C-1), 149.3 (C-3), 145.7 (C-4), 131.4 (C-5), 126.4 (C-2), 60.5, 28.1 (C-7), 14.4, 13.8 (C-8). **FTIR** (thin film) ν 2982, 1712, 1668, 1638, 1605, 1367, 1247, 1230, 1160, 1117, 1045, 985, 893, 836, 602, 537 cm⁻¹. **HRMS** (ESI): Calculated for C₁₀H₁₅O₃⁺ [M+H]⁺ 183.1016; found 183.1015.

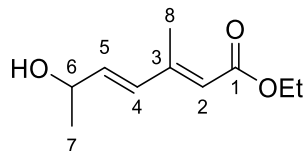
Diethyl (2*E*,4*E*,9*E*)-8-hydroxy-3,9-dimethyl-6-oxoundeca-2,4,9-trienedioate, **474**



R_f: 0.50 (pet. ether/EtOAc = 1:1). **¹H NMR** (500 MHz, CDCl₃) δ 7.16 (d, *J* = 15.0 Hz, 1H, H-4), 6.47 (d, *J* = 15.0 Hz, 1H, H-5), 6.10 – 6.08 (m, 1H, H-2), 6.05 – 6.02 (m, 1H, H-10), 4.60 (d, *J* = 8.3 Hz, 1H, H-8), 4.23 – 4.12 (m, 4H), 3.28 (br. s, 1H, OH), 2.93 – 2.86 (m, 1H, H-7a), 2.80 (dd, *J* = 17.3, 9.3 Hz, 1H, H-7b), 2.27 (d, *J* = 5.0 Hz, 3H, H-12), 2.13 (d, *J* = 5.0 Hz, 3H, H-13), 1.31 – 1.24 (m, 6H). **¹³C NMR** (125 MHz, CDCl₃) δ 199.4 (C-6), 166.8 (C-11), 166.0 (C-1), 157.5 (C-9), 148.8 (C-3), 146.3 (C-4), 130.2 (C-5), 127.3 (C-2), 115.8 (C-10), 72.0 (C-8), 60.5, 59.9, 45.8 (C-7), 15.4 (C-13), 14.4, 14.3, 13.7 (C-12). **FTIR** (thin film) ν 3483, 2981, 1710, 1654, 1597, 1444, 1367, 1353, 1277, 1226,

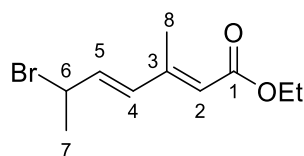
1152, 1093, 1041, 979, 875, 825, 538 cm^{-1} . **HRMS** (ESI): Calculated for $\text{C}_{17}\text{H}_{24}\text{NaO}_6^+$ $[\text{M}+\text{Na}]^+$ 347.1471; found 347.1477.

Preparation of ethyl (2*E*,4*E*)-6-hydroxy-3-methylhepta-2,4-dienoate, **475**



To a solution of ketone **359** (13.0 g, 71.3 mmol, 1.0 equiv.) and cerium (III) chloride heptahydrate (26.8 g, 72.0 mmol, 1.01 equiv.) in methanol (185 mL) was added sodium borohydride (1.89 g, 49.9 mmol, 0.7 equiv.) at 0 °C. Then the reaction mixture was stirred at 0 °C for 2 hours and then quenched by slow addition of distilled water (300 mL). The organic solvent was then removed under reduce pressure and the resulting aqueous mixture was extracted with ethyl acetate (3 × 150 mL). The combined organic phase was washed with brine, dried over anhydrous Na_2SO_4 , filtered, and then concentrated by rotary evaporation to afford the title compound (13.0 g, yield 99%) as a colourless oil, which was used directly for the next step without further purification. **^1H NMR** (500 MHz, CDCl_3) δ 6.26 (d, J = 15.7 Hz, 1H, H-4), 6.11 (dd, J = 15.7, 5.9 Hz, 1H, H-5), 5.76 (s, 1H, H-2), 4.43 (quintet, J = 6.2 Hz, 1H, H-6), 4.16 (q, J = 7.0 Hz, 2H), 2.26 (s, 3H, H-8), 1.89 (br. s, 1H, OH), 1.32 (d, J = 6.4 Hz, 3H, H-7), 1.27 (t, J = 7.0 Hz, 3H). **^{13}C NMR** (125 MHz, CDCl_3) δ 167.0 (C-1), 151.5 (C-3), 139.2 (C-5), 132.4 (C-4), 119.6 (C-2), 68.4 (C-6), 59.8, 23.3 (C-7), 14.3, 13.8 (C-8). **FTIR** (thin film) ν 3401, 2976, 2930, 1708, 1692, 1638, 1611, 1445, 1387, 1366, 1351, 1231, 1226, 1146, 1094, 1039, 966, 942, 875, 827, 545, 462, 419 cm^{-1} . **HRMS** (ESI): Calculated for $\text{C}_{10}\text{H}_{17}\text{O}_3^+$ $[\text{M}+\text{H}]^+$ 185.1172; found 185.1185.

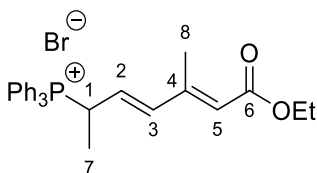
Preparation of ethyl (2*E*,4*E*)-6-bromo-3-methylhepta-2,4-dienoate, **462**



To a solution of alcohol **475** (3.81 g, 0.207 mol, 1.0 equiv.) in anhydrous DCM (5.8 mL) was added dropwise a solution of phosphorus tribromide (0.89 mL, 9.5 mmol, 0.46 equiv.) in anhydrous DCM (5.8 mL) by syringe pump over 30 minutes at 1 – 2 °C. Then the reaction mixture was stirred at that temperature for 3 hours. Upon completion, 60 mL

saturated aqueous NaHCO₃ solution was added slowly to the reaction mixture at 0 – 4 °C. The aqueous phase was then separated and extracted with DCM (3 × 50 mL). The combined organic phase was dried with anhydrous Na₂SO₄, filtered, and then concentrated by rotary evaporation at room temperature to afford the pure title compound as a yellow oil (4.96 g, yield 97%), which was used for the next step without further purification. **¹H NMR** (500 MHz, CDCl₃): δ 6.30 – 6.20 (m, 2H, H-4, H-5), 5.80 (s, 1H, H-2), 4.81 – 4.74 (m, 1H, H-6), 4.18 (q, *J* = 7.1 Hz, 2H), 2.27 (s, 3H, H-8), 1.84 (d, *J* = 6.5 Hz, 3H, H-7), 1.29 (t, *J* = 7.0 Hz, 3H). **¹³C NMR** (125 MHz, CDCl₃): δ 166.6 (C-1), 150.5 (C-3), 137.0 (C-5), 133.8 (C-4), 120.9 (C-2), 59.9, 48.4 (C-6), 25.7 (C-7), 14.3, 13.8 (C-8). **FTIR** (thin film) ν 2979, 1707, 1634, 1612, 1442, 1367, 1354, 1275, 1236, 1148, 1095, 1074, 1042, 1019, 1004, 962, 879, 845, 614, 571, 452 cm⁻¹. **HRMS** (ESI): Calculated for C₁₀H₁₆BrO₂⁺ [M+H]⁺ 247.0328; found 247.0417.

Preparation of ((3*E*,5*E*)-7-ethoxy-5-methyl-7-oxohepta-3,5-dien-2-yl)triphenylphosphonium bromide, **476**



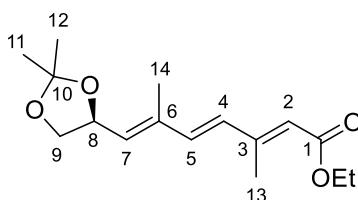
To a solution of bromide **462** (349 mg, 1.41 mmol, 1.0 equiv.) in toluene (1.7 mL) was added triphenylphosphine (378 mg, 1.43 mmol, 1.01 equiv.). The reaction mixture was stirred at room temperature for 48 hours. The precipitate was filtered and washed with Et₂O (3 × 3 mL) to provide the title compound as a white solid. **¹H NMR** (500 MHz, CDCl₃): δ 8.08 – 8.01 (m, 6H), 7.80 – 7.74 (m, 3H), 7.70 – 7.74 (m, 6H), 6.79 (dp, *J* = 15.2, 7.5 Hz, 1H, H-1), 6.65 (dd, *J* = 15.6, 4.9 Hz, 1H, H-3), 5.74 (s, 1H, H-5), 5.70 (dd, *J* = 15.3, 8.0 Hz, 1H, H-2), 4.11 (q, *J* = 7.1 Hz, 2H), 2.02 (s, 3H, H-8), 1.46 (dd, *J* = 19.0, 6.7 Hz, 3H, H-7), 1.26 (t, *J* = 7.4 Hz, 3H). **¹³C NMR** (125 MHz, CDCl₃): δ 166.7 (d, *J*_{C-P} = 1.8 Hz, C-6), 149.4 (d, *J*_{C-P} = 4.3 Hz, C-4), 141.2 (d, *J*_{C-P} = 13.2 Hz, C-3), 134.8 (d, *J*_{C-P} = 3.2 Hz), 134.1 (d, *J*_{C-P} = 9.3 Hz), 130.3 (d, *J*_{C-P} = 12.2 Hz), 126.3 (d, *J*_{C-P} = 7.7 Hz, C-2), 121.8 (d, *J*_{C-P} = 4.0 Hz, C-5), 117.6 (d, *J*_{C-P} = 82.5 Hz), 59.9, 30.4 (d, *J*_{C-P} = 44.6 Hz, C-1), 14.7 (d, *J*_{C-P} = 3.0 Hz, C-7), 14.2, 13.5 (C-8). **FTIR** (thin film) ν 3035, 3009, 2979, 2929, 2817, 1705, 1630, 1608, 1588, 1487, 1459, 1438, 1399, 1365, 1318, 1300, 1286, 1240, 1155, 1110, 1092, 1040, 985, 954, 887, 839, 754, 723, 711, 690, 663, 637, 550, 531, 521, 508,

488, 469, 458, 446 cm^{-1} . **HRMS** (ESI): Calculated for $\text{C}_{28}\text{H}_{30}\text{O}_2\text{P}$ $[\text{M}]^+$ 429.1983; found 429.1988.

Preparation of trienoate **477** and **478**

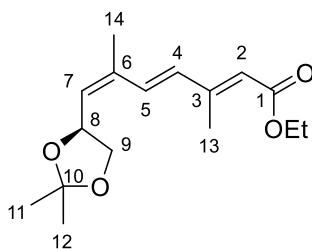
To a solution of phosphonium salt **476** (78 mg, 0.154 mmol, 2.0 equiv.) in anhydrous THF (1.8 mL) was added *n*-BuLi (69 μL , 2.0 M in cyclohexane, 0.139 mmol, 1.8 equiv.) dropwise at $-50\text{ }^\circ\text{C}$. Then the reaction mixture was allowed to room temperature at stirred at room temperature for 2 hours. The resulting orange solution was cooled to $-40\text{ }^\circ\text{C}$ prior to the addition of a solution of aldehyde **322** (10 mg, 0.077 mmol, 1.0 equiv.) in anhydrous THF (0.5 mL). The reaction mixture was then allowed to warm up to $-4\text{ }^\circ\text{C}$ over 2 hours. The reaction was then quenched with saturated NH_4Cl solution (4 mL) and extracted with Et_2O ($3 \times 10\text{ mL}$). The combined organic phase was washed with brine, dried over anhydrous Na_2SO_4 , filtered, and then concentrated by rotary evaporation. The crude material was purified by flash silica chromatography (pet. ether/ EtOAc = 10/1) to afford a 62/38 ratio of **477** and **478** (11.4 mg, yield 53%) as a yellow oil.

Ethyl (2*E*,4*E*,6*E*)-7-((*S*)-2,2-dimethyl-1,3-dioxolan-4-yl)-3,6-dimethylhepta-2,4,6-trienoate, **477**



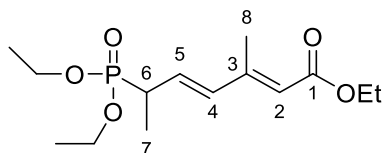
^1H NMR (500 MHz, CDCl_3): δ 6.61 (d, $J = 15.8\text{ Hz}$, 1H, H-5), 6.27 (d, $J = 15.8\text{ Hz}$, 1H, H-4), 5.82 (s, 1H, H-2), 5.68 – 5.64 (m, overlapped, 1H, H-7), 4.97 – 4.90 (m, overlapped, 1H, H-8), 4.17 (q, 2H), 4.14 – 4.10 (m, overlapped, 1H, H-9a), 3.60 – 3.55 (m, overlapped, 1H, H-9b), 2.30 (s, 3H, H-13), 1.87 (s, 3H, H-14), 1.44 (s, overlapped, 3H, H-11 or H-12), 1.41 (s, overlapped, 3H, H-11 or H-12), 1.28 (t, $J = 7.2\text{ Hz}$). **^{13}C NMR** (125 MHz, CDCl_3): δ 167.0 (C-1), 152.0 (C-3), 137.8 (C-5), 137.4 (C-6), 132.3 (C-7), 131.9 (C-4), 119.8 (C-2), 109.3 (C-10), 72.8 (C-8), 69.33 (C-9), 59.7, 26.7 (C-11 or C-12), 25.95 (C-12 or C-11), 14.3, 13.7 (C-13), 12.93 (C-14).

Ethyl (2*E*,4*E*,6*Z*)-7-((*S*)-2,2-dimethyl-1,3-dioxolan-4-yl)-3,6-dimethylhepta-2,4,6-trienoate, 478



¹H NMR (500 MHz, CDCl₃): δ 7.84 (d, *J* = 16.2 Hz, 1H, H-5), 6.61 (d, *J* = 16.2 Hz, 1H, H-4), 5.70 (s, 1H, H-2), 5.68 – 5.64 (m, overlapped, 1H, H-7), 4.97 – 4.90 (m, overlapped, 1H, H-8), 4.16 (q, *J* = 7.2 Hz, 2H), 4.14 – 4.10 (m, overlapped, 1H, H-9a), 3.60 – 3.55 (m, overlapped, 1H, H-9b), 2.02 (s, 3H, H-13), 1.93 (s, 3H, H-14), 1.44 (s, overlapped, 3H, H-11 or H-12), 1.41 (s, overlapped, 3H, H-11 or H-12), 1.29 (t, *J* = 7.2 Hz). **¹³C NMR** (125 MHz, CDCl₃): δ 166.4 (C-1), 150.8 (C-3), 139.1 (C-4), 138.3 (C-6), 132.5 (C-7), 126.1 (C-5), 117.7 (C-2), 109.30 (C-10), 72.89 (C-8), 69.34 (C-9), 59.7, 26.7 (C-11 or C-12), 25.92 (C-12 or C-11), 20.9 (C-13), 13.7, 12.97 (C-14).

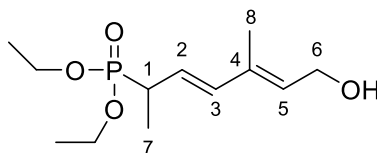
Preparation of ethyl (2*E*,4*E*)-6-(diethoxyphosphoryl)-3-methylhepta-2,4-dienoate, 481



A mixture of bromide **462** (17.5 g, 71.0 mmol, 1.0 equiv.) and triethyl phosphite (36.5 ml, 213 mmol, 3.0 equiv.) was heated at 140 °C with vigorous stirring under argon atmosphere for 23 hours. Then the unreacted triethyl phosphite was removed by oil pump at 70 °C. The residue was purified by flash silica chromatography (pet. ether/EtOAc = 1:1) to afford the title compound (10.8 g, yield 50%) as a yellow oil. **R_f**: 0.20 (pet. ether/EtOAc = 1:1). **¹H NMR** (500 MHz, CDCl₃): δ 6.20 (dd, *J* = 15.8, 4.6 Hz, 1H, H-4), 6.12 – 6.05 (m, 1H, H-5), 5.74 (s, 1H, H-2), 4.16 (q, *J* = 6.9 Hz, 2H), 4.14 – 4.04 (m, 4H), 2.76 (dp, *J* = 21.9, 7.1 Hz, 1H, H-6), 2.27 (s, 3H, H-8), 1.37 – 1.22 (m, 12H, overlapped, H-7). **¹³C NMR** (125 MHz, CDCl₃): δ 167.0 (d, *J*_{C-P} = 1.3 Hz, C-1), 151.5 (d, *J*_{C-P} = 3.8 Hz, C-3), 135.8 (d, *J*_{C-P} = 13.8 Hz, C-4), 132.2 (d, *J*_{C-P} = 10.0 Hz, C-5), 119.5 (d, *J*_{C-P} = 2.5 Hz, C-2), 62.4 (d, *J*_{C-P} = 6.3 Hz), 62.2 (d, *J*_{C-P} = 7.5 Hz), 59.9, 36.3 (d, *J*_{C-P} = 139 Hz, C-6), 16.59 (d, *J*_{C-P} = 0.9 Hz), 16.55 (d, *J*_{C-P} = 0.9 Hz), 14.4, 13.90 (d, *J*_{C-P} = 6.3 Hz, C-7),

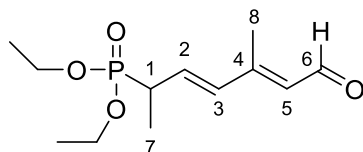
13.89 (C-8). **FTIR** (thin film) ν 2981, 2936, 1708, 1635, 1612, 1444, 1392, 1367, 1353, 1237, 1152, 1096, 1046, 1019, 959, 878, 836, 785, 700, 560, 500, 467 cm^{-1} . **HRMS** (ESI): Calculated for $\text{C}_{14}\text{H}_{26}\text{O}_5\text{P}^+$ $[\text{M}+\text{H}]^+$ 305.1512; found 305.1516.

Preparation of diethyl ((3*E*,5*E*)-7-hydroxy-5-methylhepta-3,5-dien-2-yl)phosphonate, **482**



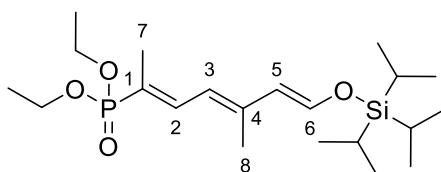
To a solution of ester **481** (521 mg, 1.71 mmol, 1.0 equiv.) in anhydrous DCM (30 mL) was added slowly diisobutylaluminium hydride (4.3 mL, 1.0 M in cyclohexane, 2.5 equiv.) at $-78\text{ }^{\circ}\text{C}$. Then the reaction mixture was stirred at $-78\text{ }^{\circ}\text{C}$ for 1 hour and then quenched by addition of saturated aqueous potassium sodium tartrate (40 mL) solution. The resulting mixture was stirred at room temperature for 2 hours and the aqueous phase was extracted with ethyl acetate ($10 \times 20\text{ mL}$). The combined organic phase was washed with brine, dried over anhydrous Na_2SO_4 , filtered, concentrated under reduced pressure to afford the title compound (446 mg, yield 99%) as a yellow oil. **^1H NMR** (500 MHz, CDCl_3): δ 6.18 (dd, $J = 15.7, 4.5\text{ Hz}$, 1H, H-3), 5.70 – 5.61 (m, 2H, H-2, H-5), 4.28 (d, $J = 6.8\text{ Hz}$, 2H, H-6), 4.13 – 4.01 (m, 4H), 2.70 (dp, $J = 21.9, 7.1\text{ Hz}$, 1H, H-1), 1.79 (s, 3H, H-8), 1.36 – 1.26 (m, 12H, overlapped, H-7). **^{13}C NMR** (125 MHz, CDCl_3): δ 136.4 (d, $J_{\text{C-P}} = 13.6\text{ Hz}$, C-3), 135.7 (d, $J_{\text{C-P}} = 4.1\text{ Hz}$, C-4), 129.9 (d, $J_{\text{C-P}} = 3.8\text{ Hz}$, C-5), 125.3 (d, $J_{\text{C-P}} = 10.3\text{ Hz}$, C-2), 62.22 (d, $J = 7.2\text{ Hz}$), 61.98 (d, $J = 7.0\text{ Hz}$), 59.3 (C-6), 35.8 (d, $J_{\text{C-P}} = 139.7\text{ Hz}$, C-1), 16.52, 16.48, 14.1 (d, $J = 6.2\text{ Hz}$, C-7), 12.6 (C-8). **FTIR** (thin film) ν 3390, 2980, 2935, 1444, 1391, 1228, 1163, 1096, 1049, 1018, 960, 771, 700, 560, 525, 480 cm^{-1} . **HRMS** (ESI): Calculated for $\text{C}_{14}\text{H}_{24}\text{O}_4\text{P}^+$ $[\text{M}+\text{H}]^+$ 263.1407; found 263.1413.

Preparation of diethyl ((3*E*,5*E*)-5-methyl-7-oxohepta-3,5-dien-2-yl)phosphonate, 483



To solution of alcohol **482** (161 mg, 0.377 mmol, 1.0 equiv.) in anhydrous DCM (30 mL) was added freshly prepared active manganese dioxide (1.86 g, 21.4 mmol, 57 equiv.). The reaction mixture was stirred vigorously at room temperature for 14 hours. Then the reaction mixture was filtered by a Büchner funnel and the precipitate was rinsed with ethyl acetate (3 × 30 mL). The combined filtrate was then concentrated under reduced pressure at 30 °C to afford the title compound (84 mg, yield 52%) as a yellow oil. **¹H NMR** (500 MHz, CDCl₃): δ 10.12 (d, *J* = 7.8 Hz, 1H, H-6), 6.34 – 6.22 (m, 2H, H-2, H-3), 5.93 (d, *J* = 7.7 Hz, 1H, H-5), 4.16 – 4.04 (m, 4H), 2.88 – 2.74 (m, 1H, H-1, d. quintet), 2.27 (s, 3H, H-8), 1.42 – 1.28 (m, 9H, overlapped, H-7). **¹³C NMR** (125 MHz, CDCl₃): δ 191.4 (C-6), 153.7 (d, *J*_{C-P} = 3.4 Hz, C-4), 135.3 (d, *J*_{C-P} = 10.9 Hz, C-3), 134.2 (d, *J*_{C-P} = 8.7 Hz, C-2), 129.6 (d, *J*_{C-P} = 2.5 Hz, C-5), 62.3 (d, *J*_{C-P} = 5.8 Hz), 62.2 (d, *J*_{C-P} = 5.6 Hz), 36.4 (d, *J*_{C-P} = 115.5 Hz, C-1), 16.5 (d, *J*_{C-P} = 4.7 Hz), 16.3 (d, *J*_{C-P} = 3.7 Hz), 13.7 (d, *J*_{C-P} = 5.2 Hz, C-7), 13.1 (C-8). **FTIR** (thin film) ν 2982, 2934, 1663, 1629, 1598, 1443, 1389, 1241, 1207, 1162, 1112, 1048, 1017, 960, 774, 731, 702, 564, 538, 484 cm⁻¹. **HRMS** (ESI): Calculated for C₁₂H₂₁O₄P⁺ [M+H]⁺ 260.1177; found 260.1147.

Preparation of diethyl ((2*E*,4*E*,6*E*)-5-methyl-7-((triisopropylsilyl)oxy)hepta-2,4,6-trien-2-yl)phosphonate, 485



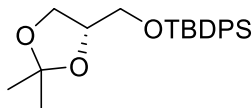
To a solution of KHMDS (40 μ L, 0.5 in toluene, 0.020 mmol, 1.0 equiv.) in anhydrous THF (0.2 mL) was added a solution of aldehyde **483** (5.2 mg, 0.020 mmol, 1.0 equiv.) in anhydrous THF (0.2 mL) at -78 °C. Then resulting mixture was stirred at 0 °C for 30 minutes, followed by dropwise addition of a solution of triisopropylsilyl chloride (5 μ L, 0.024 mmol, 1.22 equiv.) in anhydrous THF (0.1 mL) at -78 °C. Then the reaction mixture was allowed to be stirred at room temperature for 30 minutes and then hydrolysed at 0 °C with distilled water (0.2 mL). Then the reaction mixture was diluted with ethyl acetate (2

mL) and saturated NH_4Cl aqueous solution (2 mL). The aqueous phase was separated and extracted with ethyl acetate (3×5 mL). The combined organic phase was washed with brine, dried over anhydrous Na_2SO_4 , filtered, concentrated under reduced pressure. The crude material was purified by flash silica chromatography (pet. ether/EtOAc = 2:1) to afford the title compound (3.7 mg, yield 31%) as a colourless oil. **R_f**: 0.43 (pet. ether/EtOAc = 2:1). **¹H NMR** (500 MHz, CDCl_3) δ 7.33 (ddd, $J = 22.8, 11.9, 1.6$ Hz, 1H, H-2), 6.84 (d, $J = 11.9$ Hz, 1H, H-6), 6.09 (d, $J = 12.0$ Hz, 1H, H-5), 4.14 – 3.97 (m, 4H), 1.93 (s, 3H, H-8), 1.87 (dd, $J = 15.1, 1.4$ Hz, 2H, H-7), 1.31 (t, $J = 7.0$ Hz, 6H), 1.22 – 1.14 (m, 3H), 1.10 – 1.03 (m, 18H). **¹³C NMR** (125 MHz, CDCl_3) δ 145.2 (C-6), 140.7 (C-4), 138.5 (d, $J_{\text{C-P}} = 12.0$ Hz, C-2), 120.3 (d, $J_{\text{C-P}} = 22.4$ Hz, C-5), 120.2 (d, $J_{\text{C-P}} = 182.4$ Hz, C-1), 117.9 (C-3), 61.45, 61.41, 17.64, 16.37, 16.32, 13.2 (C-8), 12.7 (d, $J_{\text{C-P}} = 9.8$ Hz, C-7), 11.9. **(FTIR)** (thin film) ν 2943, 2868, 1689, 1632, 1603, 1463, 1390, 1243, 1236, 1183, 1167, 1121, 1098, 1053, 1024, 967, 882, 798, 686, 558, 534 cm^{-1} . **HRMS** (ESI): Calculated for $\text{C}_{21}\text{H}_{42}\text{O}_4\text{PSi}^+$ $[\text{M}+\text{H}]^+$ 417.2584; found 417.2584.

6.4 Experimental for Chapter Four

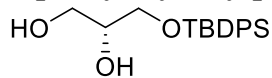
6.4.1 Attempted Synthesis of Aldehyde (*R*)-509

Preparation of (*R*)-*tert*-butyl((2,2-dimethyl-1,3-dioxolan-4-yl)methoxy)diphenylsilane, 503



To a solution of (*S*)-solketal **502** (3.00 g, 22.7 mmol, 1.0 equiv.) in anhydrous DMF (10 mL) was added imidazole (3.63 g, 53.3 mmol, 2.35 equiv.) and *tert*-butyldiphenylchlorosilane (6.86 g, 25.0 mmol, 1.1 equiv.) slowly at room temperature. Then the reaction mixture was stirred at room temperature for 1.5 hour. Upon completion, the reaction was diluted in ethyl acetate (200 mL) and then washed with distilled water (3 × 80 mL). The combined aqueous layers were then separated and extracted with ethyl acetate (3 × 20 mL). The combined organic phase was dried with anhydrous Na₂SO₄, filtered, and then concentrated by rotary evaporation. The crude material was purified by flash silica chromatography (pet. ether/ethyl acetate = 50/1) to afford the title compound as a light-yellow oil (8.0 g, yield 96%). **R_f**: 0.59 (pet. ether/EtOAc = 10:1). **¹H NMR** (500 MHz, CDCl₃) δ 7.69 – 7.63 (m, 4H), 7.45 – 7.35 (m, 6H), 4.24 – 4.17 (m, 1H), 4.07 (dd, *J* = 8.2, 6.4 Hz, 1H), 3.91 (dd, *J* = 8.2, 6.0 Hz, 1H), 3.73 (dd, *J* = 10.4, 4.5 Hz, 1H), 3.65 (dd, *J* = 10.4, 6.5 Hz, 1H), 1.39 (s, 3H), 1.36 (s, 3H), 1.05 (s, 9H). **¹³C NMR** (125 MHz, CDCl₃): δ 136.0, 135.2, 133.8, 130.2, 130.1, 128.1, 109.6, 67.3, 65.0, 27.2, 27.1, 27.0, 25.9, 19.7. These characterisation data match those reported in the literature.³⁵⁵

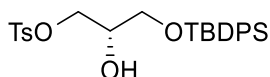
Preparation of (*R*)-3-((*tert*-butyldiphenylsilyl)oxy)propane-1,2-diol, 504



Silyl ether compound **503** (8.09 g, 21.8 mmol, 1.0 equiv.) was mixed with 100 mL of 90% AcOH. After heating to reflux for 10 min, the solution was allowed to cool to room temperature slowly. The solvent was removed under vacuum and the resulting oil was purified by flash silica chromatography (dichloromethane/methanol/acetic acid = 95/5/3) to afford an off-white crystal (6.12 g, yield 84%). **R_f**: 0.22 (DCM/MeOH = 50:1). **¹H NMR** (500 MHz, CDCl₃) δ 7.67 – 7.65 (m, 4H), 7.47 – 7.37 (m, 6H), 3.84 – 3.77 (m, 1H), 3.76 – 3.60 (m, 4H), 2.56 (d, *J* = 5.0 Hz, 1H), 1.96 (br. s, 1H), 1.07 (s, 9H). **¹³C NMR**

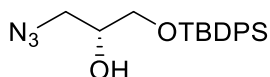
NMR (125 MHz, CDCl₃): δ 135.5, 132.9, 130.0, 127.9, 71.9, 65.2, 63.9, 26.9, 19.2. These characterisation data match those reported in the literature.³⁵⁶

Preparation of (*S*)-3-((*tert*-butyldiphenylsilyl)oxy)-2-hydroxypropyl 4-methylbenzenesulfonate, **505**



Diol compound **504** (512 mg, 1.55 mmol, 1.0 equiv.), 4-toluenesulfonyl chloride (295mg, 1.55 mmol, 1.0 equiv.) and dibutyltin oxide (77mg, 0.31 mmol, 0.2 equiv.) were mixed in a 50 mL round-bottom flask under nitrogen atmosphere. Then anhydrous DCM (15 mL) and triethylamine (0.22 ml, 1.55 mmol, 1.0 equiv.) were added to the flask. The reaction mixture was stirred at room temperature for 20 hours. Distilled water (10 mL) was then added to the reaction mixture and the aqueous layer was separated and extracted with distilled ethyl acetate (3 × 10 mL). The combined organic phase was dried with anhydrous Na₂SO₄, filtered, and then concentrated by rotary evaporation. The crude material was purified by flash silica chromatography (pet. ether/ethyl acetate = 4/1) to afford the title compound as a colourless oil (576 mg, yield 77%). **R_f**: 0.50 (pet. ether/EtOAc = 3:1). **¹H NMR** (500 MHz, CDCl₃) δ 7.82 – 7.75 (m, 2H), 7.82 – 7.75 (m, 4H), 7.47 – 7.42 (m, 2H), 7.41 – 7.36 (m, 4H), 7.34 – 7.30 (m, 2H), 4.14 (dd, *J* = 10.1, 5.0 Hz, 1H), 4.06 (dd, *J* = 10.1, 5.9 Hz, 1H), 3.92 – 3.86 (m, 1H), 3.66 (d, *J* = 5.1 Hz, 2H), 2.44 (s, 3H), 1.01 (s, 9H). **¹³C NMR** (125 MHz, CDCl₃): δ 135.5, 130.0, 129.9, 128.0, 127.9, 70.3, 69.5, 63.7, 26.7, 21.69, 19.2. These characterisation data match those reported in the literature.³⁵⁷

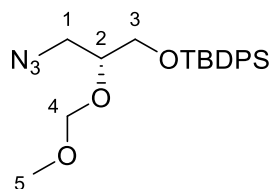
Preparation of (*R*)-1-azido-3-((*tert*-butyldiphenylsilyl)oxy)propan-2-ol, **506**



To a solution of tosylate **505** (6.70 g, 13.8 mmol, 1.0 equiv.) in anhydrous DMF (40 mL) was added sodium azide (2.24 g, 34.6 mmol, 2.5 equiv.) at room temperature. Then the reaction mixture was stirred at 90 °C for 23 hours. Then the reaction mixture was cooled down to room temperature and poured into 100 mL ice-cold water. The aqueous layers were extracted with diethyl ether (3 × 100 mL). The combined organic phase was washed with brine, dried with anhydrous Na₂SO₄, filtered, and then concentrated by rotary evaporation. The crude material was purified by flash silica chromatography (pet.

ether/ethyl acetate = 8/1) to afford the title compound as a colourless oil (3.12 g, yield 64%). **R_f**: 0.53 (pet. ether/EtOAc = 3:1). **¹H NMR** (500 MHz, CDCl₃) δ 7.67 – 7.61 (m, 4H), 7.48 – 7.37 (m, 6H), 3.87 (sextet, *J* = 5.0 Hz, 1H), 3.71 – 3.63 (m, 2H), 3.37 (d, *J* = 5.0 Hz, 2H), 1.07 (s, 9H). **¹³C NMR** (125 MHz, CDCl₃) δ 135.5, 132.7, 130.0, 127.9, 70.9, 64.9, 53.2, 26.8, 19.2. **FTIR** (thin film) ν 3443, 3071, 2930, 2858, 2099, 1589, 1472, 1427, 1391, 1362, 1264, 1189, 1112, 1105, 1006, 998, 937, 873, 823, 800, 739, 700, 622, 614, 554, 504, 487, 437 cm⁻¹. **HRMS** (ESI): Calculated for C₁₉H₂₅N₃NaO₂Si⁺ [M+Na]⁺ 378.1614; found 378.1642. [α]_D²⁶ +16 (*c* = 1.57, DCM). These characterisation data match those reported in the literature.³⁵⁸

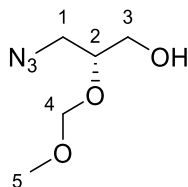
Preparation of (*R*)-5-(azidomethyl)-9,9-dimethyl-8,8-diphenyl-2,4,7-trioxa-8-siladecane, **507**



To a solution of azide **506** (3.12 g, 8.8 mmol, 1.0 equiv.) and 4-DMAP (0.43 g, 3.52 mmol, 0.4 equiv.) in anhydrous DCM (88 mL) were sequentially added *N*, *N*-diisopropylethylamine (23 mL, 132 mmol, 15 equiv.) and MOMCl (8.25 mL, purity 90%, 88 mmol, 10.0 equiv.) at 0 °C. Then the reaction mixture was allowed to warm up to room temperature and stirred at room temperature for 17 hours. Then the reaction mixture was heated at reflux for 6 hours. The reaction was quenched by addition of 20 mL NaHCO₃ aqueous solution. Then the aqueous layers were separated and extracted with diethyl ether (3 × 30 mL). The combined organic phase was washed with brine, dried with anhydrous Na₂SO₄, filtered, and then concentrated by rotary evaporation. The crude material was purified by flash silica chromatography (pet. ether/ethyl acetate = 14/1) to afford the title compound as a colourless oil (3.22 g, yield 92%). **R_f**: 0.28 (pet. ether/EtOAc = 10:1). **¹H NMR** (500 MHz, CDCl₃) δ 7.68 – 7.62 (m, 4H), 7.48 – 7.37 (m, 6H), 4.66 – 4.62 (m, 2H, H-4), 3.82 – 3.77 (m, 1H, H-2), 3.73 (dd, *J* = 10.6, 4.9 Hz, 1H, H-3a), 3.68 (dd, *J* = 10.6, 6.4 Hz, 1H, H-3b), 3.52 (dd, *J* = 12.8, 3.8 Hz, 1H, H-1a), 3.44 (dd, *J* = 12.8, 6.1 Hz, 1H, H-1b), 3.33 (s, 3H, H-5), 1.05 (s, 9H). **¹³C NMR** (125 MHz, CDCl₃) δ 135.6, 135.5, 133.1, 133.0, 129.8, 127.78, 127.76, 96.1 (C-4), 76.5 (C-2), 63.4 (C-3), 55.6 (C-5), 52.3 (C-1), 26.8, 19.2. **FTIR** (thin film) ν 2931, 2888, 2858, 2098, 1472, 1428, 1281, 1154, 1105,

1030, 998, 919, 823, 794, 739, 700, 622, 614, 504, 488 cm^{-1} . **HRMS** (ESI): Calculated for $\text{C}_{21}\text{H}_{30}\text{N}_3\text{O}_3\text{Si}^+$ $[\text{M}+\text{H}]^+$ 400.2051; found 400.2050. $[\alpha]_D^{26} +16$ ($c = 1.24$, DCM).

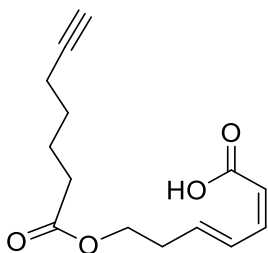
Preparation of (*R*)-3-azido-2-(methoxymethoxy)propan-1-ol, **508**



To a solution of azide **507** (307mg, 0.77 mmol, 1.0 equiv.) in anhydrous THF (10 mL) was added tetrabutylammonium fluoride (1.50 mL, 1.0 M in THF, 1.50 mmol, 1.95 equiv.) at room temperature and the reaction mixture was stirred at room temperature for 2 hours. Saturated aqueous NH_4Cl solution (10 mL) was then added to the reaction mixture and the resulting mixture was stirred for 10 minutes. The aqueous phase was then separated and extracted with ethyl acetate (3×10 mL). The combined organic phase was washed with brine, dried with anhydrous Na_2SO_4 , filtered, and then concentrated by rotary evaporation. The crude material was purified by flash silica chromatography (pet. ether/ethyl acetate = 2/1) to afford the title compound as a colourless oil (117 mg, yield 94%). **R_f**: 0.16 (pet. ether/EtOAc = 2:1). **¹H NMR** (500 MHz, CDCl_3) δ 4.79 – 4.74 (m, 2H, H-4), 3.80 – 3.73 (m, 1H, H-2), 3.68 (dd, $J = 12.0, 2.9$ Hz, 1H, H-3a), 3.63 (dd, $J = 11.9, 6.1$ Hz, 1H, H-3b), 3.45 (s, 3H, H-5), 3.42 (dd, $J = 12.9, 6.4$ Hz, 1H, H-1a), 3.37 (dd, $J = 12.9, 4.7$ Hz, 1H, H-1b), 2.59 (br. s, 1H, -OH). **¹³C NMR** (125 MHz, CDCl_3) δ 96.9 (C-4), 79.5 (C-2), 63.2 (C-3), 55.9 (C-5), 51.8 (C-1). **FTIR** (thin film) ν 3423, 2927, 2096, 1443, 1280, 1212, 1151, 1105, 1022, 917, 811, 621, 554 cm^{-1} . **HRMS** (ESI): Calculated for $\text{C}_{21}\text{H}_{30}\text{N}_3\text{O}_3\text{Si}^+$ $[\text{M}+\text{H}]^+$ 162.0873; found 162.1010. $[\alpha]_D^{21} -56.7$ ($c = 0.97$, DCM).

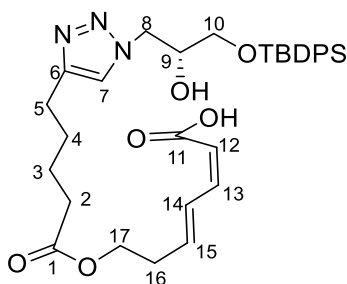
6.4.2 Synthesis of Macrocyclic Alcohol 523

Preparation of (2*Z*,4*E*)-7-(hept-6-ynoyloxy)hepta-2,4-dienoic acid, 414



To a solution of lactone **364** (60.0 mg, 0.240 mmol, 1.0 equiv.) in THF (4.4 mL) was added a solution of tetrabutylammonium fluoride (0.96 mL, 1.0 M in THF, 0.96 mmol, 2.0 equiv.) at 0 °C. The reaction mixture was stirred at room temperature for 2 hours. Then the reaction mixture was washed with 2% H₂SO₄ aqueous solution (3 × 20 mL). The organic phase was washed with brine, dried with anhydrous Na₂SO₄, filtered, and then concentrated by rotary evaporation to afford the title compound as a colourless oil (43 mg, yield 99%). *R_f*: 0.64 (pet. ether/EtOAc = 1:1). ¹H NMR (500 MHz, CDCl₃) δ 7.41 (dd, *J* = 15.6, 11.1 Hz, 1H), 6.65 (t, *J* = 11.3 Hz, 1H), 6.06 (dd, *J* = 15.0, 7.2 Hz, 1H), 5.65 (d, *J* = 11.3 Hz, 1H), 4.18 (t, *J* = 6.5 Hz, 2H), 2.55 (dt, *J* = 6.9, 6.6 Hz, 2H), 2.34 (t, *J* = 7.3 Hz, 2H), 2.21 (t, *J* = 7.0 Hz, 2H), 1.96 – 1.93 (m, 1H), 1.74 (quin, *J* = 6.9 Hz, 2H), 1.56 (quin, *J* = 7.0 Hz, 2H). ¹³C NMR (125 MHz, CDCl₃) 173.4, 171.5, 146.6, 140.9, 129.1, 116.0, 83.9, 68.6, 62.8, 33.7, 32.3, 27.8, 23.9, 18.1. These characterisation data match those reported in the literature.¹³⁴

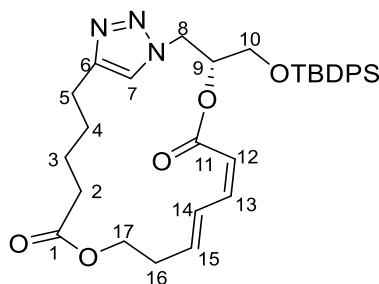
Preparation of (2*Z*,4*E*)-7-((5-(1-((*R*)-3-((*tert*-butyldiphenylsilyl)oxy)-2-hydroxypropyl)-1*H*-1,2,3-triazol-4-yl)pentanoyl)oxy)hepta-2,4-dienoic acid, 514



To a solution of CuSO₄ (2.0 mg, 0.008 mmol, 0.09 equiv.) and sodium ascorbate (7.3 mg, 0.037 mmol, 0.5 equiv.) in distilled water (2.0 mL) was added a solution of alkyne **414** (22.2 mg, 0.088 mmol, 1.1 equiv.) and azide **506** (28.8 mg, 0.081 mmol, 1.0 equiv.) in THF (2.0 mL). The reaction mixture was stirred at room temperature in dark for 12 hours. Then the reaction mixture was directly extracted with ethyl acetate (3 × 5 mL). The

combined organic phase was washed with brine, dried with anhydrous Na_2SO_4 , filtered, and then concentrated by rotary evaporation. The crude material was purified by flash silica chromatography (pet. ether/ethyl acetate = 1/2) to afford the title compound as a colourless oil (43 mg, yield 88%). **R_f**: 0.24 (pet. ether/EtOAc = 1:1). **¹H NMR** (500 MHz, CDCl_3) δ 7.66 – 7.60 (m, 4H), 7.47 – 7.36 (m, 8H, overlapped, H-7, H-14), 6.60 (t, J = 11.3 Hz, 1H, H-13), 6.04 (dt, J = 14.3, 6.7 Hz, 1H, H-15), 5.63 (d, J = 11.3 Hz, 1H, H-12), 4.53 (d, J = 14.0 Hz, 1H, H-8a), 4.32 (dd, J = 13.9, 7.7 Hz, 1H, H-8b), 4.19 (t, J = 5.7 Hz, 2H, H-17), 4.16 – 4.09 (m, 1H, H-9), 3.70 – 3.60 (m, 2H, H-10), 2.73 – 2.66 (m, 2H, H-5), 2.56 – 2.48 (m, 2H, H-16), 2.38 – 2.29 (m, 2H, H-2), 1.72 – 1.60 (m, 4H, H-3, H-4), 1.07 (s, 9H). **¹³C NMR** (125 MHz, CDCl_3) 173.7 (C-1), 169.9 (C-11), 147.6 (C-6), 145.5 (C-13), 140.1 (C-15), 135.68, 135.67, 132.81, 132.78, 130.2, 129.4 (C-14), 128.1, 122.6 (C-7), 116.9 (C-12), 70.9 (C-9), 65.1 (C-10), 62.7 (C-17), 53.0 (C-8), 34.1 (C-2), 32.2 (C-16), 28.9 (C-4 or C-3), 27.0, 25.2 (C-5), 24.5 (C-3 or C-4), 19.4. **FTIR** (thin film) ν 3493, 3156, 2929, 2858, 1708, 1639, 1601, 1427, 1361, 1219, 1179, 1111, 1065, 998, 964, 823, 741, 701, 690, 614, 504, 489 cm^{-1} . **HRMS** (ESI): Calculated for $\text{C}_{33}\text{H}_{43}\text{N}_3\text{NaO}_6\text{Si}^+$ $[\text{M}+\text{Na}]^+$ 628.2819; found 628.2860. $[\alpha]_D^{25} +7.8$ (c = 1.02, DCM).

Preparation of (14Z,3R,6Z,8E)-3-(((*tert*-butyldiphenylsilyl)oxy)methyl)-1'*H*-4,12-dioxo-1(1,4)-triazolacycloheptadecaphane-6,8-diene-5,13-dione, **515**

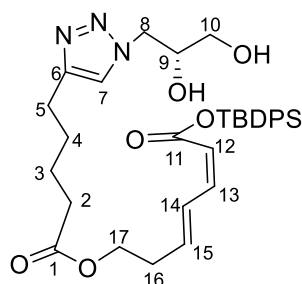


To a mixture of acid **514** (21.0 mg, 0.0347 mmol, 1.0 equiv.) and solid NaHCO_3 (717 mg, 8.5 mmol, 246 equiv.) in anhydrous DCM (80 mL) was added 2-bromo-1-ethylpyridinium tetrafluoroborate (233 mg, 0.85 mmol, 24.6 equiv.). The reaction mixture was stirred in dark under argon atmosphere at room temperature for 23 hours. The reaction was quenched by addition of distilled water (3.6 mL). The aqueous phase was separated and extracted ethyl acetate (3×5 mL). The combined organic phase was dried with anhydrous Na_2SO_4 , filtered, and then concentrated by rotary evaporation. The crude material was purified by flash silica chromatography (pet. ether/EtOAc = 2/1 to pet.

ether/EtOAc = 1/3) to afford the title compound **515** as a colourless oil (8.1 mg, yield 40%) and the silyl ester by-product **516** (9.6 mg, yield 46%) as a colourless oil.

515, *R_f*: 0.34 (pet. ether/EtOAc = 1:1). **¹H NMR** (500 MHz, CDCl₃): δ 7.70 – 7.61 (m, 4H), 7.48 – 7.36 (m, 6H), 7.24 (s, 1H, H-7), 7.15 (t, *J* = 15.0 Hz, 1H, H-14), 6.54 (t, *J* = 11.2 Hz, 1H, H-13), 5.99 (dt, *J* = 14.8, 7.2 Hz, 1H, H-15), 5.50 (d, *J* = 10.0 Hz, 1H, H-12), 5.49 – 5.42 (overlapped, m, 1H, H-9), 4.72 (d, *J* = 14.5 Hz, 1H, H-8a), 4.56 (dd, *J* = 13.9, 10.6 Hz, 1H, H-8b), 4.30 (t, *J* = 10.3 Hz, 1H, H-17a), 4.24 – 4.14 (m, 1H, H-17b), 3.87 (dd, *J* = 11.1, 4.0 Hz, 1H, H-10a), 3.81 (dd, *J* = 11.0, 4.6 Hz, 1H, H-10b), 2.73 (dt, *J* = 14.4, 7.0 Hz, 1H, H-5a), 2.63 (dt, *J* = 14.6, 7.1 Hz, 1H, H-5b), 2.56 – 2.47 (m, 1H, H-16a), 2.47 – 2.39 (m, 1H, H-16b), 2.28 (dtd, *J* = 21.5, 14.6, 14.0, 7.0 Hz, 2H, H-2), 1.74 – 1.61 (m, 2H, H-4, overlapped), 1.61 – 1.51 (m, 2H, H-3, overlapped), 1.08 (s, 9H). **¹³C NMR** (125 MHz, CDCl₃): 173.6 (C-1), 164.6 (C-11), 146.8 (C-6), 146.4 (C-13), 142.0 (C-15), 135.76, 135.69, 132.88, 132.84, 130.20, 130.18, 128.6 (C-14), 128.09, 128.05, 121.5 (C-7), 114.9 (C-12), 110.2, 71.2 (C-9), 63.8 (C-10), 62.0 (C-17), 51.5 (C-8), 34.9 (C-2), 34.0, 33.2 (C-16), 28.8 (C-4), 26.7, 25.4 (C-5), 24.5 (C-3), 19.5. **FTIR** (thin film) ν 2957, 2930, 2858, 1725, 1640, 1602, 1472, 1460, 1428, 1389, 1362, 1308, 1261, 1168, 1126, 1114, 1050, 998, 965, 823, 779, 742, 703, 622, 615, 505, 495, 490, 475, 468, 451, 433 cm⁻¹. **HRMS** (ESI): Calculated for C₃₃H₄₂N₃O₅SSi⁺ [M + H]⁺ 588.2888; found 588.2892. [α]_D²³ +23.8 (*c* = 0.41, DCM).

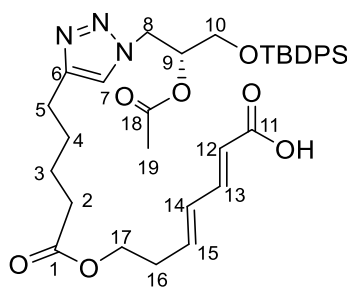
***Tert*-butyldiphenylsilyl (2*Z*,4*E*)-7-((5-(1-((*R*)-2,3-dihydroxypropyl)-1*H*-1,2,3-triazol-4-yl)pentanoyl)oxy)hepta-2,4-dienoate, 516**



R_f: 0.10 (pet. ether/EtOAc = 1:1). **¹H NMR** (500 MHz, CDCl₃): δ 7.66 – 7.56 (m, 4H), 7.48 – 7.34 (m, 8H, overlapped, H-7, H-14), 6.72 (t, *J* = 11.2 Hz, 1H, H-13), 6.14 (dt, *J* = 14.6, 7.1 Hz, 1H, H-15), 5.62 (d, *J* = 11.1 Hz, 1H, H-12), 4.52 (d, *J* = 14.2 Hz, 1H, H-8a), 4.32 (dd, *J* = 13.6, 6.9 Hz, 1H, H-8b), 4.17 (t, *J* = 6.1 Hz, 2H, H-17), 4.14 – 4.07 (m,

1H, H-9), 3.70 – 3.59 (m, 2H, H-10), 2.73 – 2.67 (m, 2H, H-5), 2.59 – 2.48 (m, 2H, H-16), 2.36 – 2.30 (m, 2H, H-2), 1.73 – 1.59 (m, 4H, H-3, H-4), 1.07 (s, 9H). ¹³C NMR (125 MHz, CDCl₃): 173.6 (C-1), 161.6 (C-11), 149.0 (C-13), 147.7 (C-6), 143.1 (C-15), 135.7, 132.82, 132.79, 130.2, 129.2 (C-14), 128.1, 122.4 (C-7), 115.0 (C-12), 70.9 (C-9), 65.0 (C-10), 62.8 (C-17), 52.8 (C-8), 34.1 (C-2), 32.7 (C-16), 28.9 (C-4), 27.0, 25.4 (C-5), 24.6 (C-3), 19.4. **FTIR** (thin film) ν 3386, 3234, 3153, 3069, 2930, 2857, 1773, 1734, 1654, 1636, 1589, 1560, 1472, 1461, 1428, 1391, 1361, 1308, 1258, 1214, 1112, 1034, 964, 930, 888, 824, 743, 703, 691, 663, 615, 589, 546, 507, 466, 454, 448, 442, 431 cm⁻¹. **HRMS** (ESI): Calculated for C₃₃H₄₄N₃O₆SSi⁺ [M+H]⁺ 606.2994; found 606.2974. $[\alpha]_D^{23} +5.6$ ($c = 0.48$, DCM).

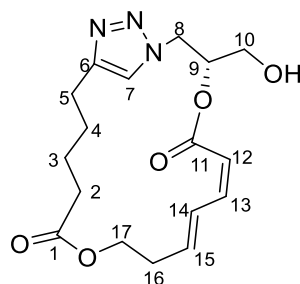
Preparation of (2*E*,4*E*)-7-((5-(1-((*R*)-2-acetoxy-3-((*tert*-butyldiphenylsilyl)oxy)propyl)-1*H*-1,2,3-triazol-4-yl)pentanoyl)oxy)hepta-2,4-dienoic acid, *E,E*-522



To a solution of diol **516** (11.3 mg, 0.019 mmol, 1.0 equiv.) in DCM (1.0 mL) was added pyridine (60 μ L, 0.72 mmol, 38 equiv.) and acetyl chloride (26 μ L, 0.36 mmol, 20.0 equiv.) at 0 °C. Then the reaction mixture was stirred at room temperature for 4 days. The reaction was then quenched by addition of saturated aqueous NaHCO₃ solution (2 mL). The aqueous phase was separated and extracted ethyl acetate (3 \times 5 mL). The combined organic phase was dried with anhydrous Na₂SO₄, filtered, and then concentrated by rotary evaporation. The crude material was purified by flash silica chromatography (pet. ether/EtOAc = 3/2) to afford the title compound as a colourless oil (7.5 mg, yield 62%). **R_f**: 0.12 (pet. ether/EtOAc = 1:1). **¹H NMR** (500 MHz, CDCl₃): δ 7.68 – 7.56 (m, 4H), 7.48 – 7.35 (m, 6H), 7.35 – 7.27 (overlapped, m, 1H, H-13), 7.28 (s, 1H, H-7), 6.26 (dd, $J = 15.2, 11.8$ Hz, 1H, H-14), 6.14 – 6.06 (m, 1H, H-15), 5.83 (d, $J = 15.6$ Hz, 1H, H-12), 5.26 – 5.18 (m, 1H, H-9), 4.68 (dd, $J = 14.3, 4.4$ Hz, 1H, H-8a), 4.60 (dd, $J = 14.3, 7.4$ Hz, 1H, H-8b), 4.16 (t, $J = 6.6$ Hz, 2H, H-17), 3.77 – 3.66 (m, 2H, H-10), 2.76 – 2.66 (m, 2H, H-5), 2.56 – 2.46 (m, 2H, H-16), 2.34 (t, $J = 5.8$ Hz, 2H, H-2), 1.98 (s, 3H, H-19),

1.75 – 1.61 (m, 4H, H-3, H-4), 1.08 (s, 9H). ^{13}C NMR (125 MHz, CDCl_3): 173.4 (C-1), 170.2 (C-11), 169.9 (C-18), 147.8 (C-6), 146.3 (C-13), 134.0 (C-15), 135.54, 135.46, 132.66, 132.64, 130.4 (C-14), 130.0, 127.86, 127.83, 121.5 (C-7), 119.4 (C-12), 72.1 (C-9), 62.6 (C-17), 62.4 (C-10), 49.8 (C-8), 33.9 (C-2), 32.3 (C-16), 28.8 (C-4), 26.8, 25.2 (C-5), 24.4 (C-3), 20.8 (C-19), 19.3. FTIR (thin film) ν 3140, 2955, 2930, 2858, 1735, 1701, 1697, 1643, 1589, 1461, 1428, 1389, 1374, 1301, 1230, 1185, 1133, 1113, 1059, 998, 823, 803, 742, 703, 692, 505, 492 cm^{-1} . HRMS (ESI): Calculated for $\text{C}_{35}\text{H}_{46}\text{N}_3\text{O}_7\text{Si}^+$ $[\text{M}+\text{H}]^+$ 648.3100; found 648.3108. $[\alpha]_D^{23} +11$ ($c = 0.33$, DCM).

Preparation of (1⁴Z,3R,6Z,8E)-3-(hydroxymethyl)-1¹H-4,12-dioxa-1(1,4)-triazolacycloheptadecaphane-6,8-diene-5,13-dione, 523



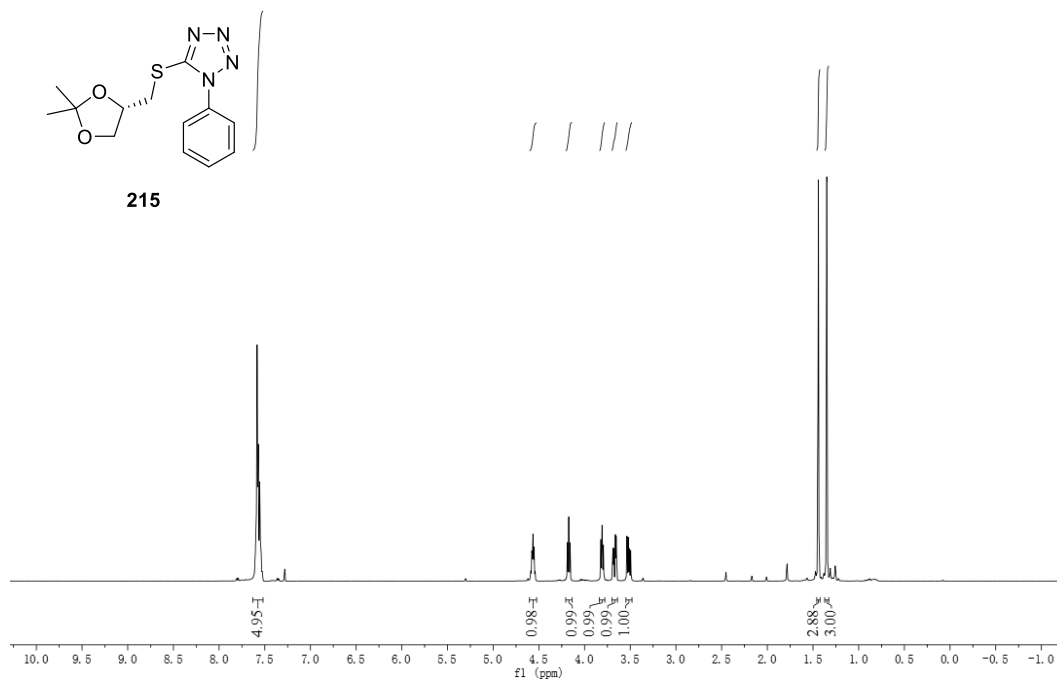
To a solution of compound **515** (34.4 mg, 0.059 mmol, 1.0 equiv.) and acetic acid (16 μL , 0.280 mmol, 4.78 equiv.) in anhydrous THF (0.8 mL) was slowly added tetrabutylammonium fluoride (116 μL , 1.0 M in THF, 0.116 mmol, 2.0 equiv.) over 20 minutes at 0 $^\circ\text{C}$. Then the reaction mixture was allowed to warm up to room temperature and stirred at room temperature for 28 hours. The reaction mixture was then diluted with ethyl acetate (10 mL) and added saturated aqueous NaHCO_3 solution (5 mL). The aqueous phase was separated and extracted ethyl acetate (3×5 mL). The combined organic phase was dried with anhydrous Na_2SO_4 , filtered, and then concentrated by rotary evaporation. The crude material was purified by flash silica chromatography (DCM/MeOH = 20/1) to afford the title compound (16.9 mg, yield 83%) as a colourless oil. R_f : 0.25 (DCM/MeOH = 10/1). ^1H NMR (500 MHz, CDCl_3) δ 7.24 (s, 1H, H-7), 7.13 – 7.07 (m, 1H, H-14), 6.55 (t, $J = 11.4$ Hz, 1H, H-13), 6.00 (ddd, $J = 14.8, 8.8, 5.3$ Hz, 1H, H-15), 5.54 (d, $J = 11.3$ Hz, 1H, H-12), 5.43 (dtd, $J = 9.6, 4.8, 2.6$ Hz, 1H, H-9), 4.70 (dd, $J = 14.6, 2.6$ Hz, 1H, H-8a), 4.59 (dd, $J = 14.6, 9.7$ Hz, 1H, H-8b), 4.33 – 4.27 (m, 1H, H-17a), 4.23 – 4.18 (m, 1H, H-17b), 3.86 (dd, $J = 12.0, 4.6$ Hz, 1H, H-10a), 3.82 (dd, $J = 12.0, 4.9$ Hz, 1H, H-10b), 2.72 (dt, $J = 14.3, 6.9$ Hz, 1H, H-5a), 2.63 (dt, $J = 14.8, 7.2$

Hz, 1H, H-5b), 2.57 – 2.48 (m, 1H, H-16a), 2.47 – 2.40 (m, 1H, H-16b), 2.35 – 2.22 (m, 2H, H-2), 1.70 – 1.62 (m, 2H, H-4), 1.58 – 1.51 (m, 2H, H-3). **¹³C NMR** (125 MHz, CDCl₃) δ 173.5 (C-1), 164.6 (C-11), 147.8 (C-6), 146.6 (C-13), 142.3 (C-15), 128.5 (C-14), 121.7 (C-7), 114.7 (C-12), 71.5 (C-9), 62.3 (C-10), 62.0 (C-17), 50.9 (C-8), 34.9 (C-2), 33.2 (C-16), 28.7 (C-4), 25.3 (C-5), 24.5 (C-3). **FTIR** (thin film) ν 3355, 2923, 2854, 1719, 1639, 1602, 1524, 1458, 1420, 1380, 1260, 1172, 1131, 1057, 1002, 964, 817, 759 cm⁻¹. **HRMS** (ESI): Calculated for C₁₇H₂₄N₃O₅⁺ [M+H]⁺ 350.1710; found need re-do. $[\alpha]_D^{25}$ –137 (*c* = 0.125, DCM).

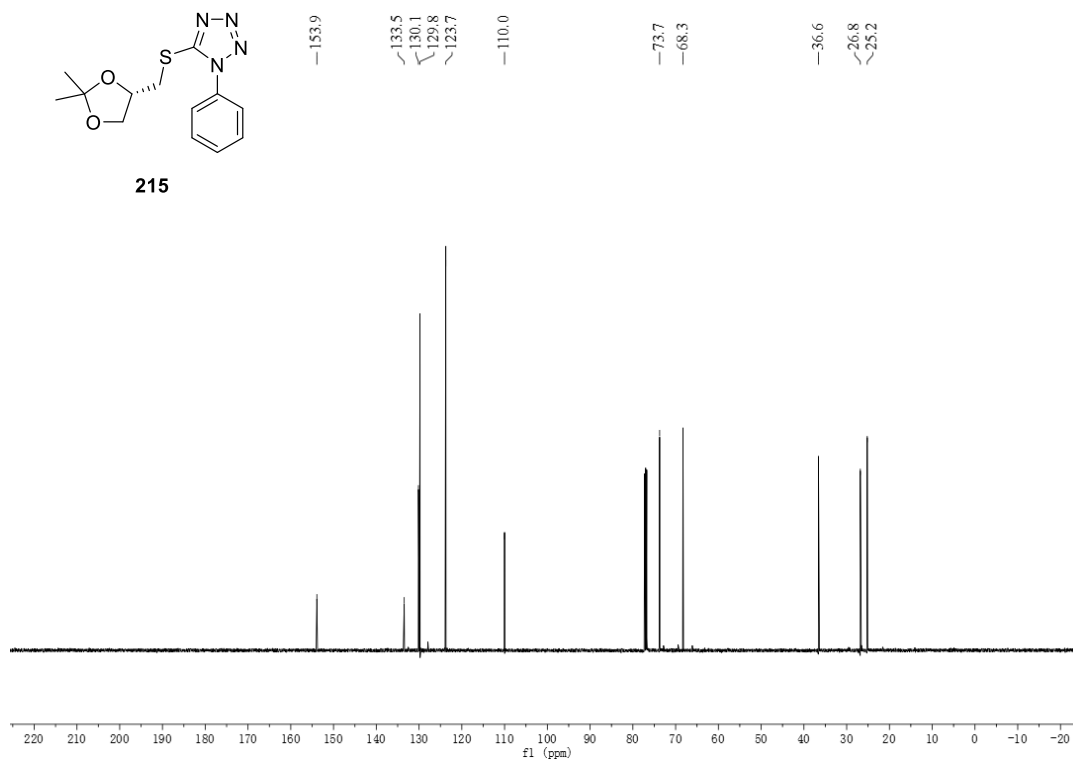
NMR Spectra of Novel Compounds

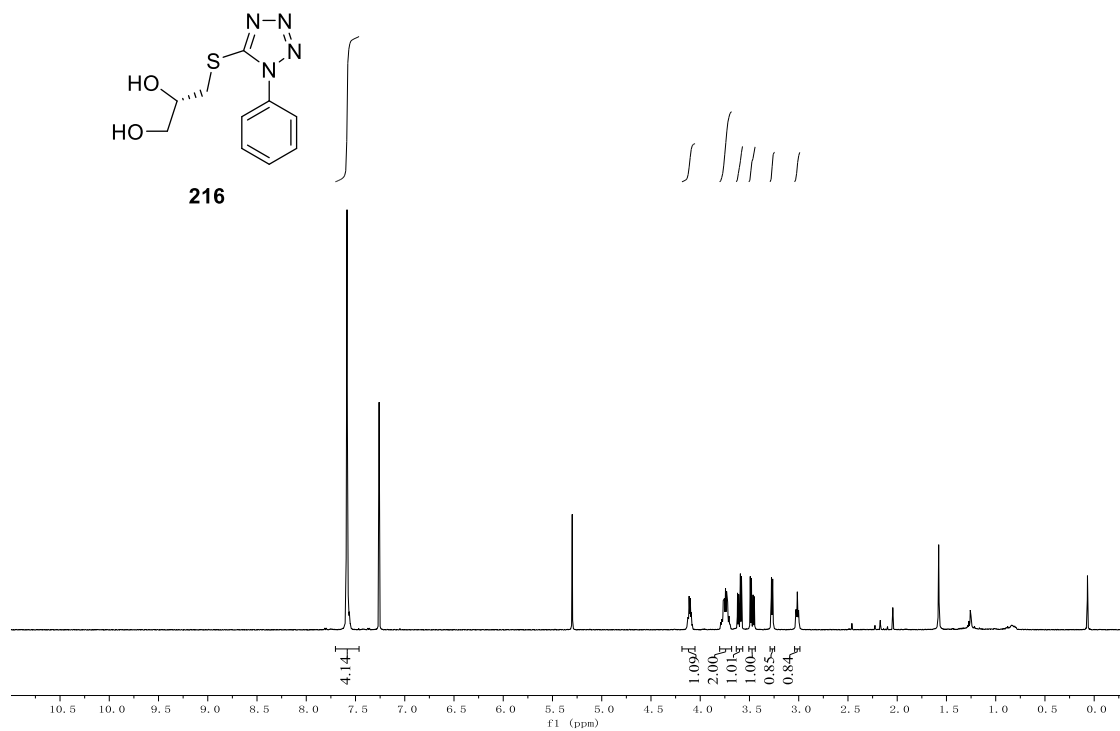
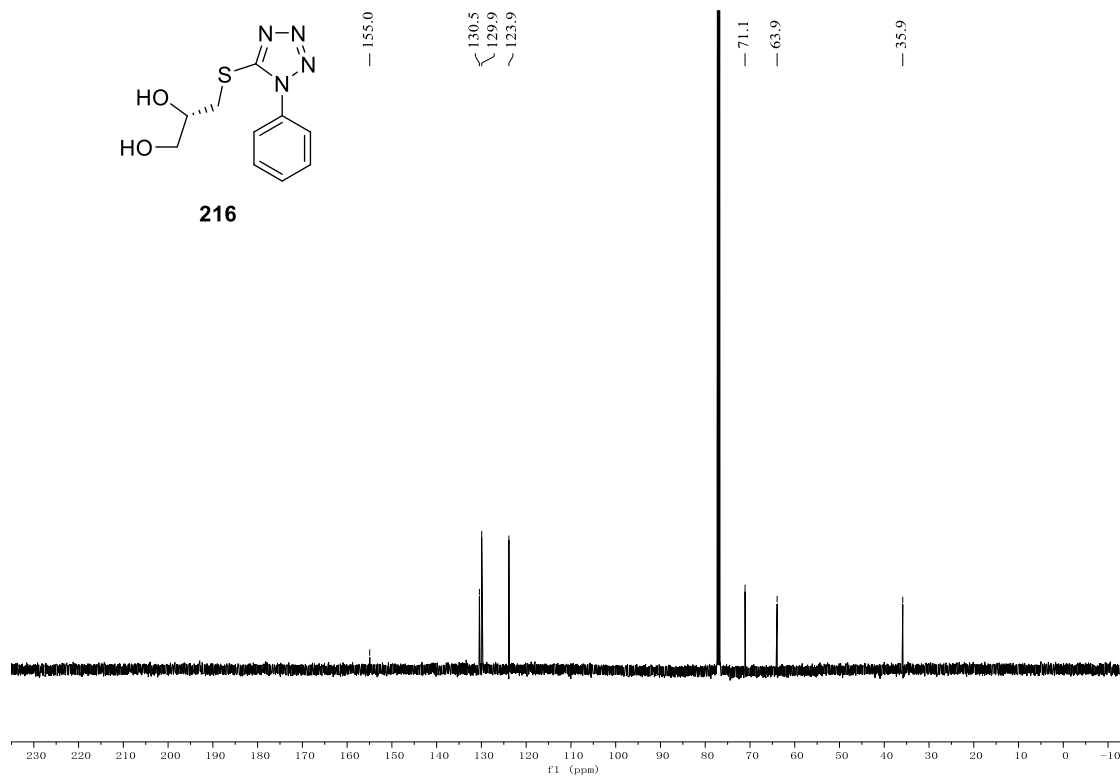
Spectra of Chapter Two

^1H NMR (500 MHz, CDCl_3)

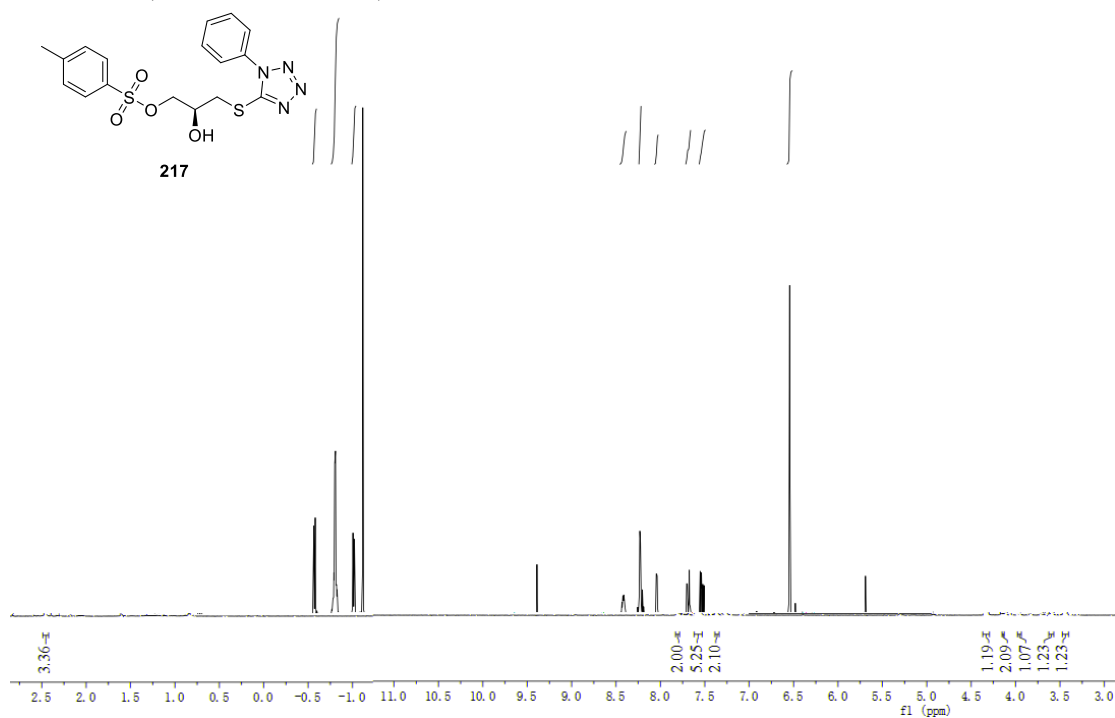


^{13}C NMR (125 MHz, CDCl_3)

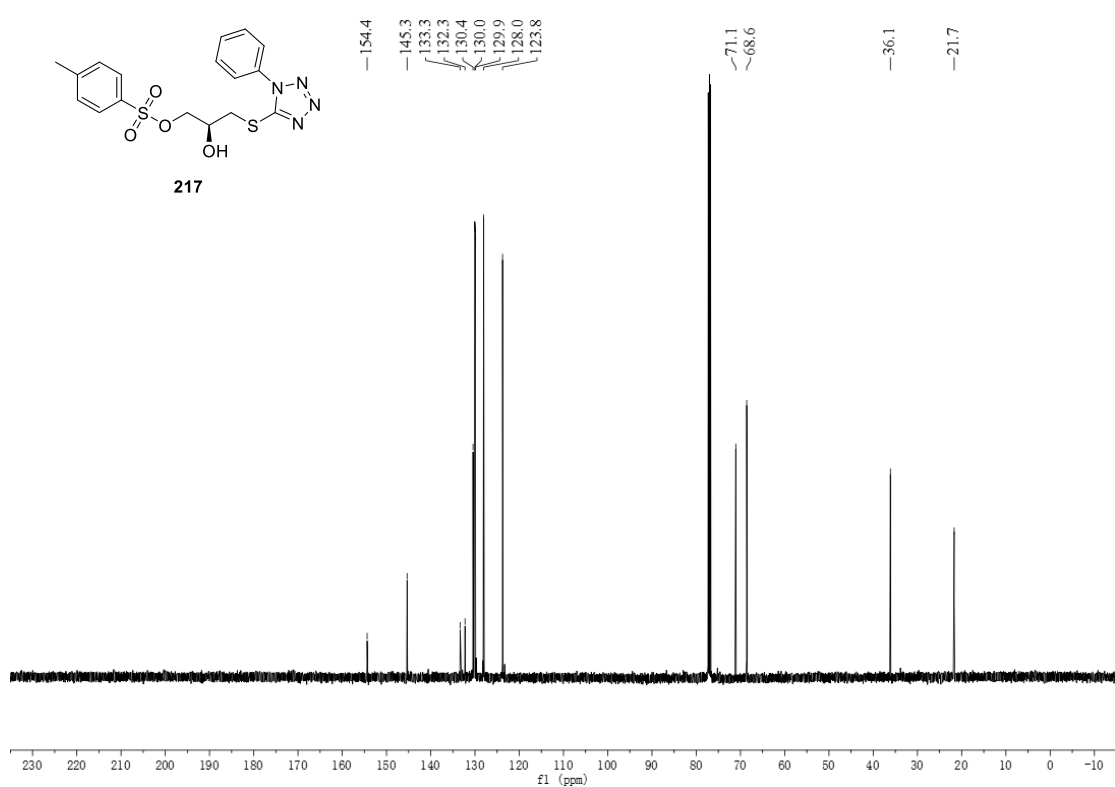


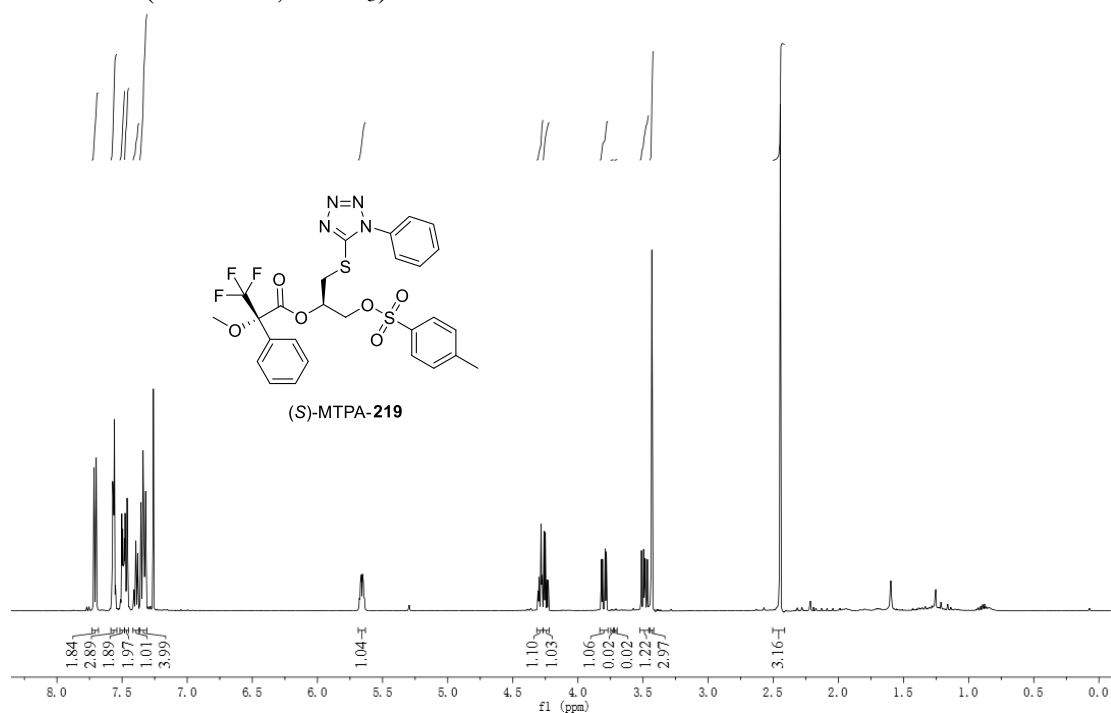
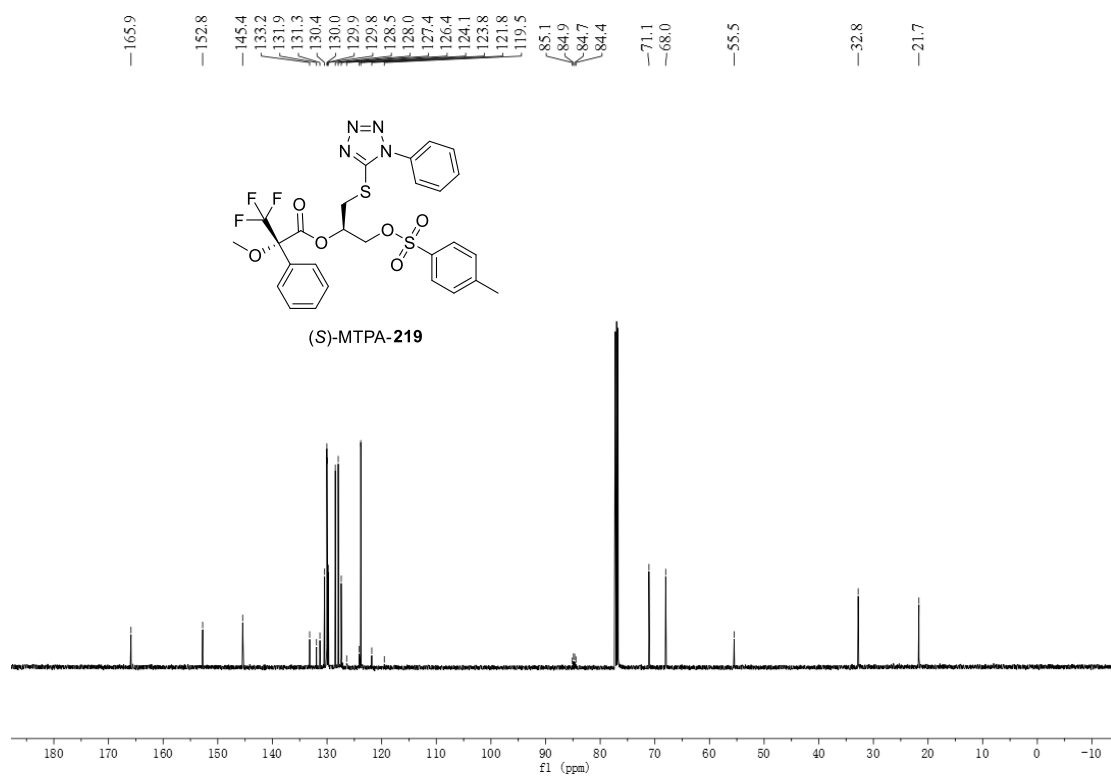
^1H NMR (500 MHz, CDCl_3) ^{13}C NMR (125 MHz, CDCl_3)

^1H NMR (500 MHz, CDCl_3)

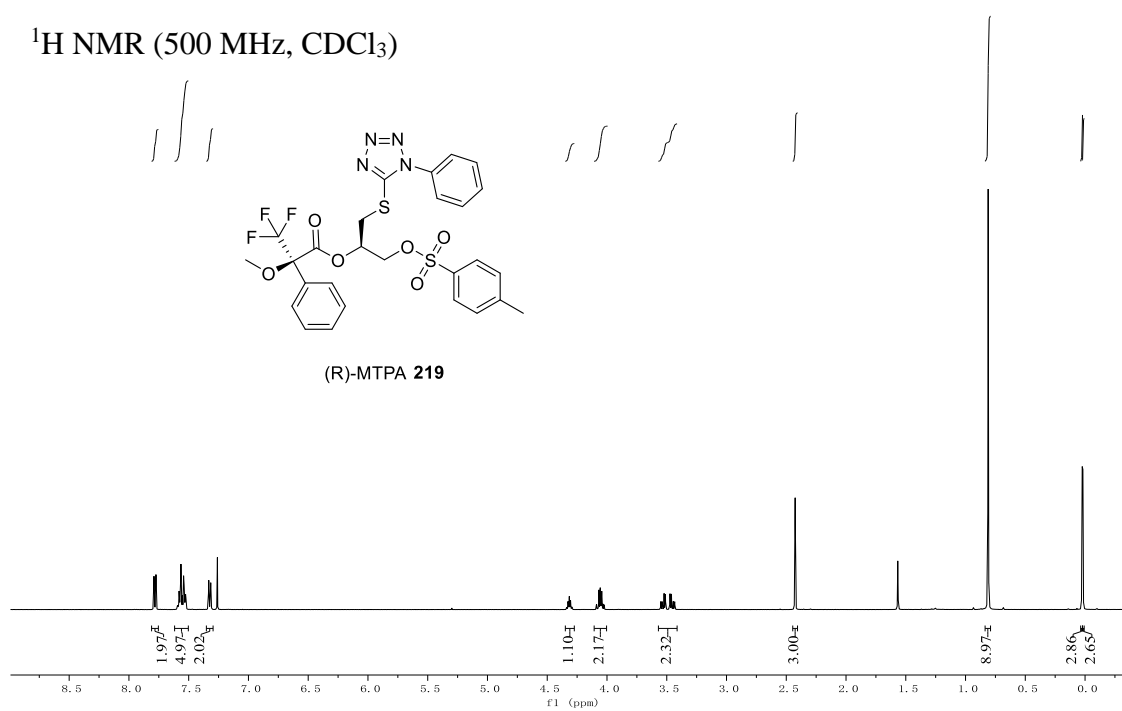


^{13}C NMR (125 MHz, CDCl_3)

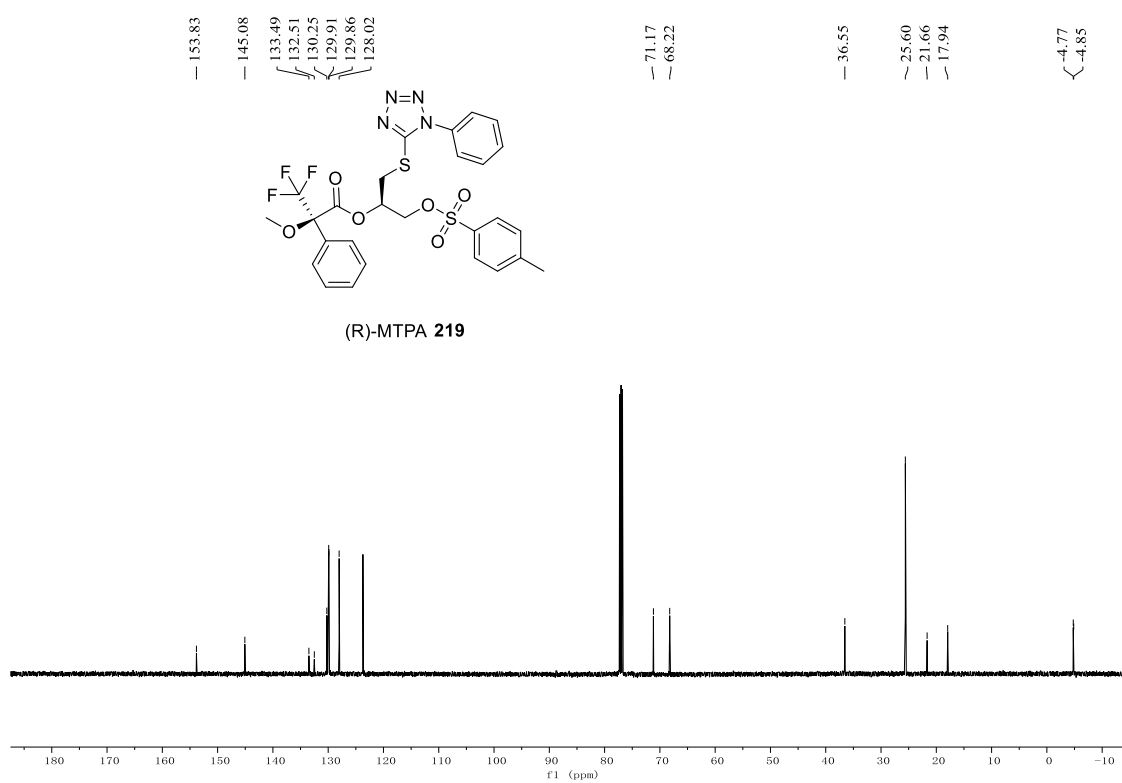


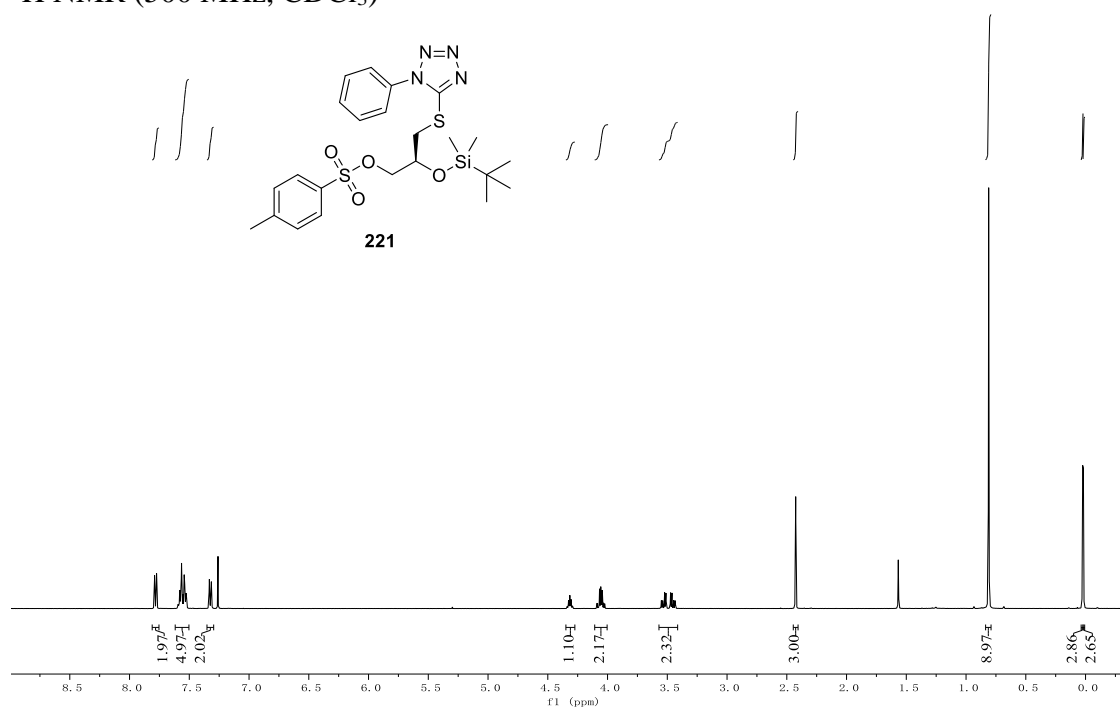
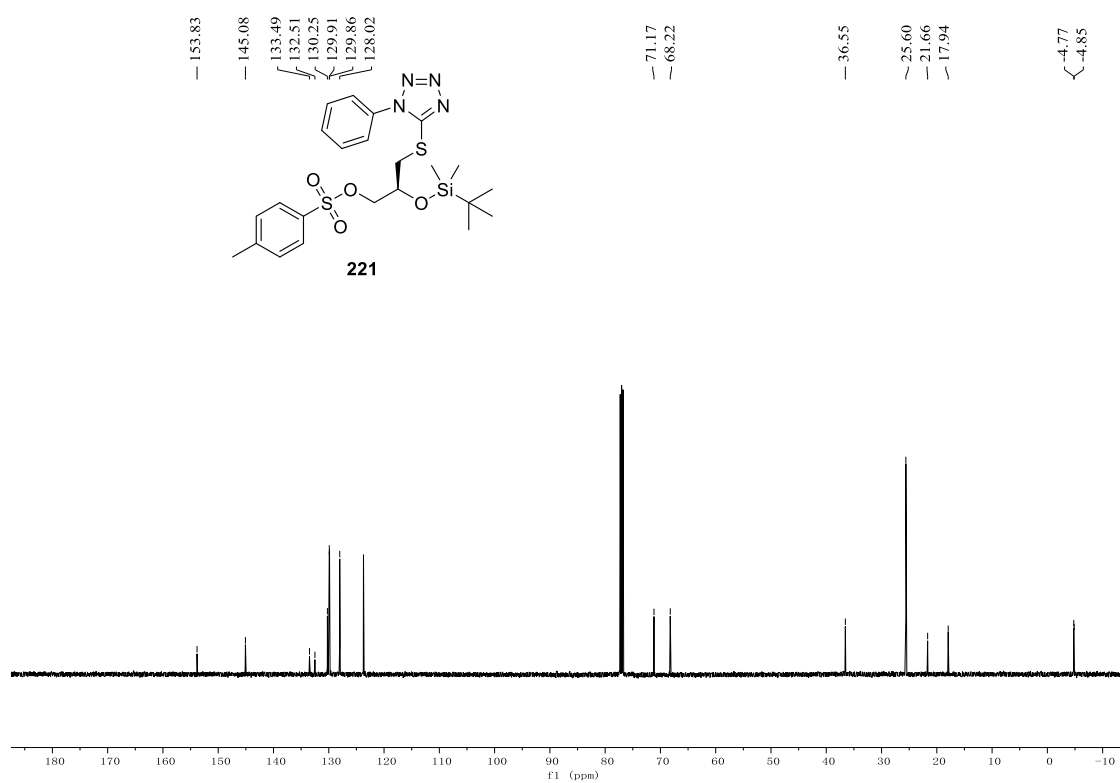
^1H NMR (500 MHz, CDCl_3) ^{13}C NMR (125 MHz, CDCl_3)

^1H NMR (500 MHz, CDCl_3)

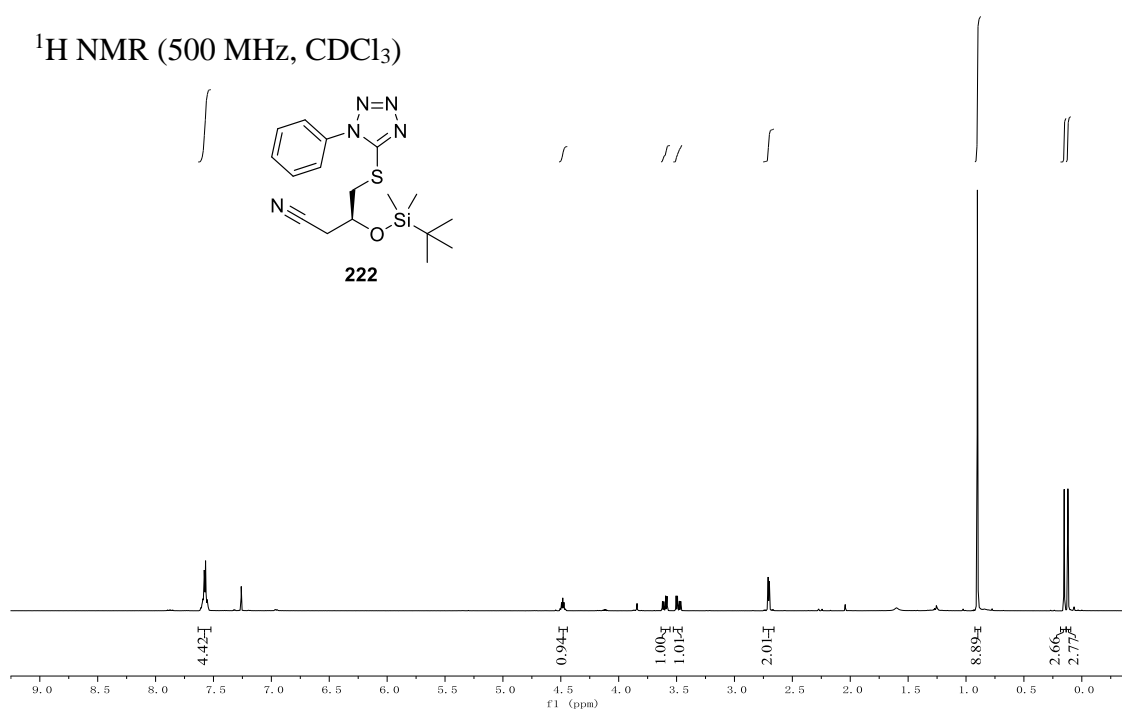


^{13}C NMR (125 MHz, CDCl_3)

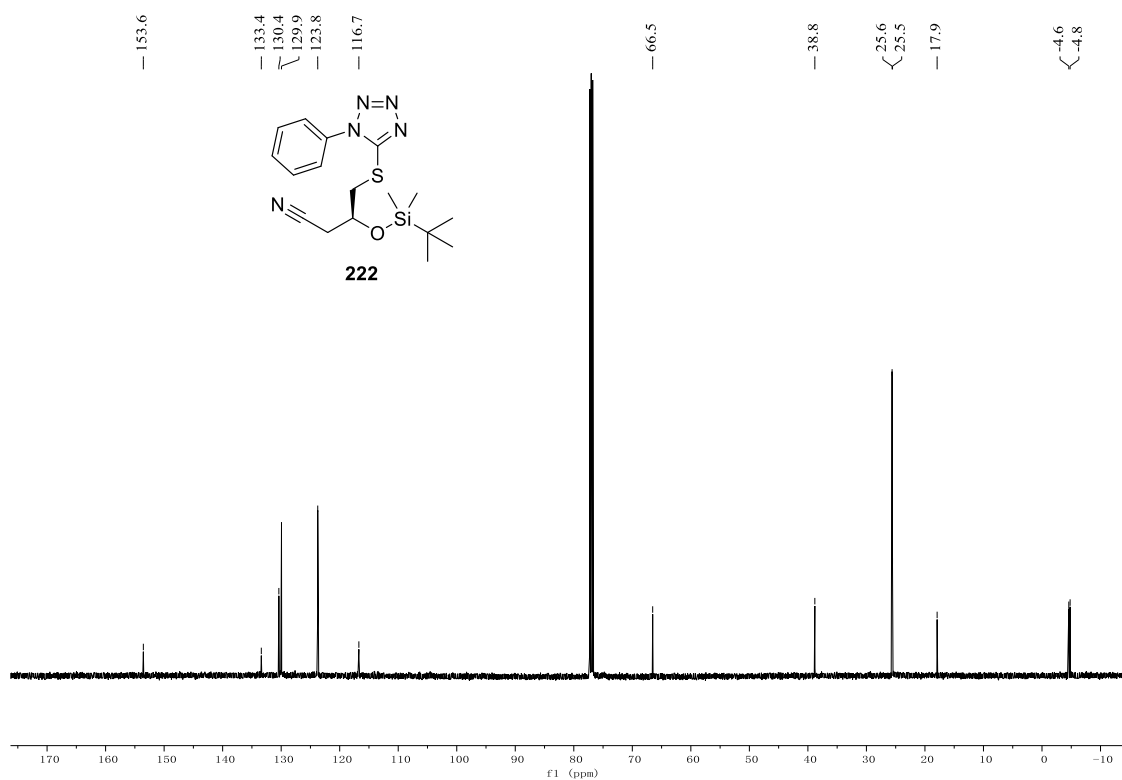


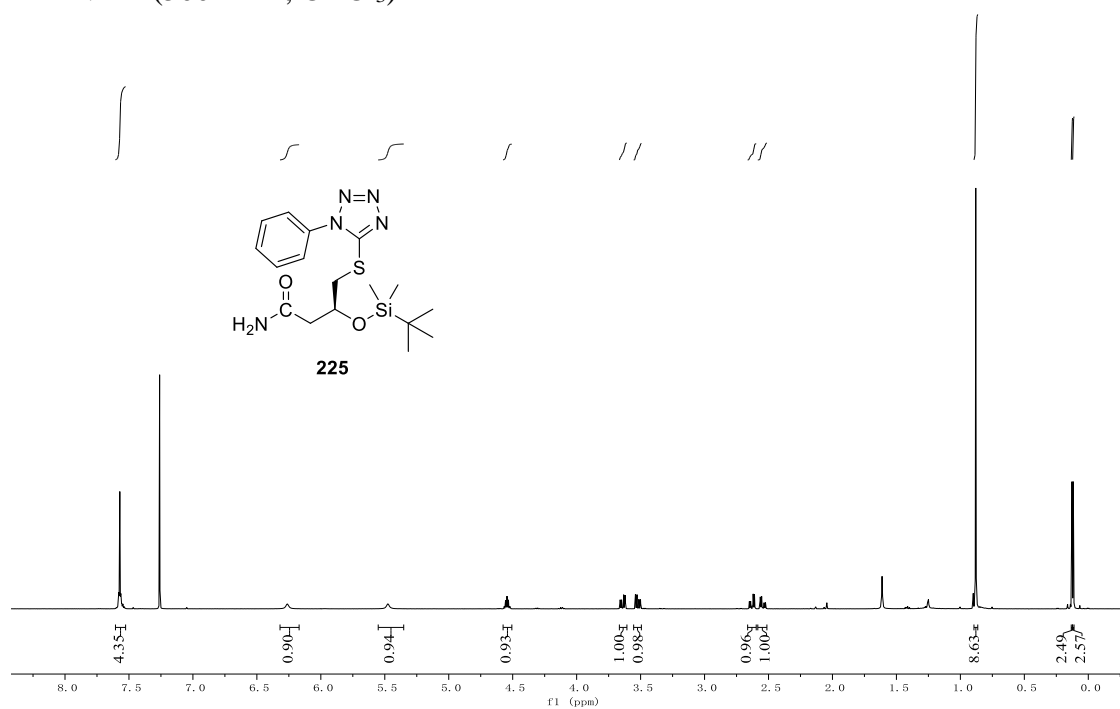
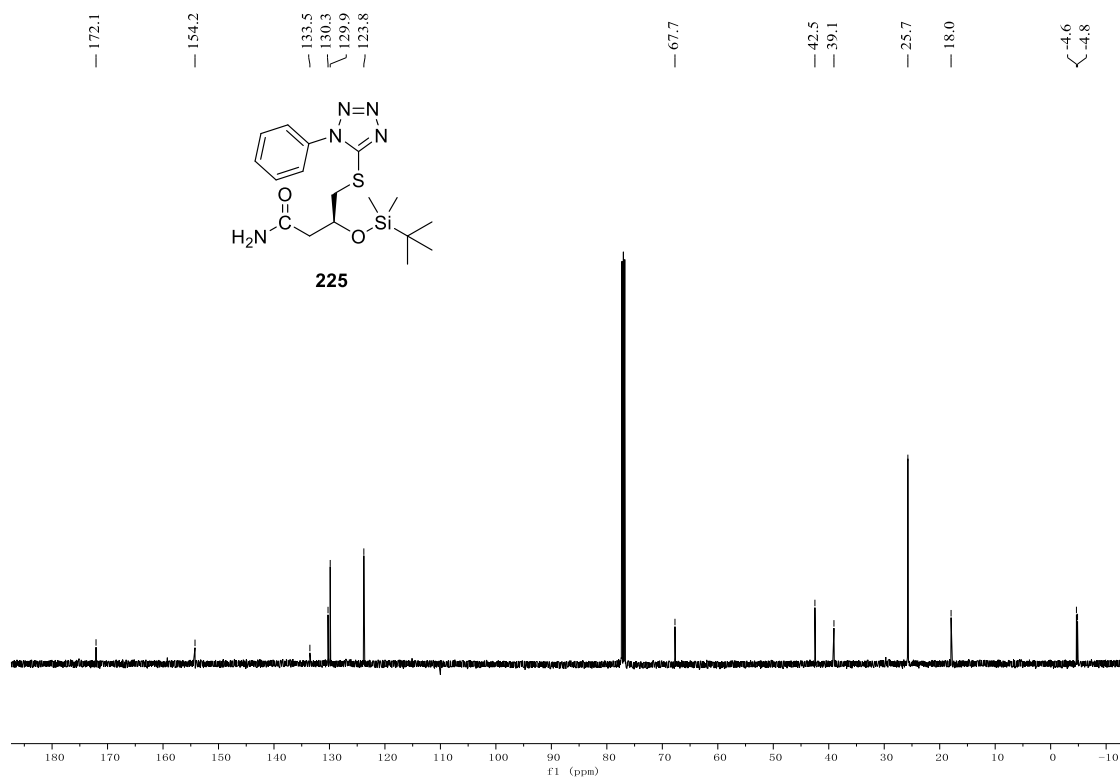
^1H NMR (500 MHz, CDCl_3) ^{13}C NMR (125 MHz, CDCl_3)

^1H NMR (500 MHz, CDCl_3)

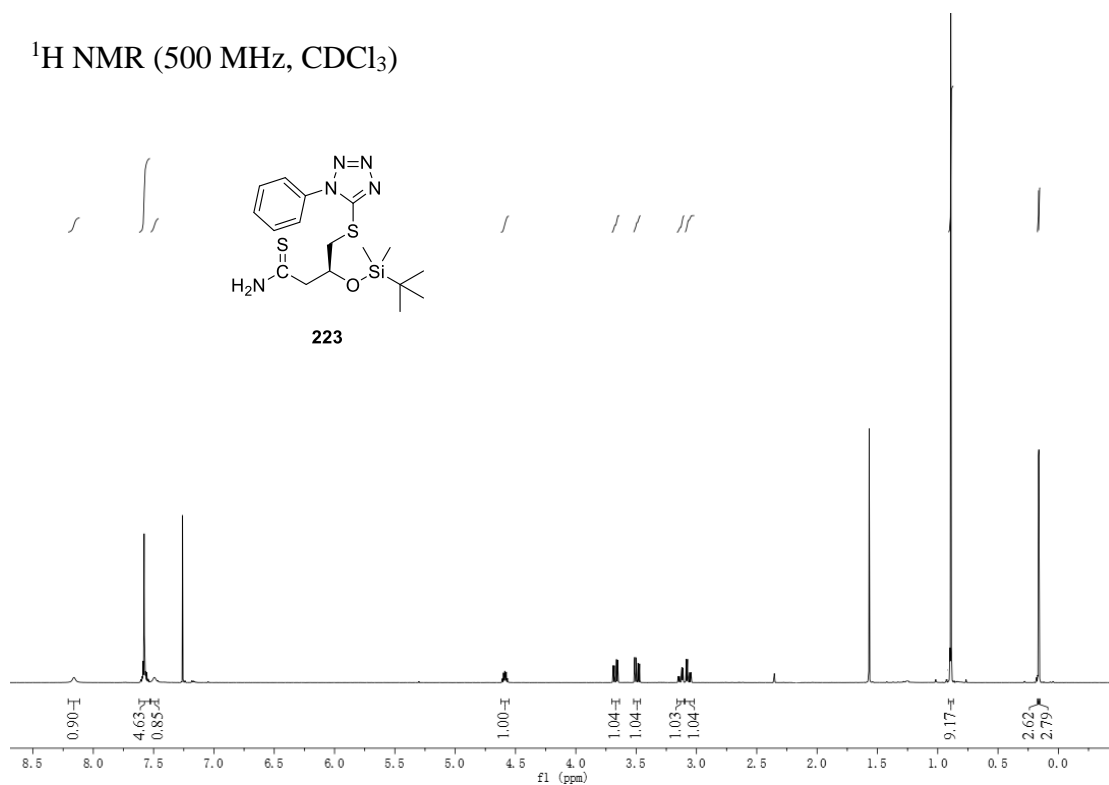


^{13}C NMR (125 MHz, CDCl_3)

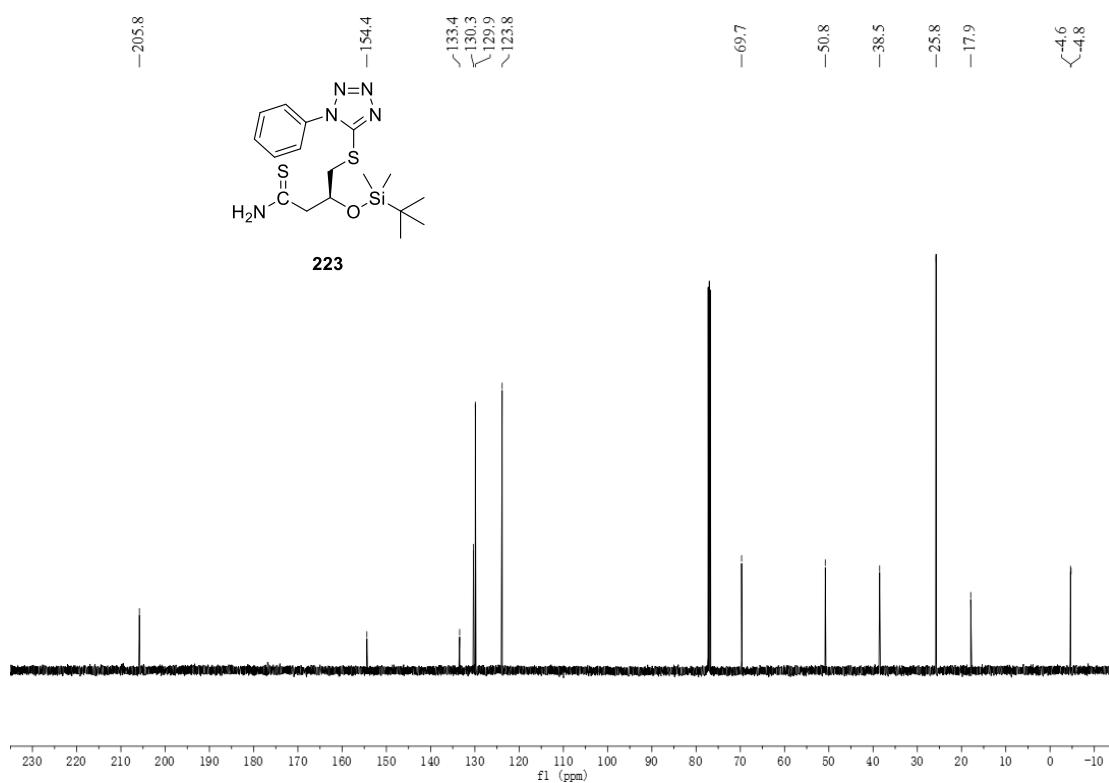


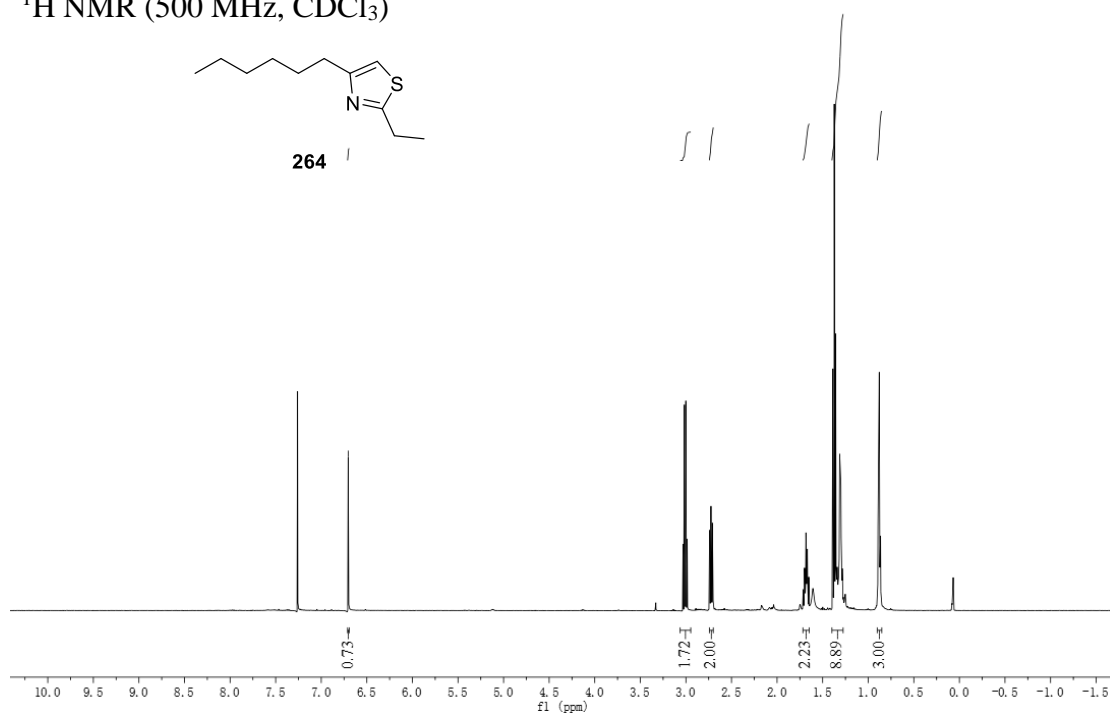
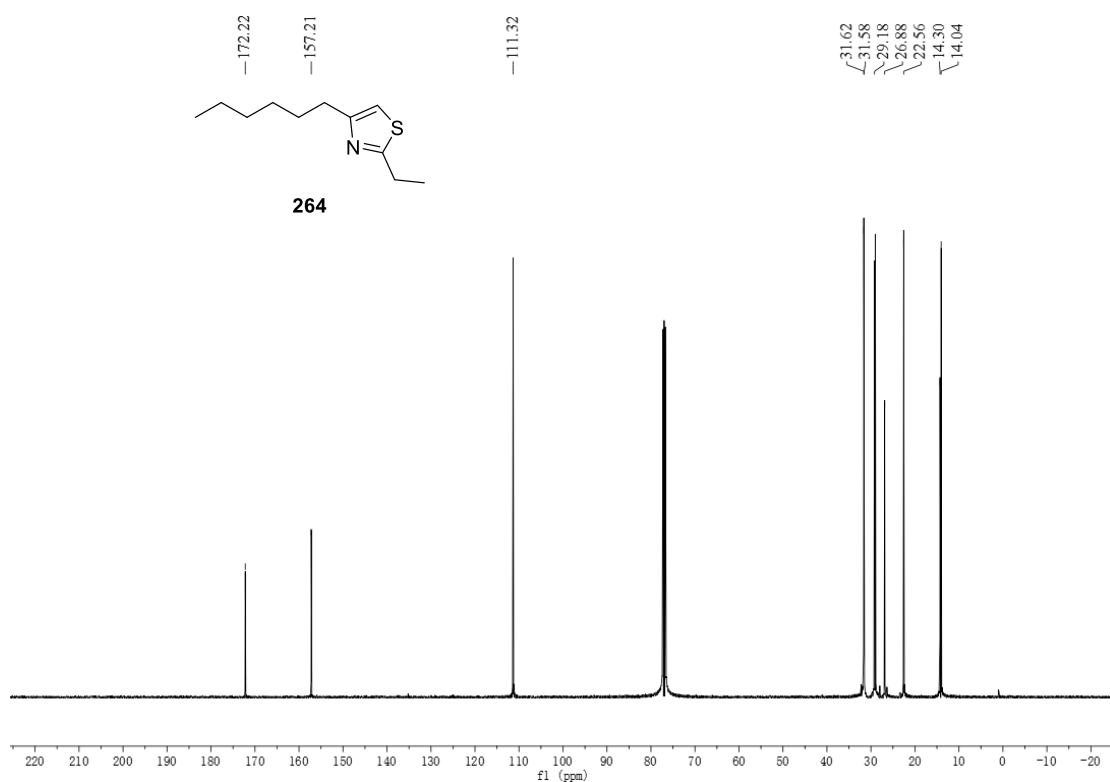
^1H NMR (500 MHz, CDCl_3) ^{13}C NMR (125 MHz, CDCl_3)

^1H NMR (500 MHz, CDCl_3)

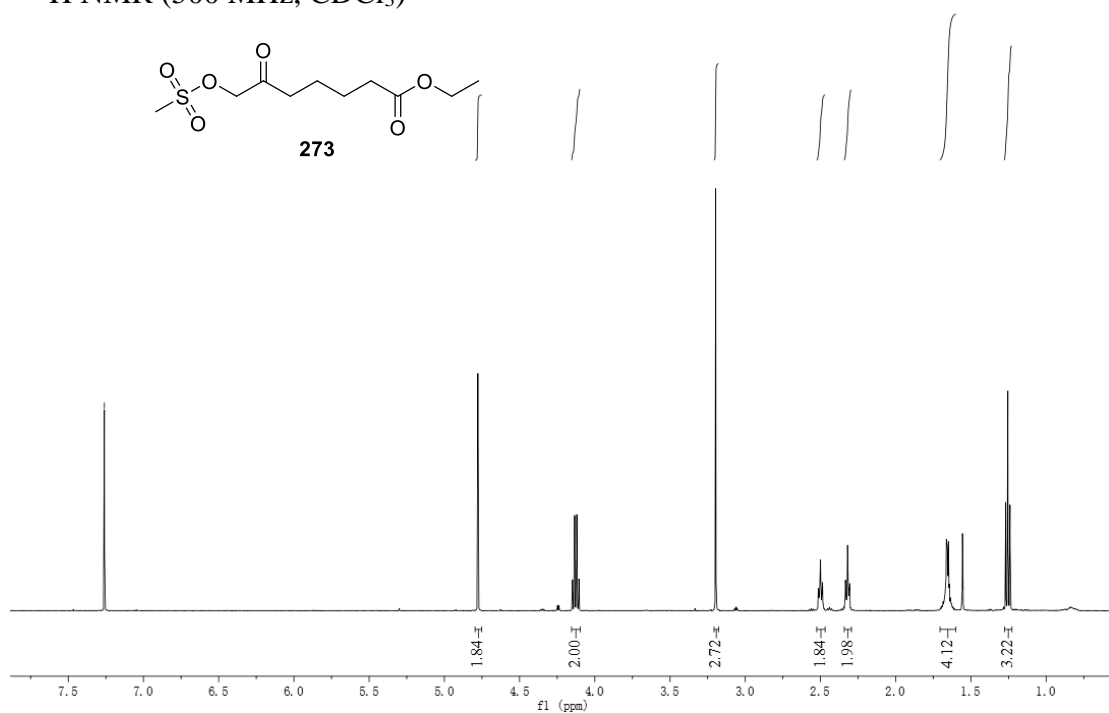


^{13}C NMR (125 MHz, CDCl_3)

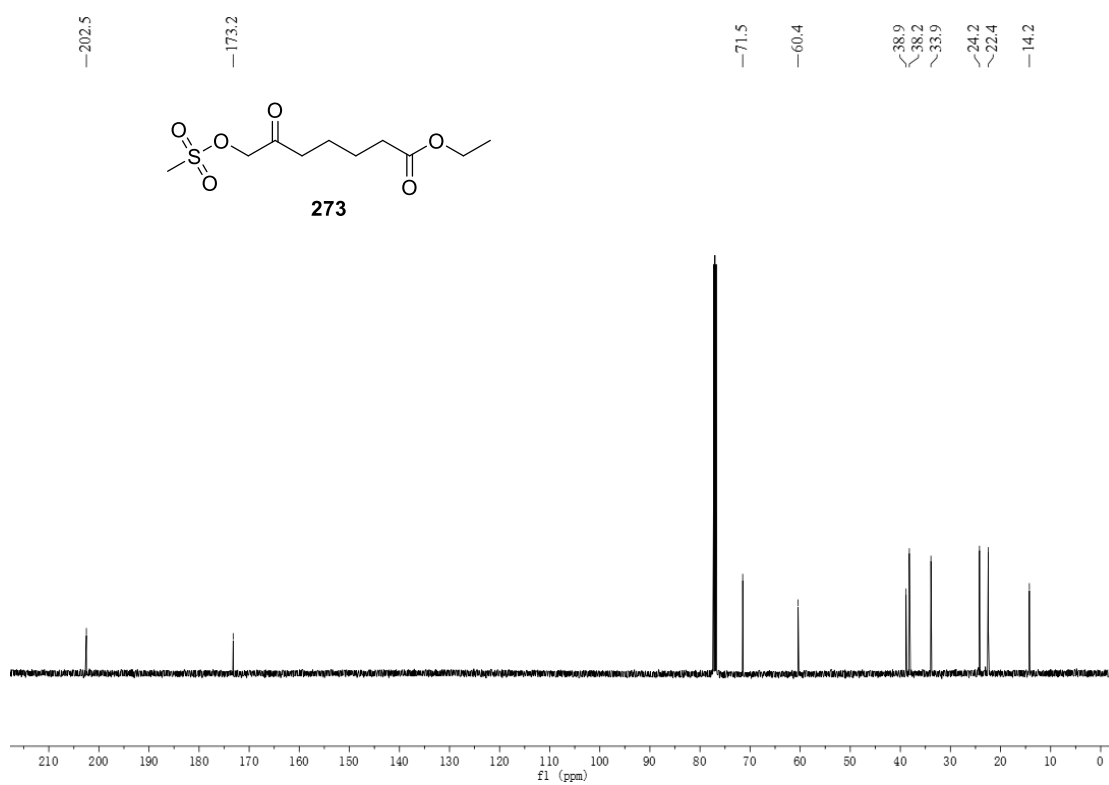


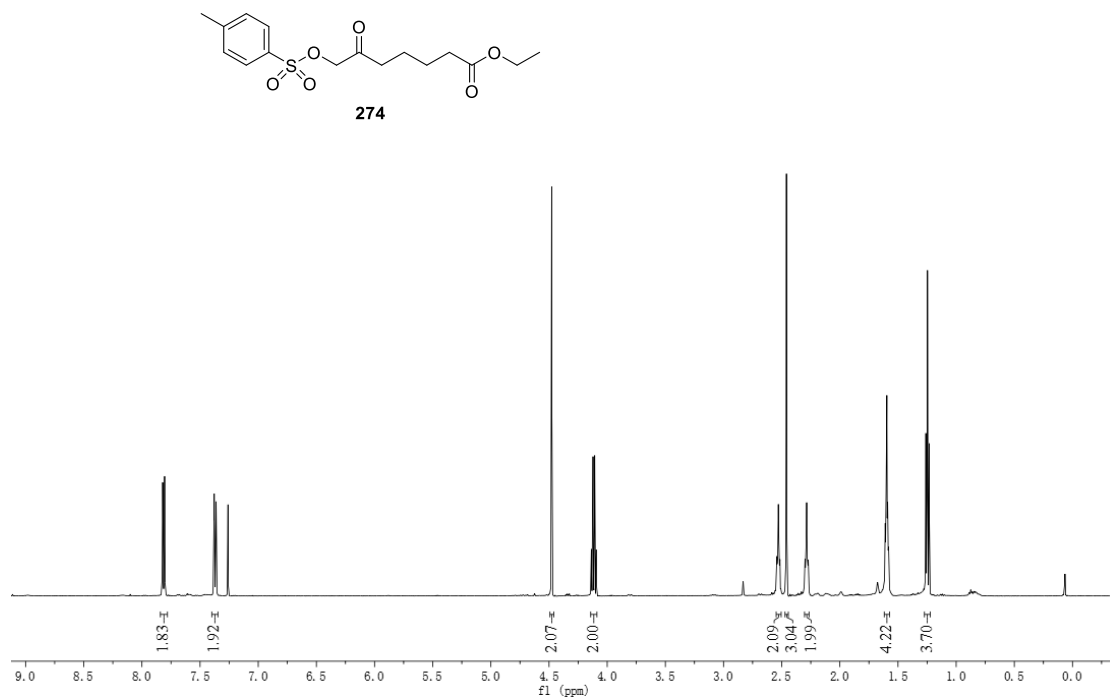
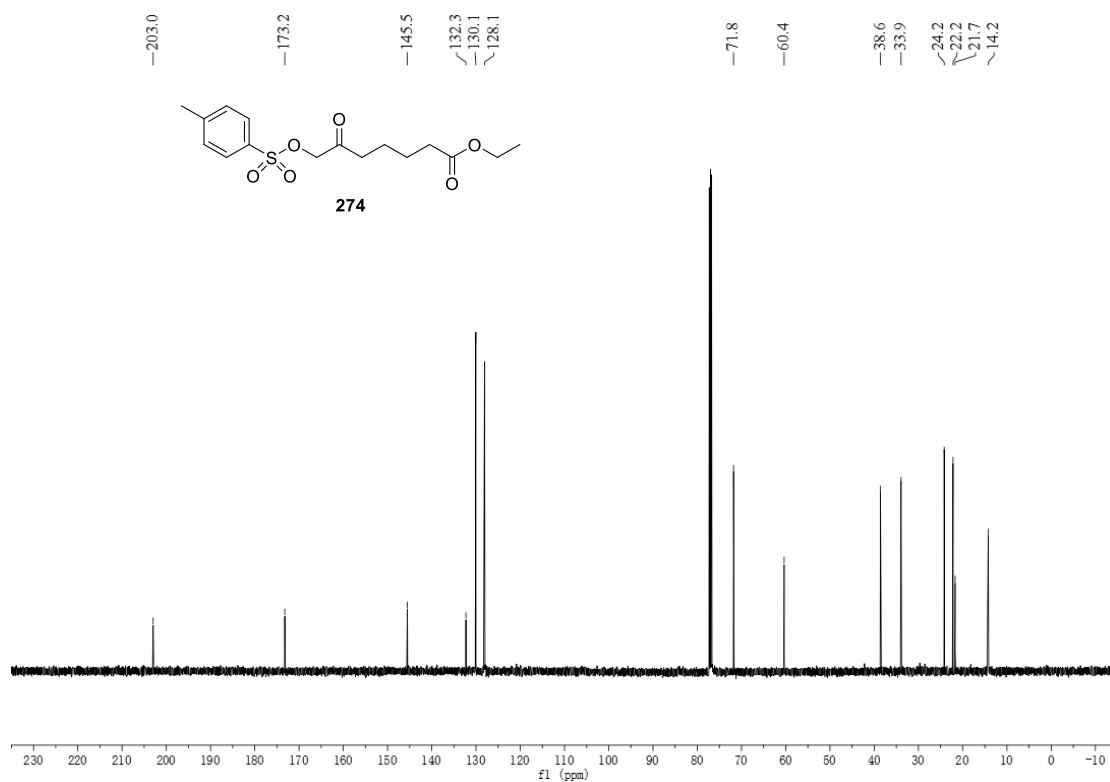
^1H NMR (500 MHz, CDCl_3) ^{13}C NMR (125 MHz, CDCl_3)

^1H NMR (500 MHz, CDCl_3)

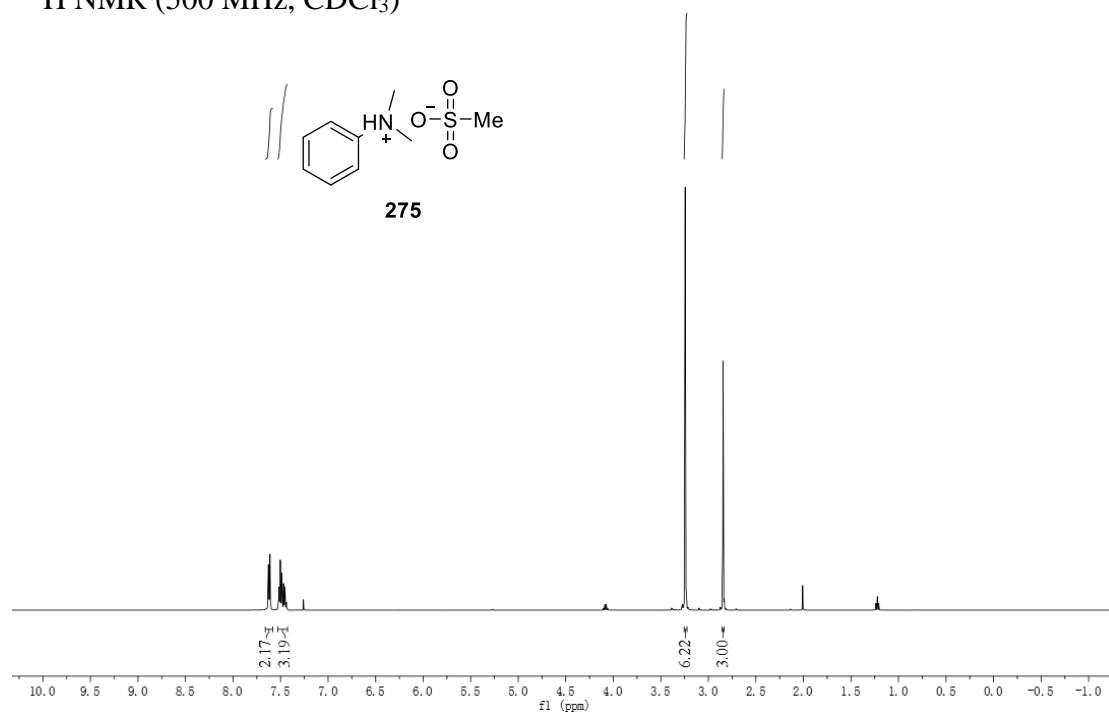


^{13}C NMR (125 MHz, CDCl_3)

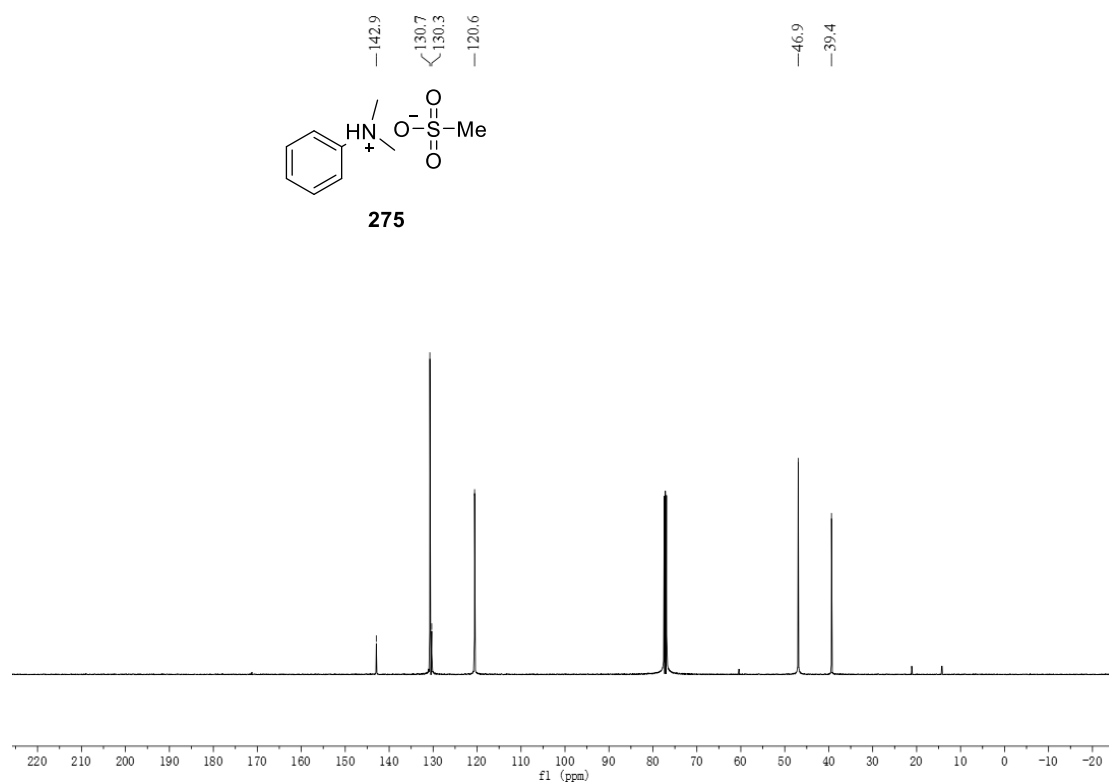


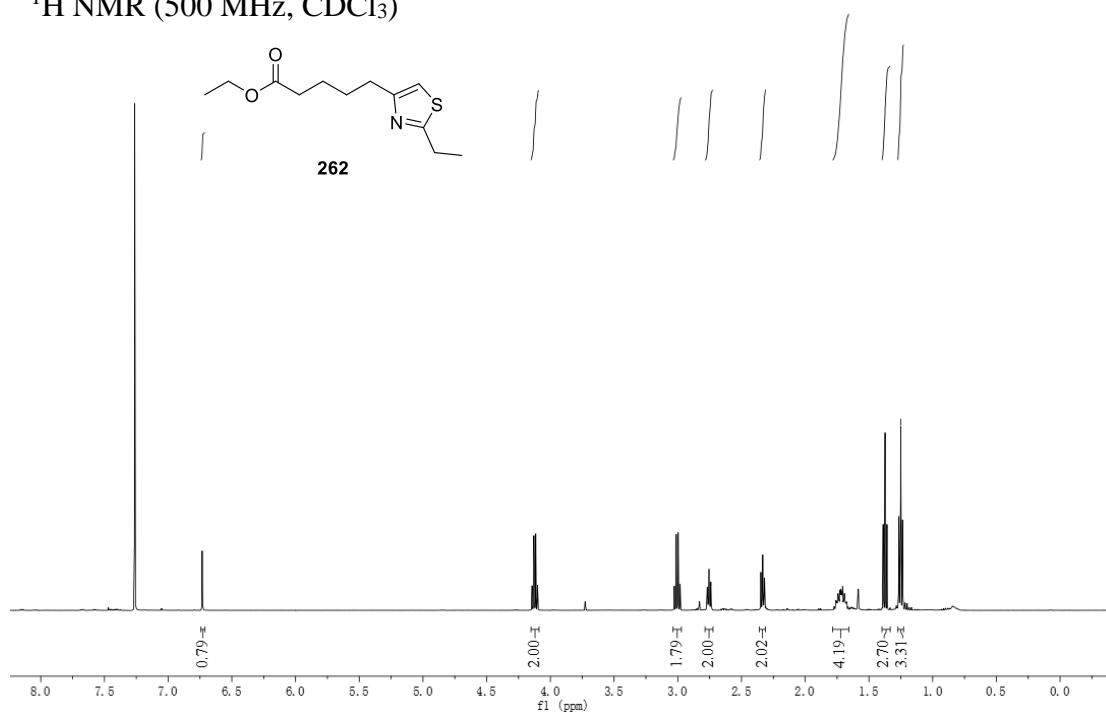
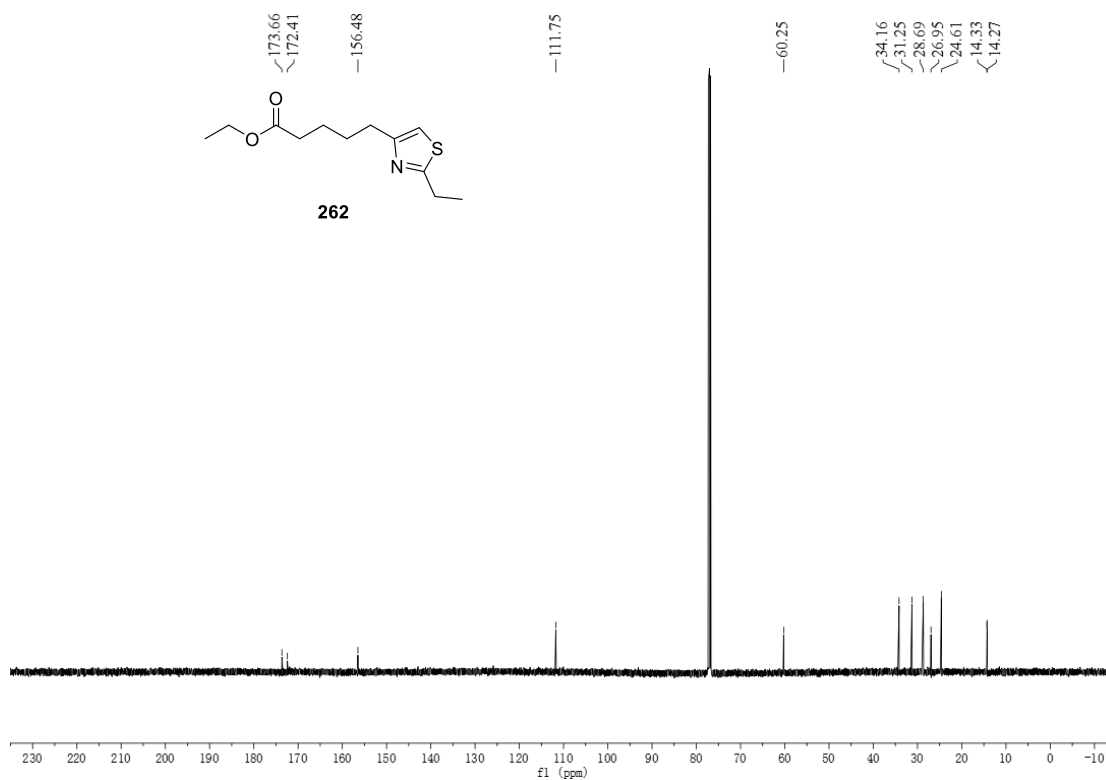
^1H NMR (500 MHz, CDCl_3) ^{13}C NMR (125 MHz, CDCl_3)

^1H NMR (500 MHz, CDCl_3)

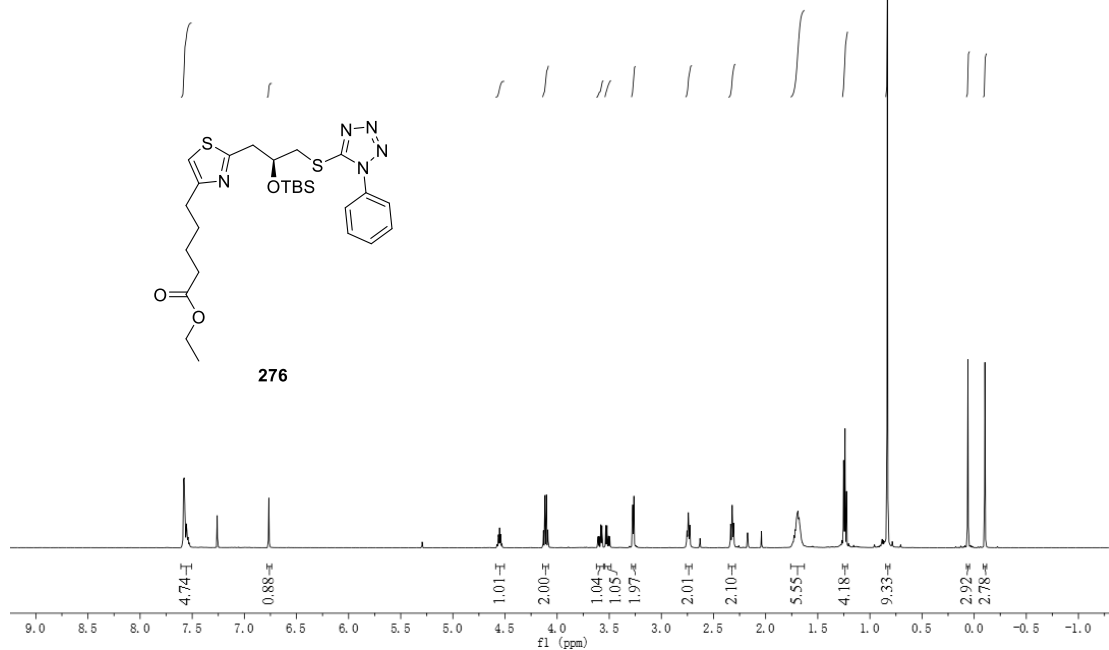


^{13}C NMR (125 MHz, CDCl_3)

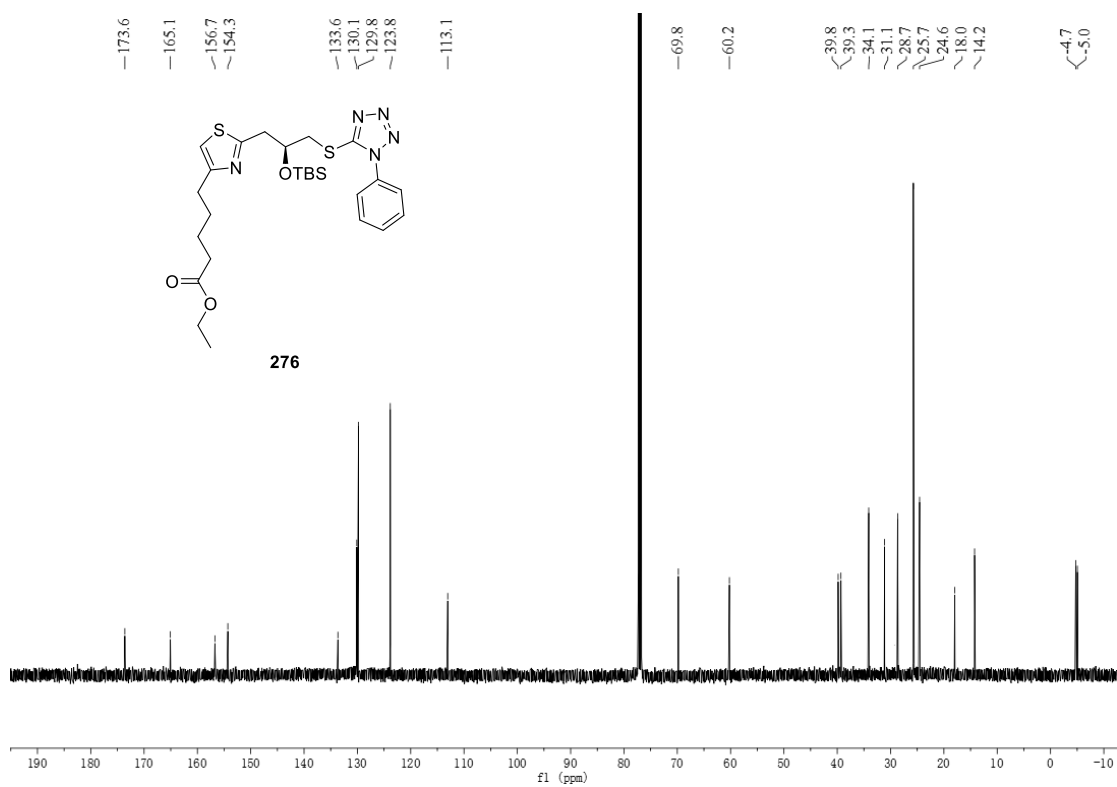


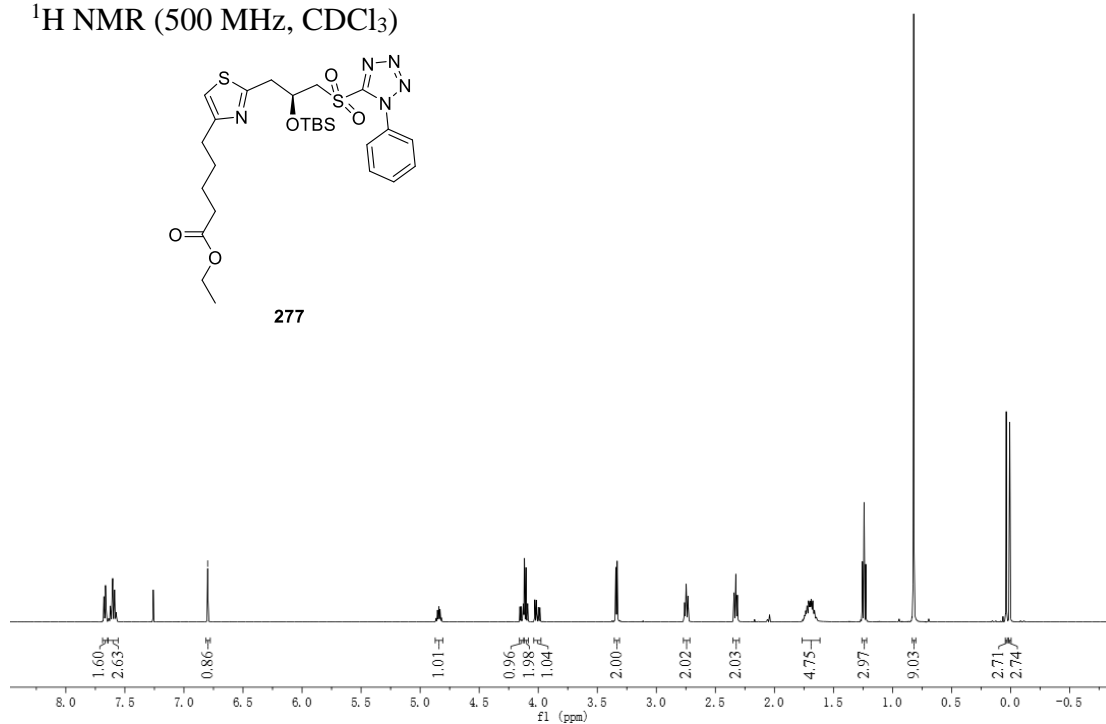
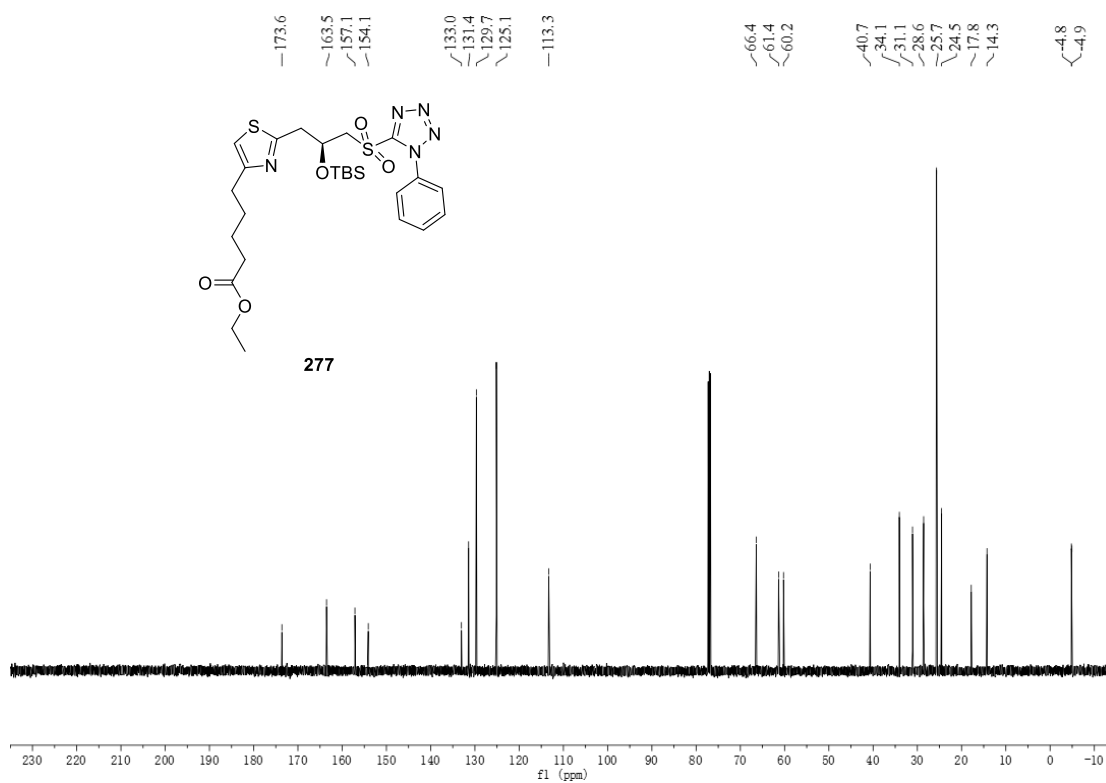
^1H NMR (500 MHz, CDCl_3) ^{13}C NMR (125 MHz, CDCl_3)

^1H NMR (500 MHz, CDCl_3)

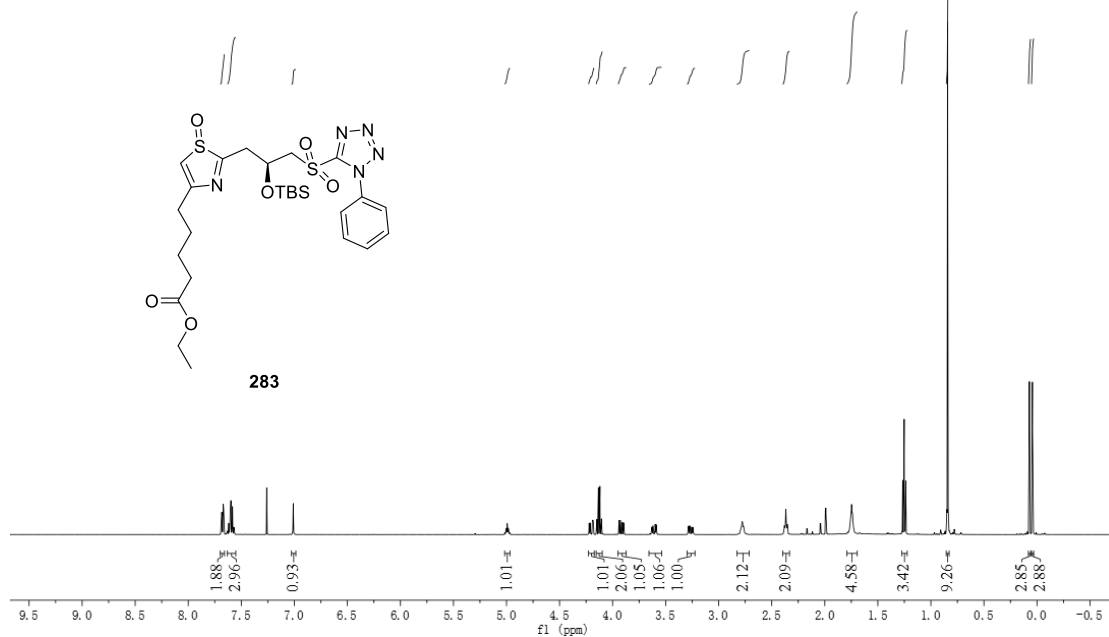


^{13}C NMR (125 MHz, CDCl_3)

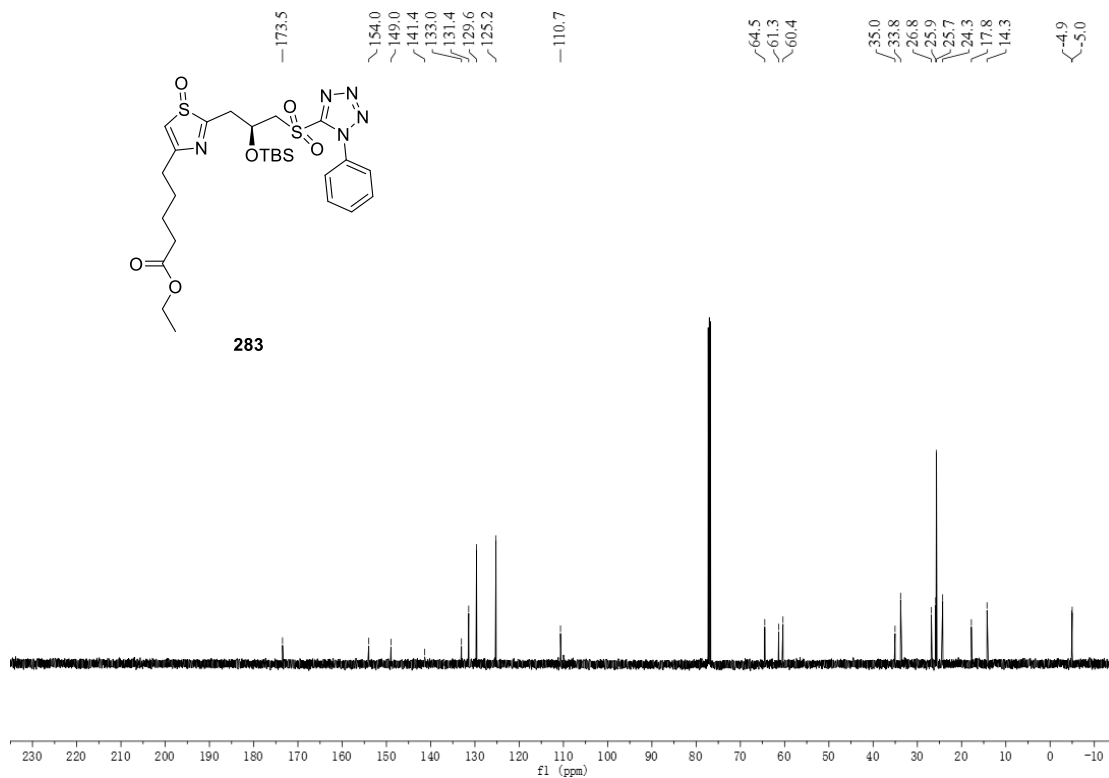


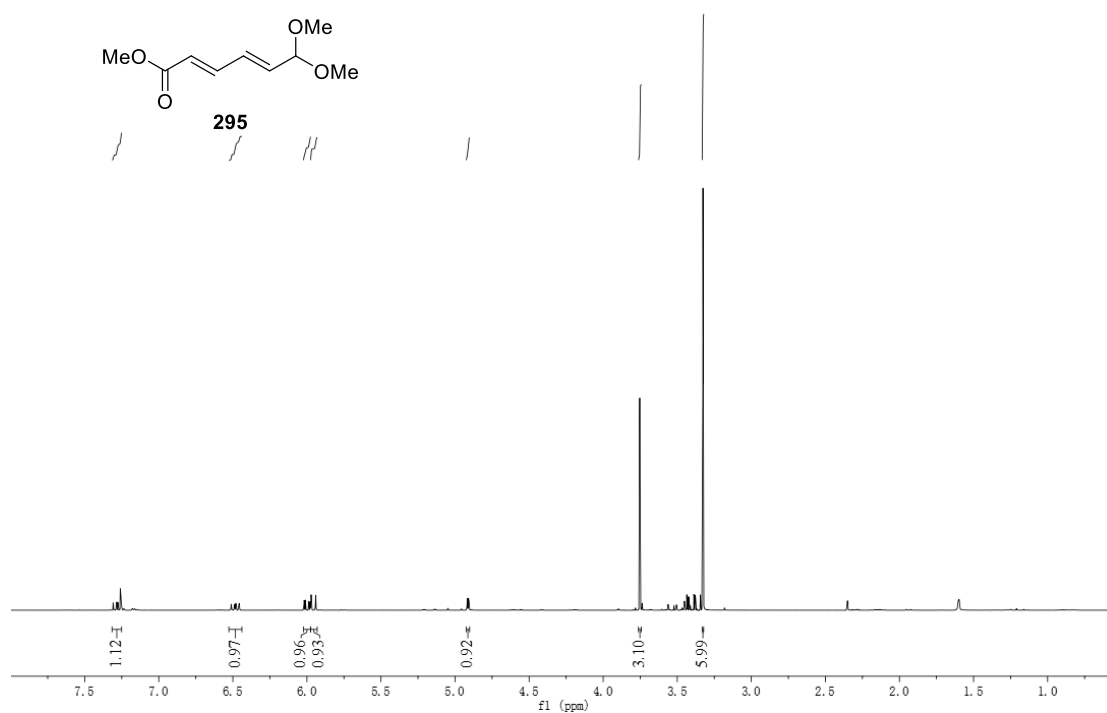
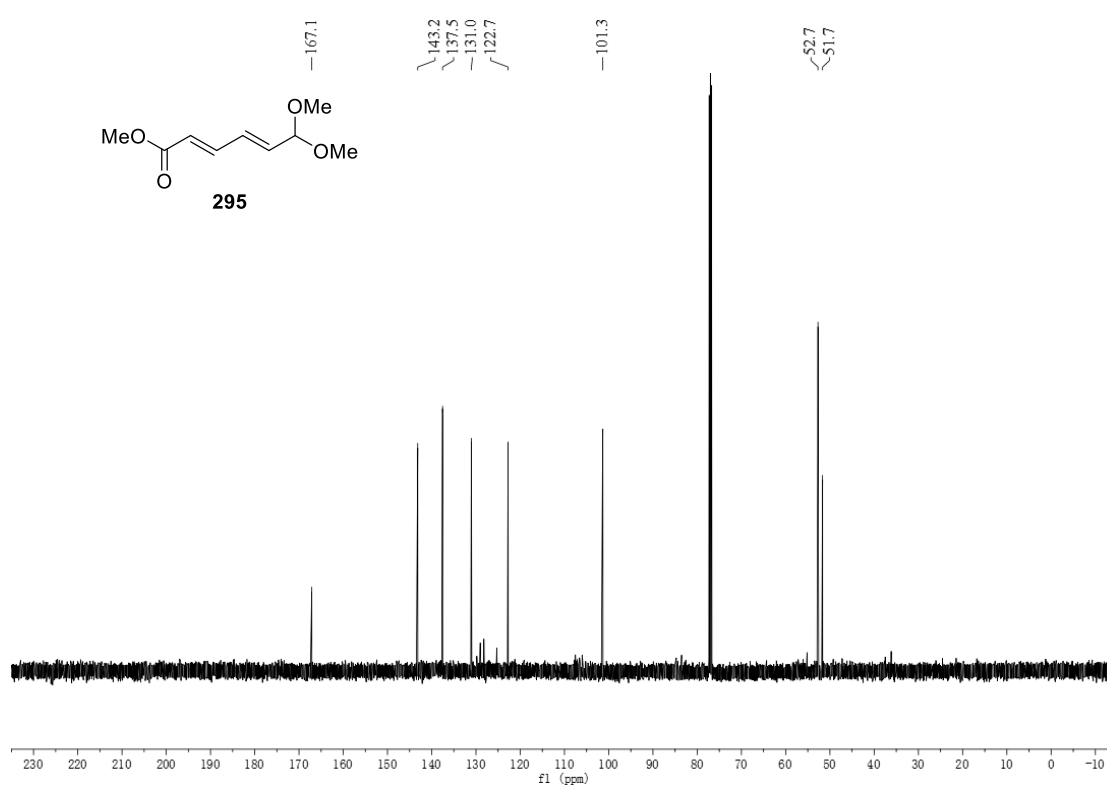
^1H NMR (500 MHz, CDCl_3) ^{13}C NMR (125 MHz, CDCl_3)

^1H NMR (500 MHz, CDCl_3)

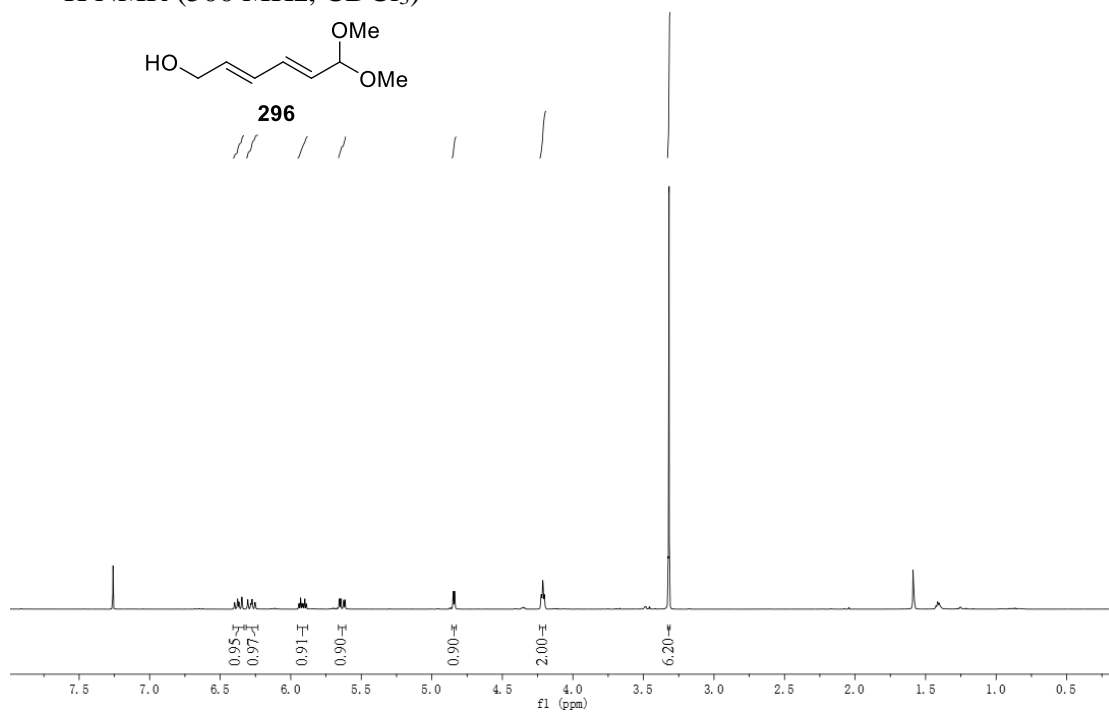


^{13}C NMR (125 MHz, CDCl_3)

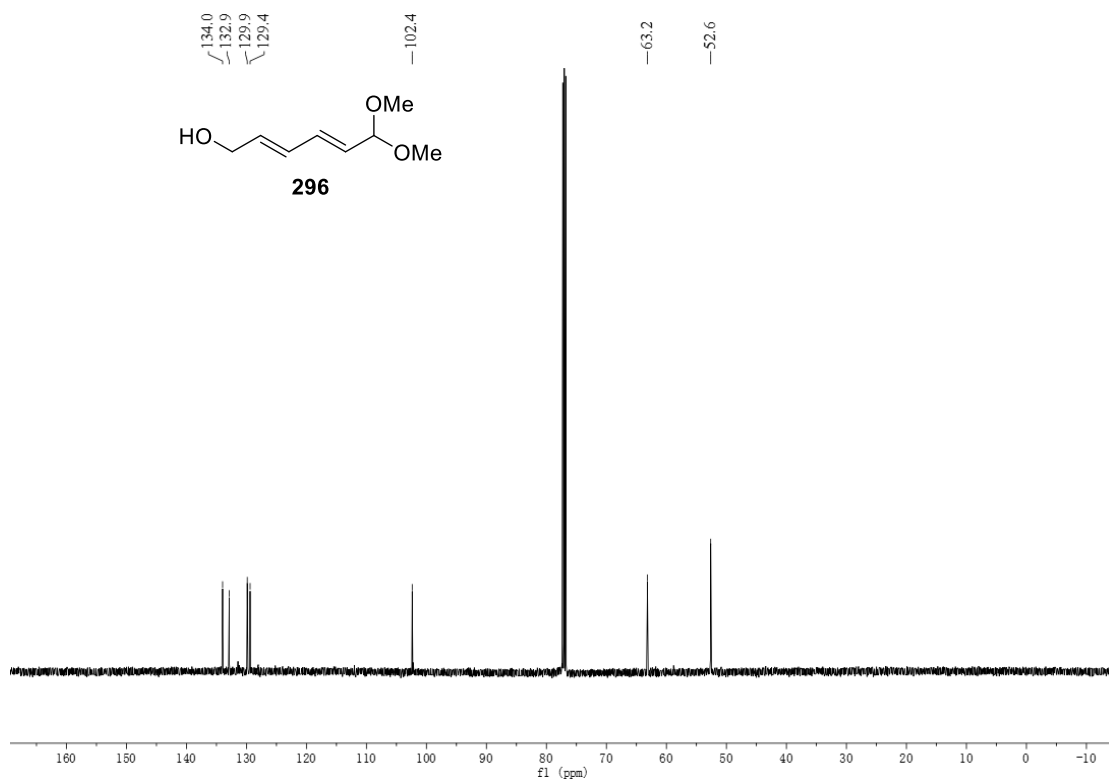


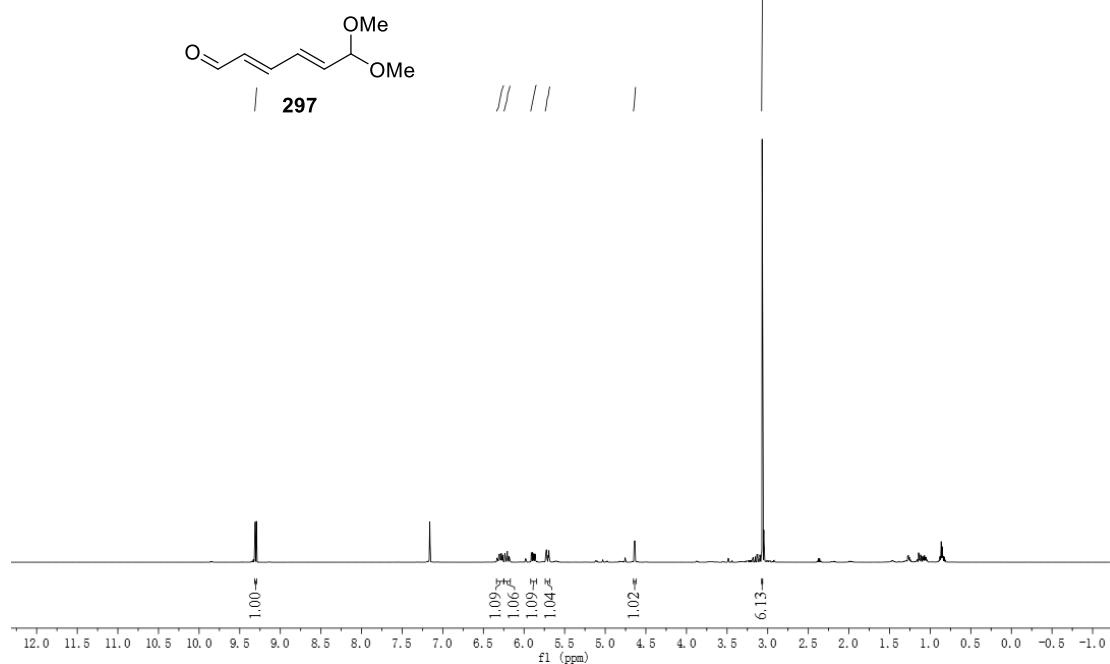
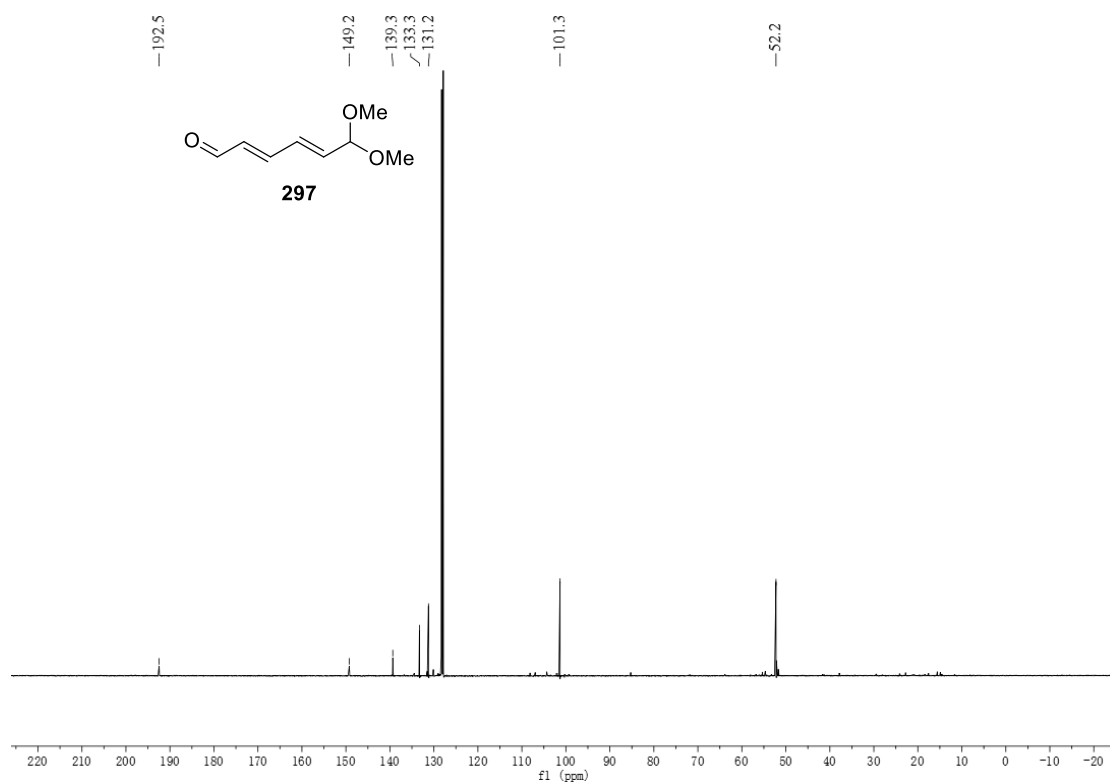
^1H NMR (500 MHz, CDCl_3) ^{13}C NMR (125 MHz, CDCl_3)

^1H NMR (500 MHz, CDCl_3)

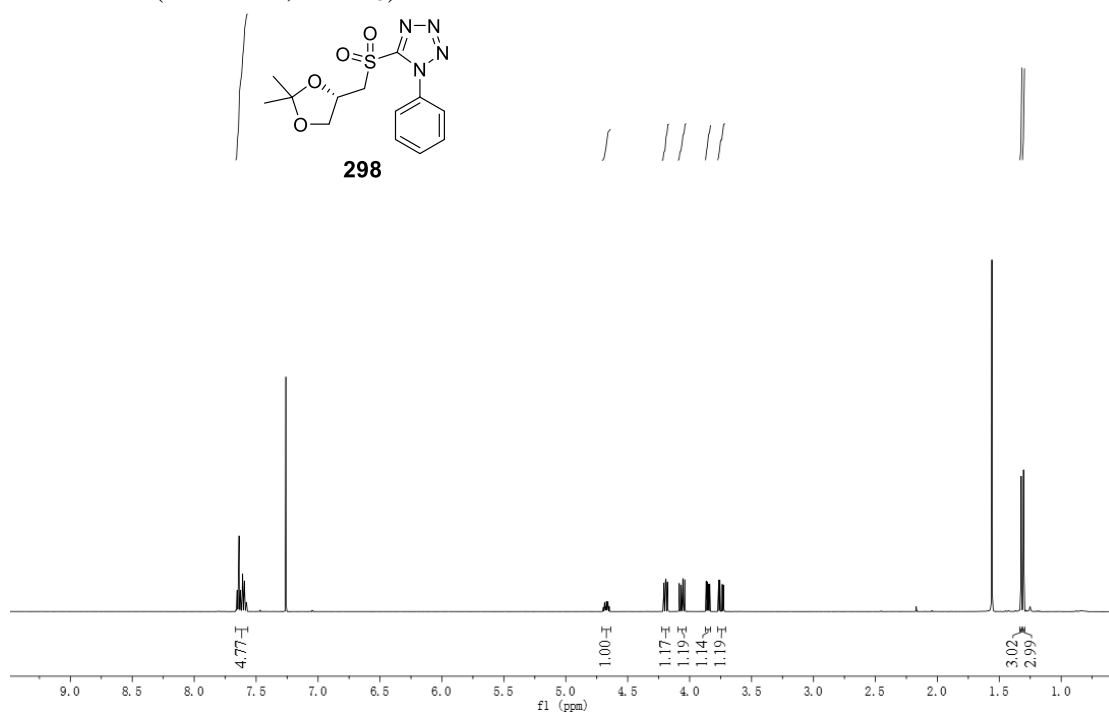


^{13}C NMR (125 MHz, CDCl_3)

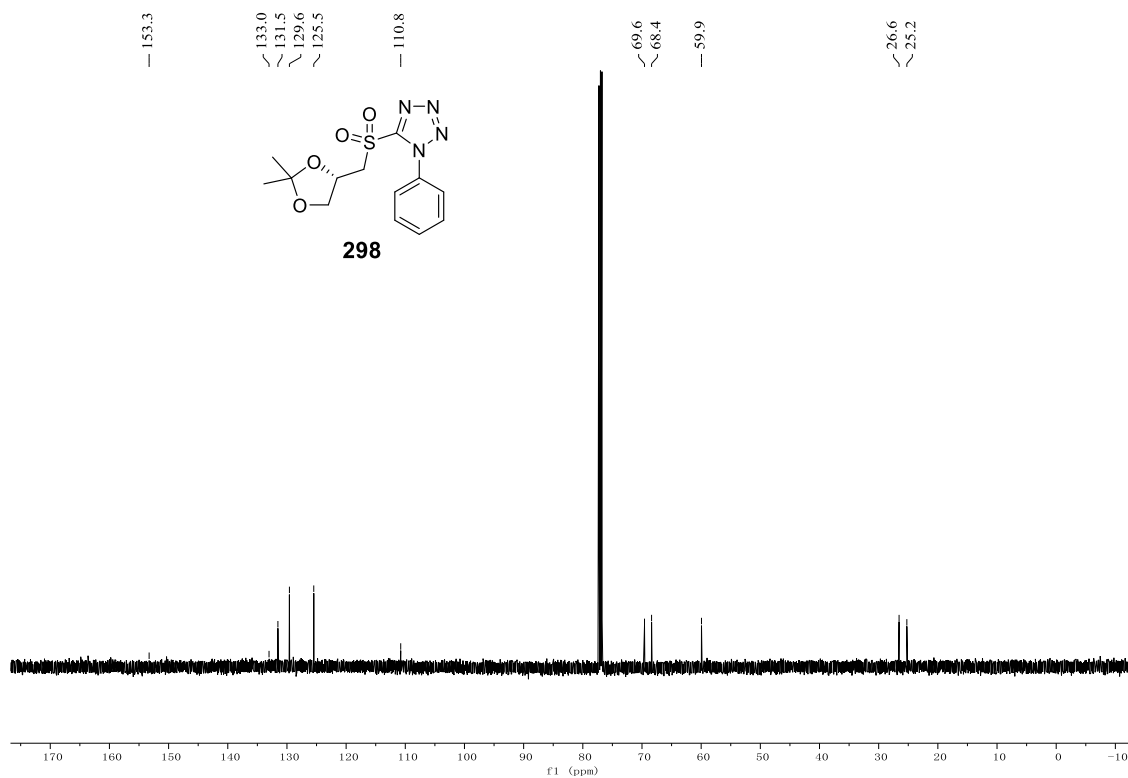


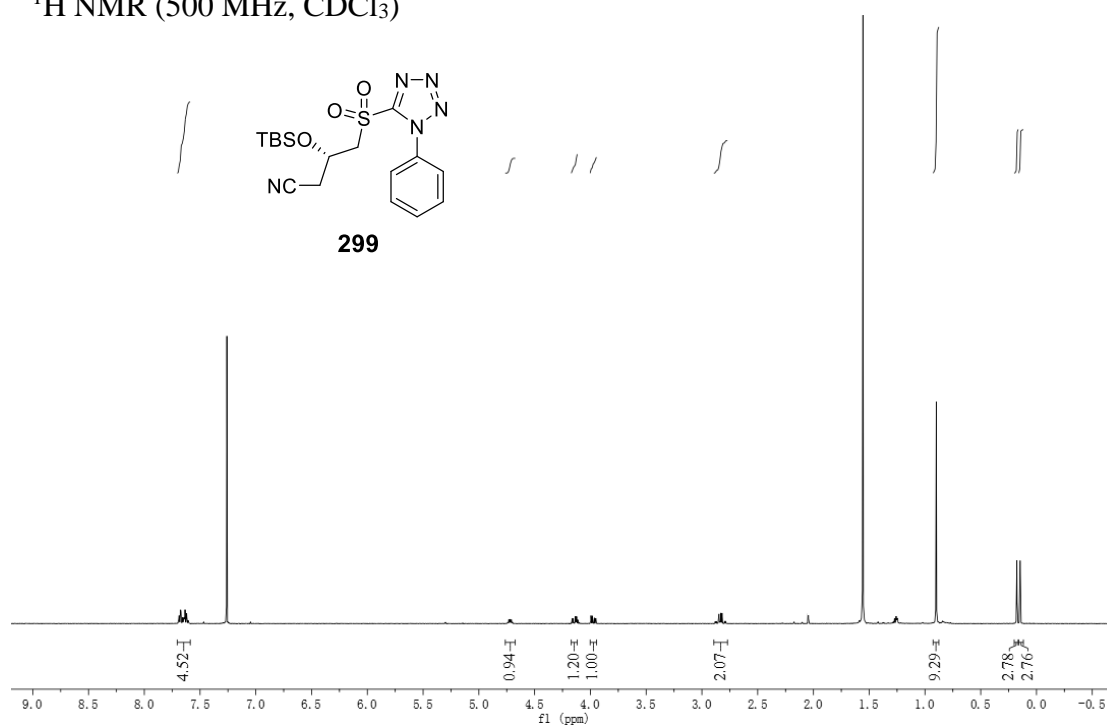
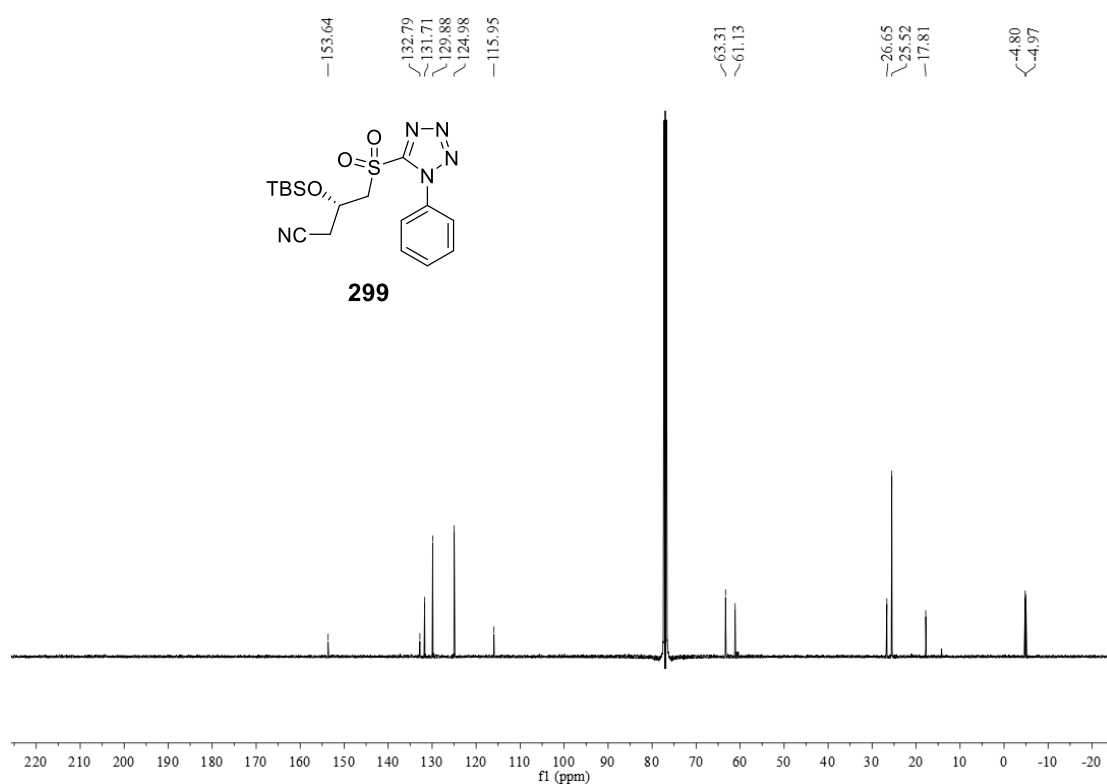
^1H NMR (500 MHz, C_6D_6) ^{13}C NMR (125 MHz, C_6D_6)

^1H NMR (500 MHz, CDCl_3)

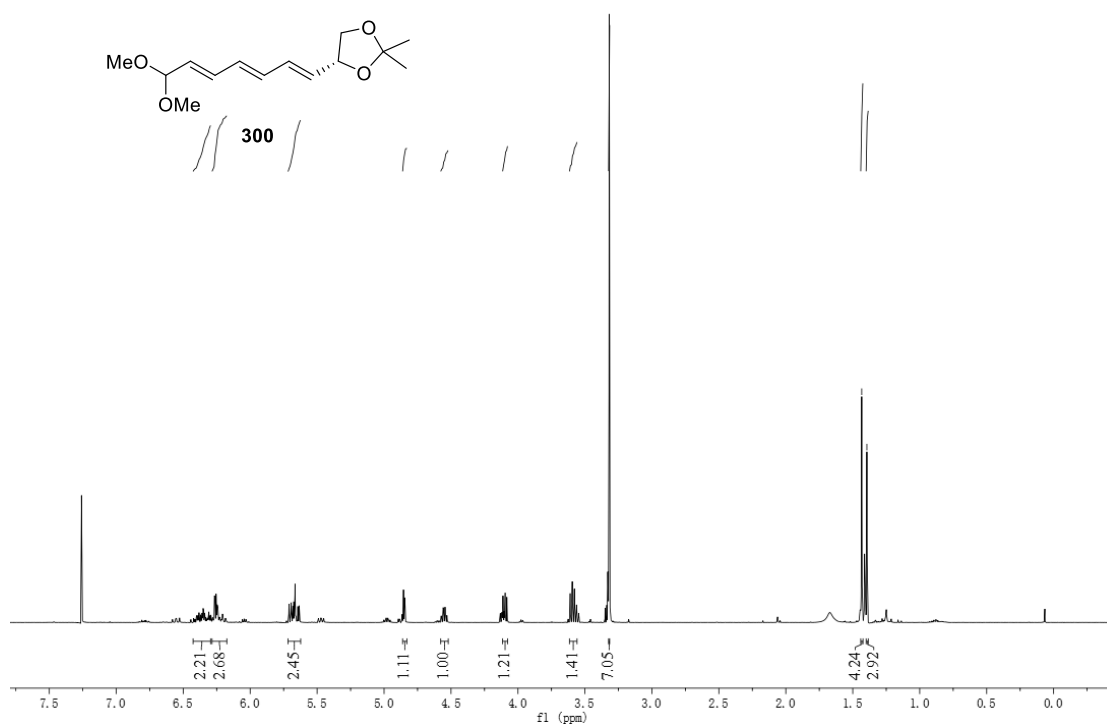


^{13}C NMR (125 MHz, CDCl_3)

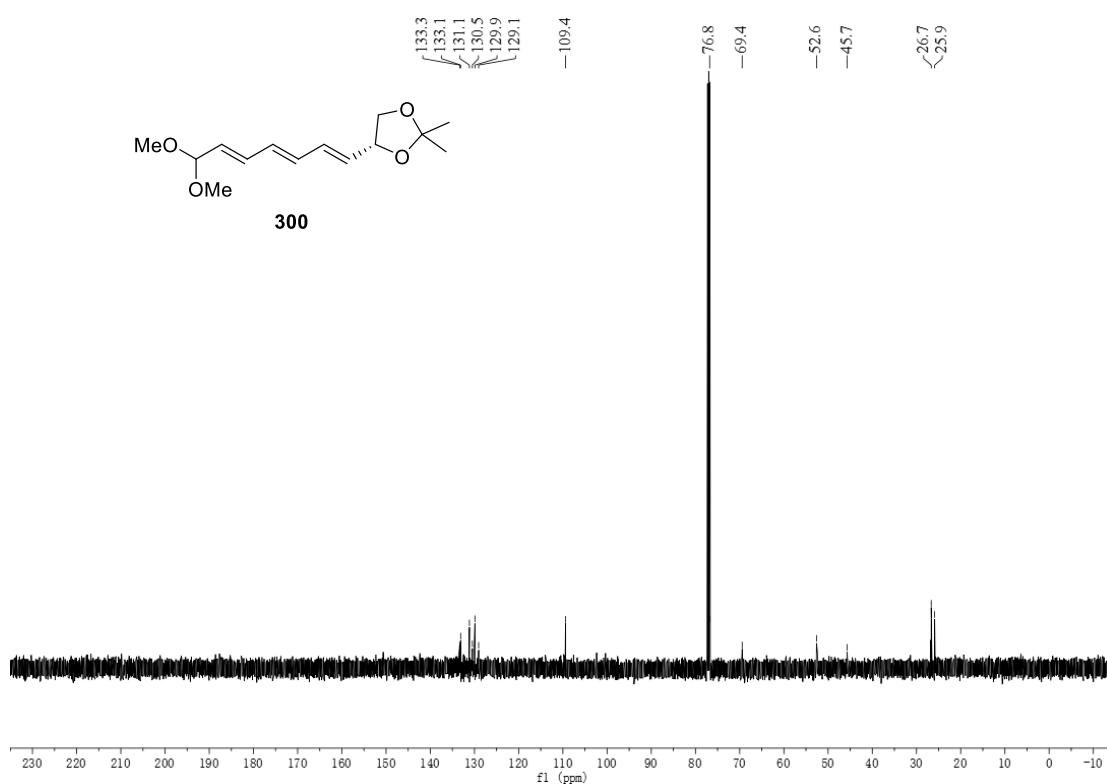


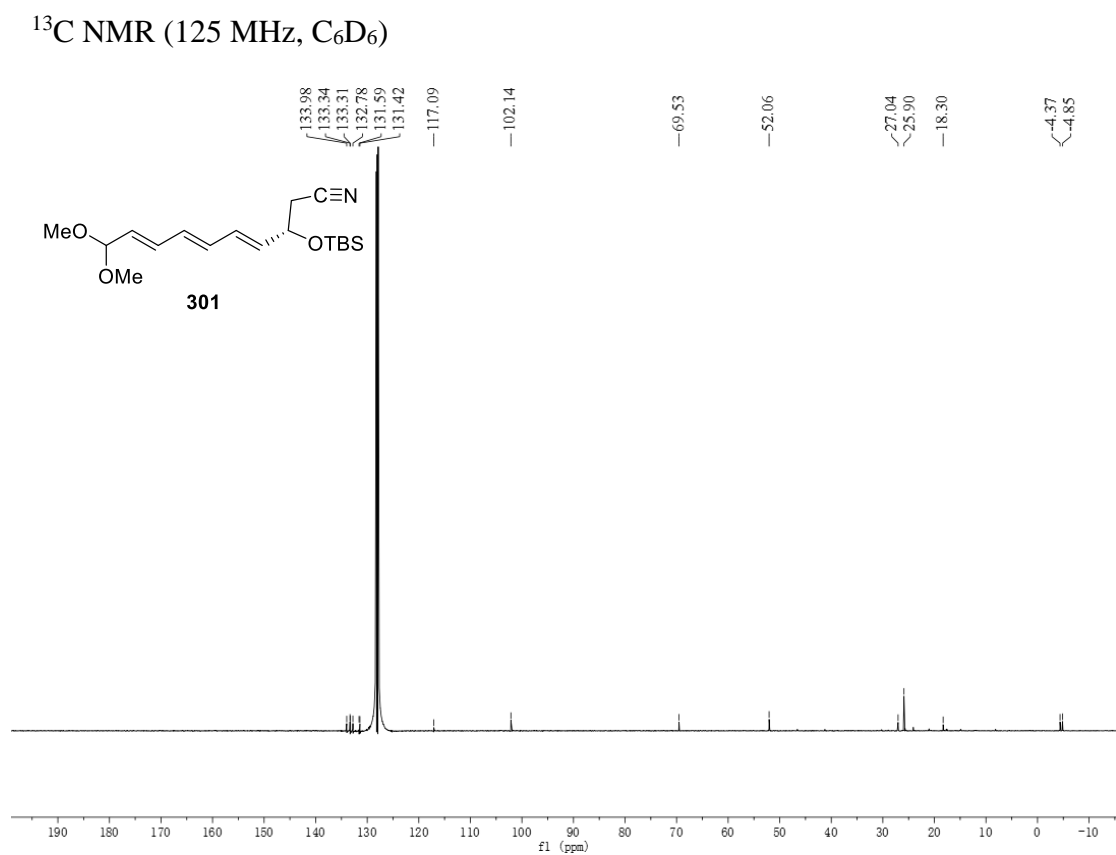
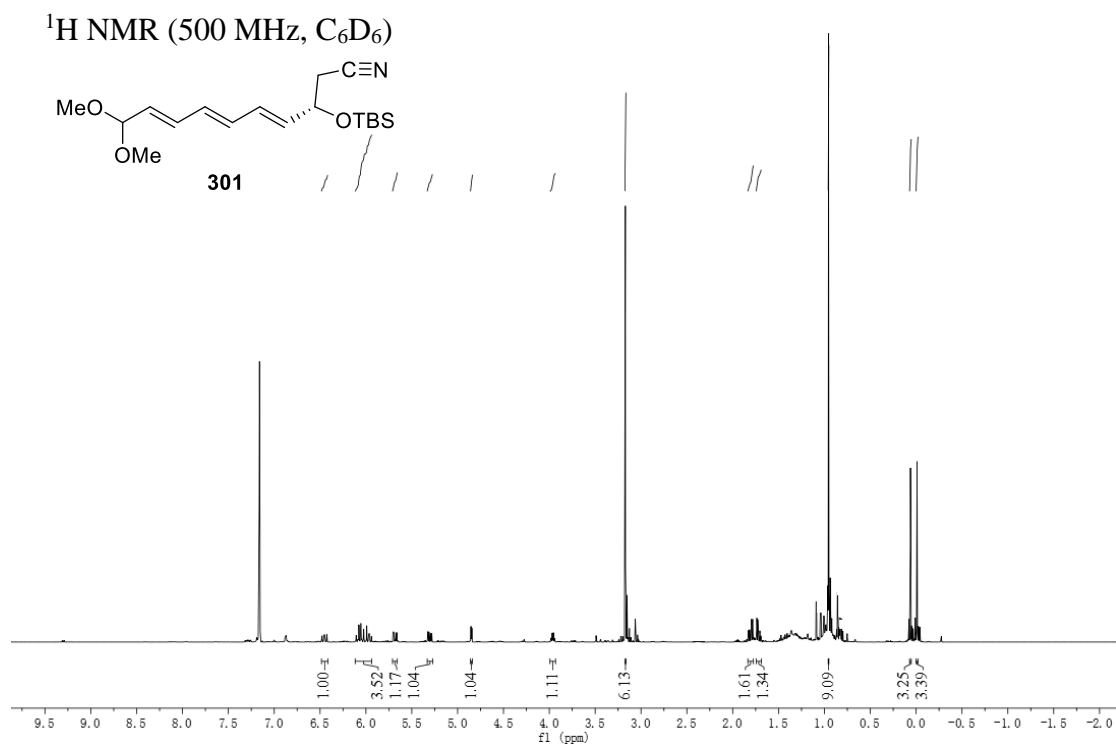
^1H NMR (500 MHz, CDCl_3) ^{13}C NMR (125 MHz, CDCl_3)

^1H NMR (500 MHz, CDCl_3)

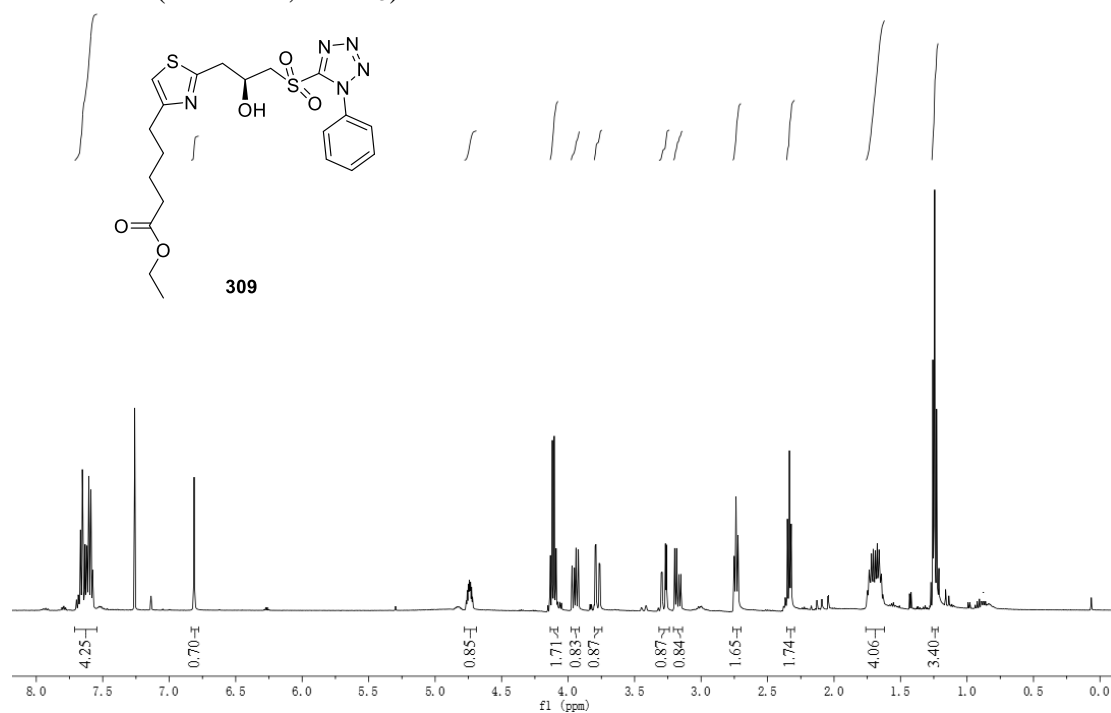


^{13}C NMR (125 MHz, CDCl_3)

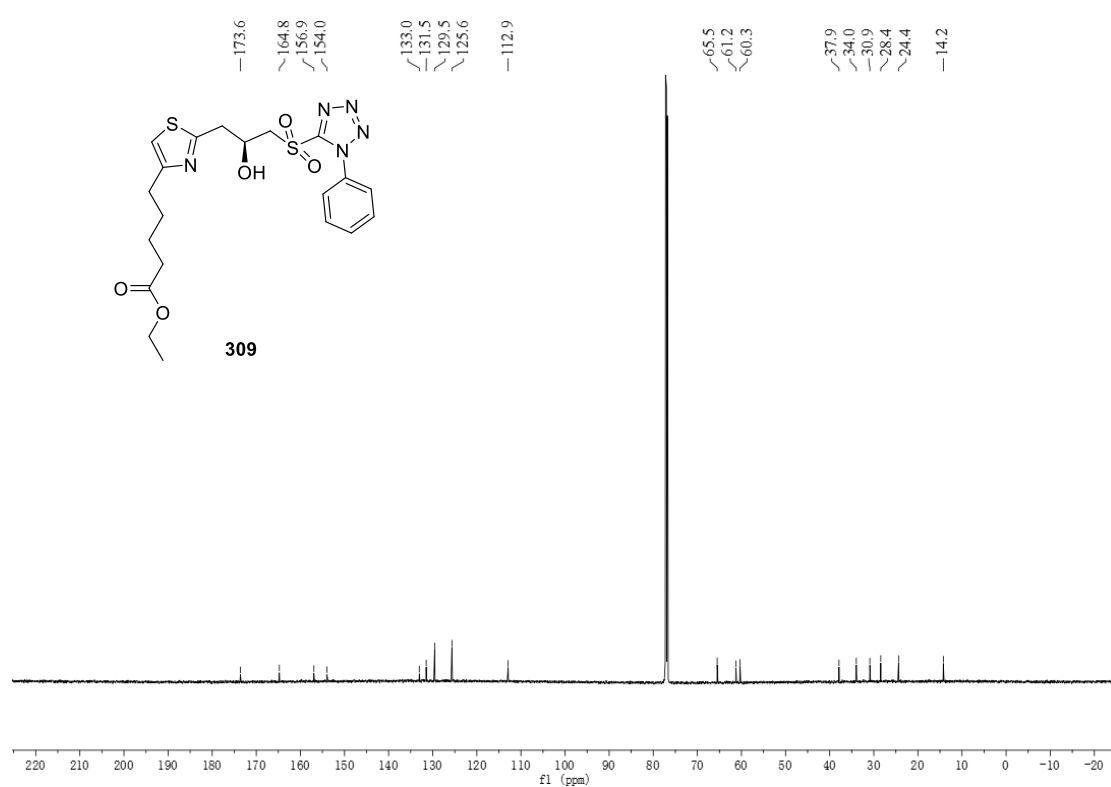


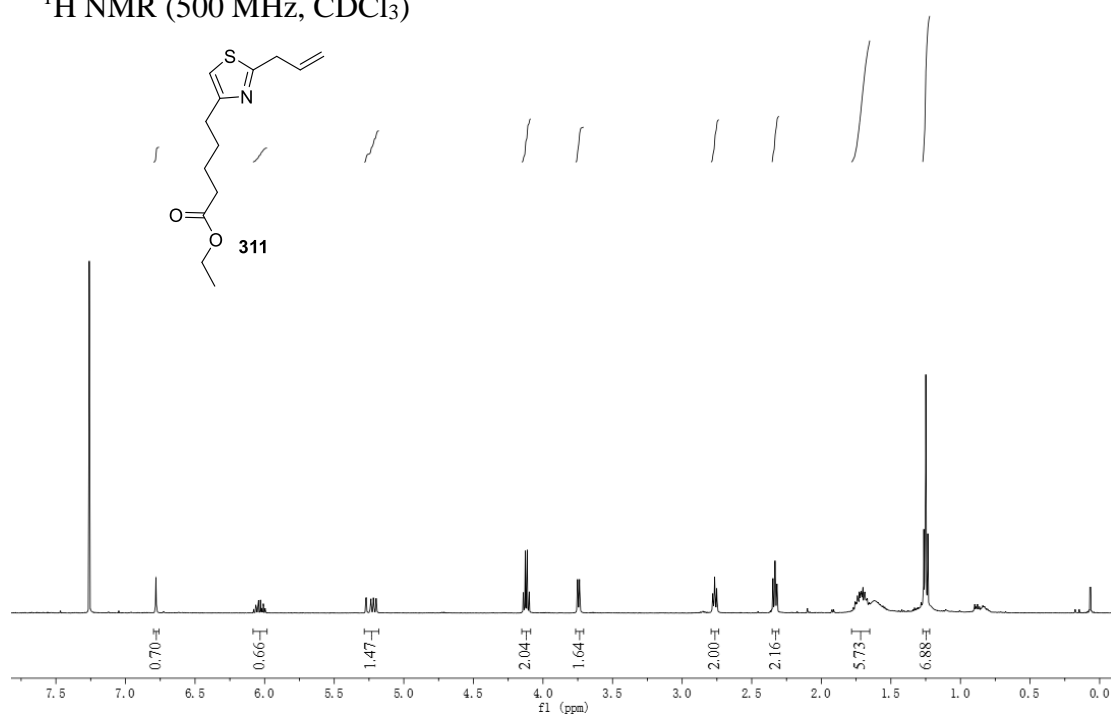
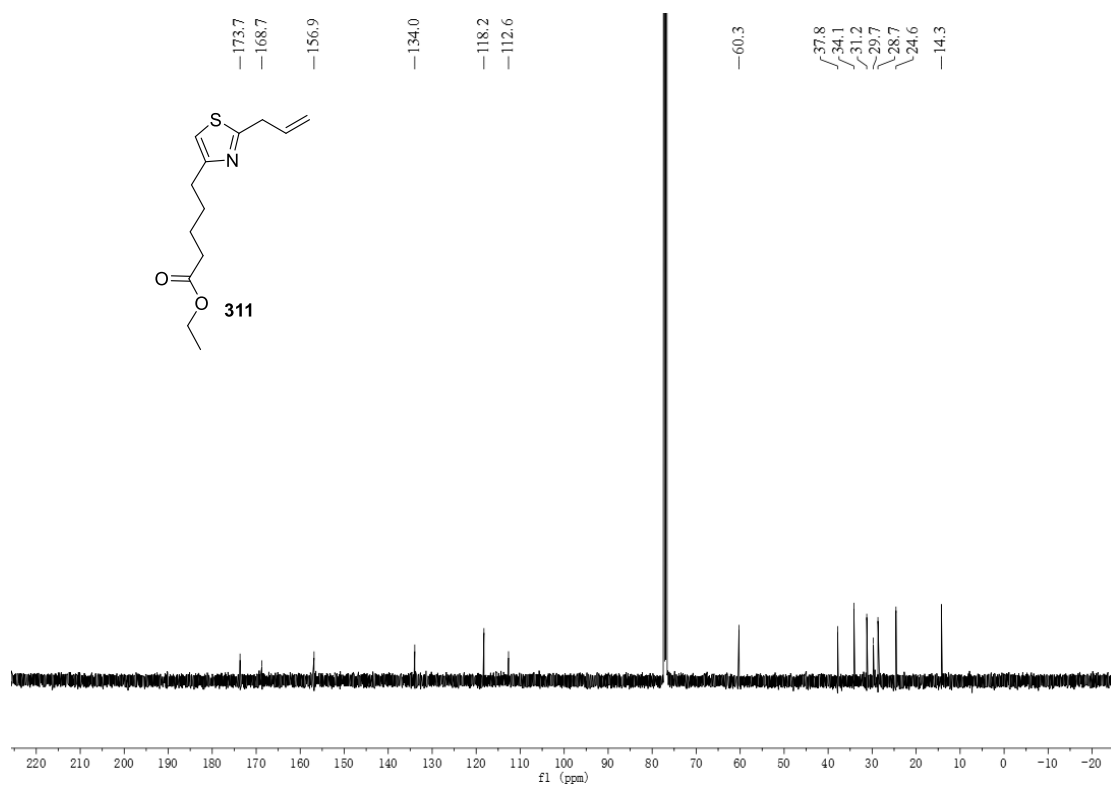


^1H NMR (600 MHz, CDCl_3)

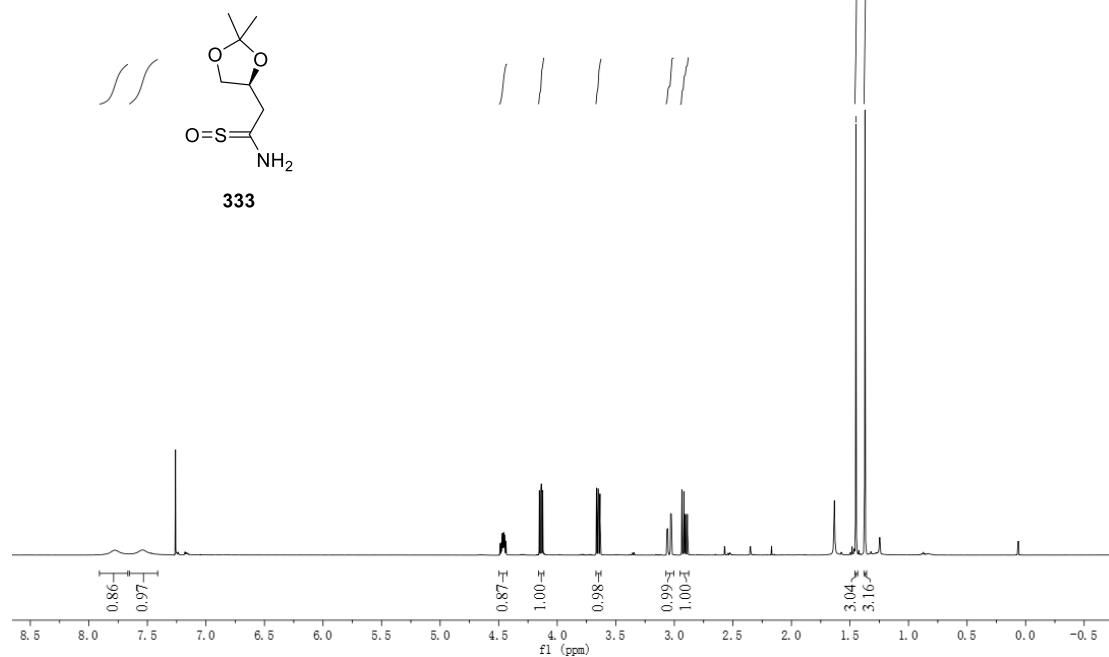


^{13}C NMR (150 MHz, CDCl_3)

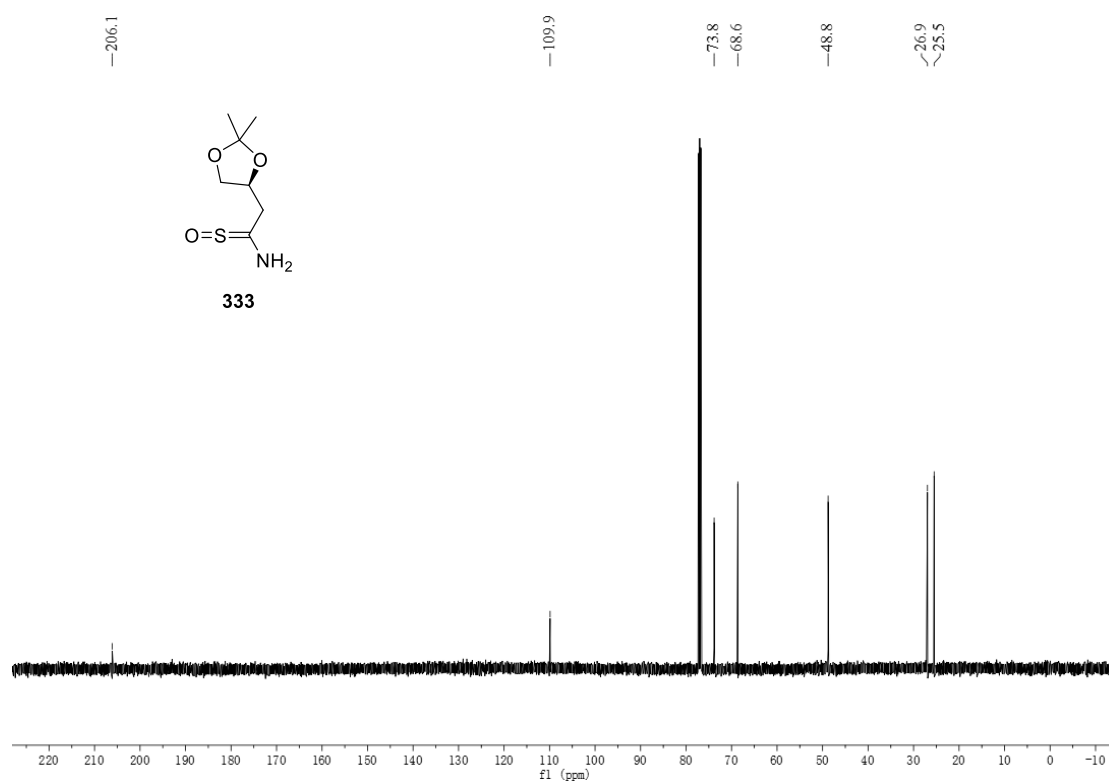


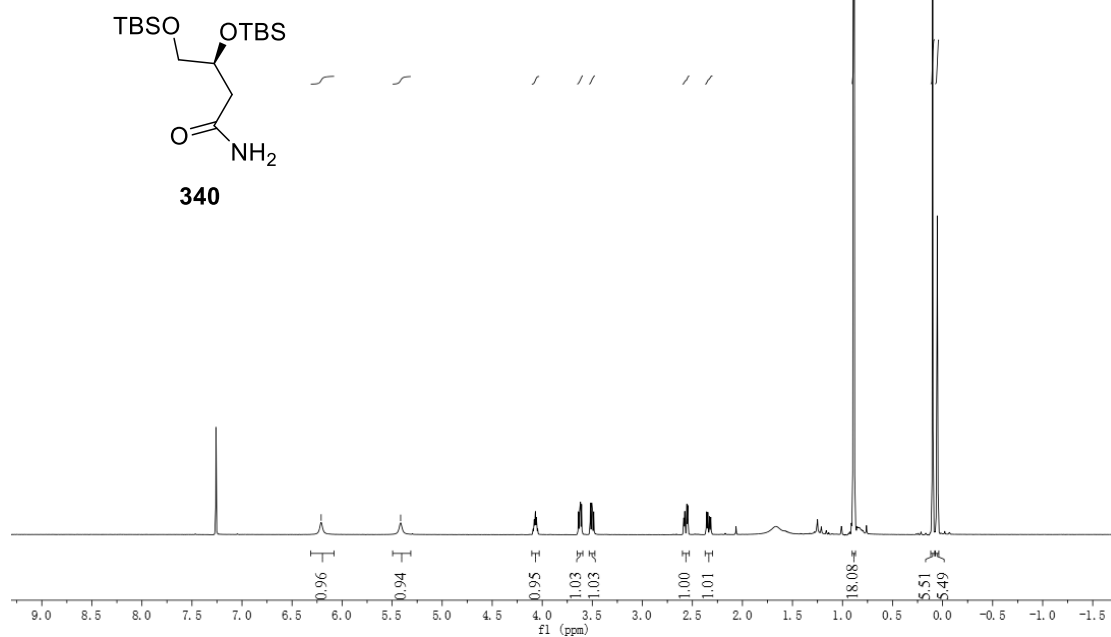
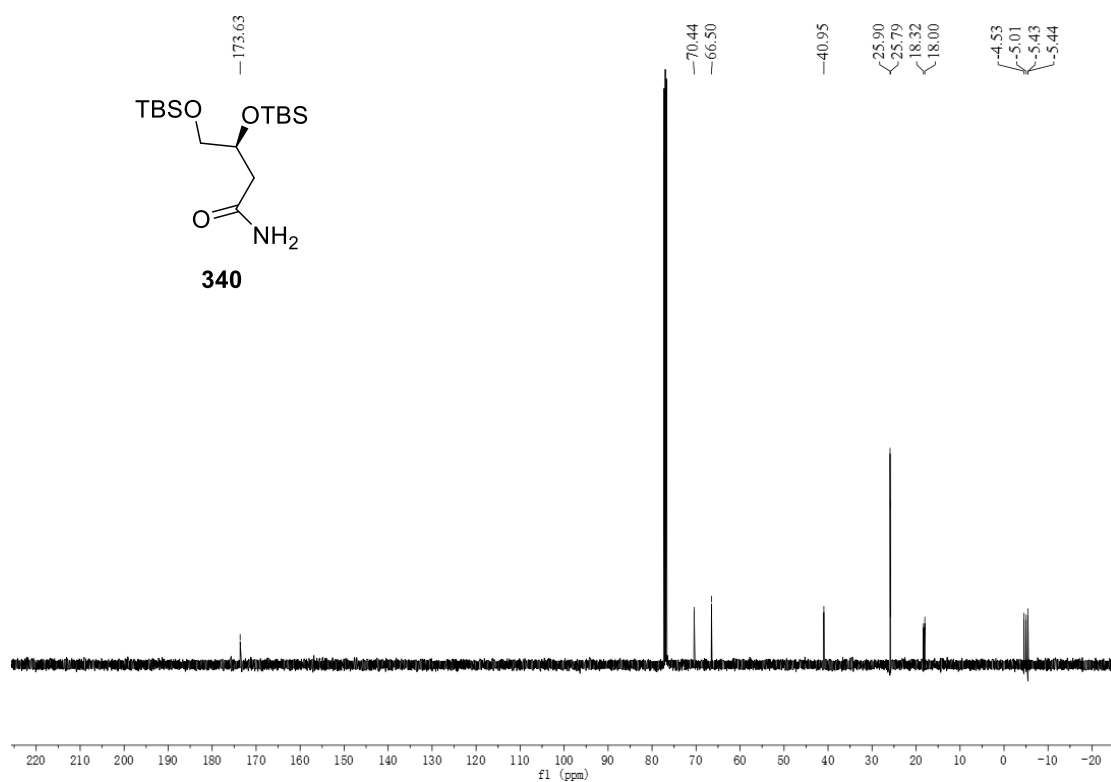
^1H NMR (500 MHz, CDCl_3) ^{13}C NMR (125 MHz, CDCl_3)

^1H NMR (500 MHz, CDCl_3)

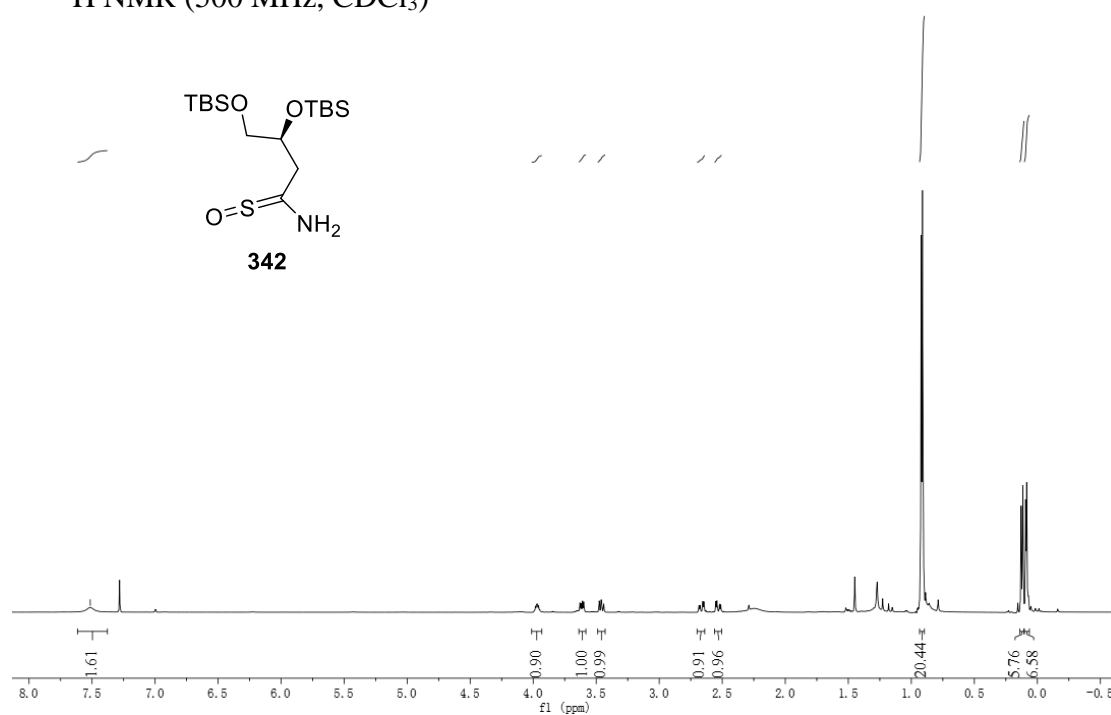


^{13}C NMR (125 MHz, CDCl_3)

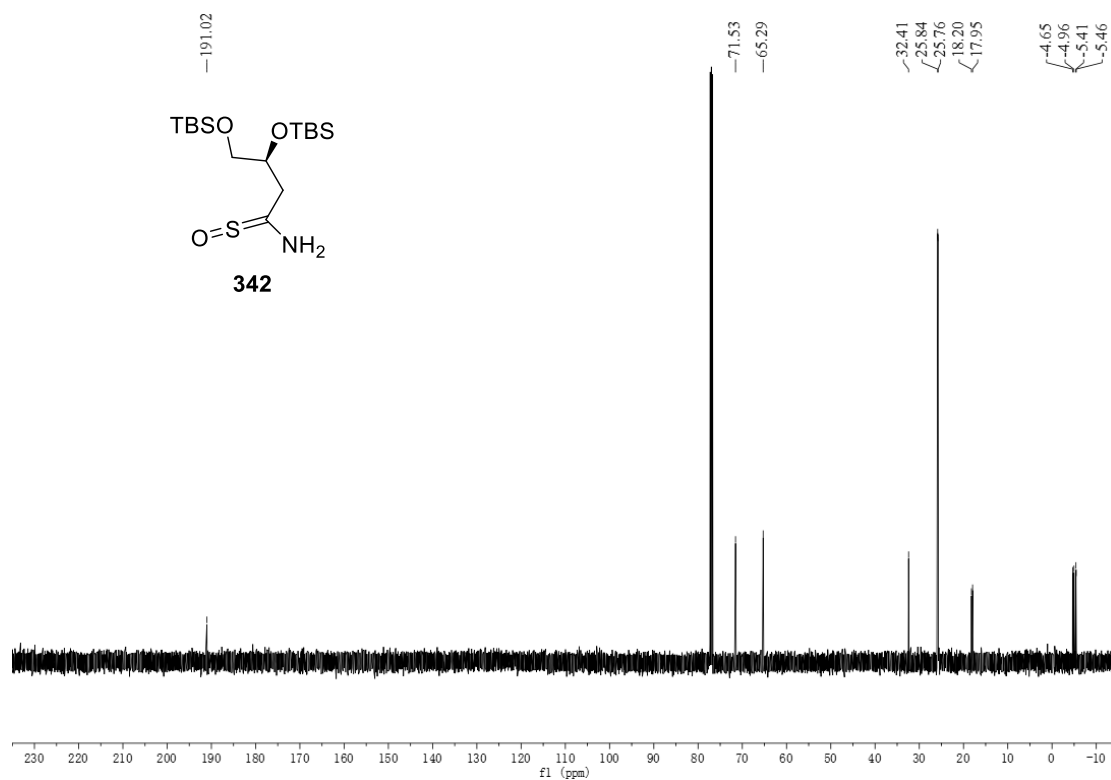


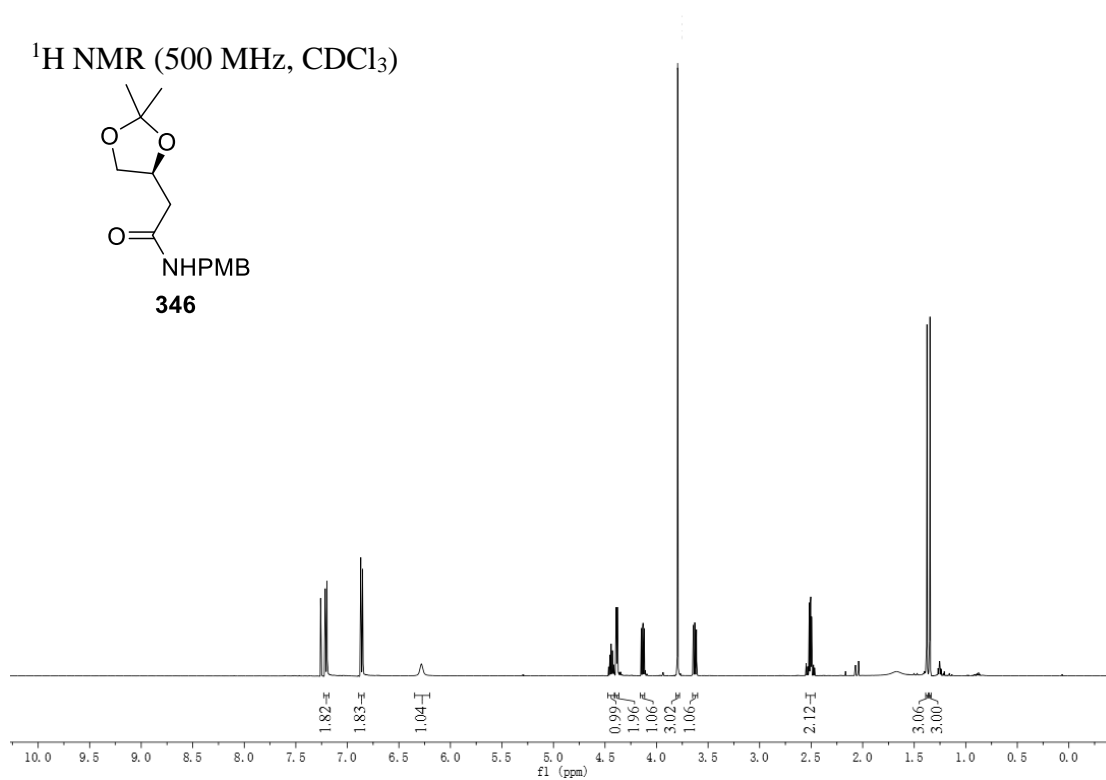
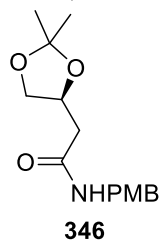
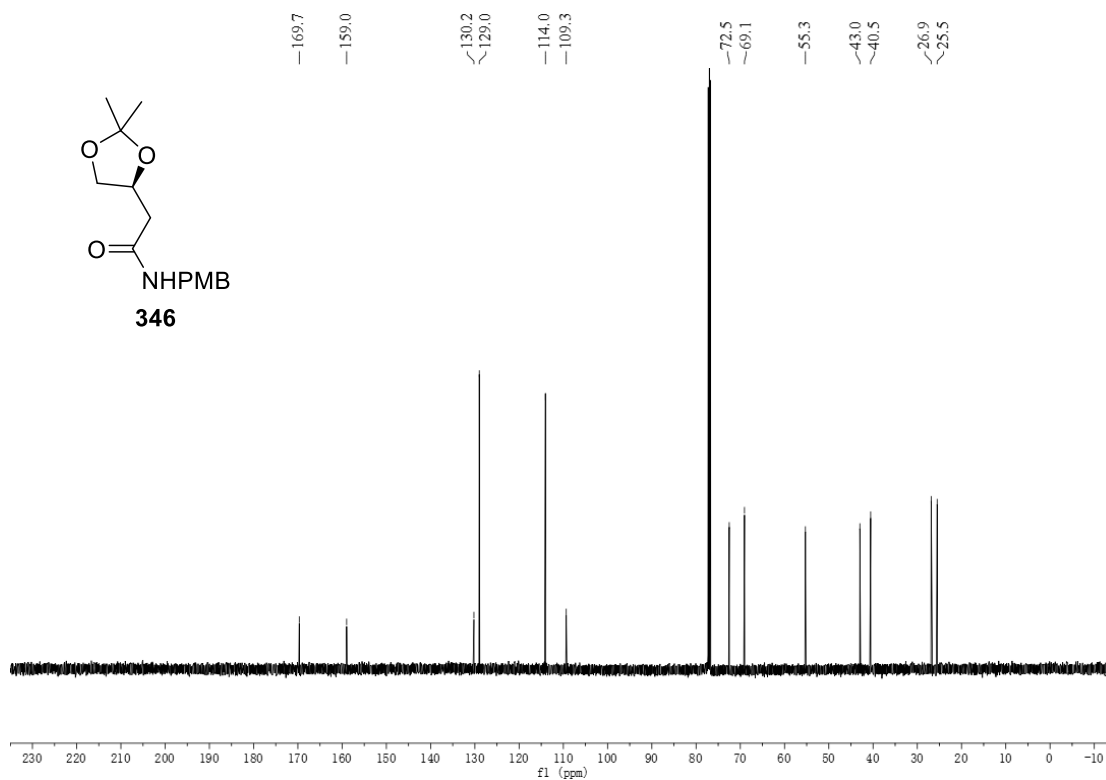
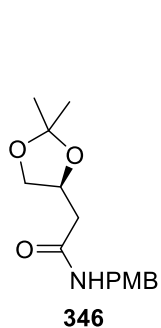
^1H NMR (500 MHz, CDCl_3) ^{13}C NMR (125 MHz, CDCl_3)

^1H NMR (500 MHz, CDCl_3)

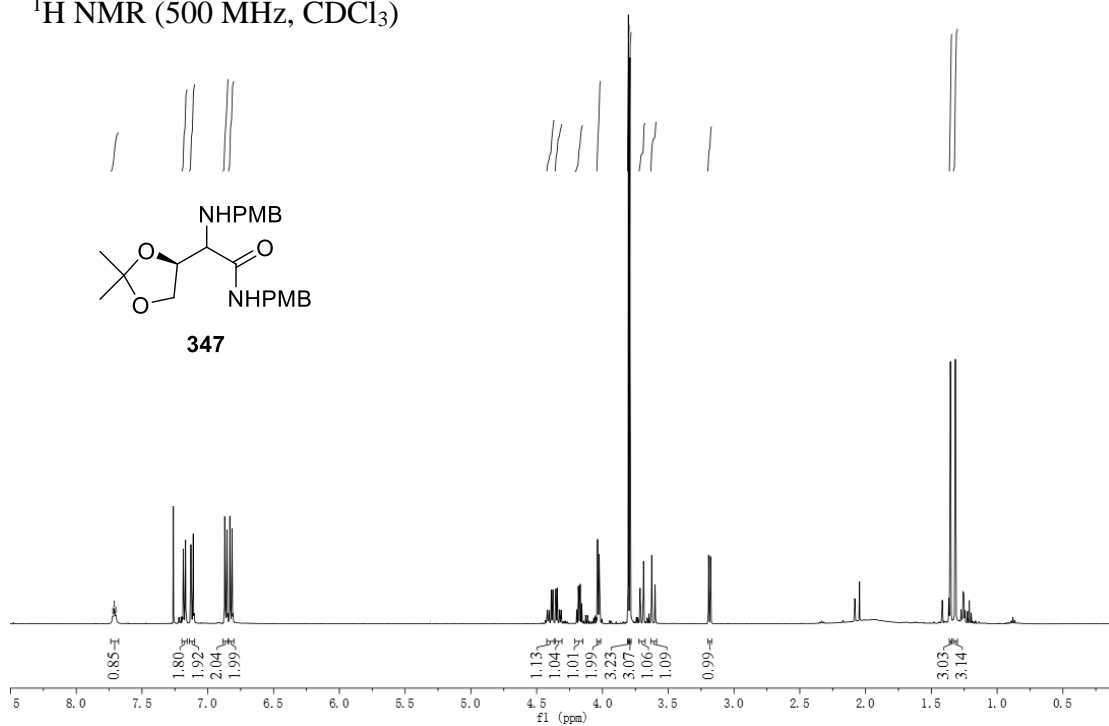


^{13}C NMR (125 MHz, CDCl_3)

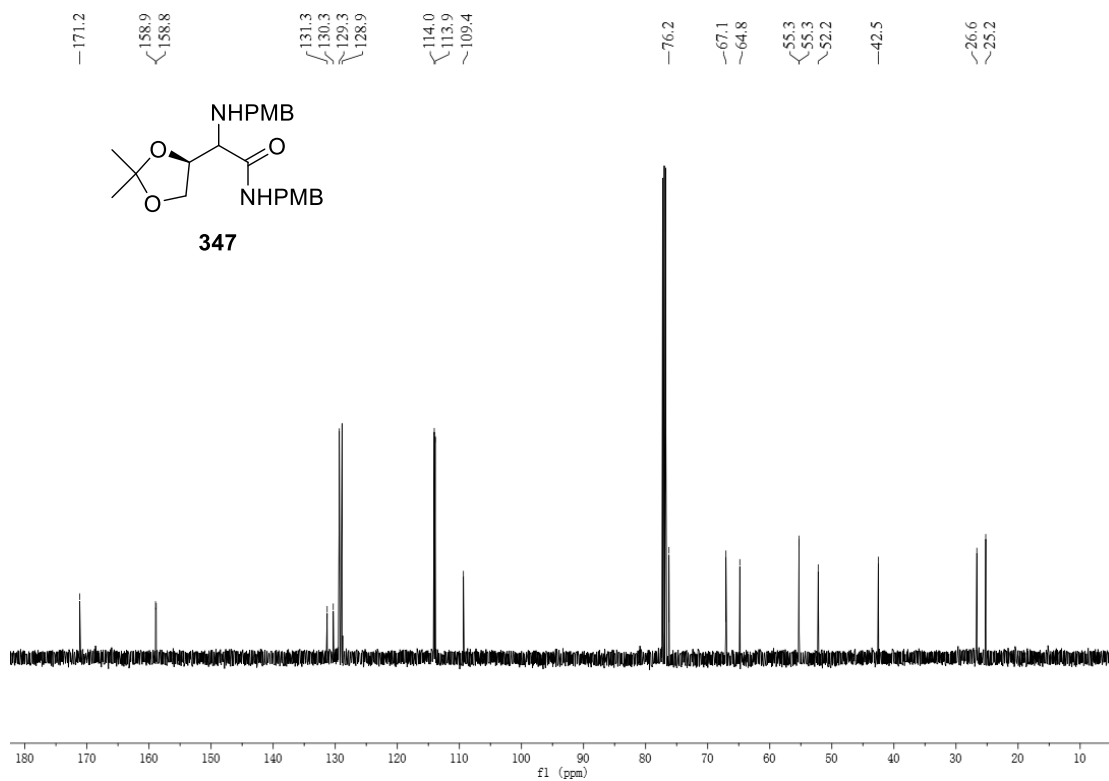


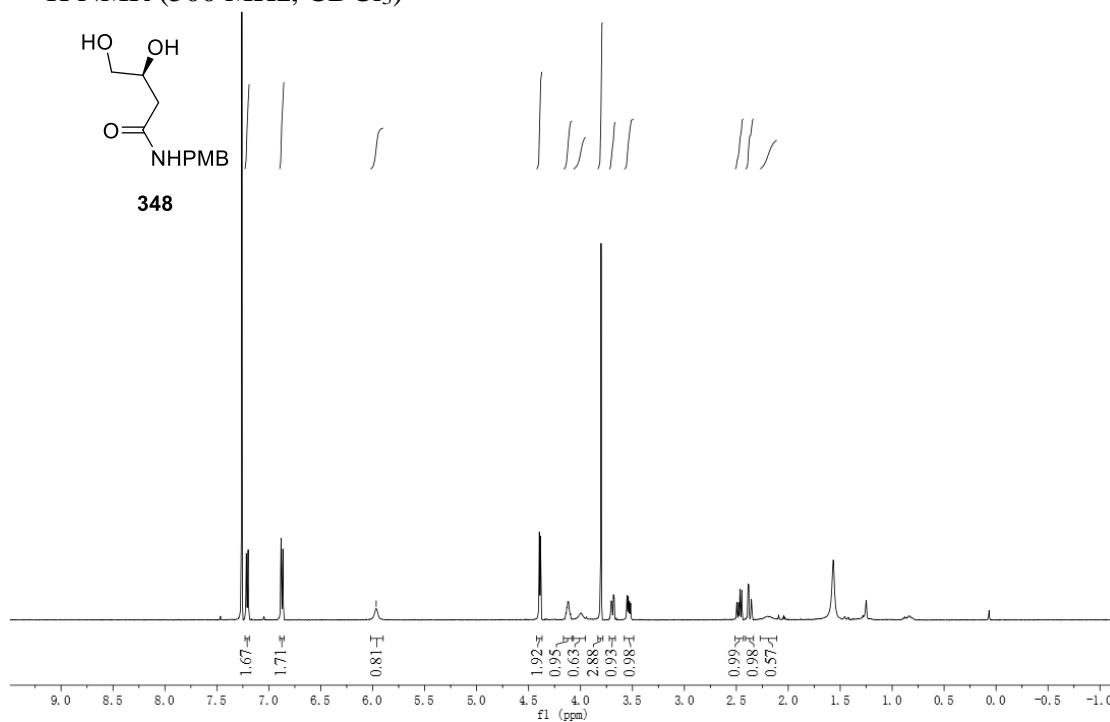
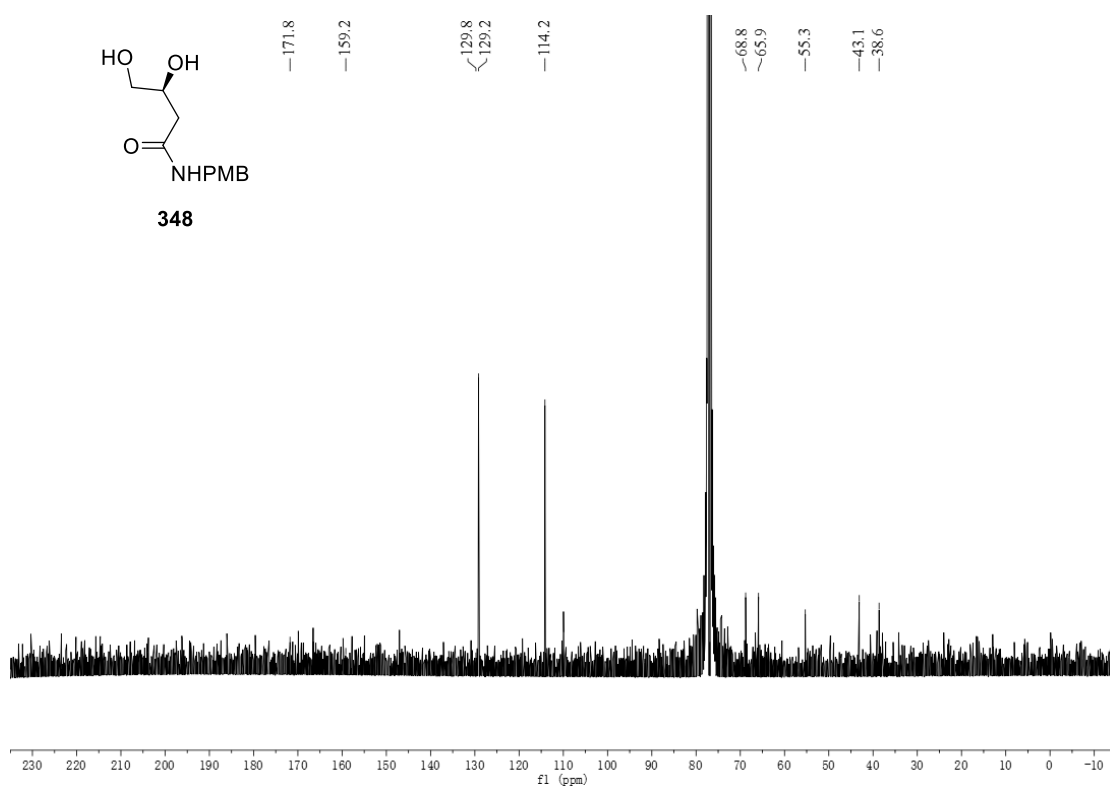
¹H NMR (500 MHz, CDCl₃)¹³C NMR (125 MHz, CDCl₃)

^1H NMR (500 MHz, CDCl_3)

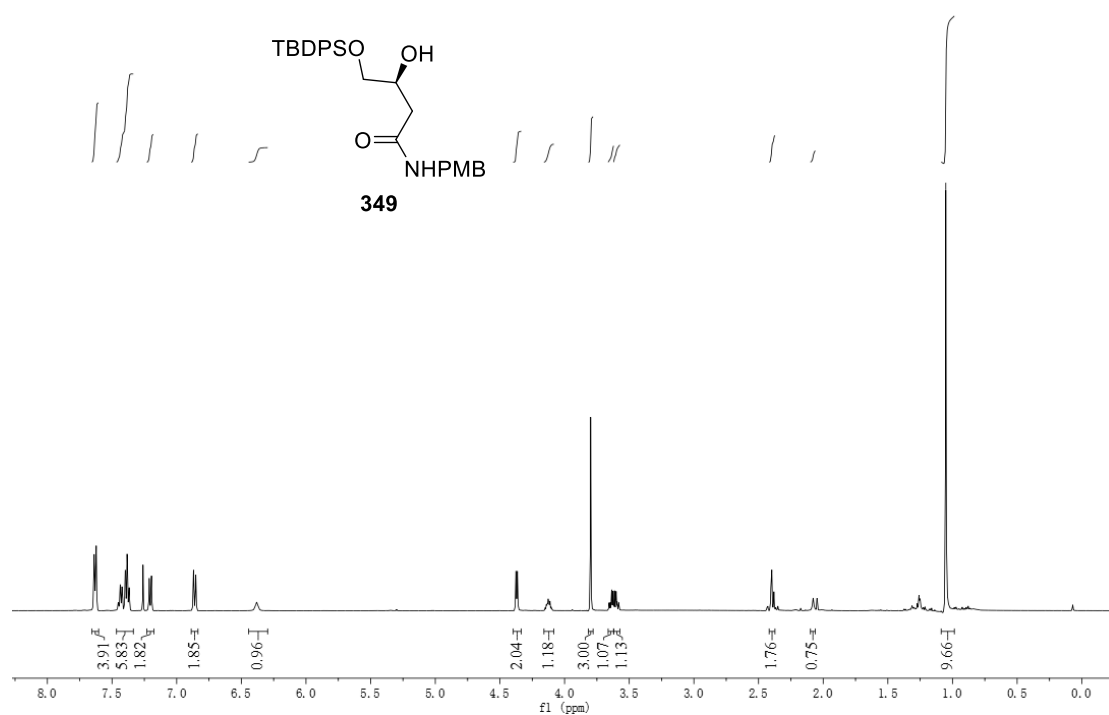


^{13}C NMR (125 MHz, CDCl_3)

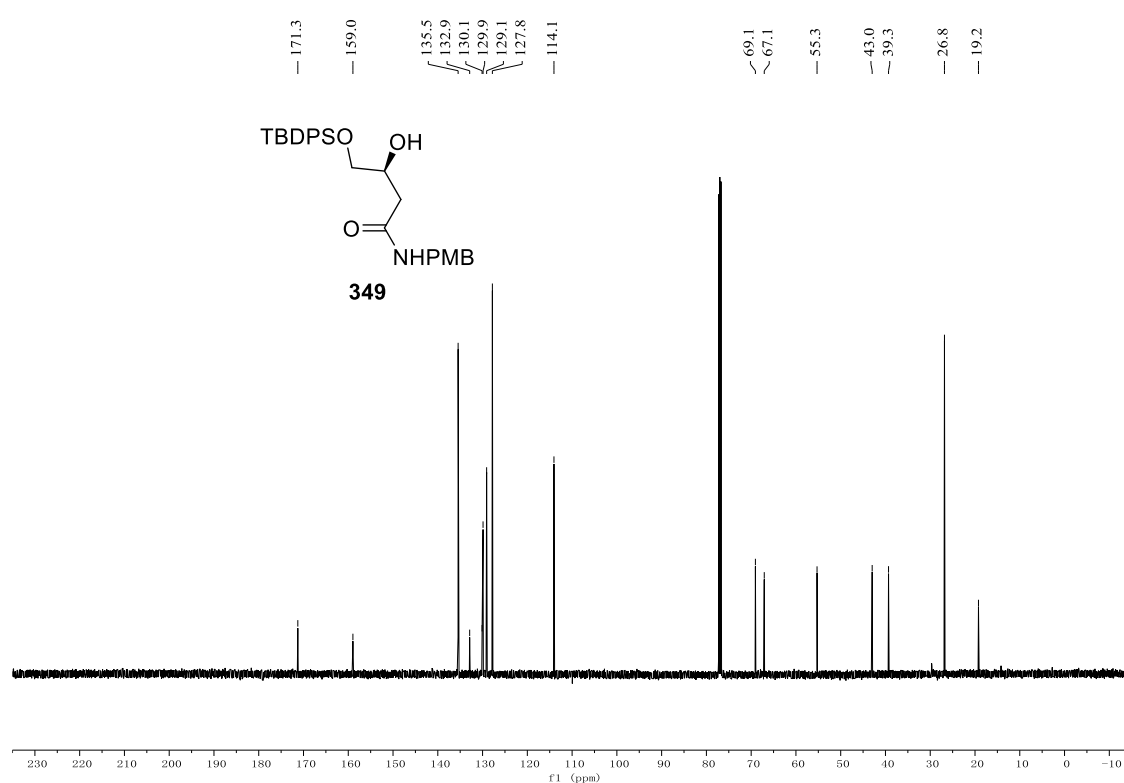


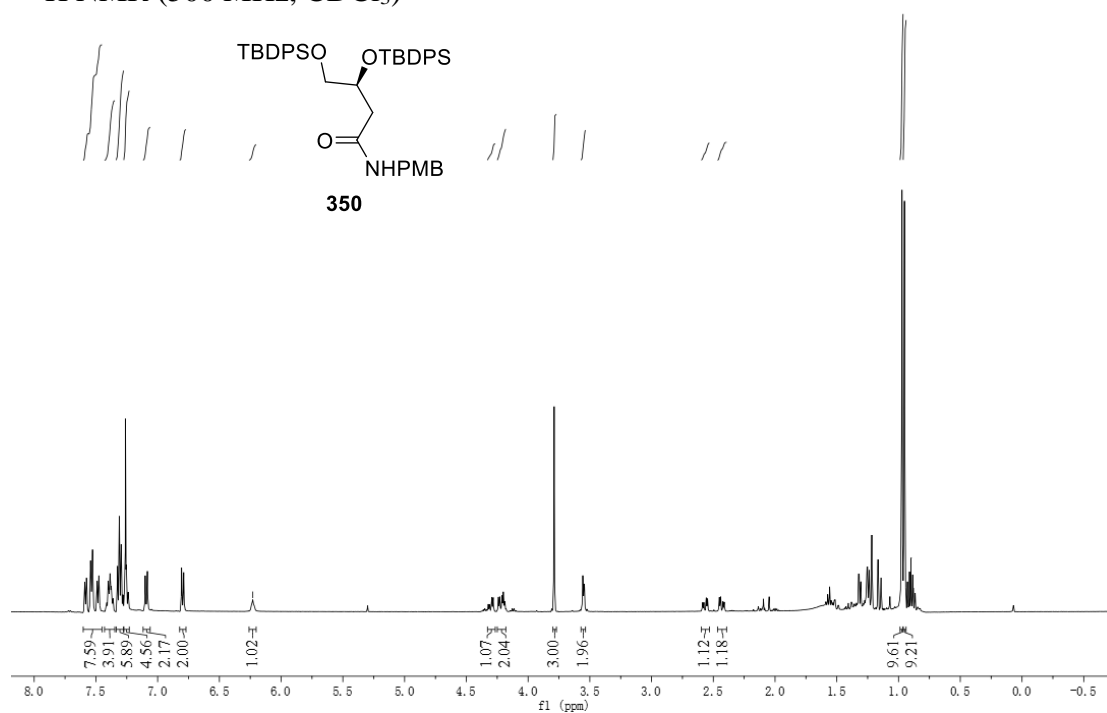
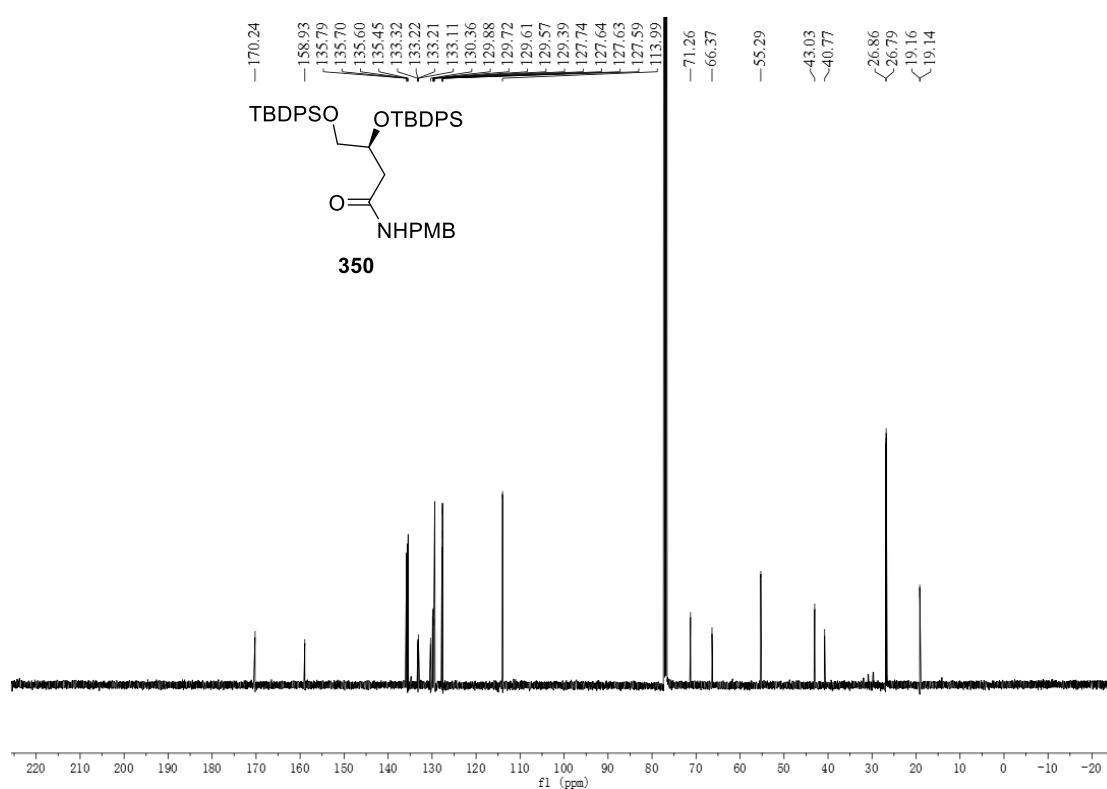
^1H NMR (500 MHz, CDCl_3) ^{13}C NMR (125 MHz, CDCl_3)

^1H NMR (500 MHz, CDCl_3)

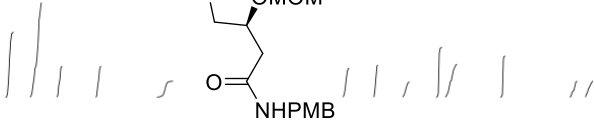


^{13}C NMR (125 MHz, CDCl_3)

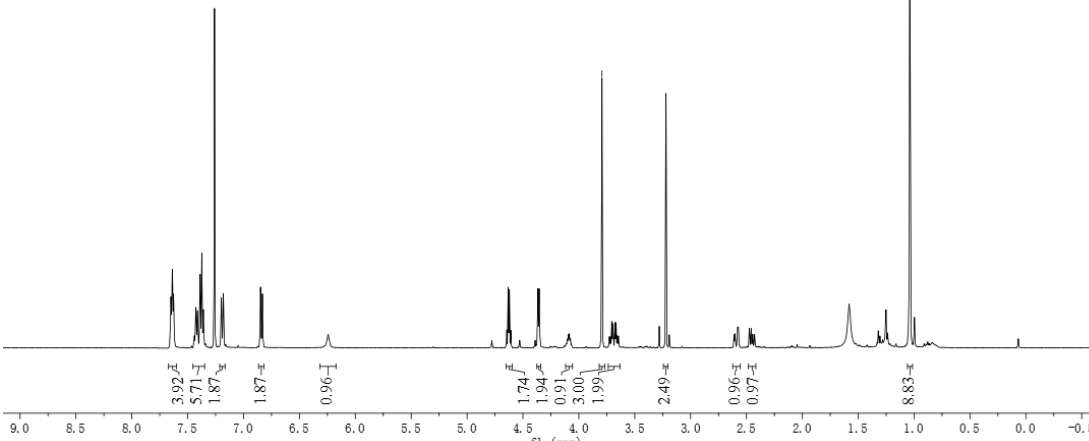


^1H NMR (500 MHz, CDCl_3) ^{13}C NMR (125 MHz, CDCl_3)

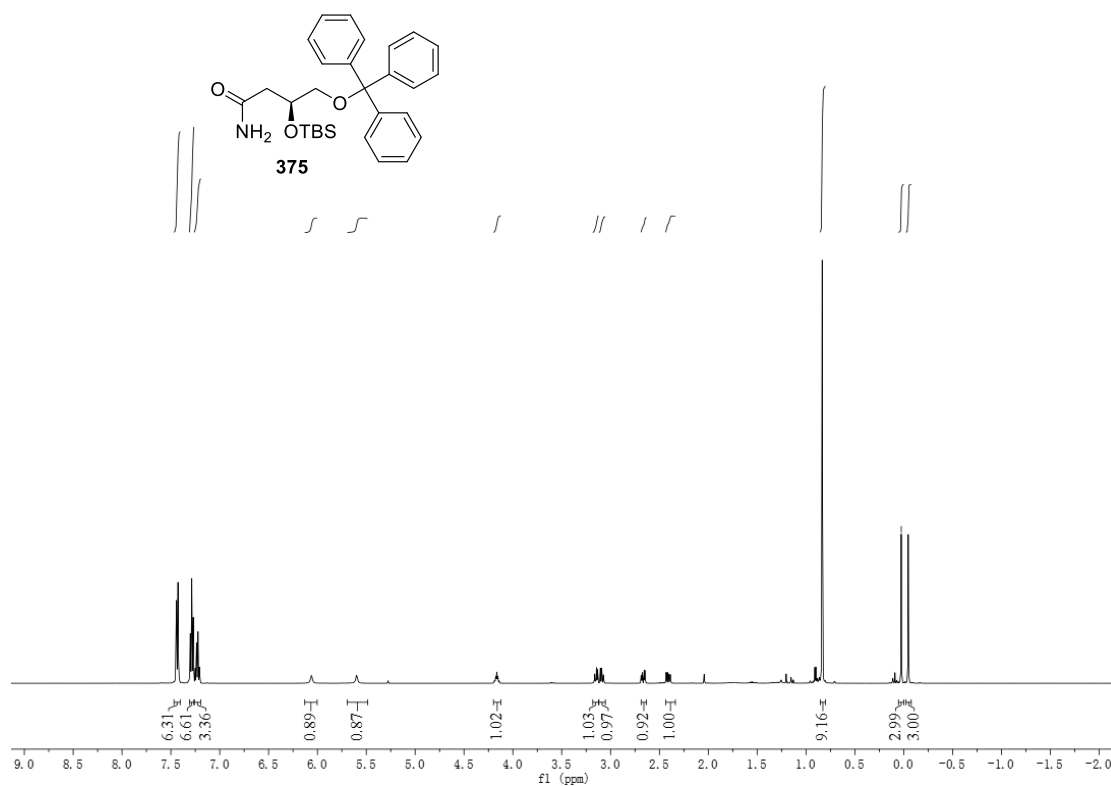
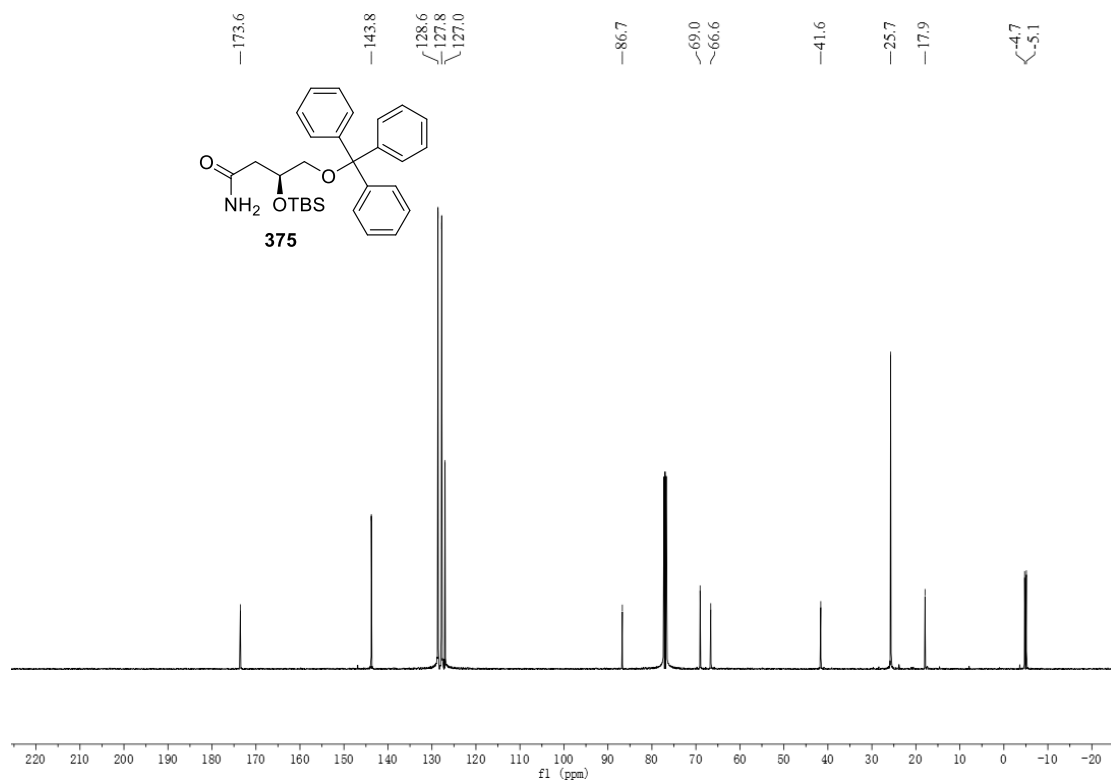
¹H NMR (500 MHz, CDCl₃)



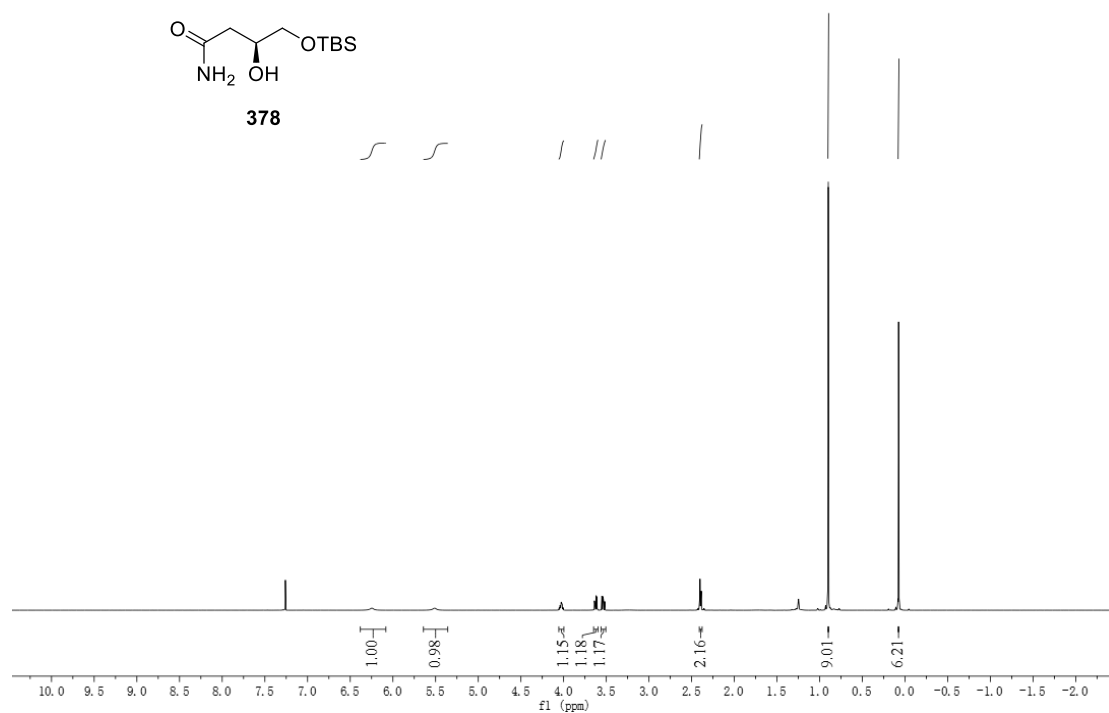
351



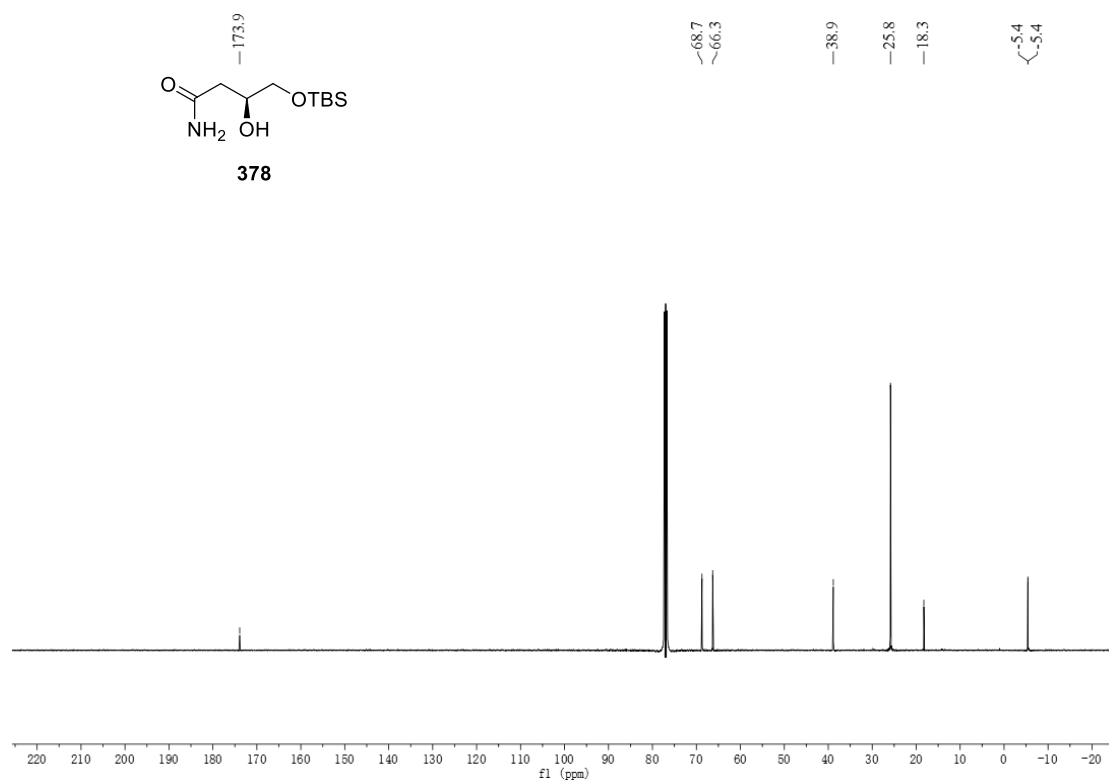
Chemical structure of compound **351** is shown above the spectrum. The structure is a derivative of NHPMB, featuring a TBDPSO group and an OMOM group. The spectrum displays the ¹³C NMR data, with the x-axis representing the chemical shift in ppm (f1) from 180 to -10. The spectrum shows several peaks, with the most prominent ones labeled with their chemical shifts: 170.4, 158.9, 135.5, 133.1, 130.3, 129.8, 129.2, 127.7, 114.0, 96.4, 75.3, 65.6, 55.6, 55.3, 43.1, 39.5, 26.8, and 19.2.

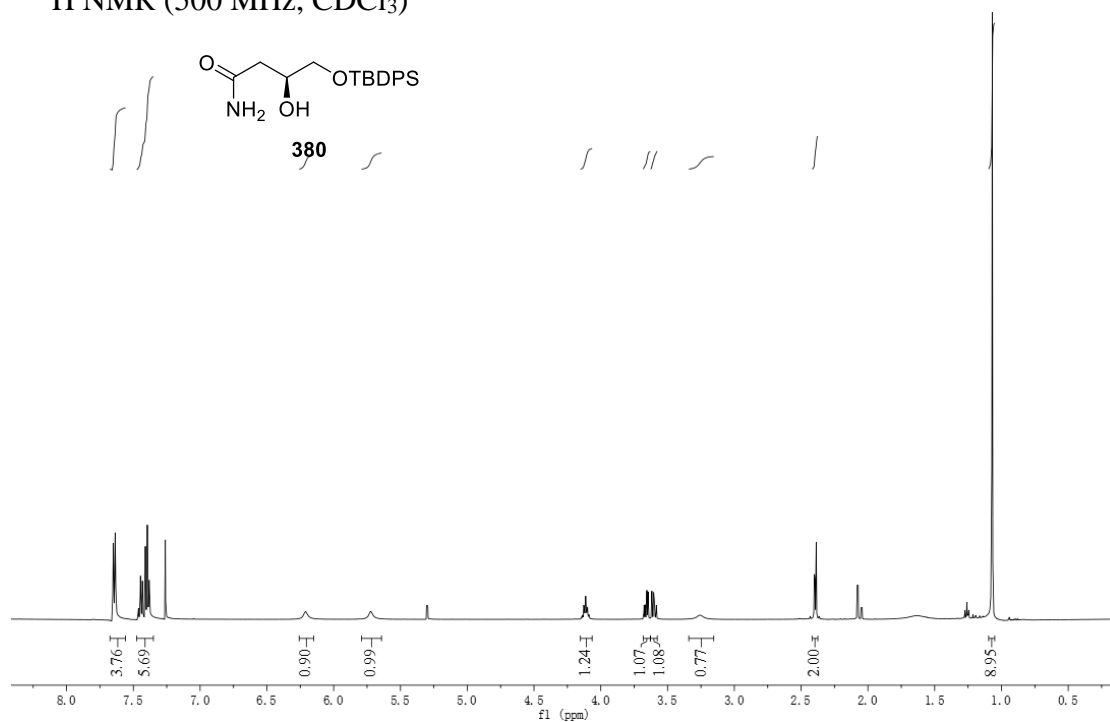
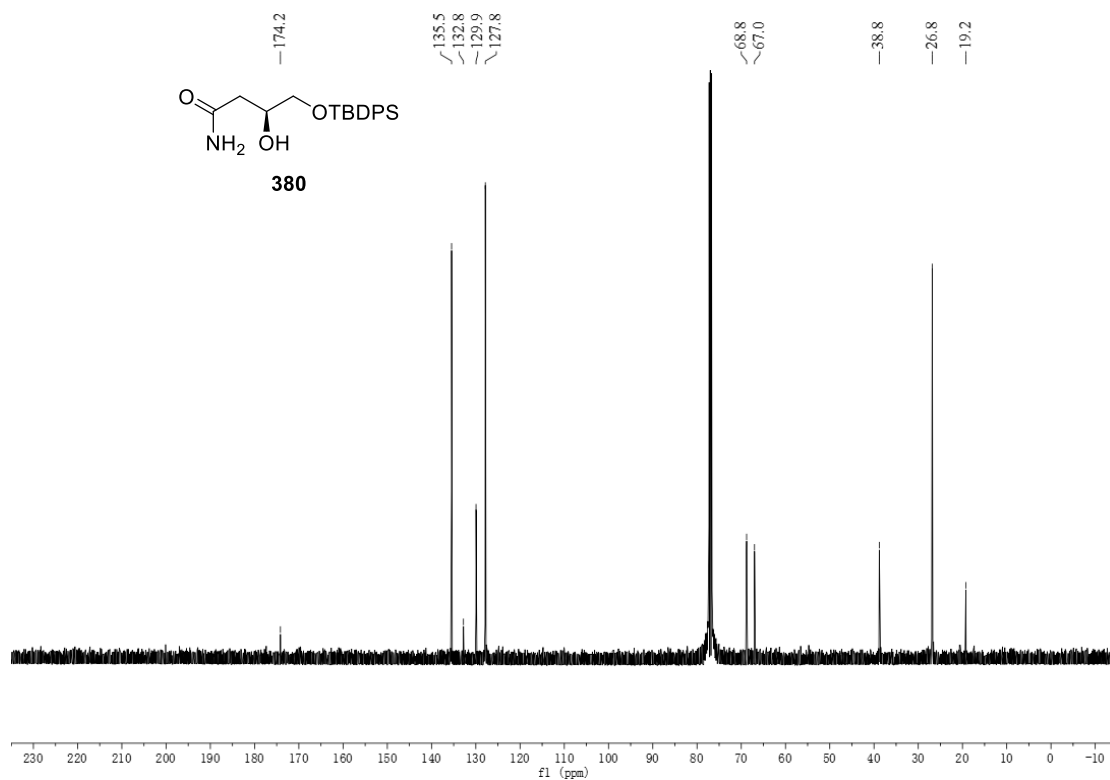
Spectra of Chapter Three ^1H NMR (500 MHz, CDCl_3) ^{13}C NMR (125 MHz, CDCl_3)

^1H NMR (500 MHz, CDCl_3)

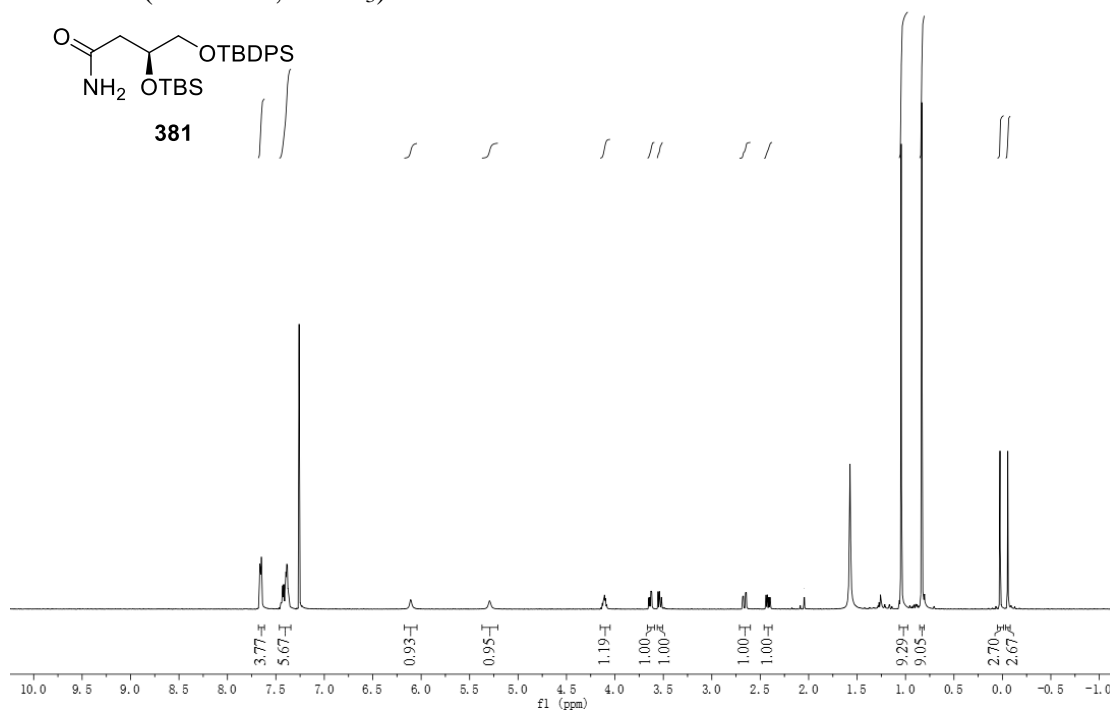


^{13}C NMR (125 MHz, CDCl_3)

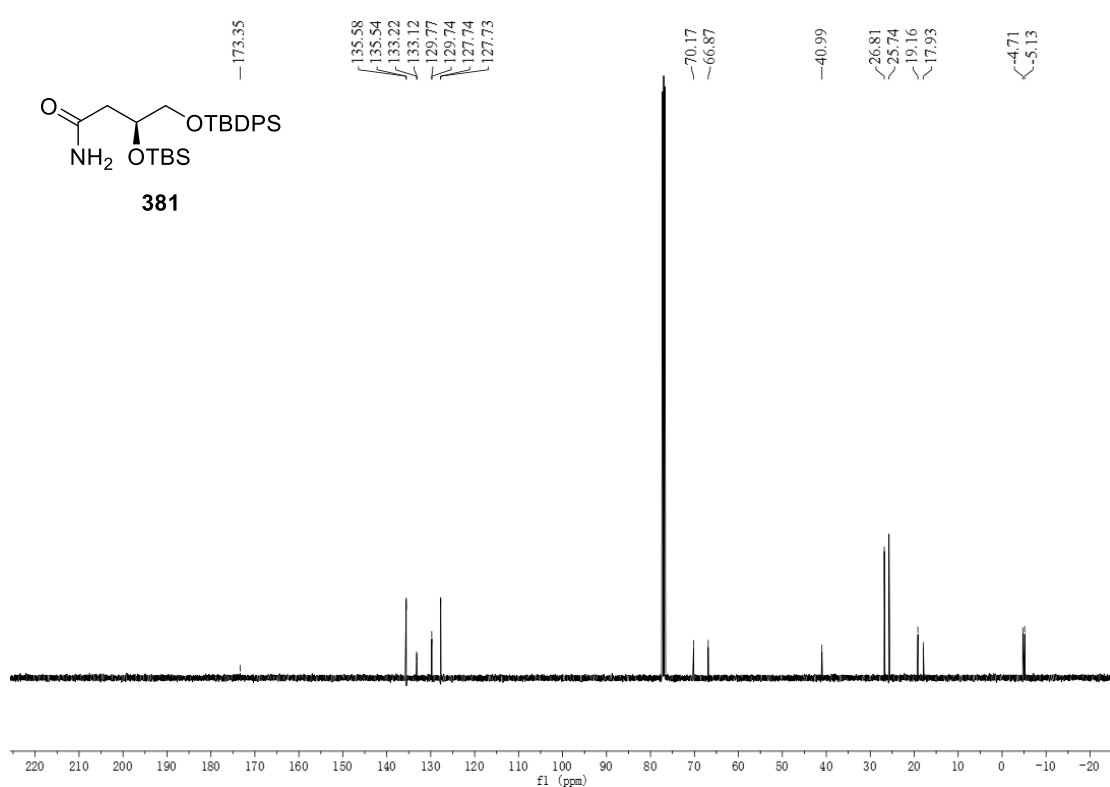


^1H NMR (500 MHz, CDCl_3) ^{13}C NMR (125 MHz, CDCl_3)

^1H NMR (500 MHz, CDCl_3)



^{13}C NMR (125 MHz, CDCl_3)



[illegible]

Chemical structure of compound **382** is shown above the spectrum. The structure is a thioamide derivative with a chiral center, an amine group, and a silyl ether group.

The spectrum displays the following chemical shifts (ppm):

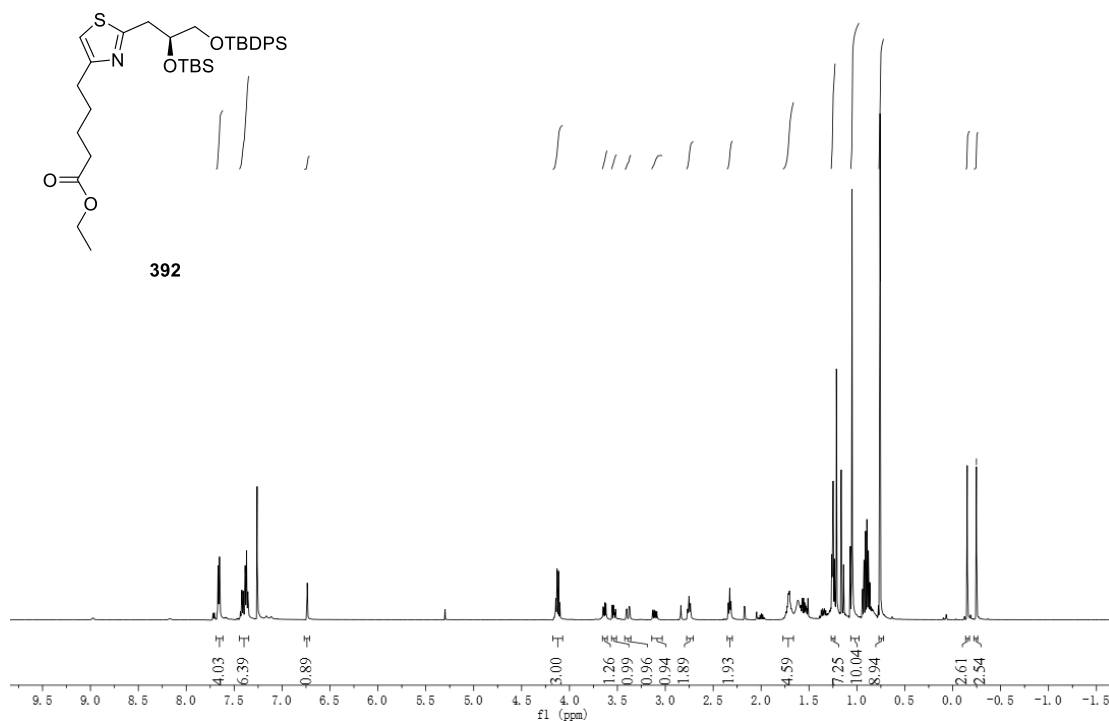
- 207.68
- 135.59
- 135.54
- 133.11
- 132.93
- 129.81
- 129.77
- 127.74
- 72.31
- 66.37
- 49.66
- 26.81
- 25.76
- 19.17
- 17.91
- 4.74
- 5.04

Chemical structure of compound **382** is shown above the spectrum. The structure is a thioamide derivative with a chiral center, an amine group, and a silyl ether group.

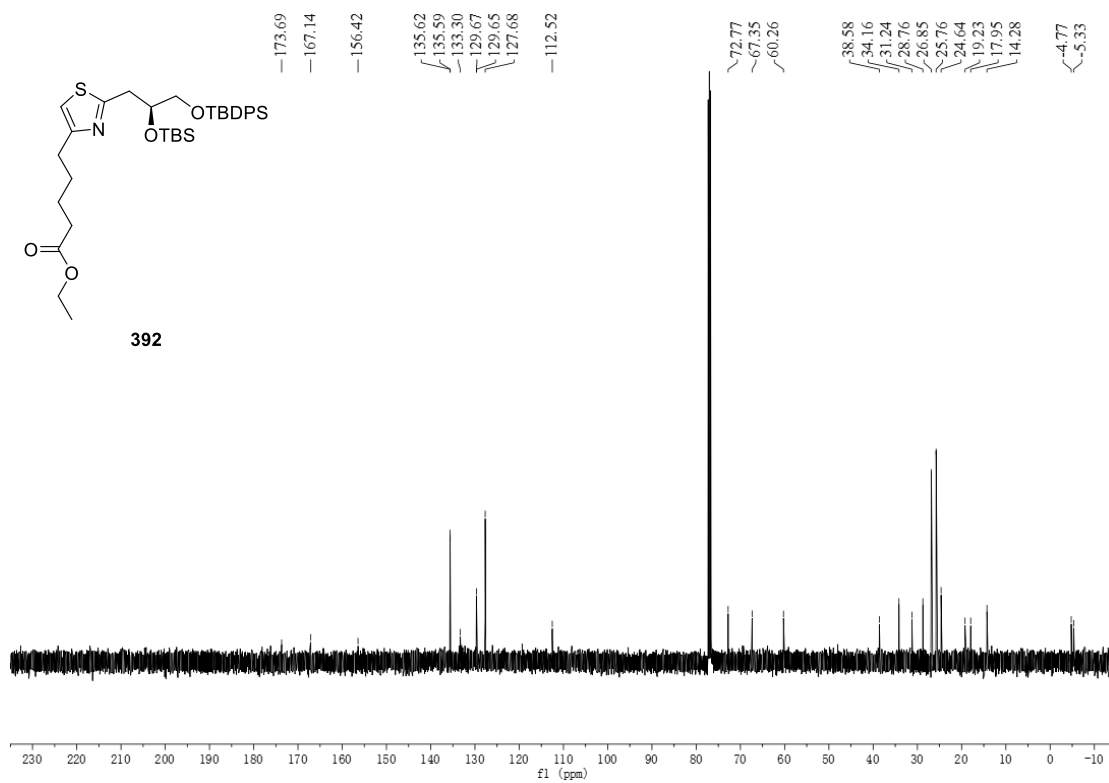
The spectrum displays the following chemical shifts (ppm):

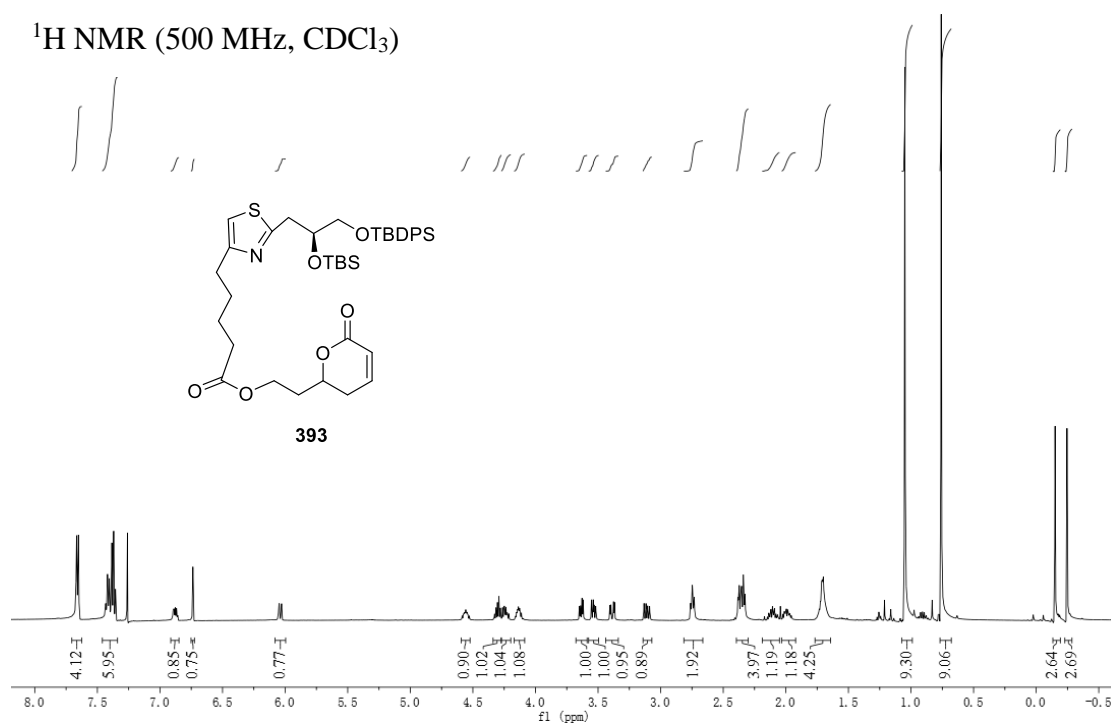
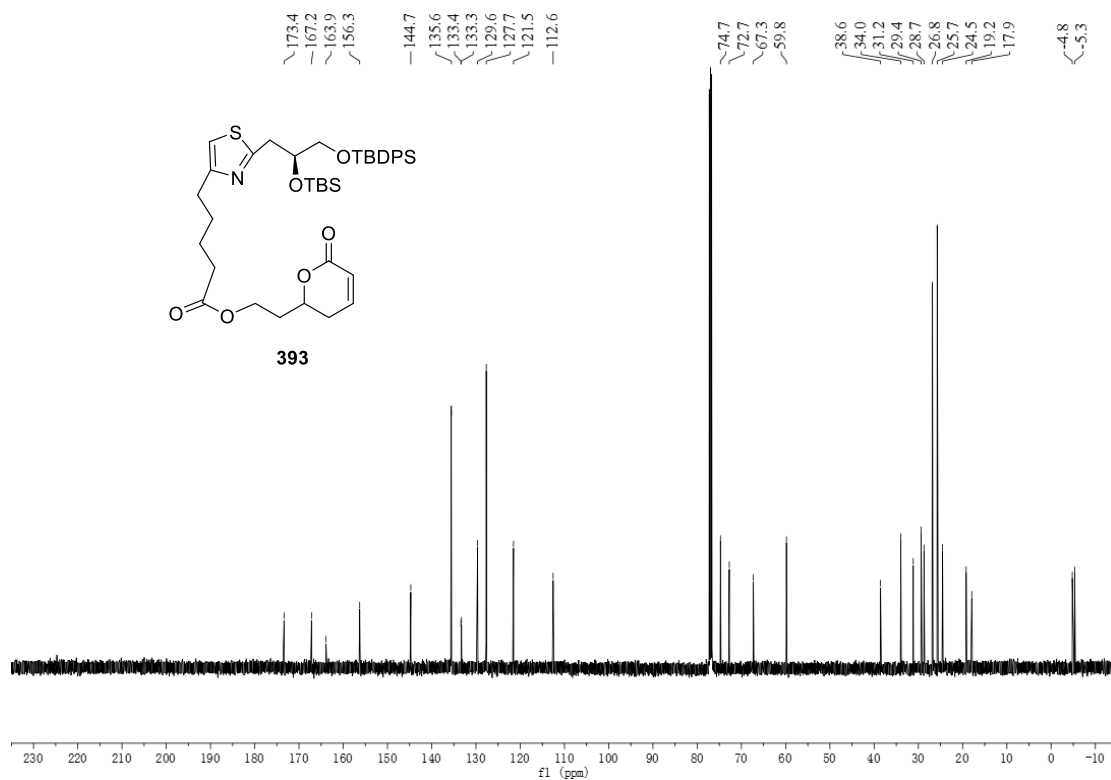
- 207.68
- 135.59
- 135.54
- 133.11
- 132.93
- 129.81
- 129.77
- 127.74
- 72.31
- 66.37
- 49.66
- 26.81
- 25.76
- 19.17
- 17.91
- 4.74
- 5.04

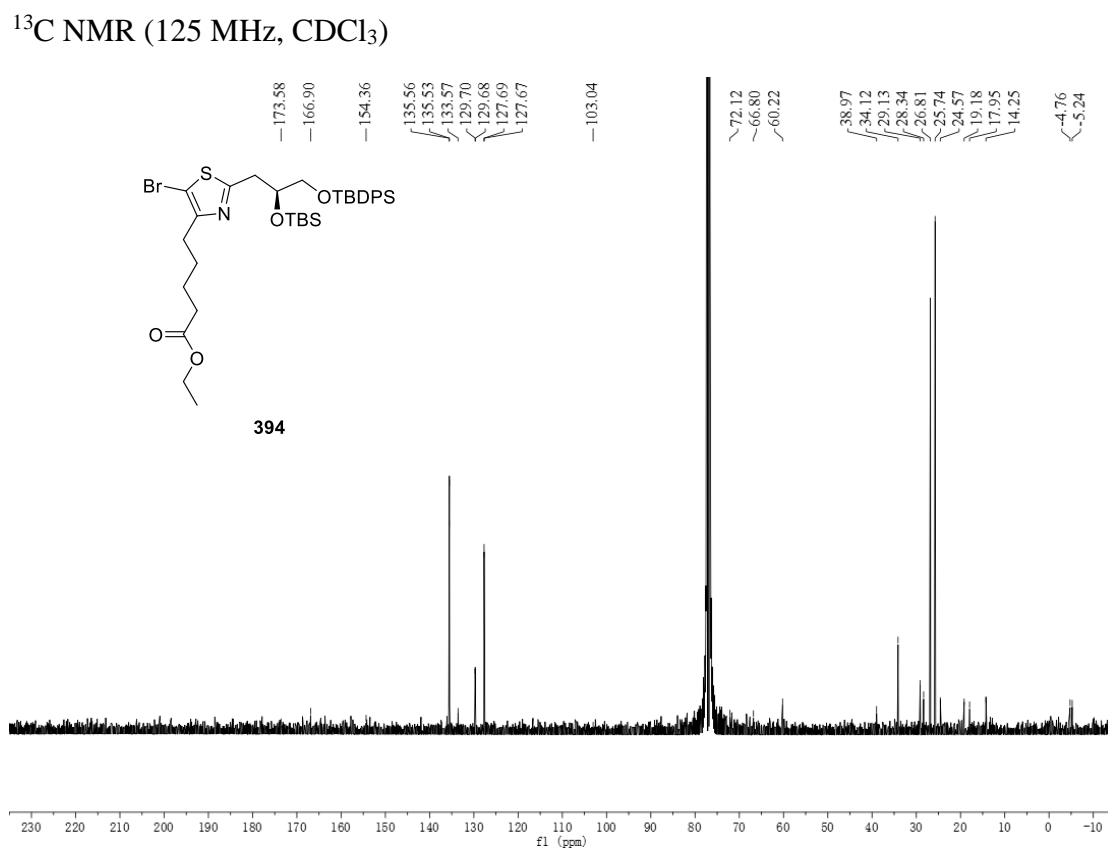
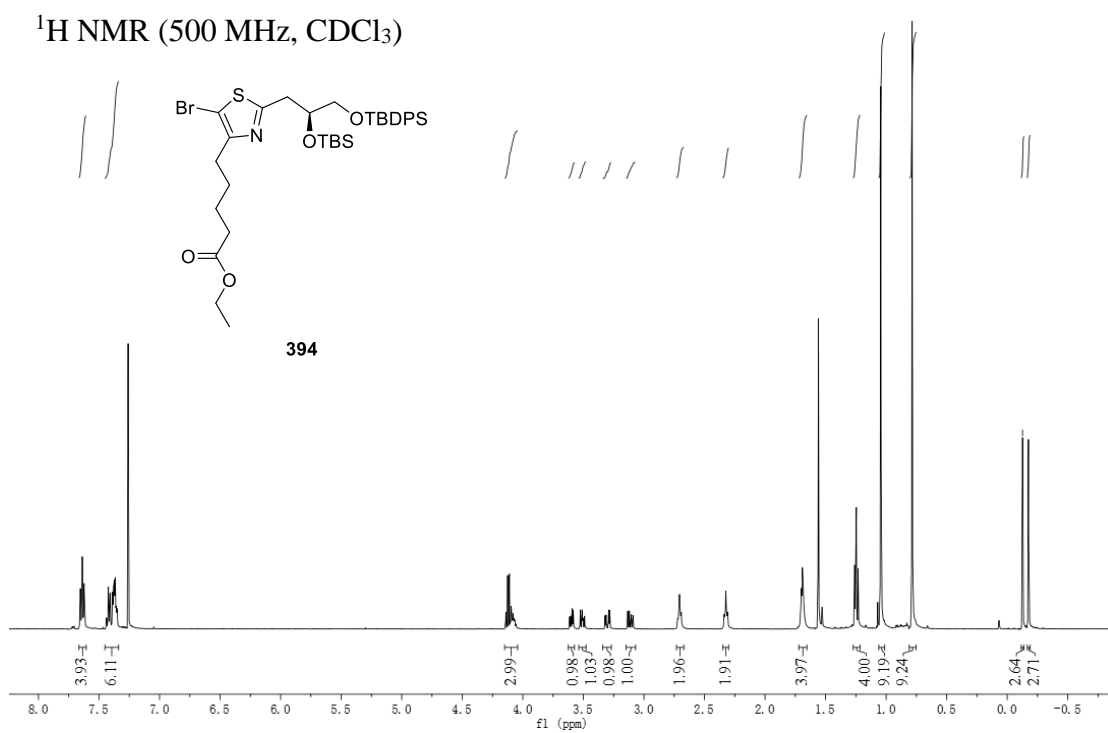
^1H NMR (500 MHz, CDCl_3)

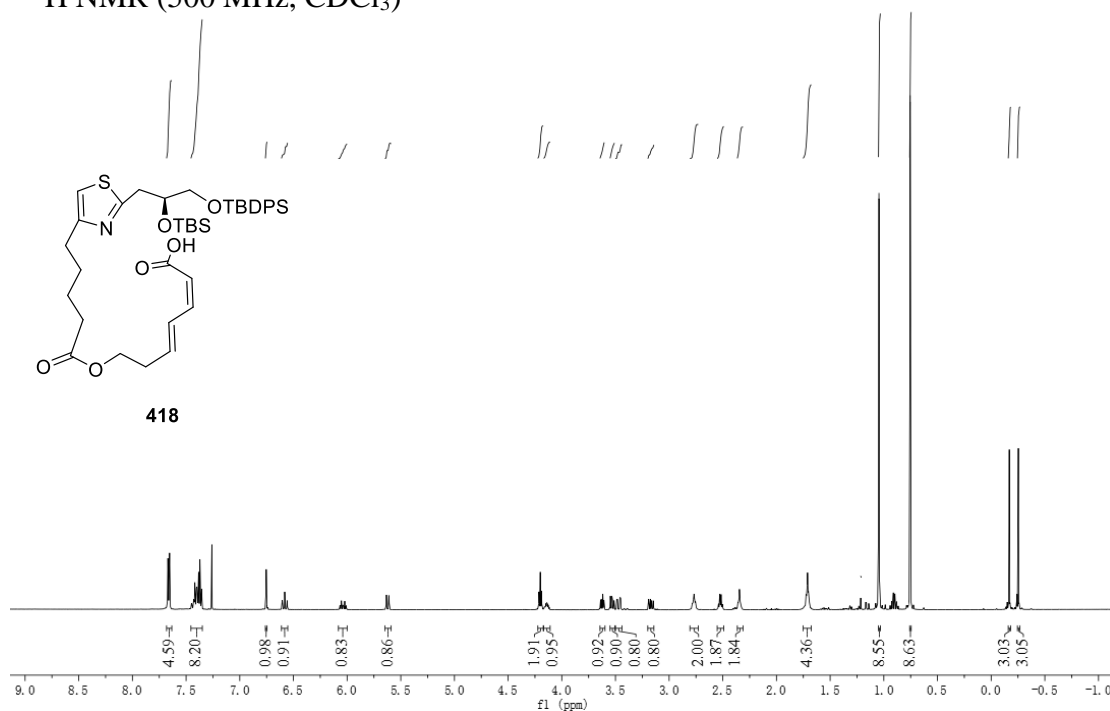
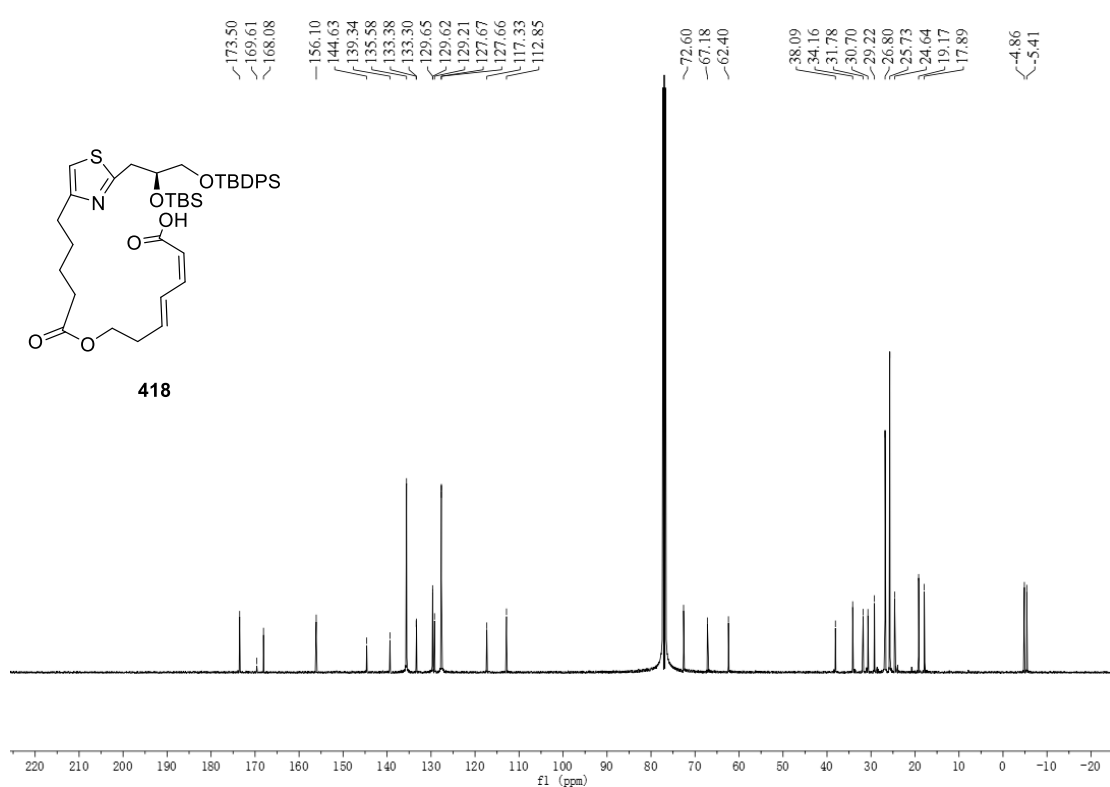


^{13}C NMR (125 MHz, CDCl_3)

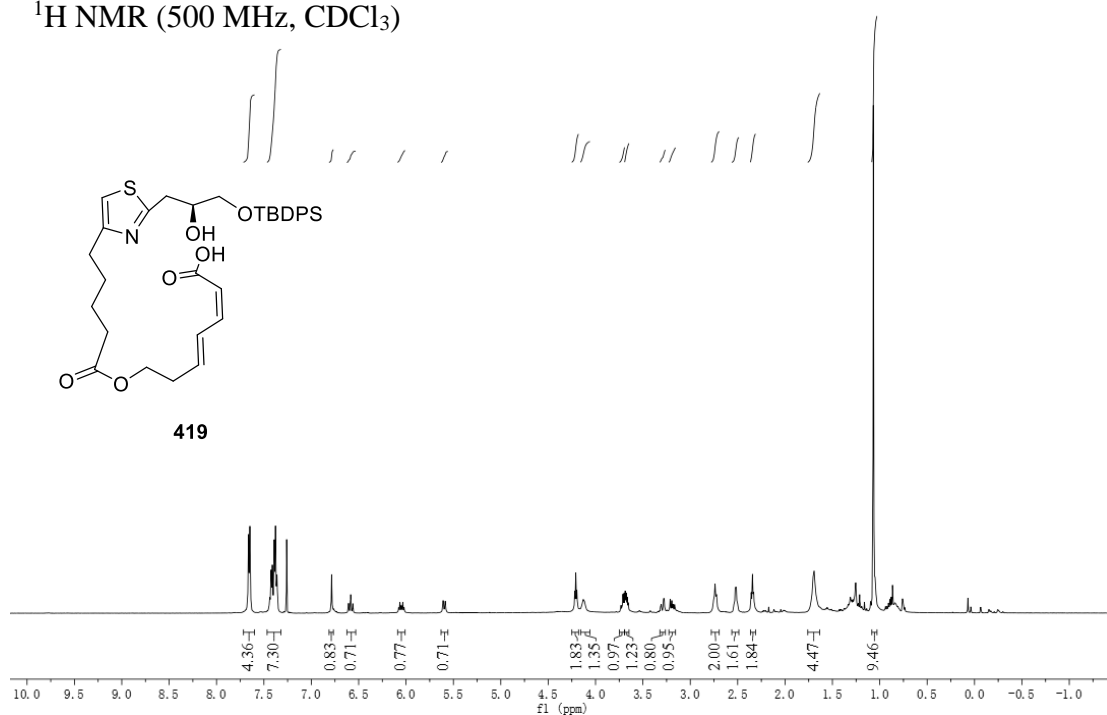


^1H NMR (500 MHz, CDCl_3) ^{13}C NMR (125 MHz, CDCl_3)

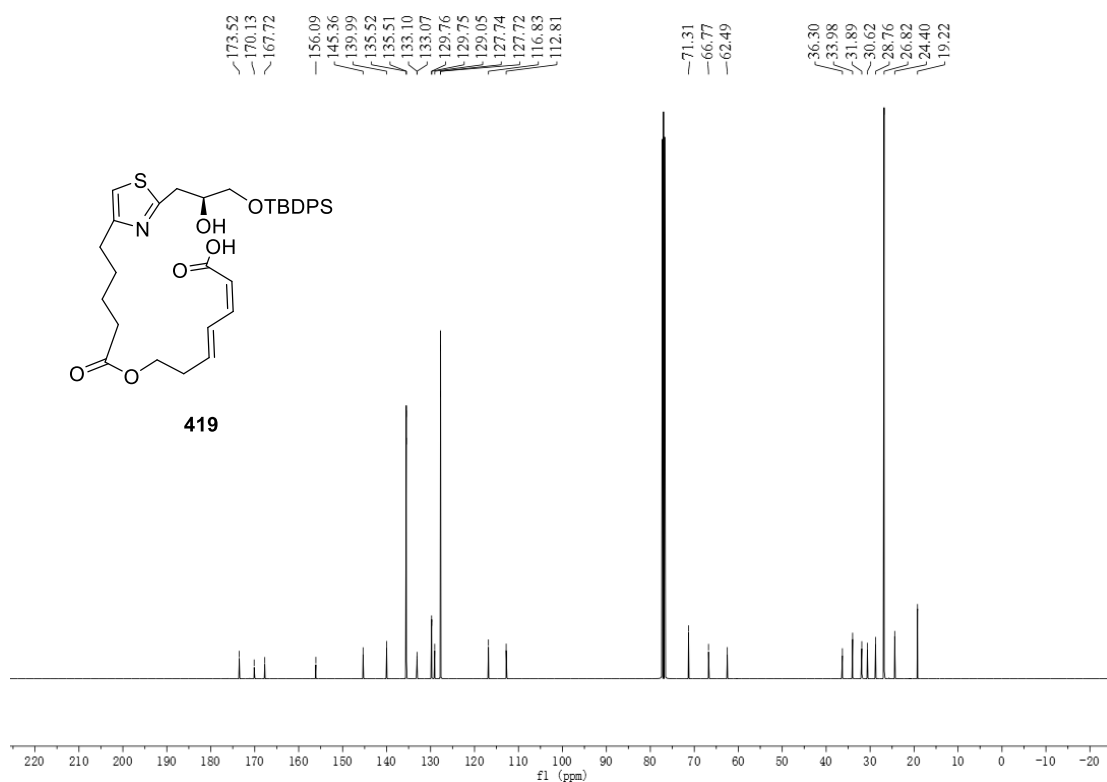


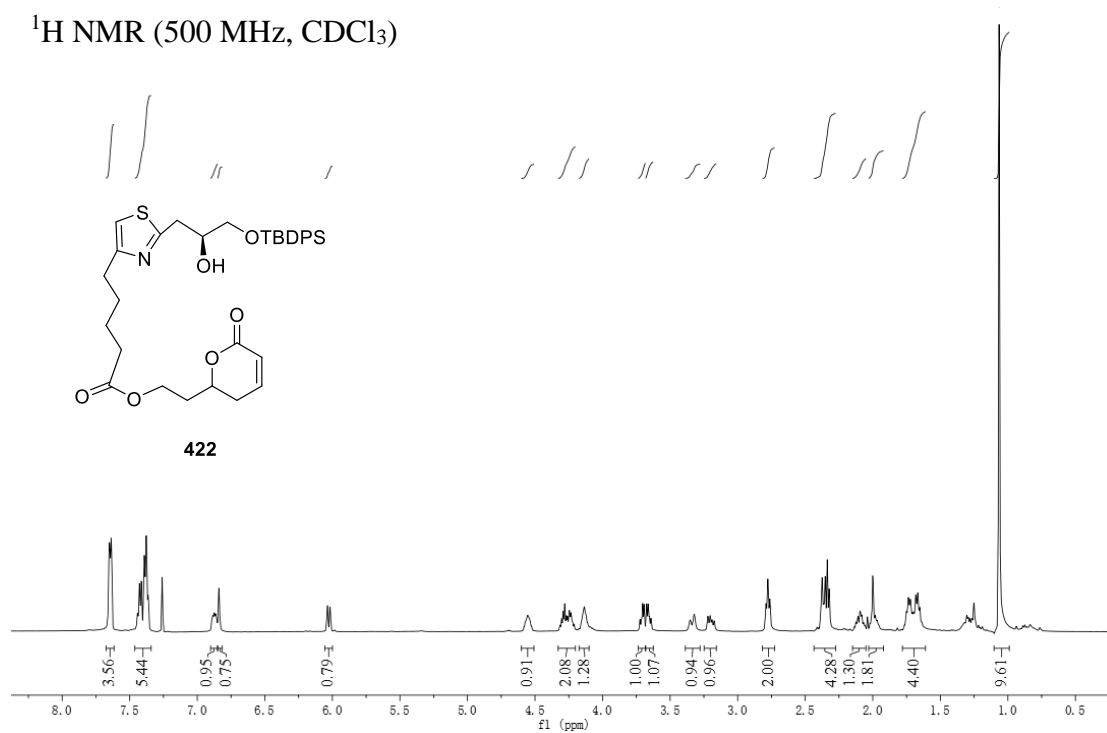
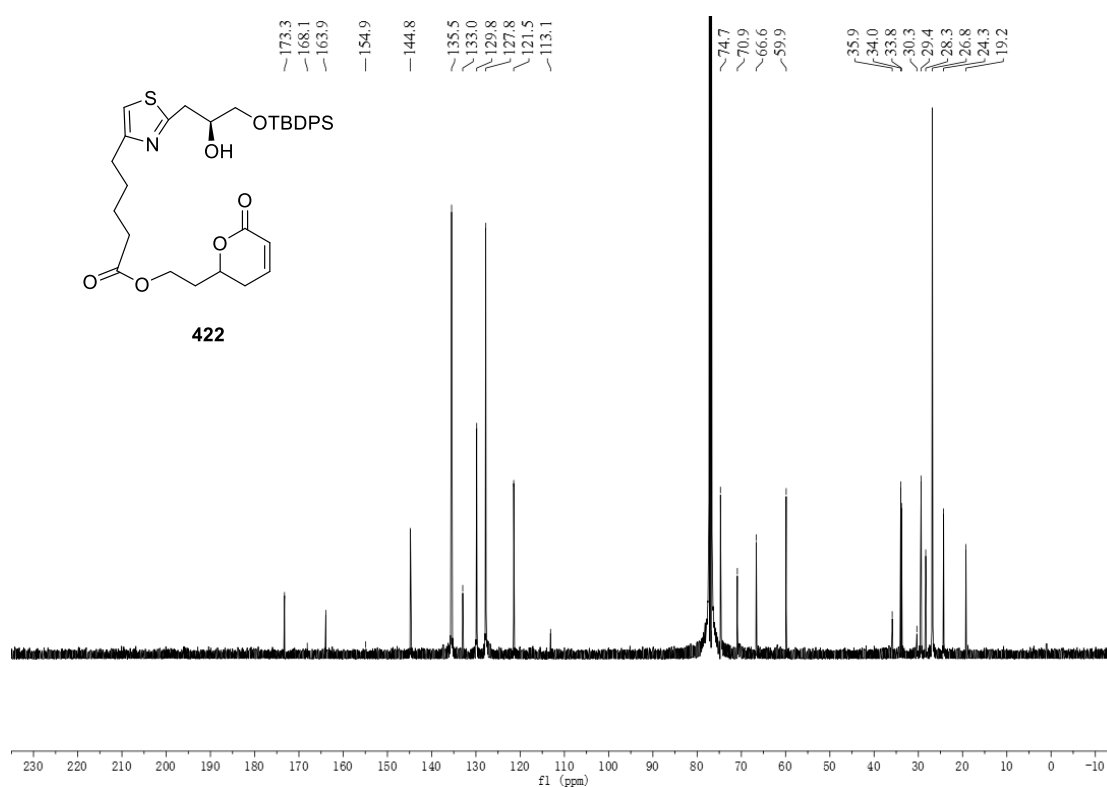
^1H NMR (500 MHz, CDCl_3) ^{13}C NMR (125 MHz, CDCl_3)

^1H NMR (500 MHz, CDCl_3)

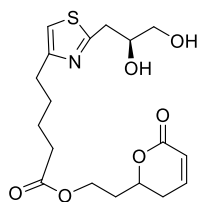


^{13}C NMR (125 MHz, CDCl_3)

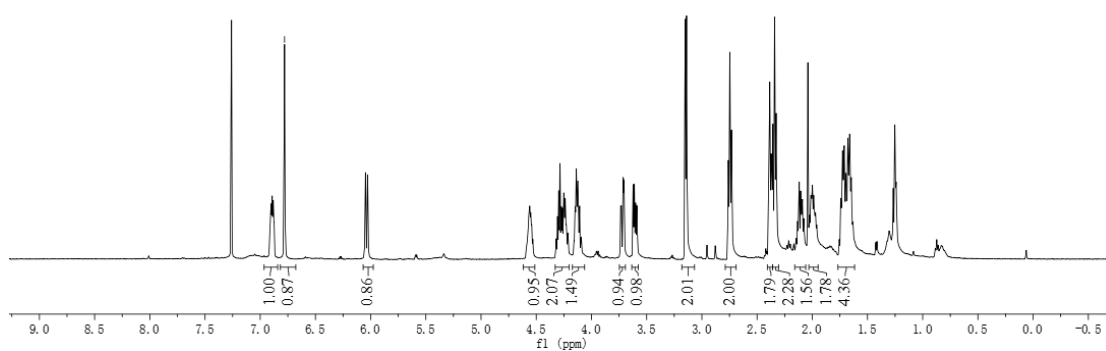


^1H NMR (500 MHz, CDCl_3) ^{13}C NMR (125 MHz, CDCl_3)

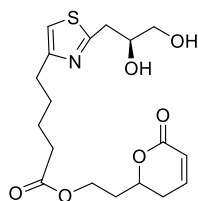
^1H NMR (500 MHz, CDCl_3)



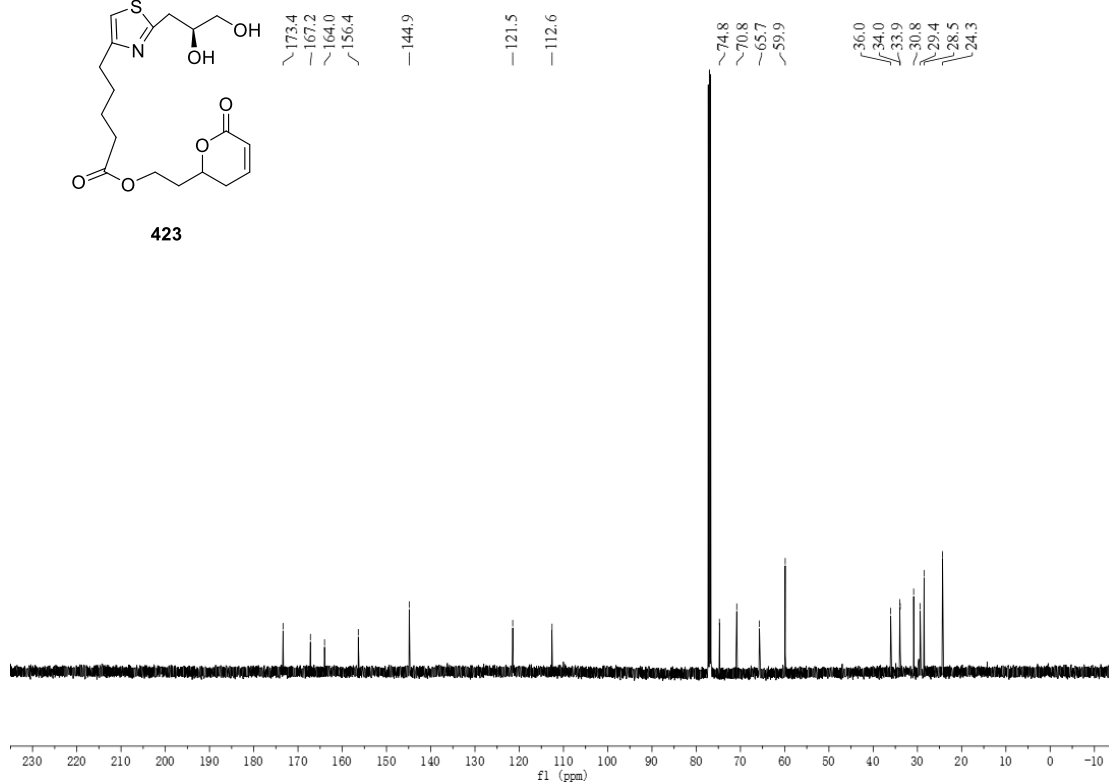
423

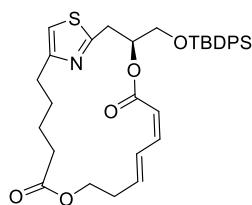


^{13}C NMR (125 MHz, CDCl_3)

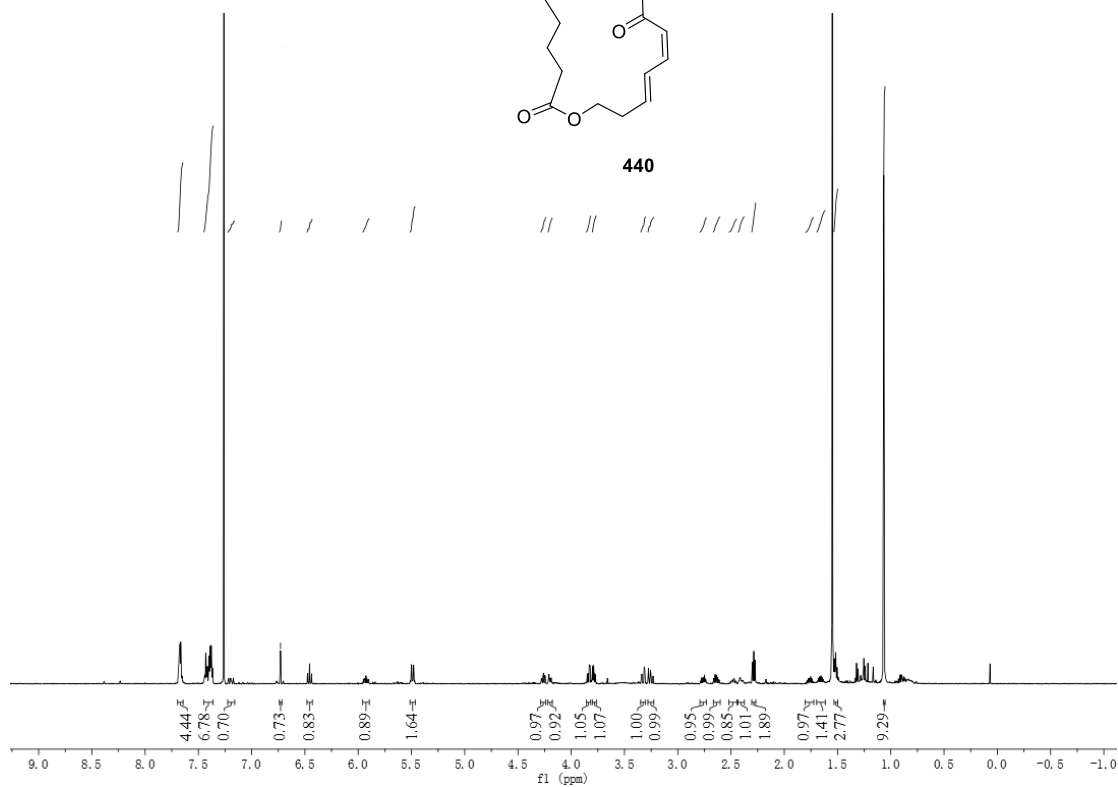
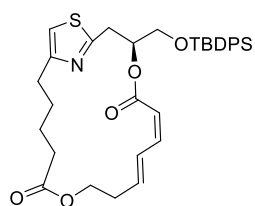


423

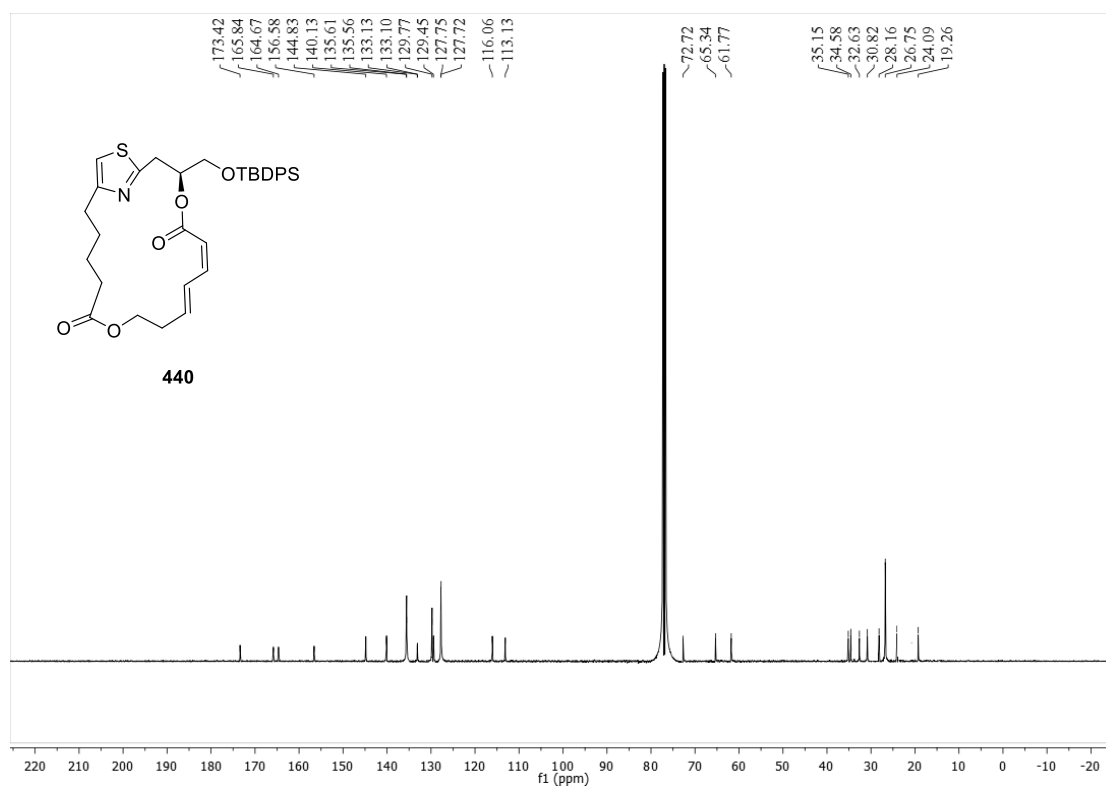


¹H NMR (600 MHz, CDCl₃)

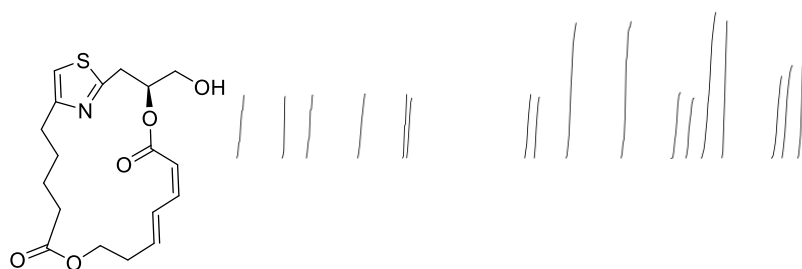
440

 ^{13}C NMR (150 MHz, CDCl_3)

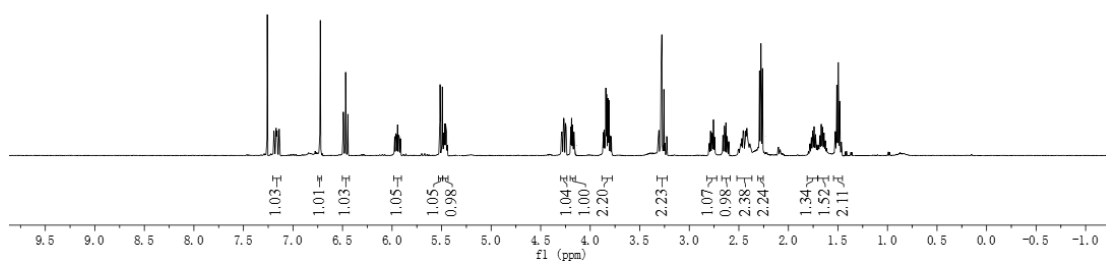
440



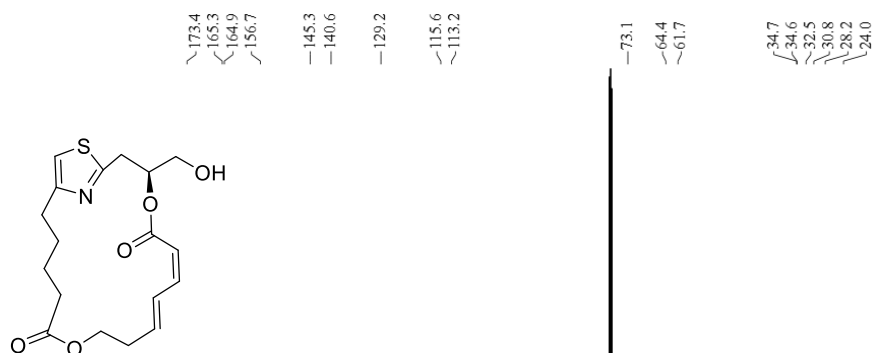
^1H NMR (600 MHz, CDCl_3)



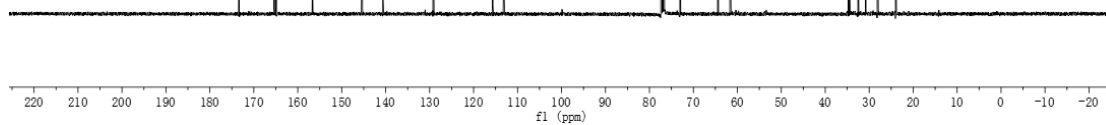
441

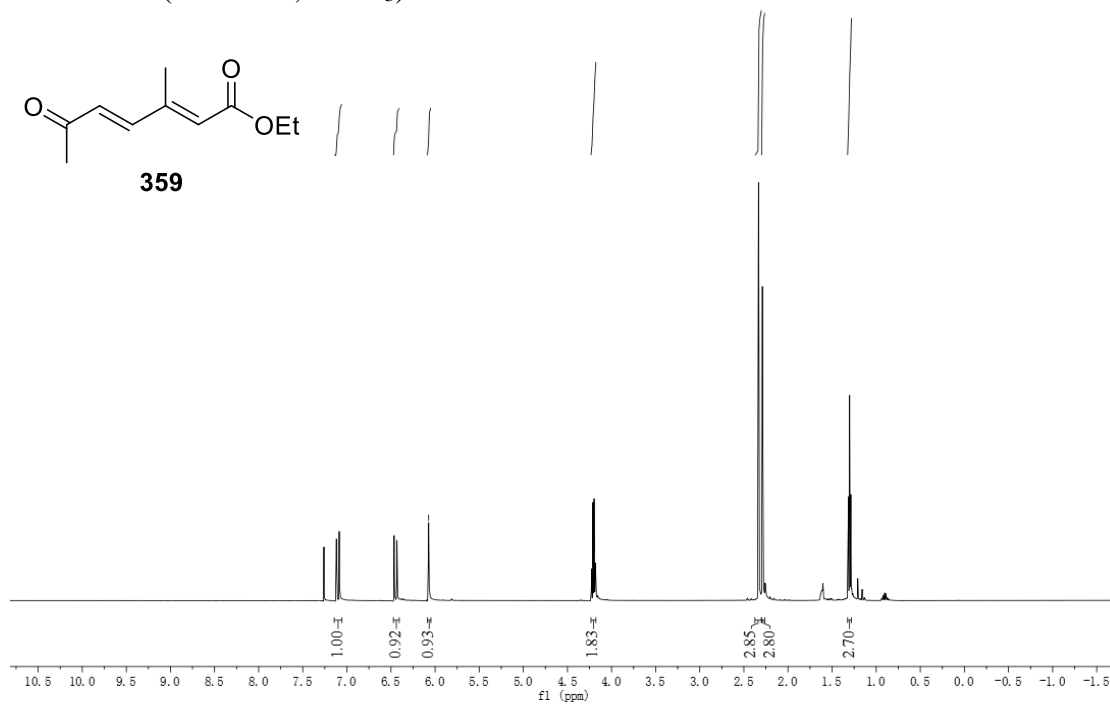
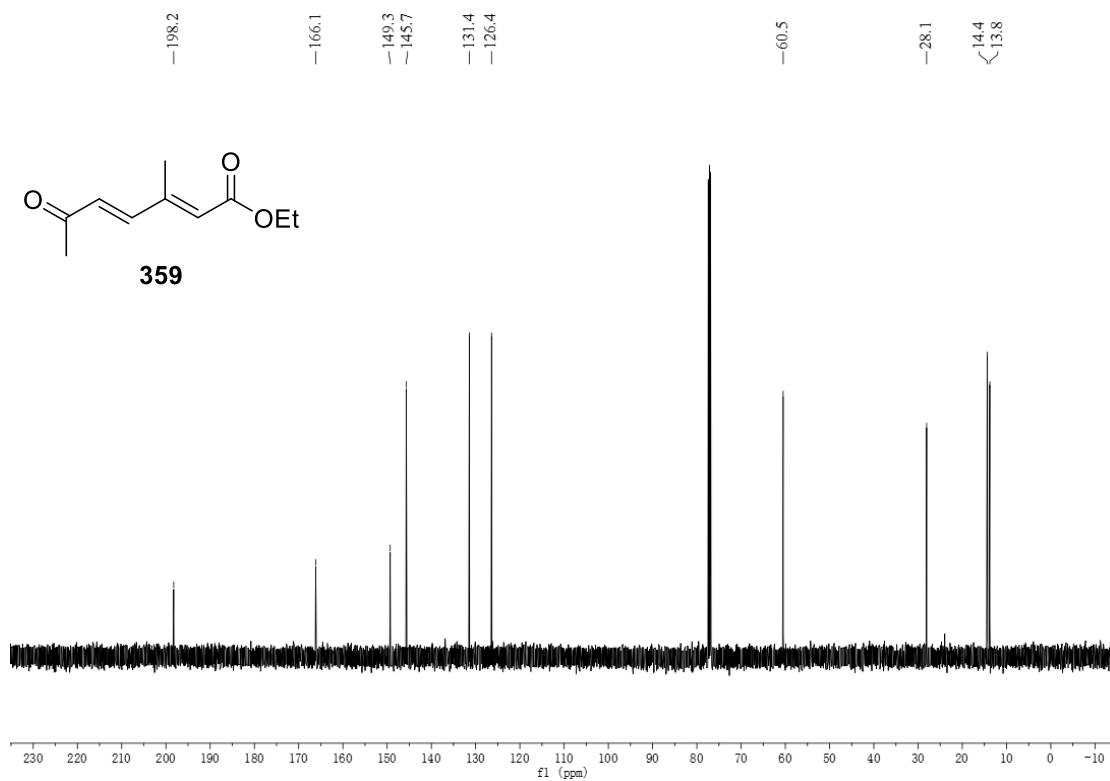


^{13}C NMR (150 MHz, CDCl_3)

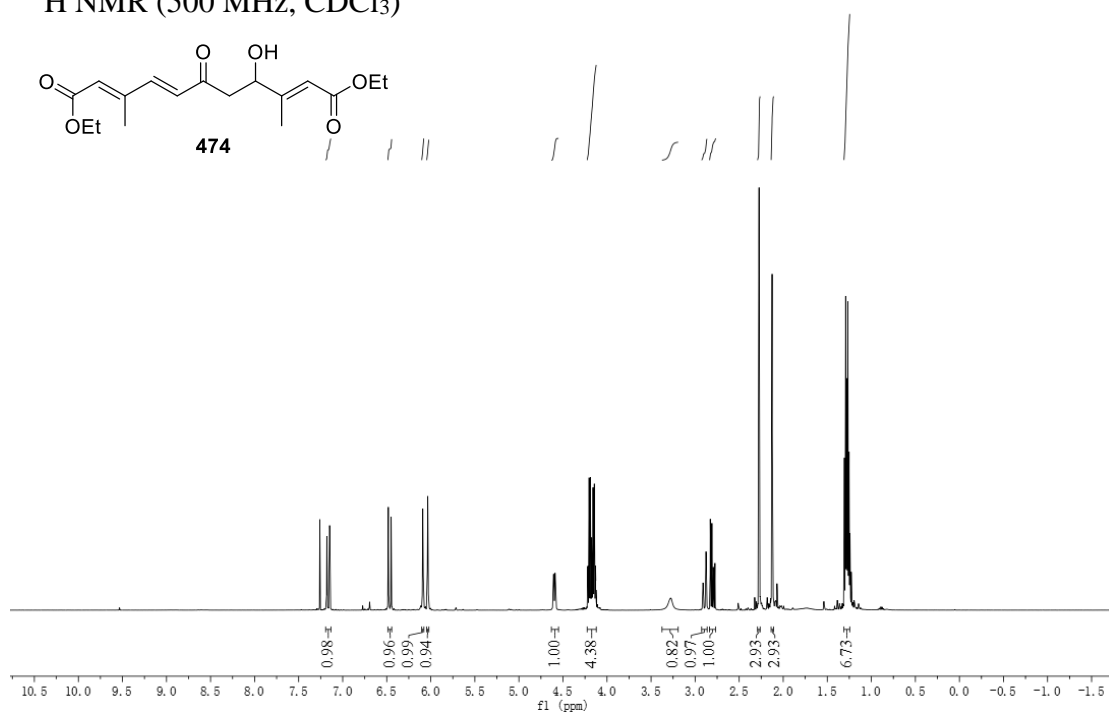


441

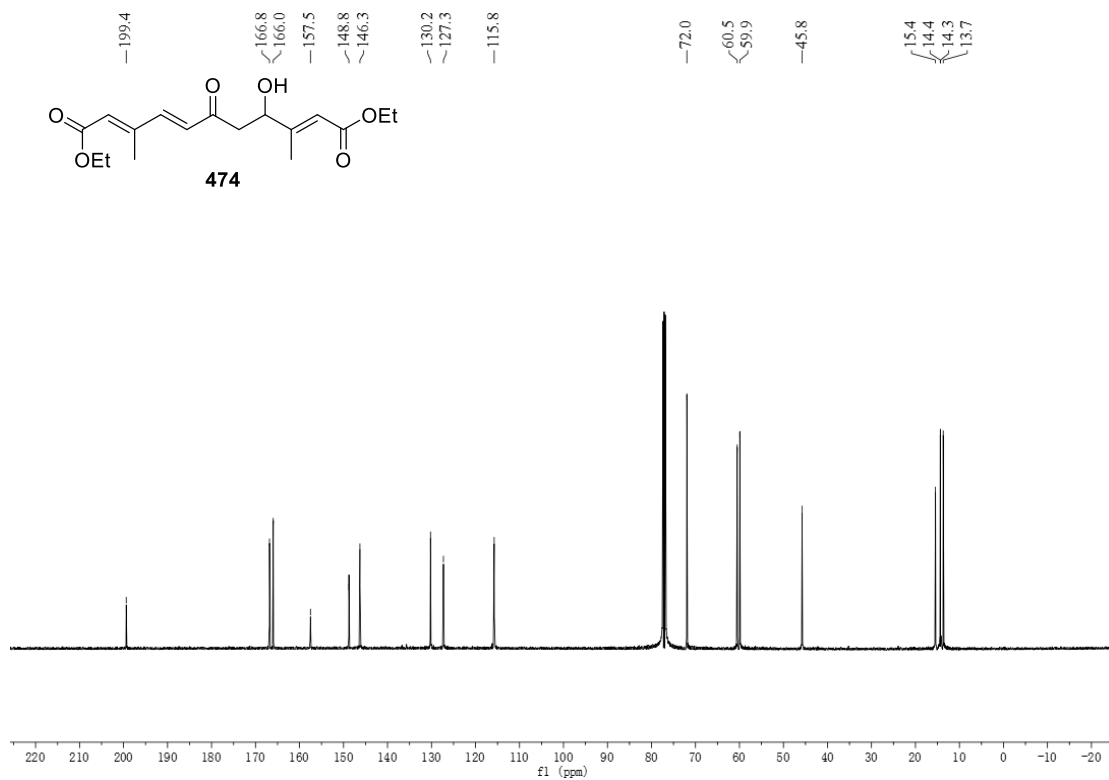


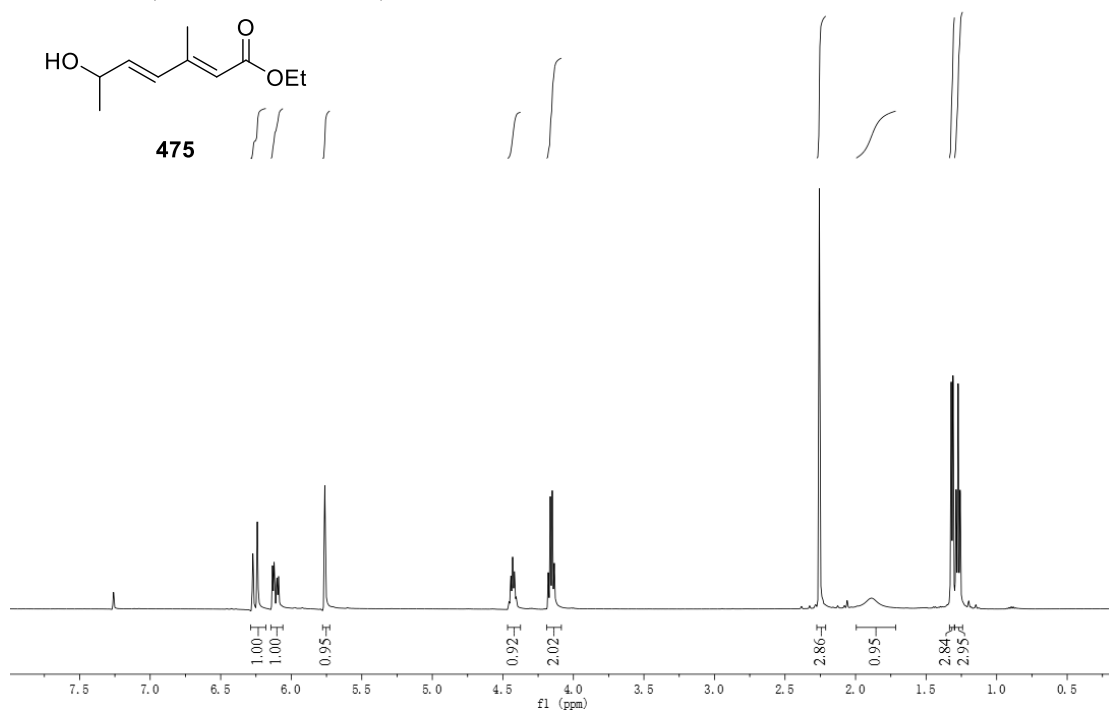
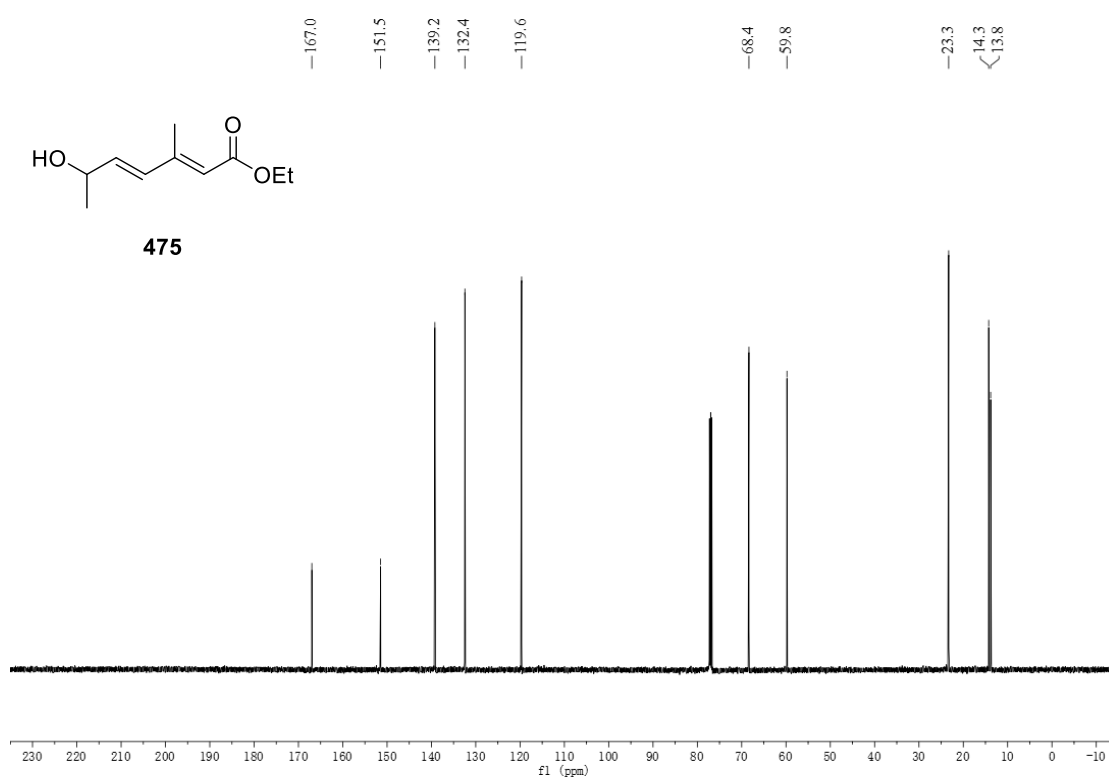
¹H NMR (500 MHz, CDCl₃)¹³C NMR (125 MHz, CDCl₃)

^1H NMR (500 MHz, CDCl_3)

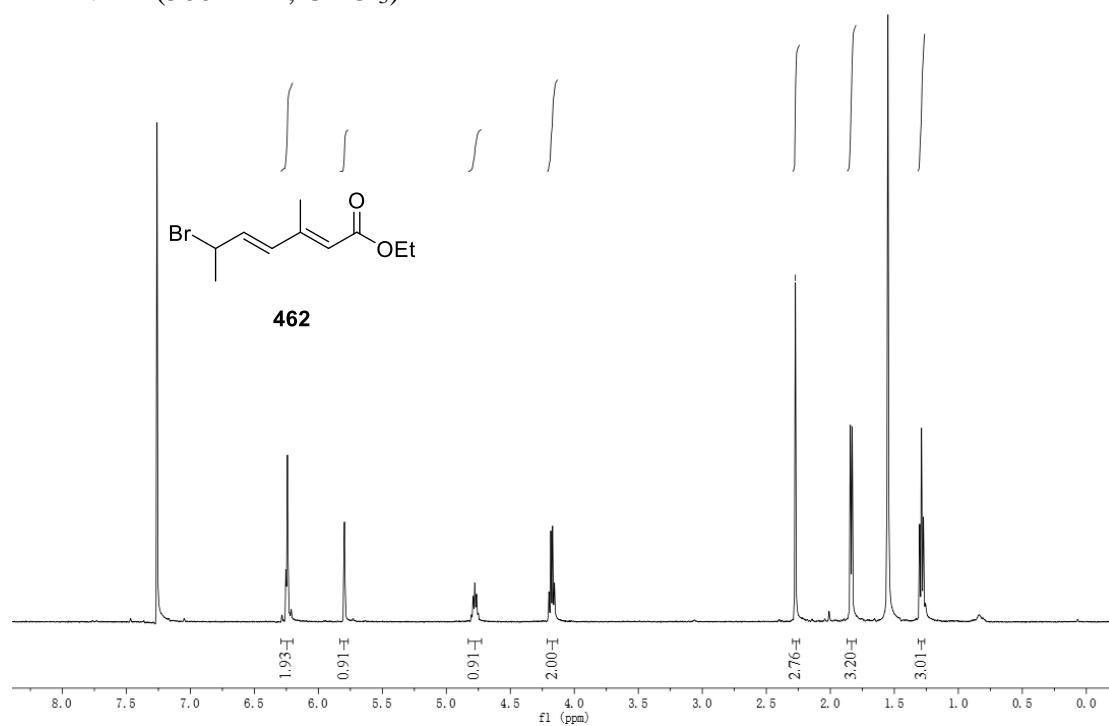


^{13}C NMR (125 MHz, CDCl_3)

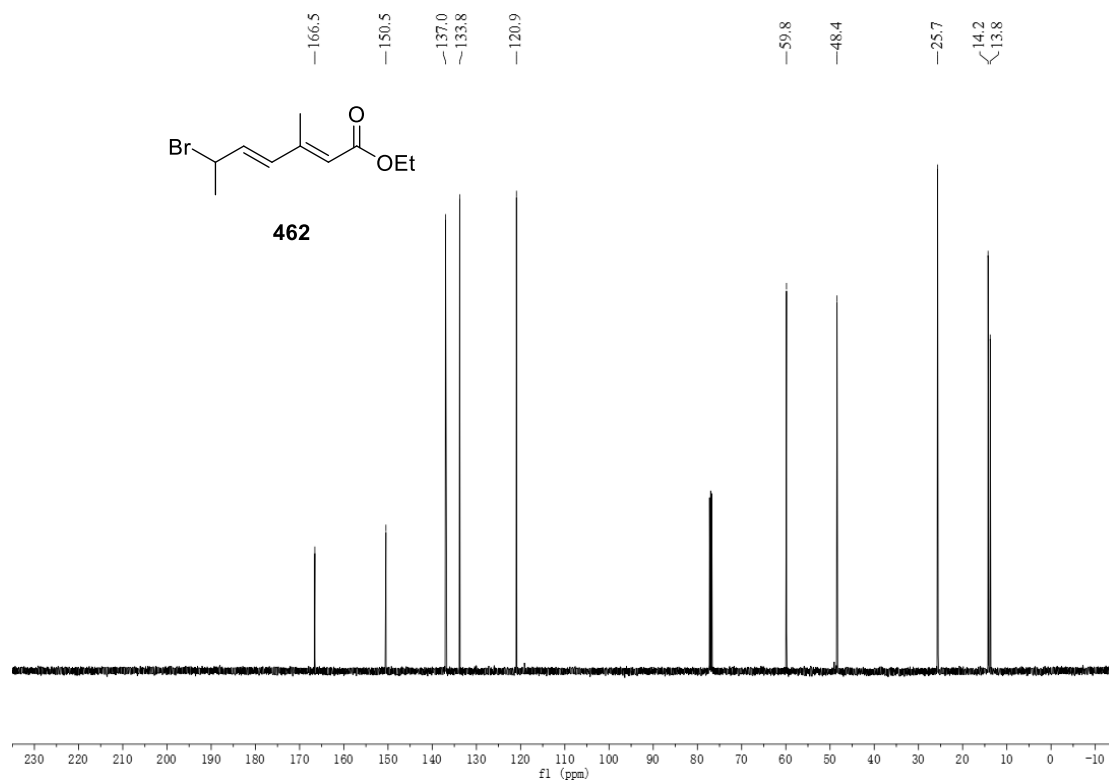


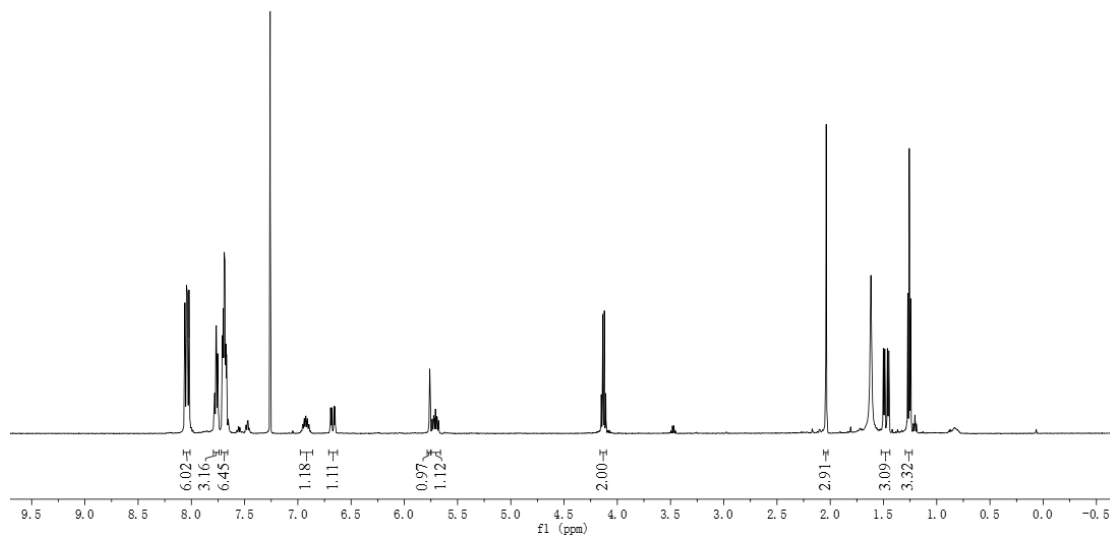
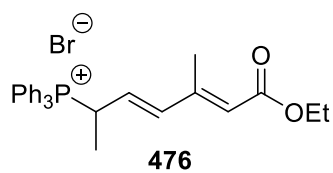
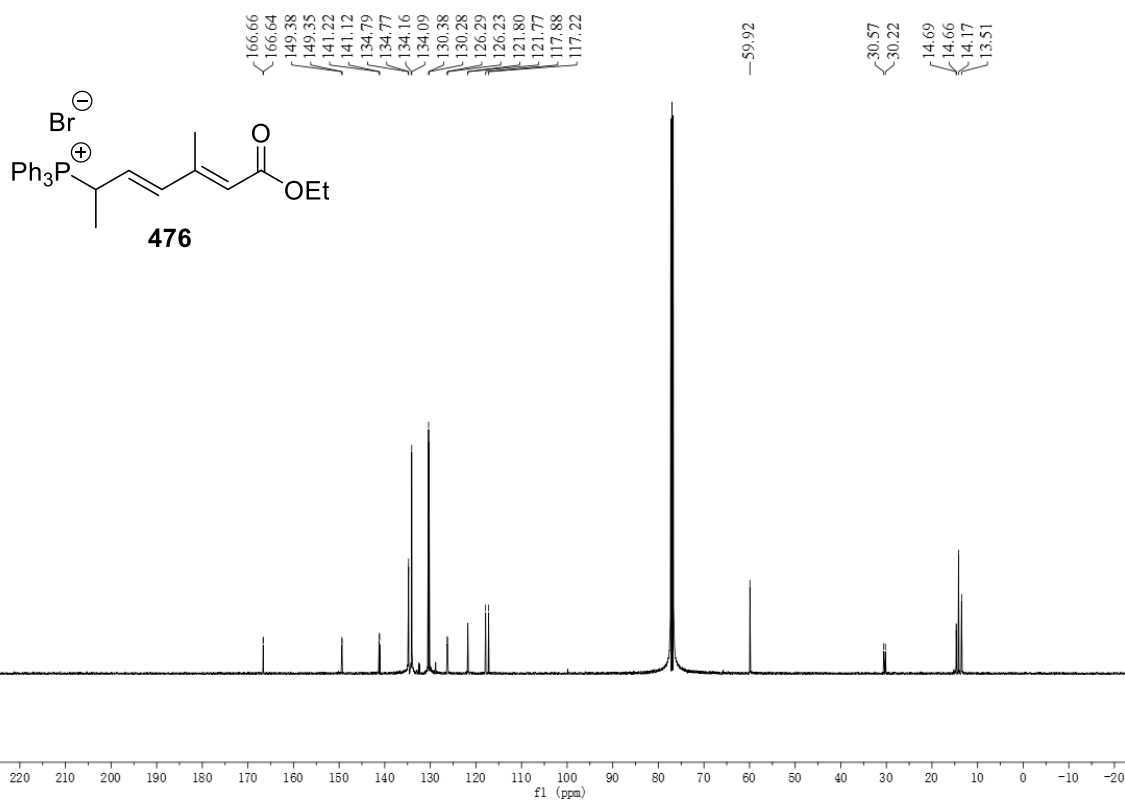
^1H NMR (500 MHz, CDCl_3) ^{13}C NMR (125 MHz, CDCl_3)

^1H NMR (500 MHz, CDCl_3)

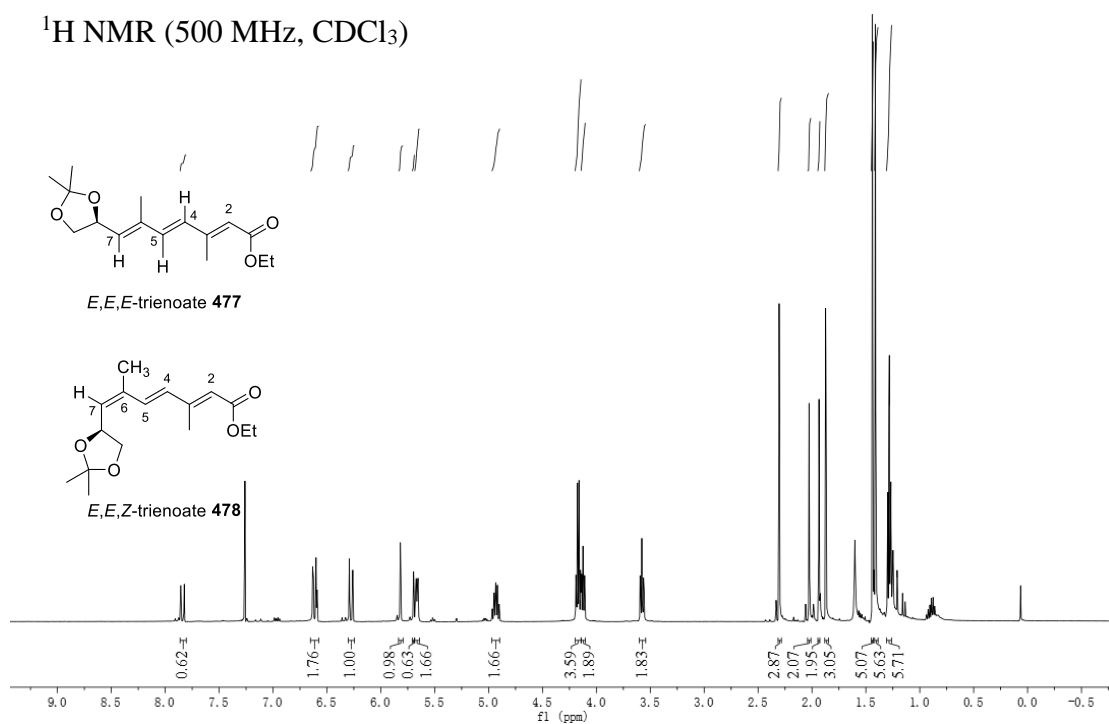


^{13}C NMR (125 MHz, CDCl_3)

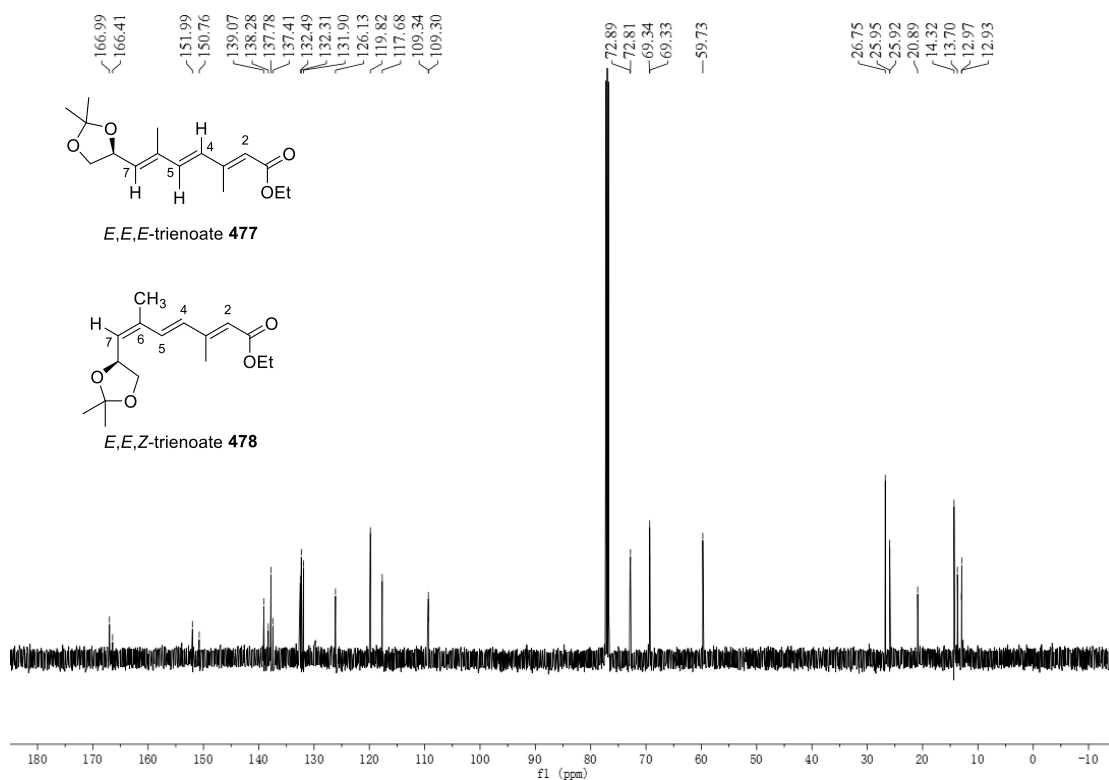


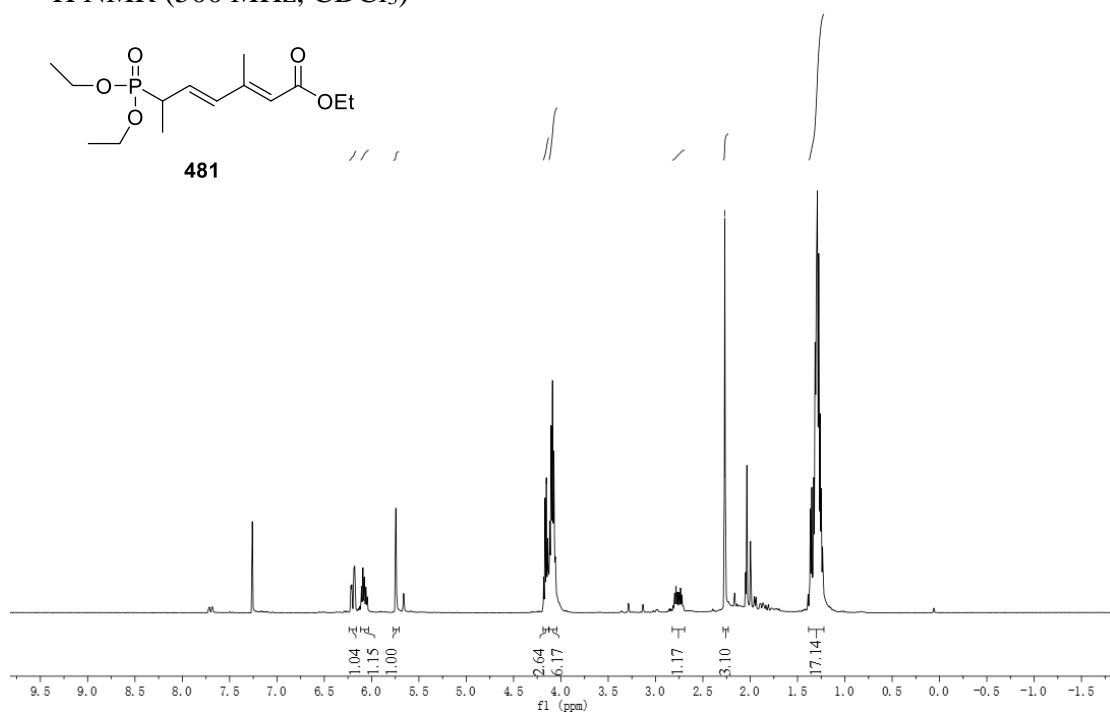
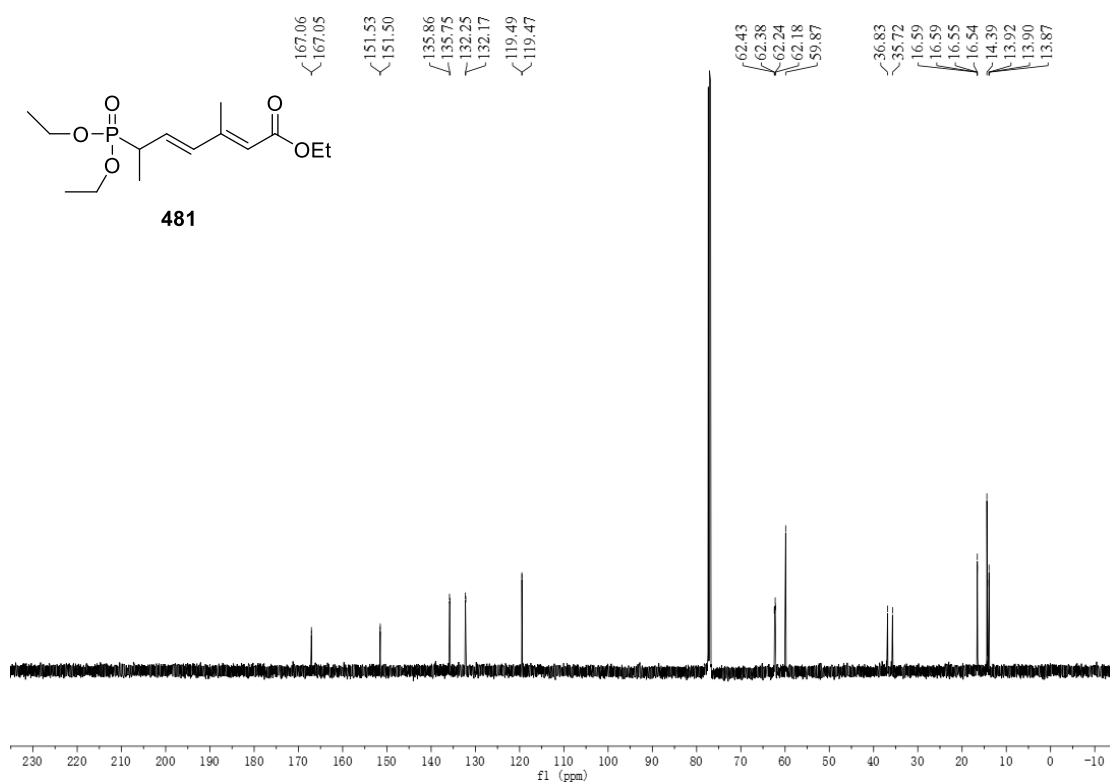
^1H NMR (500 MHz, CDCl_3) ^{13}C NMR (125 MHz, CDCl_3)

^1H NMR (500 MHz, CDCl_3)

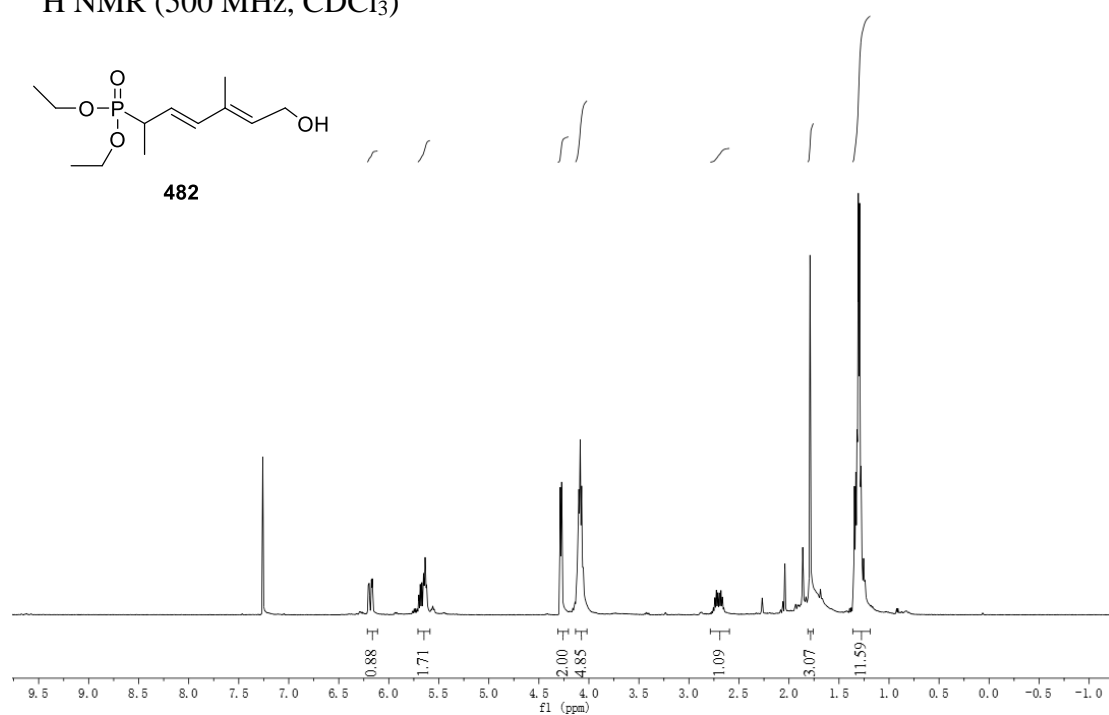


^{13}C NMR (125 MHz, CDCl_3)

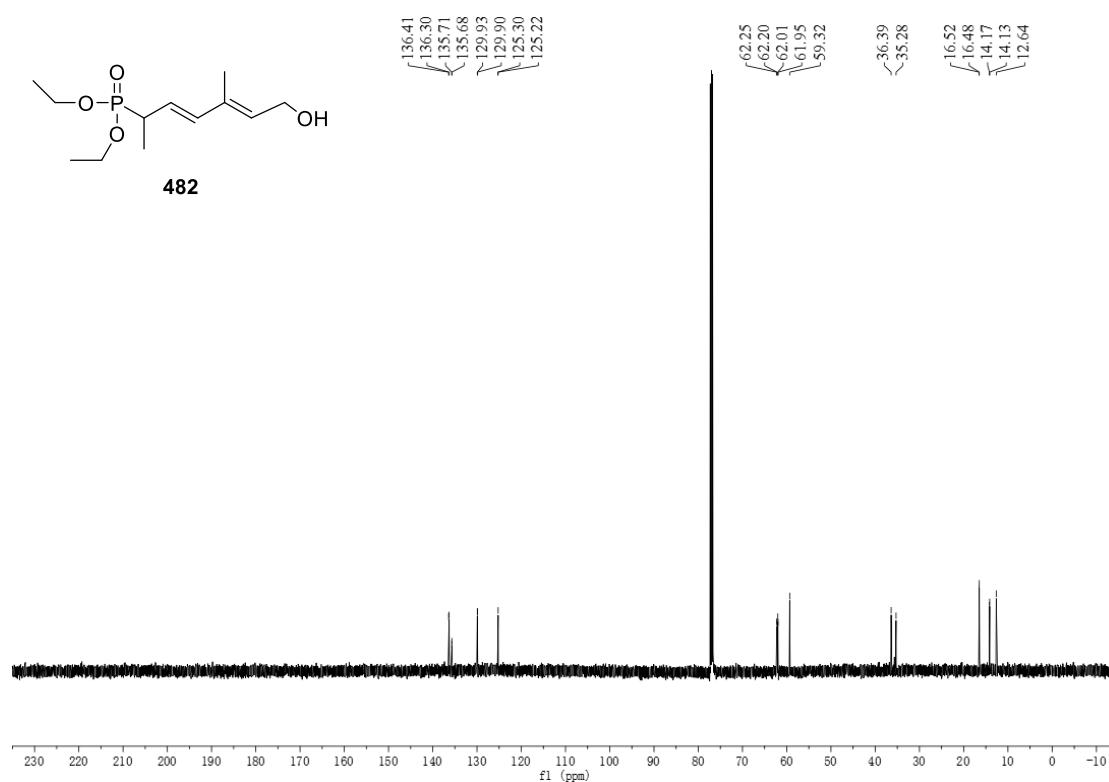


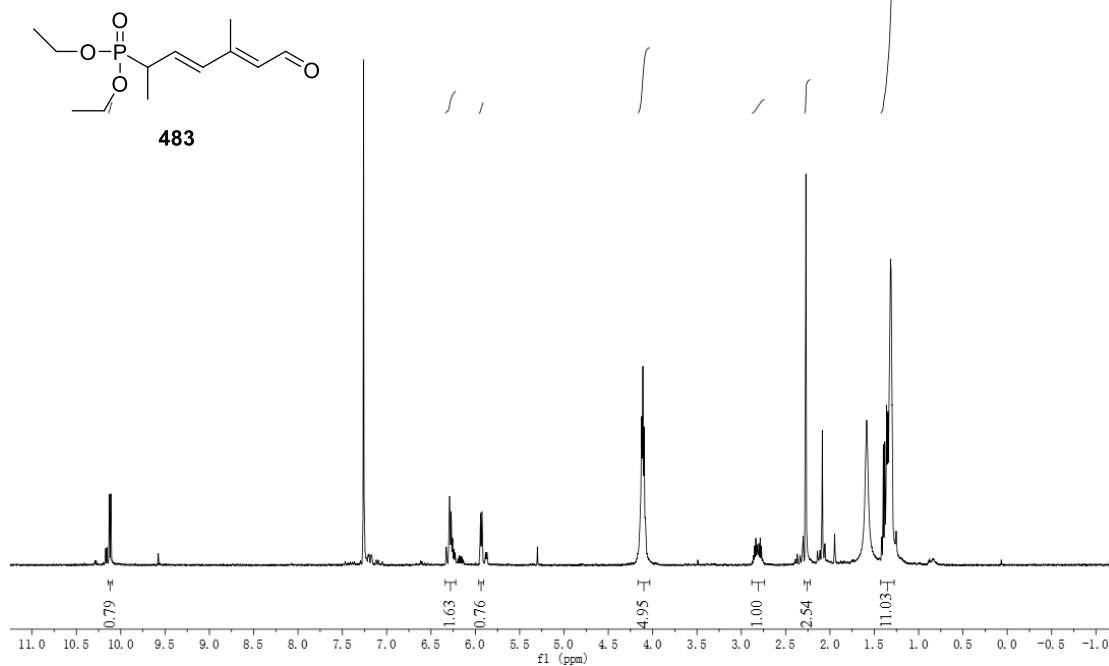
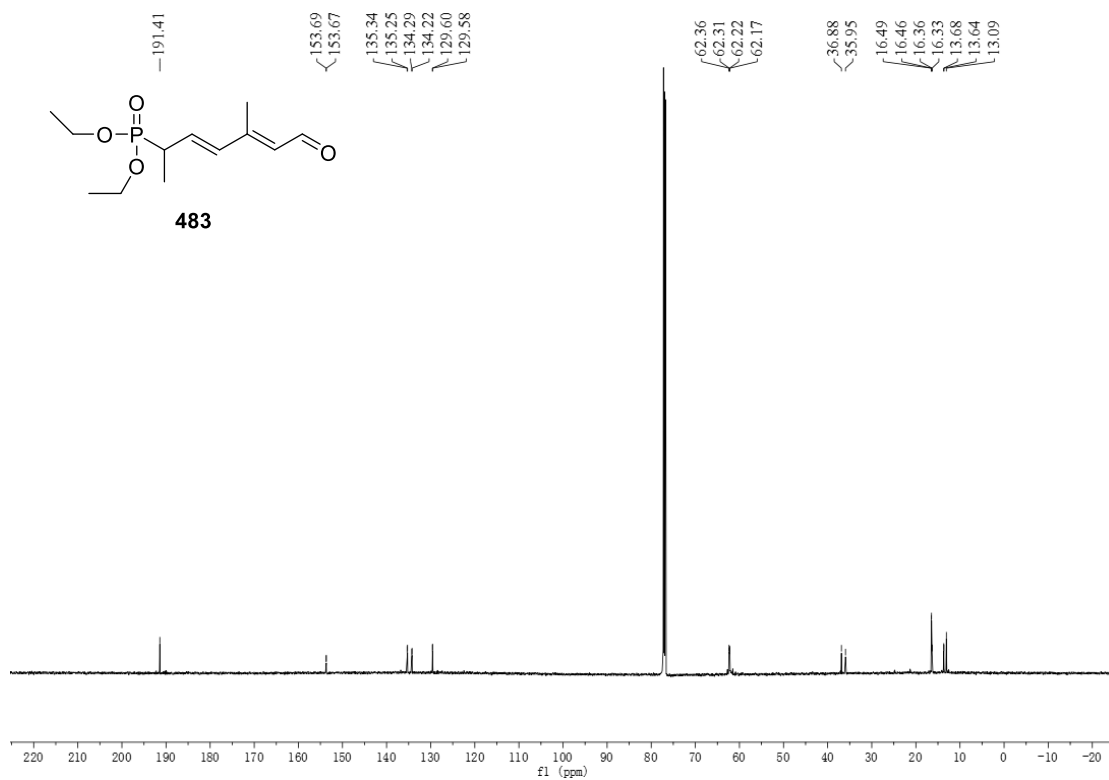
^1H NMR (500 MHz, CDCl_3) ^{13}C NMR (125 MHz, CDCl_3)

^1H NMR (500 MHz, CDCl_3)

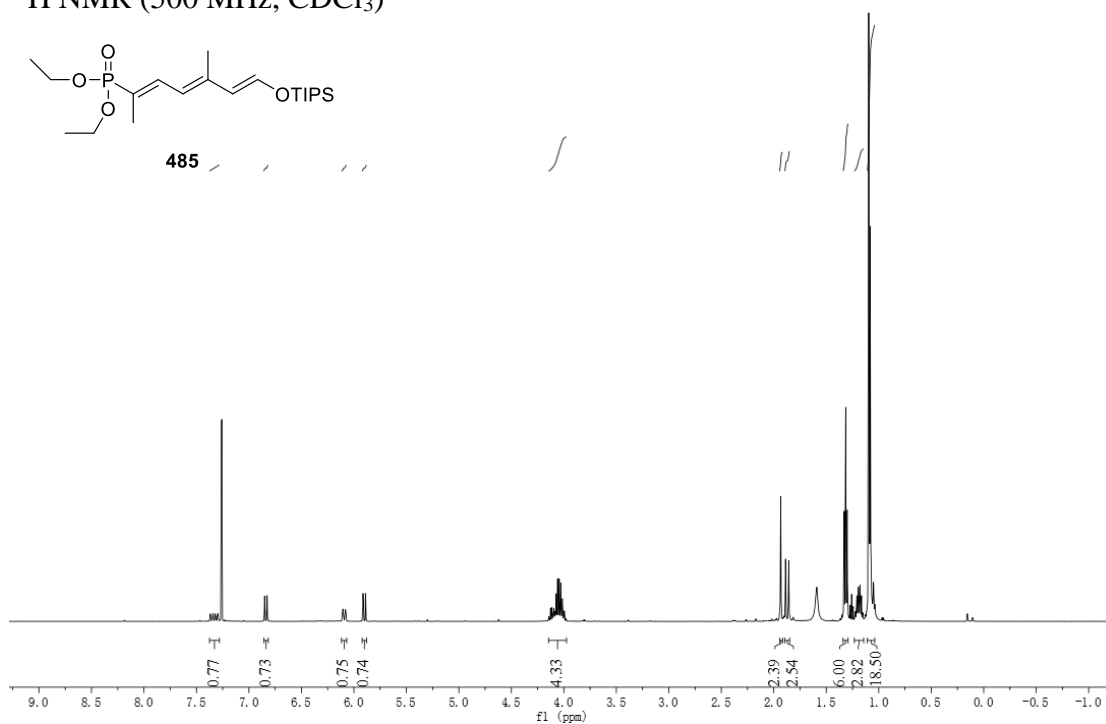


^{13}C NMR (125 MHz, CDCl_3)

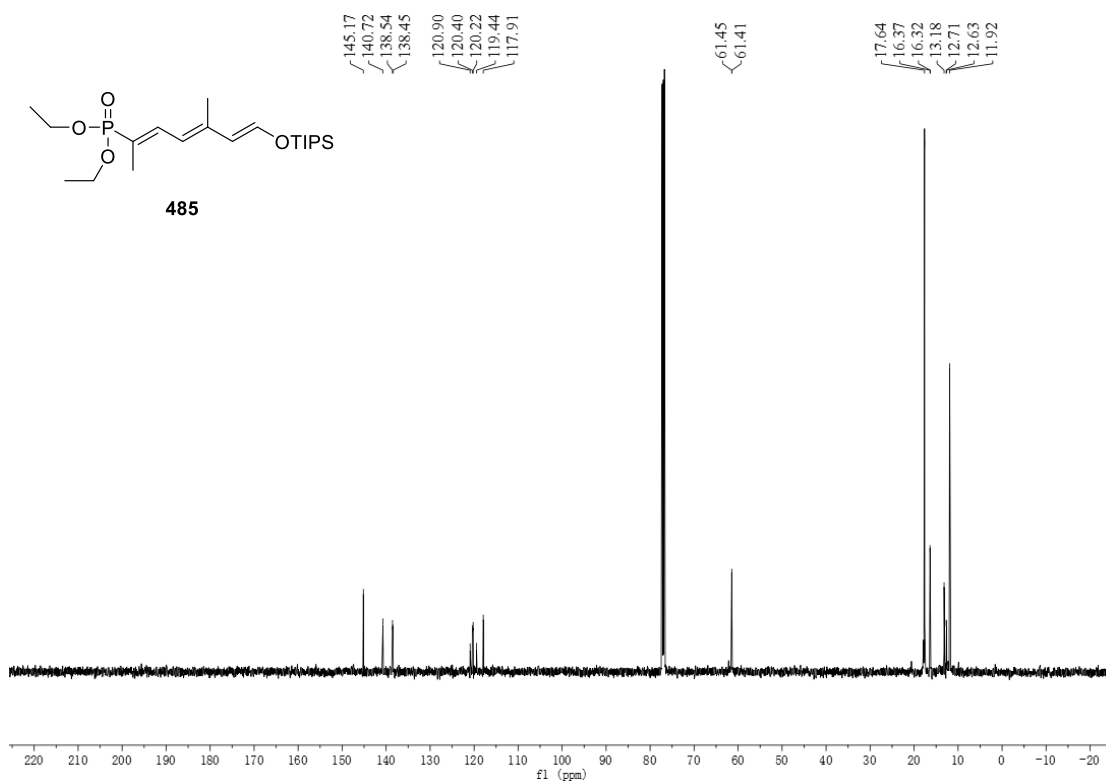


^1H NMR (500 MHz, CDCl_3) ^{13}C NMR (125 MHz, CDCl_3)

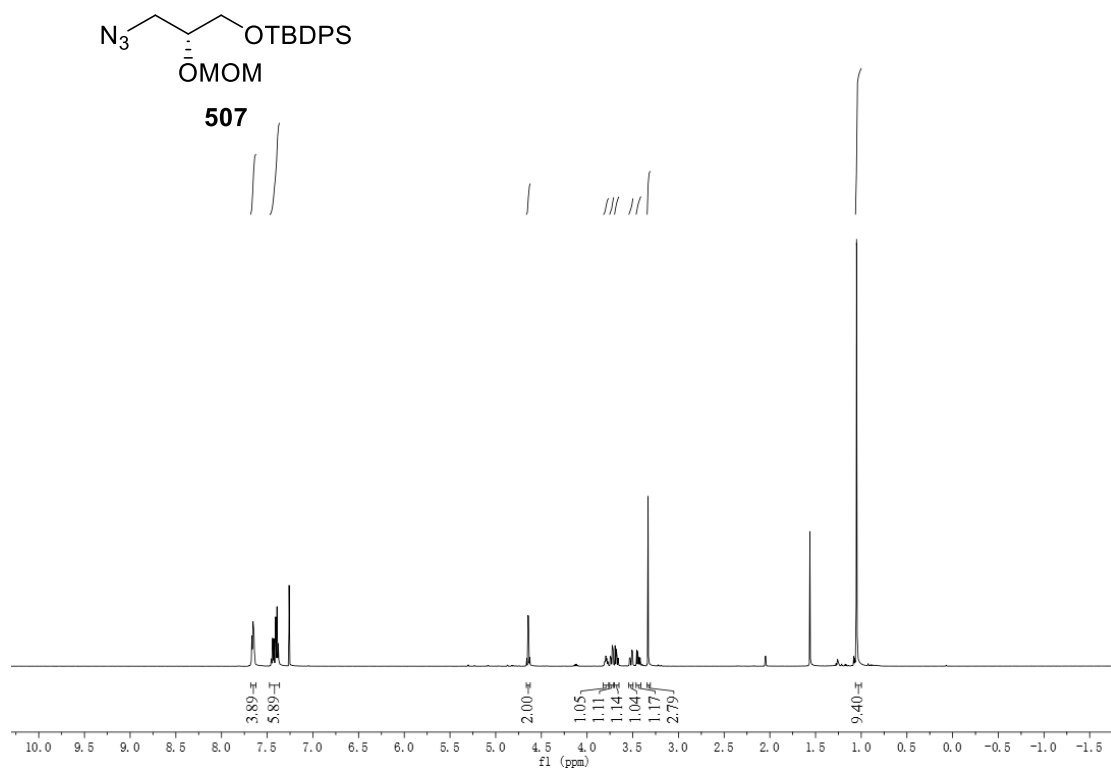
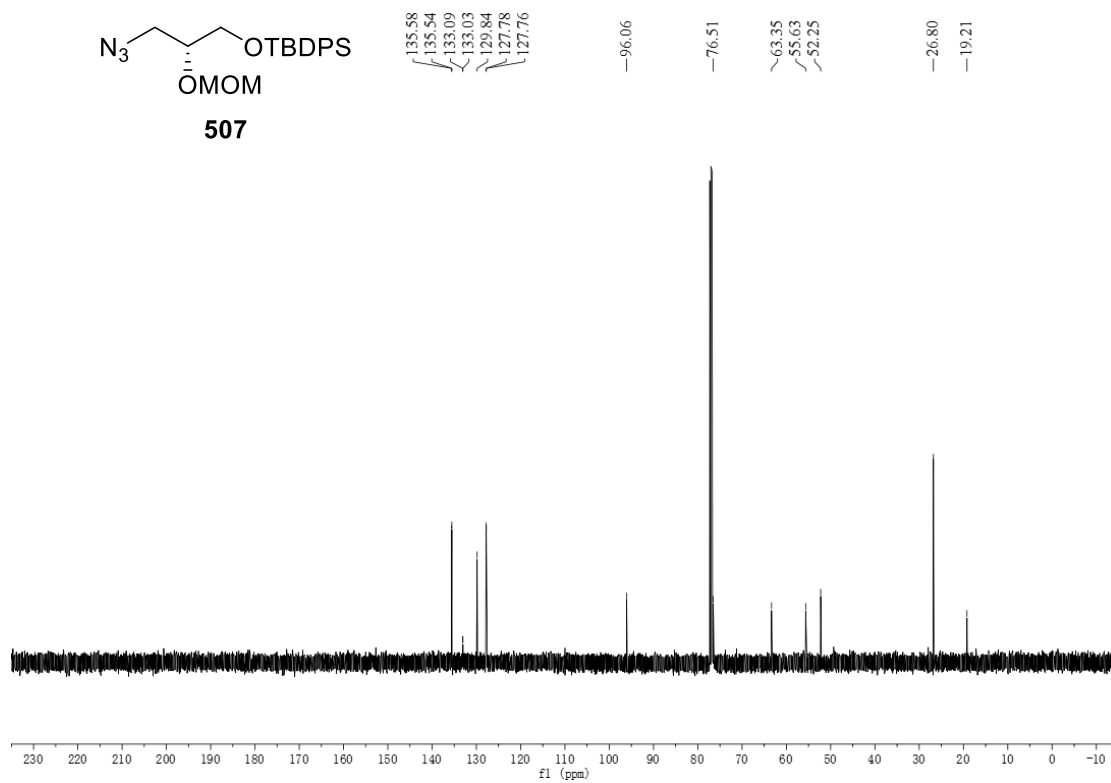
^1H NMR (500 MHz, CDCl_3)



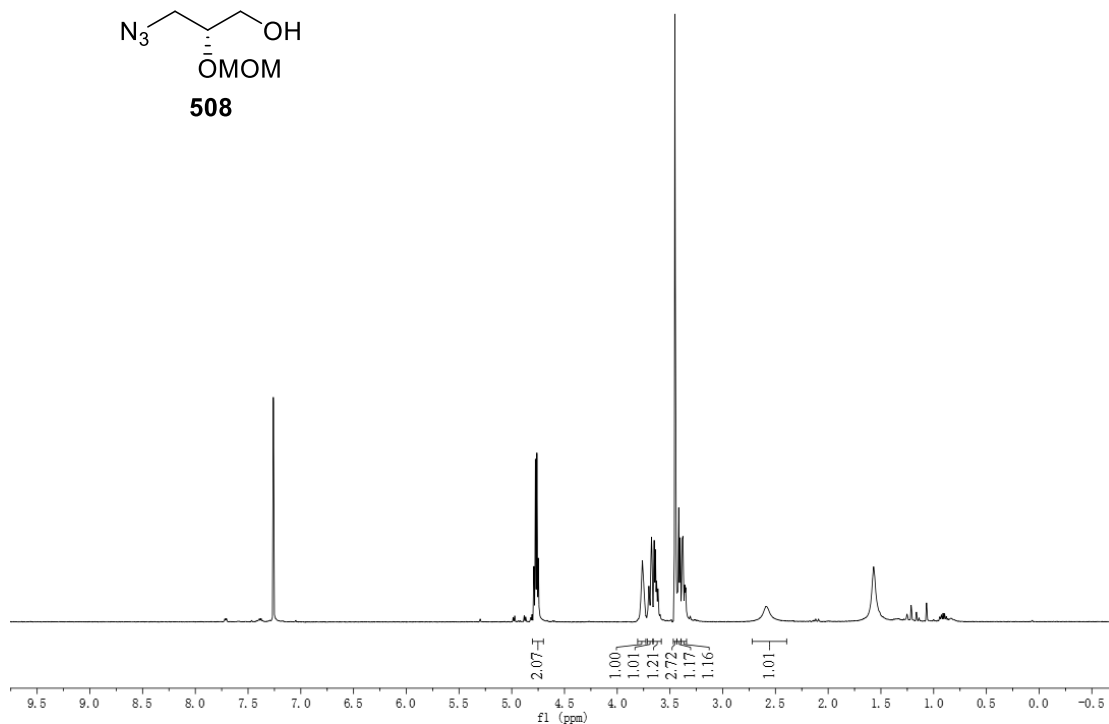
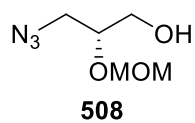
^{13}C NMR (125 MHz, CDCl_3)



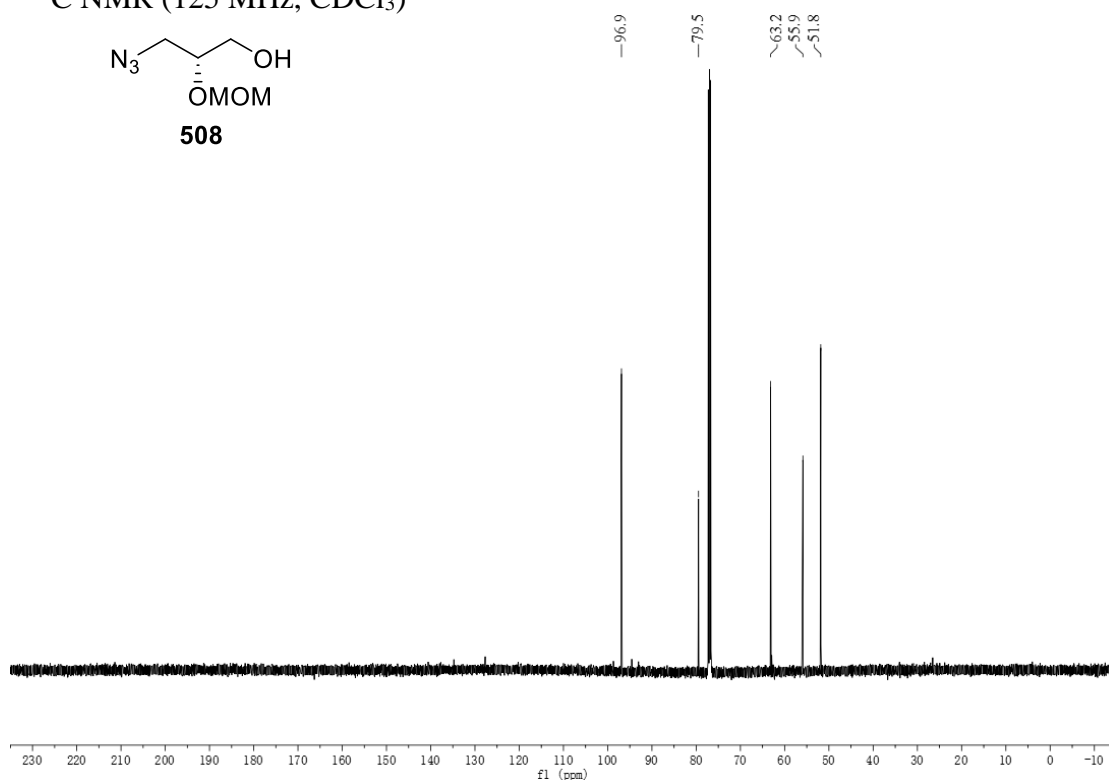
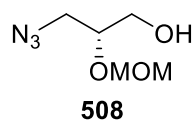
Spectra of Chapter Four

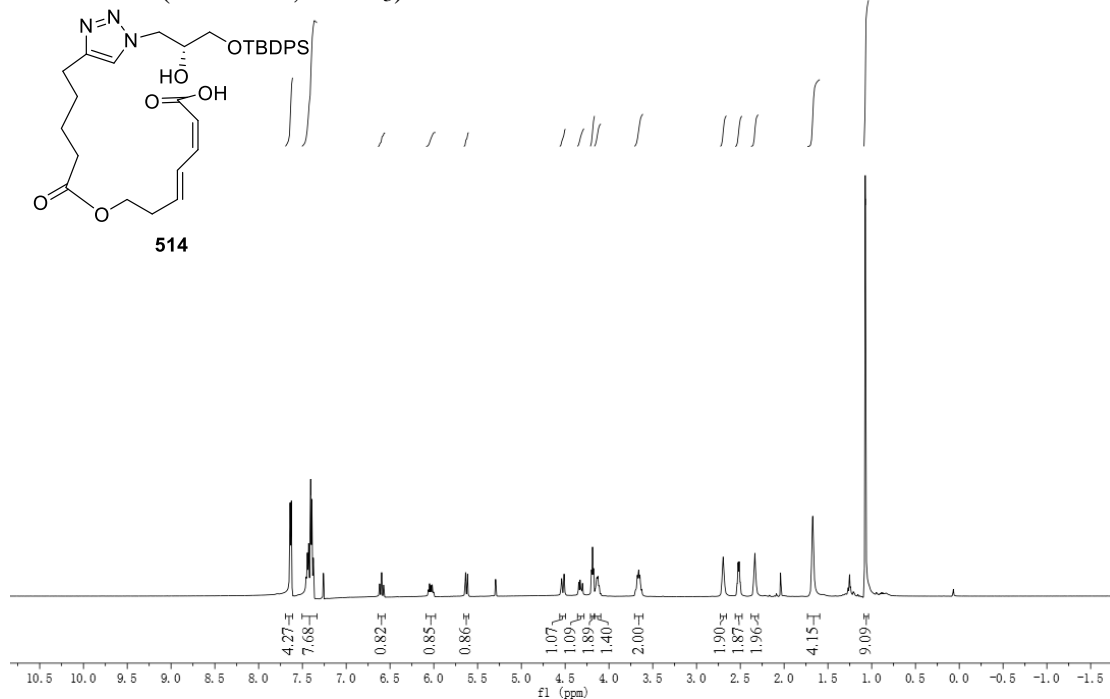
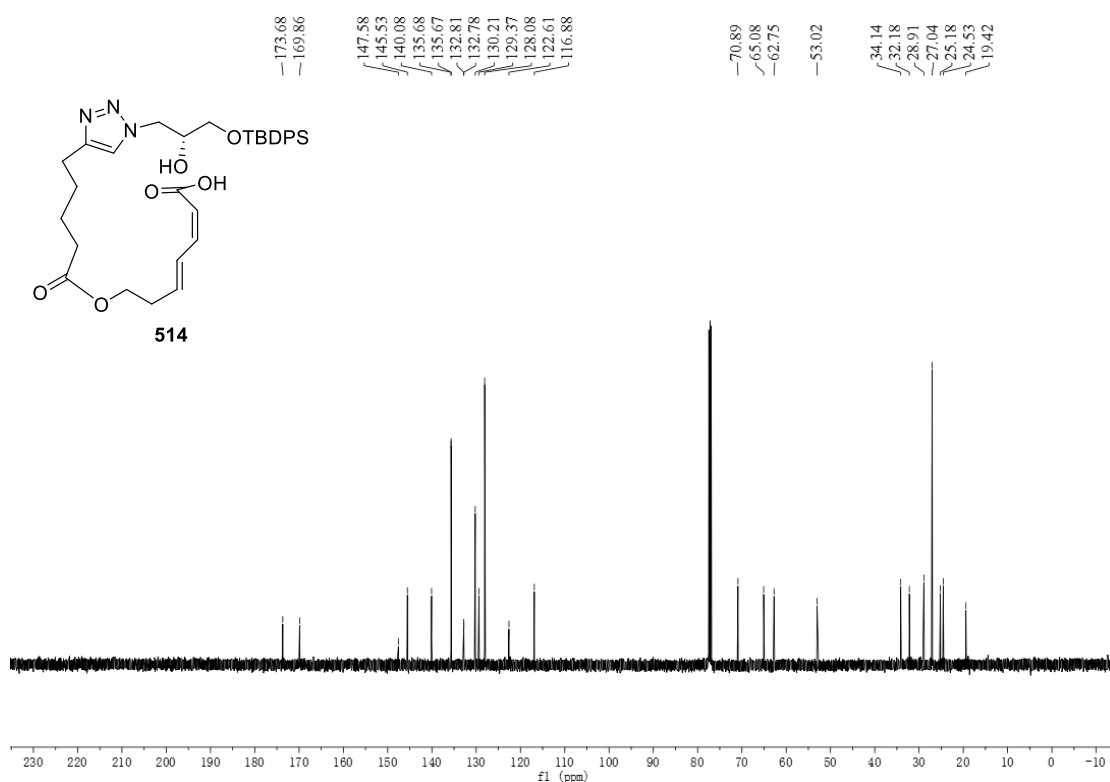
 ^1H NMR (500 MHz, CDCl_3) ^{13}C NMR (125 MHz, CDCl_3)

^1H NMR (500 MHz, CDCl_3)

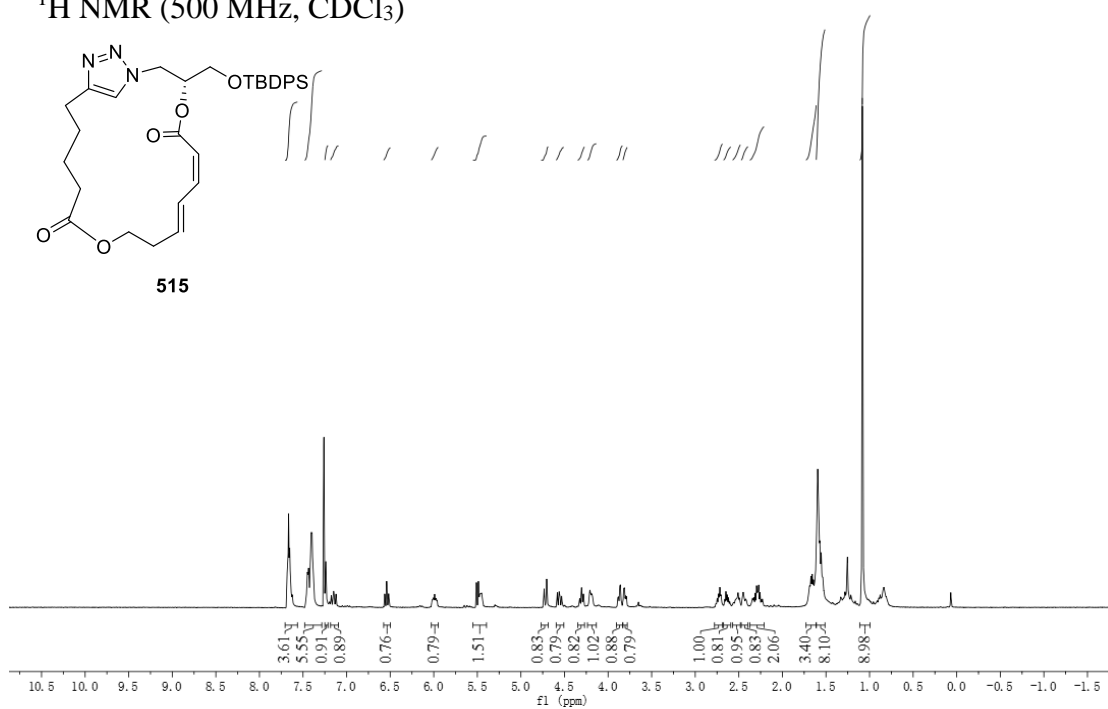


^{13}C NMR (125 MHz, CDCl_3)

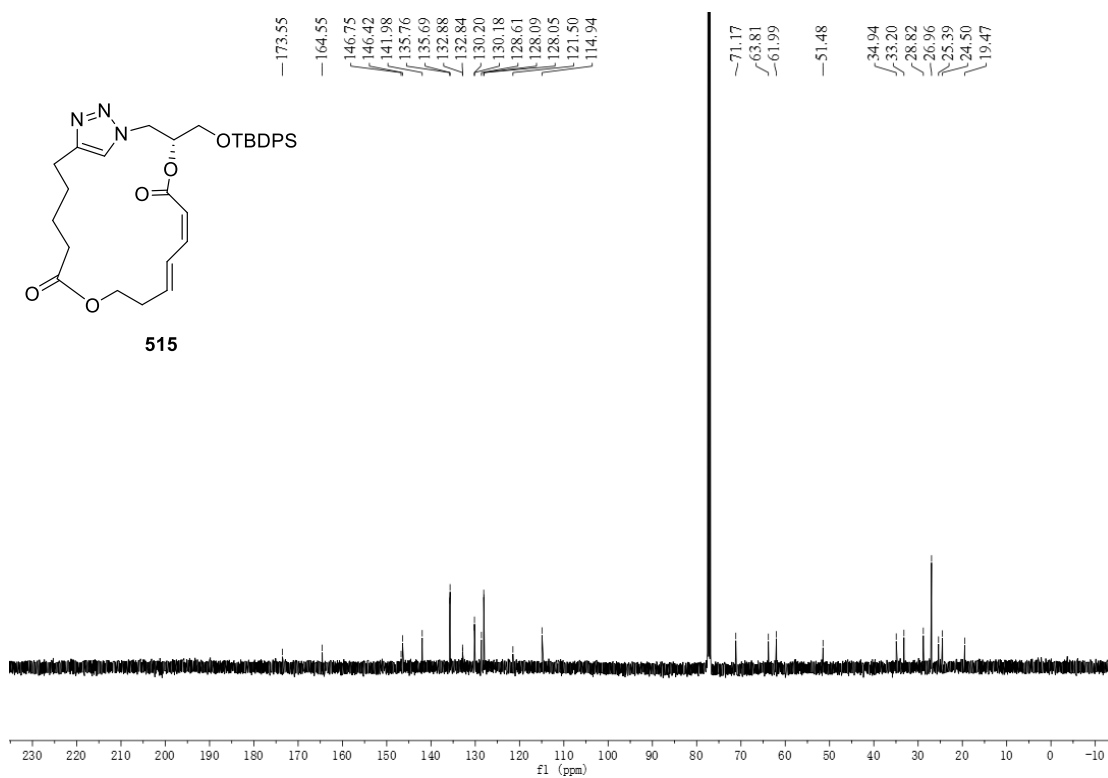


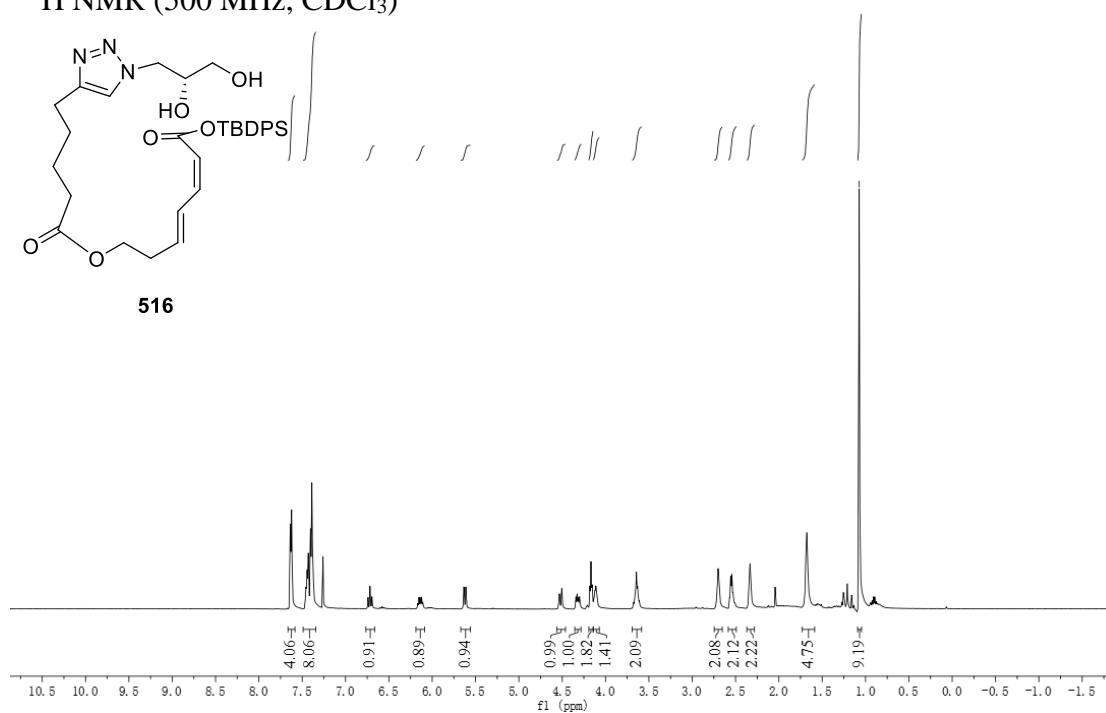
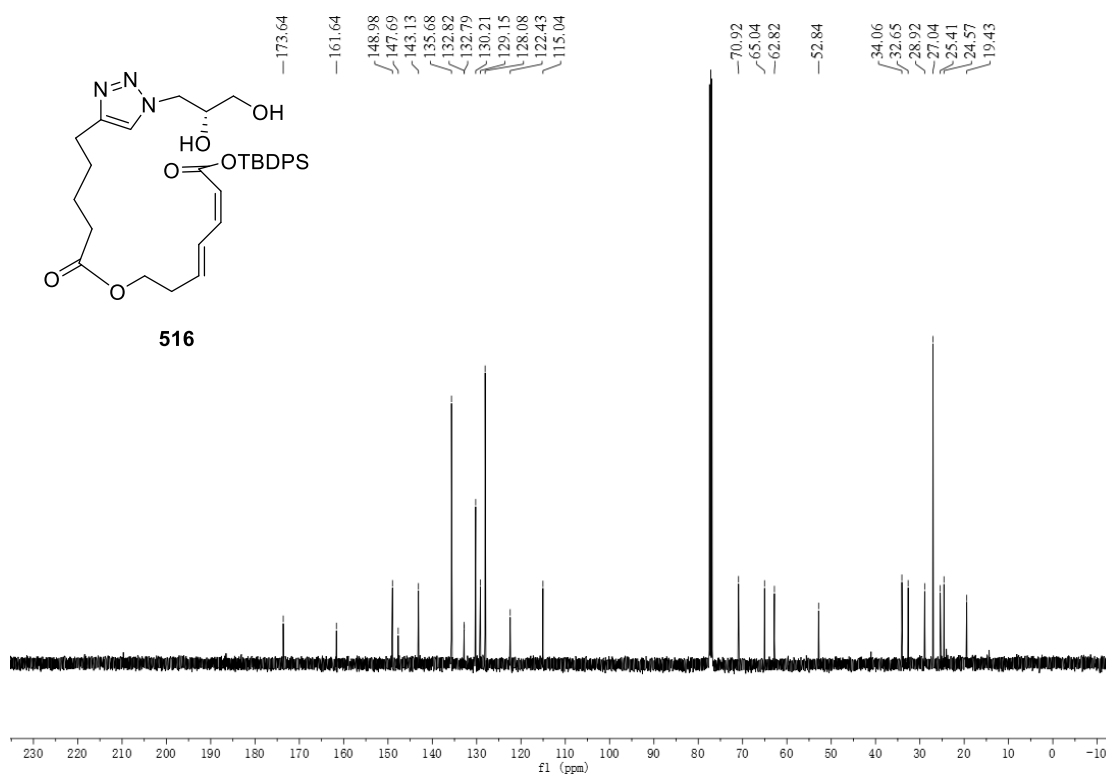
¹H NMR (500 MHz, CDCl₃)¹³C NMR (125 MHz, CDCl₃)

^1H NMR (500 MHz, CDCl_3)

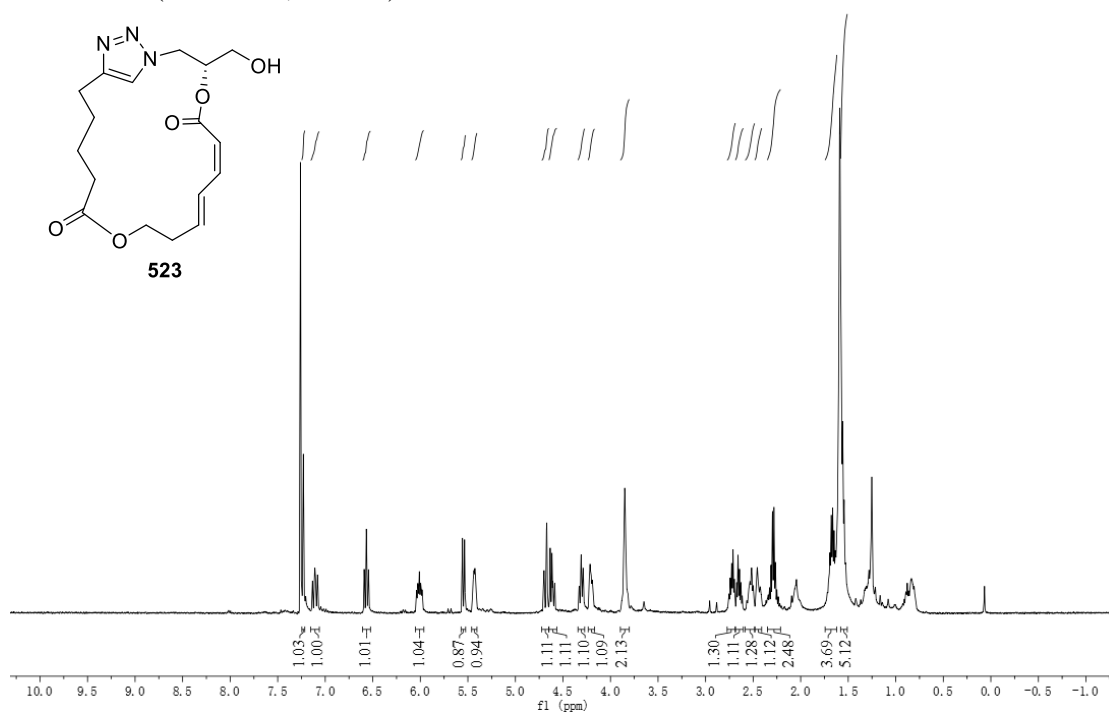


^{13}C NMR (125 MHz, CDCl_3)

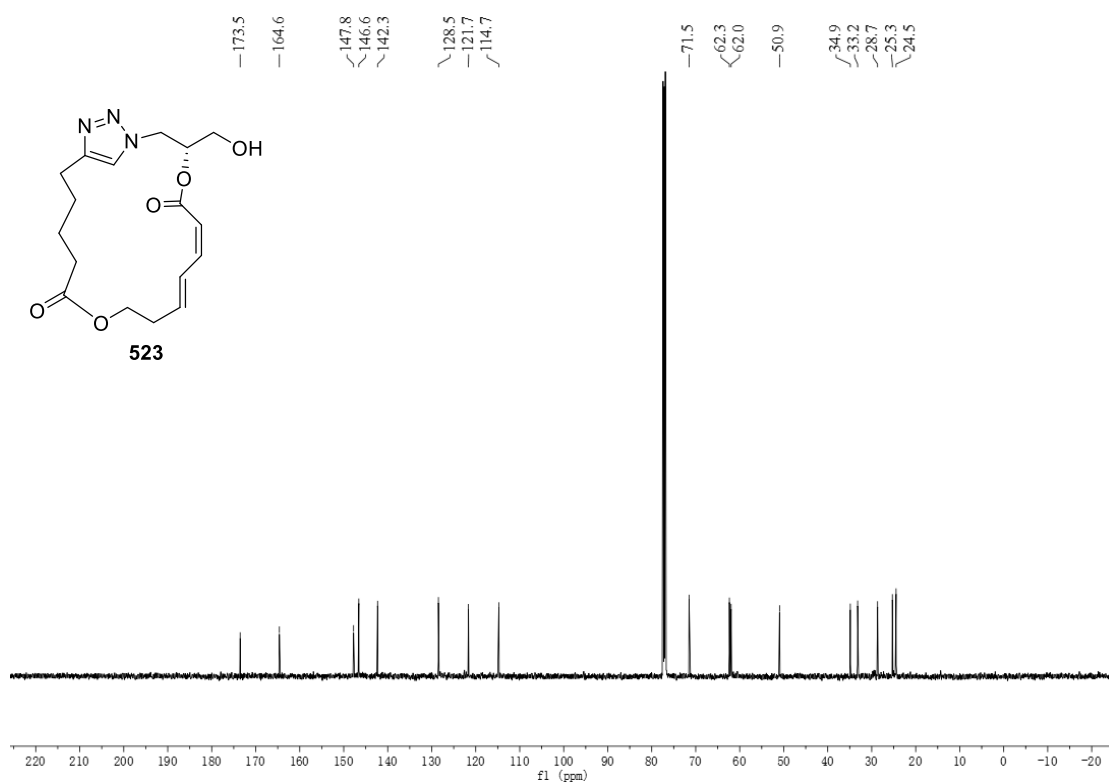


^1H NMR (500 MHz, CDCl_3) ^{13}C NMR (125 MHz, CDCl_3)

^1H NMR (500 MHz, CDCl_3)



^{13}C NMR (125 MHz, CDCl_3)



Bibliography

1. Dias, D. A.; Urban, S.; Roessner, U., A historical overview of natural products in drug discovery. *Metabolites* **2012**, 2 (2), 303-336.
2. Hong, J., Role of natural product diversity in chemical biology. *Curr. Opin. Chem. Biol.* **2011**, 15 (3), 350-354.
3. Ortholand, J.-Y.; Ganesan, A., Natural products and combinatorial chemistry: back to the future. *Curr. Opin. Chem. Biol.* **2004**, 8 (3), 271-280.
4. Newman, D. J.; Cragg, G. M., Natural Products as Sources of New Drugs from 1981 to 2014. *J. Nat. Prod.* **2016**, 79 (3), 629-661.
5. Molinski, T. F.; Dalisay, D. S.; Lievens, S. L.; Saludes, J. P., Drug development from marine natural products. *Nat. Rev. Drug Discov.* **2009**, 8 (1), 69-85.
6. Simmons, T. L.; Andrianasolo, E.; McPhail, K.; Flatt, P.; Gerwick, W. H., Marine natural products as anticancer drugs. *Mol. Cancer Ther.* **2005**, 4 (2), 333.
7. Rinehart, K. L.; Gloer, J. B.; Hughes, R. G.; Renis, H. E.; McGovren, J. P.; Swynenberg, E. B.; Stringfellow, D. A.; Kuentzel, S. L.; Li, L. H., Didemnins: antiviral and antitumor depsipeptides from a caribbean tunicate. *Science* **1981**, 212 (4497), 933.
8. Rinehart, K. L.; Gloer, J. B.; Cook, J. C.; Mizsak, S. A.; Scahill, T. A., Structures of the didemnins, antiviral and cytotoxic depsipeptides from a Caribbean tunicate. *J. Am. Chem. Soc.* **1981**, 103 (7), 1857-1859.
9. Andrew Dorr, F.; Kuhn, J. G.; Phillips, J.; Von Hoff, D. D., Phase I clinical and pharmacokinetic investigation of didemnin B, a cyclic depsipeptide. *Eur. J. Cancer Clin. Oncol.* **1988**, 24 (11), 1699-1706.
10. Stewart, J. A.; Low, J. B.; Roberts, J. D.; Blow, A., A phase i clinical trial of didemnin B. *Cancer* **1991**, 68 (12), 2550-2554.
11. Maroun, J. A.; Stewart, D.; Verma, S.; Eisenhauer, E., Phase I clinical study of didemnin B. *Invest. New Drug* **1998**, 16 (1), 51-56.
12. Shin, D. M.; Holoye, P. Y.; Murphy, W. K.; Forman, A.; Papasozomenos, S. C., Phase I/II clinical trial of didemnin B in non-small-cell lung cancer: neuromuscular toxicity is dose-limiting. *Cancer Chemother. Pharmacol.* **1991**, 29 (2), 145-149.
13. Benvenuto, J. A.; Newman, R. A.; Bignami, G. S.; Raybould, T. J. G.; Raber, M. N.; Esparza, L.; Walters, R. S., Phase II clinical and pharmacological study of didemnin B in patients with metastatic breast cancer. *Invest. New Drug* **1992**, 10 (2), 113-117.
14. Shin, D. M.; Holoye, P. Y.; Forman, A.; Winn, R.; Perez-Soler, R.; Dakhil, S.; Rosenthal, J.; Raber, M. N.; Hong, W. K., Phase II clinical trial of didemnin B in previously treated small cell lung cancer. *Invest. New Drug* **1994**, 12 (3), 243-249.

15. Goss, G.; Muldal, A.; Lohmann, R.; Taylor, M.; Lopez, P.; Armitage, G.; Steward, W. P., Didemnin B in favourable histology non-Hodgkin's lymphoma. *Invest. New Drug* **1995**, *13* (3), 257-260.
16. Kucuk, O.; Young, M. L.; Habermann, T. M.; Wolf, B. C.; Jimeno, J.; Cassileth, P. A., Phase II Trial of didemnin B in previously treated non-Hodgkin's lymphoma: an Eastern Cooperative Oncology Group (ECOG) study. *Am. J. Clin. Oncol.* **2000**, *23* (3).
17. Hochster, H.; Oratz, R.; Ettinger, D. S.; Borden, E., A phase II study of didemnin B (NSC 325319) in advanced malignant melanoma: an Eastern Cooperative Oncology Group study (PB687). *Invest. New Drug* **1998**, *16* (3), 259-263.
18. Mittelman, A.; Chun, H. G.; Puccio, C.; Coombe, N.; Lansen, T.; Ahmed, T., Phase II clinical trial of didemnin B in patients with recurrent or refractory anaplastic astrocytoma or glioblastoma multiforme (NSC 325319). *Invest. New Drug* **1999**, *17* (2), 179-182.
19. Taylor, S. A.; Giroux, D. J.; Jaeckle, K. A.; Panella, T. J.; Dakhil, S. R.; Schold, S. C., Phase II study of didemnin B in central nervous system tumors: A Southwest Oncology Group study. *Invest. New Drug* **1998**, *16* (4), 331-332.
20. Rinehart, K. L.; Holt, T. G.; Fregeau, N. L.; Stroh, J. G.; Keifer, P. A.; Sun, F.; Li, L. H.; Martin, D. G., Ecteinascidins 729, 743, 745, 759A, 759B, and 770: potent antitumor agents from the Caribbean tunicate *Ecteinascidia turbinata*. *J. Org. Chem.* **1990**, *55* (15), 4512-4515.
21. Wright, A. E.; Forleo, D. A.; Gunawardana, G. P.; Gunasekera, S. P.; Koehn, F. E.; McConnell, O. J., Antitumor tetrahydroisoquinoline alkaloids from the colonial ascidian *Ecteinascidia turbinata*. *J. Org. Chem.* **1990**, *55* (15), 4508-4512.
22. Pommier, Y.; Kohlhagen, G.; Bailly, C.; Waring, M.; Mazumder, A.; Kohn, K. W., DNA sequence- and structure-selective alkylation of guanine N2 in the DNA minor groove by Ecteinascidin 743, a potent antitumor compound from the Caribbean tunicate *Ecteinascidia turbinata*. *Biochemistry* **1996**, *35* (41), 13303-13309.
23. Leimgruber, W.; Stefanović, V.; Schenker, F.; Karr, A.; Berger, J., Isolation and characterization of anthramycin, a new antitumor antibiotic. *J. Am. Chem. Soc.* **1965**, *87* (24), 5791-5793.
24. Harvey, A. L.; Edrada-Ebel, R.; Quinn, R. J., The re-emergence of natural products for drug discovery in the genomics era. *Nat Rev Drug Discov* **2015**, *14* (2), 111-129.
25. Debbab, A.; Aly, A. H.; Lin, W. H.; Proksch, P., Bioactive compounds from marine bacteria and fungi. *Microb. Biotechnol.* **2010**, *3* (5), 544-563.
26. Proksch, P.; Edrada-Ebel, R.; Ebel, R., Drugs from the sea-opportunities and obstacles. *Mar. Drugs* **2003**, *1* (1), 5-17.

27. Cuevas, C.; Pérez, M.; Martín, M. J.; Chicharro, J. L.; Fernández-Rivas, C.; Flores, M.; Francesch, A.; Gallego, P.; Zarzuelo, M.; de la Calle, F.; García, J.; Polanco, C.; Rodríguez, I.; Manzanares, I., Synthesis of ecteinascidin ET-743 and phthalascidin Pt-650 from cyanosafracin B. *Org. Lett.* **2000**, 2 (16), 2545-2548.
28. He, W.; Zhang, Z.; Ma, D., A Scalable total synthesis of the antitumor agents ET-743 and lurbinectedin. *Angew. Chem. Int. Ed.* **2019**, 58 (12), 3972-3975.
29. Searle, P. A.; Molinski, T. F.; Brzezinski, L. J.; Leahy, J. W., Absolute configuration of phorboxazoles A and B from the marine sponge *Phorbas sp. I*. macrolide and hemiketal rings. *J. Am. Chem. Soc.* **1996**, 118 (39), 9422-9423.
30. Uemura, D.; Takahashi, K.; Yamamoto, T.; Katayama, C.; Tanaka, J.; Okumura, Y.; Hirata, Y., Norhalichondrin A: an antitumor polyether macrolide from a marine sponge. *J. Am. Chem. Soc.* **1985**, 107 (16), 4796-4798.
31. Hirata, Y.; Uemura, D., Halichondrins-antitumor polyether macrolides from a marine sponge. *Pure Appl. Chem.* **1986**, 58 (5), 701-710.
32. Bai, R. L.; Paull, K. D.; Herald, C. L.; Malspeis, L.; Pettit, G. R.; Hamel, E., Halichondrin B and homohalichondrin B, marine natural products binding in the vinca domain of tubulin. Discovery of tubulin-based mechanism of action by analysis of differential cytotoxicity data. *J. Biol. Chem.* **1991**, 266 (24), 15882-15889.
33. Dabydeen, D. A.; Burnett, J. C.; Bai, R.; Verdier-Pinard, P.; Hickford, S. J. H.; Pettit, G. R.; Blunt, J. W.; Munro, M. H. G.; Gussio, R.; Hamel, E., Comparison of the activities of the truncated halichondrin B analog NSC 707389 (E7389) with those of the parent compound and a proposed binding site on tubulin. *Mol. Pharmacol.* **2006**, 70 (6), 1866-1875.
34. Aicher, T. D.; Buszek, K. R.; Fang, F. G.; Forsyth, C. J.; Jung, S. H.; Kishi, Y.; Matelich, M. C.; Scola, P. M.; Spero, D. M.; Yoon, S. K., Total synthesis of halichondrin B and norhalichondrin B. *J. Am. Chem. Soc.* **1992**, 114 (8), 3162-3164.
35. Munro, M. H. G.; Blunt, J. W.; Dumdei, E. J.; Hickford, S. J. H.; Lill, R. E.; Li, S.; Battershill, C. N.; Duckworth, A. R., The discovery and development of marine compounds with pharmaceutical potential. *J. Biotechnol.* **1999**, 70 (1-3), 15-25.
36. Stamos, D. P.; Chen, S. S.; Kishi, Y., New synthetic route to the C.14-C.38 segment of halichondrins. *J. Org. Chem.* **1997**, 62 (22), 7552-7553.
37. Wang, Y.; Habgood, G. J.; Christ, W. J.; Kishi, Y.; Littlefield, B. A.; Yu, M. J., Structure-activity relationships of halichondrin B analogues: modifications at C30 – C38. *Bioorg. Med. Chem. Lett.* **2000**, 10 (10), 1029-1032.
38. Littlefield, B. A.; Palme, M. H.; Seletsky, B. M.; Towle, M. J.; Yu, M. J.; Zheng, W., Macrocyclic analogs and methods of their use and preparation. Eisai R&D Management Co. Ltd. **2001**, US6214865B1.

39. Towle, M. J.; Salvato, K. A.; Budrow, J.; Wels, B. F.; Kuznetsov, G.; Aalfs, K. K.; Welsh, S.; Zheng, W.; Seletsky, B. M.; Palme, M. H., *In vitro* and *in vivo* anticancer activities of synthetic macrocyclic ketone analogues of halichondrin B. *Cancer Res.* **2001**, *61* (3), 1013-1021.
40. Swami, U.; Shah, U.; Goel, S., Eribulin in cancer treatment. *Mar. Drugs* **2015**, *13* (8).
41. Pettit, G. R.; Herald, C. L.; Doubek, D. L.; Herald, D. L.; Arnold, E.; Clardy, J., Isolation and structure of bryostatin 1. *J. Am. Chem. Soc.* **1982**, *104* (24), 6846-6848.
42. Sudek, S.; Lopanik, N. B.; Waggoner, L. E.; Hildebrand, M.; Anderson, C.; Liu, H.; Patel, A.; Sherman, D. H.; Haygood, M. G., Identification of the putative bryostatin polyketide synthase gene cluster from "*Candidatus Endobugula sertula*", the uncultivated microbial symbiont of the marine bryozoan *Bugula neritina*. *J. Nat. Prod.* **2007**, *70* (1), 67-74.
43. Hennings, H.; Blumberg, P. M.; Pettit, G. R.; Herald, C. L.; Shores, R.; Yuspa, S. H., Bryostatin 1, an activator of protein kinase C, inhibits tumor promotion by phorbol esters in SENCAR mouse skin. *Carcinogenesis* **1987**, *8* (9), 1343-1346.
44. Sun, M.-K.; Hongpaisan, J.; Nelson, T. J.; Alkon, D. L., Poststroke neuronal rescue and synaptogenesis mediated *in vivo* by protein kinase C in adult brains. *Proc. Natl. Acad. Sci. USA* **2008**, *105* (36), 13620-13625.
45. Way, K. J.; Katai, N.; King, G. L., Protein kinase C and the development of diabetic vascular complications. *Diabet. Med.* **2001**, *18* (12), 945-959.
46. Schrott, L. M.; Jackson, K.; Yi, P.; Dietz, F.; Johnson, G. S.; Basting, T. F.; Purdum, G.; Tyler, T.; Rios, J. D.; Castor, T. P., Acute oral bryostatin-1 administration improves learning deficits in the APP/PS1 transgenic mouse model of Alzheimer's disease. *Curr. Alzheimer Res.* **2015**, *12* (1), 22-31.
47. Schaufelberger, D. E.; Koleck, M. P.; Beutler, J. A.; Vatakis, A. M.; Alvarado, A. B.; Andrews, P.; Marzo, L. V.; Muschik, G. M.; Roach, J.; Ross, J. T.; Lebherz, W. B.; Reeves, M. P.; Eberwein, R. M.; Rodgers, L. L.; Testerman, R. P.; Snader, K. M.; Forenza, S., The large-scale isolation of bryostatin 1 from *Bugula neritina* following current good manufacturing practices. *J. Nat. Prod.* **1991**, *54* (5), 1265-1270.
48. Keck, G. E.; Poudel, Y. B.; Cummins, T. J.; Rudra, A.; Covell, J. A., Total synthesis of bryostatin 1. *J. Am. Chem. Soc.* **2011**, *133* (4), 744-747.
49. Wender, P. A.; DeBrabander, J.; Harran, P. G.; Jimenez, J.-M.; Koehler, M. F. T.; Lipka, B.; Park, C.-M.; Siedenbiedel, C.; Pettit, G. R., The design, computer modeling, solution structure, and biological evaluation of synthetic analogs of bryostatin 1. *Proc. Natl. Acad. Sci. USA* **1998**, *95* (12), 6624-6629.
50. Wender, P. A.; De Brabander, J.; Harran, P. G.; Jimenez, J.-M.; Koehler, M. F. T.; Lipka, B.; Park, C.-M.; Shiozaki, M., Synthesis of the first members of a new class of biologically active bryostatin analogues. *J. Am. Chem. Soc.* **1998**, *120* (18), 4534-4535.

51. Wender, P. A.; Baryza, J. L.; Brenner, S. E.; De Christopher, B. A.; Loy, B. A.; Schrier, A. J.; Verma, V. A., Design, synthesis, and evaluation of potent bryostatin analogs that modulate PKC translocation selectivity. *Proc. Natl. Acad. Sci. USA* **2011**, *108* (17), 6721-6726.
52. Wender, P. A.; Cribbs, C. M.; Koehler, K. F.; Sharkey, N. A.; Herald, C. L.; Kamano, Y.; Pettit, G. R.; Blumberg, P. M., Modeling of the bryostatins to the phorbol ester pharmacophore on protein kinase C. *Proc. Natl. Acad. Sci. USA* **1988**, *85* (19), 7197-7201.
53. Pettit, G. R.; Kamano, Y.; Herald, C. L.; Tuinman, A. A.; Boettner, F. E.; Kizu, H.; Schmidt, J. M.; Baczynskyj, L.; Tomer, K. B.; Bontems, R. J., The isolation and structure of a remarkable marine animal antineoplastic constituent: dolastatin 10. *J. Am. Chem. Soc.* **1987**, *109* (22), 6883-6885.
54. Harrigan, G. G.; Luesch, H.; Yoshida, W. Y.; Moore, R. E.; Nagle, D. G.; Paul, V. J.; Mooberry, S. L.; Corbett, T. H.; Valeriote, F. A., Symplostatin 1: A dolastatin 10 analogue from the marine cyanobacterium *Symploca hydnoidea*. *J. Nat. Prod.* **1998**, *61* (9), 1075-1077.
55. Luesch, H.; Moore, R. E.; Paul, V. J.; Mooberry, S. L.; Corbett, T. H., Isolation of dolastatin 10 from the marine cyanobacterium *Symploca* species VP642 and total stereochemistry and biological evaluation of its analogue symplostatin 1. *J. Nat. Prod.* **2001**, *64* (7), 907-910.
56. Pettit, G. R.; Singh, S. B.; Hogan, F.; Lloyd-Williams, P.; Herald, D. L.; Burkett, D. D.; Clewlow, P. J., Antineoplastic agents. Part 189. The absolute configuration and synthesis of natural (–)-dolastatin 10. *J. Am. Chem. Soc.* **1989**, *111* (14), 5463-5465.
57. Bai, R.; Pettit, G. R.; Hamel, E., Dolastatin 10, a powerful cytostatic peptide derived from a marine animal: inhibition of tubulin polymerization mediated through the vinca alkaloid binding domain. *Biochem. Pharmacol.* **1990**, *39* (12), 1941-1949.
58. Bai, R. L.; Pettit, G. R.; Hamel, E., Binding of dolastatin 10 to tubulin at a distinct site for peptide antimitotic agents near the exchangeable nucleotide and vinca alkaloid sites. *J. Biol. Chem.* **1990**, *265* (28), 17141-17149.
59. Ludueña, R. F.; Roach, M. C.; Prasad, V.; Pettit, G. R., Interaction of dolastatin 10 with bovine brain tubulin. *Biochem. Pharmacol.* **1992**, *43* (3), 539-543.
60. Pitot, H. C.; McElroy, E. A.; Reid, J. M.; Windebank, A. J.; Sloan, J. A.; Erlichman, C.; Bagniewski, P. G.; Walker, D. L.; Rubin, J.; Goldberg, R. M., Phase I trial of dolastatin-10 (NSC 376128) in patients with advanced solid tumors. *Clin. Cancer Res.* **1999**, *5* (3), 525-531.
61. Vaishampayan, U.; Glode, M.; Du, W.; Kraft, A.; Hudes, G.; Wright, J.; Hussain, M., Phase II study of dolastatin-10 in patients with hormone-refractory metastatic prostate adenocarcinoma. *Clin. Cancer Res.* **2000**, *6* (11), 4205-4208.
62. Hoffman, M. A.; Blessing, J. A.; Lentz, S. S., A phase II trial of dolastatin-10 in recurrent platinum-sensitive ovarian carcinoma: a Gynecologic Oncology Group study. *Gynecol. Oncol.* **2003**, *89* (1), 95-98.

63. Miyazaki, K.; Kobayashi, M.; Natsume, T.; Gondo, M.; Mikami, T.; Sakakibara, K.; Tsukagoshi, S., Synthesis and antitumor activity of novel dolastatin 10 analogs. *Chem. Pharm. Bull. (Tokyo)* **1995**, *43* (10), 1706-1718.
64. Kobayashi, M.; Natsume, T.; Tamaoki, S.; Watanabe, J.-i.; Asano, H.; Mikami, T.; Miyasaka, K.; Miyazaki, K.; Gondo, M.; Sakakibara, K.; Tsukagoshi, S., Antitumor activity of TZT-1027, a novel dolastatin 10 derivative. *Jpn. J. Clin. Oncol.* **1997**, *88* (3), 316-327.
65. Tamura, K.; Nakagawa, K.; Kurata, T.; Satoh, T.; Nogami, T.; Takeda, K.; Mitsuoka, S.; Yoshimura, N.; Kudoh, S.; Negoro, S.; Fukuoka, M., Phase I study of TZT-1027, a novel synthetic dolastatin 10 derivative and inhibitor of tubulin polymerization, which was administered to patients with advanced solid tumors on days 1 and 8 in 3-week courses. *Cancer Chemother. Pharmacol.* **2007**, *60* (2), 285-293.
66. Yamamoto, N.; Andoh, M.; Kawahara, M.; Fukuoka, M.; Niitani, H., Phase I study of TZT-1027, a novel synthetic dolastatin 10 derivative and inhibitor of tubulin polymerization, given weekly to advanced solid tumor patients for 3 weeks. *Cancer Sci.* **2009**, *100* (2), 316-321.
67. Riely, G. J.; Gadgeel, S.; Rothman, I.; Saidman, B.; Sabbath, K.; Feit, K.; Kris, M. G.; Rizvi, N. A., A phase 2 study of TZT-1027, administered weekly to patients with advanced non-small cell lung cancer following treatment with platinum-based chemotherapy. *Lung Cancer* **2007**, *55* (2), 181-185.
68. Horti, J.; Juhasz, E.; Monostori, Z.; Maeda, K.; Eckhardt, S.; Bodrogi, I., Phase I study of TZT-1027, a novel synthetic dolastatin 10 derivative, for the treatment of patients with non-small cell lung cancer. *Cancer Chemother. Pharmacol.* **2008**, *62* (1), 173-180.
69. Miyazaki, K.; Kobayashi, M.; Natsume, T.; Gondo, M.; Mikami, T.; Sakakibara, S., Synthesis and antitumor activity of novel dolastatin 10 analogs. *Chem. Pharm. Bull. (Tokyo)* **1995**, *43* (10), 1706-1718.
70. Talpir, R.; Benayahu, Y.; Kashman, Y.; Pannell, L.; Schleyer, M., Hemiasterlin and geodiamolide TA; two new cytotoxic peptides from the marine sponge *Hemiasterella minor* (Kirkpatrick). *Tetrahedron Lett.* **1994**, *35* (25), 4453-4456.
71. Coleman, J. E.; de Silva, E. D.; Kong, F.; Andersen, R. J.; Allen, T. M., Cytotoxic peptides from the marine sponge *Cymbastela* sp. *Tetrahedron* **1995**, *51* (39), 10653-10662.
72. Nieman, J. A.; Coleman, J. E.; Wallace, D. J.; Piers, E.; Lim, L. Y.; Roberge, M.; Andersen, R. J., Synthesis and antimitotic/cytotoxic activity of hemiasterlin analogues. *J. Nat. Prod.* **2003**, *66* (2), 183-199.
73. Loganzo, F.; Discafani, C. M.; Annable, T.; Beyer, C.; Musto, S.; Hari, M.; Tan, X.; Hardy, C.; Hernandez, R.; Baxter, M., HTI-286, a synthetic analogue of the tripeptide hemiasterlin, is a potent antimicrotubule agent that circumvents P-glycoprotein-mediated resistance *in vitro* and *in vivo*. *Cancer Res.* **2003**, *63* (8), 1838-1845.

74. Schwartz, R. E.; Hirsch, C. F.; Sesin, D. F.; Flor, J. E.; Chartrain, M.; Fromtling, R. E.; Harris, G. H.; Salvatore, M. J.; Liesch, J. M.; Yudin, K., Pharmaceuticals from cultured algae. *J. Ind. Microbiol.* **1990**, *5* (2), 113-123.
75. Trimurtulu, G.; Ohtani, I.; Patterson, G. M. L.; Moore, R. E.; Corbett, T. H.; Valeriote, F. A.; Demchik, L., Total structures of cryptophycins, potent antitumor depsipeptides from the blue-green alga *Nostoc sp.* strain GSV 224. *J. Am. Chem. Soc.* **1994**, *116* (11), 4729-4737.
76. Golakoti, T.; Ogino, J.; Heltzel, C. E.; Le Husebo, T.; Jensen, C. M.; Larsen, L. K.; Patterson, G. M. L.; Moore, R. E.; Mooberry, S. L., Structure determination, conformational analysis, chemical stability studies, and antitumor evaluation of the cryptophycins. Isolation of 18 new analogs from *Nostoc sp.* strain GSV 224. *J. Am. Chem. Soc.* **1995**, *117* (49), 12030-12049.
77. Wagner, M. M.; Paul, D. C.; Shih, C.; Jordan, M. A.; Wilson, L.; Williams, D. C., *In vitro* pharmacology of cryptophycin 52 (LY355703) in human tumor cell lines. *Cancer Chemother. Pharmacol.* **1999**, *43* (2), 115-125.
78. Northcote, P. T.; Blunt, J. W.; Munro, M. H. G., Pateamine: a potent cytotoxin from the New Zealand Marine sponge, *mycale sp.* *Tetrahedron Lett.* **1991**, *32* (44), 6411-6414.
79. Rzasas, R. M.; Romo, D.; Stirling, D. J.; Blunt, J. W.; Munro, M. H. G., Structural and synthetic studies of the pateamines: Synthesis and absolute configuration of the hydroxydienoate fragment. *Tetrahedron Lett.* **1995**, *36* (30), 5307-5310.
80. Blincoe, S. N., *Studies on some compounds from the Mycale species*. Master's thesis, University of Canterbury, Christchurch, New Zealand. **1994**.
81. Stirling, D. J. *Studies on marine natural products*. Doctoral dissertation, University of Canterbury, Christchurch, New Zealand. **1996**.
82. Rzasas, R. M.; Shea, H. A.; Romo, D., Total synthesis of the novel immunosuppressive agent (–)-pateamine A from *Mycale sp.* employing a β -lactam-based macrocyclization. *J. Am. Chem. Soc.* **1998**, *120* (3), 591-592.
83. Hood, K. A.; West, L. M.; Northcote, P. T.; Berridge, M. V.; Miller, J. H., Induction of apoptosis by the marine sponge (*Mycale*) metabolites, mycalamide A and pateamine. *Apoptosis* **2001**, *6* (3), 207-219.
84. Romo, D.; Rzasas, R. M.; Shea, H. A.; Park, K.; Langenhan, J. M.; Sun, L.; Akhiezer, A.; Liu, J. O., Total synthesis and immunosuppressive activity of (–)-pateamine A and related compounds: implementation of a β -lactam-based macrocyclization. *J. Am. Chem. Soc.* **1998**, *120* (47), 12237-12254.
85. Bordeleau, M.-E.; Matthews, J.; Wojnar, J. M.; Lindqvist, L.; Novac, O.; Jankowsky, E.; Sonenberg, N.; Northcote, P.; Teesdale-Spittle, P.; Pelletier, J., Stimulation of mammalian translation initiation factor eIF4A activity by a small molecule inhibitor of eukaryotic translation. *Proc. Natl. Acad. Sci. USA* **2005**, *102* (30), 10460-10465.

86. Low, W.-K.; Dang, Y.; Schneider-Poetsch, T.; Shi, Z.; Choi, N. S.; Merrick, W. C.; Romo, D.; Liu, J. O., Inhibition of eukaryotic translation initiation by the marine natural product pateamine A. *Mol. Cell* **2005**, *20* (5), 709-722.
87. Pause, A.; Méthot, N.; Sonenberg, N., The HRIGRXXR region of the DEAD box RNA helicase eukaryotic translation initiation factor 4A is required for RNA binding and ATP hydrolysis. *Mol. Cell. Biol.* **1993**, *13* (11), 6789-6798.
88. Conroy, S. C.; Dever, T. E.; Owens, C. L.; Merrick, W. C., Characterization of the 46,000-Dalton subunit of eIF4F. *Arch. Biochem Biophys.* **1990**, *282* (2), 363-371.
89. Yoder-Hill, J.; Pause, A.; Sonenberg, N.; Merrick, W. C., The p46 subunit of eukaryotic initiation factor eIF4F exchanges with eIF4A. *J. Biol. Chem.* **1993**, *268* (8), 5566-5573.
90. Kapp, L. D.; Lorsch, J. R., The molecular mechanics of eukaryotic translation. *Annu. Rev. Biochem.* **2004**, *73* (1), 657-704.
91. Merrick, W. C., Cap-dependent and cap-independent translation in eukaryotic systems. *Gene* **2004**, *332*, 1-11.
92. Shibuya, T.; Tange, T. Ø.; Sonenberg, N.; Moore, M. J., eIF4AIII binds spliced mRNA in the exon junction complex and is essential for nonsense-mediated decay. *Nat. Struct. Mol. Biol.* **2004**, *11* (4), 346-351.
93. Palacios, I. M.; Gatfield, D.; St Johnston, D.; Izaurralde, E., An eIF4AIII-containing complex required for mRNA localization and nonsense-mediated mRNA decay. *Nature* **2004**, *427* (6976), 753-757.
94. Hellen, C. U. T.; Sarnow, P., Internal ribosome entry sites in eukaryotic mRNA molecules. *Gene Dev.* **2001**, *15* (13), 1593-1612.
95. Grifo, J. A.; Abramson, R. D.; Satler, C. A.; Merrick, W. C., RNA-stimulated ATPase activity of eukaryotic initiation factors. *J. Biol. Chem.* **1984**, *259* (13), 8648-8654.
96. Rogers, G. W.; Richter, N. J.; Merrick, W. C., Biochemical and kinetic characterization of the RNA helicase activity of eukaryotic initiation factor 4A. *J. Biol. Chem.* **1999**, *274* (18), 12236-12244.
97. Pestova, T. V.; Kolupaeva, V. G., The roles of individual eukaryotic translation initiation factors in ribosomal scanning and initiation codon selection. *Gene Dev.* **2002**, *16* (22), 2906-2922.
98. Korneeva, N. L.; First, E. A.; Benoit, C. A.; Rhoads, R. E., Interaction between the NH₂-terminal domain of eIF4A and the central domain of eIF4G modulates RNA-stimulated ATPase activity. *J. Biol. Chem.* **2005**, *280* (3), 1872-1881.
99. Bordeleau, M.-E.; Cencic, R.; Lindqvist, L.; Oberer, M.; Northcote, P.; Wagner, G.; Pelletier, J., RNA-mediated sequestration of the RNA helicase eIF4A by pateamine A inhibits translation initiation. *Chem. Biol.* **2006**, *13* (12), 1287-1295.

100. Stroupe, M. E.; Tange, T. Ø.; Thomas, D. R.; Moore, M. J.; Grigorieff, N., The three-dimensional architecture of the EJC Core. *J. Mol. Biol.* **2006**, *360* (4), 743-749.
101. Ballut, L.; Marchadier, B.; Baguet, A.; Tomasetto, C.; Séraphin, B.; Le Hir, H., The exon junction core complex is locked onto RNA by inhibition of eIF4AIII ATPase activity. *Nat. Struct. Mol. Biol.* **2005**, *12* (10), 861-869.
102. Le Hir, H.; Izaurralde, E.; Maquat, L. E.; Moore, M. J., The spliceosome deposits multiple proteins 20 – 24 nucleotides upstream of mRNA exon–exon junctions. *EMBO J.* **2000**, *19* (24), 6860-6869.
103. Dostie, J.; Dreyfuss, G., Translation is required to remove Y14 from mRNAs in the cytoplasm. *Curr. Biol.* **2002**, *12* (13), 1060-1067.
104. Lejeune, F.; Ishigaki, Y.; Li, X.; Maquat, L. E., The exon junction complex is detected on CBP80-bound but not eIF4E-bound mRNA in mammalian cells: dynamics of mRNP remodeling. *EMBO J.* **2002**, *21* (13), 3536.
105. Tange, T. Ø.; Nott, A.; Moore, M. J., The ever-increasing complexities of the exon junction complex. *Curr. Opin. Cell. Biol.* **2004**, *16* (3), 279-284.
106. Le Hir, H.; Saulière, J.; Wang, Z., The exon junction complex as a node of post-transcriptional networks. *Nat. Rev. Mol.* **2015**.
107. Chang, Y.-F.; Imam, J. S.; Wilkinson, M. F., The nonsense-mediated decay RNA surveillance pathway. *Annu. Rev. Biochem.* **2007**, *76* (1), 51-74.
108. Schweingruber, C.; Rufener, S. C.; Zünd, D.; Yamashita, A.; Mühlemann, O., Nonsense-mediated mRNA decay—mechanisms of substrate mRNA recognition and degradation in mammalian cells. *BBA-Gene Regul. Mech.* **2013**, *1829* (6), 612-623.
109. Kervestin, S.; Jacobson, A., NMD: a multifaceted response to premature translational termination. *Nat. Rev. Mol.* **2012**, *13* (11), 700-712.
110. Dang, Y.; Low, W.-K.; Xu, J.; Gehring, N. H.; Dietz, H. C.; Romo, D.; Liu, J. O., Inhibition of nonsense-mediated mRNA decay by the natural product pateamine A through eukaryotic initiation factor 4AIII. *J. Biol. Chem.* **2009**, *284* (35), 23613-23621.
111. Ziehr, B.; Lenarcic, E.; Cecil, C.; Moorman, N. J., The eIF4AIII RNA helicase is a critical determinant of human cytomegalovirus replication. *Virology* **2016**, *489*, 194-201.
112. Clardy, J., Stopping trouble before it starts. *ACS Chem. Biol.* **2006**, *1* (1), 17-19.
113. Aguilar, E.; Meyers, A. I., Reinvestigation of a modified Hantzsch thiazole synthesis. *Tetrahedron Lett.* **1994**, *35* (16), 2473-2476.
114. Li, G.; Pattel, D.; Hruby, V. J., Asymmetric synthesis of (2*R*, 3*S*) and (2*S*, 3*R*) precursors of β-methyl-histidine, -phenylalanine and -tyrosine. *Tetrahedron: Asymmetry* **1993**, *4* (11), 2315-2318.
115. Aksela, R.; Oehlschlager, A. C., Stannylmetallation of conjugated enynes. *Tetrahedron* **1991**, *47* (7), 1163-1176.

116. Corey, E. J.; Fuchs, P. L., A synthetic method for formyl→ethynyl conversion ($\text{RCHO} \rightarrow \text{RC}=\text{CH}$ or $\text{RC}=\text{CR}'$). *Tetrahedron Lett.* **1972**, 13 (36), 3769-3772.
117. Palomo, C.; Aizpurua, J. M.; Cuevas, C.; Mielgo, A.; Galarza, R., A mild method for the alcoholysis of β -lactams. *Tetrahedron Lett.* **1995**, 36 (49), 9027-9030.
118. Remuiñón, M. J.; Pattenden, G., Total synthesis of (–)-pateamine, a novel polyene bis-macrolide with immunosuppressive activity from the sponge *Mycale* sp. *Tetrahedron Lett.* **2000**, 41 (38), 7367-7371.
119. Critcher, D. J.; Pattenden, G., Synthetic studies towards pateamine, a novel thiazole-based 19-membered bis-lactone from *Mycale* sp. *Tetrahedron Lett.* **1996**, 37 (50), 9107-9110.
120. Zhuo, C.-X.; Fürstner, A., Catalysis-based total syntheses of pateamine A and DMDA-Pat A. *J. Am. Chem. Soc.* **2018**, 140 (33), 10514-10523.
121. Jung, H.-Y.; Feng, X.; Kim, H.; Yun, J., Copper-catalyzed boration of activated alkynes. Chiral boranes via a one-pot copper-catalyzed boration and reduction protocol. *Tetrahedron* **2012**, 68 (17), 3444-3449.
122. Rupnicki, L.; Saxena, A.; Lam, H. W., Aromatic heterocycles as activating groups for asymmetric conjugate addition reactions. Enantioselective copper-catalyzed reduction of 2-alkenylheteroarenes. *J. Am. Chem. Soc.* **2009**, 131 (30), 10386-10387.
123. Smith, A. B.; Dong, S.; Brennen, J. B.; Fox, R. J., Total synthesis of (+)-sorangicin A. *J. Am. Chem. Soc.* **2009**, 131 (34), 12109-12111.
124. Fürstner, A.; Funel, J.-A.; Tremblay, M.; Bouchez, L. C.; Nevado, C.; Waser, M.; Ackermann, J.; Stimson, C. C., A versatile protocol for Stille–Migita cross coupling reactions. *Chem. Commun. (Camb.)* **2008**, (25), 2873-2875.
125. Srogl, J.; Allred, G. D.; Liebeskind, L. S., Sulfonium salts. Participants par excellence in metal-catalyzed carbon–carbon bond-forming reactions. *J. Am. Chem. Soc.* **1997**, 119 (50), 12376-12377.
- 126.
127. Low, W.-K.; Li, J.; Zhu, M.; Kommaraju, S. S.; Shah-Mittal, J.; Hull, K.; Liu, J. O.; Romo, D., Second-generation derivatives of the eukaryotic translation initiation inhibitor pateamine A targeting eIF4A as potential anticancer agents. *Bioorg. Med. Chem.* **2014**, 22 (1), 116-125.
128. Zhuo, C.-X.; Fürstner, A., Concise synthesis of a pateamine A analogue with *in vivo* anticancer activity based on an iron-catalyzed pyrone ring opening/cross-coupling. *Angew. Chem. Int. Ed.* **2016**, 55 (20), 6051-6056.
129. Maquat, L., *Nonsense-Mediated mRNA Decay*. CRC Press: **2006**; pp 71-80.
130. Kuznetsov, G.; Xu, Q.; Rudolph-Owen, L.; TenDyke, K.; Liu, J.; Towle, M.; Zhao, N.; Marsh, J.; Agoulnik, S.; Twine, N., Potent *in vitro* and *in vivo* anticancer activities of des-methyl, des-amino pateamine A, a synthetic analogue of marine natural product pateamine A. *Mol.*

Cancer Ther. **2009**, 8 (5), 1250-1260.

131. Low, W.-K.; Dang, Y.; Bhat, S.; Romo, D.; Liu, J. O., Substrate-dependent targeting of eukaryotic translation initiation factor 4A by pateamine A: negation of domain-linker regulation of activity. *Chemistry & Biology* **2007**, 14 (6), 715-727.

132. Mackay, I. R.; Rose, N. R., *The Autoimmune Diseases*. Elsevier Science: **2013**; pp 429-458.

133. Frischmeyer, P. A.; Dietz, H. C., Nonsense-mediated mRNA decay in health and disease. *Hum. Mol. Genet.* **1999**, 8 (10), 1893-1900.

134. Cumming, A. H.; Brown, S. L.; Xu, T.; Cuyamendous, C.; Field, J. J.; Miller, J. H.; Harvey, J. E.; Teesdale-Spittle, P. H., Synthesis of a simplified triazole analogue of pateamine A. *Org. Biomol.Chem.* **2016**, 14 (22), 5117-5127.

135. Cumming, A. H. *Design and synthesis of simplified analogues of pateamine A*. Doctoral dissertation, Victoria University of Wellington, New Zealand. **2014**.

136. Burton, A. G.; Frampton, R. D.; Johnson, C. D.; Katritzky, A. R., The kinetics and mechanism of the electrophilic substitution of heteroaromatic compounds. Part XXVIII. The preparation and kinetic nitration of 2-, 3-, and 4-dimethylaminopyridines and their 1-oxides in sulphuric acid. *J. Chem. Soc., Perkin Trans. 2* **1972**, (13), 1940-1949.

137. Jencks, W. P.; Regenstein, J., Ionization constants of acids and bases. In *Handbook of Biochemistry and Molecular Biology, Fourth edition*. CRC Press: **2010**; pp 595-635.

138. Barreiro, E. J.; Kümmerle, A. E.; Fraga, C. A. M., The methylation effect in medicinal chemistry. *Chem. Rev.* **2011**, 111 (9), 5215-5246.

139. Schönherr, H.; Cernak, T., Profound methyl effects in drug discovery and a call for new C-H methylation reactions. *Angew. Chem. Int. Ed.* **2013**, 52 (47), 12256-12267.

140. Meldal, M.; Tornøe, C. W., Cu-catalyzed azide-alkyne cycloaddition. *Chem. Rev.* **2008**, 108 (8), 2952-3015.

141. Wu, G.; Zheng, R.; Nelson, J.; Zhang, L., One-step synthesis of methanesulfonyloxymethyl ketones via gold-catalyzed oxidation of terminal alkynes: a combination of ligand and counter anion enables high efficiency and a one-pot synthesis of 2,4-disubstituted thiazoles. *Adv. Synth. Catal.* **2014**, 356 (6), 1229-1234.

142. Rostovtsev, V. V.; Green, L. G.; Fokin, V. V.; Sharpless, K. B., A stepwise Huisgen cycloaddition process: Copper(I)-catalyzed regioselective “ligation” of azides and terminal alkynes. *Angew. Chem. Int. Ed.* **2002**, 41 (14), 2596-2599.

143. Tornøe, C. W.; Christensen, C.; Meldal, M., Peptidotriazoles on solid phase: [1,2,3]-triazoles by regiospecific copper(I)-catalyzed 1,3-dipolar cycloadditions of terminal alkynes to azides. *J. Org. Chem.* **2002**, *67* (9), 3057-3064.
144. Cinellu, M. A., Gold-Alkene Complexes. In *Modern Gold Catalyzed Synthesis*, Wiley: **2012**, pp 175-199.
145. Wiberg, K. B.; Rush, D. J., Solvent effects on the thioamide rotational barrier: an experimental and theoretical study. *J. Am. Chem. Soc.* **2001**, *123* (9), 2038-2046.
146. Mykhaylychenko, S. S.; Pikun, N. V.; Shermolovich, Y. G., Acylation of primary polyfluoroalkanethioamides. *J. Fluor. Chem.* **2012**, *140*, 76-81.
147. Takahata, H.; Yamazaki, T., Synthesis of heterocycles using thioamide groups. *J. Synth. Org. Chem Jpn.* **1987**, *45* (7), 682-690.
148. Satoh, T.; Miura, M., Catalytic direct arylation of heteroaromatic compounds. *Chem. Lett.* **2006**, *36* (2), 200-205.
149. Xiong, Z.; Wang, N.; Dai, M.; Li, A.; Chen, J.; Yang, Z., Synthesis of novel palladacycles and their application in Heck and Suzuki reactions under aerobic conditions. *Org. Lett.* **2004**, *6* (19), 3337-3340.
150. Kanchanadevi, A.; Ramesh, R.; Semeril, D., Efficient and recyclable Ru (II) arene thioamide catalysts for transfer hydrogenation of ketones: Influence of substituent on catalytic outcome. *J. Organomet. Chem.* **2016**, *808*, 68-77.
151. Hurd, R. N.; DeLaMater, G., The Preparation and chemical properties of thionamides. *Chem. Rev.* **1961**, *61* (1), 45-86.
152. Willgerodt, C., Ueber die einwirkung von gelbem schwefelammonium auf ketone und chinone. *Ber. Dtsch. Chem. Ges.* **1887**, *20* (2), 2467-2470.
153. Rekunge, D. S.; Khatri, C. K.; Chaturbuj, G. U., Rapid and efficient protocol for Willgerodt-Kindler's thioacetamides catalyzed by sulfated polyborate. *Monatsh. Chem.* **2017**, *148* (12), 2091-2095.
154. Nguyen, T. B.; Retailleau, P., Methyl ketone break-and-rebuild: a strategy for full α -heterofunctionalization of acetophenones. *Green Chem.* **2017**, *19* (22), 5371-5374.
155. Murai, T., Synthesis of Thioamides. In *Chemistry of Thioamides*, Murai, T., Ed. Springer Singapore: Singapore, **2019**; pp 45-73.
156. Demselben, Ueber die verbindungen des phosphors mit schwefel. *Justus Liebigs Ann. Chem.* **1843**, *46* (3), 251-281.
157. Davy, H., A direct conversion of carboxylic acids into dithioesters. *J. Chem. Soc., Chem. Commun.* **1982**, (8), 457-458.
158. Lecher, H. Z.; Greenwood, R. A.; Whitehouse, K. C.; Chao, T. H., The phosphonation of aromatic compounds with phosphorus pentasulfide. *J. Am. Chem. Soc.* **1956**, *78* (19), 5018-5022.

159. Choi, Y.; Ishikawa, H.; Velcicky, J.; Elliott, G. I.; Miller, M. M.; Boger, D. L., Total synthesis of (–)- and ent-(+)-vindoline. *Org. Lett.* **2005**, 7 (20), 4539-4542.
160. Zhang, W.; Ding, M.; Li, J.; Guo, Z.; Lu, M.; Chen, Y.; Liu, L.; Shen, Y.-H.; Li, A., Total synthesis of hybridaphniphylline B. *J. Am. Chem. Soc.* **2018**, 140 (12), 4227-4231.
161. Cherkasov, R. A.; Kuttyrev, G. A.; Pudovik, A. N., Tetrahedron report number 186: Organothiophosphorus reagents in organic synthesis. *Tetrahedron* **1985**, 41 (13), 2567-2624.
162. Cava, M. P.; Levinson, M. I., Thionation reactions of Lawesson's reagents. *Tetrahedron* **1985**, 41 (22), 5061-5087.
163. Jesberger, M.; Davis, T. P.; Barner, L., Applications of Lawesson's reagent in organic and organometallic Syntheses. *Synthesis* **2003**, 2003 (13), 1929-1958.
164. Bailey, P. D.; Mills, T. J.; Pettecrew, R.; Price, R. A., 5.06 - Amides. In *Comprehensive Organic Functional Group Transformations II*, Katritzky, A. R.; Taylor, R. J. K., Eds. Elsevier: Oxford, **2005**; pp 201-294.
165. Oremus, V.; Heimgartner, H., Reaction of 1, 4-Dihydro-1-phenyltetrazole-5-thione with Epoxides; Formation of 1-[(1-Phenyl-1*H*-tetrazol-5-yl) thio] alkan-2-ols. *J. Chem. Research (S)* **1991**, 10, 296-297.
166. Saikia, B.; Devi, T. J.; Barua, N. C., Stereoselective total synthesis of both (6*R*, 9*R*, 10*S*, 7*E*)-and (6*S*, 9*R*, 10*S*, 7*E*)-epimers of oxylipin (9*R*, 10*S*, 7*E*)-6, 9, 10-trihydroxyoctadec-7-enoic acid. *Tetrahedron* **2013**, 69 (9), 2157-2166.
167. Pellissier, H., Catalytic non-enzymatic kinetic resolution. *Adv. Synth. Catal.* **2011**, 353 (10), 1613-1666.
168. Schaus, S. E.; Brandes, B. D.; Larrow, J. F.; Tokunaga, M.; Hansen, K. B.; Gould, A. E.; Furrow, M. E.; Jacobsen, E. N., Highly selective hydrolytic kinetic resolution of terminal epoxides catalyzed by chiral (salen)Co^{III} complexes. Practical synthesis of enantioenriched terminal epoxides and 1,2-diols. *J. Am. Chem. Soc.* **2002**, 124 (7), 1307-1315.
169. Fleming, F. F.; Wang, Q.; Steward, O. W., Hydroxylated α,β -unsaturated nitriles: stereoselective synthesis. *J. Org. Chem.* **2001**, 66 (6), 2171-2174.
170. Mete, E.; Maraş, A.; Seçen, H., A short synthesis of 4-amino-3-hydroxybutyric acid (GABOB) via allyl cyanide. *Russ. Chem. Bull.* **2003**, 52 (8), 1879-1881.
171. Herzberger, J.; Frey, H., Epicyanohydrin: polymerization by monomer activation gives access to nitrile-, amino-, and carboxyl-functional poly(ethylene glycol). *Macromolecules* **2015**, 48 (22), 8144-8153.
172. Dale, J. A.; Mosher, H. S., Nuclear magnetic resonance enantiomer reagents. Configurational correlations via nuclear magnetic resonance chemical shifts of diastereomeric mandelate, O-methylmandelate, and .alpha.-methoxy-.alpha.-trifluoromethylphenylacetate (MTPA) esters. *J. Am. Chem. Soc.* **1973**, 95 (2), 512-519.

173. Torok, D. S.; Figueroa, J. J.; Scott, W. J., 1,3-Dioxolane formation *via* Lewis acid-catalyzed reaction of ketones with oxiranes. *J. Org. Chem.* **1993**, 58 (25), 7274-7276.
174. Saha, S.; Mandal, S. K.; Roy, S. C., Fe(III) chloride catalyzed conversion of epoxides to acetones. *Tetrahedron Lett.* **2008**, 49 (41), 5928-5930.
175. Díez, D.; Beneitez, M. T.; Marcos, I. S.; Garrido, N. M.; Basabe, P.; Urones, J. G., Enantioselective synthesis of a 2,3,4-trisubstituted pyrrolidine from 1-hydroxymethyl-4-phenylsulfonylbutadiene. *Synlett* **2001**, 2001 (05), 0655-0657.
176. Meskens, F. A. J., Methods for the preparation of acetals from alcohols or oxiranes and carbonyl compounds. *Synthesis* **1981**, 1981 (07), 501-522.
177. Martinelli, M. J.; Nayyar, N. K.; Moher, E. D.; Dhokte, U. P.; Pawlak, J. M.; Vaidyanathan, R., Dibutyltin oxide catalyzed selective sulfonylation of α -chelatable primary alcohols. *Org. Lett.* **1999**, 1 (3), 447-450.
178. Ohtani, I.; Kusumi, T.; Kashman, Y.; Kakisawa, H., High-field FT NMR application of Mosher's method. The absolute configurations of marine terpenoids. *J. Am. Chem. Soc.* **1991**, 113 (11), 4092-4096.
179. Tsuruoka, A.; Negi, S.; Yanagisawa, M.; Nara, K., Practical oxirane ring opening with *in situ* prepared LiCN; synthesis of (2*S*,3*R*)-3-(2,4-difluorophenyl)-3-hydroxy-2-methyl-4-(1*H*-1,2,4-triazol-1-yl)-1-butanenitrile. *Synth. Commun.* **1997**, 27 (20), 3547-3557.
180. Jackman, L. M.; Lange, B. C., Methylation of lithioisobutyrophenone in weakly polar aprotic solvents. The effect of aggregation. *J. Am. Chem. Soc.* **1981**, 103 (15), 4494-4499.
181. Spychała, J., Convenient syntheses of *N*-methylthioamides: A migration of the H₂S molecule in the thioamide-nitrile system. *J. Sulfur Chem.* **2006**, 27 (3), 203-212.
182. Nagl, M.; Panuschka, C.; Barta, A.; Schmid, W., The BF₃·OEt₂-assisted conversion of nitriles into thioamides with Lawesson's Reagent. *Synthesis* **2008**, 2008 (24), 4012-4018.
183. Carey, F. A.; Sundberg, R. J., Functional Group Interconversion by Substitution, Including Protection and Deprotection. In *Advanced Organic Chemistry: Part B: Reactions and Synthesis*, Carey, F. A.; Sundberg, R. J., Eds. Springer US: Boston, MA, **2007**; pp 215-288.
184. Lee, J.; Kim, M.; Chang, S.; Lee, H.-Y., Anhydrous hydration of nitriles to amides using aldoximes as the water Source. *Org. Lett.* **2009**, 11 (24), 5598-5601.
185. Petrie, C. R.; Revankar, G. R.; Dalley, N. K.; George, R. D.; McKernan, P. A.; Hamill, R. L.; Robins, R. K., Synthesis and biological activity of certain nucleoside and nucleotide derivatives of pyrazofurin. *J. Med. Chem.* **1986**, 29 (2), 268-278.
186. Lajoie, G.; Lépine, F.; Maziak, L.; Belleau, B., Facile regioselective formation of thiopeptide linkages from oligopeptides with new thionation reagents. *Tetrahedron Lett.* **1983**, 24 (36), 3815-3818.
187. Charette, A. B.; Grenon, M., Mild method for the conversion of amides to thioamides. *J. Org. Chem.* **2003**, 68 (14), 5792-5794.

188. Voss, J.; Voss, J., 2,4-Bis(4-methoxyphenyl)-1,3,2,4-dithiadiphosphetane 2,4-disulfide. *eEROS* **2001**.
189. Cava, M. P.; VanMeter, J. P., Condensed cyclobutane aromatic compounds. XXX. Synthesis of some unusual 2, 3-naphthoquinonoid heterocycles. A synthetic route to derivatives of naphtho [2,3-b] biphenylene and anthra[b]cyclobutene. *J. Org. Chem.* **1969**, 34 (3), 538-545.
190. Thomsen, I.; Clausen, K.; Scheibye, S.; Lawesson, S. O., Thiation with 2,4-Bis(4-methoxyphenyl)-1,3,2,4-dithiadiphosphetane 2,4-disulfide: *N*-methylthiopyrrolidone. *Org. Synth.* **1984**, 158-158.
191. Arora, P.; Narang, R.; Nayak, S. K.; Singh, S. K.; Judge, V., 2,4-Disubstituted thiazoles as multitargeted bioactive molecules. *Med. Chem. Res.* **2016**, 25 (9), 1717-1743.
192. T Chhabria, M.; Patel, S.; Modi, P.S Brahmksatriya, P., Thiazole: a review on chemistry, synthesis and therapeutic importance of its derivatives. *Curr. Top. Med. Chem.* **2016**, 16 (26), 2841-2862.
193. Moradi, A. V.; Peyghan, A. A.; Hashemian, S.; Baei, M. T., Theoretical study of thiazole adsorption on the (6,0) zigzag single-walled boron nitride nanotube. *Bull.Korean Chem. Soc.* **2012**, 33 (10), 3285-3292.
194. Cui, S.; Wang, Y.; Lv, J.; Damu, G.; Zhou, C., Recent advances in application of thiazole compounds. *Sci. Sin. Chim.* **2012**, 42 (8), 1105-1131.
195. de Souza, M. V. N., Synthesis and biological activity of natural thiazoles: An important class of heterocyclic compounds. *J. Sulfur Chem.* **2005**, 26 (4-5), 429-449.
196. Gribble, G. W.; Joule, J. A., Five-Membered Ring Systems: With N and S Atom. In *Progress in Heterocyclic Chemistry*, Eds. Elsevier: **2015**; pp 287-303.
197. Menche, D.; Hassfeld, J.; Li, J.; Rudolph, S., Total synthesis of archazolid A. *J. Am. Chem. Soc.* **2007**, 129 (19), 6100-6101.
198. Zhu, B.; Panek, J. S., Total aynthesis of epothilone A. *Org. Lett.* **2000**, 2 (17), 2575-2578.
199. Patt, W. C.; Massa, M. A., The total synthesis of the natural product endothelin converting enzyme (ECE) inhibitor, WS75624 B. *Tetrahedron Lett.* **1997**, 38 (8), 1297-1300.
200. Merritt, E. A.; Bagley, M. C., Holzapfel-Meyers-Nicolaou modification of the Hantzsch thiazole synthesis. *Synthesis* **2007**, 2007 (22), 3535-3541.
201. Bredenkamp, M. W.; Holzapfel, C. W.; van Zyl, W. J., The chiral synthesis of thiazole amino acid enantiomers. *Synth. Commun.* **1990**, 20 (15), 2235-2249.
202. Nicolaou, K. C.; Safina, B. S.; Zak, M.; Lee, S. H.; Nevalainen, M.; Bella, M.; Estrada, A. A.; Funke, C.; Zécri, F. J.; Bulat, S., Total synthesis of thiostrepton. Retrosynthetic analysis and construction of key building blocks. *J. Am. Chem. Soc.* **2005**, 127 (31), 11159-11175.
203. Bruno, P.; Peña, S.; Just-Baringo, X.; Albericio, F.; Álvarez, M., Total synthesis of aeruginazole A. *Org. Lett.* **2011**, 13 (17), 4648-4651.

204. Nicolaou, K. C.; Zak, M.; Safina, B. S.; Estrada, A. A.; Lee, S. H.; Nevalainen, M., Total synthesis of thiostrepton. Assembly of key building blocks and completion of the synthesis. *J. Am. Chem. Soc.* **2005**, *127* (31), 11176-11183.
205. Kriek, M.; Martins, F.; Leonardi, R.; Fairhurst, S. A.; Lowe, D. J.; Roach, P. L., Thiazole synthase from *Escherichia coli* an investigation of the substrates and purified proteins required for activity *in vitro*. *J. Biol. Chem.* **2007**, *282* (24), 17413-17423.
206. Xu, Z.; Ye, T., Thiazoline and thiazole and their Derivatives. In *Heterocycles in Natural Product Synthesis*, Wiley: **2011**; pp 459-505.
207. Raman, P.; Razavi, H.; Kelly, J. W., Titanium (IV)-mediated tandem deprotection–cyclodehydration of protected cysteine *N*-amides: biomimetic syntheses of thiazoline-and thiazole-containing heterocycles. *Org. Lett.* **2000**, *2* (21), 3289-3292.
208. Boyce, R. J.; Mulqueen, G. C.; Pattenden, G., Total synthesis of thiagazole, a novel inhibitor of HIV-1 from polyangium sp. *Tetrahedron Lett.* **1994**, *35* (31), 5705-5708.
209. Sugiyama, H.; Yokokawa, F.; Shioiri, T., Asymmetric total synthesis of (–)-mycothiazole. *Org. Lett.* **2000**, *2* (14), 2149-2152.
210. DeRoy, P. L.; Charette, A. B., Total synthesis of (+)-cystothiazole A. *Org. Lett.* **2003**, *5* (22), 4163-4165.
211. Tang, X.; Yang, J.; Zhu, Z.; Zheng, M.; Wu, W.; Jiang, H., Access to thiazole via copper-catalyzed [3+1+1]-type condensation reaction under redox-neutral conditions. *J. Org. Chem.* **2016**, *81* (22), 11461-11466.
212. Zhang, G.; Chen, B.; Guo, X.; Guo, S.; Yu, Y., Iron(II)-promoted synthesis of 2-aminothiazoles via C-N bond formation from vinyl azides and potassium thiocyanate. *Adv. Synth. Catal.* **2015**, *357* (5), 1065-1069.
213. Luo, Y.; Ji, K.; Li, Y.; Zhang, L., Tempering the reactivities of postulated α -oxo gold carbenes using bidentate ligands: implication of tricoordinated gold intermediates and the development of an expedient bimolecular assembly of 2,4-disubstituted oxazoles. *J. Am. Chem. Soc.* **2012**, *134* (42), 17412-17415.
214. Horneff, T.; Chuprakov, S.; Chernyak, N.; Gevorgyan, V.; Fokin, V. V., Rhodium-catalyzed transannulation of 1,2,3-triazoles with nitriles. *J. Am. Chem. Soc.* **2008**, *130* (45), 14972-14974.
215. He, W.; Xie, L.; Xu, Y.; Xiang, J.; Zhang, L., Electrophilicity of α -oxo gold carbene intermediates: halogen abstractions from halogenated solvents leading to the formation of chloro/bromomethyl ketones. *Org. Biomol. Chem.* **2012**, *10* (16), 3168-3171.
216. Ji, K.; Zhao, Y.; Zhang, L., Optimizing P,N-bidentate ligands for oxidative gold catalysis: efficient intermolecular trapping of α -oxo gold carbenes by carboxylic acids. *Angew. Chem. Int. Ed.* **2013**, *52* (25), 6508-6512.

217. Rong, D.; Phillips, V. A.; Rubio, R. S.; Ángeles Castro, M.; Wheelhouse, R. T., A safe, convenient and efficient method for the preparation of heterocyclic *N*-oxides using urea-hydrogen peroxide. *Tetrahedron Lett.* **2008**, 49 (48), 6933-6935.
218. Subbaraman, L. R.; Subbaraman, J.; Behrman, E. J., Reaction of nucleic acid components with *m*-chloroperoxybenzoic acid. *Biochemistry* **1969**, 8 (7), 3059-3066.
219. Xu, M.; Ren, T.-T.; Li, C.-Y., Gold-catalyzed oxidative rearrangement of homopropargylic ether *via* oxonium ylide. *Org. Lett.* **2012**, 14 (18), 4902-4905.
220. Kumar, D.; Kumar, N. M.; Patel, G.; Gupta, S.; Varma, R. S., A facile and eco-friendly synthesis of diarylthiazoles and diarylimidazoles in water. *Tetrahedron Lett.* **2011**, 52 (16), 1983-1986.
221. Wu, G.; Wang, X.; Liu, H., Highly efficient one-pot synthesis of 2,4-disubstituted thiazoles using Au(I) catalyzed oxidation system at room temperature. *Catalysts* **2016**, 6 (8), 126.
222. Zhang, L., A non-diazo approach to α -oxo gold carbenes *via* gold-catalyzed alkyne oxidation. *Acc. Chem. Res.* **2014**, 47 (3), 877-888.
223. Blakemore, P. R.; Cole, W. J.; Kociński, P. J.; Morley, A., A stereoselective synthesis of trans-1,2-disubstituted alkenes based on the condensation of aldehydes with metallated 1-phenyl-1*H*-tetrazol-5-yl sulfones. *Synlett* **1998**, 1998 (01), 26-28.
224. Baudin, J. B.; Hareau, G.; Julia, S. A.; Lorne, R.; Ruel, O., Stereochemistry of direct olefin formation from carbonyl compounds and lithiated heterocyclic sulfones. *Bull. Soc. Chim. Fr.* **1993**, 130 (6), 856-878.
225. Legnani, L.; Porta, A.; Caramella, P.; Toma, L.; Zanoni, G.; Vidari, G., Computational mechanistic study of the Julia–Kociński reaction. *J. Org. Chem.* **2015**, 80 (6), 3092-3100.
226. Chatterjee, B.; Bera, S.; Mondal, D., Julia–Kociński olefination: a key reaction for the synthesis of macrolides. *Tetrahedron: Asymmetry* **2014**, 25 (1), 1-55.
227. Blakemore, P. R.; Kociński, P. J.; Marzcek, S.; Wicha, J., The modified Julia olefination in vitamin D₂ synthesis. *Synthesis* **1999**, 1999 (07), 1209-1215.
228. Grée, R.; Tourbah, H.; Carrié, R., Fumaraldehyde monodimethyl acetal: an easily accessible and versatile intermediate. *Tetrahedron Lett.* **1986**, 27 (41), 4983-4986.
229. Valeev, R. F.; Bikzhanov, R. F.; Miftakhov, M. S., Synthesis of the C₆–C₂₁ fragment of epothilone analogues. *Mendeleev Commun.* **2014**, 6 (24), 372-373.
230. Takano, D.; Nagamitsu, T.; Ui, H.; Shiomi, K.; Yamaguchi, Y.; Masuma, R.; Kuwajima, I.; Ōmura, S., Total synthesis of nafuredin, a selective NADH-fumarate reductase inhibitor. *Org. Lett.* **2001**, 3 (15), 2289-2291.
231. Greene, T. W.; Wuts, P. G. M., Protection for the Hydroxyl Group, Including 1,2- and 1,3-Diols. In *Protective Groups in Organic Synthesis*, Wiley: **1999**; pp 17-245.
232. Gupta, M. K.; Li, Z.; Snowden, T. S., Preparation of one-carbon homologated amides from aldehydes or primary alcohols. *Org. Lett.* **2014**, 16 (6), 1602-1605.

233. Reeve, W.; Tsuk, R., Reactions of trihalomethylcarbinols with aqueous potassium hydroxide. *J. Org. Chem.* **1980**, *45* (25), 5214-5215.
234. Schmid, C. R.; Bryant, J. D.; Dowlatzedah, M.; Phillips, J. L.; Prather, D. E.; Schantz, R. D.; Sear, N. L.; Vianco, C. S., Synthesis of 2,3-*O*-isopropylidene-D-glyceraldehyde in high chemical and optical purity: observations on the development of a practical bulk process. *J. Org. Chem.* **1991**, *56* (12), 4056-4058.
235. Corey, E. J.; Link, J. O.; Shao, Y., Two effective procedures for the synthesis of trichloromethyl ketones, useful precursors of chiral α -amino and α -hydroxy acids. *Tetrahedron Lett.* **1992**, *33* (24), 3435-3438.
236. Cafiero, L. R.; Snowden, T. S., General and practical conversion of aldehydes to homologated carboxylic acids. *Org. Lett.* **2008**, *10* (17), 3853-3856.
237. Schmidt, A.-K. C.; Stark, C. B. W., TPAP-catalyzed direct oxidation of primary alcohols to carboxylic acids through stabilized aldehyde hydrates. *Org. Lett.* **2011**, *13* (16), 4164-4167.
238. Li, Z.; Gupta, M. K.; Snowden, T. S., One-carbon homologation of primary alcohols and the reductive homologation of aldehydes involving a Jovic-Type reaction. *Eur. J. Org. Chem.* **2015**, *2015* (32), 7009-7019.
239. Epp, J. B.; Widlanski, T. S., Facile preparation of nucleoside-5'-carboxylic Acids. *J. Org. Chem.* **1999**, *64* (1), 293-295.
240. Shin, C.-g.; Nakamura, Y.; Yamada, Y.; Yonezawa, Y.; Umemura, K.; Yoshimura, J., Syntheses of 2-[(1*S*, 3*S*)-1-amino-3-carboxy-3-hydroxypropyl] thiazole-4-carboxylic acid and the tripeptide skeleton of nosiheptide containing the acid. *Bull. Chem. Soc. Jpn.* **1995**, *68* (11), 3151-3160.
241. Murray, R. W.; Agarwal, S. K., Singlet oxygen oxidation of substituted thiobenzamides. *J. Photochem.* **1984**, *25* (2), 335-343.
242. Crank, G.; Mursyidi, A., Photochemical reactions of thioamides. *J. Photochem. Photobiol. A: Chem.* **1990**, *53* (3), 301-310.
243. Jensen, F.; Greer, A.; Clennan, E. L., Reaction of organic sulfides with singlet oxygen: a revised mechanism. *J. Am. Chem. Soc.* **1998**, *120* (18), 4439-4449.
244. Sarma, D.; Hanzlik, R. P., Synthesis of carbon-14, carbon-13 and deuterium labeled forms of thioacetamide and thioacetamide *S*-oxide. *J. Labelled Compd. Radiopharm.* **2011**, *54* (13), 795-798.
245. Pattenden, G.; Critcher, D. J.; Remuiñán, M., Total synthesis of (–)-pateamine A, a novel immunosuppressive agent from *Mycale* sp. *Can. J. Chem.* **2004**, *82* (2), 353-365.
246. Yamaura, M.; Suzuki, T.; Hashimoto, H.; Yoshimura, J.; Okamoto, T.; Shin, C.-G., Oxidative removal of *N*-(4-methoxybenzyl) group on 2,5-piperazinediones with Cerium(IV) diammonium nitrate. *Bull. Chem. Soc. Jpn.* **1985**, *58* (5), 1413-1420.
247. Allen, D. A.; Tomaso, A. E.; Priest, O. P.; Hindson, D. F.; Hurlburt, J. L., Mosher amides:

determining the absolute stereochemistry of optically-active amines. *J. Chem. Educ.* **2008**, 85 (5), 698.

248. Kojić-Prodić, B.; Molcanov, K., The nature of hydrogen bond: new insights into old theories. *Acta. Chim. Slov.* **2008**, 55, 692-708.

249. Martinelli, M. J.; Vaidyanathan, R.; Pawlak, J. M.; Nayyar, N. K.; Dhokte, U. P.; Doecke, C. W.; Zollars, L. M. H.; Moher, E. D.; Khau, V. V.; Košmrlj, B., Catalytic regioselective sulfonylation of α -chelatable alcohols: scope and mechanistic insight. *J. Am. Chem. Soc.* **2002**, 124 (14), 3578-3585.

250. Newhouse, T.; Baran, P. S.; Hoffmann, R. W., The economies of synthesis. *Chem. Soc. Rev.* **2009**, 38 (11), 3010-3021.

251. Moriyama, K.; Nakamura, Y.; Togo, H., Oxidative debenzoylation of *N*-benzyl amides and *O*-benzyl ethers using alkali metal bromide. *Org. Lett.* **2014**, 16 (14), 3812-3815.

252. Mulzer, J.; Schöllhorn, B., Multiple 1,2-*O,O*-Shift of *tert*-butyldiphenylsilyl groups in polyols. *Angew. Chem. Int. Ed.* **1990**, 29 (4), 431-432.

253. Mosley, A. P., Acrylic Plastics. In *Brydson's Plastics Materials (Eighth Edition)*, Gilbert, M., Ed. Butterworth-Heinemann: 2017; pp 441-456.

254. Srinivasan, S.; Lee, M. W.; Grady, M. C.; Soroush, M.; Rappe, A. M., Self-initiation mechanism in spontaneous thermal polymerization of ethyl and *n*-butyl acrylate: a theoretical study. *J. Phys. Chem. A* **2010**, 114 (30), 7975-7983.

255. Ballard, N.; Asua, J. M., Radical polymerization of acrylic monomers: an overview. *Prog. Polym. Sci.* **2018**, 79, 40-60.

256. Greene, T., W., Wuts, P., G., M., Protection for the Hydroxyl Group, Including 1,2- and 1,3-Diols. In *Greene's Protective Groups in Organic Synthesis*, Wiley: **2006**; pp 123-130.

257. Ganapathi, K.; Kulkarni, K. D. Part V. Fine Structure and Orientation. In *Chemistry of the Thiazoles*, Springer: **1953**; pp 45-57.

258. Pola, S., Significance of Thiazole-based Heterocycles for Bioactive Systems. In *Scope of Selective Heterocycles from Organic and Pharmaceutical Perspective*, InTech Rijeka, Croatia: **2016**. DOI: 10.5772/62077

259. Wang, J.; Sánchez-Roselló, M.; Aceña, J. L.; del Pozo, C.; Sorochinsky, A. E.; Fustero, S.; Soloshonok, V. A.; Liu, H., Fluorine in pharmaceutical industry: fluorine-containing drugs introduced to the market in the last decade (2001–2011). *Chem. Rev.* **2014**, 114 (4), 2432-2506.

260. Cho, E. J.; Senecal, T. D.; Kinzel, T.; Zhang, Y.; Watson, D. A.; Buchwald, S. L., The palladium-catalyzed trifluoromethylation of aryl chlorides. *Science* **2010**, 328 (5986), 1679-1681.

261. Alonso, C.; Martínez de Marigorta, E.; Rubiales, G.; Palacios, F., Carbon trifluoromethylation reactions of hydrocarbon derivatives and heteroarenes. *Chem. Rev.* **2015**, 115 (4), 1847-1935.

262. Dürrenberger, F.; Burgert, M.; Burckhardt, S.; Buhr, W.; Kalogerakis, A.; Reim, S.,

- Manolova, V., Boyce, S., Yarnold, C., J., Pena, P., Shepherd, J., Lecci, C., Jarjes-Pike, R., Scott, J., Novel ferroportin inhibitors. **2017**, WO2017068090.
263. Grushin, V. V.; Marshall, W. J., Unexpected H₂O-Induced Ar–X Activation with trifluoromethylpalladium(II) aryls. *J. Am. Chem. Soc.* **2006**, *128* (14), 4632-4641.
264. Grushin, V. V.; Marshall, W. J., Facile Ar–CF₃ bond formation at Pd. Strikingly different outcomes of reductive elimination from [(Ph₃P)₂Pd(CF₃)Ph] and [(Xantphos)Pd(CF₃)Ph]. *J. Am. Chem. Soc.* **2006**, *128* (39), 12644-12645.
265. Mestre, J.; Lishchynskiy, A.; Castellón, S.; Boutureira, O., Trifluoromethylation of electron-rich alkenyl iodides with fluoroform-derived “ligandless” CuCF₃. *J. Org. Chem.* **2018**, *83* (15), 8150-8160.
266. Yu, X.; Sun, D., Macrocyclic drugs and synthetic methodologies toward macrocycles. *Molecules* **2013**, *18* (6), 6230-6268.
267. Ridge, C. D.; Mazzola, E. P.; Coles, M. P.; Hinkley, S. F. R., Isolation and characterization of roridin E. *Magn. Reson. Chem.* **2017**, *55* (4), 337-340.
268. Yadav, J. S.; Rajender, V., Studies directed towards the total synthesis of (–)-dictyostatin. *Eur. J. Org. Chem.* **2010**, *2010* (11), 2148-2156.
269. Eisner, U.; Elvidge, J. A.; Linstead, R. P., 281. Polyene acids. Part VI. A new (*cis-trans*)-isomer of sorbic acid and its relation to hexenolactones. *J. Chem. Soc. (Resumed)* **1953**, (0), 1372-1379.
270. Cardillo, G.; Orena, M.; Sandri, S., Synthesis of compounds containing the isoprene unit: a stereospecific synthesis of dehydronerol isovalerate, a component of *anthemis Montana* L. *Tetrahedron* **1976**, *32* (1), 107-108.
271. Masamune, S.; Imperiali, B.; Garvey, D. S., Synthesis of ansamycins: the ansa chain of rifamycin S. *J. Am. Chem. Soc.* **1982**, *104* (20), 5528-5531.
272. Constantino, M. G.; Losco, P.; Castellano, E. E., A novel synthesis of (±)-abscisic acid. *J. Org. Chem.* **1989**, *54* (3), 681-683.
273. Feng, Y.; Liu, J.; Carrasco, Y. P.; MacMillan, J. B.; De Brabander, J. K., Rifamycin biosynthetic congeners: isolation and total Synthesis of rifsaliniketal and total synthesis of salinisporamycin and saliniketals A and B. *J. Am. Chem. Soc.* **2016**, *138* (22), 7130-7142.
274. Nakata, T.; Hata, N.; Oishi, T., A stereoselective synthesis of (2*Z*,4*E*)-dienoic acid involving masked functional groups: *n*-Bu₄NF-induced ring opening of α,β-unsaturated δ-lactone. *ChemInform* **1990**, *21* (34).
275. Bridgwood, K. A. *Towards the total synthesis of leustroducsin B*. Doctoral dissertation, University of Cambridge, Great Britain. **2009**.
276. Li, H.-Y.; Sun, H.; DiMagno, S. G., Tetrabutylammonium fluoride. *e-EROS* **2007**.

277. Olofson, R. A.; Landesberg, J. M.; Houk, K. N.; Michelman, J. S., The deprotonation of thiazole and related bases. *J. Am. Chem. Soc.* **1966**, *88* (18), 4265-4266.
278. Davies, J. S.; Higginbotham, C. L.; Tremeer, E. J.; Brown, C.; Treadgold, R. C., Protection of hydroxy groups by silylation: use in peptide synthesis and as lipophilicity modifiers for peptides. *J. Chem. Soc., Perkin Trans. 1* **1992**, (22), 3043-3048.
279. Gillard, J. W.; Fortin, R.; Morton, H. E.; Yoakim, C.; Quesnelle, C. A.; Daignault, S.; Guindon, Y., Symmetrical alkoxysilyl ethers. A new class of alcohol-protecting groups. Preparation of *tert*-butoxydiphenylsilyl ethers. *J. Org. Chem.* **1988**, *53* (11), 2602-2608.
280. Nicolaou, K. C.; Baker, T. M.; Nakamura, T., Synthesis of the WXYZA' domain of maitotoxin. *J. Am. Chem. Soc.* **2010**, *133* (2), 220-226.
281. Yu, J.; Sun, J.; Niu, Y.; Li, R.; Liao, J.; Zhang, F.; Yu, B., Synthetic access toward the diverse ginsenosides. *Chem. Sci.* **2013**, *4* (10), 3899-3905.
282. Smith Iii, A. B.; Smits, H.; Kim, D.-S., Spirastrellolide studies. Synthesis of the C(1)–C(25) southern hemispheres of spirastrellolides A and B, exploiting anion relay chemistry. *Tetrahedron* **2010**, *66* (33), 6597-6605.
283. Loh, T.-P.; Feng, L.-C., Progress towards the total synthesis of tedanolide: an efficient assembly of the C1–C11 subunit. *Tetrahedron Lett.* **2001**, *42* (34), 6001-6005.
284. Prakash, C.; Saleh, S.; Blair, I. A., Selective de-protection of silyl ethers. *Tetrahedron Lett.* **1989**, *30* (1), 19-22.
285. Ganapathi, K.; Kulkarni, K. D., Chemistry of the thiazoles. *Proc. Natl. Acad. Sci. India. Sect. A* **1953**, *38* (1), 45-57.
286. Willwacher, J.; Heggen, B.; Wirtz, C.; Thiel, W.; Fürstner, A., Total Synthesis, stereochemical revision, and biological reassessment of mandelalide A: chemical mimicry of intrafamily relationships. *Chem. Eur. J.* **2015**, *21* (29), 10416-10430.
287. Wang, M.; Li, C.; Yin, D.; Liang, X.-T., A mild and efficient approach for the deprotection of silyl ethers by sodium periodate. *Tetrahedron Lett.* **2002**, *43* (48), 8727-8729.
288. Kawahara, S.-i.; Wada, T.; Sekine, M., 1:1 and 1:2 complexes of Bu₄NF and BF₃·Et₂O: unique properties as reagents for cleavage of silyl ethers. *Tetrahedron Lett.* **1996**, *37* (4), 509-512.
289. Corey, E. J.; Venkateswarlu, A., Protection of hydroxyl groups as *tert*-butyldimethylsilyl derivatives. *J. Am. Chem. Soc.* **1972**, *94* (17), 6190-6191.
290. Ouellette, R. J.; Rawn, J. D., Amines and Amides. In *Organic Chemistry (Second Edition)*, Ouellette, R. J.; Rawn, J. D., Eds. Academic Press: **2018**; pp 763-800.
291. Gille, A.; Hiersemann, M., (–)-Lytophilippine A: synthesis of a C1–C18 building block. *Org. Lett.* **2010**, *12* (22), 5258-5261.
292. Frank, A. T.; Farina, N. S.; Sawwan, N.; Wauchope, O. R.; Qi, M.; Brzostowska, E. M.; Chan, W.; Grasso, F. W.; Haberfield, P.; Greer, A., Natural macrocyclic molecules have a possible limited structural diversity. *Mol. Divers.* **2007**, *11* (3-4), 115-118.

293. Wessjohann, L. A.; Ruijter, E.; Garcia-Rivera, D.; Brandt, W., What can a chemist learn from nature's macrocycles? – A brief, conceptual view. *Mol. Divers.* **2005**, *9* (1), 171-186.
294. Lafontaine, J. A.; Provencal, D. P.; Gardelli, C.; Leahy, J. W., Enantioselective total synthesis of the antitumor macrolide rhizoxin D. *J. Org. Chem.* **2003**, *68* (11), 4215-4234.
295. Prunet, J., Progress in metathesis through natural product synthesis. *Eur. J. Org. Chem.* **2011**, *2011* (20-21), 3634-3647.
296. Peng, L.; Zhang, F.; Mei, T.; Zhang, T.; Li, Y., Studies on novel macrocyclization methods of cembrane-type diterpenoids: a Stille cyclization approach to (\pm)-isocembrene. *Tetrahedron Lett.* **2003**, *44* (31), 5921-5923.
297. Kobayashi, K.; Fujii, Y.; Hirayama, Y.; Kobayashi, S.; Hayakawa, I.; Kigoshi, H., Design, synthesis, and biological evaluations of aplyronine A–mycalolide B hybrid compound. *Org. Lett.* **2012**, *14* (5), 1290-1293.
298. Illuminati, G.; Mandolini, L., Ring closure reactions of bifunctional chain molecules. *Acc. Chem. Res.* **1981**, *14* (4), 95-102.
299. Rossa, L.; Vögtle, F. In *Synthesis of Medio- and Macrocyclic Compounds by High Dilution Principle Techniques*, Cyclophanes I, Ed. Springer Berlin Heidelberg: **1983**; pp 1-86.
300. Parenty, A.; Moreau, X.; Niel, G.; Campagne, J. M., Update 1 of: Macrolactonizations in the total synthesis of natural products. *Chem. Rev.* **2013**, *113* (1), PR1-PR40.
301. Inanaga, J.; Hirata, K.; Saeki, H.; Katsuki, T.; Yamaguchi, M., A rapid esterification by means of mixed anhydride and its application to large-ring lactonization. *Bull. Chem. Soc. Jpn.* **1979**, *52* (7), 1989-1993.
302. Kobayashi, Y.; Fukuda, A.; Kimachi, T.; Ju-ichi, M.; Takemoto, Y., Asymmetric synthetic study of macrolactin analogues. *Tetrahedron* **2005**, *61* (10), 2607-2622.
303. Hikota, M.; Sakurai, Y.; Horita, K.; Yonemitsu, O., Synthesis of erythronolide a *via* a very efficient macrolactonization under usual acylation conditions with the Yamaguchi reagent. *Tetrahedron Lett.* **1990**, *31* (44), 6367-6370.
304. Shin, Y.; Fournier, J.-H.; Brückner, A.; Madiraju, C.; Balachandran, R.; Raccor, B. S.; Edler, M. C.; Hamel, E.; Sikorski, Rachel P.; Vogt, A.; Day, B. W.; Curran, D. P., Synthesis and biological evaluation of (–)-dictyostatin and stereoisomers. *Tetrahedron* **2007**, *63* (35), 8537-8562.
305. Schrof, R.; Altmann, K.-H., Studies toward the total synthesis of the marine macrolide salarin C. *Org. Lett.* **2018**, *20* (23), 7679-7683.
306. Zhu, W.; Jiménez, M.; Jung, W.-H.; Camarco, D. P.; Balachandran, R.; Vogt, A.; Day, B. W.; Curran, D. P., Streamlined syntheses of (–)-dictyostatin, 16-desmethyl-25,26-dihydrodictyostatin, and 6-*epi*-16-desmethyl-25,26-dihydrodictyostatin. *J. Am. Chem. Soc.* **2010**, *132* (26), 9175-9187.

307. Smith, A. B.; Dong, S.; Fox, R. J.; Brennehan, J. B.; Vanecko, J. A.; Maegawa, T., (+)-Soranicin A: evolution of a viable synthetic strategy. *Tetrahedron* **2011**, 67 (51), 9809-9828.
308. Li, P.; Xu, J.-C., 1-Ethyl 2-halopyridinium salts, highly efficient coupling reagents for hindered peptide synthesis both in solution and the solid-phase. *Tetrahedron* **2000**, 56 (41), 8119-8131.
309. Gu, Y.; Tian, S.-K., Olefination Reactions of Phosphorus-Stabilized Carbon Nucleophiles. In *Stereoselective Alkene Synthesis*, Wang, J., Ed. Springer Berlin Heidelberg: **2012**; pp 197-238.
310. Vedejs, E.; Marth, C. F., Mechanism of the Wittig reaction: the role of substituents at phosphorus. *J. Am. Chem. Soc.* **1988**, 110 (12), 3948-3958.
311. Vedejs, E.; Fleck, T. J., Kinetic (not equilibrium) factors are dominant in Wittig reactions of conjugated ylides. *J. Am. Chem. Soc.* **1989**, 111 (15), 5861-5871.
312. Tian, X.-Y.; Han, J.-W.; Zhao, Q.; Wong, H. N. C., Asymmetric synthesis of 3,3,5,5-tetrasubstituted 1,2-dioxolanes: total synthesis of epiplakinic acid F. *Org. Biomol. Chem.* **2014**, 12 (22), 3686-3700.
313. Kahl, U.; Andernach, L.; Opatz, T., Total Synthesis of *epi*-Trichosetin. *J. Org. Chem.* **2018**, 83 (24), 15170-15177.
314. Tamura, R.; Saegusa, K.; Kakihana, M.; Oda, D., Stereoselective *E* and *Z* olefin formation by Wittig olefination of aldehydes with allylic phosphorus ylides. Stereochemistry. *J. Org. Chem.* **1988**, 53 (12), 2723-2728.
315. Bhatt, U.; Christmann, M.; Quitschalle, M.; Claus, E.; Kalesse, M., The first total synthesis of (+)-ratjadone. *J. Org. Chem.* **2001**, 66 (5), 1885-1893.
316. Edmonds, M.; Abell, A., The Wittig Reaction. In *Modern Carbonyl Olefination* Wiley: **2003**, pp 1-17.
317. Wang, Z., Horner-Wadsworth-Emmons Olefination. In *Comprehensive Organic Name Reactions and Reagents*, Wiley: **2010**, pp 1484-1490.
318. Blakemore, P. R., 1.15 Olefination of Carbonyl Compounds by Main-Group Element Mediators. In *Comprehensive Organic Synthesis II (Second Edition)*, Knochel, P., Ed. Elsevier: Amsterdam, 2014; pp 516-608.
319. Simoni, D.; Rossi, M.; Rondanin, R.; Mazzali, A.; Baruchello, R.; Malagutti, C.; Roberti, M.; Invidiata, F. P., Strong bicyclic guanidine base-promoted Wittig and Horner-Wadsworth-Emmons Reactions. *Org. Lett.* **2000**, 2 (24), 3765-3768.
320. Chintareddy, V. R.; Ellern, A.; Verkade, J. G., P[N(*i*-Bu)CH₂CH₂]₃N: Nonionic Lewis base for promoting the room-temperature synthesis of α,β -unsaturated esters, fluorides, ketones, and nitriles using Wadsworth-Emmons phosphonates. *J. Org. Chem.* **2010**, 75 (21), 7166-7174.
321. Iorga, B.; Eymery, F.; Mouriès, V.; Savignac, P., Phosphorylated aldehydes: preparations and synthetic uses. *Tetrahedron* **1998**, 54 (49), 14637-14677.

322. Haugan, J. A.; Lobkovskyb, E.; Liaaen-Jensena, S., Total synthesis of C₃₁-methyl ketone apocarotenoids 3. On the structure of hopkinsiaxanthin: first total synthesis of (all-*E*)-(3*S*)- and (9*Z*)-(3*S*)-7'-apohopkinsiaxanthin. *Acta Chem. Scand.* **1997**, *51*, 1201-1216.
323. Zhao, Y.-J.; Loh, T.-P., Practical synthesis of 1,5-dimethyl substituted conjugated polyenes from geranyl acetate. *Tetrahedron* **2008**, *64* (22), 4972-4978.
324. Mohamed-Hachi, A.; About-Jaudet, E.; Combret, J.-C.; Collignon, N., 4-Diethoxyphosphonyl-2-methyl-1,3-dienolates and their O-acylated and O-silylated derivatives: new, efficient and highly stereoselective polyvinylolation reagents. *Synthesis* **1999**, 1999 (07), 1188-1192.
325. Lengkeek, N. A.; Greenwood, P. F.; Nguyen, B.; Koutsantonis, G. A.; Piggott, M. J., Making mixtures to solve structures: structural elucidation *via* combinatorial synthesis. *J. Comb. Chem.* **2010**, *12* (1), 141-150.
326. Luche, J.-L.; Rodriguez-Hahn, L.; Crabbé, P., Reduction of natural enones in the presence of cerium trichloride. *J. Chem. Soc., Chem. Commun.* **1978**, (14), 601-602.
327. Arbusow, B. A., Michaelis-Arbusow-und perkow-reaktionen. *Pure Appl. Chem.* **1964**, *9* (2), 307-336.
328. Bhattacharya, A. K.; Thyagarajan, G., Michaelis-Arbuzov rearrangement. *Chem. Rev.* **1981**, *81* (4), 415-430.
329. Hari Babu, B.; Syam Prasad, G.; Naga Raju, C.; Venkata Basaveswara Rao, M., Synthesis of phosphonates *via* Michaelis-Arbuzov reaction. *Curr. Org. Synth.* **2017**, *14* (6), 883-903.
330. Iranpoor, N.; Firouzabadi, H.; Rajabi Moghadam, K.; Etemadi-Davan, E., Triphenylphosphine/2,3-dichloro-5,6-dicyanobenzoquinone (PPh₃/DDQ) system for conversion of alcohols and thiols into trialkyl phosphonates. *Asian J. Org. Chem.* **2015**, *4* (11), 1289-1293.
331. Ma, X.; Xu, Q.; Li, H.; Su, C.; Yu, L.; Zhang, X.; Cao, H.; Han, L.-B., Alcohol-based Michaelis-Arbuzov reaction: an efficient and environmentally-benign method for C-P (O) bond formation. *Green Chem.* **2018**, *20* (15), 3408-3413.
332. Thirumurugan, P.; Matosiuk, D.; Jozwiak, K., Click chemistry for drug development and diverse chemical-biology applications. *Chem. Rev.* **2013**, *113* (7), 4905-4979.
333. Yang, M.; Li, J.; Chen, P. R., Transition metal-mediated bioorthogonal protein chemistry in living cells. *Chem. Soc. Rev.* **2014**, *43* (18), 6511-6526.
334. Kempe, K.; Krieg, A.; Becer, C. R.; Schubert, U. S., "Clicking" on/with polymers: a rapidly expanding field for the straightforward preparation of novel macromolecular architectures. *Chem. Soc. Rev.* **2012**, *41* (1), 176-191.
335. Kolb, H. C.; Finn, M. G.; Sharpless, K. B., Click chemistry: diverse chemical function from a few good reactions. *Angew. Chem. Int. Ed.* **2001**, *40* (11), 2004-2021.

336. Fürstner, A.; Bonnekessel, M.; Blank, J. T.; Radkowski, K.; Seidel, G.; Lacombe, F.; Gabor, B.; Mynott, R., Total synthesis of myxovirescin A1. *Chem. Eur. J.* **2007**, *13* (31), 8762-8783.
337. De Luca, L.; Giacomelli, G.; Porcheddu, A., A very mild and chemoselective oxidation of alcohols to carbonyl compounds. *Org. Lett.* **2001**, *3* (19), 3041-3043.
338. Denmark, S. E.; Edwards, M. G., On the mechanism of the selenolactonization reaction with selenenyl halides. *J. Org. Chem.* **2006**, *71* (19), 7293-7306.
339. Meyers, S. R.; Juhn, F. S.; Griset, A. P.; Luman, N. R.; Grinstaff, M. W., Anionic amphiphilic dendrimers as antibacterial agents. *J. Am. Chem. Soc.* **2008**, *130* (44), 14444-14445.
340. Dams, I.; Chodyński, M.; Krupa, M.; Pietraszek, A.; Zezula, M.; Cmoch, P.; Kosińska, M.; Kutner, A., A novel convergent synthesis of the potent antiglaucoma agent travoprost. *Tetrahedron* **2013**, *69* (5), 1634-1648.
341. Lee, Y.-S.; Park, S. M.; Kim, B. H., Synthesis of 5-isoxazol-5-yl-2'-deoxyuridines exhibiting antiviral activity against HSV and several RNA viruses. *Bioorg. Med. Chem. Lett.* **2009**, *19* (4), 1126-1128.
342. Ripperger, H., Zur darstellung und selektiven reduktion von geschützten endothiopeptiden. *J. Prakt. Chem.* **1987**, *329* (6), 1039-1044.
343. Henrion, G.; Chavas, T. E. J.; Le Goff, X.; Gagosz, F., Biarylphosphonite gold(I) complexes as superior catalysts for oxidative cyclization of propynyl arenes into indan-2-ones. *Angew. Chem. Int. Ed.* **2013**, *52* (24), 6277-6282.
344. Parsons, S. R.; Hooper, J. F.; Willis, M. C., *O*-Substituted alkyl aldehydes for rhodium-catalyzed intermolecular alkyne hydroacylation: the utility of methylthiomethyl ethers. *Org. Lett.* **2011**, *13* (5), 998-1000.
345. Mahammed, K. A.; Jayashankara, V. P.; Prem Sai Rai, N.; Mohana Raju, K.; Arunachalam, P. N., A mild and versatile synthesis of thioamides. *Synlett* **2009**, *2009* (14), 2338-2340.
346. Frederico, D.; Donate, P. M.; Constantino, M. G.; Bronze, E. S.; Sairre, M. I., A short and efficient synthesis of crocetin-dimethylester and crocetinindial. *J. Org. Chem.* **2003**, *68* (23), 9126-9128.
347. Manley, D. W.; McBurney, R. T.; Miller, P.; Walton, J. C.; Mills, A.; O'Rourke, C., Titania-promoted carboxylic acid alkylations of alkenes and cascade addition-cyclizations. *J. Org. Chem.* **2014**, *79* (3), 1386-1398.
348. Ella-Menye, J.-R.; Sharma, V.; Wang, G., New synthesis of chiral 1,3-oxazinan-2-ones from carbohydrate derivatives. *J. Org. Chem.* **2005**, *70* (2), 463-469.
349. Hernández, D.; Lindsay, K. B.; Nielsen, L.; Mittag, T.; Bjerglund, K.; Friis, S.; Mose, R.; Skrydstrup, T., Further studies toward the stereocontrolled synthesis of silicon-containing peptide mimics. *J. Org. Chem.* **2010**, *75* (10), 3283-3293.

350. Gao, X.; Han, H.; Krische, M. J., Direct generation of acyclic polypropionate stereopolyads *via* double diastereo- and enantioselective iridium-catalyzed crotylation of 1,3-diols: beyond stepwise carbonyl addition in polyketide construction. *J. Am. Chem. Soc.* **2011**, *133* (32), 12795-12800.
351. Mohapatra, D. K.; Reddy, D. S.; Janaki Ramaiah, M.; Ghosh, S.; Pothula, V.; Lunavath, S.; Thomas, S.; Pushpa Valli, S. N. C. V. L.; Bhadra, M. P.; Yadav, J. S., Rugulactone derivatives act as inhibitors of NF- κ B activation and modulates the transcription of NF- κ B dependent genes in MDA-MB-231 cells. *Bioorg. Med. Chem. Lett.* **2014**, *24* (5), 1389-1396.
352. Kirsch, S. F.; Klahn, P.; Menz, H., The use of COP-OAc in the catalyst-controlled syntheses of 1,3-polyols. *Synthesis* **2011**, *2011* (22), 3592-3603.
353. Lengkeek, N. A.; Greenwood, P. F.; Nguyen, B.; Koutsantonis, G. A.; Piggott, M. J., Making mixtures to solve structures: structural elucidation *via* combinatorial synthesis. *J. Comb. Chem.* **2009**, *12* (1), 141-150.
354. Magoulas, G. E.; Bariamis, S. E.; Athanassopoulos, C. M.; Haskopoulos, A.; Dedes, P. G.; Krokidis, M. G.; Karamanos, N. K.; Kletsas, D.; Papaioannou, D.; Maroulis, G., Syntheses, antiproliferative activity and theoretical characterization of acitretin-type retinoids with changes in the lipophilic part. *Eur. J. Med. Chem.* **2011**, *46* (2), 721-737.
355. Kim, K.; Punna, V.; Karri, P.; Krishnamurthy, R., Synthesis of phosphoramidites of isoGNA, an isomer of glycerol nucleic acid. *Beilstein J. Org. Chem.* **2014**, *10*, 2131-2138.
356. Singh, S.; Gajulapati, V.; Kim, M.; Goo, J.-I.; Lee, J. K.; Lee, K.; Lee, C.-K.; Jeong, L. S.; Choi, Y., A divergent approach for the synthesis of d- and l-4'-ethynyl dioxolane nucleosides with potent anti-HIV activity. *Synthesis* **2016**, *48* (18), 3050-3056.
357. Leftheris, K.; Goodman, M., Synthesis and β -adrenergic antagonist activity of stereoisomeric practolol and propranolol derivatives. *J. Med. Chem.* **1990**, *33* (1), 216-223.
358. Doboszewski, B.; Groaz, E.; Herdewijn, P., Synthesis of phosphonoglycine backbone units for the development of phosphono peptide nucleic acids. *Eur. J. Org. Chem.* **2013**, *2013* (22), 4804-4815.